Nitrogen, Oxygen and Fluorine Rich *N*-(Hetero)Aryl-1,2,3-Triazoles: A Resource For High Energy Materials

A Thesis
Submitted for the Degree of
DOCTOR OF PHILOSOPHY

In

Chemistry

By

Ambarkar Sudheer Kumar

ACRHEM, School of Chemistry
University of Hyderabad
Hyderabad 500 046
Telangana State
INDIA

August, 2015

DEDICATION

My Family Members

	Page No.
Statement	i
Certificate	iii
Acknowledgements	v
List Abbreviations	ix
Chapter 1: Introduction to High Energy Materials	1
1.1. History & Background of High Energy Materials	3
1.2. Definition and Introduction	4
1.3. Explosophores	4
1.4. Factors which must be considered for the synthesis of novel energetic materials are	4
1.5. Classification of High Energy Materials	5
1.5.1 Explosives	5
1.5.1.1. Explosives and its Classification	5
1.5.1.1.1. Thermally Stable Explosives	7
1.5.1.1.2. High Performance Explosives	8
1.5.1.1.3. Melt-Cast Explosives	9
1.5.1.1.4. Insensitive Explosives	9
1.5.2. Propellants	10
1.5.3. Pyrotechnics	12
1.6. Different terms involved in High Energy Materials Science	12
1.7. Role Azole Derivatives in High Energy Materials	15
1.7.1. Introduction of nitrogen-rich heterocyclic rings	15
1.7.2. Energetic five membered N-heterocyclic derivatives	16
1.7.3. Energetic six membered N-heterocycles derivatives	17
1.7.4. Fused heterocycles	18
1.8. Importance of Strained and Benzene Rings	18
1.8.1. Energetic materials having strained rings	18
1.8.2. Energetic materials having benzene ring	18
1.9. Challenges to Discover the Modern Energetic Materials	18
1.10. Objective of the thesis	19
1.11. References	20
Chapter 2: Synthesis of Thermally Stable Energetic 1,2,3-Triazole Derivatives	25
2.1. Introduction	27
2.1.1. Precedents and Strategies for 1H-1,2,3-triazole derivatives towards energetic-materials applications	28
2.1.2. Motivation and Design Plan	33
2.2. Results and Discussion	33
2.3. X-Ray Crystallography	42
2.4. Energetic Properties	45
2.5. Potential Energy Diagrams	47
2.6. Conclusion	49

2.7. Future Work 49
2.8. Experimental 51
2.8.1. Caution 51
2.8.2. General Experimental Information 51
2.8.3. X-ray Crystallography Information 52
2.8.4. Theoretical Study Information 52
2.8.5. Materials 53
2.8.6. General procedure for the synthesis of azides (GP-1) 53
2.8.7. General Cycloaddition Procedure (GP-2) 53
2.8.8. General procedure for the synthesis of compounds 5a–11 (GP-3) 54
2.8.9. General procedure for the synthesis of compounds 15–22 (GP-4) 54
2.8.10. General procedure for the formation of the N-oxides (GP-5) 54
2.9. Spectral and Analytical Data of the Compounds 55
2.10. References 69
2.11. Spectra 73
2.12. Applications 84

Chapter 3: Synthesis of Triflurомethyl-Substituted N-Aryl Poly-1,2,3-Triazole-Derivatives 85

3.1. Introduction 87
3.1.1. Background of –CF3 substituted-1,2,3-triazole based energetic compounds 87
3.1.2. Motivation and Design Plan 88
3.2. Results and Discussion 89
3.3. X-Ray Crystallography 96
3.4. Energetic Properties 99
3.5. Potential Energy Diagrams 101
3.6. Conclusion 104
3.7. Future Work 104
3.8. Experimental 105
3.8.1. Caution 105
3.8.2. General Experimental Information 105
3.8.3. X-ray Crystallography Information 105
3.8.4. Theoretical Study Information 106
3.8.5. Isodesmic reactions for the titled compounds 107
3.8.6. Materials 110
3.8.7. General procedure for the synthesis of azides (GP-1) 110
3.8.8. General Cycloaddition Procedure (GP-2) 110
3.8.9. General procedure for the synthesis of compounds 3a–3m (GP-3) 111
3.8.10. General procedure for the synthesis of compounds 5–15 (GP-4) 111
3.9. Spectral and Analytical Data of the Compounds 111
3.10. References 128
3.11. Spectra 131

Chapter 4: Synthesis and Energetic Studies of Nitrogen-Rich *N*-Hetero-Aryl-Azole Derivatives 157

4.1. Introduction 159
4.1.1. Background of pirydyl-/pyrimidyl-tethered azoles for energetic materials applications 159
4.1.2. Motivation and Design Plan 163
4.2. Results and Discussion 164
4.3. X-Ray Crystallography 171
4.4. Energetic Properties 174
4.5. Potential Energy Diagrams 176
4.6. Conclusion 177
4.7. Future Work 178
4.8. Experimental 179
4.8.1. General Experimental Information 179
4.8.2. Safety Precautions 179
4.8.3. X-ray Crystallography Information 179
4.8.4. Theoretical Study Information 179
4.8.5. Isodesmic reactions for the titled compounds 179
4.8.6. Materials 181
4.8.7. General Procedure for the Synthesis of Compounds 39a, 39b-39b', 46-51, 58a-58d and 61a-61d (GP-1) 181
4.8.8. General Procedure for the Synthesis of Compounds 42 and 43+44 (GP-2) 181
4.8.9 General procedure for the synthesis of azides (GP-3) 181
4.8.10 General Cycloaddition Procedure for the Synthesis of Compounds 54-55 (GP-4) 182
4.9. Spectral and Analytical Data of the Compounds 182
4.10. References 191
4.11. Spectra 194

List of Publications 209

Conference attended 211

STATEMENT

I hereby declare that the matter embodied in the thesis **entitled** "**Nitrogen, Oxygen and Fluorine Rich *N*-(Hetero)Aryl-1,2,3-Triazoles: A Resource For High Energy Materials**" is the result of investigation carried out by me in the Advanced Center of Research in High Energy Materials (ACRHEM) and School of Chemistry, University of Hyderabad, Hyderabad, India, under the supervision of **Dr. Akhila Kumar Sahoo**.

In keeping with the general practice of reporting scientific observations, due acknowledgements have been made on the basis of the findings of other investigators. Any omission, which might have occurred by oversight or error, is regretted. This research work is free from Plagiarism. I hereby agree that my thesis can be deposited in shodganga/INFLIBNET. A report on plagiarism statistics from the University Librarian is enclosed.

Ambarkar Sudheer Kumar
10ACPA02

Dr. Akhila Kumar Sahoo
Supervisor

University of Hyderabad
August, 2015

Dr. A. K. Sahoo
Associate Professor
Work: +91-40-23134822
Fax: +91-40-23012460
e-mail: akssc@uohyd.ernet.in/
akhilkumar_s@yahoo.com

School of Chemistry
University of Hyderabad
Prof. C. R. Rao Road, Gachi Bowli
Hyderabad – 500 046
INDIA

CERTIFICATE

Certified that the work contained in the thesis entitled "**Nitrogen, Oxygen and Fluorine Rich *N*-(Hetero)Aryl-1,2,3-Triazoles: A Resource For High Energy Materials**" has been carried out by ***Mr. Ambarkar Sudheer Kumar*** under my supervision. I declare that this work has not been submitted previously in part or in full to this university or other university or institution for the award of any degree.

DIRECTOR
ACRHEM

Dr. Akhila Kumar Sahoo
(Supervisor)

Dean
School of Chemistry

Dean
School of Physics

Acknowledgements

I wish to express my deep sincere heartfelt gratitude to my supervisor **Dr. Akhila Kumar Sahoo** for his splendid guidance, patience, suggestions, encouragement, constant support, inspiration, valuable discussions, advices, and personal freedom rendered to me during my research period. His endless enthusiasm, good mannerism and respective attitude will always remain a source of inspiration for me. I will be always obliged to him for his friendly behavior with me. I am fortunate enough to join under his supervision. His powerful words are motivated me a lot in my life and his best wishes which made me what I am today. He considered me as a one the family member. I consider my association with him as a cherishable memory in my life.

It's my privilege to thank Dr. K. Venkateswara Rao, Director, Advanced Center of Research in High Energy Materials (ACRHEM), University of Hyderabad and Prof. S. P. Tewari, (former Director of ACRHEM) for their support, encouragement and helpful discussions throughout my research work. I extend my sincere thanks to Prof. M. Durga Prasad, Dean, School of Chemistry for providing work place and experimental facilities. I also thank to former Deans Prof. M. V. Rajasekharan, Prof. D. Basavaiah, Prof. M. Periasamy and all the faculty members, School of Chemistry for their co-operation on various aspects. Prof. M. Durga Prasad and Prof. S. Mahapatra are thanked for their support and valuable suggestions in computational chemistry. I also want to thank the CMSD, University of Hyderabad, for providing computational facilities.

I am grateful to thank my doctoral committee members Dr. K. Muralidharan and Dr. P. K. Panda for their support, encouragement, helpful suggestions, and strict evaluation on doctoral committee reports. I sincerely thank all the faculty and non-teaching staff of the School of Chemistry and ACRHEM for their assistance on various occasions.

I am very happy to collaborate and indebted to Dr. Anil K. Choudary for his support, valuable discussions and guidance in physics which has been helped to extend my knowledge and helpful for my research work. His association was joyful.

I would like to thank Dr. A. K. Sikder and HEMRL team members Dr. Radha Krishna, Dr. Anniyappan, Dr. Shfee Khan and Mr. Abhijit Singh for their support, guidance and helpful discussions during RAB meetings.

I would like to acknowledge DRDO, HEMRL and ACRHEM for the fellowship and financial support. Sincere thanks to ACRHEM and University Purse Grant (UPE-Phase-II) for providing the financial assistance for attending the international conference "NTREM-

2015" held at University of Pardubice, Pardubice, Czech Republic, European Union during 15th April-17th April-2015.

My heart full thanks to my senior cum friend Dr. Vikas D. Ghule. Without his support, encouragement and kind help my Ph.D work unsuccessful. He has shown the path in my Ph.D tenure with lots of patience. In addition, he only taught me all the computational calculations. His help in my life is highly obliged.

My Special thanks go to Dr. M. Bhanuchandra for his support, encouragement, respect, best wishes during my Ph.D work. His valuable discussions and suggestions are helped me a lot to increase my subject in chemistry. He treated me as a brother. After my parents he is the only person who has not hurts me with his words. He helped me a lot as professionally and personally. I am lucky enough to have such kind of person in my life.

Sincere thanks to my co-worker and friend Nagarjuna Kommu for his help, encouragement, pleasant company, respect, and cooperation during my tenure. His valuable discussions and suggestions are highly appreciable. Especially while my thesis corrections he helped me lot and his contribution and suggestions are outstanding for the progress of my thesis work. He is very kind, honest, gentle and encouraging person.

I take this opportunity to thank my college Dr. J. Raveendra. He is the one person who taught me fundamentals of chemistry during my pre Ph.D. viva. His patience and encouragement is highly appreciable.

From the bottom of my heart I thank to my friends and labmates Dr. Bhanuchandra, Dr. K. Malleshwararao, Dr. M. Ramu Yadav, Dr. Nayan Ghosh, Dr. Raja K. Rit, Dr. Sanatan Nayak, Dr. Nagarjuna Kommu, Dr. J. Raveendra, Koushik Ghosh, Prabagar, Shankar Majji, E. Ramesh, Rajender Mallick, Suman Dana, Rangu Prasad and Kallol Mukharjee for their helpful discussion, pleasant company, creating cheerful work atmosphere and cooperation during my Ph.D. tenure. Especially, I appreciate the support of Dr. Ramu Yadav, Dr. Raja K. Rit, Dr. Sanatan Nayak, Dr. Nagarjuna Kommu, Dr. J. Raveendra and Mr. Koushik Ghosh. Without their support, help and encouragement it is not possible to complete the Ph. D work. I also thank to UGC networking project students for their help during my thesis work.

I am lucky enough to have family friends Dr. A. K. Sahoo, Smt. Rashmita Sahoo and cute Amlesh Sahoo (sonu). I am specially wishing to Amlesh Sahoo (sonu) for his bright future. My special thanks to Madam for her patience in preparing a many variety of dishes, when our lab members are gathered in home. Finally, I would like to say hats off to Sahoo family for their patience and heartfelt thanks to them for considering me as family member.

My sincere thanks to Prof. F. Nawaz Khan, VIT University, Vellore, Tamil Nadu for his marvelous training in research and honorable support during my M.Sc. project.

I feel fortunate to have my close friend P. B. Raj (Manager, Perkin Elmer (India) Pvt. Ltd., Hyderabad) who has supported me personally, professionally and financially throughout my Ph.D career. My heart full thanks to him for his outstanding encouragement.

I am indeed fortunate to have friends like Mr. Y. Daniel, Mr. Nirmal, Mr. Eeswar Karki and Mr. Rafi Shaik. These are the people always supported and encouraged during my entire Ph.D career.

I appreciate the support of Dr. P. Raghaviah, Dr. Naba K. Nath, Dr. S. Sudalai Kumar, Dr. D. Maddileti, and Mr. P. Krishna Chary (School of Chemistry, the University of Hyderabad) for performing the X-ray crystallography studies.

I would like to acknowledge ACRHEM friends Dr. P. Gopala Krishana, Dr. Syed Ahmad and Mr. K. S. Rao for their support.

It is great pleasure to thank my family members, A. Suabsh Chandra Rao, A. Satyavathi, A. Madhu Sudhana Rao, A. Raviteja, and A. Nagini for their support, love and affection. My family is always cared and loved me. Without their support I could not reached at this stage. I owe everything to them. I would like to thank all my relatives for their help and close association with me.

Finally, I thank all of them who are involved directly or indirectly for the successful completion of this Ph.D thesis.

Ambarkar Sudheer Kumar

University of Hyderabad
August, 2015

List of Acronyms

NMR	-	Nuclear Magnetic Resonance
FTIR	-	Fourier Transform Infrared
GC-MS	-	Gas Chromatography-Mass Spectrometry
LC-MS	-	Liquid Chromatography-Mass Spectrometry
HPLC	-	High Pressure Liquid Chromatography
GPC	-	Gas Phase Chromatography
EI	-	Electron Ionization
ESI	-	Electron-Spray Ionization
XRD	-	X-Ray Diffraction
s	-	singlet
d	-	doublet
m	-	multiplet
q	-	quartet
bs	-	broad singlet
bd	-	broad doublet
dd	-	double doublet
Hz	-	Hertz
J	-	Coupling Constant in Hertz
mp	-	Melting Point
TMS	-	Trimethylsilyl
DMSO	-	Dimethylsulfoxide
DMF	-	Dimethylformamide
THF	-	Tetrahydrofuran
EtoAc	-	Ethyl acetate
MeOH	-	Methanol
DCM	-	Dichloromethane
tBuOH	-	Tertiary Butanol
RT	-	Room Temperature
^{o}C	-	Degree Celsius
m-CPBA	-	*m*-chloroperbenzoic acid
reflns	-	Reflections
GOF	-	Good of Fitness

DFT	-	Density Functional Theory
CVFF	-	Consistence Valence Force Field
ZPE	-	Zero Point Energies
AM1	-	Austin Model 1
PM1	-	Parameterization Method 3
PM6	-	Parameterization Method 6
DSC	-	Differential Scanning Calorimetry
TGA	-	Thermogravimetic Analysis
DTA	-	Decomposition Temperature Analysis
HOF	-	Heat of Formation
VOD	-	Velocity of Detonation
DP	-	Detonation Pressure
T_m	-	Thermal Melting
T_d	-	Thermal Decomposition
GPa	-	Gigapascal
Is	-	Impact Sensitivity
Fs	-	Friction Sensitivity
ESD	-	Electrostatic Discharge
kcal	-	Kilo Calorie
kJ	-	Kilo Joule
km	-	Kilometer
sec	-	second
TNT	-	Trinitrotoluene
HNS	-	Hexanitrostilbene
TATB	-	Triaminotrinitrobenzene
RDX	-	1,3,5-Trinitro-1,3,5-triazinane
HMX	-	1,3,5,7-Tetranitro-1,3,5,7-tetrazocane
CL-20	-	2,4,6,8,10,12-Hexanitro-2,4,6,8,10,12-hexaazaisowurtzitane

Chapter 1

Introduction to High Energy Materials

Abstract

This chapter describes the brief history, introduction of the high energy materials and classification of explosives, propellants and pyrotechnics. The general terms used in the "High Energy Materials Science" are enumerated. The strength and utility of azole and azine (five membered and six membered heterocycles) derivatives for the development of various energetic materials is also shown. Main features of energetic materials, challenges and goals pertaining to the discovery of novel energetic materials are also emphasized. The objective of the thesis revolves for the design and synthesis of insensitive energetic materials. The potential application of high energy materials for military, space and civilian purposes is also highlighted.

1.1. History & Background of High Energy Materials

Discovery of black powder by Chinese alchemists in 220 BC and its utility in weapons as gun powder has made significant impact in the sustainable development of energetic materials.[1] Awareness of black powder was at first conceived by the German monk Berthold Schwartz in the 14th century. Black powder has been used for blasting purposes.[2] In 19th century, nitroglycerine (NG) has been invented by the Italian chemist Ascanio Sobrero; NG was initially used for the medication of heart disease and later it has been used as potential energetic material. NG is highly sensitive and therefore not useful for military and civil applications.[3] In 1875 Alfard Nobel invented dynamite, a combination of NG and kiselghur, which is less sensitive and easy to handle compared to pure NG. Later, the Swedish chemists Ohlsson and Norrbin found that addition of ammonium nitrate to dynamite improves its explosive nature. The emergent use of dynamite in coal mines promotes in the development of new energetic materials picric acid and trinitrotoluene (TNT).[4] Picric acid is highly acidic and suffers with considerable drawbacks, whereas the less sensitive TNT has been used in the 1st World War. Later in the early Second World War, nitramine bearing explosives RDX and HMX are successfully used.[4,5] Until 20th century the less sensitive RDX has been found greater use and more powerful than other common explosives, for example pentaerythritol tetranitrate (PETN), triaminotrinitrobenzene (TATB), hexanitrobenzene (HNB) and so on.[4,5] Structures of some of the common explosives are shown in Figure 1.1.[5]

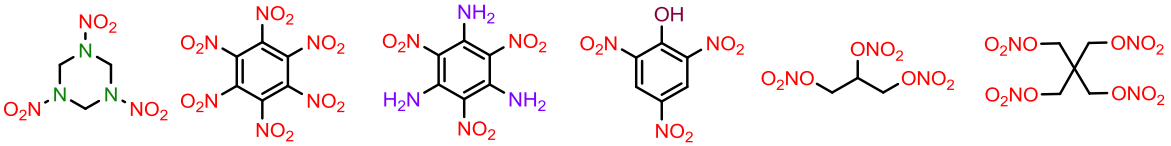

Figure 1.1. Common explosives and their structures

Development of novel energetic materials is highly essential, as its applications are widely sensed to military and civilian applications. Therefore considerable research activities are aimed in the synthesis of thermal stable, biodegradable, green powerful energetic N, O-rich small strained molecular scaffolds with high velocity of detonation and detonation pressure compared to the known benchmark energetic compounds.[6] Thus, design of energetic materials is envisaged on the basis of stability and performance of the molecule. Furthermore, effective application of thermally stable energetic materials to military and civilian use needs detailed investigation.

1.2. Definition & Introduction

The energetic material can be defined as "a substance on initiation by heat, spark or flame undergoes rapid chemical reaction with the evolution of large amount of heat and pressure".[1]

Energetic materials are generally composed of readily oxidizable nitro, azido and hydrazino groups. Oxidation is a process when explosive materials undergo decomposition or detonation and release energy. The organic explosive materials mainly consist of carbon, hydrogen, oxygen, nitrogen and fluorine elements. Thus, combustion of organic explosive materials readily converts carbon to CO_2 and hydrogen to H_2O. Similarly, nitrogen translates to N_2 gas during detonation; as molecular nitrogen possesses low internal energy than the oxides of nitrogen (NO, NO_2, N_2O_3, etc.). Accordingly, $–NO_2$ and $–ONO_2$ groups are the source of oxygen in the molecule, which in turn significantly assists for detonation or combustion process.[2-5]

The nitrogen-rich high energetic materials find versatile utility; as a consequence development of novel high nitrogen content (HNC) materials is always important. In general, high nitrogen content (HNC) materials derive energy through high positive heat of formation rather than the oxidation of carbon backbone. Usually high nitro-/nitrogen content in the molecule contribute enhancing density, detonation performance and generate large quantity of gases per gram.[6,7]

1.3. Explosophores

The groups rapidly converted to gaseous products during detonation of the molecule are called explosophores.[4] The nitrogen and oxygen bearing nitro, nitroso, nitramine, nitrate ester, and azido moieties are explosophoric groups. The oxygen content in the explosophoric groups is useful for the conversion of molecular backbone to gaseous byproducts NO_2, CO_2, CO, and H_2O.[5]

1.4. Factors responsible for the synthesis of novel energetic materials are[6]

i) the easy and cost efficient availability of raw materials with eco-friendly nature
ii) the production of non-toxic and non-hygroscopic by-products during detonation
iii) the thermal and chemical stability of the compounds for long-time storage
iv) the insensitivity of the compound to stimuli for safe transportation and handling
v) the delivery of high enthalpy of formation and density for better performance
vi) the compound with better oxygen balance useful for complete combustion

1.5. Classification of High Energy Materials

Energetic materials are typically classified as explosives, propellants, and pyrotechnics. These classes of compounds are distinguished on the basis of the generation of products and the rate of reaction.[4] The classification is schematically depicted in Figure 1.2.

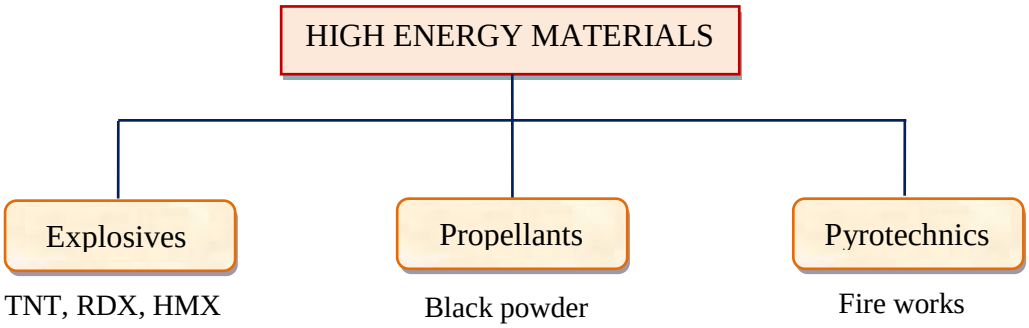

Figure 1.2. Classification of high energy materials

1.5.1. Explosives:

Explosive is a substance with large amount of stored potential energy. It is capable of making

explosion by its own energy through rapid and self propagating decomposition of compounds. Oxidation of materials led to decomposition; this process thus releases energy through heat and therefore exothermic.[8-10] Classification of explosives is made on the basis of the chemical behavior and performance of the compounds (Figure 1.3).

1.5.1.1. Explosives and its classification

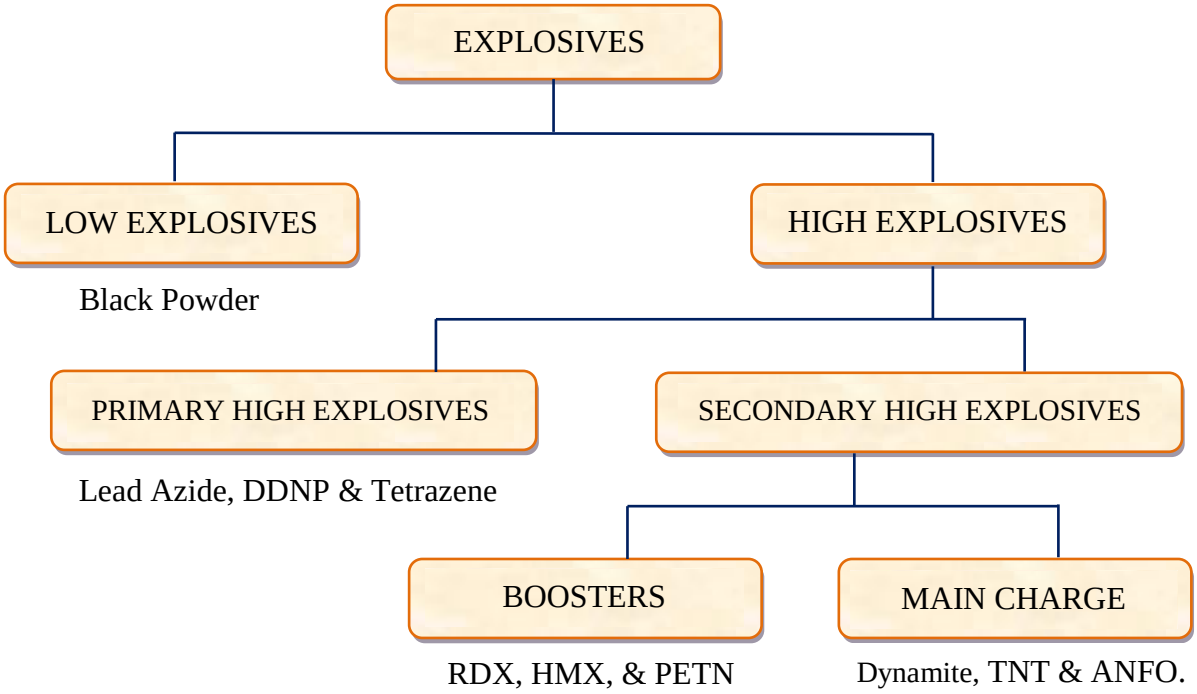

Figure 1.3. Classification of chemical explosives

Low explosives: Low explosive is combustible materials; this material directly burn but do not explode. Thus, the oxygen required for burning is present within the compound. Finally, gas produced in the burning process causes explosion. Under normal conditions, low explosives deflagrates in a rate of few centimeters per second to 400 meters per second.[8] Detonation of low explosive occurs when ignited in a confined space.[10]

Examples: black powder, flash powder and smokeless powder.

High explosive compounds are capable of sustaining detonation shockwave to produce powerful blast. Detonation occurs under the influence of shock of the suitable primary explosive. Mostly, these compounds are ignited by a flame; some cases the small amount generally burn tranquilly and easily extinguished.[11] A high explosive compound (primary & secondary) detonates at rates ranging from 1,000 to 9,000 meters per second and is conventionally subdivided into two explosives classes, which is differentiated by sensitivity:

Primary high explosives or **initiators** explode or detonate when they are heated or subjected to shock. The detonation velocity ranges from 3500–5500 m s^{-1}. They do not burn; sometimes they do not even contain the elements necessary for combustion. These materials themselves explode and ignite the secondary explosives. These materials are generally sensitive to heat and shock.[8,9]

Examples: $Hg(CNO)_2$ (mercury fulminate) and $Pb(N_3)_2$ (lead azide)

Secondary high explosives also called base explosives. These explosives are generally less sensitive to shock, friction, and heat and more stable than primary explosives. They may burn when exposed to heat or flame in small unconfined quantities. They require much more energy to detonate than primary explosives, but explode with greater violence. However, secondary explosives are safer to handle, store and have broad utility than primary explosives.[9] Based on performance, stability, and sensitivity, classification of secondary explosives are made and shown in Figure 1.4.[9,10]

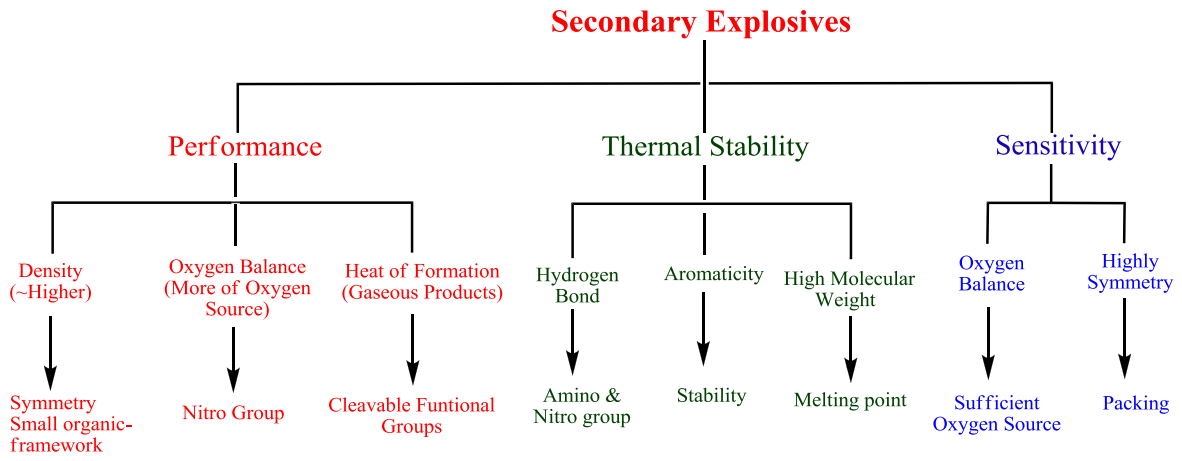

Figure 1.4. Classification of secondary explosives

1.5.1.1.1. Thermal stable explosives

1.5.1.1.2. High performance explosives

1.5.1.1.3. Melt-castable explosives

1.5.1.1.4. Insensitive explosives

1.5.1.1.1. Thermal Stable Explosives:

Thermal stability is an important characteristic of the energetic materials. Explosives with decomposition at high-temperature (preferably > 200 ^{o}C) are typically called as thermally stable explosives.[12-18] Improved thermal stability ensures safer production, increased shelf-life of ammunitions and low vulnerability to accidental initiations. Some of the high performance and good thermal stable explosives are cyclotrimethylene trinitramine (RDX) and cyclotetramethylene tetranitramine (HMX) (>200 ^{o}C).[14] Thus, development of thermal stable high energy materials with better decomposition temperatures than RDX and HMX are always in demand.

Modification of the molecular scaffold would significantly contribute enhancing decomposition temperature of the material. The structural modification of the molecular entities can be suitably performed through:

- induction of poly-N-cataining triazole ring
- introduction of amino groups and conjugation moieties
- salt formation

Some of the representative thermal stable energetic materials are highlighted in Figure 1.5.

Figure 1.5. Examples of thermally stable explosives

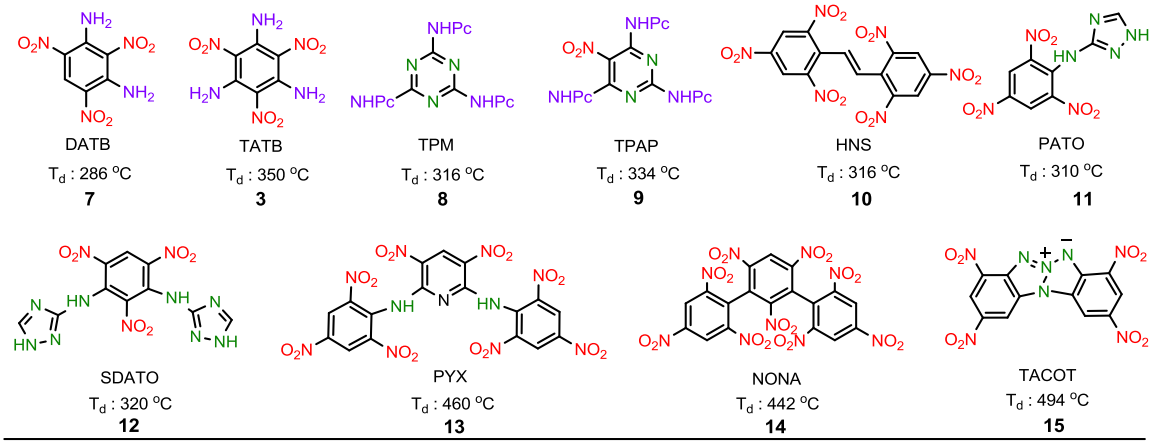

DATB: 1,3-Diamino-2,4,6-trinitrobenzene; TATB: 1,3,5-Triamino-2,4,6-trinitrobenzene; TPM: *N*,*N*-nitropicrylmelamine; TPAP: Tris(picrylamino)pyrimidine; HNS: 2,2',4,4',6,6'-Hexanitrostilbene; PATO: 3-Picrylamino-1,2,4-triazole; SDATO: 2,4-Bis-(3-amino-1,2,4-triazole)-1,3,5-trinitrobenzene; PYX: 2,6-Bis-(picrylamino)-3,5-dinitropyridine; TACOT: Tetranitrodibenzo-3,3a,4,4a-tetrazapentalene; NONA: 2,2',2",4,4',4",6,6',6"- Nonanitrote rphenyl; T_d = Thermal decomposition temperature

1.5.1.1.2. High Performance Explosives:

High performance explosives essentially possess high density (ρ) and high velocity of detonation (vD). These explosive are used in warhead applications.[19,20] Density is the primary physical parameter that determines detonation performance of the molecule. The detonation velocity and pressure of the explosives increases proportionally with the packing density and square of it, respectively. On the other hand, an increase in oxygen balance (O.B.) and heat of formation generally increases the sensitivity as well as performance of the energetic material.[21] Introduction of some coordinating functional groups would enhance density and performance of the materials, as:

- ✓ insertion of trifluoromethyl, pentafluorosulfonyl and nitrogen difluoride (CF_3, SF_5 & NF_2) groups
- ✓ introduction of nitro ($-NO_2$) group and trinitromethyl functionality
- ✓ presence of cage or strained structures in the molecular skeleton

Some of the representative high performance energetic materials are shown in Figure 1.6:

Figure 1.6: Examples of high performance explosives

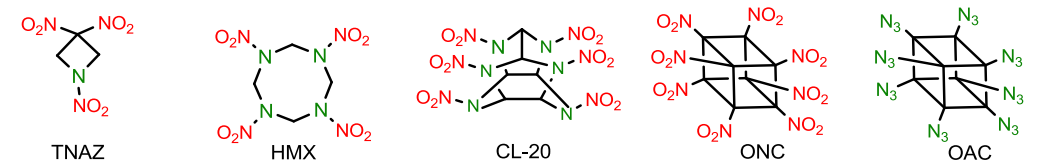

TNAZ: 1,3,3-Trinitroazetidine; CL-20: 2,4,6,8,10,12-Hexanitro-2,4,6,8,10,12-hexaazaisowurtzitane; HMX: Octahydro-1,3,5,7-tetranitro-1,3,5,7-tetrazocine; ONC: Octanitrocubane; OAC: Octaazidocubane; VOD = Velocity of detonation; DP = Detonation pressure

1.5.1.1.3. Melt-Castable Explosives:

The molecules with large variation of melting-point <90 °C and decomposition temperature >250 °C are normally called melt-cast explosives. Most of the melt cast explosives are used in mortars, grenades, artillery shells, warheads and antipersonnel mines.[22,23]

The introduction of methyl (–CH_3), methoxy (–OCH_3) groups in the compound substantially decreases the melting point of the molecule.[23] Some of the melt-cast explosives are mentioned in Figure 1.7.

Figure 1.7. Examples of melt-cast explosives

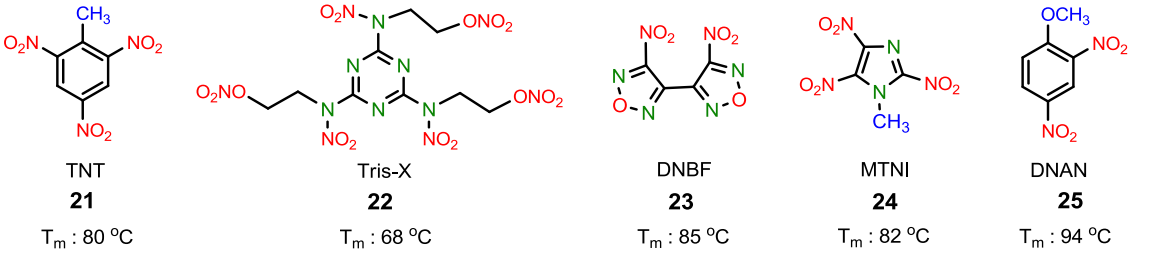

TNT: 2,4,6-Trinitrotoluene; Tris-X: 2,4,6-Tris(2-nitroxyethylnitramino)-1,3,5-triazine; DNBF: 4,4'-Dinitro-3,3'-bifurazan; MTNI: 1-Methyl-2,4,5-trinitroimidazole; DNAN: 2,4-Dinitroanisole; T_m = Thermal melting temperature

1.5.1.1.4. Insensitive Explosives:

The materials with high performance, and insensitive enough to handle, and transport are called ideal insensitive explosives. TNT, RDX and HMX are some of the most common highly useful performance explosives; however, some of these compounds are sensitive to impact and shock; as a result, easy transportation of

these materials is restricted.[5] Thus, the well-known explosive material satisfying insensitivity and high performance are insignificant.

Introduction of a nitrogen-rich heterocycles and *N*-oxides or a nitro and amino groups in the ring *ortho* to each other contributes infringing insensitivity.[24,25] Few insensitive energetic molecules are shown in Figure 1.8.

Figure 1.8. Examples of insensitive explosives

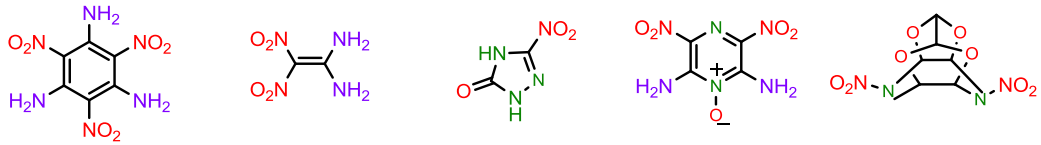

TATB	FOX-7	NTO	LLM -105	TEX
3	**26**	**27**	**28**	**29**
Is (h 50%): >177 cm	Is (h 50%): >126 cm	Is (h 50%): 93 cm	Is (h 50%): 117 cm	Is (h 50%): >177 cm

TATB: 2,4,6-Triamino-1,3,5-trinitrobenzene; FOX-7: 1,1-diamino-2,2-dinitroethylene; NTO: 3-Nitro-1,2,4-triazol-5-one; LLM-105: 2,6-diamino-3,5-dinitropyrazine-1-oxide; TEX: 4,10-Dinitro-4,10-diaza-2,6,8,12-tetraoxaisowurtzitane; Is = Impact sensitivity.

1.5.2. Propellants:

Propellant undergoes rapid and predictable combustion (without detonation) and produce large volume of gas. This gas can be used to propel a projectile, *i.e.* a bullet or a missile, or gas generators.[5]

Propellants only burn and do not explode; the process is initiated by flame or spark, and subsequently converted to gaseous state slowly (*i.e.* milliseconds). In addition, propellants are self-combustible; thus, it holds required amount of oxygen for full combustion.[2-5] Propellants are categorized in two classes: a homogeneous propellant (monopropellant) contains both fuel and oxidizer component in the same molecule, *i.e.* nitrocellulose. Whereas a heterogeneous propellant (bipropellant) is the combination of different compounds related to fuel and oxidizer. For instance, gun propellants are known to be homogeneous, whereas rocket propellants are heterogeneous.[9]

Propellants are typically classified as gun and rocket propellant. The classification is schematically depicted in Figure 1.9.

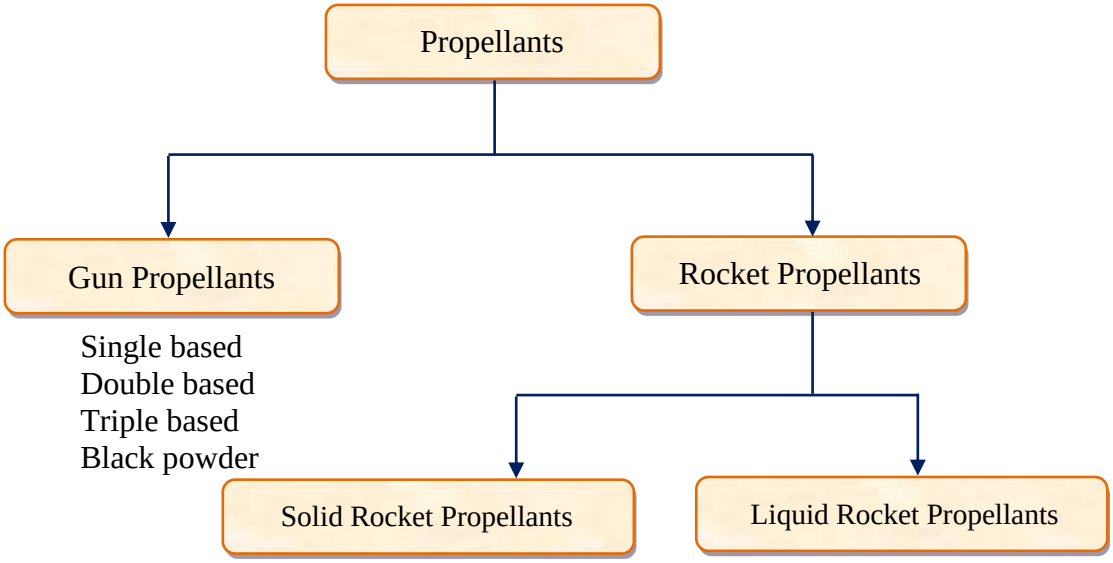

Figure 1.9. Classification of propellants

Gun Propellants: Gun propellants provide thrust to propel projectiles at high kinetic energy.

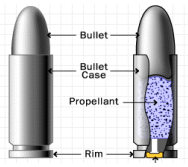

They are generally smokeless on firing, without performing detonation. Gun propellants have traditionally been fabricated from nitrocellulose-based materials.[9] The size of the propellant grains depend on the size of the gun. The shape of the propellant grain is also very important.[13,14]

Rocket Propellants: **R**ocket propellant produces exhaust, which is useful to fly the object using motor device; in this process the chemical energy is transformed into energy of motion. In aircraft, direct combustion of fuel led to propellant. For space exploration and military applications, both solid and liquid propellants are used (Figure 1.10). In view of safety, reliability, simplicity, and long storage life, solid propellants are preferred over liquid propellants. The solid rocket propellants are classified into double-base homogeneous and composite propellants. Composite propellant consists of fuel and oxidizer (*e.g.* aluminum and ammonium perchlorate) bound together in a polymeric matrix. Oxidizer (positive oxygen balance) plays vital for the development of solid propellants.[14]

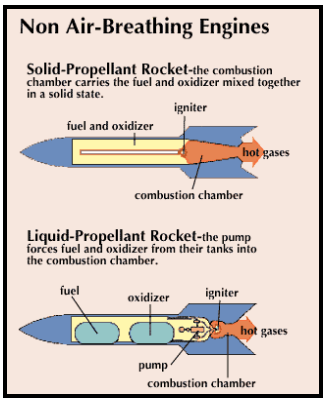

Figure 1.10. Classification of rocket propellants

1.5.3. Pyrotechnics:

The name pyrotechnic is derived from the Greek words 'pyr' (fire) and 'techne' (an art). Pyrotechnic materials evolve huge amount of heat compared to propellants and explosives, releasing less gaseous products. Pyrotechnic compounds are of three types: a) heat generating, b) smoke generating and c) light emitting materials (Figure 1.11). Heat generating pyrotechnics are used for detonation, fire compositions. Smoke generating pyrotechnics are used for camouflage and signalling purposes. The light emitting pyrotechnics are used either for illumination (visible and infra-red), fireworks or decoy flares.[5,6] In explosives, the gaseous products evolve at the highest speed of reaction with high pressure shock; whereas in propellants, the products evolve at a slow reaction rate with low pressure. In case of pyrotechnics, the formation of solid residues and gases are visible.[15,]

Pyrotechnic compositions contain a fuel and an oxidizer, responsible for the production of lot of energy. This energy led to produce flame or glow *(i.e.* a matchstick), when it combines with other volatile substances to produce smoke and light ***(i.e.*** fireworks), or produce large quantities of gas (firework rockets and bangers).[16]

Figure 1.11. Effect of the pyrotechnics and crackers

1.6. Different terms involved in High Energy Material Science

a) Oxygen Balance: Oxygen balance (OB, or OB %) indicates the degree to which an explosive is oxidized. The molecule having zero oxygen balance indicates presence of adequate amount of oxygen responsible for the complete conversion of carbon to CO_2, hydrogen to H_2O. The molecule with positive oxygen balance shows the presence of excess oxygen. While the molecule of negative oxygen balance displays the presence of insufficient oxygen, indicating incomplete combustion of the molecule. The sensitivity, strength, and performance of an explosive solely depend on oxygen balance of the molecule. Oxygen balance is calculated from the empirical formula of a compound as shown below.[17]

$$OB\% = \frac{-1600}{Mol.\ wt.\ of\ compound} \mathbf{X}\ (2x + y/2 - z)$$

x = number of atoms of carbon, y = number of atoms of hydrogen, z = number of atoms of oxygen.

b) Density: Density (ρ) is one of the important parameter useful to evaluate the performance of explosives. Density of loading refers to the mass of an explosive per unit volume. Several loading methods are known, which includes pellet loading, cast loading, and press loading. Sensitivity can be reduced through high load density, as more amount of mass will resist internal friction. Furthermore, increased load density permits the use of more explosive material for efficient warhead.[10]

c) Detonation Velocity and Pressure: Velocity of detonation (*vD*) and detonation pressure (*P*) are important parameters of explosive material. Performance of explosive invariably depends on the velocity of detonation and pressure. Detonation velocity is proportional to the density of the energetic material. Detonation velocity is hard to measure, as the velocity of explosive is faster than the local speed of sound. Detonation velocity of commercial mining explosives ranges from 1800 m s^{-1} to 9000 m s^{-1}. Detonation pressure data derived from measurements of shock waves transmitted into water by the detonation of explosive of standard size.[10]

d) Stability: Thermal stability signifies the stability of the molecule at high temperature. The molecule resist to decomposition at high temperature shows more stability and are called "heat-resistant" or "thermally stable" compounds. The stability of the molecule is determined by the glass transition temperature, initial decomposition temperature, degradation temperature and the melting temperature range. High thermal stability allows safe handling and long time storage of the explosive material. Thermal stability is measured by thermo gravimetric analysis (TGA) and differential scanning calorimetry (DSC).[8]

e) Sensitivity: Sensitivity of an explosive refers to the ease of ignition or detonation. Sensitivity signifies the release of energy contained in the molecule through external stimuli. External stimuli could be mechanical (impact / friction) or electrostatic sources.[8] The level of sensitivity of energetic materials to impact and friction will permit the issues of safety and handling.[5 ,8, 17]

Important parameters required for the sensitivity studies are:

Impact Sensitivity: Impact sensitivity is the blow of explosive material to the falling weight.[8,9] Impact sensitivity is calculated in Joule (*J*), given by the product *mgh*, where '*m*' is the mass of the falling weight, '*g*' is the acceleration and '*h*' is the height of the falling

weight. It is denoted as "Is". Impact sensitivity of the explosives is measured using the standardized BAM drop-hammer instrument.

Friction Sensitivity: Friction sensitivity is the response of the material to the scraping with weighted pendulum. In this process, the material undergoes either to ignition, turn to black, crack or explosion. It is represented as "Fs" and the friction energy reported in newton (*N*).[9]

f) Heat of Combustion: Heat of combustion (ΔHc°) is the energy released when a compound undergoes complete combustion with oxygen under standard conditions. It is expressed as energy/mole of fuel (kJ mol^{-1}), energy/mass of fuel and energy/volume of fuel. The heat of combustion is conventionally measured with a bomb calorimeter.[18]

g) Heats of Formation: The standard enthalpy of formation or standard heat of formation measures the energy content of an energetic material obtained during decomposition through ignition, explosion by heat, and impact. It is represented as ΔH°_{f} or HOF. The unit of heats of formation can be represented as kcal mol^{-1} or kJ mol^{-1}.[18] In general; HOF is calculated from heats of combustion. Usually, heat of combustion (ΔHc°) of energetic material is determined through bomb calorimetric measurements, producing inconsistent results.

h) Heat of Explosion: The liberation of energy in the form of heat during the detonation of the explosive under adiabatic conditions is called the heat of explosion; it is represented as Q. The propellants effectiveness is determined by the heat of explosion; for instance, secondary explosives show high Q value. It is represented as kJ kg^{-1} or cal g^{-1}.[18]

i) Toxicity: The explosive materials produce toxic and environmental-harmful pollutants during detonation. For example, primary explosives lead azide and lead styphnate, and secondary explosives TNT, RDX and HMX contain toxic or polluting components like heavy metals, and nitramines. Lead (Pb), cadmium (Cd), and mercury (Hg) are highly toxic and environmentally harmful by-products generated during detonation of common explosive materials. Some of the organic energetic compounds also produce hazardous and carcinogenic components upon decomposition. Whereas production of harmless carbon dioxide, N_2 gas and water from the decomposition of molecule is always advantageous.[18,19]

Therefore, development of green explosives that produce low toxic ingredient is highly desirable.

j) Decomposition: Chemical decomposition of an explosive material may take years, days, hours, or a fraction of a second. The slow decomposition of materials allows for extended storage. Precisely, deflagration and detonation are the two rapid forms of decomposition.[19]

k) Deflagration: Deflagration is the exothermic chemical reaction propagating through heat transfer at subsonic speed. This process helps in igniting the cold material. For instance, fire to flames, which eventually leads to explosion is termed deflagration.[19] Thus, deflagration is an intermediate process between combustion and detonation.[6-8] Deflagration of propellants proceeds through normal burning without the presence of atmospheric oxygen.

l) Detonation: Detonation involves a supersonic exothermic front accelerating through a medium. Energy released during combustion is determined by the speed at which the material transmits the shockwave, not by the rate of heat transfer. The efficient HEM decomposes via the passage of heat through shock waves with velocity of about 9000 m s^{-1}.[20]

m) Oxidizer: An oxidizer is source of oxygen; this fuel component is useful for burning explosive. The rocket propellants carry oxidizer, which in turn helps to burn and provide thrust for the rocket to reach the target.[19,20] Liquid oxygen, concentrated H_2O_2, nitric acid, N_2O_4, $KClO_3$, $KClO_4$, NH_4ClO_4, NH_4NO_3, $NH_4N(NO_2)_2$ and hydrazinum nitroformate (HNF) are some of the well-known oxidizers.[10]

n) Igniters: Igniters are used to initiate the explosive material to efficiently burn and detonate.[20]

1.7. Role of Azole and Azine Derivatives in High Energetic Materials

1.7.1. Introduction of nitrogen-rich heterocyclic rings

The nitrogen-rich molecules are widely found in the compounds of pharmaceutical importance, natural products; moreover, the N-bearing molecules are useful as potential ligands in coordination chemistry. The presence of nitrogen in the compounds enhances density of the molecule.[28] Thus, N-bearing molecular entities are extensively found in high energetic materials. [29]

The presence of large number of N–N and C–N bonds in the N-rich compounds holds the energy-content of the molecule. The bond energy of N–N single bond (160 kJ mol^{-1}), N=N double bond (418 kJ mol^{-1}) and N≡N triple bond (954 kJ mol^{-1}); thus, decomposition or detonation of N-rich molecules produce N_2 molecule with the release of energy and therefore *N*-heterocycles showed high positive heat of formation (ΔH_f). The presence of more N-atoms in the molecule contributes lowering C–H content, enhancing density, and releasing more energy during decomposition. Thus, design and development of novel *N*-heterocyclic energetic compounds for explosive and propellant applications are always desirable.

1.7.2. Energetic five membered *N*-heterocyclic derivatives

Imidazole, pyrazole, triazole, and tetrazole are some of the five membered N-containing natural frameworks inherently present in many energetic materials. With the induction of explosophores nitro ($–NO_2$), nitroamino ($–NHNO_2$), azido ($–N_3$) groups in the *N*-heterocycles, performance of the molecule is substantially enhanced.[25] Among various explosophores, nitro group in the molecules enhances density and oxygen balance; this will contribute enhancing velocity of detonation and detonation pressure.[25,26] Heat of formation, nitrogen percentages and density of common five-membered *N*-heterocycles are shown in Table 1.1.

Table 1.1. Energetic properties of five-membered azole derivatives.[24a-24c]

Comp.	Structure	Name	Formula	N (%)	HOF (kJ mol^{-1})	ρ (g cm^{-3})
30	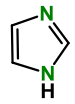	Imidazole	$C_3H_4N_2$	41.1	129.5	1.23
31		Pyrazole	$C_3H_4N_2$	41.1	179.4	1.12
32		1,2,4-Triazole	$C_2H_3N_3$	60.8	192.7	1.39
33		1,2,3-Triazole	$C_2H_3N_3$	60.8	271.7	1.19
34	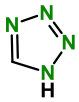	1,2,3,4-Tetrazole	CH_2N_4	79.9	326.0	1.48

Imidazole and pyrazole are the class of five-membered ring structure composed of three carbon atoms and two nitrogen atoms; the two nitrogen atoms are contiguous in pyrazole.[27] Imidazole or pyrazole readily undergo salt formation through protonation or substitution at nitrogen. Some of these salts are used as ionic liquids.[27,28]

Triazoles are nitrogen-containing five-membered heterocycles with molecular formula $C_2H_3N_3$ and exist in two isomers 1,2,3-triazole and 1,2,4-triazole. Incorporation of a triazole (1,2,4-triazole and 1,2,3-triazole) rings in the molecule substantially increases thermal stability of the compound.[29] 1,2,3-Triazole possesses high positive heat of formation (in gas phase: 271 kJ mol^{-1}) than 1,2,4- triazole (in gas phase: 194 kJ mol^{-1}). Triazole derivatives are

susceptible to produce energetic salts. Accordingly, many triazole containing explosives have been designed and synthesized.[29,30]

Tetrazole is comprised of four nitrogen and one carbon atom. The high nitrogen content (80 %), large number of N–N bonds, and ring strain, tetrazole moiety possess high density and better positive heat of formation (326 kJ mol^{-1}).[31-32] The tetrazole moiety can readily modified with the introduction of various functional groups. A large array of tetrazole-bearing high-performance explosives are developed, synthesized and successfully used.

The tetrazole-based molecules are generally employed as primary explosives, sensitizers, or igniters. For instance, 5-aminotetrazole is an essential component of gas generators in automobile airbags.[33,34] These molecules produce high-temperature, non-toxic reaction products, with high burn rate and are also stable.[35-37]

1.7.3. Energetic six membered *N*-heterocyclic derivatives

Pyridine, pyrimidine, triazine and tetrazine derivatives are the potential six membered *N*-heterocycles extensively used for high-energy density materials (HEDMs).[38-42] The more nitrogen content bearing scaffolds 1,3,5-triazine and 1,2,4,5-tetrazine are integral part of many energetic materials.[43-46] Diazine, triazine and tetrazine based energetic compounds are used as energetic additive in high performance propellants and smoke-free pyrotechnic ingredients.[47-49]

The heat of formation and nitrogen percentages of six-membered heterocycles is shown in Table 1.2

Table 1.2. Energetic properties of six-membered azine derivatives.[24a-24c]

Comp.	Structure	Name	Formula	N (%)	HOF (kJ mol^{-1})
35		Pyridine	C_5H_5N	17.7	143.0
36		Pyrazine	$C_4H_4N_2$	34.9	285.3
37		Pyrimidine	$C_4H_4N_2$	34.9	190.3
38		Pyridazine	$C_4H_4N_2$	34.9	209.9

39		1,3,5-Triazine	$C_3H_3N_3$	51.8	229.1
40		1,2,4,5-Tetrazine	$C_2H_2N_4$	68.2	489.7
41		Pentazine	CHN_5	84.3	676.3

1.7.4. Fused heterocycles

The ring-strain in fused-heterocycles assists enhancing density and performance of the molecule. Some of the pyrazolo-pyrazole, benzofuroxans and benzotriazoles fused heterocycles have been used for energetic applications. With the introduction of explosophore groups in the fused heterocycles, the resulting molecules showed better energetic performance.[50-52]

1.8. Importance of strained and benzene ring

1.8.1. Energetic materials having strained rings

The strain-rings bearing energetic materials showed better heat of formation over the molecules with unstrained system.[53] The ring-strain makes the molecule more rigid and compact with decreased molecular motion, which results showing increased density and performance.[54,55] For example, 1,3,3-trinitroazetidine (TNAZ) is a nitramine caged compound powerful than RDX, and suitable for plasticizer applications.[56-58]

1.8.2. Energetic materials having benzene ring

In general, the presence of aryl-moieties in the form of energetic polynitroarenes lowers the hygroscopic nature of a material, as well as its synthetic cost; this group also decreases the sensitivity of the material to impact, shock, and friction. Moreover, the presence of a benzene moiety enhances stability of the molecule due to conjugation. Therefore, these polynitroarenes would be useful as thermally stable energetic materials. Benzene is used as a fuel component for internal combustion engines and it is an excellent octane enhancer.[59,60]

1.9. Challenges to Discover the Modern Energetic Materials

High performance, low sensitivity, and high thermal stability are some of the crucial parameters that determine potential utility of the molecule for high energy material applications. However, most of the high-performance energetic materials are sensitive and

produce toxic by-products.[61,62] For instance, the well-known insensitive TNT, TATB are high thermal stable explosives possessing *less performance*. The poly nitramine compounds RDX and HMX showed outstanding performance with poor sensitivity and moderate thermal stability. The extensively used TNT and RDX during decomposition delivers toxic gases, affecting plants and microorganisms.[63-70] It is therefore desirable to design and construct ideal High Energy Density Materials (HEDMs). Accordingly, HEDMs should be hydrolytic stable, producing water-soluble gas-byproducts upon detonation. In addition, the fundamental parameters required for the development of HEDMs is sketched in Table 1.3.

Table 1.3. Goals for the preparation of novel high energy materials.[24c, 64-70]

Performance	Detonation velocity Detonation pressure Heat of explosion	$vD > 8000$ m s^{-1} $P > 35$ GPa $Q > 6200$ kJ kg^{-1}
Stability & Sensitivity	Thermal stability Impact sensitivity Friction sensitivity Electrostatic sensitivity	$T_d \geq 200$ °C Is > 10 J Fs > 120 N ESD > 0.2 J
Chemical properties	Hydrolytically stable, non-toxic & non-corrosive smoke-free combustion and long-term stability	

1.10. Objective of the thesis

Development of novel energetic materials for civil, military and space applications is always in great demand. The challenges involved in the synthesis of energetic materials are, safety in terms of stability and sensitivity, reliability in terms of large scale synthesis, yields, and synthetic costs. The following factors related to i) high detonation velocity (*vD*), ii) high detonation pressure (*P*), iii) high density (ρ), iv) high heat of formation ($\Delta_f H^o$), v) good thermal stability, vi) good environmental compatibility, and vii) low sensitivity toward impact and friction are especially considered for the design and synthesis of energetic compounds for vast applications

This thesis aims in the design and development of novel high energy density materials (HEDMs) with high performance combined with high thermal stabilities, a potential replacement to TNT and RDX.

1.11. References

1) J. P. Agarwal, *Combust. Explos. Shock Waves (USSR)*, **2005**, *30*, 316.
2) J. Akhavan, *The chemistry of explosives*, RSC Paperbacks, Cambridge, **1998**.
3) S. Fordham, *High explosives and propellants*, Pergamon, Press, Oxford, **1980**.
4) A. Bailey, S. G. Murrey, *Explosives propellants and pyrotechnics*, Brassey's, London, **2000**.
5) T. M. Klapotke, *Chemistry of High Energy Materials*, **2011**.
6) J. P. Agarwal, *High Energy Materials: Propellants, Explosives and Pyrotechnics*, Wiley-vch Verlag Gmbh & Co, Weinheim, **2010.**
7) T. M. Klapotke, *Structure and Bonding: High Energy Density Materials* 1st ed., **2007**, Springer (**2010**).
8) G. I. Brown, *Explosives*, the history press ltd, **2010**.
9) N. Kubota, *Propellants and explosives*, John Wiley & Sons, **2007**.
10) T. J. Janssen, *Explosive energetic materials*, Nova science publisher's inc. **2011**.
11) R. M. Matyas, J. Pachman, *Primary Explosives*, Springer-Verlag Berlin and Heidelberg GmbH & Co. K, **2013**.
12) C. D. Kalb, *Manual of explosives*, Biblio Bazaar, LLC, **2009**.
13) W. R. Quinan, *High explosives*, Biblio Bazaar, LLC, **2009**.
14) N. Kubota, *Propellants and explosives: Thermochemical aspects of combustion*, Wiley-VCH, **2007**.
15) E. Barlow, R. H. Barth, J. E. Snow, *The pentaerythritols*, Reinhold, New York, **1958**.
16) F. D. Miles, *Cellulose nitrate*, Oliver & Boyd, London, **1955**.
17) S. Nauckhoff, O. Bergstrom, *Nitroglycerine and dynamite, Nitroglycerin*, Sweden, **1959**.
18) J. P. Agrawal, R. D. Hodgson, *Organic chemistry of explosives*, John Willey and Sons Ltd, The Atrium, Chichester, England, **2007**.
19) G. S. George, U. M. Barsode, S. A. Kanavade, B. R. Mhaske, *Applied science II*, Technical publications, **2007**.

20) M. Hudlicky, *Chemistry of organic fluorine compounds*, 2nd ed., Halstead Press, New York, **1976**.

21) H. Gao, J. M. Shreeve, *Chem. Rev*., **2011**, *111*, 7377.

22) R. Meyer, J. Kohler, A. Homburg, *Explosives*, Wiley, **2008**.

23) J. P. Agrawal, *Prog. Energy Combust. Sci.* **1998**, *24*, 1.

24) a) M. H. Rao, *Dissertation*, ACRHEM, University of Hyderabad, **2013,** p. 22; b) V. D. Ghule, *Dissertation*, ACRHEM, University of Hyderabad, **2011,** p. 9-11; c) N. Kommu, Dissertation, ACRHEM, University of Hyderabad, 2015, p. 9-12; d) M. Cheng, H. Ho, C. S. Lam, W. K. Li J. Serb. Chem. Soc., 2002, 67, 257.

25) S. M. Danali, R. S. Palaiah, K. C. Raha, *Def. Sci. J.*, **2010**, *60*, 152.

26) A. K. Sikder, N. Sikder, *J. Hazard. Mater.* **2004**, *112*, 1.

27) D. M. Badgujar, M. B. Talawar, S. N. Asthana, P. P. Mahulikar, *J. Hazard. Mater.* **2008**, *151*, 289.

28) D. E. Chavez, B. C. Tappan, B. A. Mason, *Propell. Explos. Pyrotech.* **2009**, *34*, 475.

29) D. E. Chavez, D. A. Parrish, *J. Heterocyclic Chem.* **2009**, *46*, 88.

30) H. H. Licht, H. Ritter, *Propell. Explos. Pyrotech.* **1997**, *22*, 333.

31) H. Xue, Y. Gao, B. Twamley, J. M. Shreeve, *Chem. Mater.* **2005**, *17*, 191.

32) E. E. Gilbert, *Propell. Explos. Pyrotech.* **1980**, *5*, 15.

33) D. E. Bliss, S. L. Christian, W. S. Wilson, *J. Energ. Mater*. **1991**, *9*, 319.

34) R. A. Henry, R. C. Makosky, G. B. L. Smith, *J. Am. Chem. Soc*. **1951**, *73*, 474.

35) A. Hammerl, M. A. Hiskey, G. Holl, T. M. Klapotke, K. Polborn, J. Stierstorfer, J. Weigand, *J. Chem. Mater*. **2005**, *17*, 3784.

36) D. R. Miller, D. C. Swenson, E. G. Gillan, *J. Am. Chem. Soc*. **2004**, *126*, 5372.

37) C. Ye, G. L. Gard, R. W. Winter, R. G. Syvret, B. Twamley, J. M. Shreeve, *Org. Lett.* **2007**, *9*, 3841.

38) X. Su, X. Cheng, C. Meng, X. Yuan, *J. Hazard. Mater*. **2009**, *161*, 551.

39) M. E. Sitzmann, W. H. Gilligan, D. L. Omellas, J. S. Trasher, *J. Energ. Mater*. **1990**, *8*, 352.

40) G. Doddi, P. Mencarelli, A. Razzini, F. Stegel, *J. Org. Chem.* **1979**, *44*, 2321.

41) W. W. Edwards, C. George, R. Gilardi, J. C. Hinshaw, *J. Heterocycl. Chem.* **1992,** *29*, 1721.

42) M. D. Coburn, U. S Pat. 4028154, **1977**.

43) R. L. Atkins, A. T. Nielsen, W.P. Norris, U. S Pat. 4248798, **1981**.

44) S. G. Cho, J. R. Cho, E. M. Goh, J. K. Kim, R. Damavarapu, R. Surapaneni, *Propell. Explos. Pyrotech.* **2005**, *30*, 445.

45) H. Gao, C. F. Ye, O. D. Gupta, J. C. Xiao, M. A. Hiskey, B. Twamley, J. M. Shreeve, *Chem. Eur. J.* **2007**, *13*, 3853.

46) R. Duddu, P. R. Dave, R. Damavarapu, N. Gelber, D. Parrish, *Tetrahedron Lett*. **2010**, *51*, 399.

47) L. L. Dalinger, V. I. Gulevskaya, M. I. Kanishchev, S. A. Shevelev, T. K. Shkineva, B. I. Ugrak, *Russ. Chem. Bull*. **1993**, *42*, 1063.

48) P. Badol, F. Goujon, J. Guillard, D. Poullain, *Tetrahedron Lett*. **2003**, *44*, 5943.

49) P. A. Ivanov, N. V. Latypov, M. S. Pevzner, V. A. Silevich, *Chem. Heterocyclic Compd.* **1976**, *12*, 1355.

50) M. B. Talawar, R. Sivabalan, N. Senthilkumar, G. Prabhu, S. N. Asthana, *J. Hazard. Mater*. **2004**, *113*, 11.

51) M. D. Coburn, U. S Pat. 3414570, **1968**.

52) A. Gunasekaran, J. H. Boyer, *Heteroatom. Chem*. **1993**, *4*, 521.

53) R. L. Willer, U. S Pat. 4503229, **1985**.

54) D. W. Moore, R. L. Willer, *J. Org. Chem*. **1985**, *50*, 5123.

55) A. B. Sheremetev, V. G. Andrianov, E. V. Mantseva, E. V. Shatunova, N. S. Aleksandrova, I. L. Yudin, D. E. Dmitriev, B. B. Averkiev, M. Y. Antipin, *Russ. Chem. Bull*. **2004**, *53*, 596.

56) A. L. Fridman, G. S. Ismagilova, A. D. Nikolaeva, *Chem. Heterocyclic Compd*. **1971**, *7*, 804.

57) J. K. Berlin, M. D. Coburn, *J. Heterocyclic Chem*. **1975**, *12*, 235.

58) R. V. Kendall, R. A. Olofson, *J. Org Chem*. **1970**, *35*, 2246.

59) G. S. Lee, A. R. Mitchell, P. F. Pagoria, R. D. Schmidt, *Thermochimi. Acta* **2002**, *384*, 187.

60) G. W. Drake, T. W. Hawkins, L. A. Hall, J. A. Boatz, A. J. Brand, *Propell. Explos. Pyrotech*. **2005**, *30*, 329.

61) A. T. Baryshnikov, V. I. Erashko, N. I. Zubanova, B. I. Ugrak, S. A. Shevelev, A. A. Fainzilberg, A. L. Laikhter, L. G. Melnikova, V. V. Semenov, *Bull. Russ. Acad. Sci. Chem. Ser*. **1992**, *41*, 751.

62) C. D. Bedford, J. C. Bottaro, C. George, R. Gilardi, R. J. Schmitt, *J. Org. Chem.* **1990**, *55*, 1916.

63) D. A. Dixon, D. Feller, K. O. Christe, W. W. Wilson, A. Vij, V. Vij, H. D. B. Brooke, M. R. Olson, M. S. R. Gordon, *J. Am. Chem. Soc*. **2004**, *126*, 834.

64) H. G. Adolph, M. Chaykovsky, *J. Energ. Mater*. **1990**, *8*, 392.

65) R. A. Henry, R. L. Willer, *J. Org. Chem*. **1988**, *53*, 5371.

66) T. M. Klapotke, F. X. Steemann, *Propell. Explos. Pyrotech*. **2010**, *35*, 114.

67) Klapotke, T. M.; Laub, H. A.; Stierstorfer, J. *Propell. Explos. Pyrotech*. **2008**, *33*, 421.

68) K. Karaghiosoff, T. M. Klapotke, P. Mayer, H. Piotrowski, K. Polborn, R. L. Willer, J. J. Weigand, *J. Org. Chem*. **2006**, *71*, 1295.

69) K. Karaghiosoff, T. M. Klapotke, P. Mayer, C. M. Sabate, A. Penger, J. M. Welch, *Inorg. Chem*. **2008**, *47*, 1007.

70) Klapotke, T. M.; Mayer, P.; Sabate, C. M.; Welch, J. M.; Weigand, J. *J. Inorg. Chem*. **2008**, *47*, 6014.

Chapter 2

Synthesis of Thermally Stable Energetic 1,2,3-Triazole Derivatives

Abstract

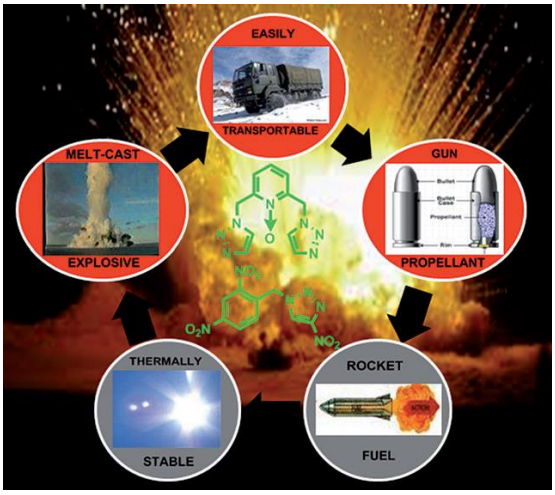

Various thermally stable energetic polynitro-aryl-1,2,3-triazoles have been synthesized through Cu-catalyzed [3+2] cycloaddition reactions between their corresponding azides and alkynes, followed by nitration. These compounds were characterized by analytical and spectroscopic methods and the solid-state structures of most of these compounds have been determined by using X-ray diffraction techniques. Most of the polynitro-bearing triazole derivatives decomposed within the range 142–319 ^{o}C and their heats of formation and crystal densities were determined from computational studies. By using the Kamlet–Jacobs empirical relation, their detonation velocities and pressures were calculated from their heats of formation and crystal densities. Most of these newly synthesized compounds exhibited high positive heats of formation, good thermal stabilities, reasonable densities, and acceptable detonation properties that were comparable to those of TNT.

Reference:

A. Sudheer Kumar, Vikas D. Ghule, S. Subrahmanyam and Akhila K. Sahoo*
Chem. Eur. J, **2013**, *9*, 509–518

2.1. Introduction

Development of thermally stable and less sensitive energetic materials requires a detailed investigation into the design of N- and O-rich molecules, the determination of their energy content through computational studies, as well as the demonstration of reliable strategies for their synthesis.[1] Therefore, synthesis of small organic molecular frameworks that have high N- and O-content as thermally stable energetic materials from readily available precursors is always desirable.[2] Thermal stability is an important characteristic of the energetic materials (safe working limit >225 ^{o}C). Improved thermal stability of the material ensures safer production, increased self-life of ammunitions and low vulnerability to accidental initiations. Thus, challenges always remain for the construction of thermal stable high energy explosive materials with better performance than RDX and HMX (>220 ^{o}C).[1] In general, presence of aryl moiety enhances stability of the molecule due to conjugation. Thus, aryl-moiety bearing energetic polynitroarenes are generally non-hygroscopic and insensitive to impact, shock, and friction; furthermore, the methods used for the synthesis of aryl-containing energetic materials are cost effective. Moreover, arene-moieties are octane enhancer; these moieties significantly contribute raising fuel-composition of the material through internal combustion.[3] Apart from high thermal stability, high oxygen balance and high density improve detonation performance of the compound and make the molecule a better-performing energetic material. Incorporation of nitro (–NO_2) groups into a molecular backbone enhances oxygen balance and detonation performance of the compound.[4]

Five-membered azole heterocycles behave as a source of energy owing to the high N-content. The high N-content of these compounds often leads to high crystal density which directly contributes to performance. In addition, the high percentage nitrogen bearing energetic materials release nitrogen (N_2) gas during combustion and therefore environmentally friendly.[4] Therefore, nitrogen-rich aromatic-triazole-based energetic materials have invariably been used in civil, military and aerospace propellant applications. Essentially 1,2,3-triazoles are one of the most promising backbones used for the fabrication of nitrogen rich energetic materials; as they possess high positive heats of formation with reduced sensitivity, owing to the N–N and C–N bonds and ring-strain.[5,1g] Moreover, the aromatic nature of triazole moiety makes the molecule thermally stable. On the basis of theoretical calculation studies, 1H-1,2,3-triazole possesses high positive heat of formation (in gas phase: 271 kJ mol^{-1}) than 1,2,4-triazole (in gas phase: 194 kJ mol^{-1}). Accordingly, molecules with large number of 1H-1,2,3-triazole derivatives produce good amount of energy

during combustion. Gratifyingly, construction of 1H-1,2,3-triazole can reliably be perceived through Click reaction involving a formal [3+2]-cycloaddition between terminal alkynes with azides under Cu-catalysis.[9]

Karl Berry Sharpless introduced the terminology "Click chemistry". This reaction broadly defines the quick generation of highly-selective products from terminal-alkynes and azides under Cu-catalysts.[9-11]

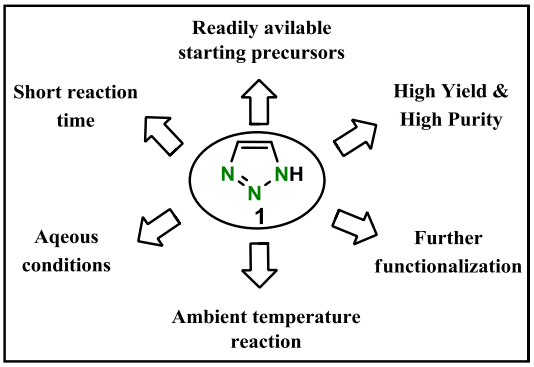

Figure 2.1. Advantages of "Click-Chemistry"

Development and synthesis of 1H-1,2,3-triazole bearing materials for energetic applications is briefly summarized herewith.

2.1.1. Precedents and strategies for 1H-1,2,3-triazole derivatives towards energetic material applications

In 1971, a series of tri- and tetranitro-*N*-aryl-1,2,3-triazolyl derivatives (**4** & **8**–**9**) were synthesized involving coupling and cycloaddition reactions followed by nitration (Scheme 2.1). Crystal density, impact sensitivity, thermal stability of the synthesized compounds were determined.[8a] Most of the polynitro-substituted *N*-aryl-1,2,3-triazole derivatives showed high positive HOF (110–1070 kJ mol^{-1}), good density (1.69–1.85 g cm^{-3}), moderate thermal stability (150–335 ^{o}C); disappointingly, these compounds are sensitive towards impact.

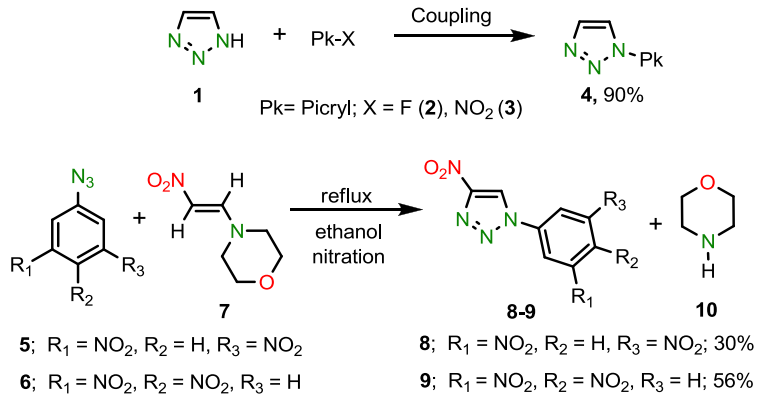

Scheme 2.1. Polynitro derivatives of phenyl 1H-1,2,3-triazoles

Shreeve group demonstrated the synthesis of five catenated nitrogen bearing 1-nitroamino-1,2,3-triazole (**12**). The compound **12** was synthesized from 1-amino-1,2,3-triazole (**11**) with mixture of nitric acid and sulphuric acid. The structure of **12** was established by single-crystal X-ray analysis (Scheme 2.2).[8b] Detonation properties of the compound **12** (*P* = 33.0 GPa, *vD* = 8743 m s^{-1}) is comparable with RDX. A new family of 1-nitroamino-1,2,3-triazolate salts **13**–**18** were synthesized from compound **12** by using acid base reactions; most of the compounds exhibited high positive HOF (205.4–888.3 kJ mol^{-1}), good density (1.43–1.82 g cm^{-3}) and moderate thermal stability (105–240 °C). The calculated detonation pressure (*P*) of the salts **13**–**18** fall between 18.6 GPa to 24.4 GPa, and the detonation velocities (*vD*) are distributed from 7282 m s^{-1} to 8366 m s^{-1}. Although the denotation data are lower than the corresponding values of RDX, most of them are superior to TNT (*P* = 20.6 GPa, *vD* = 6850 m s^{-1}). *Unfortunately, compound **12** is extremely shock-sensitive with an impact sensitivity of <1 J and should be handled with all possible care*.

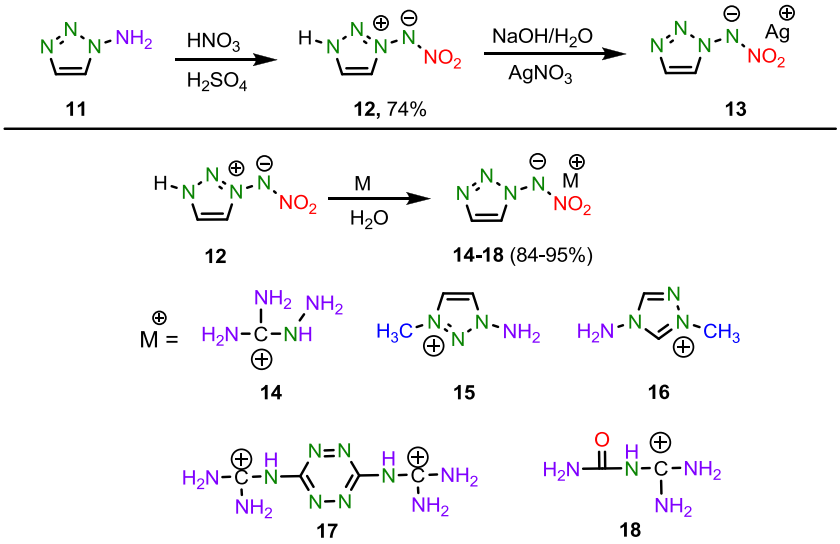

Scheme 2.2. Synthesis of 1-nitroamino-1,2,3-triazole and their salts

Synthesis and energetic properties of 5-(1,2,3-triazol-1-yl)tetrazole derivatives (**22**–**28**) are studied by the Shreeve group; the respective compounds are constructed involving Cu^{I}-catalyzed 1,3-dipolar azide–alkyne cycloaddition reaction (Scheme 2.3).[5a] The reaction of isopropyl(trifluoromethyl)diazene (**19**) with sodium azide produced 5-azido-N-(propan-2-ylidene)-1H-tetrazole (**20**) in good yield. This compound **20** was used as the starting azide for click reactions with alkynes (**21a–g**) to obtain new 1,2,3-triazolyltetrazoles (**22**–**28**). The synthesized 1,2,3-triazole derivatives (**22**–**28**) exhibit poor density (1.27-1.64 g cm^{-3}), moderate detonation performance (*vD* = 5995–7251 m s^{-1}; *P* = 10.4–16.5 GPa), negative heat of formation (-37.9–730.5 kJ mol^{-1}), thermally unstable nature (149–177 ^{o}C) and are insensitive to impact (35–40 J).

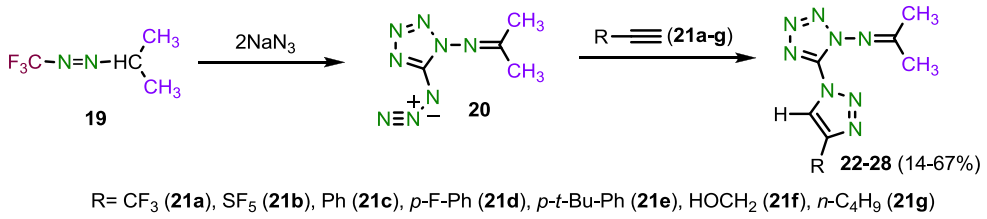

Scheme 2.3. Synthesis of 5-(1,2,3-triazol-1-yl)tetrazole derivatives via click chemistry

Condensation between 1-amino-1,2,3-triazole (**11**) and sodium dichloroisocyanurate led to the synthesis of 1,1'-azobis-1,2,3-triazole (**29**), a report disclosed from the Pang group (Scheme 2.4).[5c] The molecule 1,1'-azobis-1,2,3-triazole (**29**) possesses eight-nitrogen in a chain showing density (1.62 g cm^{-3}), decomposition temperature (193.8 ^{o}C) with high positive heat of formation (962 kJ mol^{-1}). Unfortunately, compound **29** seems to be sensitive. The H_{50} value of **29** is 16.6 cm [less sensitive than TAAT (tetra(azido)azo triazine; 6.2 cm) and PETN (11 cm), but slightly more sensitive than RDX (28 cm)].

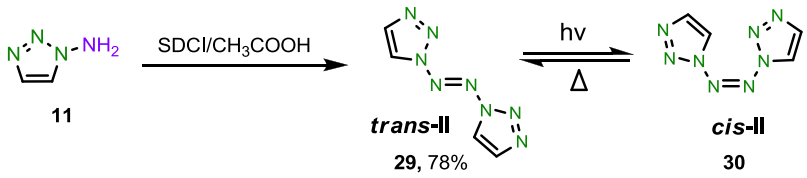

Scheme 2.4. Synthesis of 1,1'-azobis-1,2,3-triazole

In 2012, Shreeve group reported the synthesis of *N*-substituted nitro and chloro derivatives of triazoles (**33–35**) and the metal salts of tris(triazolo)benzene **36–38** in high yields (Scheme 2.5).[5d] The new tris(triazolo)benzene derivatives **33–35** were obtained via diazo-couling, cyclization, nitration reactions and exhibit density in the range of 1.69–1.94 g cm^{-3} superior

to those of TNT and PETN. Gratifyingly, sodium, potassium, and silver salts of the triazole-derivatives **36–38** exhibited density in the range of 2.1–2.8 g cm^{-3}. Furthermore, some of the tris-(triazolo)benzene compounds were found to be powerful hypergolic oxidizers with better ignition delay times over white fuming nitric acid (WFNA). Although tris-(triazolo)benzene compounds and its salts **33–38** display high thermal stability (>250 °C), high density (1.69–2.80 g cm^{-3}), good positive heats of formation (463–711 kJ mol^{-1}), and detonation properties (*vD* = 7032–8376 m s^{-1}; *P* = 13.67–31.20 GPa), however most of the compounds are more sensitive to impact (3–5 J).

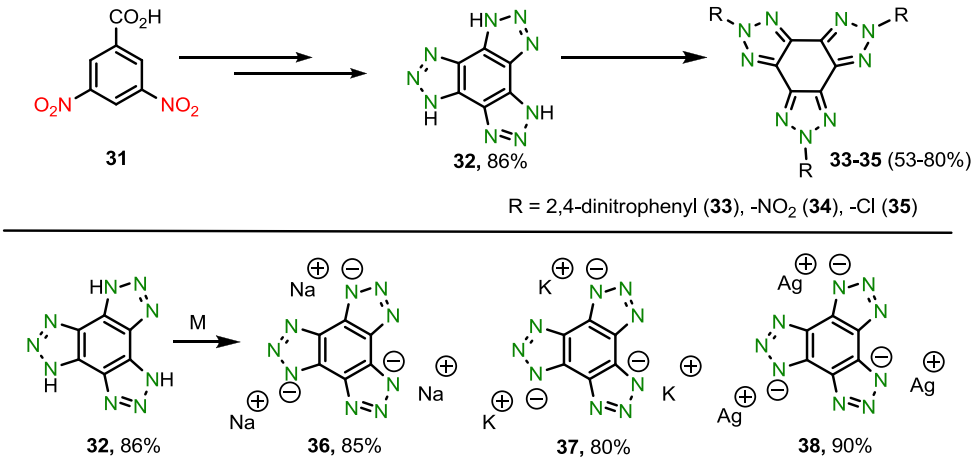

Scheme 2.5. Synthesis of tris(triazolo)benzene and its energetic salts

A report revealed from the Klapotke group showed the nitration of 1,3-diamino-1,2,3-triazolium nitrate (**39**) and nitronium tetrafluoroborate leading to the synthesis of 1,3-bis-(nitroimido)-1,2,3-triazolate anion (**40**); (Scheme 2.6).[5e] The energetic salts **41–46** are readily constructed from compound **40** by treating with corresponding chlorides and bromides. The salts **41**–**46** exhibited good detonation performance (*vD* = 8823–9426 m s^{-1}; *P* = 32.6–40.7 GPa) with less thermal stability (T_d = 149–210 °C) and sensitive to mechanical stimuli (1–5 J).

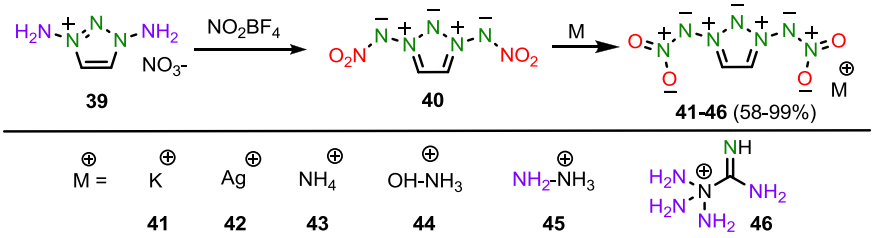

Scheme 2.6. Synthesis of 1,3-bis(nitroimido)-1,2,3-triazolate and its salts

Recently, Shreeve group demonstrated the synthesis of 1,2,3-triazolo-[4,5-*e*]furazano[3,4-*b*]pyrazine 6-oxide (**51**) and its energetic salts **52**–**56** as insensitive energetic materials (Scheme 2.7).[5f] The synthesis of diamino furazan (**47**) was achieved from commercially available glyoxal. The condensation of **47** with oxalic acid produced 5,6-dihydroxyfurazano[3,4-*b*]pyrazine (**48**) and hydroxyl groups were substituted by chlorine atoms with a mixture of phosphorous pentachloride & phosphorus oxychloride to produce 5,6-dichlorofurazano-[3,4-b]pyrazine (**49**). When **49** was treated with aqueous ammonia solution, 5,6-diaminofurazano-[3,4-*b*]pyrazine (**50**) was obtained. The 1,2-diamino compound (**50**) converted to the corresponding 1,2,3-triazole N-oxide (**51**) by treating with a nitration mixture from nitric acid and acetic anhydride. Reaction of **51** with ammonia, hydrazine, hydroxylamine, 3,4,5-triamino-1,2,4-triazole, and bis(guanidinium)tetrazine produced the corresponding salts **52**–**56** almost in quantitative yield. Finally, synthesis of di(trinitroethylamino) derivative **57** was achieved, when **50** was treated with formaldehyde followed by trinitromethane at room temperature.

The compounds **51**-**57** exhibit good physical and detonation properties, such as high positive heats of formation (110–1070 kJ mol^{-1}), good densities (1.69–1.85 g cm^{-3}), moderate thermal stabilities (141–301 ^{o}C), acceptable detonation velocities (7871–8532 m s^{-1}) and pressures (24–30.3 GPa).

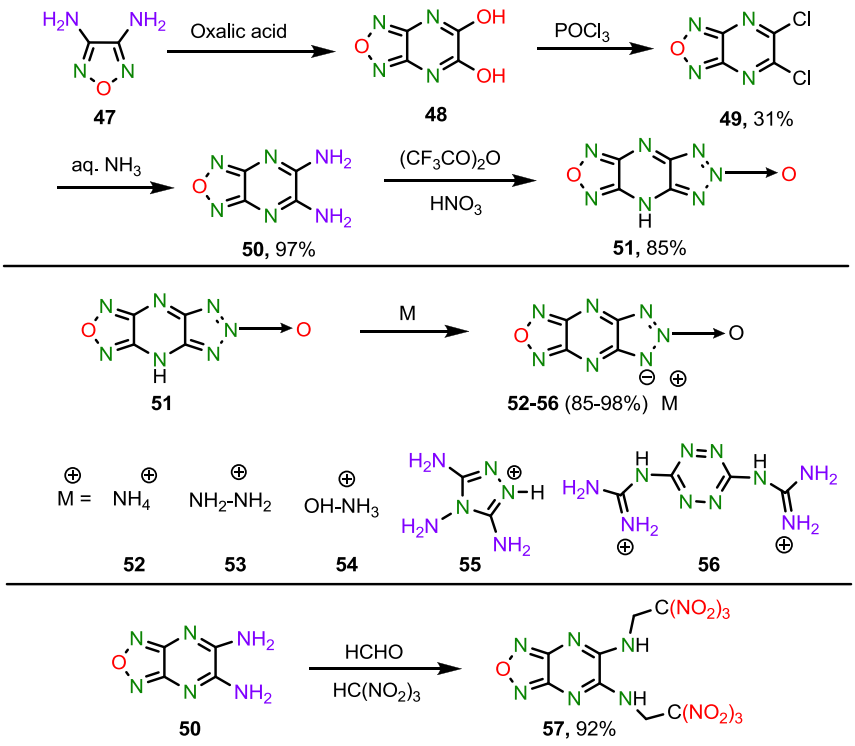

Scheme 2.7. Synthesis of 1,2,3-triazolo[4,5,-*e*]furazano[3,4,-*b*]pyrazine 6-oxide & its salts

2.1.2. Motivation and Design Plan

The development of less sensitive and thermally stable high performance energetic materials with high N- and O-content is challenging. In general, the super explosive molecules are sensitive, whereas the insensitive molecules showed poor energetic performance. We thus envisioned in the design and synthesis of insensitive and thermally stable energetic materials with high N- and O- content molecules.

In this chapter a detailed discussion on the synthesis of various *N*-benzyl-/aryl and/or pyridyl-tethered 1,2,3-triazoles and its derivatives using the known Cu-catalyzed [3+2] cycloaddition reaction between the corresponding azides and terminal alkynes are enumerated. Nitration on these precursors delivered a wide range of nitro-/nitrogen-rich 1,2,3-triazole derivatives as thermally stable energetic materials (Scheme 2.8).

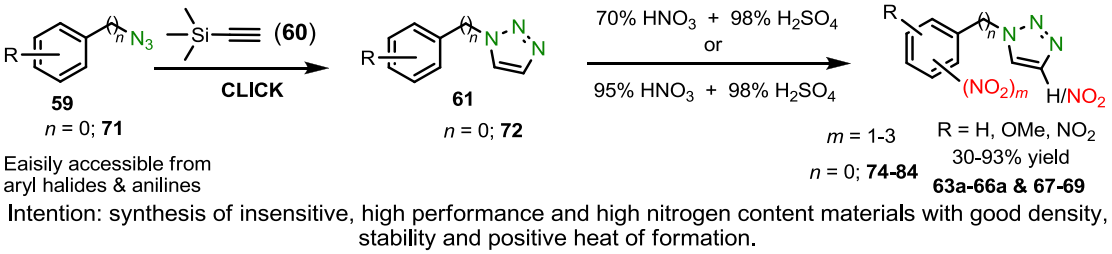

Scheme 2.8. Synthesis of thermally stable energetic 1,2,3-triazole derivatives

2.2. Results and Discussion

The development of simple and efficient approaches for the creation of triazole skeletons in small molecular entities has always attracted considerable attention.[9] Importantly, the Cu-catalyzed [3+2] cycloaddition reaction between an azide and an alkyne, termed the "click reaction", is a reliable synthetic strategy for the efficient formation of 1,2,3-triazole skeletons in high yields with affordable cost and high regioselectivity.[10] Herein, we report the synthesis of nitro-rich benzyl-/aryl- and pyridyl-tethered 1,2,3-triazoles as new thermally stable energetic materials.

In general, electron-rich azides (dipoles) and electron poor alkynes (dipolarophiles) favor the cycloaddition reaction, whereas steric bulk on the acetylene retards the rate of the reaction.[11] It has been reported that the cycloaddition reaction of electron-rich dipolarophiles proceeds well in water and in protic solvents.[12] The base-mediated deprotection of the C–Si bond occurs smoothly in protic solvent at ambient temperature.[13] With these facts in mind, the cycloaddition reactions between readily accessible benzyl azides and electron-rich TMS-acetylene (**60**) were carried out under the previously reported conditions involving sodium

ascorbate, $CuSO_4$, and K_2CO_3 as a base in MeOH/water at room temperature for 24 h (Table 2.1).[14] Benzyl azides were prepared from the commercially available benzyl bromides by nucleophilic displacement with NaN_3 in DMSO almost quantitative yields.[15]

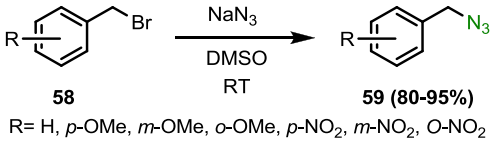

Scheme 2.9. Synthesis of aryl azides from aryl halides

The electronically neutral benzyl azide **59a** reacted smoothly with **60** to give compound **61a** in 92% yield; the corresponding TMS-substituted 1,2,3-triazole **62a** was also isolated in trace amount (Table 2.1, entry 1). An activated aryl azide that had a nitro group at the 4-position on the phenyl ring underwent cycloaddition with **60**, thereby producing compound **61b** in 87% yield (Table 2.1, entry 2).

Table 2.1. Cu-catalyzed 1,3-dipolar cycloaddition of benzyl azides and TMS-acetylene (**60**).[a]

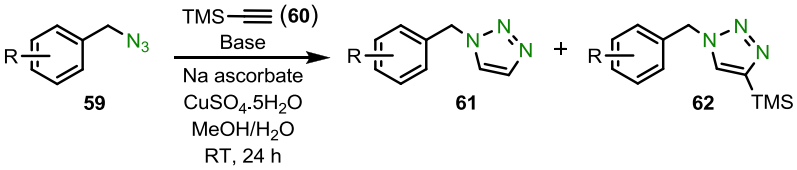

entry	**59**	R	Base	**61**	Yield (%)[b]	**62**	
1	**59a**	H	K_2CO_3	**61a**	92	**62a**	03
2	**59b**	4-NO_2	K_2CO_3	**61b**	87	**62b**	00
3	**59c**	3-NO_2	KOAc	**61c**	83	**62c**	09
4	**59d**	2-NO_2	K_2CO_3	**61d**	53	**62d**	00
5	**59e**	4-OMe	K_2CO_3	**61e**	92	**62e**	00
6	**59f**	3-OMe	K_2CO_3	**61f**	79	**62f**	00
7	**59g**	2-OMe	K_2CO_3	**61g**	52	**62g**	00

[a]All reactions were carried out with azide (1.0 equiv), TMS-acetylene (1.5 equiv), base (potassium carbonate or potassium acetate, 1.2 equiv), sodium ascorbate (0.4 equiv), and $CuSO_4 \cdot 5H_2O$ (0.2 equiv) in a mixture of MeOH/water (1:1, 0.5 mL for 1 mmol) at room temperature for 24 h. [b]Yield of isolated product.

A poor yield of compound **61c** was obtained when the reaction of 3-nitrobenzyl azide (**59c**) with **60** was conducted under the optimized conditions. Interestingly, KOAc was found to be suitable as the base and the desired compound, **61c**, was isolated in 83% yield (Table 2.1, entry 3). Sterically demanding 2-nitro-substituted benzyl azide **59d** reacted poorly with compound **60** and only afforded compound **61d** in moderate yield, with a fair amount of

recovered unreacted compound **59d**. A similar trend of reactivity and selectivity was observed in the reactions of MeO-substituted benzyl azides **59e**–**59g** with **60** under the optimized conditions, thus delivering their corresponding products, **61e**–**61g**, in good yields (Table 2.1, entries 5–7).

With a series of triazole-based molecules in hand, the nitration of compounds **61a**–**61g** was independently performed in either a mixture of 70% HNO_3 and 98% H_2SO_4 (Conditions A) or 95% HNO_3 and 98% H_2SO_4 (Conditions B), as shown in Equation (1).

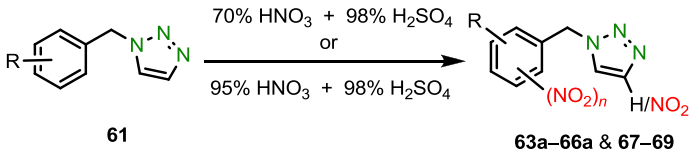

61 **63a–66a & 67–69** [Eq. (**1**)]

Table 2.2 summarizes the nitration of the *N*-benzyl-substituted-1,2,3-triazoles (**61**). At first, compound **61a** was heated under the conditions A at 120 ^{o}C for 24 h. Nitro-rich regioisomeric products **63a**–**66a** were detected and purified easily by column chromatography on silica gel in an overall 83% yield (Table 2.2, entry 1). In non-polar trinitro-bearing compound **63a**, which was isolated in 15% yield, the two nitro groups were substituted at the *o*- and *p*-positions on the *N*-benzyl ring, whilst the other nitro group was inserted at the 4-position of the triazole moiety. As expected, the *o*,*p*-dinitro-substituted compound **64a** was isolated in 39% yield as the major product. Interestingly, the *m*,*m*- and *m*,*p*-dinitro substituted compounds **65a** and **66a**, respectively, were also isolated, albeit in poor yields. The factors that were responsible to the formation of these unlikely *meta*-substituted products (**65a** and **66a**) remain unclear. The introduction of more nitro groups onto the molecular framework usually enhances density and detonation properties of a compound. Therefore, we speculate that the use of 95% HNO_3 in the nitration reactions could influence the formation of the tetranitro substituted products. Therefore, the nitration of compound **61a** was carried out under the conditions B at 100 ^{o}C. Although compound **61a** was completely consumed within 12 h, products **63a**–**66a** were exclusively formed (Table 2.2, entry 1), as observed previously. Next, nitration of nitro-substituted triazoles **61b**–**61d** were independently conducted under conditions A and B. The products, **63a** (12%), **64a** (70%), and **66a** (11%), were obtained from **61b** under conditions A at 120 ^{o}C, whereas the same reaction under conditions B at 70 ^{o}C gave compounds **64a** and **66a** in overall good yields (Table 2.2, entry 2).

Table 2.2. Nitration reactions of triazoles **61**

entry	**61**	T (°C)	t (h)	Polynitro derivatives of benzyl-1,2,3-triazoles[c]			
				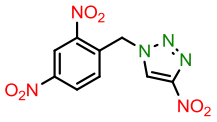	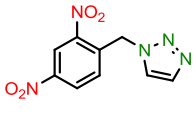	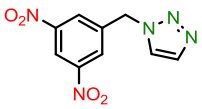	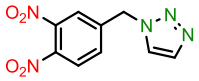
1	**61a**			**63a**	**64a**	**65a**	**66a**
		120[a]	24[a]	15%	39%	20%	9%
		100[b]	12[b]	14%	35%	25%	10%
2	**61b**	120[a]	24[a]	12%	70%	–	11%
		70[b]	6[b]	–	64%	–	13%
3	**61c**	80[a]	12[a]	–	–	60%	25%
		60[b]	10[b]	–	–	62%	30%
4	**61d**	60[a]	8[a]	–	88%	–	–
		45[b]	6[b]	–	93%	–	–
5	**61e**	rt[a]	2[a]	–	–	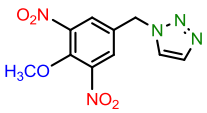 **67** (71[a] & 76%[b])	–
		rt[b]	2[b]				
6	**61f**	rt[a]	2[a]	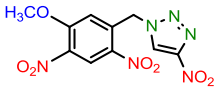 **68** (75[a] & 81%[b])	–	–	–
		rt[b]	2[b]				
7	**61g**	rt[a]	6[a]	–	–	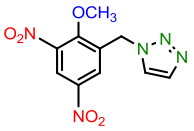 **69** (48[a] & 64%[b])	–
		rt[b]	2[b]				

[a]Mixture of 70% HNO_3 and 98% H_2SO_4. [b]Mixture of 95% HNO_3 and 98% H_2SO_4. [c]Yield of isolated product.

Similarly, the nitration of compound **61c** under conditions A or B delivered **65a** and **66a** as the major and minor products, respectively (Table 2.2, entry 3). Compound **64a** was exclusively obtained from the nitration of *o*-nitro-substituted triazole **61d** under both sets of conditions (Table 2.2, entry 4). Thus, variously substituted nitro-containing products (**64a**, **65a**, and **66a**) can be directly prepared from **61** in good yields. In general, electron-rich

aromatic compounds undergo electrophilic substitution reactions with ease. Therefore, we anticipated that the OMe group on the aryl moiety in benzyl triazoles would facilitate the introduction of more nitro groups onto the aromatic skeleton. Thus, the nitration of 4-OMe-substituted triazole **61e** was independently carried out under conditions A and B; the di-*ortho*-nitro-substituted product **67** was exclusively isolated in good yield (Table 2.2, entry 5). Gratifyingly, the trinitration product, **68**, was obtained in 81% yield when *m*-methoxy-bearing triazole **61f** was exposed to conditions B at RT for 2 h (Table 2.2, entry 6). On the other hand, the sterically demanding compound **61g** delivered the *o*, *p*-dinitration product (**69**) as a thick liquid in moderate yield (Table 2.2, entry 7). These results reveal that conditions B are milder than conditions A. In addition, more reactive and highly productive nitration reactions are observed under conditions B in comparison to conditions A. *X*-ray diffraction analysis confirmed the structures of compounds **63a**, **64a**, **65a**, **66a**, and **67**, as depicted in Figure 2.2.

Next, we turned our attention to explore the nitration reactions of aryl-1,2,3-triazoles and the synthesis of various polynitroaryl triazoles. We anticipate that these nitro-containing *N*-aryl triazoles would show better energetic properties compared to the corresponding nitro-substituted *N*-benzyl triazoles, because of low-carbon content. In addition, the presence of triazole skeleton on the aryl ring (C–N bond) would facilitate the electrophilic-nitration process.

The Cu-catalyzed cycloaddition reaction between an aryl azide and TMS-acetylene (**60**) is a reliable method for the synthesis of aryl triazoles (Table 2.3).[14] Aryl azides are easily accessible in good yields from the corresponding commercially available aryl amines, through diazotization followed by azide substitution.[15]

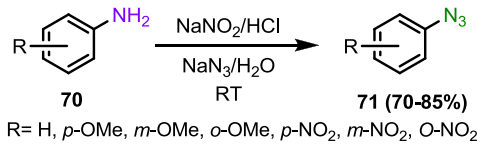

Scheme 2.10. Synthesis of aryl azides from anilines

The reaction between phenyl azide (**71a**) and **60** was successfully conducted under previously optimized conditions (sodium ascorbate, $CuSO_4$, and K_2CO_3 as a base in MeOH/water at room temperature) and the product **72a** was isolated in 66% yield (Table 2.3, entry 1). *p/m*-nitro/methoxy-substituted aryl azides efficiently underwent cycloaddition with **1**, thereby delivering triazoles **72b**,**c** and **72e**,**f** in good to excellent yields (Table 2.3, entries 2–3 and 5–

6). However, cycloaddition reactions of *ortho*-substituted aryl azides **71d** and **71g** were successfully performed in the presence of KOAc base: the corresponding 1-substituted-1,2,3-triazoles **72d** and **72g** were isolated in moderate yields and TMS-bearing 1,4-disubstituted-triazoles **73d** and **73g** were also formed in fairly good amounts (Table 2.3, entries 4 and 7). The desilylation of compounds **73d** and **73g** with K_2CO_3 in MeOH readily gave the corresponding products **72d** and **72g**.[13]

Table 2.3. [3+2] Cycloaddition reactions between aryl azides and TMS acetylene.[a]

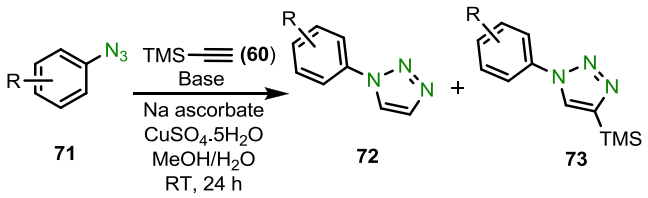

entry	**71**	R	Base	**72**	Yield (%)[b]	**73**	Yield (%)[b]
1	**71a**	H	K_2CO_3	**72a**	66	**73a**	00
2	**71b**	4-NO_2	K_2CO_3	**72b**	45	**73b**	00
3	**71c**	3-NO_2	K_2CO_3	**72c**	73	**73c**	00
4	**71d**	2-NO_2	KOAc	**72d**	30	**73d**	59
5	**71e**	4-OMe	K_2CO_3	**72e**	85	**73e**	00
6	**71f**	3-OMe	K_2CO_3	**72f**	79	**73f**	00
7	**71g**	2-OMe	KOAc	**72g**	41	**73g**	29

[a]All reactions were carried out with azide (1.0 equiv), TMS-acetylene (1.5 equiv), base (potassium carbonate or potassium acetate, 1.2 equiv), sodium ascorbate (0.4 equiv), and $CuSO_4 \cdot 5H_2O$ (0.2 equiv) in a mixture of MeOH/water (1:1, 0.5 mL for 1 mmol) at room temperature for 24 h. [b]Yield of the isolated product.

The nitration of *N*-aryl-substituted 1,2,3-triazoles was independently examined under conditions A and B (Table 2.4). Our attempts to nitrate compound **72a** under conditions A were unsuccessful; however, heating compound **72a** at reflux under conditions B gave mono-nitro derivatives **74** and **75** in poor yields (Table 2.4, entry 1). The *m*, *p*-dinitro-substituted product (**76**) and trinitro benzene (**77**) were obtained in poor yields when compound **72c** was reacted under conditions B at 160 ^oC (Table 2.4, entry 2). Unfortunately, cleavage of the C–N linkage of the aryl triazole was observed when the reaction was conducted in strong acids at higher temperatures.[16] The presence of a nitro group at the *ortho*/*para* position with respect to the triazole made the aryl ring highly electron deficient and, therefore, compounds **72b** and

72d failed to undergo nitration under both sets of conditions, even when the reaction was performed at elevated temperature. Therefore, we investigated the nitration reactions of electron-rich methoxy-substituted aryl triazoles. Owing to the *o*- and *p*-directing nature of the OMe group, nitration of 4-MeO-substituted phenyl triazole **72e** exclusively produced the di-*ortho*-nitro-containing product **78** in 85% yield under conditions B at room temperature (Table 2.4, entry 3).

Table 2.4. Nitration reactions of compounds **72**.[a]

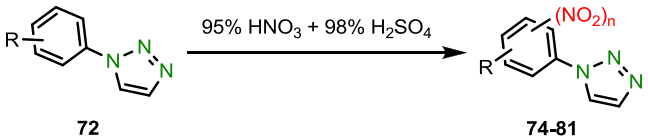

entry	72	T (°C)	t (h)	Nitro Derivatives of Phenyl 1,2,3- Triazoles[b]	
1	**72a**	100	24	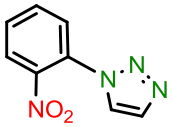 **74** (5%)	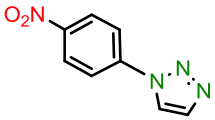 **75** (25%)
2	**72c**	160	24	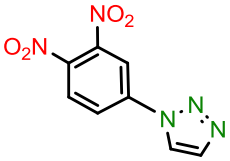 **76** (18%)	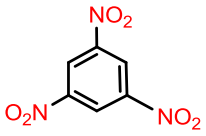 **77** (16%)
3	**72e**	rt	2	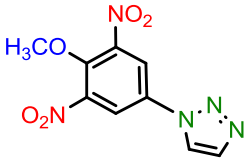 **78** (85%)	
4	**72f**	rt	2	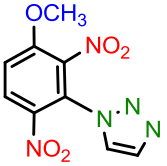 **79** (33%)	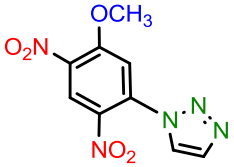 **80** (46%)
5	**72g**	rt	2	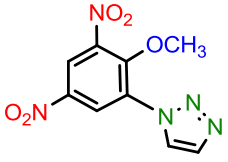 **81** (82%)	

[a]Mixture of 95% HNO_3 and 98% H_2SO_4. [b]Yield of isolated product is shown in parenthesis. 70% HNO_3 and 98% H_2SO_4 (Conditions A) or 95% HNO_3 and 98% H_2SO_4 (Conditions B).

A regioisomeric mixture of *o*, *p*-dinitro substituted products **79** and **80** were obtained from the nitration of 3-OMe-substituted triazole **72f** in good overall yield (Table 2.4, entry 4). The sterically encumbered compound **72g** delivered **81** in 82% yield, when the reaction was carried out under conditions B at room temperature for 2 h. Unfortunately, our efforts to achieve the tri- and/or tetranitro substituted aryl triazole were futile. The structures of compounds **79**, **80**, and **81** were confirmed by single-crystal *X*-ray analysis (Figure 2.2).

Heat of formation (HOF) is a valuable factor that determines the nature and efficiency of highly energetic materials.[6] The synthesized polynitro-1,2,3-triazole derivatives (**63a**–**69** and **74**–**81**) showed positive HOFs that varied from 197–401 kJ mol^{-1}. These results reveal that 1,2,3-triazole skeleton is beneficial to a positive HOF value. Therefore, we believe that the incorporation of more triazole rings would enhance the heat of formation of the molecule. The fact that a pyridine moiety contributes more energy than a benzene ring is well-established.[17] Based on this information, new molecular entities **83**, in which two triazole skeletons are attached onto a pyridine template, were proposed and the synthesis was commenced through a cycloaddition reaction between 2,6-bis(azidomethyl)-pyridine (**82**) and the corresponding alkynes (Table 2.5).

Table 2.5. Synthesis of bis-1,2,3-triazoles from the corresponding azides and alkynes.[a]

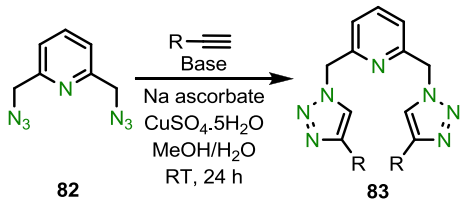

82 **83**

entry	**82**	R	Base	**83**	Yield (%)[b]
1	**82a**	TMS (**60**)	K_2CO_3	**83a**	74
2	**82b**	$H_2COCOEt$ (**60'**)	KOAc	**83b**	88

[a]All reactions were carried out using 1.0 equiv of azide, 3.0 equiv of TMS acetylene, 2.4 equiv of base (potassium carbonate or potassium acetate), 0.8 equiv of sodium ascorbate, 0.4 equiv of $CuSO_4 \cdot 5H_2O$, in a mixture of methanol:H_2O (1:1, 1 mL for 1 mmol) at room temperature for 24 h. [b]Isolated yields.

The precursor **82** was obtained from the commercially available 2,6-bis(bromomethyl)pyridine by the nucleophilic displacement of bromide by NaN_3 in good yield.[18] The cycloaddition of compound **82** to TMS-acetylene (**60**) under the optimized conditions gave **83a** in 74% yield at room temperature (Table 2.5, entry 1). Similarly, the reaction between compound **82** and propargyl propionate (**60'**) in the presence of KOAc afforded **83b** in excellent yield (Table 2.5, entry 2).

Our efforts to nitrate compound **83a** failed, even when the reaction was performed at high temperature under conditions A and B. Presumably, protonation of pyridine-N atom by the acids hindered the electrophilic nitration of the pyridine moiety. However, oxidation of compound **83a** with *m*-CPBA in $CHCl_3$ at 70 ^oC delivered the corresponding N-oxide product **84a** in 35% yield (Table 2.6, entry 1). X-ray diffraction studies establish the structure of **84a** (Figure 2.2).

A recent report by Shreeve and co-workers[19] inspired us to introduce more nitro groups onto the methylene hydrogen atoms of compound **83b**. However, we noted the formation of the mono-nitro derivative of compound **83b** under conditions B at room temperature. Subsequently, the purified nitro-containing product was reacted with *m*-CPBA at room temperature and the desired N-oxide product **84b** was isolated in 41% yield over two steps (Table 2.6, entry 2).

Table 2.6. Synthesis of pyridine-N-oxides **84a** and **84b**

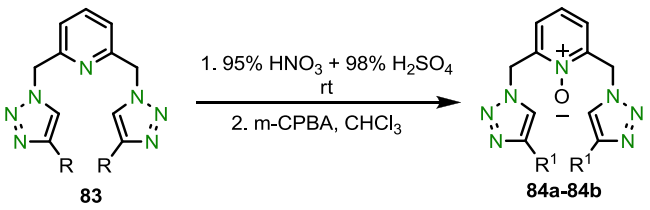

83 **84a-84b**

entry	**83**	R	temp (^oC)	time (h)	**84**	R^1	Yield (%)[a]
1[b]	**83a**	H	70	48	**84a**	H	35
2	**83b**	$H_2COCOEt$	rt	24	**84b**	H_2CNO_2	41

[a]Yield of isolated product. [b]Nitration failed, even at high temperature.

2.3. X-ray crystallography

Single crystals were grown by the slow evaporation of solutions of **63a**, **64a**, **65a**, **66a**, **67**, **79**, **80**, **81**, and **84a** in EtOAc at room temperature and atmospheric pressure. The structures of **63a**, **64a**, **65a**, **66a**, **67**, **79**, **80**, **81**, and **84a** were unambiguously elucidated by single-crystal *X*-ray diffraction analysis. The molecular structures of **63a**, **64a**, **65a**, **66a**, **67**, **79**, **80**, **81**, and **84a** are shown in Figure 2.2. Compounds **63a**, **65a**, **66a**, **67**, **79**, and **84a** crystallized in monoclinic space groups $P2_1/n$, $P2_1/c$, and $C2/c$, with cell volumes of 557.09(10), 1016.72(14), 1074.68(14), 1240.45(14), 2316.6(6), and 1182.7(4) Å^3, respectively, whereas **64a**, **80**, and **81** crystallized in the orthorhombic space group $P2_12_12_1$ with cell volumes of 1075.07(12), 1112.8(8), 1141(4) Å^3, respectively. The crystallographic data of all of these compounds are detailed in Table 2.7 & Table 2.8.

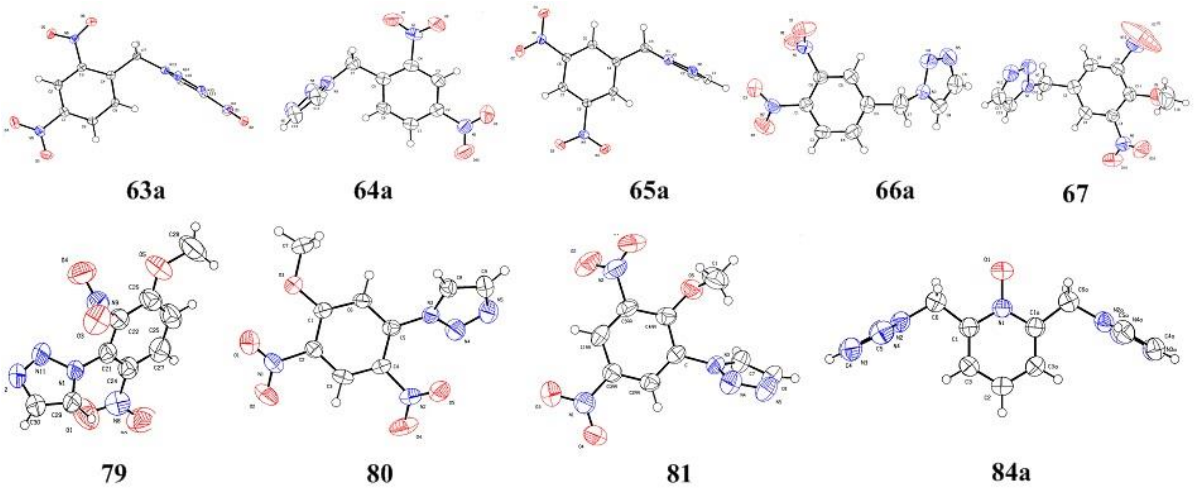

Figure 2.2. Molecular structures of compounds **63a**, **64a**, **65a**, **66a**, **67**, **79**, **80**, **81**, and **84a**; thermal ellipsoids are set at 50% probability and hydrogen atoms are unlabeled for clarity

Table 2.7. Crystallographic data for compounds **63a**, **64a**, **65a**, **66a**, and **67**

Compoud	**63a**	**64a**	**65a**	**66a**	**67**
CCDC	895107	895108	895109	895110	896656
Formula	$C_9H_5N_6O_6$	$C_9H_7N_5O_4$	$C_9H_7N_5O_4$	$C_9H_7N_5O_4$	$C_{10}H_9N_5O_5$
F_w	293.19	249.20	249.20	249.20	279.22
Crystal system	Monoclinic	Orthorhombic	Monoclinic	Monoclinic	Monoclinic
Space group	$P2_1$	$P2_12_12_1$	$P2_1/n$	$P2_1/c$	$P2_1/n$
T (K)	100	298	100	293	293 K
a (Å)	5.5245(6)	5.5436(4)	10.0567(8)	8.6097(7)	11.6392(8)
b (Å)	5.5719(6)	11.9190(8)	9.2416(7)	11.3982(8)	5.4843(3)
c (Å)	18.1323(19)	16.2706(10)	10.9434(9)	11.0544(7)	19.6637(14)
α (°)	90	90	90	90	90
β (°)	93.521(2)	90	91.5180(10)	97.843(7)	98.790(7)
γ (°)	90	90	90	90	90
Z	2	4	4	4	4
V (Å^3)	557.09(10)	1075.07(12)	1016.72(14)	1074.68(14)	1240.45(14)
D_{calc}/g cm^{-3}	1.748	1.540	1.628	1.540	1.495
μ/mm^{-1}	0.151	1.077	0.132	0.125	0.123
Reflns collected	5787	3071	8988	4709	3255
Unique reflns	2177	1851	1763	2408	2811
Observed reflns	2098	1700	1603	1687	1688
$R_1[I > 2\sigma(I)]$	0.0355	0.0381	0.0350	0.0450	0.0733
wR_2 [all]	0.0879	0.0982	0.0806	0.1282	0.2306
GOF	1.114	1.073	1.088	0.863	1.241
Diffractometer	SMART APEX CCD	Xcalibur Gemini Eos CCD	SMART APEX CCD	SMART APEX CCD	Xcalibur Gemini Eos CCD

Table 2.8. Crystallographic data for **79**, **80**, **81** and **84a**

Compound	**79**	**80**	**81**	**84a**
CCDC	895111	895112	895113	895114
Formula	$C_9H_7N_5O_5$	$C_9H_7N_5O_5$	$C_9H_7N_5O_5$	$C_{11}H_{11}N_7O_1$
F_w	265.20	265.20	265.20	257.27
Crystal system	Monoclinic	Orthorhombic	Orthorhombic	Monoclinic
Space group	$P2_1/c$	$P2_12_12_1$	$P2_12_12_1$	$C2/c$
T (K)	298	298	298	298
a (Å)	10.8498(16)	5.6454(18)	5.554(3)	14.179(3)
b (Å)	12.1869(18)	13.486(7)	12.461(6)	7.7450(17)
c (Å)	18.249(3)	14.616(5)	16.49(6)	10.792(2)
α (°)	90	90	90	90
β (°)	106.253(2)	90	90	93.667 (4)
γ (°)	90	90	90	90
Z	8	4	4	4
V (Å^3)	2316.6(6)	1112.8(8)	1141(4)	1182.7(4)
D_{calc}/g cm^{-3}	1.521	1.583	1.544	1.445
μ/mm^{-1}	0.127	0.132	0.129	0.102
Reflns collected	20797	3131	2165	5768
Unique reflns	3933	2095	1451	1137
Observed reflns	3303	1545	1264	901
$R_1[I > 2\sigma(I)]$	0.0682	0.0366	0.0889	0.0504
wR_2 [all]	0.1823	0.0835	0.2440	0.1245
GOF	1.122	0.968	1.082	1.126
Diffractometer	SMART APEX CCD	Xcalibur Gemini Eos CCD	Xcalibur Gemini Eos CCD	Xcalibur Gemini Eos CCD

2.4. Energetic Properties

This work demonstrates the synthesis of polynitrobenzyl-(**63a**–**69**), polynitro-*N*-aryl- (**74**–**81**), and polynitropyridyl containing triazoles (**85a** and **84b**). Essential parameters, such as heat of formation (HOF), density (ρ), detonation velocity (D), and detonation pressure (P), determine the nature and efficiency of energetic materials. Table 2.9 summarizes the energetic properties of these materials. HOF is indicative of the energy content of high-energy materials; the newly synthesized triazole derivatives showed positive HOFs, that is, in the range 197–683 kJ mol^{-1}. Of the benzyl substituted triazole derivatives, compound **63a** possessed the highest HOF (390.3 kJ mol^{-1}), owing to the presence of three nitro groups in the molecular backbone. Compound **63a** showed better density and performance than the other nitro-bearing benzyl derivatives **64a**–**66a** and **67**–**69**, because it contained one more nitro group than the latter compounds. Changes in the positions of the nitro groups in the molecular structure did not affect the HOF values, as observed in compounds **64a**, **65a**, and **66a**. Similar trends were observed in polynitro-*N*-aryl-triazole derivatives **78**–**81**. Of the triazole derivatives, pyridyl-based compound **84a** showed higher HOF, which can be attributed to the presence of triazole and pyridine rings in its molecular structure. In general, pyridine contributes 140.12 kJ mol^{-1} energy, whereas benzene offers only 82.84 kJ mol^{-1}; thus, the N-oxide-bearing pyridine–triazole molecules **84a** and **84b** possess higher HOFs.[17] Density is a primary physical parameter that determines the detonation performance of a molecule. The detonation velocity increases with packing density and the detonation pressure varies proportionally with respect to the square of the density. The density of the triazole derivatives were in the range 1.38–1.64 g cm^{-3}. As evident in Table 2.9, the predicted density (from their cvff force fields) closely matched with the observed crystal density. The incorporation of nitro groups into a framework improves its density. As a consequence, a noticeable variation in density was clearly visible between compounds **75** and **76**; a similar trend was observed among compounds **63a** and **64a**, **65a** and **66a**, and **84a** and **84b**. The velocity of detonation (vD) is a function of the energy that is produced by explosive decomposition. The density, heat of formation, and atomic composition can be integrated into an empirical formula to predict the performance of a proposed explosive. The detonation velocity and detonation pressure of the triazole derivatives were computed by Kamlet–Jacobs empirical equations and the results are shown in Table 2.9. Detonation performance mainly depends on the crystal density, whereas, contribution of HOF to the detonation properties is negligible. For example, compounds **84a** and **84b** show poor detonation performance, apart

from high HOFs. Of the synthesized triazole derivatives, compound **63a** demonstrated best performance, owing to its high crystal density. Thus, compound **63a** possessed *vD* = 7414 m s^{-1} and *P* = 21.34 GPa.

Table 2.9. Energetic properties of 1,2,3-triazole derivatives

Comp.	OB[a] (%)	ρ[b] (g cm^{-3})	*vD*[c] (m s^{-1})	*P*[d] (GPa)	T_m[e] (^oC)	T_d[f] (^oC)	HOF[g] (kJ mol^{-1})
63a	-81.6	1.64 (1.75)	6998 (7414)	20.07 (21.34)	195	256	390.3
64a	-112.4	1.53 (1.54)	6269 (6738)	15.73 (15.87)	145	220	381.9
65a	-112.4	1.53 (1.63)	6276 (6716)	15.77 (15.77)	131	312	364.8
66a	-112.4	1.58 (1.54)	6479 (6955)	17.16 (17.24)	88	215	387.0
67	-111.7	1.54 (1.49)	5928 (6748)	14.08 (15.77)	90	170	232.6
68	-83.8	1.61	6505 (7224)	17.52 (19.72)	–	237	224.2
69	-111.7	1.53	5909 (6664)	14.08 (15.18)	–	209	197.4
74	-143.0	1.49	5152 (6439)	10.46 (13.40)	197	271	401.6
75	-143.0	1.48	5131 (6361)	10.33 (13.01)	92	259	383.2
76	-98.6	1.57	6209 (6944)	15.69 (17.53)	125	268	394.9
78	-99.5	1.57	6378 (6921)	16.59 (17.31)	–	319	263.1
79	-99.5	1.58 (1.52)	6404 (6963)	16.82 (17.58)	168	221	263.1
80	-99.5	1.59 (1.58)	6411 (6993)	16.89 (17.68)	200	230	253.5
81	-99.5	1.57 (1.54)	6343 (6910)	16.41 (17.23)	–	152	253.5
84a	-164.8	1.38 (1.44)	4429 (6541)	7.32 (12.56)	62	228	682.8
84b	-117.2	1.49	5757 (6802)	13.05 (15.22)	110	142	585.7
TNT	-74.0	1.65	6881	19.50	80	300	-67.0

[a] Oxygen balance. [b] Calculated density; the experimental crystal density is shown in parenthesis. [c] Velocity of detonation is calculated with Kamlet–Jacobs equations; the *vD* is calculated with Explo5 *version* 6.02 is shown in parenthesis.[41] [d] Detonation pressure is calculated with Kamlet–Jacobs equations; the *P* is calculated with Explo5 *version* 6.02 is shown in parenthesis.[41] [e] Melting point. [f] Decomposition temperature under nitrogen gas (10 ^oC min^{-1}). [g] Heat of formation.

Thermal stabilities of the triazole derivatives were determined by DSC-TGA measurements. The triazole derivatives decomposed in the range 142–319 ^{o}C. Interestingly, compounds **64a** and **78** showed good thermal stabilities (>300 ^{o}C). Compounds **68**, **69**, **78**, and **81** decomposed without melting. Owing to a large variation of melting (<92 ^{o}C) and decomposition temperatures (>170 ^{o}C), compounds **65a**, **67**, **75**, and **84a** could be useful as melt-cast explosives.

2.5. Potential Energy Diagrams

The distribution of electron density is a useful parameter for understanding the reactivity and stability of the molecular systems. The molecular electrostatic potential represents the charge density and polarization effects within the molecule. Figure 2.8 showed the theoretical molecular electrostatic potential graphs obtained from DFT calculations at the B3LYP/6-311G** (d,p) level, with the electronegative and electropositive regions in the molecule. The surface is taken to be the 0.001 au (electrons/Bohr^3) outline of the electronic density, as proposed by Bader et al.[19c]

For compounds **63a**–**66a**, **67**–**69**, and **74**–**81**, a large electropositive region is located in the vicinity of the benzene ring due to the high electron withdrawing nature of –NO_2 groups and the negative charge density is mostly located on the triazole rings because of the strong electronegative nitrogen's. In pyridine derivative **84a**, charge densities were found negative on the triazole and pyridine ring. Similarly, a small electropositive potential generated over the triazole and pyridine ring because of the strong electron withdrawing effect of the nitro (–NO_2) groups in the compound **84b**. This is cleary shown in potential energy diagrams (Figure 2.3).

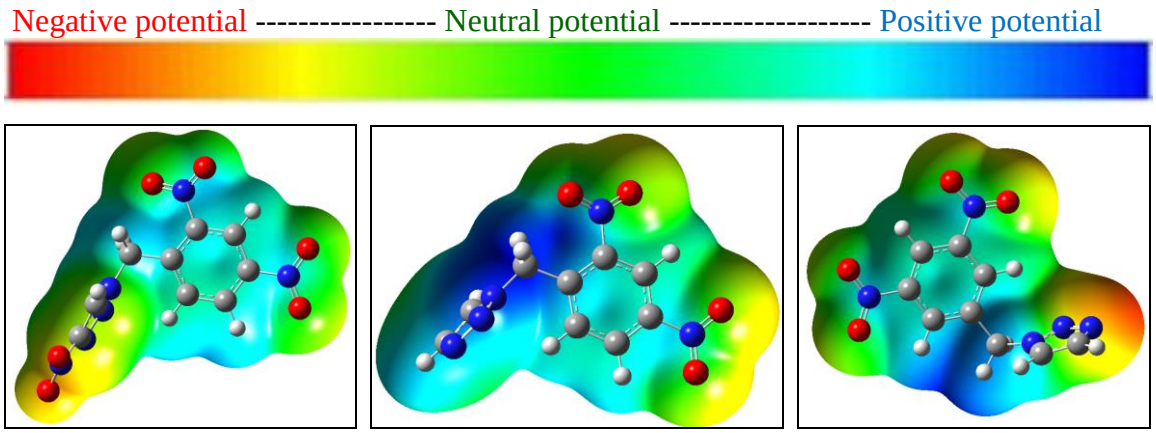

63a **64a** **65a**

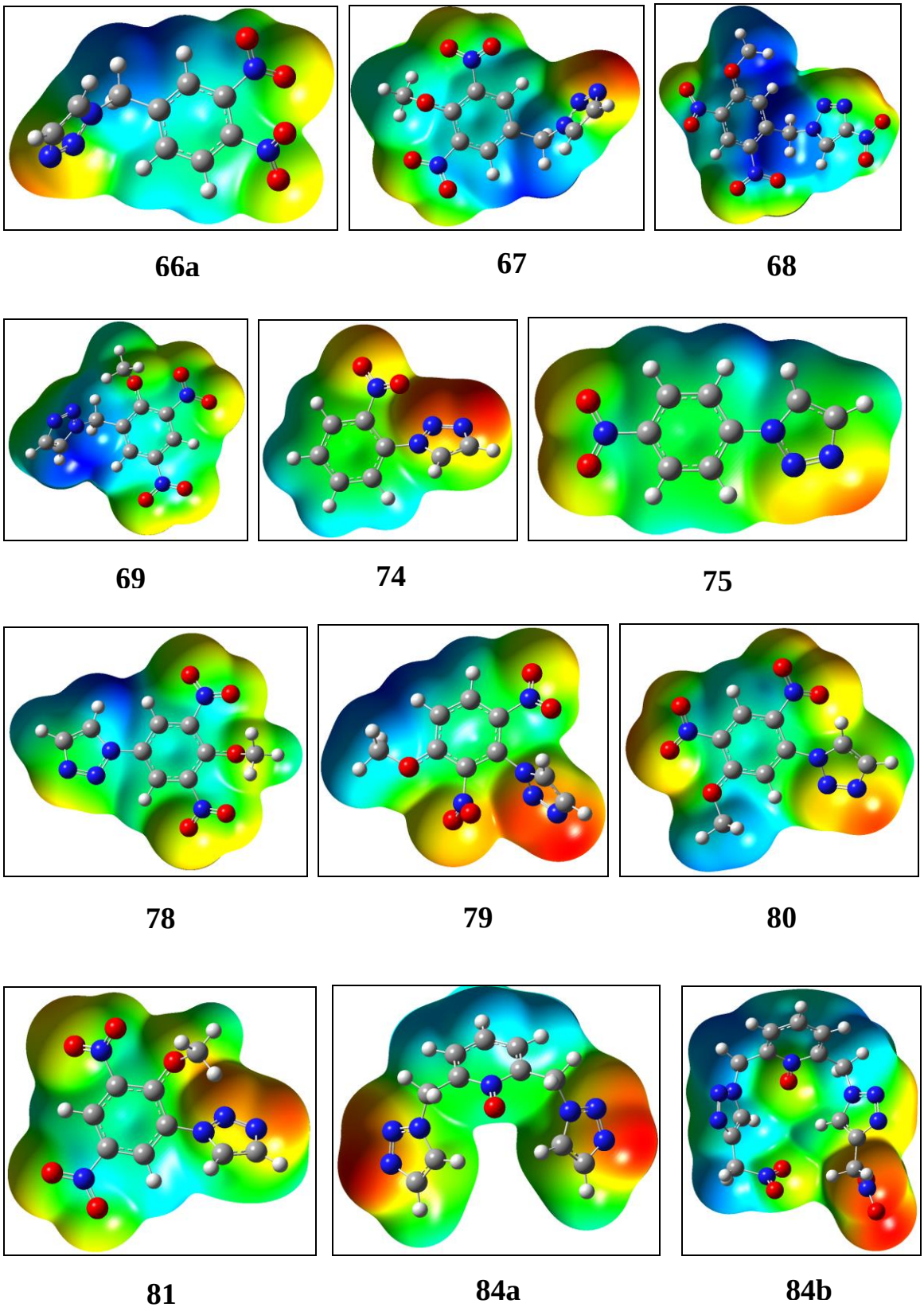

Figure 2.3. Optimized structures and electrostatic potential surfaces of compounds **63a**–**66a**, **67**–**69**, **74**–**81** and **84a**-**84b** (B3LYP/6-311G** (d,p)), 0.001 au electron/Bohr^3 iso-surface. The red and blue regions of the ruler (from left to right) indicate regions of more negative (electron-rich) and positive (electron deficient) charges, respectively. Gray = carbon; white = hydrogen; blue = nitrogen; red = oxygen.

2.6. Conclusion

In summary, wide varieties of new thermally stable nitro rich benzyl-/aryl- and pyridyl-tethered 1,2,3-triazole-based energetic materials have been efficiently synthesized through a cycloaddition reaction between the corresponding readily available benzyl-/aryl- and pyridyl-tethered azides and commercially available alkynes, followed by nitration of the triazole derivatives; the molecules were thoroughly characterized by analytical and spectroscopic methods. The structures of most of these newly synthesized molecules were determined by X-ray diffraction analysis. Most of the nitro derivatives of 1,2,3-triazoles decomposed in the range 142–319 ^{o}C; therefore, these molecules are considered to be thermally stable energetic materials. Most of these compounds exhibited moderate detonation performance: Compound **63a** (*P* = 21.34 GPa, *vD* = 7414 m s^{-1}) showed comparable detonation properties to TNT (*P* = 19.50 GPa, *vD* = 6881 m s^{-1}). Our predicted results revealed that the synthesized compounds possessed high positive HOFs; in particular, the pyridyl-tethered nitro derivative **84a** showed HOF of 682.8 kJ mol^{-1}. Some of these molecules might be useful as melt-cast explosives and energetic oxidizers, owing to their low melting points and high thermal stabilities. Fabrication of complex structures with more triazole moieties on pyridine templates is currently being pursued in our laboratory.

2.7. Future Work

The present work successfully demonstrates the synthesis of thermally stable energetic 1,2,3-triazole derivatives from easily accessible benzyl-/aryl- and pyridyl-tethered azides and commercially available alkynes via click chemistry, followed by nitration of the triazole derivatives. The synthesized 1,2,3-triazole derivatives exhibit high thermal stability and positive heat of formation. As density and detonation properties (VOD & DP) of the synthesized molecules showed moderate (less than RDX), we thus envisaged the design of new molecular frameworks **87**–**88** & **93**–**96** by incorporating more nitro groups on the molecular segment (Scheme 2.11 & 2.12).[8] We believe most of the molecules designed would exhibit better density and detonation performance than RDX.

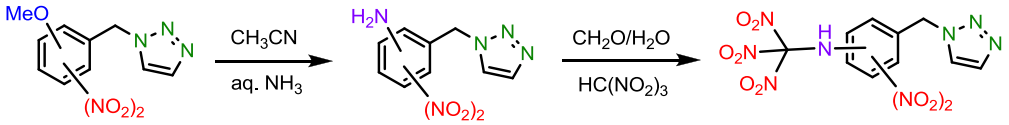

67, 69 **85, 86** **87-88**

67 4-OMe, 3,5-di-NO_2 **85** 4-NH_2, 3,5-di-NO_2 **87** 4-NH-$C(NO_2)_3$, 3,5-di-NO_2

69 2-OMe, 3,5-di-NO_2 **86** 2-NH_2, 3,5-di-NO_2 **88** 2-NH-$C(NO_2)_3$, 3,5-di-NO_2

Scheme 2.11. Synthesis of benzyl-substituted polynitro containing 1H-1,2,3-triazole derivatives

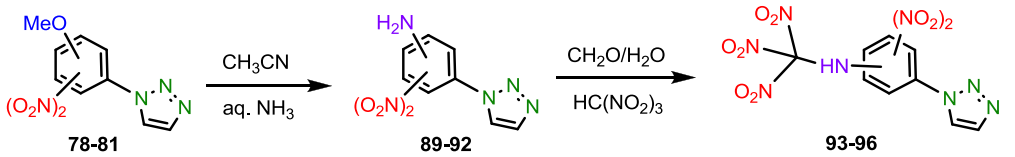

78-81 **89-92** **93-96**

78 4-OMe, 3,5-di-NO_2 **89** 4-NH_2, 3,5-di-NO_2 **93** 4-NH-$C(NO_2)_3$, 3,5-di-NO_2

79 3-OMe, 2,6-di-NO_2 **90** 3-NH_2, 2,6-di-NO_2 **94** 3-NH-$C(NO_2)_3$, 2,6-di-NO_2

80 3-OMe, 4,6-di-NO_2 **91** 3-NH_2, 4,6-di-NO_2 **95** 3-NH-$C(NO_2)_3$, 4,6-di-NO_2

81 2-OMe, 3,5-di-NO_2 **92** 2-NH_2, 3,5-di-NO_2 **96** 2-NH-$C(NO_2)_3$, 3,5-di-NO_2

Scheme 2.12. Synthesis of phenyl-substituted polynitro containing 1H-1,2,3-triazole derivatives

2.8. Experimental

2.8.1. Caution! Working with azides should always be done carefully. Organic azides, in particular those of low molecular weight or with high nitrogen content, are potentially explosive. Heat, light, and pressure can cause decomposition of the azides. Any experiments in which azides are to be heated in the presence of copper should involve the use of a blast shield. All nitro derivatives of 1,2,3-triazoles are dangerous when heating at high temperature. We prepared all of these compounds on the milligram scale. None of the compounds described herein exploded or were detonated during the course of this research; in any case, these materials should be handled with care by using proper safety precautions. Safety shields, safety glasses, face shields, leather gloves, and protective clothing, such as leather suits and ear plugs, must be worn. Ignoring safety precautions can lead to serious injury.

2.8.2. General Experimental Information for all the work in this Thesis

All the reactions were performed in an oven-dried Schlenk flask/ pressure tubes under an argon atmosphere or in open air conditions. Commercial grade solvents were distilled prior to use. Column chromatography was performed using silica gel procured from Merck (100-200 Mesh) eluting with hexanes and ethyl acetate mixture. Flash column chromatography was performed using silica gel procured from Acme's (230-400 Mesh) eluting with hexanes and ethyl acetate mixture. Thin layer chromatography (TLC) was performed on silica gel GF254 (Merck) plates. Visualization of spots on TLC plate was accomplished with UV light (254 nm) and staining over I_2 chamber.

Proton and carbon nuclear magnetic resonance spectra (^{1}H NMR, ^{13}C NMR and ^{19}F NMR) were recorded on a Bruker Avance 400 (^{1}H NMR, 400 MHz; ^{13}C NMR, 101 MHz; ^{19}F NMR, 376 MHz) spectrometer, Bruker Avance 500 (^{1}H NMR, 500 MHz; ^{13}C NMR, 126 MHz; ^{19}F NMR, 470 MHz) spectrometer having solvent resonance as internal standard (^{1}H NMR: $CDCl_3$ at δ=7.26 ppm, [D6]DMSO at δ=2.50 and 3.50 ppm; ^{13}C NMR: $CDCl_3$ at δ=77.0 ppm, [D6]DMSO at δ=44.0 ppm). Few cases tetramethylsilane (TMS) at 0.00 ppm was used as reference standard. Data for ^{1}H NMR are reported as follows: chemical shift (ppm), multiplicity (s = singlet; bs = broad singlet; d = doublet; bd = broad doublet, t = triplet; bt = broad triplet; q = quartet; m = multiplet), coupling constants, *J*, in (Hz), and integration. Data for ^{13}C NMR, ^{19}F NMR were reported in terms of chemical shift (ppm). IR spectra were recorded on JASCO FT/IR-5300 spectrometer and reported in cm^{-1}. LC-MS spectra were

obtained with a Shimadzu 2010A (EI-positive/ negative mode) with ionization voltage of 70eV; data was reported in the form of m/z (intensity relative to base peak = 100). Elemental (C, H, N) analysis were carried out using THERMO FINNIGAN FLASH EA 1112 analyzer. GC analysis was performed on a Shimadzu GCMS QP2010 equipped with a ZB-1 column (30 m × 0.25 mm, pressure = 20.0 kPa, detector = EI, 300 °C) with helium gas as carrier. High resolution mass spectrum (HRMS) was recorded on a Bruker maxis mass spectrometer using ESI (electrospray ionization). Melting points and decomposition temperatures (DTA) were determined by using DSC–TGA measurements. Single-crystal X-ray data were collected at 298 K on SMART APEX CCD and Xcalibur Gemini Eos CCD single-crystal diffractometers by using graphite-monochromated MoKa radiation (0.71073 Å).

2.8.3. X-ray crystallography: X-ray reflections for compounds **63a**, **65a**, **66a**, and **79** were collected on a Bruker SMART APEX CCD diffractometer that was equipped with a graphite monochromator and a Mo Kα fine-focus sealed tube (λ=0.71073 Å). Data integration was done by using SAINT.[20] The intensities of the absorption were corrected by using SADABS.[21] Structure solution and refinement were carried out by using Bruker SHELX-TL.[22] X-ray reflections for compounds **64a**, **67**, **80**, **81**, and **84a** were collected on an Oxford Xcalibur Gemini Eos CCD diffractometer by using Mo Kα radiation. Data reduction was performed by using CrysAlisPro (*version* 1.171.33.55). The OLEX2–1.0[23] and SHELX-TL 97 programs were used to solve and refine the data. All non-hydrogen atoms were refined anisotropically and the C–H hydrogen atoms were placed at fixed positions.
CCDC-895107 (**63a**), CCDC-895108 (**64a**), CCDC-895109 (**65a**), CCDC-895110 (**66a**), CCDC-896656 (**67**), CCDC-895111 (**79**), CCDC-895112 (**80**), CCDC-895113 (**81**), and CCDC-895114 (**84a**) contain the supplementary crystallographic data for this paper. These data can be obtained free of charge from The Cambridge Crystallographic Data Centre via www.ccdc.cam.ac.uk/data_request/cif.

2.8.4. Theoretical study: Density function theory (DFT) has been universally applied to study energetic materials and has been shown to be reliable. Electronic-structure calculations were performed with the Gaussian 09 suite.[24] The geometries of the molecules were calculated at the B3LYP level in conjugation with the 6–311G** basis set.[25] The optimized geometries were submitted to the polymorph module of the Material studio suite for density calculations by using the CVFF force field.[26] The heats of formation of the triazole derivatives were obtained by using semi-empirical methods (Austin Model 1 (AM1),

Parameterization Method 3 (PM3), and Parameterization Method 6 (PM6)).[27] The detonation properties (*vD* and *P*) of the compounds were evaluated by using the Kamlet–Jacobs equations,[28] based on their predicted densities and HOFs, according to Equations (2) and (3), where *vD* is detonation velocity (m s^{-1}), *P* is the detonation pressure (GPa), *N* is the number of moles of gaseous detonation products per gram of explosives, *M* is the average molecular weight of the gaseous products, *Q* is the chemical energy of detonation (cal g^{-1}), which is defined as the difference between the HOFs of the products and the reactants, and 1 is the density of the explosive (g cm^{-3}):

$$vD = 1.01\ (NM^{0.5}Q^{0.5})^{0.5}\ (1 + 1.30\rho_o) \qquad \text{[Eq. (2)]}$$

$$P = 1.55\ \rho_o^{\,2}\ NM^{0.5}\ Q^{0.5} \qquad \text{[Eq. (3)]}$$

2.8.5 Materials: Unless otherwise noted, all the substrates Benzyl bromide, 4-nitrobenzyl bromide, 3-nitrobenzyl bromide, 2-nitrobenzyl bromide, 4-methoxybenzyl chloride, 3-methoxybenzyl bromide, 2-methoxybenzyl chloride, Aniline, 4-nitro aniline, 3-nitro aniline, 2-nitro aniline, 4-methoxy aniline, 3-methoxy aniline, 2-methoxy aniline, 2,6-bis(bromomethyl)pyridine, trimethylsilylacetylene, propargyl propionate, potassium carbonate, potassium acetate, sodium ascorbate, copper sulphate pentahydrate, m-chloroperbenzoic acid purchased from Sigma Aldrich Ltd, and used as received.

2.8.6. General procedure for the synthesis of azides (**GP-1**)**:** All azides were prepared following the reported procedures.[29] Benzyl azide (**59a**), 4-nitrobenzyl azide (**59b**), 3-nitrobenzyl azide (**59c**), 2-nitrobenzyl azide, (**59d**), 4-methoxybenzyl azide (**59e**), 3-methoxybenzyl azide (**59f**), 2-methoxybenzyl azide (**59g**), 2,6-bis(azidomethyl)pyridine (**82**) were prepared from the corresponding bromides or chlorides by reacting with NaN_3 in DMSO at room temperature.[29] Phenyl azide (**71a**), 4-nitrophenyl azide (**71b**)**,** 3-nitrophenyl azide (**71c**)**,** 2-nitrophenyl azide (**71d**)**,** 4-methoxyphenyl azide (**71e**)**,** 3-methoxyphenyl azide (**71f**)**,** 2-methoxyphenyl azide (**71g**) were prepared through the diazotization of their corresponding anilines with $NaNO_2$ and HCl at room temperature.[29]

2.8.7. General Cycloaddition Procedure (GP-2):

A mixture of the azide (1.0 equiv), trimethylsilyl (TMS)-acetylene (1.5 equiv), potassium carbonate (1.2 equiv), $CuSO_4$ (0.2 equiv), and sodium ascorbate (0.4 equiv) was dissolved in MeOH/water (1:1, 5 mL for 10 mmol) in a 20 mL vial. The vial was sealed with a screw cap and the resulting mixture was stirred rapidly at RT for 24 h. Upon completion of the reaction,

aqueous ammonium hydroxide (5%) was added to the reaction mixture, the organic layer was separated, and the aqueous layer was extracted with EtOAc (3 times). The combined extracts were washed with water (twice) and brine and dried over Na_2SO_4. The solvent was filtered off and evaporated under reduced pressure. The crude residue was purified by column chromatography on silica gel.

According to this above-mentioned procedure, known triazole compounds **61a**–**61g**, **62a**, and **72a**–**72g** were prepared in good-to-excellent yields.

2.8.8. General procedure for the synthesis of compounds 63a–69 (GP-3):

A mixture of 98% sulfuric acid (15 mL) and 70% nitric acid (10 mL) was added to compound **61** (12 mmol) at 0 ^oC and the reaction was carried out under the respective conditions shown in the Table 1.2. Upon completion, the reaction mixture was cooled by the addition of ice and neutralized with a saturated aqueous solution of $NaHCO_3$. The organic layer was separated and the aqueous layer was extracted with the minimum amount of EtOAc (3x20 mL). The combined extracts were washed with water (2x20 mL) and brine (25 mL) and dried over Na_2SO_4. The solvent was filtered off and evaporated under vacuum. The crude residue was purified by column chromatography on silica gel to afford the desired nitration products in good overall yields. A similar procedure was adopted for the nitration reactions that were carried out with a mixture of 95% nitric acid and 98% sulfuric acid.

2.8.9. General procedure for the synthesis of compounds 74–81 (GP-4):

A mixture of 98% sulfuric acid (15 mL) and 95% nitric acid (10 mL) was added to compound **72** (12 mmol) at 0 ^oC and the reaction was carried out under the respective conditions shown in the Table 1.4. Upon completion, the reaction mixture was cooled by the addition of ice and neutralized with a saturated aqueous solution of $NaHCO_3$. The organic layer was separated and the aqueous layer was extracted with the minimum amount of EtOAc (3x20 mL). The combined extracts were washed with water (2x20 mL) and brine (25 mL) and dried over Na_2SO_4. The solvent was filtered off and evaporated under vacuum. The crude residue was purified by column chromatography on silica gel to afford the desired nitration products in good overall yields.

2.8.10. General procedure for the formation of the N-oxides (GP-5):

A solution of the bistriazole-containing pyridine (**83**) (1.0 equiv) and *m*-chloroperbenzoic acid (*m*-CPBA, 1.5 equiv) in $CHCl_3$ (2 mL for 1 mmol) was placed in a 10 mL screw-capped vial. The vial was sealed and the mixture was stirred at 70 ^oC for 48 h. Upon completion of

the reaction, the mixture was cooled and dissolved in water. The organic layer was separated and the aqueous layer was extracted with Et_2O (twice). The combined extracts were washed with water and brine and dried over Na_2SO_4. The solvent was filtered off and evaporated under reduced pressure. The crude residue was purified by column chromatography on silica gel. The desired N-oxide products were obtained in good yields.

2.9. Spectral and Analytical Data of the Compounds:

1-benzyl-1H-1,2,3-triazole (61a) and 1-benzyl-4-(trimethylsilyl)-1H-1,2,3-triazole (62a):[30,31]

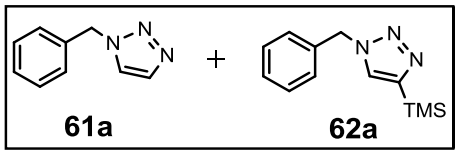

Following the general procedure (GP-2), a mixture of benzyl azide (**59a**; 1.0 g, 7.52 mmol), trimethylsilylacetylene (1.11 g, 11.2 mmol), K_2CO_3 (1.25 g, 9.02 mmol), sodium ascorbate (0.60 g, 3.01 mmol) and $CuSO_4$ (0.37 g, 1.50 mmol) in methanol: water (10 mL, 1:1) was stirred at room temperature for 24 h. Upon usual work-up, the crude mixture was purified by silica gel column chromatography eluting with hexane: ethyl acetate (2.3:1) to afford 1-benzyl-4-(trimethylsilyl)-1H-1,2,3-triazole (**62a**) (0.05 g) in 3% yield and **61a** (1.10 g) in 92% yield as brown color solids. For **61a:** ^{1}H NMR (400 MHz, $CDCl_3$) δ 7.69 (s, 1H), 7.48 (s, 1H), 7.35 (d, *J* = 6.0 Hz, 3H), 7.25 (d, *J* = 5.2 Hz, 2H), 5.56 (s, 2H); ^{13}C NMR (101 MHz, $CDCl_3$) δ 134.6, 134.1, 128.9, 128.6, 127.9, 123.3, 53.8.

For **62a**: ^{1}H NMR (400 MHz, $CDCl_3$) δ 7.43 (s, 2H), 7.33 (s, 2H), 7.27 (s, 2H), 5.53 (s, 2H), 0.29 (s, 9H); ^{13}C NMR (101 MHz, $CDCl_3$) δ 134.6, 134.1, 128.9, 128.6, 127.9, 123.2, 53.8, -1.31.

1-(4-nitrobenzyl)-1H-1,2,3-triazole (61b):[32]

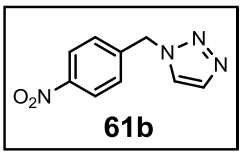

Following the general procedure (GP-2); a mixture of 4-nitrobenzyl azide (**59b**; 8.0 g, 44.9 mmol), trimethylsilylacetylene (6.61 g, 67.3 mmol), K_2CO_3 (7.44 g, 53.8 mmol), sodium ascorbate (3.55 g, 17.9 mmol) and $CuSO_4$ (2.24 g, 8.98 mmol) in methanol: water (80 mL, 1:1) was stirred at room temperature for 24 h. Upon usual work-up, the crude mixture was purified by silica gel column chromatography eluting with hexane: ethyl acetate (1.5:1) to afford **61b** (8.04 g) in 87% yield as brown color solid. ^{1}H NMR (400 MHz, $CDCl_3$) δ 8.23 (t, *J* = 2.0 Hz, 2H), 7.79 (s, 1H), 7.58 (s, 1H), 7.39 (d, *J* = 8.8 Hz, 2H), 5.70 (s, 2H); ^{13}C NMR (101 MHz, $CDCl_3$) δ 147.9, 141.9, 134.6, 128.5, 124.2, 123.9, 52.9.

1-(3-nitrobenzyl)-1H-1,2,3-triazole (**61c**)[33] and **1-(3-nitrobenzyl)-4-(trimethylsilyl)-1H-1,2,3-triazole** (**62c**)**:**

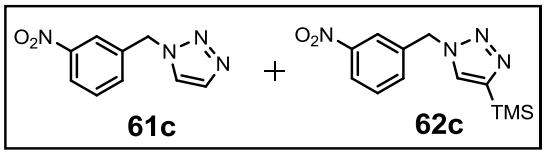

Following the general procedure (GP-2); a mixture of 3-nitrobenzyl azide (**59c**; 7.86 g, 44.1 mmol), trimethylsilylacetylene (6.5 g, 66.2 mmol), KOAc (5.19 g, 52.9 mmol), sodium ascorbate (3.49 g, 17.6 mmol) and $CuSO_4$ (2.2 g, 8.82 mmol) in methanol: water (80 mL, 1:1) was stirred at room temperature for 24 h. Upon usual work-up, the crude mixture was purified by silica gel column chromatography eluting with hexane: ethyl acetate (2.3:1) to afford 1-(3-nitrobenzyl)-4-(trimethylsilyl)-1H-1,2,3-triazole (**62c**) (0.85 g) in 9% yield as colorless solid and **61c** (7.51 g) in 83% yield as brown color solid. For **61c**: ^{1}H NMR (400 MHz, $CDCl_3$) δ 8.18 (d, *J* = 2 .0 Hz, 1H), 8.12 (s, 1H), 7.77 (s, 1H), 7.62 (s, 1H), 7.55 (m, 2H), 5.69 (s, 2H); ^{13}C NMR (101 MHz, $CDCl_3$) δ 148.6, 136.9, 134.7, 133.9, 130.3, 123.8, 122.8, 52.9.

For **62c**: R_f = 0.45 (4:1 *n*-hexane/EtOAc); ^{1}H NMR (400 MHz, $CDCl_3$) δ 7.94 (s, 1H), 7.86 (d, *J* = 8.0 Hz, 1H), 7.72 (s, 1H), 7.45 (d, *J* = 8 Hz, 1H), 7.30 (m, 1H), 5.58 (s, 2H), 0.03 (s, 9H); ^{13}C NMR (101 MHz, $CDCl_3$) δ 148.1, 146.9, 137.5, 134.1, 129.9, 129.8, 123.1, 122.7, 52.1, -1.31; IR (Neat) 2959, 1732, 1537, 1352, 1249, 1103, 1047, 842, 725, 630 cm^{-1}; MS (EI) *m/z* (%) 277 (M^++1, 100), 261 (11), 247 (50), 219 (33), 202 (6), 89 (6); Elemental analysis calcd (%) for $C_{12}H_{16}N_4O_2Si$: C, 52.15; H, 5.84; N, 20.27. Found: C, 52.06; H, 5.81; N, 20.35.

1-(2-nitrobenzyl)-1H-1,2,3-triazole (**61d**)**:**[33]

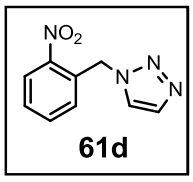

Following the general procedure (GP-2); a mixture of 2-nitrobenzyl azide (**59d**; 0.4 g, 2.24 mmol), trimethylsilylacetylene (0.33 g, 3.36 mmol), K_2CO_3 (0.37 g, 2.69 mmol), sodium ascorbate (0.17 g, 0.89 mmol) and $CuSO_4$ (0.11 g, 0.44 mmol) in methanol: water (10 mL, 1:1) was stirred at room temperature for 24 h. Upon usual work-up, the crude mixture was purified by silica gel column chromatography eluting with hexane: ethyl acetate (0.6:1) to afford **61d** (0.24 g) in 53% yield as brown color solid. ^{1}H NMR (400 MHz, $CDCl_3$) δ 8.14 (d, *J* = 8.4 Hz, 1H), 7.75 (d, *J* = 12 Hz, 2H), 7.61 (m, 1H), 7.53 (m, 1H), 7.04 (d, *J* = 4.0 Hz, 1H), 5.97 (s, 2H); ^{13}C NMR (101 MHz, $CDCl_3$) δ 147.4, 134.4, 130.7, 130.3, 129.7, 125.4, 124.7, 50.7.

1-(4-methoxybenzyl)-1H-1,2,3-triazole (61e):[34]

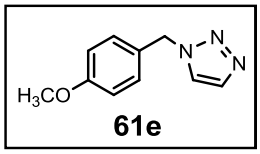

61e

Following the general procedure (GP-2); a mixture of 4-methoxybenzyl azide (**59e**; 10 g, 61.2 mmol), trimethylsilylacetylene (9.02 g, 91.2 mmol), K_2CO_3 (7.21 g, 73.5 mmol), sodium ascorbate (4.85 g, 24.5 mmol) and $CuSO_4$ (3.01 g, 12.2 mmol) in methanol: water (100 mL, 1:1) was stirred at room temperature for 24 h. Upon usual work-up, the crude mixture was purified by silica gel column chromatography eluting with hexane: ethyl acetate (4:1) to afford **61e** (10.6 g) in 92% yield as yellow color solid. ^{1}H NMR (400 MHz, $CDCl_3$) δ 7.65 (s, 1H), 7.45 (s, 1H), 7.19 (d, *J* = 8.0 Hz, 2H), 6.85 (d, *J* = 12 Hz, 2H), 5.45 (s, 2H), 3.81 (s, 3H); ^{13}C NMR (101 MHz, $CDCl_3$) δ 159.9, 134.2, 129.6, 126.7, 123.3, 114.4, 55.3, 53.5.

1-(3-methoxybenzyl)-1H-1,2,3-triazole (61f):[35]

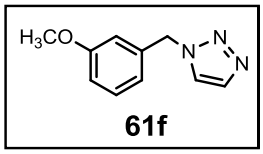

61f

Following the general procedure (GP-2); a mixture of 3-methoxybenzyl azide (**59f**; 10 g, 61.2 mmol), trimethylsilylacetylene (9.02 g, 91.2 mmol), K_2CO_3 (7.21 g, 73.5 mmol), sodium ascorbate (4.85 g, 24.5 mmol) and $CuSO_4$ (3.01 g, 12.2 mmol) in methanol: water (100 mL, 1:1) was stirred at room temperature for 24 h. Upon usual work-up, the crude mixture was purified by silica gel column chromatography eluting with hexane: ethyl acetate (1:1) to afford **61f** (9.21 g) in 79% yield as pale yellow color solid. ^{1}H NMR (400 MHz, $CDCl_3$) δ 7.60 (s, 1H), 7.51 (s, 1H), 7.16 (m, 1H) 6.73 (m, 3H), 5.41 (s, 2H), 3.64 (s, 3H); ^{13}C NMR (101 MHz, $CDCl_3$) δ 159.9, 136.2, 130.0, 124.1, 120.0, 113.9, 113.6, 55.2, 53.8.

1-(2-methoxybenzyl)-1H-1,2,3-triazole (61g):[33]

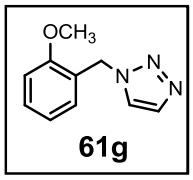

61g

Following the general procedure (GP-2); a mixture of 2-methoxybenzyl azide (**59g**; 1.08 g, 6.61 mmol), trimethylsilylacetylene (0.97 g, 9.92 mmol), K_2CO_3 (1.09 g, 7.94 mmol), sodium ascorbate (0.52 g, 2.64 mmol) and $CuSO_4$ (0.33 g, 1.32 mmol) in methanol: water (10 mL, 1:1) was stirred at room temperature for 24 h. Upon usual work-up, the crude mixture was purified by silica gel column chromatography eluting with hexane: ethyl acetate (0.6:1) to afford **61g** (0.65 g) in 52% yield as brown color solid. ^{1}H NMR (400 MHz, $CDCl_3$) δ 7.66 (s, 2H), 7.29 (d, *J* = 8.0 Hz, 1H), 7.13 (s, 1H), 6.83 (m, 1H), 6.70 (s, *J* = 8.0 Hz, 1H), 5.43 (s, 2H), 3.74 (s, 3H); ^{13}C NMR (101 MHz, $CDCl_3$) δ 156.2, 132.8, 132.4, 130.3, 130.0, 125.2, 122.9, 120.8, 112.7, 112.5, 110.7, 55.8, 48.5.

1-(2,4-Dinitrobenzyl)-4-nitro-1H-1,2,3-triazole (63a) and 1-(2,4-Dinitrobenzyl)-1H-1,2,3-triazole (64a) and 1-(3,5-Dinitrobenzyl)-1H-1,2,3-triazole (65a) and 1-(3,4-Dinitrobenzyl)-1H-1,2,3-triazole (66a):

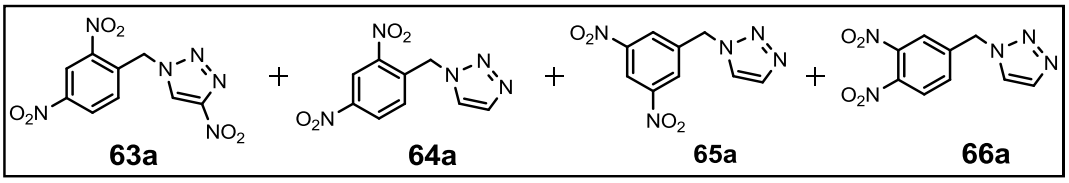

Following the general procedure (GP-3); A mixture of 98% sulfuric acid (18.4 g, 188.4 mmol, 10 mL) and 70% nitric acid (7.91 g, 125.6 mmol, 5 mL) was added to compound 1-benzyl-1H-1,2,3-triazole (**61a**; 2.0 g, 12.5 mmol) at 0 ^{o}C and the reaction was carried out under reflux at 120 ^{o}C for 24 h. Upon usual work-up, the crude mixture was purified by silica gel column chromatography eluting with hexane: ethyl acetate (1:1) to afford **63a** (0.58 g) in 15% yield as white solid**, 64a** (1.23 g) in 39% yield as pale colorless solid, **65a** (0.62 g) in 20% yield as white solid and **66a** (0.31 g) in 9% yield as dark yellow semi-solid.

For **63a**: 0.58 g, 15% Yield; colorless solid; m.p. 195 ^{o}C; DTA = 256 ^{o}C (exotherm); R_f = 0.60 (*n*-hexane/EtOAc, 1:1); ^{1}H NMR (400 MHz, [D$_6$]DMSO) δ 9.38 (s, 1H), 8.84 (s, 1H), 8.52 (d, *J* = 8.0 Hz, 1H), 7.50 (d, *J* = 8.8 Hz, 1H), 6.22 ppm (s, 2H); ^{13}C NMR (101 MHz, [D$_6$]DMSO) δ 153.5, 143.2, 134.9, 130.9, 124.1, 57.6 ppm; IR (KBr) ν_{max} 3412, 3092, 1518, 1342, 1086, 1047, 829, 723 cm^{-1}; MS (EI) m/z (%) 295 (100) [M+1]$^{+}$, 282 (6), 250 (60), 231 (14), 181 (4), 73 (48); Elemental analysis calcd (%) for $C_9H_6N_6O_6$: C 36.74, H 2.06, N 28.57; found: C 36.85, H 2.01, N 28.64.

For **64a**: 1.23 g, 39% Yield; colorless solid; m.p. 152 ^{o}C; DTA = 220 ^{o}C (exotherm); R_f = 0.28 (*n*-hexane/EtOAc, 1:1); ^{1}H NMR (400 MHz, [D$_6$]DMSO) δ 8.82 (d, *J* = 2.4 Hz, 1H), 8.52 (dd, *J* = 2.4, 8.8 Hz, 1H), 8.23 (s, 1H), 7.85 (s, 1H), 7.11 (d, *J* = 8.8 Hz, 1H), 6.14 ppm (s, 2H); ^{13}C NMR (101 MHz, [D$_6$]DMSO) δ 147.8, 147.6, 138.4, 138.3, 134.3, 131.6, 131.5, 128.8, 126.6, 120.8, 50.0 ppm; IR (KBr) ν_{max} 3132, 1608, 1535, 1346, 1221, 1070, 839, 729 cm^{-1}; MS (EI) m/z (%) 250 (100) [M+1]$^{+}$, 195 (3), 181 (3); Elemental analysis calcd (%) for $C_9H_7N_5O_4$: C 43.38, H 2.83, N 28.11; found: C 43.32, H 2.85, N 28.26.

For **65a**: 0.62 g, 20% Yield; colorless solid; m.p. 131 ^{o}C; DTA = 312 ^{o}C (exotherm); R_f = 0.20 (*n*-hexane/EtOAc, 1:1); ^{1}H NMR (400 MHz, [D$_6$]DMSO) δ 8.78 (s, 1H), 8.59 (s, 2H), 8.33 (s, 1H), 7.81 (s, 1H), 5.95 ppm (s, 2H); ^{13}C NMR (101 MHz, [D$_6$]DMSO) δ 148.7, 140.6, 134.3, 129.1, 126.1, 118.8, 51.3 ppm; IR (KBr) ν_{max} 3140, 3076, 1547, 1346, 1072, 929, 800, 729 cm^{-1}; MS (EI) m/z (%) 250 (100) [M+1]$^{+}$, 234 (5), 220 (3), 177 (5), 121 (3), 89

(9); Elemental analysis calcd (%) for $C_9H_7N_5O_4$: C 43.38, H 2.83, N 28.11; found: C 43.51, H 2.88, N 28.07.

For **66a**: 0.31 g, 9% Yield; yellow semi-solid; m.p. 88 ^oC; DTA = 215 ^oC (exotherm); R_f = 0.10 (*n*-hexane/EtOAc, 1:1); ^1H NMR (400 MHz, [D_6]DMSO) δ 8.30 (s, 1H), 8.23 (d, J = 8.4 Hz, 1H), 8.18 (s, 1H), 7.81 (s, 1 H), 7.77 (d, J = 8.4 Hz, 1H), 5.89 ppm (s, 2H); ^{13}C NMR (101 MHz, [D_6]DMSO) δ 143.8, 142.5, 141.8, 134.3, 133.9, 126.7, 126.1, 125.3, 51.5 ppm; IR (KBr) ν_{max} 2928, 1541, 1369, 1219, 1026, 846, 804 cm^{-1}; MS (EI) m/z (%) 250 (100) $[M+1]^+$, 202 (19), 192 (3), 172 (5), 159 (3); Elemental analysis calcd (%) for $C_9H_7N_5O_4$: C 43.38, H 2.83, N 28.11; found: C 43.45, H 2.81, N 28.05.

1-(4-Methoxy-3,5-dinitrobenzyl)-1H-1,2,3-triazole (67):

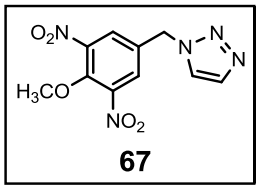

67

A mixture of 98% sulfuric acid (7.78 g, 79.4 mmol, 4.2 mL) and 70% nitric acid (3.33 g, 125.6 mmol, 2.2 mL) was added to compound 1-(4-methoxybenzyl)-1H-1,2,3-triazole (**61e**; 1.0 g, 5.29 mmol) at 0 ^oC and the reaction was carried out at room temperature for 2 h. Upon usual work-up, the crude mixture was purified by silica gel column chromatography eluting with hexane: ethyl acetate (1:1) to afford **67** (1.12 g) in 71% yield as yellow solid. 1.12 g, 71% Yield; yellow solid; m.p. 90 ^oC; DTA = 170 ^oC (exotherm); R_f = 0.51 (*n*-hexane/EtOAc, 1:1) ^1H NMR (400 MHZ, [D_6]DMSO) δ 7.98 (s, 2H), 7.79 (s, 1H), 7.72 (s, 1H), 5.69 (s, 2H), 3.98 ppm (s, 3H); ^{13}C NMR (400 MHz, [D_6]DMSO) δ 147.6, 145.3, 134.6, 131.9, 128.6, 124.4, 64.9, 51.7 ppm; IR (KBr) ν_{max} 3113, 1537, 1348, 1269, 1082, 979, 717 cm^{-1}; MS (EI) m/z (%) 280 (100) $[M+1]^+$, 211 (45), 102 (28), 70 (26); Elemental analysis calcd (%) for $C_{10}H_9N_5O_5$ C 43.02, H 3.25, N 25.08; found: C 43.15, H 3.31, N 25.19.

1-(3-Methoxy-4,5-dinitrobenzyl)-4-nitro-1H-1,2,3-triazole (68):

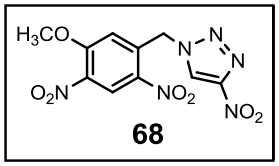

68

A mixture of 98% sulfuric acid (6.22 g, 63.4 mmol, 3.3 mL) and 70% nitric acid (2.66 g, 42.3 mmol, 1.8 mL) was added to compound 1-(3-methoxybenzyl)-1H-1,2,3-triazole (**61f**; 0.800 g, 4.23 mmol) at 0 ^oC and the reaction was carried out at room temperature for 2 h. Upon usual work-up, the crude mixture was purified by silica gel column chromatography eluting with hexane: ethyl acetate (1:1) to afford **68** (1.02 g) in 75% yield as yellow solid. 1.02 g, 75% Yield; yellow solid; DTA = 237 ^oC (exotherm); R_f = 0.71 (*n*-hexane/EtOAc, 1:1); ^1H NMR (400 MHz, [D_6]DMSO) δ 8.96 (s, 1H), 8.84 (s, 1H), 8.80 (s, 1 H), 5.88 (s, 2H), 4.28 ppm (s, 3H); ^{13}C NMR (101 MHz, [D_6]DMSO) δ 160.2, 151.3, 138.5, 132.1, 131.8, 127.5,

124.9, 123.2, 50.7, 46.9 ppm; IR (KBr) ν_{max} 3111, 1610, 1591, 1531, 1352, 1074, 792, 688 cm^{-1}; MS (EI) m/z (%) 325 (100) $[M+1]^+$, 116 (22), 102 (20), 84 (38), 70 (22); Elemental analysis calcd (%) for $C_{10}H_8N_6O_7$: C 37.05, H 2.49, N 25.92; found: C 37.12, H 2.55, N 25.86.

1-(2-Methoxy-3,5-dinitrobenzyl)-1H-1,2,3-triazole (69):

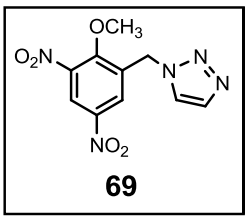

69

A mixture of 98% sulfuric acid (2.33 g, 23.8 mmol, 1.2 mL) and 70% nitric acid (0.99 g, 15.8 mmol, 0.6 mL) was added to compound 1-(2-methoxybenzyl)-1H-1,2,3-triazole (**61g**; 0.300 g, 1.58 mmol) at 0 ^oC and the reaction was carried out at room temperature for 2 h. Upon usual work-up, the crude mixture was purified by silica gel column chromatography eluting with hexane: ethyl acetate (3:7) to afford **69** (0.21 g) in 48% yield as yellow solid. 0.21 g, 48% Yield; yellow solid; DTA = 209 ^oC (exotherm); R_f = 0.67 (*n*-hexane/EtOAc, 3:7); ^1H NMR (400 MHz, $[D_6]$DMSO) δ 8.78 (d, *J* = 2.4 Hz, 1H), 8.36 (d, *J* = 2.0 Hz, 1H), 8.26 (s, 1H), 7.79 (s, 1H), 5.85 (s, 2H), 3.88 ppm (s, 3H); ^{13}C NMR(101 MHz, $[D_6]$DMSO) δ 156.2, 142.9, 142.6, 134.1, 134.0, 129.4, 126.2, 122.1, 63.7, 47.7 ppm; IR (neat) ν_{max} 1608, 1539, 1481,1346, 1265, 1091, 985 cm^{-1}; MS (EI) m/z (%) 281 (19) $[M+1]^+$, 280 (100) $[M]^+$, 235 (7), 207 (8), 162 (5), 116 (9), 84 (16); Elemental analysis calcd (%) for $C_{10}H_9N_5O_5$: C 43.02, H 3.25, N 25.08; found: C 43.11, H 3.19, N 25.15.

1-phenyl-1H-1,2,3-triazole (72a):[36]

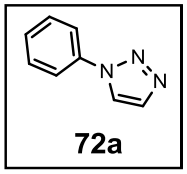

72a

Following the general procedure (GP-2); a mixture of phenyl azide (**71a**; 3.0 g, 25.2 mmol), trimethylsilylacetylene (3.71 g, 37.8 mmol), K_2CO_3 (2.96 g, 30.2 mmol), sodium ascorbate (1.99 g, 10.0 mmol) and $CuSO_4$ (1.25 g, 5.04 mmol) in methanol: water (30 mL, 1:1) was stirred at room temperature for 24 h. Upon usual work-up, the crude mixture was purified by silica gel column chromatography eluting with hexane: ethyl acetate (9:1) to afford **72a** (2.42 g) in 66% yield as brown color solid. ^1H NMR (400 MHz, $CDCl_3$) δ 8.00 (s, 1H), 7.70 (s, 1H), 7.70 (d, *J* = 8.0 Hz, 2H), 7.48 (m, 2H), 7.39 (m, 1H); ^{13}C NMR (101 MHz, $CDCl_3$) δ 136.8, 134.5, 129.7, 128.8, 121.7, 120.7.

1-(4-nitrophenyl)-1H-1,2,3-triazole (72b): [36]

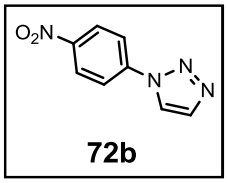

72b

Following the general procedure (GP-2); a mixture of 4-nitrophenyl azide (71**b**; 5.0 g, 30.5 mmol), trimethylsilylacetylene (4.48 g, 45.7 mmol), K_2CO_3 (5.06 g, 36.6 mmol), sodium ascorbate (2.42 g, 12.2 mmol) and $CuSO_4$ (1.52 g, 6.10 mmol) in methanol: water (50 mL, 1:1) was stirred at room temperature for 24 h. Upon usual work-up, the crude mixture was purified by silica gel column chromatography eluting with hexane: ethyl acetate (2.3:1) to afford **72b** (2.38 g) in 45% yield as brown color solid. ^{1}H NMR (400 MHz, $CDCl_3$) δ 8.44 (d, J = 9.0 Hz, 2H), 8.13 (s, 1H), 7.99 (d, J = 8.8 Hz, 2H), 7.92 (s, 1H); ^{13}C NMR (101 MHz, $CDCl_3$) δ 141.2, 135.3, 125.6, 121.7, 120.7.

1-(3-nitrophenyl)-1H-1,2,3-triazole (72c): [36]

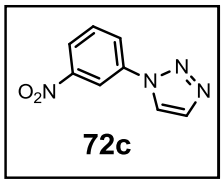

72c

Following the general procedure (GP-2); a mixture of 3-nitrophenyl azide (**71c**; 10 g, 60.9 mmol), trimethylsilylacetylene (8.97 g, 91.3 mmol), K_2CO_3 (7.17 g, 73.1 mmol), sodium ascorbate (4.82 g, 24.3 mmol) and $CuSO_4$ (3.04 g, 12.1 mmol) in methanol: water (100 mL, 1:1) was stirred at room temperature for 24 h. Upon usual work-up, the crude mixture was purified by silica gel column chromatography eluting with hexane: ethyl acetate (1.5:1) to afford **72c** (8.45 g) in 73% yield as yellow color solid. ^{1}H NMR (400 MHz, $CDCl_3$) δ 8.61 (s, 1H), 8.30 (d, J = 8.0 Hz, 1H), 8.19 (m, 2H), 7.91 (s, 1H), 7.76 (t, J = 8.4 Hz, 1H); ^{13}C NMR (101 MHz, $CDCl_3$) δ 147.4, 136.4, 133.6, 129.8, 124.7, 121.6, 114.0, 113.8, 113.7.

1-(2-nitrophenyl)-1H-1,2,3-triazole (72d)[37] **and 1-(2-nitrophenyl)-4-(trimethylsilyl)-1H-1,2,3-triazole (73d):**

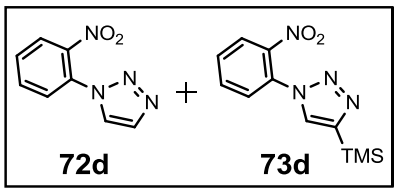

72d **73d**

Following the general procedure (GP-2); a mixture of 2-nitrophenyl azide (**71d**; 10 g, 60.9 mmol), trimethylsilylacetylene (8.97 g, 91.3 mmol), KOAc (7.17 g, 73.1 mmol), sodium ascorbate (4.82 g, 24.3 mmol) and $CuSO_4$ (3.04 g, 12.1 mmol) in methanol: water (100 mL, 1:1) was stirred at room temperature for 24 h. Upon usual work-up, the crude mixture was purified by silica gel column chromatography eluting with hexane: ethyl acetate (8:1) to afford 1-(2-nitrophenyl)-4-(trimethylsilyl)-1H-1,2,3-triazole (**73d**) (9.41 g) in 59% yield and **72d** (3.52 g) in 30% yield as brown color solids. For **73d**: mp 48–52 °C; R_f = 0.44 (1.5:1 *n*-hexane/EtOAc); ^{1}H NMR (400 MHz, $CDCl_3$) δ 8.05 (d, J = 8.4 Hz, 1H), 7.82 (s, 1H), 7.76 (d, J = 4.0 Hz, 1H), 7.67 (t, J = 6.8 Hz, 1H), 7.61 (d, J = 7.6 Hz, 1H), 0.38 (s, 9H); ^{13}C NMR (101 MHz, $CDCl_3$) δ 144.4,

133.8, 130.5, 130.4, 130.1, 127.8, 125.9, 125.4, -1.16; IR (Neat) ν_{max} 3119, 2959, 1954, 1842, 1707, 1626, 1159, 1041, 781, 630, 534, 461 cm^{-1}; MS (EI) *m/z* (%) 263 (M^++1, 61), 239 (24), 235 (39), 207 (100), 191 (43), 133 (22), 119 (29); Elemental analysis calcd (%) for $C_{11}H_{14}N_4O_2Si$: C, 50.36; H, 5.38; N, 21.36. Found: C, 50.28; H, 5.31; N, 21.42.

For **72d**: ^{1}H NMR (400 MHz, $CDCl_3$) δ 7.99 (d, *J* = 7.2 Hz, 1H), 7.91 (s, 1H), 7.77 (m, 2H), 7.66 (d, *J* = 6.4 Hz, 1H), 7.55 (d, *J* = 6.4 Hz, 1H); ^{13}C NMR (101 MHz, $CDCl_3$) δ 144.5, 134.2, 134.1, 130.1, 130.0, 127.8, 125.5, 125.4.

1-(4-methoxyphenyl)-1H-1,2,3-triazole (72e): [36]

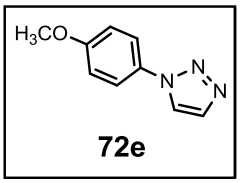

72e

Following the general procedure (GP-2); a mixture of 4-methoxyphenyl azide (**71e**; 5.0 g, 33.5 mmol), trimethylsilylacetylene (4.94 g, 50.3 mmol), K_2CO_3 (5.56 g, 40.2 mmol), sodium ascorbate (2.65 g, 13.4 mmol) and $CuSO_4$ (1.67 g, 6.70 mmol) in methanol: water (50 mL, 1:1) was stirred at room temperature for 24 h. Upon usual work-up, the crude mixture was purified by silica gel column chromatography eluting with hexane: ethyl acetate (9:1) to afford **72e** (4.98 g) in 85% yield as brown color solid. ^{1}H NMR (400 MHz, $CDCl_3$) δ 7.89 (s, 1H), 7.76 (s, 1H), 7.57 (d, *J* = 8.4 Hz, 2H), 6.96 (d, *J* = 8.8 Hz, 2H), 3.8 (s, 3H); ^{13}C NMR (101 MHz, $CDCl_3$) δ 160.6, 135.0, 129.1, 122.3, 121.7, 114.3, 55.8.

1-(3-methoxyphenyl)-1H-1,2,3-triazole (72f): [36]

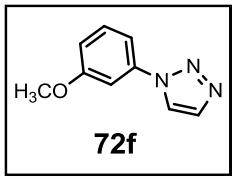

72f

Following the general procedure (GP-2); a mixture of 3-methoxyphenyl azide (**71f**; 10 g, 67.0 mmol), trimethylsilylacetylene (9.87 g, 100.5 mmol), KOAc (11.1 g, 80.4 mmol), sodium ascorbate (5.3 g, 26.8 mmol) and $CuSO_4$ (3.34 g, 13.4 mmol) in methanol: water (100 mL, 1:1) was stirred at room temperature for 24 h. Upon usual work-up, the crude mixture was purified by silica gel column chromatography eluting with hexane: ethyl acetate (9:1) to afford **72f** (9.32 g) in 79% yield as brown color solid. ^{1}H NMR (400 MHz, $CDCl_3$) δ 7.98 (s, 1H), 7.79 (s, 1H), 7.36 (t, *J* = 6.8 Hz, 1H), 7.31 (s, 1H), 7.22 (m, 1H), 6.92 (d, *J* = 8.0 Hz, 1H), 3.83 (s, 3H); ^{13}C NMR (101 MHz, $CDCl_3$) δ 160.5, 137.9, 130.5, 122.1, 114.4, 112.3, 106.4, 55.5.

1-(2-methoxyphenyl)-1H-1,2,3-triazole (72g)[38] and 1-(2-methoxyphenyl)-4-(trimethylsilyl)-1H-1,2,3-triazole (73g):

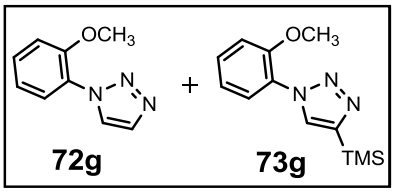

Following the general procedure (GP-2); a mixture of 2-methoxyphenyl azide (**71g**; 10 g, 67.0 mmol), trimethylsilylacetylene (9.87 g, 100.5 mmol), KOAc (11.1 g, 80.4 mmol), sodium ascorbate (5.30 g, 26.8 mmol) and $CuSO_4$ (3.34 g, 13.4 mmol) in methanol: water (100 mL, 1:1) was stirred at room temperature for 24 h. Upon usual work-up, the crude mixture was purified by silica gel column chromatography eluting with hexane: ethyl acetate (8:1) to afford 1-(2-methoxyphenyl)-4-(trimethylsilyl)-1H-1,2,3-triazole (**73g**) (4.80 g) in 29% yield as brown color liquid and **72g** (4.91 g) in 41% yield as brown color solid. For **73g**: R_f = 0.53 (4:1 *n*-hexane/EtOAc); ^{1}H NMR (400 MHz, $CDCl_3$) δ 8.00 (s, 1H), 7.65 (d, *J* = 7.6 Hz, 1H), 7.28 (m, 1H), 6.99 (d, *J* = 7.6 Hz, 2H), 3.78 (s, 3H), 0.32 (s, 9H); ^{13}C NMR (101 MHz, $CDCl_3$) δ 150.7, 144.9, 130.7, 129.4, 125.7, 124.8, 120.5, 112.0, 55.4, -1.387; IR (Neat) ν_{max} 2957, 1601, 1510, 1249, 120.5, 1118, 1035, 844, 754 cm^{-1}; MS (EI) *m/z* (%) 248 (M^++1, 44), 218 (22), 208 (10), 176 (100), 161 (10); Elemental analysis calcd (%) for $C_{12}H_{17}N_3OSi$: C, 58.26; H, 6.93; N, 16.99. Found: C, 58.37; H, 6.98; N, 16.85.

For **72g**: ^{1}H NMR (400 MHz, $CDCl_3$) δ 8.08 (s, 1H), 7.74 (s, 1H), 7.70 (dd, *J* = 15.2 Hz, 16.4, 1H), 7.35 (t, *J* = 8.0 Hz, 1H), 7.03 (m, 2H), 3.79 (s, 3H); ^{13}C NMR (101 MHz, **$CDCl_3$)** δ 150,7, 132.7, 129.8, 125.8, 125.6, 124.7, 120.5, 112.0, 55.3.

1-(2-nitrophenyl)-1H-1,2,3-triazole (74) and 1-(4-nitrophenyl)-1H-1,2,3-triazole (75):[38, 32]

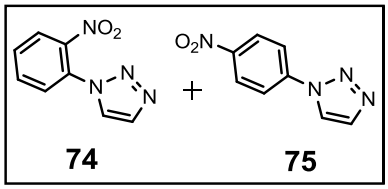

Following the general procedure (GP-4); A mixture of 98% sulphuric acid (15 ml) and 95% nitric acid (10ml) was added to 1-phenyl-1H-1,2,3-triazole (**72a**, 0.85 g, 5.85 mmol) at 0 °C and refluxed at 100 °C for 24 h. Upon usual work-up, the crude mixture was purified by silica gel column chromatography eluting with hexane: ethyl acetate (9:1) to afford **74** (0.06 g) in 5% yield and **75** (0.28 g) in 25% yield as brown color solids. For **74**: ^{1}H NMR (400 MHz, $CDCl_3$) δ 7.99 (d, *J* = 7.2 Hz, 1H), 7.91 (s, 1H), 7.77 (m, 2H), 7.66 (d, *J* = 6.4 Hz, 1H), 7.55 (d, *J* = 6.4 Hz, 1H); ^{13}C NMR (101 MHz, $CDCl_3$) δ 144.5, 134.2, 134.1, 130.1, 130.0, 127.8, 125.5, 125.4.

For **75**: ^{1}H NMR (400 MHz, $CDCl_3$) δ 8.44 (d, *J* = 9.0 Hz, 2H), 8.13 (s, 1H), 7.99 (d, *J* = 8.8 Hz, 2H), 7.92 (s, 1H); ^{13}C NMR (101 MHz, $CDCl_3$) δ 141.2, 135.3, 125.6, 121.7, 120.7.

1-(3,4-Dinitrophenyl)-1H-1,2,3-triazole (76) and 1,3,5-trinitrobenzene (77):[39]

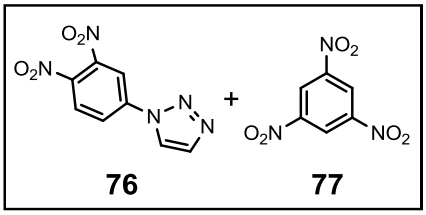

76 **77**

Following the general procedure (GP-4); A mixture of 98% sulphuric acid (15.5 g, 157.8 mmol, 8.4 mL) and 95% nitric acid (6.62 g, 105.7 mmol, 4.4 mL) was added to 1-(3-nitrophenyl)-1H-1,2,3-triazole (**72c**, 1.0 g, 10.5 mmol) at 0 °C and refluxed at 160 °C for 24 h. Upon usual work-up, the crude mixture was purified by silica gel column chromatography eluting with hexane: ethyl acetate (2:1) to afford **76** (0.19 g) in 18% yield as brown color solid and **77** (0.36 g) in 16% yield. For **76**: 0.19 g, 18% Yield; brown solid; m.p. 125 °C; DTA = 268 °C (exotherm); R_f = 0.48 (*n*-hexane/EtOAc, 2:1); ^{1}H NMR (400 MHz, $CDCl_3$) δ 9.10 (br s, 1H), 9.03 (br d, J = 4.0 Hz, 2H), 8.31 (br s, 1H), 7.99 ppm (br s, 1H); ^{13}C NMR (101 MHz, $CDCl_3$) δ 149.3, 138.6, 135.8, 121.9, 120.1, 117.9 ppm; IR (KBr) ν_{max} 3084, 2961, 1635, 1558, 1261, 1024, 798 cm^{-1}; MS (EI) m/z (%): 234 (38) $[M-1]^+$, 228 (31), 206 (100), 183 (16), 87 (7); Elemental analysis calcd (%) for $C_8H_5N_5O_4$: C 40.86, H 2.14, N 29.78; found: C 40.75, H 2.18, N 29.71.

For **77:** ^{1}H NMR (400 MHz, $CDCl_3$) δ 9.15 (s, 3H); ^{13}C NMR (101 MHz, $CDCl_3$) δ 147.2, 124.2.

1-(4-Methoxy-3,5-dinitrophenyl)-1H-1,2,3-triazole (78):

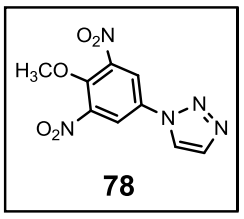

78

Following the general procedure (GP-4); A mixture of 98% sulphuric acid (16.8 g, 171.2 mmol, 9.1 mL) and 95% nitric acid (7.19 g, 114.2 mmol, 4.8 mL) was added to 1-(4-methoxyphenyl)-1H-1,2,3-triazole (**72e,** 2.0 g, 11.4 mmol) at 0 °C and the reaction was carried out at room temperature for 2 h. Upon usual work-up, the crude mixture was purified by silica gel column chromatography eluting with hexane: ethyl acetate (1:1) to afford **78** (1.10 g) in 85% yield as dark yellow solid. 1.10 g, 85% Yield; yellow solid; DTA = 319 °C (exotherm); R_f = 0.57 (*n*-hexane/EtOAc, 1:1); ^{1}H NMR (400 MHz, [D_6]DMSO) δ 9.03 (s, 1H), 8.91 (s, 2H), 8.06 (s, 1H), 4.00 ppm (s, 3H); ^{13}C NMR (101 MHz, [D_6]DMSO) δ 146.1, 145.4, 135.6, 132.2, 124.5, 121.3, 65.1 ppm; IR (KBr) ν_{max} 3157, 1541, 1346, 1271, 1053, 783 cm^{-1}; MS (EI) m/z (%) 266 (21) $[M+1]^+$, 265 (100) [M], 250 (39), 236 (26), 221 (13), 205 (5); Elemental analysis calcd (%) for $C_9H_7N_5O_5$: C 40.76, H 2.66, N 26.41; found: C 40.82, H 2.61, N 26.31.

1-(3-Methoxy-2,6-dinitrophenyl)-1H-1,2,3-triazole (79) and 1-(3-Methoxy-2,4-dinitrophenyl)-1H-1,2,3-triazole (80):

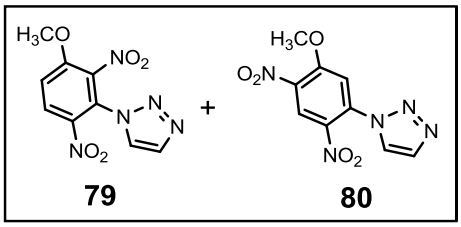

Following the general procedure (GP-4); A mixture of 98% sulphuric acid (16.8 g, 171.2 mmol, 9.1 mL) and 95% nitric acid (7.19 g, 114.2 mmol, 4.8 mL) was added to 1-(3-methoxyphenyl)-1H-1,2,3-triazole (**72f,** 2.0 g, 11.4 mmol) at 0 °C and the reaction was carried out at room temperature for 2 h. Upon usual work-up, the crude mixture was purified by silica gel column chromatography eluting with hexane: ethyl acetate (4:6) to afford **79** (0.49 g) in 33% yield and **80** (0.69 g) in 46% yield as yellow solids. For **79:** 0.49 g, 33% Yield; yellow solid; m.p. 168 °C; DTA = 221 °C (exotherm); R_f = 0.65 (*n*-hexane/EtOAc, 4:6); ^{1}H NMR (400 MHz, [D$_6$]DMSO) δ 8.68 (br s, 1H), 8.63 (d, *J* = 9.6 Hz, 1H), 8.01 (s, 1H), 7.86 (d, *J* = 9.6 Hz, 1H), 4.13 ppm (s, 3H); ^{13}C NMR (101 MHz, [D$_6$]DMSO) δ 155.2, 137.7, 137.0, 134.6, 130.2, 128.9, 124.9, 116.7, 59.0 ppm; IR (KBr) ν_{max} 3124, 1614, 1342, 1078, 989, 794, 652 cm^{-1}; MS (EI) m/z (%) 266 (58) [M+1]$^+$, 242 (26), 226 (83), 210 (100), 194 (91), 163 (72), 149 (85); Elemental analysis calcd (%) for $C_9H_7N_5O_5$: C 40.76, H 2.66, N 26.41; found: C 40.71, H 2.59, N 26.35.

For **80**: 0.69 g, 46% Yield; yellow solid; m.p. 200 °C; DTA = 230 °C (exotherm); R_f = 0.40 (*n*-hexane/EtOAc, 7:3); ^{1}H NMR (400 MHz, CDCl$_3$) δ 8.88 (s, 1H), 8.77 (br s, 1H), 8.05 (br s, 1H), 7.87 (s, 1H), 4.11 ppm (s, 3H); ^{13}C NMR (101 MHz, CDCl$_3$) δ 155.9, 138.3, 136.0, 134.7, 134.3, 127.3, 124.1, 114.4, 59.1 ppm; IR (KBr) ν_{max} 3097, 1620, 1531, 1350, 1232, 1072, 806 cm^{-1}; MS (EI) m/z (%) 266 (68) [M+1]$^+$, 242 (45), 226 (57), 210 (72), 194 (92), 164 (100), 149 (72); Elemental analysis calcd (%) for $C_9H_7N_5O_5$: C 40.76, H 2.66, N 26.41; found: C 40.85, H 2.63, N 26.35.

1-(2-Methoxy-3,5-dinitrophenyl)-1H-1,2,3-triazole (81):

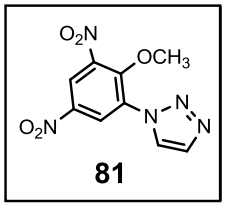

Following the general procedure (GP-4); A mixture of 98% sulphuric acid (16.8 g, 171.2 mmol, 9.1 mL) and 95% nitric acid (7.19 g, 114.2 mmol, 4.8 mL) was added to 1-(3-methoxyphenyl)-1H-1,2,3-triazole (**72g,** 2.0 g, 11.4 mmol) at 0 °C and the reaction was carried out at room temperature for 2 h. Upon usual work-up, the crude mixture was purified by silica gel column chromatography eluting with hexane: ethyl acetate (1:1) to afford **81** (1.24 g) in 82% yield as yellow solid. 1.24 g, 82% Yield; yellow solid; DTA = 152 °C (exotherm); R_f = 0.57 (*n*-hexane/EtOAc, 1:1); ^{1}H NMR (400 MHz, CDCl$_3$) δ 8.98–8.95 (m, 1H), 8.80 (br s, 1H), 8.69

(s, 1H), 8.07 (s, 1H), 3.63 ppm (s, 3H); ^{13}C NMR (101 MHz, $CDCl_3$) δ 151.5, 144.0, 142.4, 134.8, 132.1, 127.8, 126.1, 125.7, 121.9, 63.4 ppm; IR (KBr) ν_{max} 3155, 1547, 1350, 1261, 1049, 978, 733 cm^{-1}; MS (EI) m/z (%) 266 (58) $[M+1]^+$, 223 (23), 129 (56), 116 (12), 97 (100), 74 (6); Elemental analysis calcd (%) for $C_9H_7N_5O_5$: C 40.76, H 2.66, N 26.41; found: C 40.65, H 2.69, N 26.52.

2,6-Bis((1H-1,2,3-triazol-1-yl)methyl)pyridine (83a):

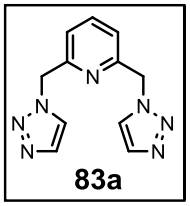

Following the general procedure (GP-2); a mixture of 2,6-bis(azidomethyl)pyridine (**82**; 1.0 g, 5.28 mmol), trimethylsilylacetylene (1.55 g, 15.8 mmol), K_2CO_3 (1.75 g, 12.7 mmol), sodium ascorbate (0.83 g, 4.22 mmol) and $CuSO_4$ (0.52 g, 2.11 mmol) in methanol : water (40 mL, 1:1) was stirred at room temperature for 24 h. Upon usual work-up, the crude mixture was purified by silica gel column chromatography eluting with hexane: ethyl acetate (9:1) to afford **83a** (1.01 g) in 79% yield as brown color solid. 1.01 g, 79% Yield; brown solid; m.p. 65–68 ^{o}C; R_f = 0.57 (EtOAc); ^{1}H NMR (400 MHz, $CDCl_3$) δ 7.65–7.54 (m, 5H), 7.02 (d, J = 7.6 Hz, 2H), 5.57 ppm (s, 4H); ^{13}C NMR (101 MHz, $CDCl_3$) δ 154.6, 138.6, 134.1, 124.5, 121.7, 54.9 ppm; IR (KBr) ν_{max} 1591, 1454, 1217, 1087, 1028, 800, 765, 690 cm^{-1}; MS (EI) m/z (%) 242 (100) $[M+1]^+$, 214 (19), 186 (14), 173 (8), 145 (16); Elemental analysis calcd (%) for $C_{11}H_{11}N_7$: C 54.76, H 4.60, N 40.64; found: C 54.63, H 4.68, N 40.52.

Diethyl-2,2'-(1,1'-(pyridine-2,6-diylbis(methylene))bis(1H-1,2,3-triazole-4,1-diyl)) diacetate (83b):

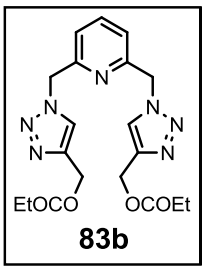

Following the general procedure (GP-2); a mixture of 2,6-bis(azidomethyl)pyridine (**82**; 1.5 g, 7.92 mmol), propargyl propionate (2.66 g, 23.7 mmol), KOAc (1.86 g, 19.0 mmol), sodium ascorbate (1.25 g, 6.34 mmol) and $CuSO_4$ (0.79 g, 3.17 mmol) in methanol : water (60 mL, 1:1) was stirred at room temperature for 24 h. Upon usual work-up, the crude mixture was purified by silica gel column chromatography eluting with only ethyl acetate to afford **83b** (2.90 g) in 88% yield as brown color solid. 2.90 g, 88% Yield; brown solid; R_f = 0.56 (EtOAc); ^{1}H NMR (400 MHz, $CDCl_3$) δ 7.72 (s, 2H), 7.66 (t, J = 8.0 Hz, 1H), 7.11 (d, J = 7.6 Hz, 2H), 5.59 (s, 4H), 5.17 (s, 4H), 2.28 (q, J = 7.6 Hz, 4H), 1.06 ppm (t, J = 7.6 Hz, 6H); ^{13}C NMR (101 MHz, $CDCl_3$) δ 173.7, 154.3, 142.7, 138.4, 124.7, 121.5, 57.1, 54.6, 26.9, 8.60 ppm; IR (neat) ν_{max} 2982, 1738, 1462, 1182, 1051, 781 cm^{-1}; MS (EI) m/z (%) 414 (45)

$[M+1]^+$, 436 (100) $[M+Na]^+$; Elemental analysis calcd (%) for $C_{19}H_{23}N_7O_4$: C 55.20, H 5.61, N 23.72; found: C 55.36, H 5.65, N 23.65.

2,6-bis((4-(nitromethyl)-1H-1,2,3-triazol-1-yl)methyl)pyridine (83'b):

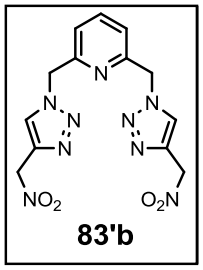

83'b

Following the general procedure (GP-4); A mixture of 98% sulphuric acid (15 ml) and 95% nitric acid (10ml) was added to (1,1'-(pyridine-2,6-diyl bis (methylene)) bis (1H-1,2,3-triazole-4,1-diyl)) bis(methylene) dipropionate (**83b**, 1.0 g, 2.42 mmol) at 0 °C. The resulting reaction mixture was stirred at room temperature for 24 h. Upon usual work-up, the crude mixture was purified by silica gel column chromatography eluting with only ethyl acetate to afford **83'b** (0.68 g) in 79% yield as colorless solid. 0.68 g, 79% yield, colorless solid, mp 92–95 °C; R_f = 0.59 (EtOAc); ^{1}H NMR (400 MHz, $CDCl_3$) δ 7.81 (s, 2H), 7.74 (t, J = 7.6 Hz, 1H), 7.23 (d, J = 7.6 Hz, 2H), 5.63 (s, 4H), 5.59 (s, 4H); ^{13}C NMR (101 MHz, $CDCl_3$) δ 154.08, 139.9, 138.9, 125.3, 122.2, 65.8, 55.1; IR (KBr) ν_{max} 1591, 1454, 1217, 1087, 1028, 800, 765, 690 cm^{-1}; MS (EI) *m/z* (%) 360 (M^++1, 100), 301 (16), 244 (27); Elemental analysis calcd (%) for $C_{13}H_{13}N_9O_4$: C, 43.46; H, 3.65; N, 35.08. Found: C, 43.29; H, 3.58; N, 35.18.

2,6-Bis((1H-1,2,3-triazol-1-yl)methyl)pyridine 1-oxide (84a):

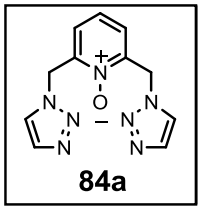
84a

Following the general procedure (GP-5); A mixture of the 2,6-bis((1H-1,2,3-triazol-1-yl)methyl)pyridine (**83a**, 0.200 g, 0.82 mmol) and *m*-chloroperbenzoic acid (*m*-CPBA, 0.21 g, 1.24 mmol) was added in $CHCl_3$ (4 mL). The resulting reaction mixture was stirred at room temperature for heated at 70 °C for 48 h. Upon usual work-up, the crude mixture was purified by silica gel column chromatography eluting with chloroform: methanol (9:1) to afford **84a** (0.08 g) in 35% yield as colorless solid. 0.08 g, 35% Yield; colorless solid; m.p. 62 °C; DTA = 228 °C (exotherm); R_f = 0.68 ($CHCl_3$/MeOH, 9:1); ^{1}H NMR (400 MHz, $CDCl_3$) δ 7.94 (s, 2H), 7.78 (s, 2 H), 7.27 (br s, 1H), 7.12 (d, J = 8.0 Hz, 2H), 5.87 ppm (s, 4H); ^{13}C NMR (101 MHz, $CDCl_3$) δ 145.8, 134.2, 125.9, 125.6, 125.4, 48.4 ppm; IR (KBr) ν_{max} 2852, 1693, 1417, 1350, 1217, 1028, 808 cm^{-1}; MS (EI) m/z (%) 258 (100) $[M+1]^+$, 242 (16), 230 (14), 174 (11), 145 (8); Elemental analysis calcd (%) for $C_{11}H_{11}N_7O_5$: C 51.36, H 4.31, N 38.11; found: C 51.28, H 4.26, N 38.29.

2,6-Bis((4-(nitromethyl)-1H-1,2,3-triazol-1-yl)methyl)pyridine 1-oxide (84b):

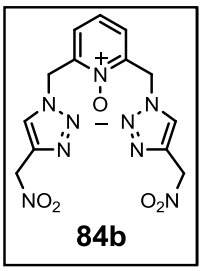

84b

Following the general procedure (GP-4); A mixture of 98% sulphuric acid (15 ml) and 95% nitric acid (10ml) was added to (1,1'-(pyridine-2,6-diylbi s(methylene))bis(1H-1,2,3-triazole-4,1-diyl))bis(methylene)di propionate (**83b**, 0.500 g, 1.21 mmol) at 0 °C. The resulting reaction mixture was stirred at room temperature for 12 h. Upon usual work-up, the crude mixture was purified by silica gel column chromatography eluting with only ethyl acetate afforded 2,6-bis((4-(nitromethyl)-1H-1,2,3-triazol-1-yl)methyl)pyridine (**83'b**) compound. To this compound **83'b** (0.100 g, 0.278 mmol) according to the general procedure (GP-5); added a solution of *m*-chloroperbenzoic acid (*m*-CPBA, 0.07 g, 0.41 mmol) in $CHCl_3$ (4 mL). The resulting reaction mixture was stirred at room temperature 24 h. Upon usual work-up, the crude mixture was purified by silica gel column chromatography eluting with chloroform: methanol (9:1) to afford **84b** (0.04 g) in 41% yield as pale-yellow solid. 0.04 g, 41% Yield; pale-yellow solid; m.p. 110 °C; DTA = 142 °C (exotherm); R_f = 0.72 ($CHCl_3$/MeOH, 9:1); ^{1}H NMR (400 MHz, [D_6]DMSO) δ 8.14 (s, 2H), 7.38–7.27 (m, 3H), 5.79 (s, 4H), 5.58 ppm (s, 4H); ^{13}C NMR (101 MHz, [D_6]DMSO) δ 145.0, 139.6, 126.8, 126.7, 126.0, 65.6, 48.8 ppm; IR (KBr) ν_{max} 2924, 1724, 1641, 1385, 1261, 1111, 1022, 850, 796 cm^{-1}; MS (EI) m/z (%) 375 (100) [M]+, 374 (100) $[M-1]^+$, 356 (13), 343 (5), 327 (24); Elemental analysis calcd (%) for $C_{13}H_{13}N_9O_5$: C 41.60, H 3.49, N 33.59; found: C 41.75, H 3.56, N 33.41.

2.10. References

1) a) H. Gao, J. M. Shreeve, *Chem. Rev*. **2011**, *111*, 7377–7436; b) M. Gobel, T. M. Klapotke, *Adv. Funct. Mater.* **2009**, *19*, 347–365; c) N. Sikder, N. R. Bulakh, A. K. Sikder, D. B. Sarwade, *J. Hazard. Mater.* **2003**, *96*, 109–119; d) T. M. Klapotke, C. M. Sabate, *Chem. Mater*. **2008**, *20*, 1750–1763; e) M. B. Talawar, R. Sivabalan, B. G. Polke, U. R. Nair, G. M. Gore, S. N. Asthana, *J. Hazard. Mater.* **2005**, *124*, 153–164; f) J. Kohler, R. Meyer, A. Homburg, *Explosives*, 6th ed., Wiley-VCH, Weinheim, **2007**; g) C. Ye, G. L. Gard, R.W. Winter, R. G. Syvret, B. Twamley, J. M. Shreeve, *Org. Lett*. **2007**, *9*, 3841–3844; h) Y. Huang, H. Gao, B. Twamley, J. M. Shreeve, *Eur. J. Inorg. Chem*. **2008**, 2560–2568.

2) a) J. E. Moses, A. D. Moorhouse, *Chem. Soc. Rev*. **2007**, *36*, 1249–1262; b) R. Sivabalan, M. Anniyappan, S. J. Pawar, M. B. Talawar, G. M. Gore, S. Venugopalan, B. R. Gandhe, *J. Hazard. Mater*. **2006**, *137*, 672 –680; c) A. Hammerl, M. A. Hiskey, G. Holl, T. M. Klapotke, P. Kurt, J. Stierstorfer, J. J. Weigand, Chem. Mater. **2005**, *17*, 3784–3793; d) T. L. Davis, *The Chemistry of Powder and Explosives*, Angriff Press, Los Angeles, **1943**; e) J. P. Agrawal, *High Energy Materials: Propellants, Explosives and Pyrotechnics*, Wiley-VCH, Weinheim, **2010**; f) N. Fischer, T. M. Klapotke, D. Piercey, S. Scheutzow, J. Stierstorfer, *Z. Anorg. Allg. Chem*. **2010**, *636*, 2357–2363; g) U. R. Nair, G. M. Gore, R. Sivabalan, S. J. Pawar, S. N. Asthana, S. Venugopalan, *J. Hazard. Mater*. **2007**, *143*, 500–505.

3) a) J. P. Agrawal, R. Mehilal, U. S. Prasad, R. N. Surve, *New J. Chem*. **2000**, *24*, 583–585; b) J. P. Agrawal, *Propellants Explos. Pyrotech*. **2005**, *30*, 316–328; c) R. Mehilal, B. Salunke, A. K. Sikder, J. P. Agrawal, *J. Hazard. Mater*. **2001**, *84*, 117–122; d) M. B. Talawar, R. Sivabalan, M. Anniyappan, G. M. Gore, S. N. Asthana, B. R. Gandhe, *Combust. Explos. Shock Waves (Engl. Transl.)* **2007**, *43*, 62–72; e) M. B. Talawar, A. P. Agarwal, M. Anniyappan, G. M. Gore, S. N. Asthana, S. Venugopalan, *J. Hazard. Mater*. **2006**, *137*, 1848–1852; f) T. M. Klapotke, B. Krumm, K. Polborn, *J. Am. Chem. Soc*. **2004**, *126*, 710–711; g) M. Mikhailov Yu, S. V. Chapyshev, V. V. Nedelko, *Russ. Chem. Bull.* **2009**, *58*, 2097–2102.

4) a) G. H. Tao, B. Twamley, J. M. Shreeve, *J. Mater. Chem*. **2009**, *19*, 5850–5854; b) C. Ye, H. Gao, J. A. Boatz, G. W. Drake, B. Twamley, J. M. Shreeve, *Angew. Chem*. **2006**, *118*, 7420–7423; c) A. Saikia, R. Sivabalan, B. G. Polke, G. M. Gore, A. Singh, A. S. Rao, A. K. Sikder, *J. Hazard. Mater*. **2009**, *170*, 306–313; d) J. P. Agrawal, R. D. Hodgson, *Organic Chemistry of Explosives*, Wiley-VCH, Weinheim, **2007**; e) J. Akhavan, *The Chemistry of Explosives*, 2nd ed., RSC, Cambridge, **2004**; f) O. Yu. Sapozhnikov, M. D. Dutov, M. A.

Korolev, V. V. Kachala, V. I. Kadentsev, S. A. Shevelev, *Russ. Chem. Bull*. **2004**, *53*, 588–595.

5) a) T. Abe, G. H. Tao, Y. H. Joo, R. W. Winter, G. L. Gard, J. M. Shreeve, *Chem. Eur. J*. **2009**, *15*, 9897–9904; b) S. Garg, J. M. Shreeve, *J. Mater. Chem*. **2011**, *21*, 4787–4794; c) Y. C. Li, C. Qi, S. H. Li, H. J. Zhang, C. H. Sun, Y. Z. Yu, Si. Ping Pang, *J. Am. Chem. Soc*. **2010**, *132*, 12172–12173; d) V. Thottempudi, F. Forohor, D. A. Parrish, J. M. Shreeve, *Angew. Chem. Int. Ed.*, **2012**, *51*, 9881–9885; e) T. M. Klapotke, C. Petermayer, D. G. Piercey, J. Stierstorfer, *J. Am. Chem. Soc*. **2012**, *134*, 20827−20836; f) V. Thottempudi, P. Yin, J. Zhang, D. A. Parrish, J. M. Shreeve, *Chem. Eur. J*. **2014**, *20*, 542–548; g) T. M. Klapotke, C. M. Sabate, *Chem. Mater*. **2008**, *20*, 3629–3637; h) T. M. Klapotke, P. Mayer, A. Schulz, J. J. Weigand, *J. Am. Chem. Soc*. **2005**, *127*, 2032–2033; i) T. M. Klapotke, F. A. Martin, J. Stierstorfer, *Angew. Chem*. **2011**, *123*, 4313–4316; *Angew. Chem. Int. Ed*. **2011**, *50*, 4227–4229.

6) a) R. P. Singh, J. M. Shreeve, Chem. Eur. J. 2011, 17, 11876–11881; b) K. Karaghiosoff, T. M. Klapotke, P. Mayer, H. Piotrowski, K. Polborn, R. L. Willer, J. J. Weigand, *J. Org. Chem*. **2006**, *71*, 1295–1305;

c) R. Damavarapu, *Propellants Explos. Pyrotech*. **2010**, *35*, 395–406; d) R. Damavarapu, C. R. Surapaneni, N. Gelber, R. G. Duddu, P. R. Dave, U. S. Patent 7304164, **2007**.

7) a) T. M. Klapotke, J. Stierstorfer, *J. Am. Chem. Soc*. **2009**, *131*, 1122–1134; b) A. K. Sikder, N. Sikder, *J. Hazard. Mater*. **2004**, *112*, 1–15; c) D. M. Badgujar, M. B. Talawar, S. N. Asthana, P. P. Mahulikar, *J. Hazard. Mater*. **2008**, *151*, 289–305; d) M. Friedrich, J. C. G. Ruiz, T. M. Klapotke, P. Mayer, B. Weber, J. J. Weigand, *Inorg. Chem*. **2005**, *44*, 8044–8052; e) S. G. Cho, J. R. Cho, E. M. Goh, J. K. Kim, *Propellants Explos. Pyrotech*. **2005**, *30*, 445–449.

8) a) P. N. Neuman, *J. Heterocycl. Chem*. **1971**, *8*, 51–56; b) Y. Huang, H. Gao, B. Twamley, J. M. Shreeve, *Eur. J. Inorg. Chem*. **2008**, 2560–2568; c) M. Gobel, K. Karaghiosoff, T. M. Klapotke, D. G. Piercey, J. Stierstorfer, *J. Am. Chem. Soc*. **2010**, *132*, 17216–17226; d) M. Anniyappan, M. B. Talawar, G. M. Gore, S. Venugopalan, B. R. Gandhe, *J. Hazard. Mater*. **2006**, *137*, 812–819; e) P. F. Pagoria, G. S. Lee, A. R. Mitchell, R. D. Schmidt, *Thermochim. Acta* **2002**, *384*, 187–204; f) Q. Zhang, J. Zhang, D. A. Parrish, J. M. Shreeve, *Chem. Eur. J*. **2013**, *19*, 11000–11006.

9) V. V. Rostovtsev, L. G. Green, V. V. Fokin, K. B. Sharpless, *Angew. Chem*. **2002**, *114*, 2708–2711; *Angew. Chem. Int. Ed*. **2002**, *41*, 2596–2599.

10) a) P. Cornago, C. Escolistico, M. D. S. Maria, R. M. Ciaramunt, *Tetrahedron* **1996**, *52*, 11075–11094; b) J. Kalisiak, K. B. Sharpless, V. V. Fokin, *Org. Lett*. **2008**, *10*, 3171.

11) a) A. Krasinski, V. V. Fokin, K. B. Sharpless, *Org. Lett*. **2004**, *6*, 1237–1240; b) L. Zhang, X. Chen, P. Xue, H. H. Y. Sun, I. D. Williams, K. B. Sharpless, V. V. Fokin, G. Jia, *J. Am. Chem. Soc*. **2005**, *127*, 15998–15999.

12) a) S. Ueda, S. Mingjuan, S. L. Buchwald, *Angew. Chem*. **2011**, *123*, 9106–9109; *Angew. Chem. Int. Ed*. **2011**, *50*, 8944–8947; b) Q. Wang, T. R. Chan, R. Hilgraf, V. V. Fokin, K. B. Sharpless, M. G. Finn, *J. Am. Chem. Soc*. **2003**, *125*, 3192–3193.

13) V. Maraval, C. Duhayon, Y. Coppel, R. Chauvin, *Eur. J. Org. Chem*. **2008**, 5144.

14) J. T. Fletcher, S. E. Walz, M. E. Keeney, *Tetrahedron Lett*. **2008**, *49*, 7030–7032.

15) V. R. Kamalraj, S. Senthil, P. Kannan, *J. Mol. Struct*. **2008**, *892*, 210–215.

16) a) B. C. Jeffrey, M. Ripudaman, D. Allen, *Synthesis* **2004**, *4*, 499–500; b) W. B. Yi, C. Cai, *J. Energ. Mater*. **2007**, *25*, 129–139.

17) a) M. V. Roux, M. Temprado, J. S. Chickos, Y. Nagano, *J. Phys. Chem. Ref. Data* **2008**, *37*, 1855–1996; b) W. N. Hubbard, F. R. Frow, G. Waddington, *J. Phys. Chem*. **1961**, *65*, 1326–1328.

18) P. Ramirez-Lopez, M. C. Torre, H. E. Montenegro, M. Asenjo, M. A. Sierra, *Org. Lett*. **2008**, *10*, 3555–3558

19) a) V. Thottempudi, H. Gao, J. M. Shreeve, *J. Am. Chem. Soc*. **2011**, *133*, 6464–6471; b) V. Thottempudi, T. K. Kim, K. H. Chung, J. S. Kim, *Bull. Korean Chem. Soc*. **2009**, *30*, 2152–2154 ; c) R. F. W. Bader, M. T. Carroll, J. R. Cheeseman, C. Chang, *J. Am. Chem. Soc*. **1987**, *109*, 7968–7979.

20) *SAINT-Plus, version 6.45*, Bruker AXS Inc., Madison, **2003**.

21) G. M. Sheldrick, *SADABS, Program for Empirical Absorption Correction of Area Detector Data*, University of Gottingen, Gottingen, **1997**.

22) a) *SMART (version 5.625), SHELX-TL (version 6.12)*, Bruker AXS Inc., Madison, **2000**; b) G. M. Sheldrick, *SHELXS-97*, University of Gottingen, Gottingen, **1997**.

23) O. V. Dolomanov, A. J. Blake, N. R. Champness, M. Schroder, *J. Appl. Crystallogr*. **2003**, *36*, 1283–1284.

24) Gaussian 09, Revision C.01, M. J. Frisch, G. W. Trucks, H. B. Schlegel, G. E. Scuseria, M. A. Robb, J. R. Cheeseman, G. Scalmani, V. Barone, B. Mennucci, G. A. Petersson, H. Nakatsuji, M. Caricato, X. Li, H. P. Hratchian, A. F. Izmaylov, J. Bloino, G. Zheng, J. L. Sonnenberg, M. Hada, M. Ehara, K. Toyota, R. Fukuda, J. Hasegawa, M. Ishida, T. Nakajima, Y. Honda, O. Kitao, H. Nakai, T. Vreven, J. A. Montgomery, Jr., J. E. Peralta, F.

Ogliaro, M. Bearpark, J. J. Heyd, E. Brothers, K. N. Kudin, V. N. Staroverov, R. Kobayashi, J. Normand, K. Raghavachari, A. Rendell, J. C. Burant, S. S. Iyengar, J. Tomasi, M. Cossi, N. Rega, J. M. Millam, M. Klene, J. E. Knox, J. B. Cross, V. Bakken, C. Adamo, J. Jaramillo, R. Gomperts, R. E. Stratmann, O. Yazyev, A. J. Austin, R. Cammi, C. Pomelli, J. W. Ochterski, R. L. Martin, K. Morokuma, V. G. Zakrzewski, G. A. Voth, P. Salvador, J. J. Dannenberg, S. Dapprich, A. D. Daniels, O. Farkas, J. B. Foresman, J. V. Ortiz, J. Cioslowski, D. J. Fox, Gaussian, Inc., Wallingford CT, **2009**.

25) a) A. D. Becke, *J. Chem. Phys*. **1993**, *98*, 5648–5652; b) C. Lee, W. Yang, R. G. Parr, *Phys. Rev*. **1988**, *B37*, 785–789.

26) *Material Studio 5.5*, Accerlys Inc. San Diego, **2010**.

27) J. J. P. Stewart, *J. Mol. Model*. **2007**, *13*, 1173–1213.

28) a) M. J. Kamlet, S. J. Jacobs, *J. Chem. Phys*. **1968**, *48*, 23; b) M. J. Kamlet, J. E. Ablard, *J. Chem. Phys*. **1968**, *48*, 36.

29) V. R. Kamalraj, S. Senthil, P. Kannan, *J. Mol. Struct.* **2008**, *892*, 210–215.

30) a) Mei Xu, C. Kuang, Z. Wang, Q. Yang, Y. Jiang, *Synthesis.* **2011**, *2*, 223–228; b) Y. Jiang, C. Kuang, Q. Yang, *Synlett.* **2009**, *19*, 3163–3166.

31) L. Harmand, M. H. Lescure, N. Candelon, M. Duttine, D. Lastecoueres, J. M. Vincent, *Tetrahedron Lett*. **2012**, *53*, 1417–1420.

32) C. Pardo, S. Graf, M. Ramos, E. Sesmilo, J. Elguero, *Synthesis*. **2000**, *32*, 385–390.

33) a) W. Richard, U.S. 4227004, **1980**; b) B. Stephandr, K. Gerf, S. Thomas, P. Arnold, N. Rainer, R. Juergen, S. Gert, DE4303657, **1994**, c) A. Miller, ZA7606188, **1977**.

34) a),S. G. Hansen, H. H. Jensen, *Synlett.* **2009**, *20*, 3275–3278, b) Burri, F. Kaspar, *Helv. Chim. Acta*. **1989**, *72*, 1416–1427.

35) H. Hedeki, T. Shinji, A. Kyoji, JP01143861, **1989**.

36) J. T. Fletcher, S. E. Walz, M. E. Keeney, *Tetrahedron Lett*. **2008**, *49*, 7030–7032.

37) S. G. Hansen, H. H. Jensen, *Synlett*. **2009**, *20*, 3275–3278.

38) L. Di Nunno, A. Scilimati, *Tetrahedron*. **1986**, *42***,** 3913–3920.

39) a) B. C. Jeffrey, M. Ripudaman, D. Allen, *Synthesis*. **2004**, *4*, 499–500, b) W. B. Yi, C. Cai, *J. Energ. Mater*. **2007**, *25*, 129–139.

40) a) K. S. Rao, F. Yehya, A. K. Chaudhary, A. S. Kumar and A. K. Sahoo, *J. Analytical and Applied pyrolysis* **2014,** *109*, 132–139; b) K. S. Rao, A. K. Chaudhary, F. Yehya, A. S. Kumar, *Spectrochim. Acta A*, **2015**, *147*, 316-323.

41) EXPLO5 *version*6.02, M. Suceska, **2014**.

2.11. Spectra

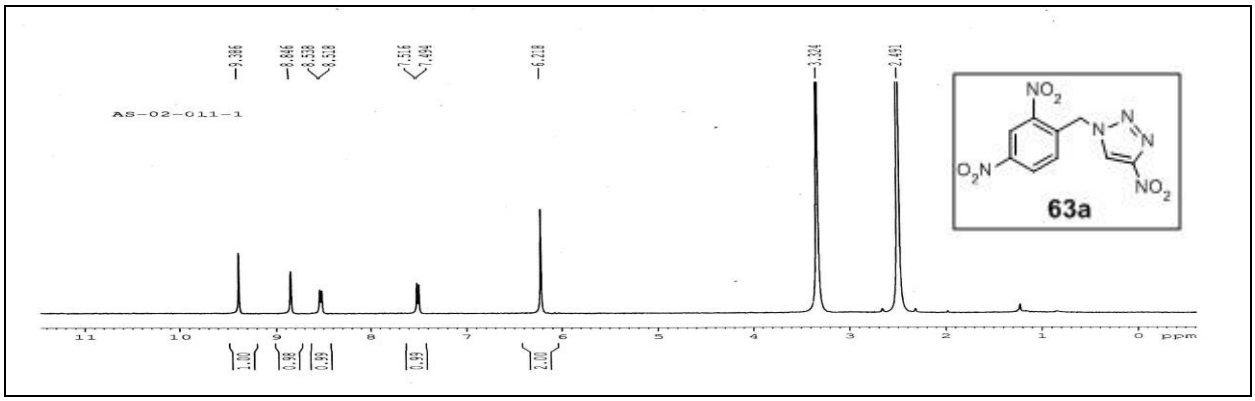
AS-02-011-1
63a

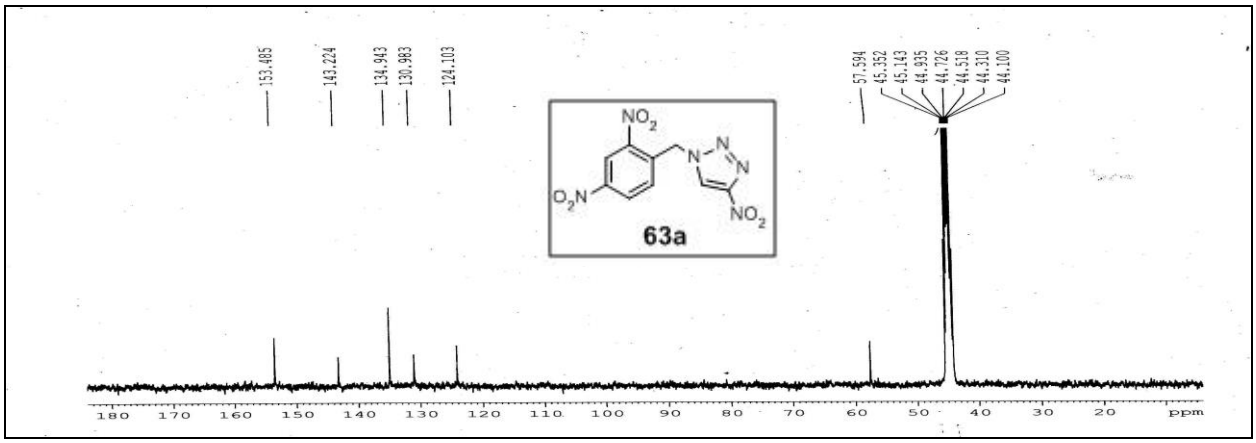
63a

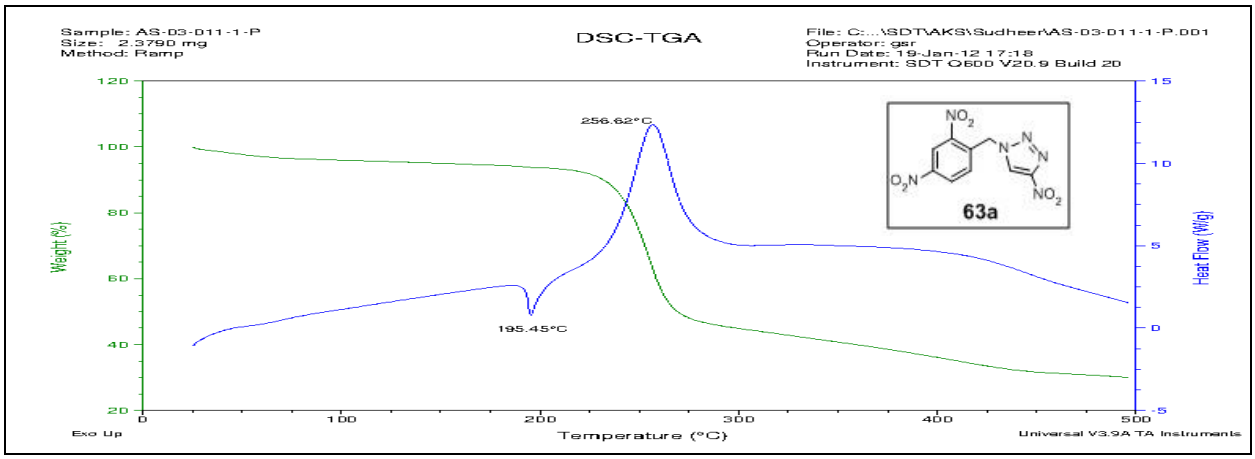
Sample: AS-03-011-1-P
Size: 2.3790 mg
Method: Ramp
DSC-TGA
File: C:...\SDT\AKS\Sudheer\AS-03-011-1-P.001
Operator: gsr
Run Date: 19-Jan-12 17:18
Instrument: SDT Q600 V20.9 Build 20
256.62°C
195.45°C
63a
Weight (%)
Heat Flow (W/g)
Temperature (°C)
Exo Up
Universal V3.9A TA Instruments

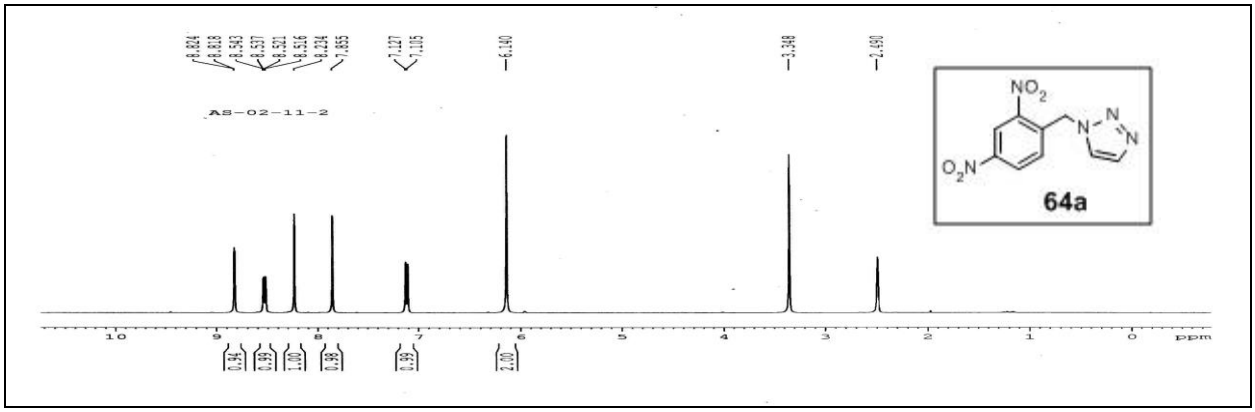
AS-02-11-2
64a

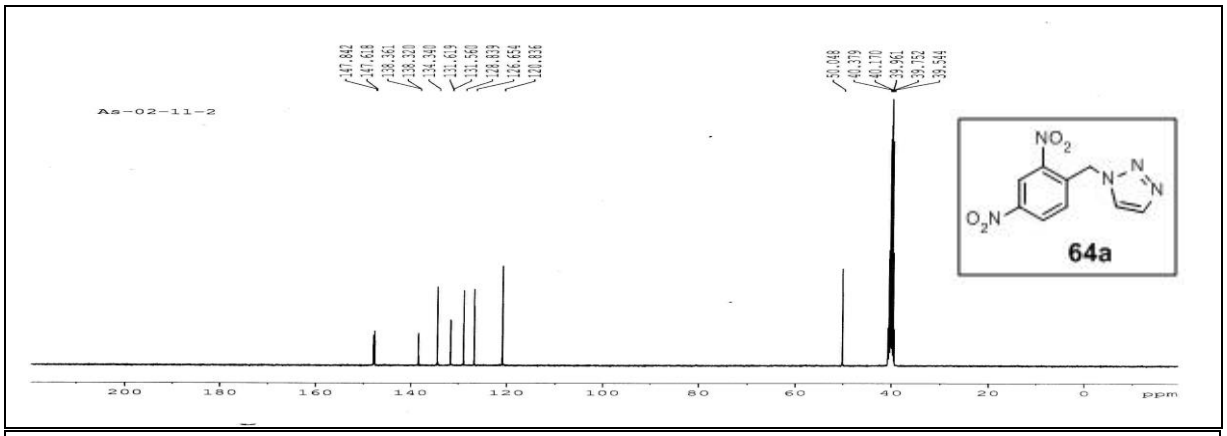
As-02-11-2
147.842
147.618
138.361
138.320
134.348
131.619
131.560
128.839
126.654
120.836
50.048
40.379
40.170
39.961
39.752
39.544
NO_2
O_2N
64a
200
180
160
140
120
100
80
60
40
20
0
ppm

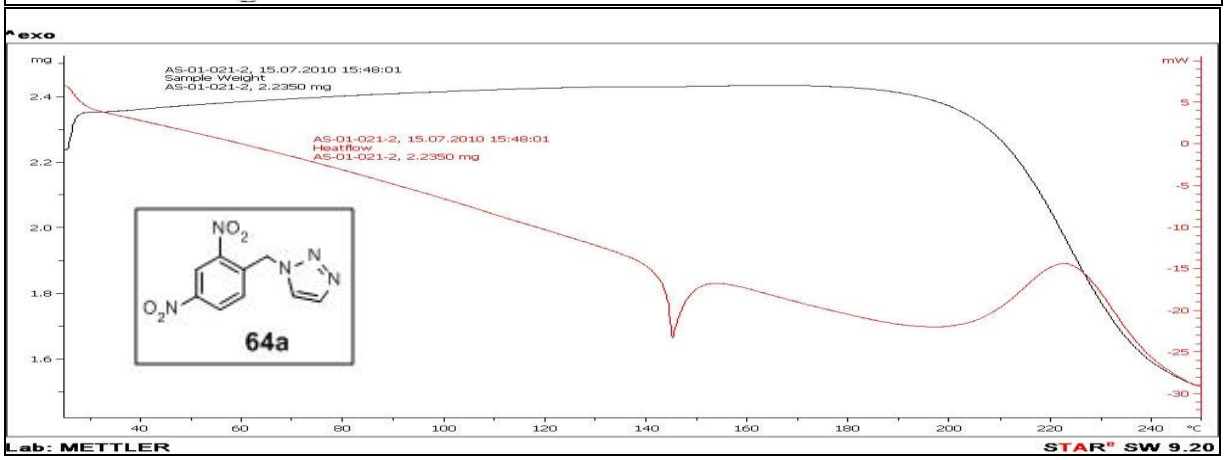
exo
mg
AS-01-021-2, 15.07.2010 15:48:01
Sample Weight
AS-01-021-2, 2.2350 mg
AS-01-021-2, 15.07.2010 15:48:01
Heatflow
AS-01-021-2, 2.2350 mg
mW
NO_2
O_2N
64a
40
60
80
100
120
140
160
180
200
220
240
°C
Lab: METTLER
STARe SW 9.20

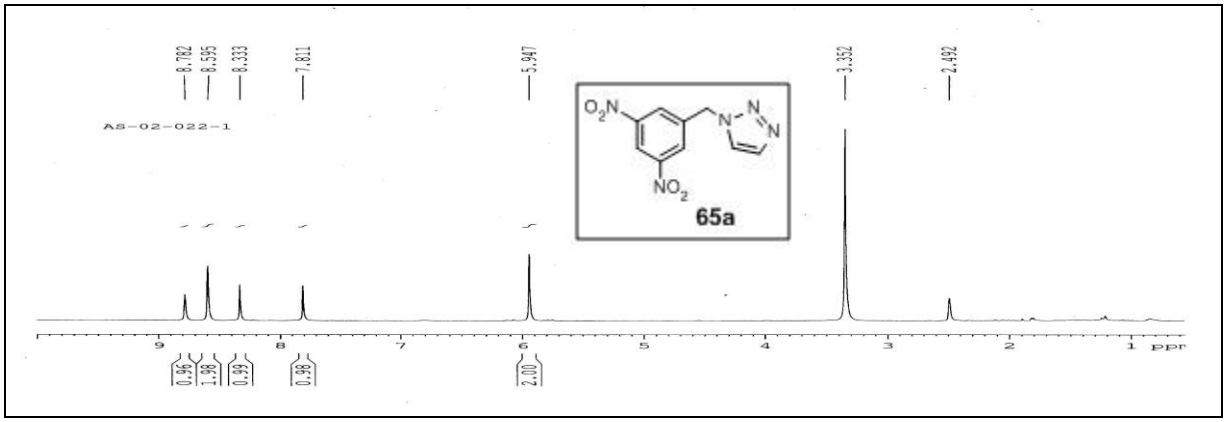
AS-02-022-1
8.782
8.595
8.333
7.811
5.947
3.352
2.492
O_2N
NO_2
65a
9
8
7
6
5
4
3
2
1
ppm
0.96
1.98
0.99
0.98
2.00

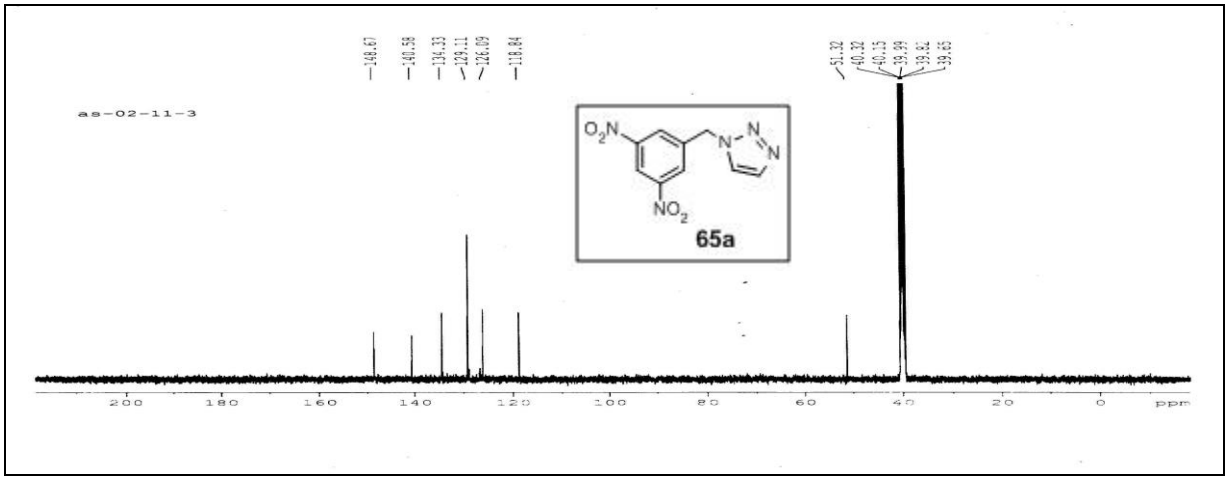
as-02-11-3
148.67
140.58
134.33
129.11
126.09
118.84
51.32
40.32
40.15
39.99
39.82
39.65
O_2N
NO_2
65a
200
180
160
140
120
100
80
60
40
20
0
ppm

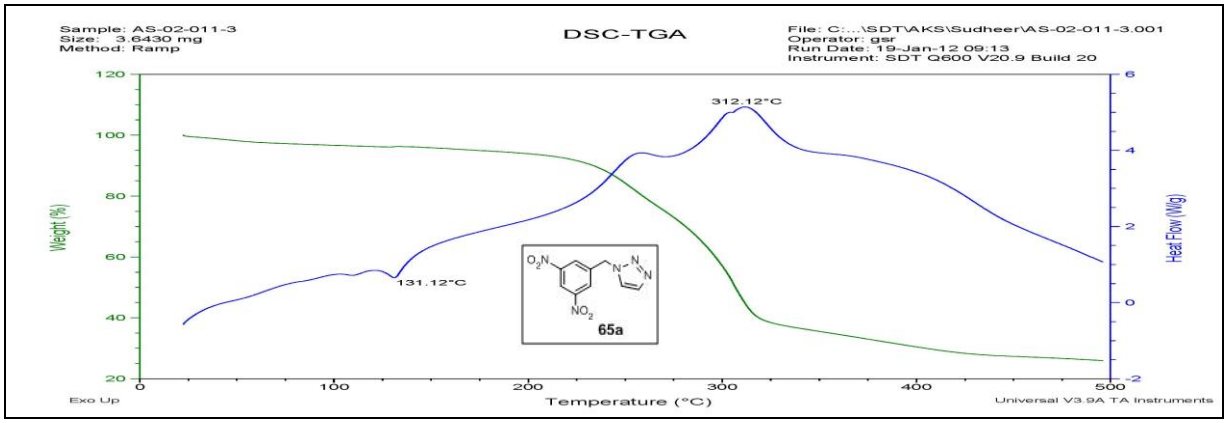
Sample: AS-02-011-3
Size: 3.6430 mg
Method: Ramp
DSC-TGA
File: C:...\SDT\AKS\Sudheer\AS-02-011-3.001
Operator: gsr
Run Date: 19-Jan-12 09:13
Instrument: SDT Q600 V20.9 Build 20
312.12°C
131.12°C
65a
Weight (%)
Heat Flow (W/g)
Temperature (°C)
Exo Up
Universal V3.9A TA Instruments

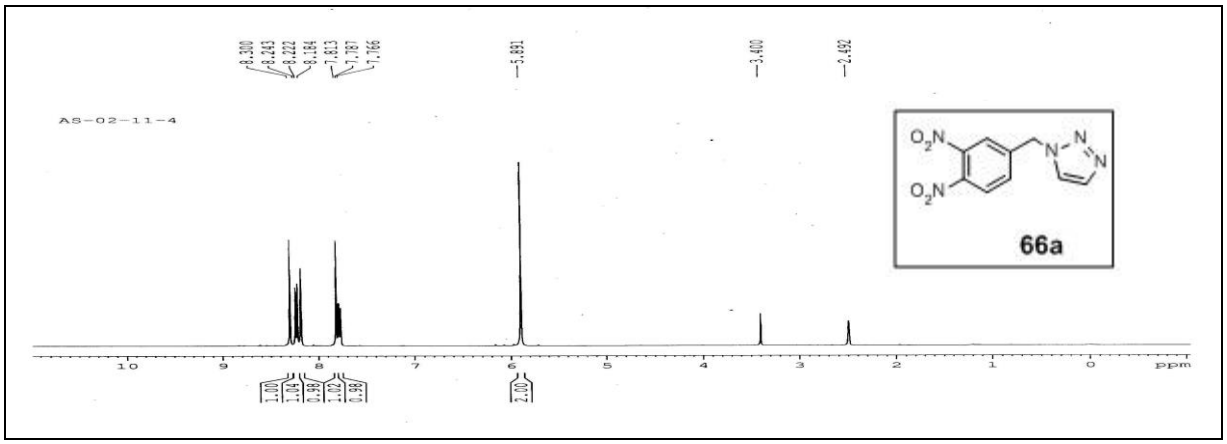
AS-02-11-4
66a
ppm

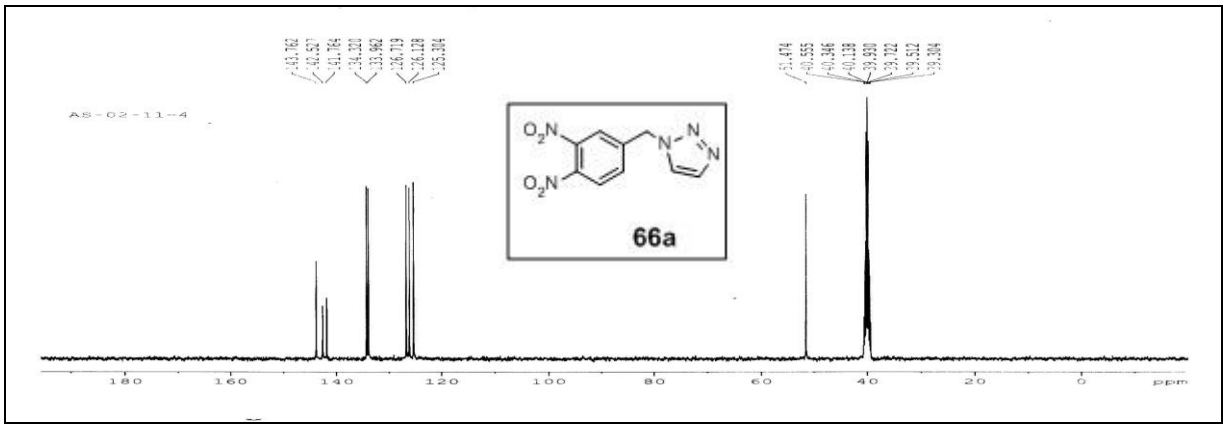
AS-02-11-4
66a
ppm

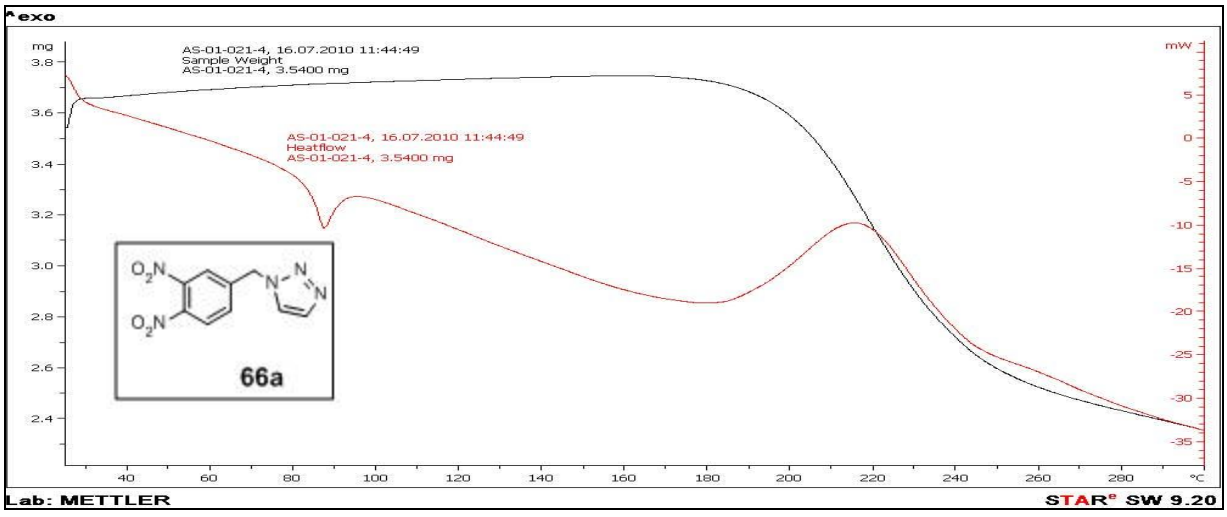
exo
AS-01-021-4, 16.07.2010 11:44:49
Sample Weight
AS-01-021-4, 3.5400 mg
AS-01-021-4, 16.07.2010 11:44:49
Heatflow
AS-01-021-4, 3.5400 mg
66a
mg
mW
°C
Lab: METTLER
STARe SW 9.20

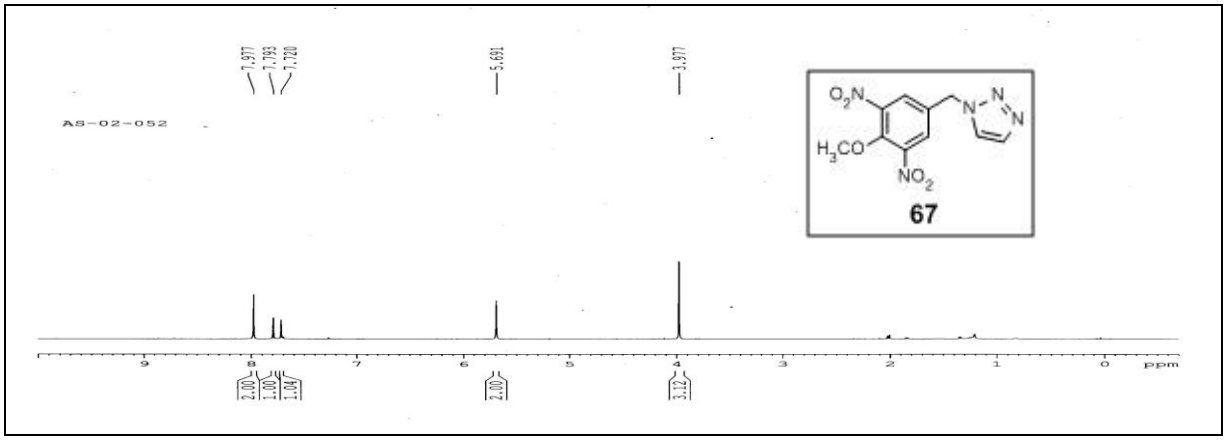
AS-02-052
7.977
7.793
7.720
5.691
3.977
67
ppm

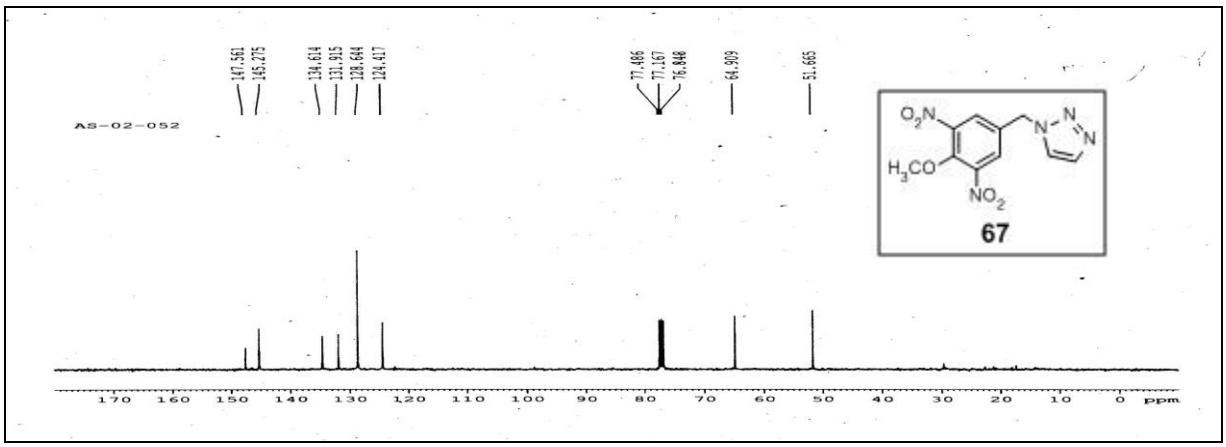
AS-02-052
147.561
145.275
134.614
131.915
128.644
124.417
77.486
77.167
76.848
64.909
51.665
67
ppm

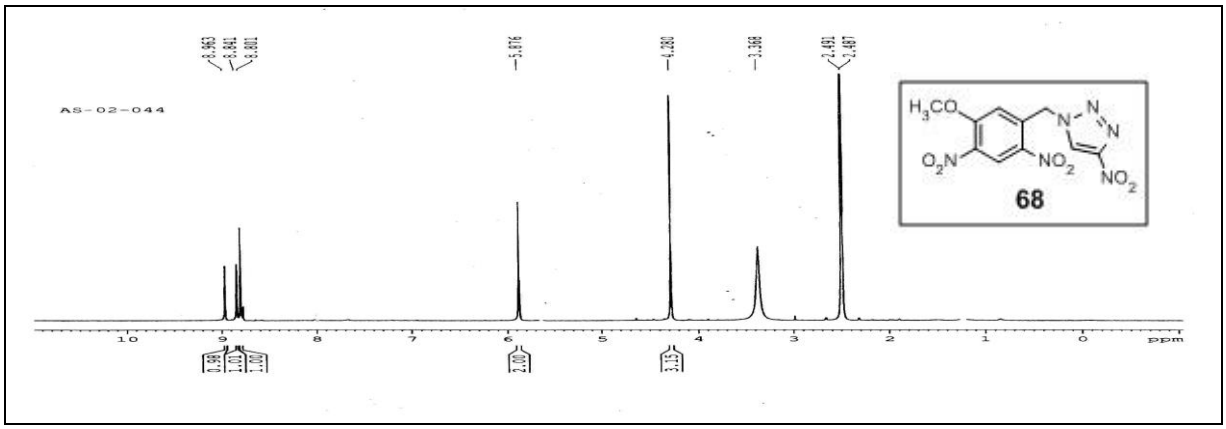
AS-02-044
8.963
8.841
8.801
5.676
4.280
3.368
2.491
2.487
68
ppm

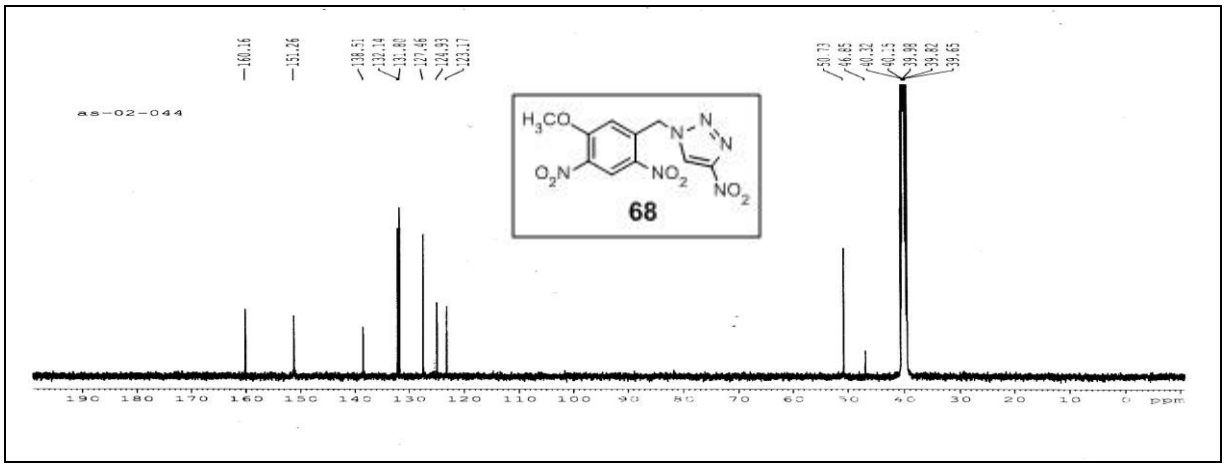
as-02-044
160.16
151.26
138.51
132.14
131.80
127.46
124.93
123.17
50.73
46.85
40.32
40.15
39.98
39.82
39.65
68
ppm

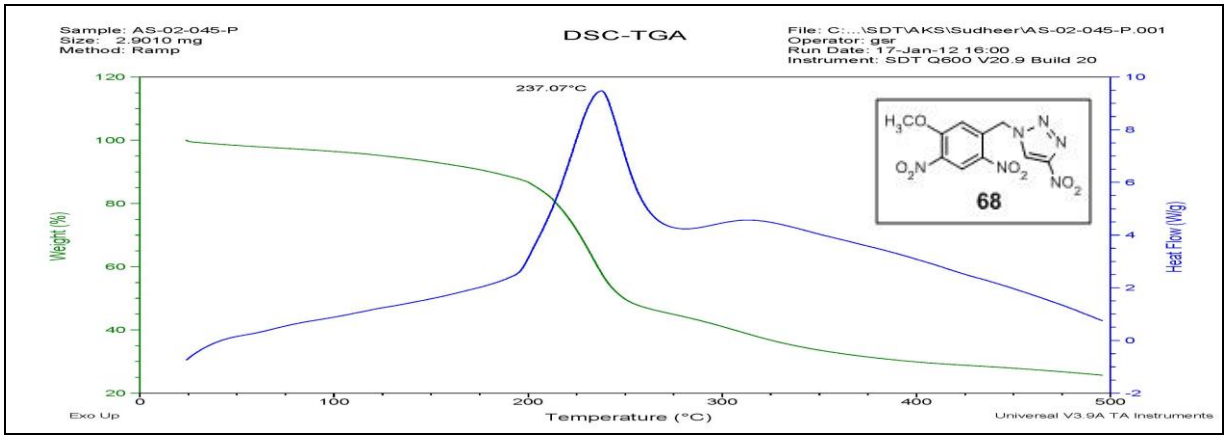
Sample: AS-02-045-P
Size: 2.9010 mg
Method: Ramp
DSC-TGA
File: C:...\SDT\AKS\Sudheer\AS-02-045-P.001
Operator: gsr
Run Date: 17-Jan-12 16:00
Instrument: SDT Q600 V20.9 Build 20
237.07°C
68
Weight (%)
Heat Flow (W/g)
Temperature (°C)
Exo Up
Universal V3.9A TA Instruments

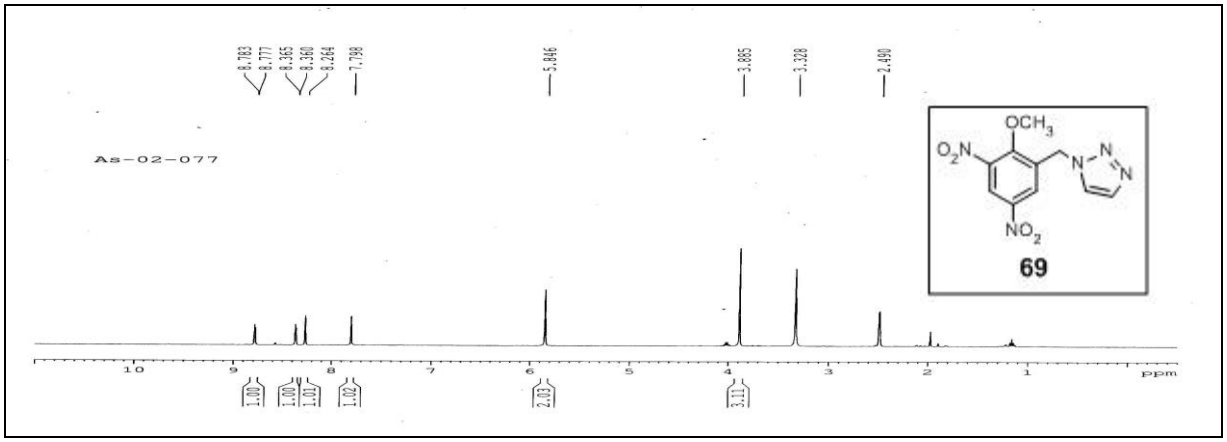
As-02-077
69
ppm

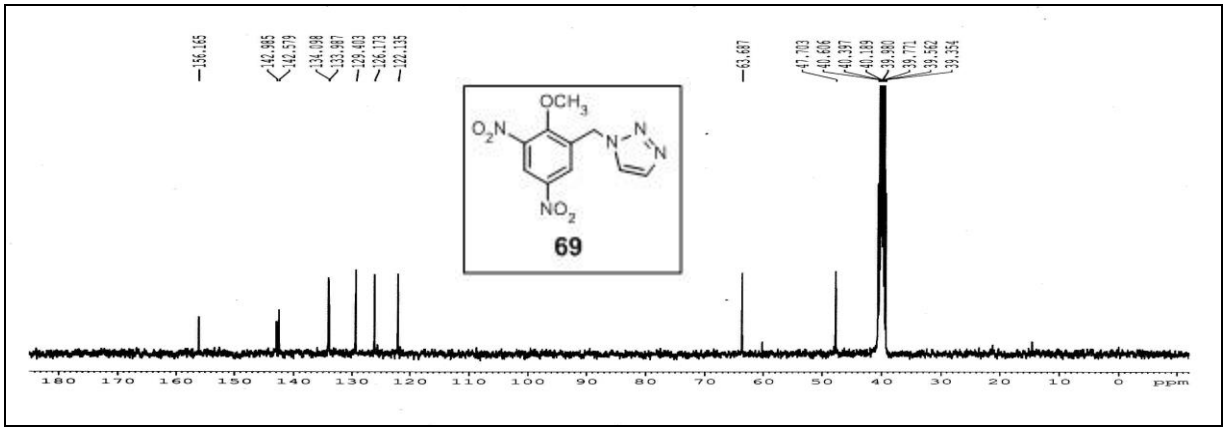
69
ppm

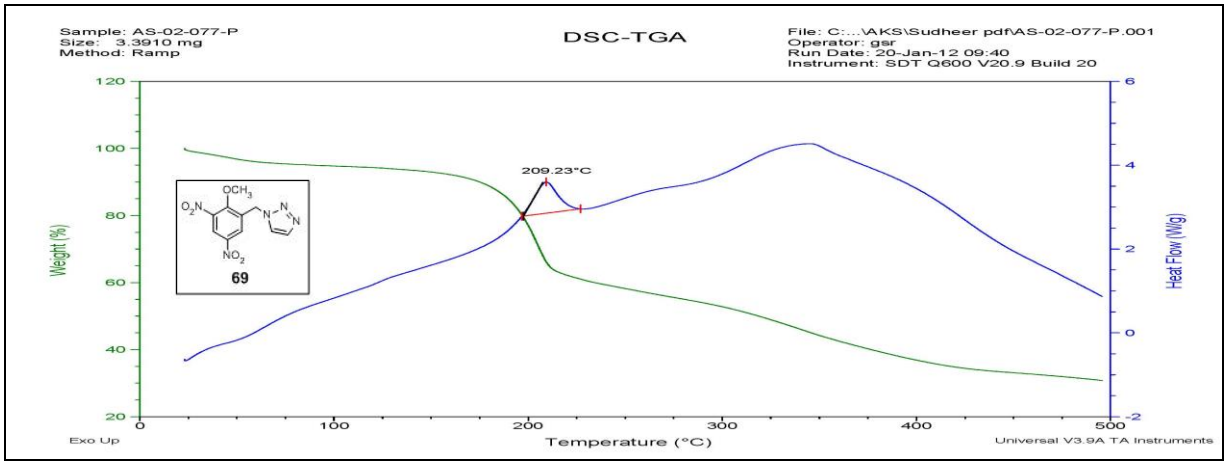
Sample: AS-02-077-P
Size: 3.3910 mg
Method: Ramp
DSC-TGA
File: C:...\AKS\Sudheer pdf\AS-02-077-P.001
Operator: gsr
Run Date: 20-Jan-12 09:40
Instrument: SDT Q600 V20.9 Build 20
209.23°C
69
Weight (%)
Heat Flow (W/g)
Temperature (°C)
Exo Up
Universal V3.9A TA Instruments

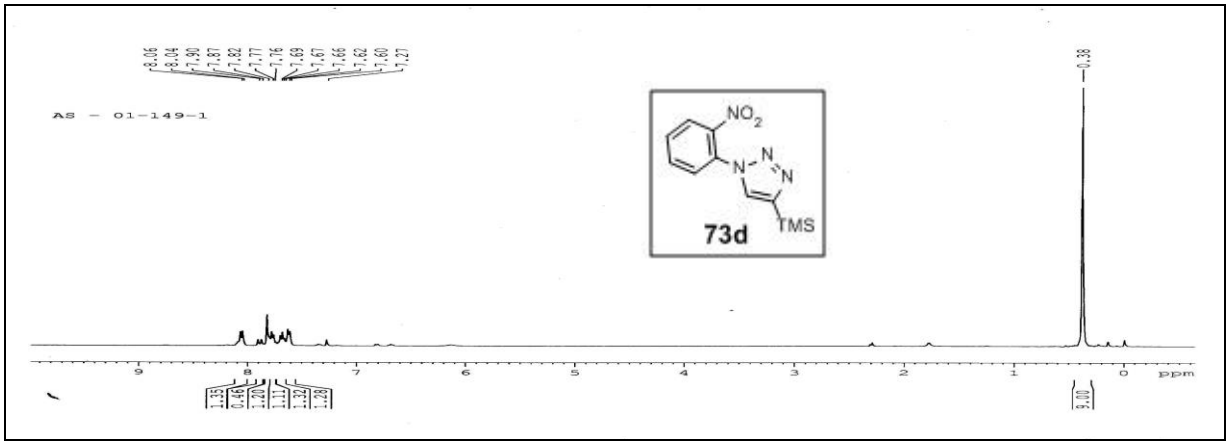
AS - 01-149-1
73d
TMS
ppm

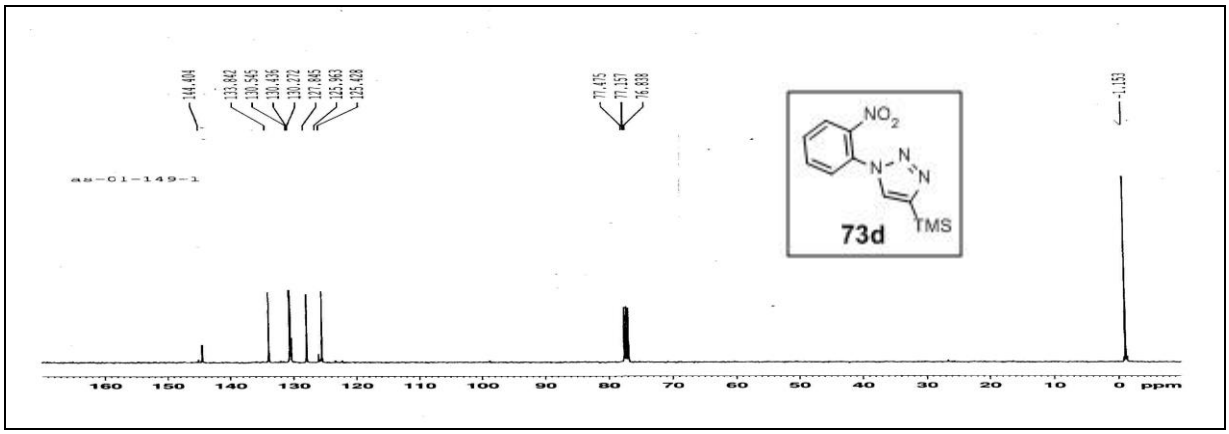
as-01-149-1
73d
TMS
ppm

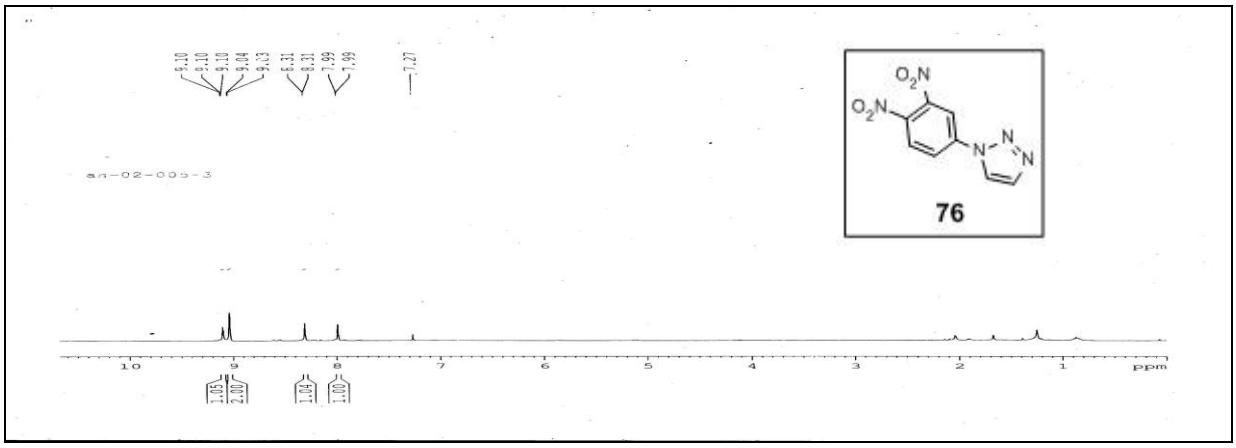
as-02-005-3
76
ppm

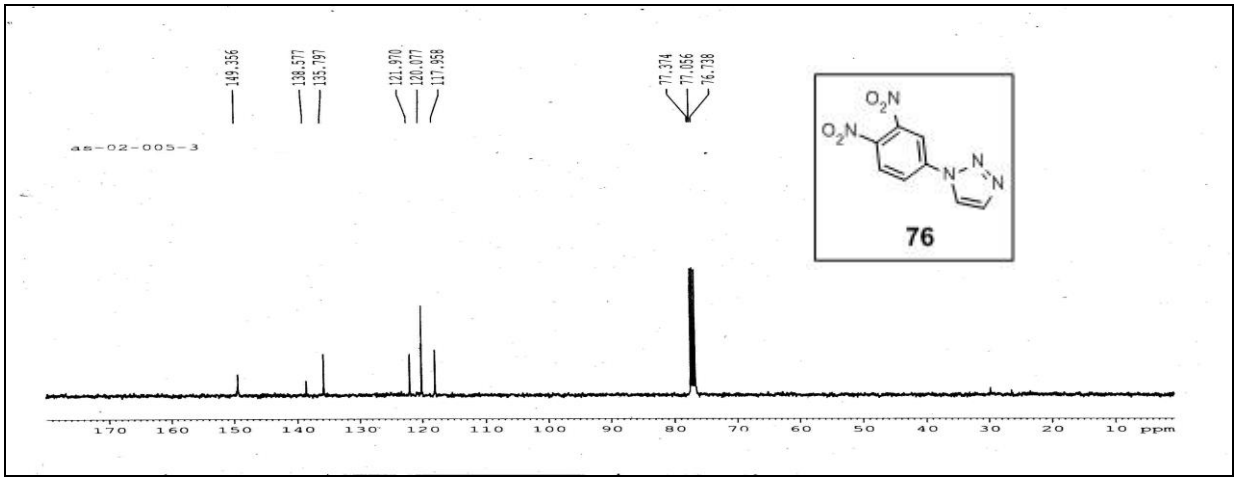
as-02-005-3
76
ppm

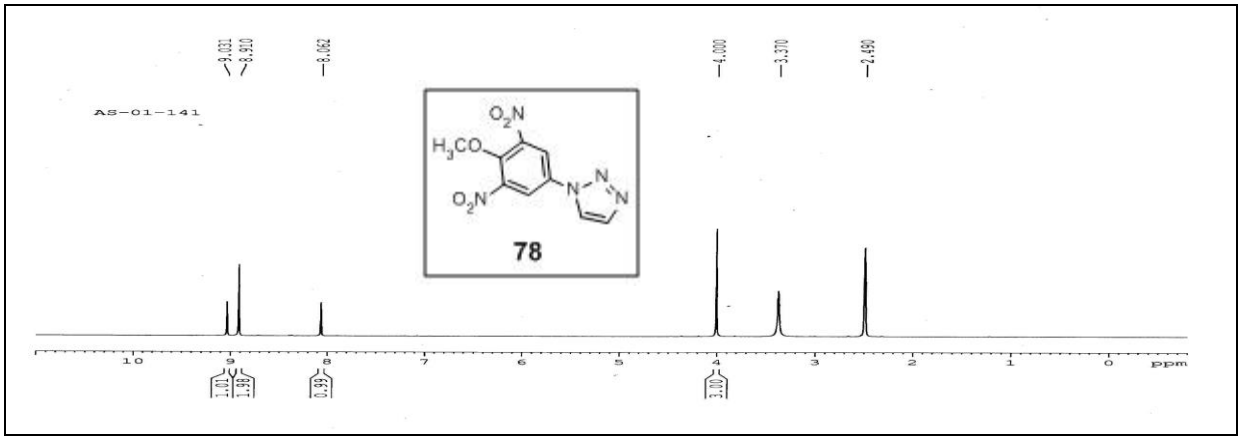
AS-01-141
9.031
8.810
8.062
4.000
3.370
2.490
78
ppm

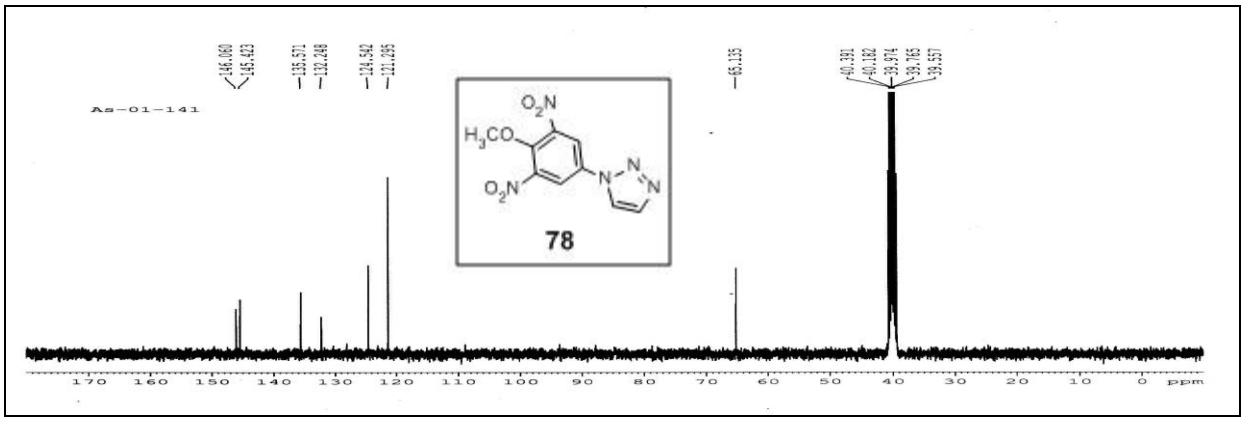
As-01-141
146.060
145.423
135.571
132.248
124.542
121.265
65.135
40.391
40.182
39.974
39.765
39.557
78
ppm

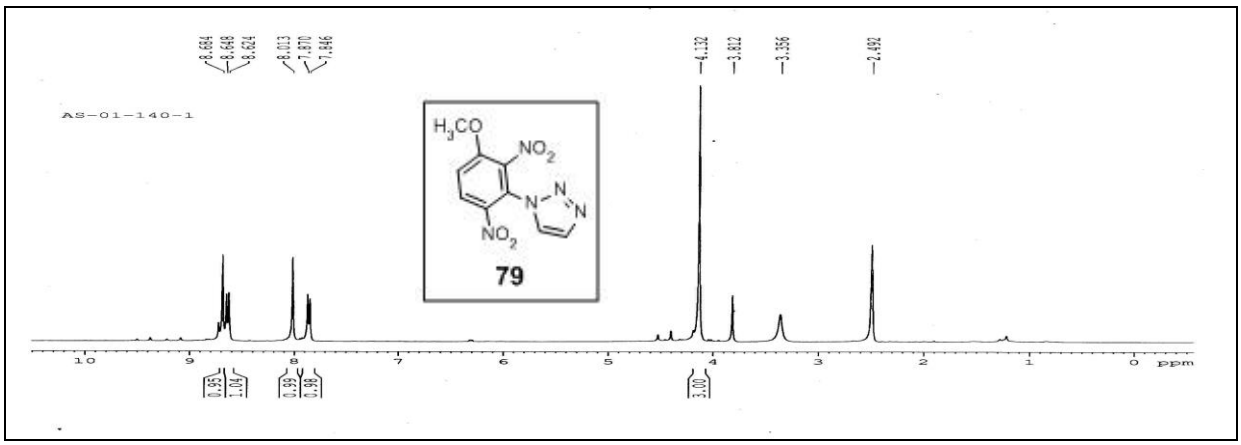
AS-01-140-1
8.684
8.648
8.624
8.013
7.870
7.846
4.132
3.812
3.356
2.492
79
ppm

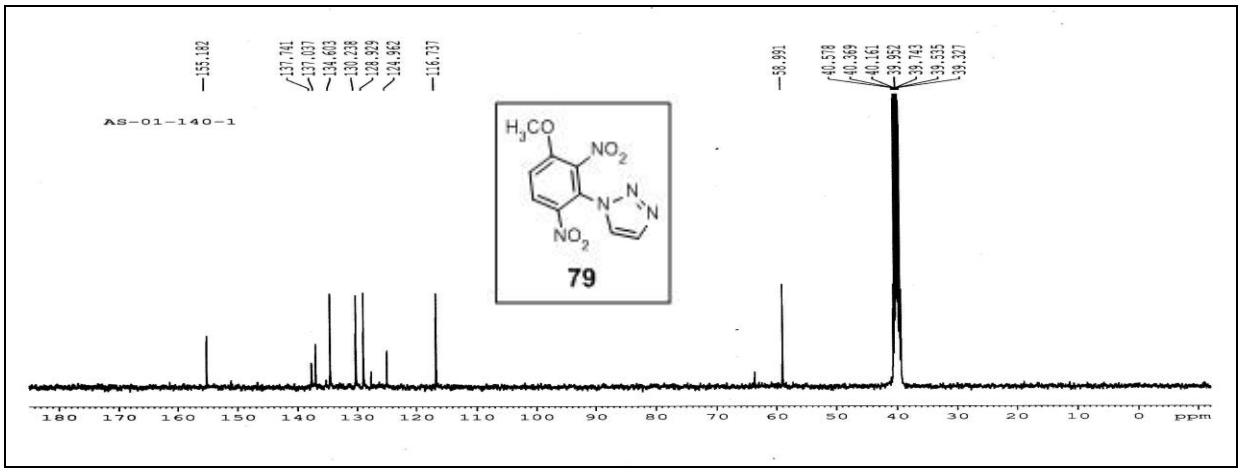
AS-01-140-1
155.182
137.741
137.037
134.603
130.238
128.929
124.962
116.737
58.991
40.578
40.369
40.161
39.952
39.743
39.535
39.327
79
ppm

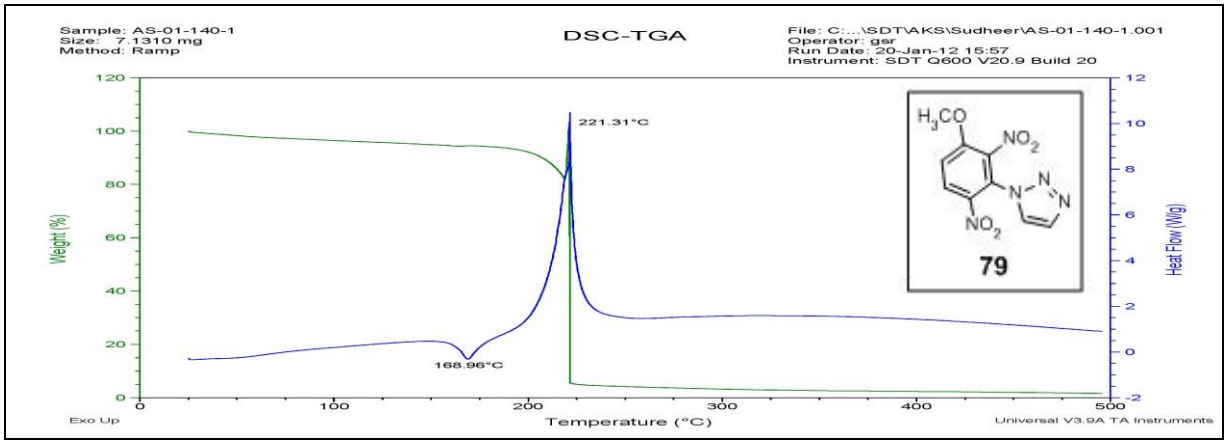
Sample: AS-01-140-1
Size: 7.1310 mg
Method: Ramp
DSC-TGA
File: C:...\SDT\AKS\Sudheer\AS-01-140-1.001
Operator: gsr
Run Date: 20-Jan-12 15:57
Instrument: SDT Q600 V20.9 Build 20
221.31°C
168.96°C
Weight (%)
Heat Flow (W/g)
Temperature (°C)
Exo Up
Universal V3.9A TA Instruments
79

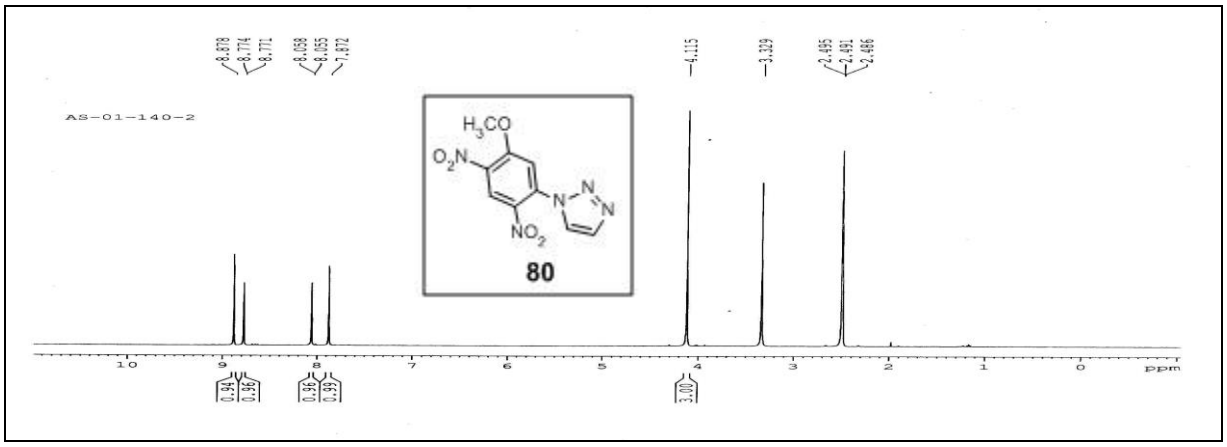
AS-01-140-2
80
ppm

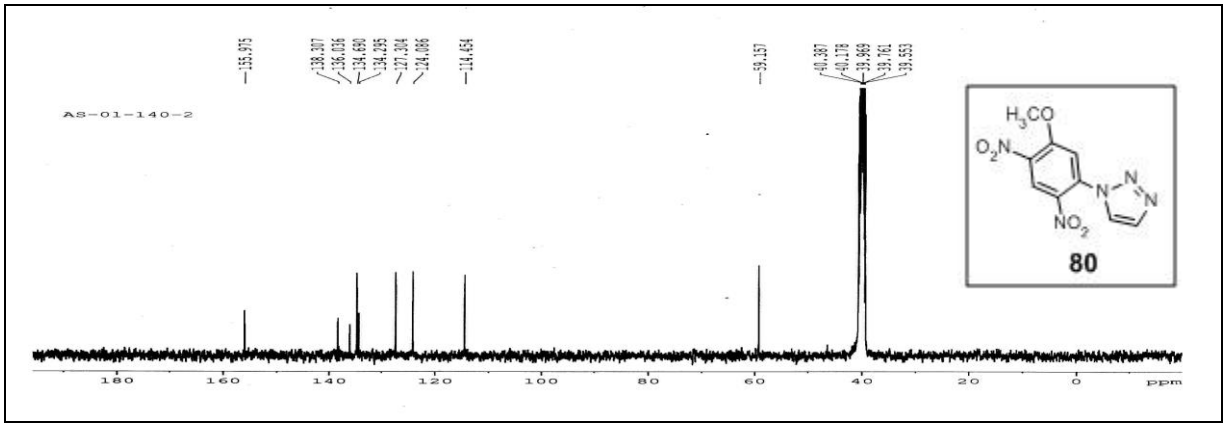
AS-01-140-2
80
ppm

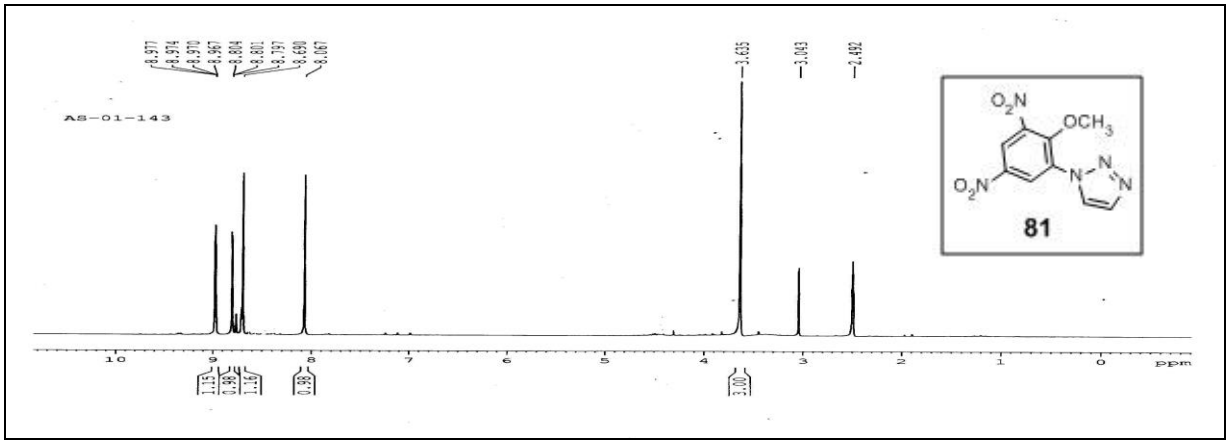
AS-01-143
81
ppm

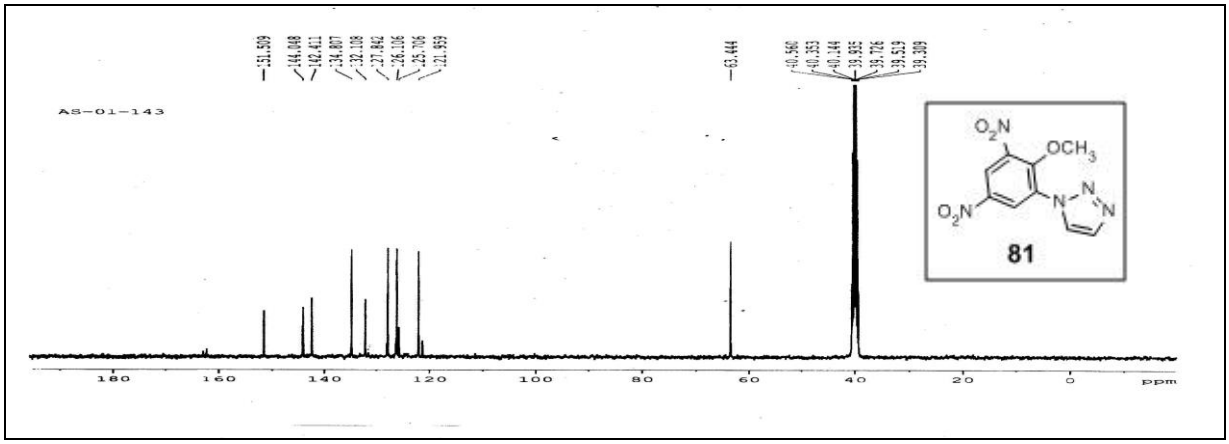
AS-01-143
81

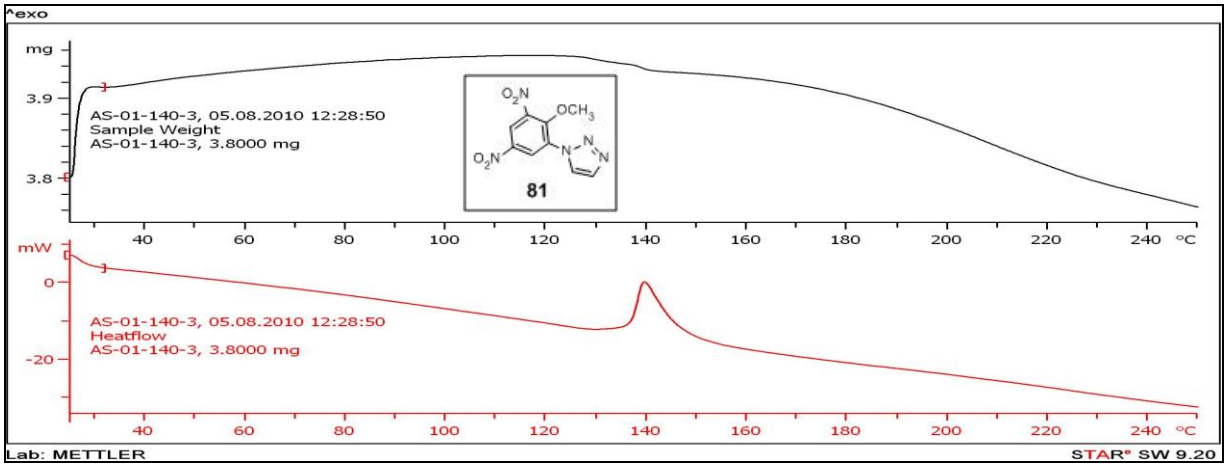
^exo
mg
AS-01-140-3, 05.08.2010 12:28:50
Sample Weight
AS-01-140-3, 3.8000 mg
81
mW
AS-01-140-3, 05.08.2010 12:28:50
Heatflow
AS-01-140-3, 3.8000 mg
°C
Lab: METTLER
STARe SW 9.20

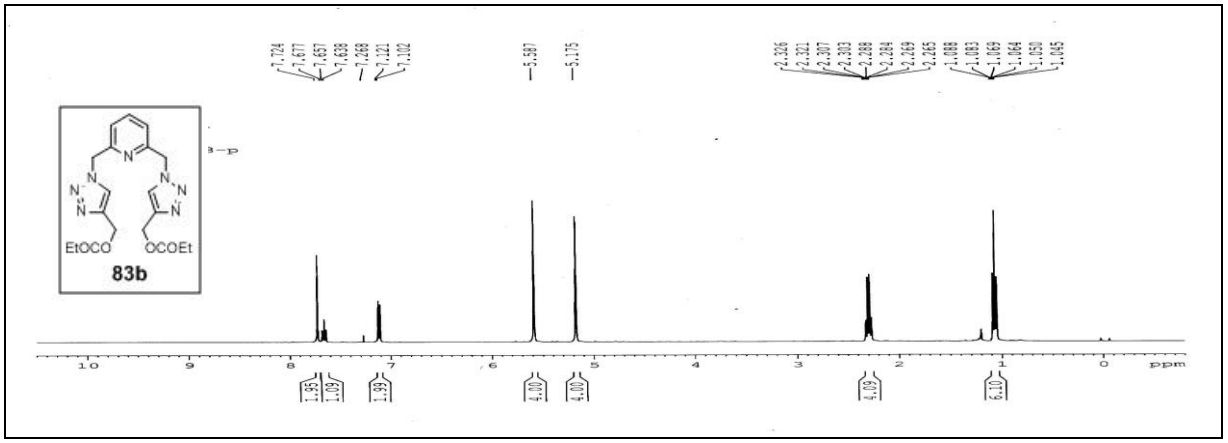
83b
ppm

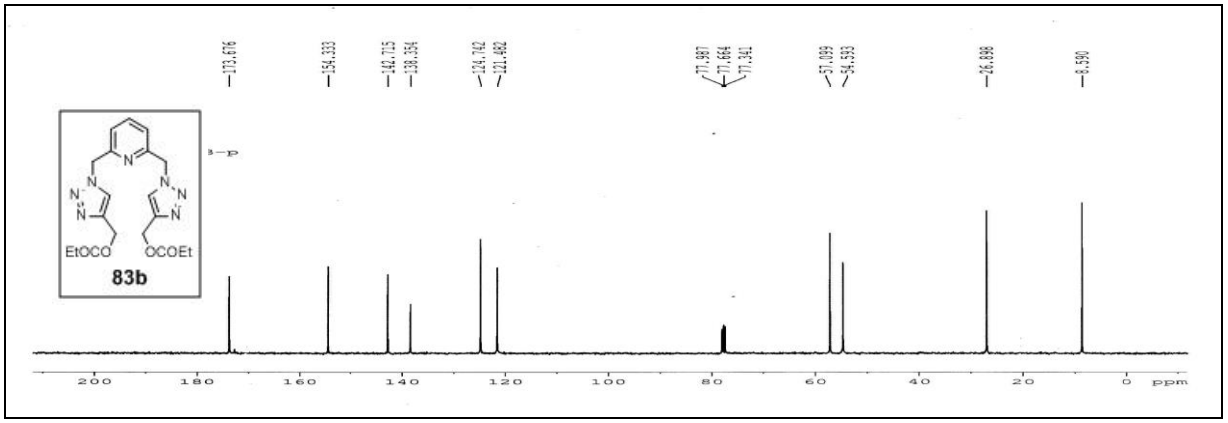
83b
ppm

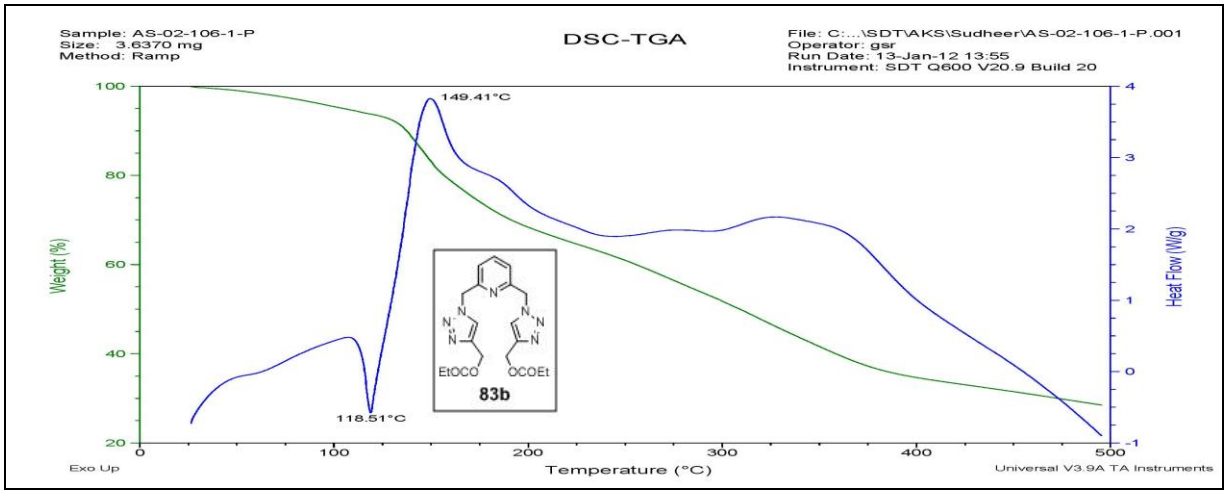
Sample: AS-02-106-1-P
Size: 3.6370 mg
Method: Ramp
DSC-TGA
File: C:...\SDT\AKS\Sudheer\AS-02-106-1-P.001
Operator: gsr
Run Date: 13-Jan-12 13:55
Instrument: SDT Q600 V20.9 Build 20
149.41°C
118.51°C
Weight (%)
Heat Flow (W/g)
Temperature (°C)
Exo Up
Universal V3.9A TA Instruments
EtOCO
OCOEt
83b

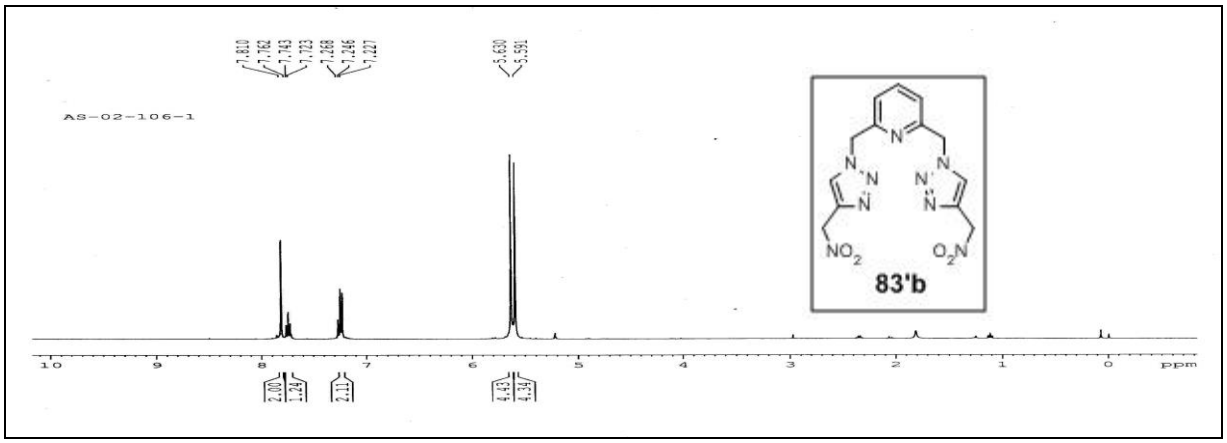
AS-02-106-1
7.810
7.762
7.743
7.723
7.268
7.246
7.227
5.630
5.591
2.00
1.24
2.11
4.43
4.34
ppm
NO2
O2N
83'b

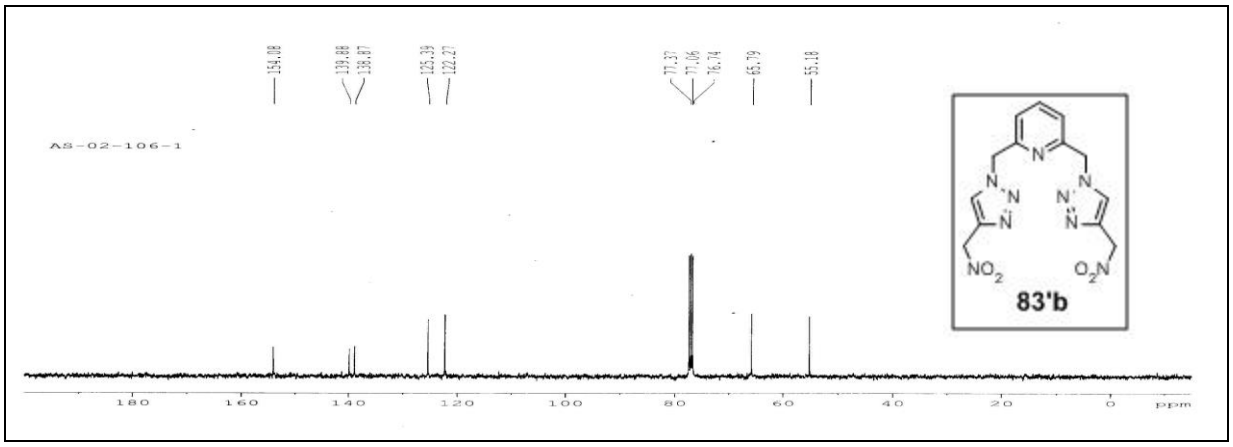
AS-02-106-1
154.08
139.88
138.87
125.39
122.27
77.37
77.06
76.74
65.79
55.18
ppm
NO2
O2N
83'b

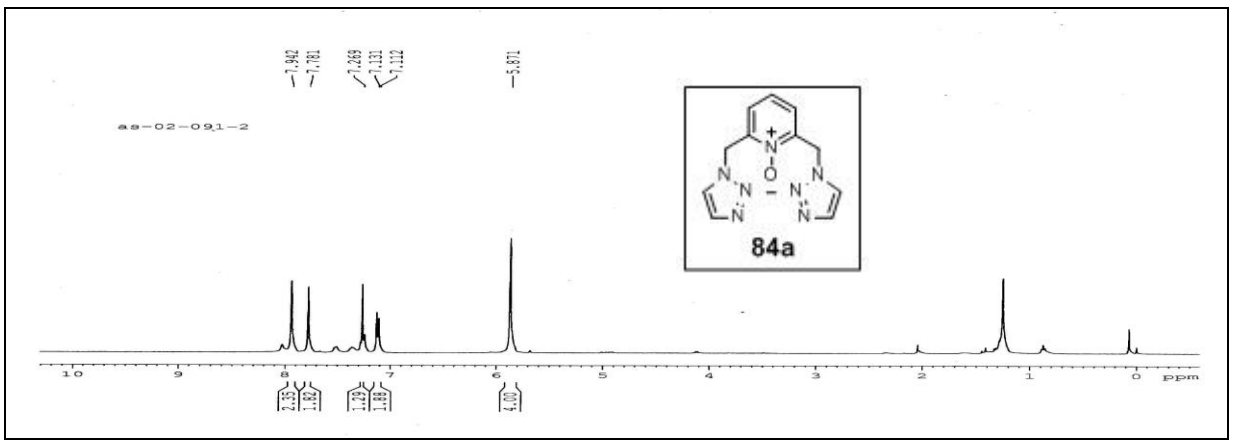
as-02-091-2
7.942
7.781
7.269
7.131
7.112
5.871
2.35
1.82
1.29
1.08
4.00
ppm
84a

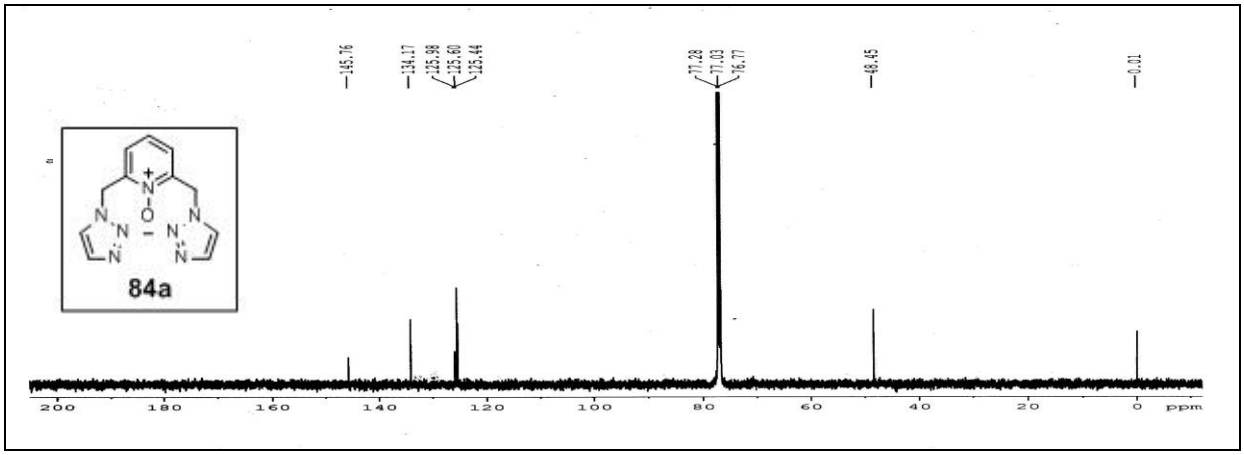
145.76
134.17
125.98
125.60
125.44
77.28
77.03
76.77
48.45
0.01
84a
200
180
160
140
120
100
80
60
40
20
0
ppm

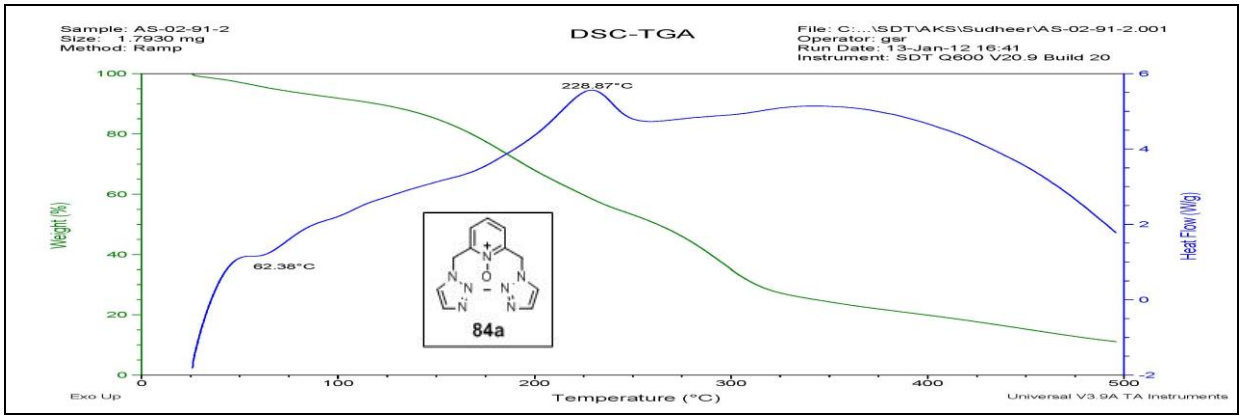
Sample: AS-02-91-2
Size: 1.7930 mg
Method: Ramp
DSC-TGA
File: C:...\SDT\AKS\Sudheer\AS-02-91-2.001
Operator: gsr
Run Date: 13-Jan-12 16:41
Instrument: SDT Q600 V20.9 Build 20
228.87°C
62.38°C
84a
Weight (%)
Heat Flow (W/g)
Temperature (°C)
Exo Up
Universal V3.9A TA Instruments

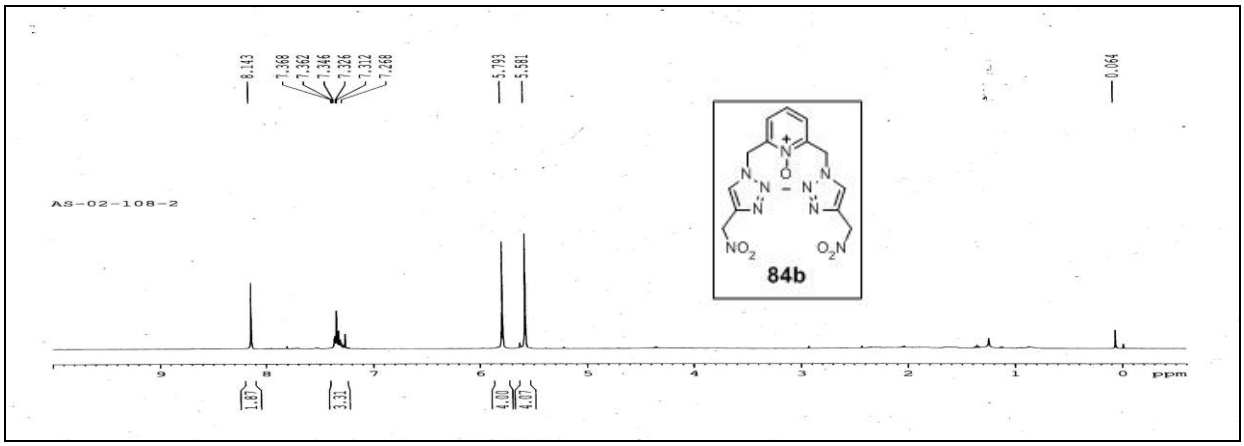
8.143
7.368
7.362
7.346
7.326
7.312
7.268
5.793
5.581
0.064
AS-02-108-2
84b
1.87
3.31
4.00
4.07
ppm

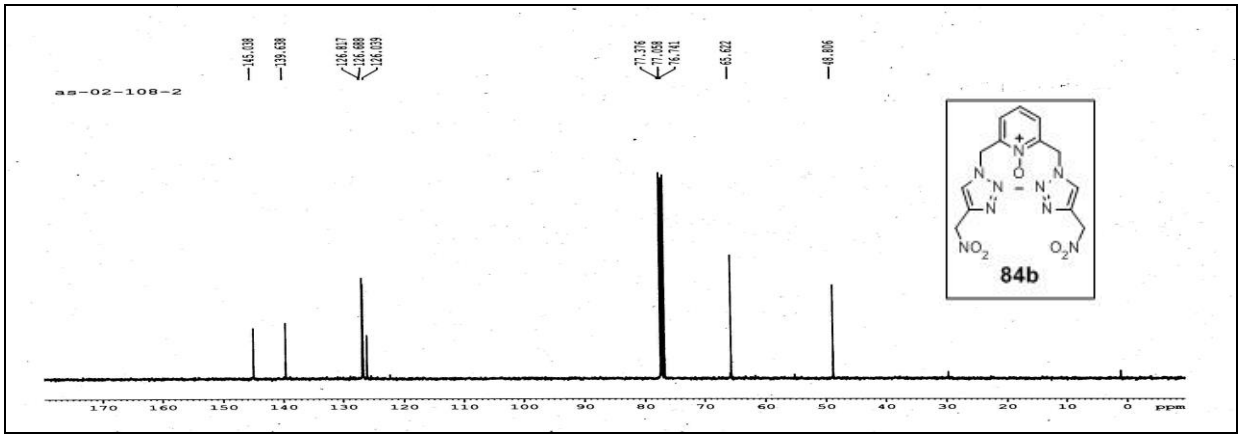
145.038
139.638
126.817
126.688
126.039
77.376
77.059
76.741
65.622
48.806
as-02-108-2
84b
ppm

2.12. Applications

Thermal stabilites of the above synthesized triazole derivatives are determined by DSC–TGA measurements and exhibits high thermally stability. We cross verified the thermal stability and decomposition of some of our synthesized 1,2,3-triazoles (**64a**, **65a**, **67, 69** and **78**) by using the photoacoustic (PA) technique employed with 532 nm and 266 nm wavelengths, respectively. The study mainly focused on freely released NO_2 molecules along with other byproducts during the pyrolysis between 30-350 ^{o}C. The photoacoustic (PA) experimental results clearly demonstrated that the synthesized triazole derivatives are thermally stable.[40]

Chapter 3

Synthesis of Trifluoromethyl-Substituted *N*-Aryl-Poly-1,2,3-Triazole Derivatives

Abstract

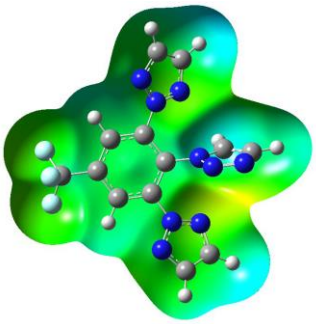

Synthesis, characterization, and energetic properties of $–CF_3$ and $–NO_2$ substituted *N*-aryl-polytriazole derivatives are reported. The molecules are prepared by a reliable Cu-catalyzed [3+2]-cycloaddition between $–CF_3$ substituted aryl azides and alkynes followed by a nitration sequence and also the base promoted nucleophilic displacement of the halo groups by the 1,2,3-triazoles. The compounds are characterized by analytical and spectroscopic methods; the solid state structures of some of the compounds are confirmed by X-ray diffraction techniques. The synthesized materials decompose in the range of 195–308 ^{o}C. Most of the $–CF_3$ and $–NO_2$ groups-bearing aryl triazoles exhibit good densities and acceptable detonation characteristics. Some of the fluorine containing polytriazole-bearing compounds showed positive heats of formation.

Reference:

A. Sudheer Kumar, Nagarjuna Kommu, Vikas D. Ghule and Akhila K. Sahoo*
J. Mater. Chem. A., **2014**, *2*, 7917–7926

3.1. Introduction

Fluorine is the strongest oxidizer; it oxidizes materials even more exothermically than oxygen does. As fluorine is the most electronegative element and can easily accept electron, consequently it oxidises other elements without being oxidised itself. Furthermore, fluorine liberated during the detonation process has a higher tendency to react with hydrogen than oxygen.[1,2] In addition, fluorine produces lot of heat during the formation of hydrated ion. Moreover, the presence of fluorine atom enhances density of a molecule due to its high molecular weight than oxygen. Thus, fluorinated nitroarene-rich molecules are useful in high-energy applications.[2] Owing to the broad utility of energetic materials, continuous demand always remains for the development of robust organic energetic compounds with enhanced thermal stability and reduced sensitivity.[3] In general, the aromatic triazole moiety enhances positive heat of formation (HOF) and thermal stability of a molecule and reduces its sensitivity due to the N–N and C–N bonds and ring strain.[4] Furthermore, the nitro ($–NO_2$) group significantly contributes towards improving the detonation performance of a molecule.[5] As the fluorine atom assists in the enhancement of the density of the molecule,[1,2] we therefore envisaged the synthesis of novel molecular entities containing the triazole moiety, $–NO_2$ group, and F atoms. Because of the presence of three F atoms in the trifuoromethyl ($–CF_3$) group, it contributes a higher density (2.25 g cm^{-3}) than that of the $–NO_2$ group (2.17 g cm^{-3}).[6] In general, the $–CF_3$ bearing molecules exhibit low surface energy, high chemical resistance, high electronegativity, excellent thermal stability, and hydrophobicity.[7] Moreover, fluorine-containing molecules are used in crystalline materials,[8] polymers[9] organic superconductors, pharmaceutical and agrochemicals.[10] Furthermore, the presence of oxidizer fluorine along with oxygen in the aluminium or boron bearing solid propellants improves metal combustion properties of the material.[10c] Apart from these properties, the high density of trifuoromethyl ($–CF_3$) group makes the compound as efficient energetic oxidizers. Therefore, incorporation of trifluoromethyl group into an organic molecule dramatically changes the energetic properties of the material.[1] Recent reports from the Shreeve group demonstrate the synthesis and energetic properties of $–CF_3$ bearing 1,2,3-triazole derivatives; these molecules are applicable as dense and stable energetic materials.[1,2]

3.1.1. Background of $–CF_3$ substituted-1,2,3-triazole based energetic compounds

In 2007, Shreeve group demonstrated the synthesis of 4-CF_3-1,2,3-triazole molecule (**III**) involving click reaction between gaseous trifluoromethylacetylene (**II**) with

trimethylsilylazide (**I**) (Scheme 3.1)[2a]. The use of gas-reagents makes this synthetic strategy cumbersome. Interestingly, compound **III** exhibits high density (1.79 g cm^{-3}), poor thermal stability (83 °C), negative HOF (–465.22 kJ mol^{-1}) and detonation performance (*vD* = 6518 m s^{-1} & *P* =14.11 GPa) less than TNT.

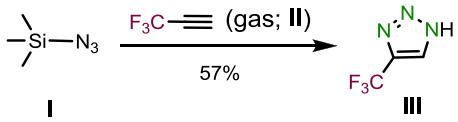

Scheme 3.1. Synthesis of 4-CF_3-1,2,3-triazole by click reaction

Later in 2011, various CF_3-substituted-1,2,3-triazole-containing molecules (C, H, N and F atoms; **Va-d**) having high densities (1.42–1.81 g cm^{-3}), good thermal stabilities (>270 °C), acceptable detonation properties (6180–7244 m s^{-1} & 11.96–17.90 GPa), and negative HOF (–251.5 to –1673.5 kJ mol^{-1}); disappointingly, some of the synthesized compounds are insensitive to impact. The Cu-catalyzed [3+2]-cycloaddition between alkyl azides (**IVa-d**) and gaseous trifluoromethyl acetylene (**II**) provided the desired CF_3-bearing triazole derivatives (**Va-d**) in good yields (Scheme 3.2).[1]

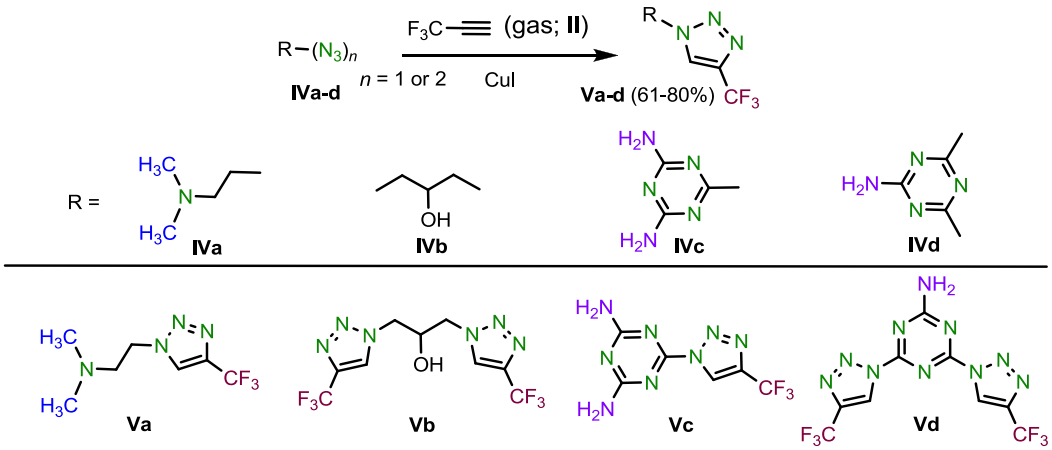

Scheme 3.2. Synthesis of –CF_3-substituted-1,2,3-triazole derivatives

3.1.2. Motivation and Design Plan

The reported CF_3 substitute 1,2,3-triazole derivatives showed good density and detonation performance, however, these molecules exhibited negative heats of formation.[1,2a] Thus, synthesis of –CF_3 and –NO_2 bearing materials with positive heats of formation is a challenging task. The lack of a general strategy for the synthesis of –CF_3, –NO_2, and triazole-containing organic molecules (C, H, N, O, and F atoms), and our recent interest in the development of dense and stable materials that exhibit positive HOFs hence motivated us to

design and synthesis of $–CF_3$ and $–NO_2$/–azido-substituted *N*-aryl-polytriazoles for energetic materials applications. The reliable cost-effective Cu-catalyzed [3+2]-cycloaddition of aryl azides with terminal alkynes and the base promoted couplings of $–CF_3$ substituted aryl halides with 1,2,3-triazole derivatives were used for the synthesis of new $–CF_3$ and $–NO_2$/–azido-substituted *N*-aryl-polytriazoles (Scheme 3.3).

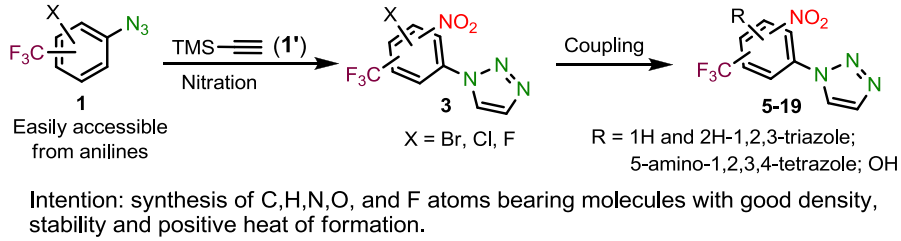

Scheme 3.3. Strategy for $–CF_3$ and $–NO_2$ substituted *N*-aryl/-poly-1,2,3-triazoles

3.2. Results and Discussion

At first, an array of CF_3-substituted-*N*-aryl-triazoles were synthesized involving Cu-catalyzed [3+2]-regioselective cycloaddition between readily accessible CF_3-substituted aryl azides (synthesized from corresponding anilines) and electron-rich TMS-acetylene (**1'**) under optimized conditions comprising of sodium ascorbate, $CuSO_4$, and K_2CO_3 or KOAc base in MeOH–H_2O at room temperature in good yields (Table 3.1).

The activated aryl azides having the CF_3-group at the 4-/3-position on the aryl ring successfully underwent cycloaddition with **1'** producing **2a**–**2h** in moderate yields (entries 1–8). The presence of an electron withdrawing group in aryl azides lowers the reactivity as well as the yields (entries 6 and 7). Disappointingly, the reaction of *ortho*-trifluoromethyl substituted aryl azides **1i**/**1j** with **1'** under the optimized conditions failed. Interestingly, the use of KOAc base is found to be suitable, giving the desired products **2i** and **2j** in 31% and 21% yields, respectively (entries 9 and 10). The other *o*-CF_3 or *o*-Cl substituted aryl azides **1k**, **1l** or **1m** reacted poorly with **1'** under the optimized conditions, affording **2k**, **2l**, and **2m**, albeit in poor yields (entries 11–13) with the recovery of the unreacted azides in a fair amount. The structures of **2h** & **2m** were confirmed by single crystal X-ray analysis (Figure 3.1 and Table 3.5).

Table 3.1. Cu-catalyzed 1,3-dipolar cycloaddition of CF_3-substituted aryl azides and TMS-acetylene (**1'**).[a]

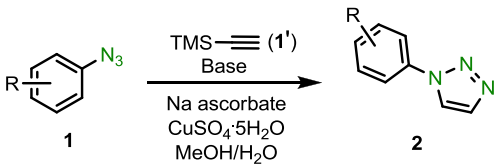

Entry	**1**	R	Base	**2**	Yield [%][f]
1[b]	**1a**	4-CF_3	K_2CO_3	**2a**	79
2[b]	**1b**	3-CF_3	K_2CO_3	**2b**	55
3[b]	**1c**	4-F-3-CF_3	K_2CO_3	**2c**	66
4[b,c]	**1d**	4-Cl-3-CF_3	K_2CO_3	**2d**	43
5[b]	**1e**	4-Br-3-CF_3	K_2CO_3	**2e**	89
6[b]	**1f**	4-NO_2-3-CF_3	K_2CO_3	**2f**	24
7[b]	**1g**	4-CN-3-CF_3	K_2CO_3	**2g**	52
8[b]	**1h**	4-CH_3-3-CF_3	K_2CO_3	**2h**	53
9[d]	**1i**	2-CF_3	KOAc	**2i**	31
10[d]	**1j**	4-NO_2-2-CF_3	KOAc	**2j**	21
11[b,e]	**1k**	4-F-2-CF_3	K_2CO_3	**2k**	27
12[b,e]	**1l**	4-Cl-2-CF_3	K_2CO_3	**2l**	22
13[b]	**1m**	2,6-Cl-4-CF_3	K_2CO_3	**2m**	28

[a]All reactions were conducted using azide (1.0 equiv), TMS acetylene (1.5 equiv), sodium ascorbate (0.4 equiv), and $CuSO_4{\cdot}5H_2O$ (0.2 equiv). [b]K_2CO_3 (1.2 equiv) and MeOH–H_2O (1:1, 2.0 mL for 1.0 mmol) were used, and the reaction performed at room temperature for 24 h. [c]Reaction conducted at 100 °C for 24 h. [d]KOAc (1.2 equiv), *t*-BuOH–H_2O (1:1, 1.0 mL for 1.0 mmol) were used, and the reaction conducted at 90 °C for 48 h. [e]Reaction conducted at 80 °C for 24 h. [f] Yield of the isolated product.

We next turned our attention performing nitrations on the –CF_3 substituted aryl triazoles **2a**–**2m** under the nitrating mixture of HNO_3 (95%) and H_2SO_4 (98%). The electrophilic substitution of the electron-poor aryl ring generally proceeds sluggishly under ambient conditions; thus, the nitrations of *N*-aryl-CF_3 substituted 1,2,3-traizoles (**2**) were conducted at 60–100 °C for 24 h. Table 3.2 summarizes the results for the nitration of **2**.

A nitro group is inserted *meta*- to the –CF_3 moiety on the aryl ring, producing exclusively **3a** from **2a** in good yield (entry 1). The nitration of *m*-CF_3-substituted phenyl-triazole **2b** gave the regioisomeric products **3b** & **3b'**; both the products were easily purified through column chromatography in 61% overall yield (entry 2). Among **3b** & **3b'**, the compound **3b** having

the *meta*-nitro to $–CF_3$ group is relatively non polar over **3b'**. The factors responsible for the formation of the unlikely major product **3b'** having the *ortho*-NO_2 to CF_3 group remain unclear. In general, insertion of the nitro group on the aryl ring possibly occurs *meta*- to the CF_3-moiety and *ortho*-/*para*- to the triazole skeleton.[4f] Thus, the nitration of 3-CF_3-4-F substituted aryl triazole **2c** gave **3c** albeit in moderate yield (entry 3). The Cl- and Br bearing CF_3-substituted aryl triazoles **2d** and **2e** underwent nitrations with HNO_3 (95%) and H_2SO_4 (98%) mixture, giving **3d** and **3e** in 30% and 38% yields, respectively (entries 4 and 5);[12] the halo group is useful for further synthetic manipulations. The presence of nitro or fluoro groups on the aryl ring makes the molecule highly electron-deficient; as a result, nitrations of 3-CF_3-4-NO_2, 2-CF_3-4-NO_2, or 2-CF_3-4-F substituted aryl triazole **2f**/**2j**/**2k** failed even under harsh conditions. Nitration of 3-CF_3-4-CN substituted aryl triazole **2g** produced **3g** in only 23% yield, while recovering the unreacted **2g** (18%) (entry 6).[12] The presence of an electron-donating group on the aryl moiety facilitates introducing the NO_2 group, thus, **2h** readily underwent nitration at an ambient temperature producing **3h** in 92% yield (entry 7). The nitrations of **2i** allowed the formation of the desired product **3i**, albeit in moderate yield (entry 8).[12] Surprisingly, insertion of a nitro group *para*- to the CF_3 and *meta*- to the triazole on **2l**, and *ortho*- to the CF_3 and *meta*- to the triazole on **2m** occurred producing **3l** and **3m**, albeit in poor yields (entries 9 and 10).[12] Unfortunately, efforts to introduce more than one nitro group on **2** were futile. The structures of **3a**, **3c** and **3l** were confirmed by single crystal X-ray analysis (Figure 3.1 and Table 3.5).

Table 3.2. Nitration reactions of triazoles **2.**

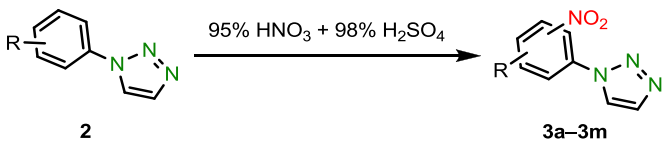

2 **3a–3m**

Entry	**2**	*T* [°C]	*t* [h]	NO_2- and CF_3-substituted-aryl-1,2,3-triazoles (**3**)	Yield [%][a]
1	**2a**	90	24	 **3a**	60
2	**2b**	80	12	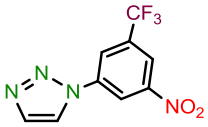 **3b** + 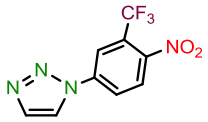 **3b'**	19+42
3	**2c**	95	12	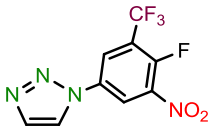 **3c**	44
4	**2d**	70	12	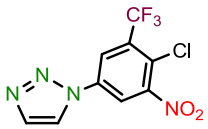 **3d**	30
5	**2e**	80	6	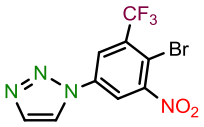 **3e**	38
6	**2g**	60	6	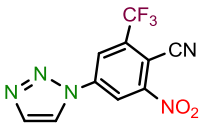 **3g**	23 (18)[b]
7	**2h**	RT	12	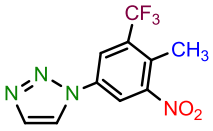 **3h**	92

8	**2i**	70	12	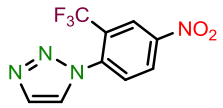 **3i**	37
9	**2l**	70	12	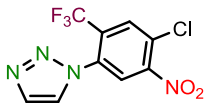 **3l**	27
10	**2m**	110	48	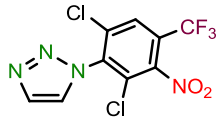 **3m**	32 (22)[b]

[a]Yield of the isolated product. [b]Yield in the parenthesis is the recovered amount of **2**.

The contribution of F atom towards the enhancement of density was evident as aryl-triazoles **2**, containing the $–CF_3$ group, showed comparable density to trinitrotoluene. The introduction of the $–NO_2$ group in **2** would further enhance the performance of the molecule. However, $–CF_3$ substituted *N*-aryl-triazoles **2** (Table 3.1) and aryl-nitro-triazoles **3** (Table 3.2) showed negative HOFs. The introduction of additional N atoms would further enhance the HOF of the molecule.[4b] With this intention, we considered investigating the base promoted replacement of the halo groups in **2** and **3** by the small molecule 1,2,3-triazole **4** (Tables 3.3 and 3.4). This would enable the achievement of novel polynitrogen compounds with positive HOFs. Thus, the CuI-catalyzed and Cs_2CO_3- promoted coupling between **2e** and **4** in DMF gave the N-1,N-2 and N-1,N-1 CF_3-substituted aryl bistriazole products **5** and **6** in 29% and 51% yields, respectively (entry 1, Table 3.3). The appearance of a doublet for the triazole moiety in the ^1H spectrum confirms the structure of **6**. Both the chloro groups in **2m** are efficiently replaced by **4**, producing the N-1,N-2,N-2 polytriazole coupled product **7** (24%) and the non-separable mixture of the N-1,N-1,N-1 and N-1,N-1,N-2 polytriazoles in 43% yield (entry 2, Table 3.3). The X-ray crystal analysis data unambiguously elucidates the structures of **5** and **7** (Figure 3.1 and Table 3.6). As anticipated, compounds **5**–**13** showed positive HOFs (45–400 kJ mol^{-1}).

Table 3.3. Reaction between haloarenes **2** with 1H-1,2,3-triazole (**4**).[a]

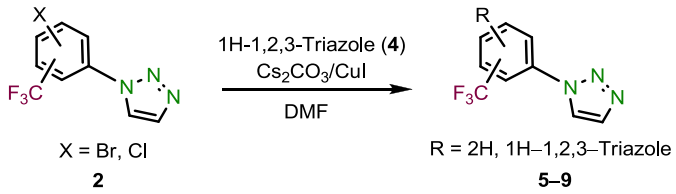

Entry	**2**	*T* [°C]	*t* [h]	CF_3-substituted-aryl-Poly 1,2,3-triazoles[b]	
1	**2e**	120	24	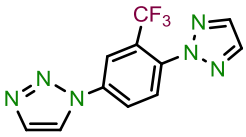 **5** 29	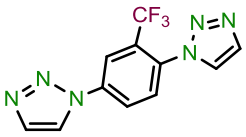 **6** 51
2	**2m**	90	12	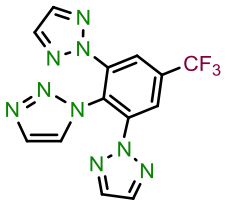 **7** 24	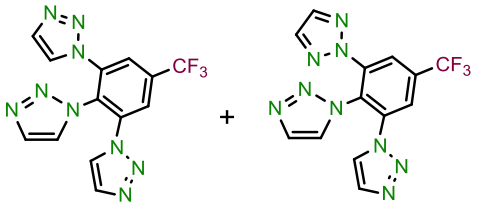 **8 + 9** 43

[a]All reactions were carried out using **2** (1.0 equiv), 1H-1,2,3-triazole (**4**, 1.5 equiv), Cs_2CO_3 (2.0 equiv), CuI (0.2 equiv) in DMF (2.0 mL for 1.0 mmol) with the respective temperature shown in Table 3.3. [b]Yield of the isolated product.

We next investigated the Cu-catalyzed couplings between the halo-, CF_3-bearing aryl-nitro-triazoles **3** and **4**. We anticipate the $–NO_2$ and $–CF_3$ substituted aryl polytriazoles would show better density, detonation performance and positive HOF. Accordingly, the reaction between **3e** and **4** delivered various $–CF_3$ substituted *N*-aryl polytriazoles **10** (8%), **11** (20%), **12** (36%), and **13** (29%) by replacing both –Br and $–NO_2$ groups in **3e** at 120 ^oC; the reaction at low temperature led to poor consumption of **3e** (entry 1, Table 3.4). The structures of **10**, **11**, and **12** were confirmed by single crystal X-ray analysis (Figure 3.1, Table 3.6).

Table 3.4. Coupling of halo-, CF_3-substituted nitroarenes **3** with **4** or 5-amino-tetrazole (**14**).[a]

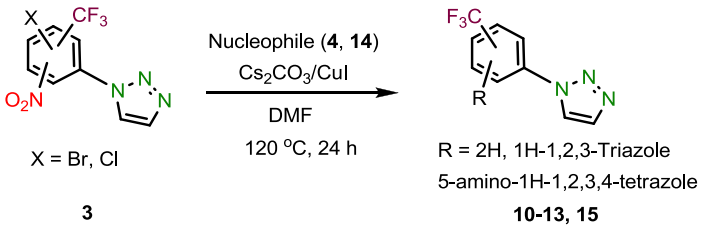

Entry	**3**	Nu^-	CF_3-substituted aryl-poly-1,2,3-triazole derivatives[b]			
1	**3e**	**4**	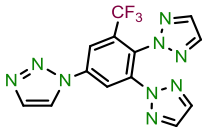	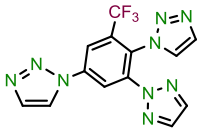	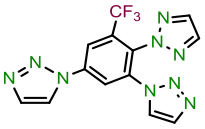	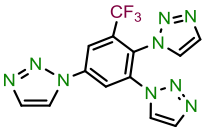
			10	**11**	**12**	**13**
			8	20	36	29
2	**3d**	**4**	**10**	**11**	–	–
			33	58	–	–
3	**3d**	**14**	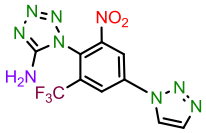	–	–	–
			15	–	–	–
			23	–	–	–

[a]All reactions were carried out using $–NO_2$, $–CF_3$ and halo-substituted aryltriazole (3, 1.0 equiv), {1H-1,2,3-triazole (**4**) or 5-amino-1H-1,2,3,4-tetrazole (**14**), 1.5 equiv}, Cs_2CO_3 (2.0 equiv), CuI (0.2 equiv) in DMF (2.0 mL for 1.0 mmol) at 120 °C for 24 h. [b]Yield of the isolated product.

Interestingly, an identical reaction between **3d** and **4** gave **10** and **11** in overall good yields (entry 2, Table 2.4). In contrast, the –Cl group in **3d** was exclusively replaced by 5-amino-1H-1,2,3,4- tetrazole (**14**) affording the $–CF_3$, $–NO_2$, and N-rich **15** in only 23% yield; the unreacted **3d** was recovered in 36% yield (entry 3, Table 3.4).

In general, the incorporation of the $–NO_2$ and –OH groups within a molecular framework enhances the density of the molecule, owing to the inherent ability of these groups to participate in H-bonding.[13] Therefore, we were interested in incorporating additional –OH groups in the molecule. Thus, the F atom in **3c** is easily converted to phenol-derivative **16**, when **3c** reacted with 30% H_2O_2 [eqn (1)].

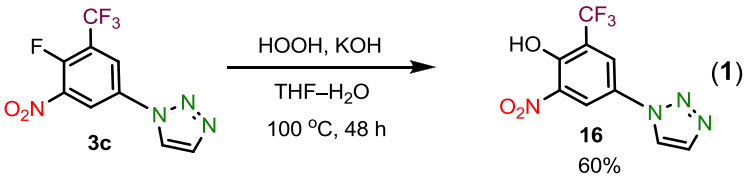

In order to have an energetic molecule with better combinations of density, detonation performance, and stability, we envisaged the synthesis of nitro and nitrogen rich heterocycle **19** from commercially available 2-chloro-1,5-dinitro-3-(trifluoromethyl)-benzene (**17**) and 3-azido-1,2,4-triazole (**18**). The desired C–N coupled product **19** was isolated with 69% yield, when **17** and **18** reacted in the presence of NaH in THF at room temperature [eqn (2)].

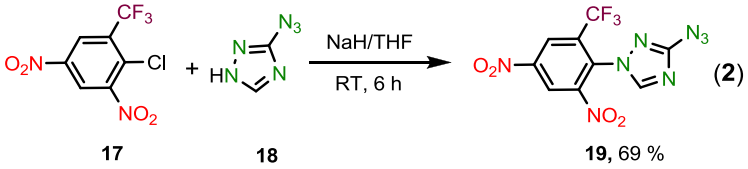

3.3. X-ray crystallography

Single crystals were grown by the slow evaporation of solutions of **2h**, **2m**, **3a**, **3c**, **3l**, **5**, **7**, **10**, **11** and **12** in EtOH at room temperature and atmospheric pressure. The structures of **2h**, **2m**, **3a**, **3c**, **3l**, **5**, **7**, **10**, **11** and **12** were unambiguously elucidated by single crystal X-ray diffraction analysis and the molecular structures are shown in Figure 3.1. Compounds **2h**, **2m**, **3a**, **3l**, **5**, **7**, **11** and **12** crystallize in the monoclinic space groups $P2_1/c$, $P2_1/n$ and C_2/c with cell volumes of 1006.66(11), 1137.67(14), 1058.17(17), 1104.6(2), 1188.3(6), 2924.5(11), 2971.9(3), and 5805(3) $Å^3$, respectively, whereas the compound **3c** crystallizes in the orthorhombic space group $P2_12_12_1$ with a cell volume of 1074.94(10) $Å^3$ and compound **10** crystallizes in the triclinic space group P_1^- with a cell volume of 733.5(3) $Å^3$. The crystallographic data for all the compounds are detailed in Tables 3.5 and 3.6.

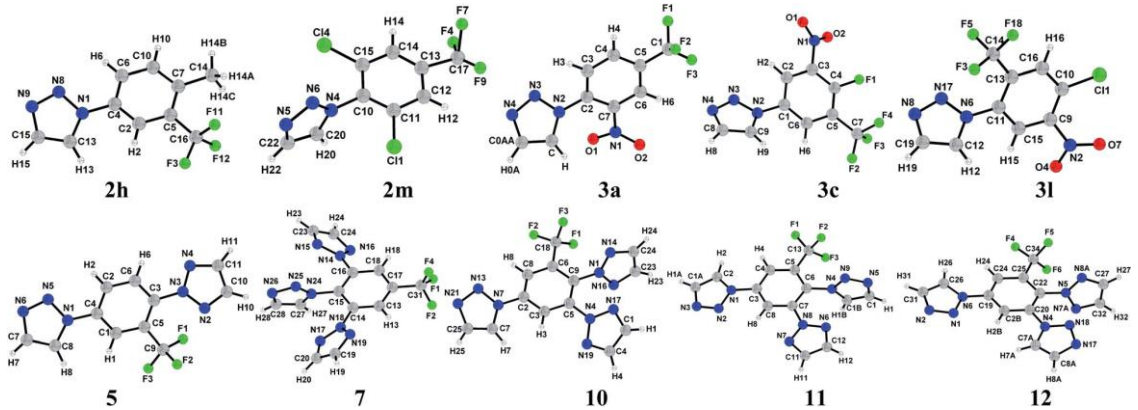

Figure 3.1. Molecular structures of compounds **2h**, **2m**, **3a**, **3c**, **3l**, **5**, **7**, **10**, **11** and **12**; thermal ellipsoids are set at 50% probability

Table 3.5. Crystallographic data for compounds **2h, 2m, 3a, 3c** and **3l**

Compound	**2h**	**2m**	**3a**	**3c**	**3l**
CCDC	949060	949061	949062	949063	949064
Formula	$C_{10}H_8F_3N_3$	$C_9H_4Cl_2F_3N_3$	$C_9H_5F_3N_4O_2$	$C_9H_4F_4N_4O_2$	$C_9H_4ClF_3N_4O_2$
M_w	227.19	282.04	258.17	276.16	292.61
Crystal system	monoclinic	monoclinic	monoclinic	orthorhombic	monoclinic
Space group	$P2_1/c$	$P2_1/c$	$P2_1/n$	$P2_12_12_1$	$P2_1/c$
T [K]	293	293	293	293	293
a [Å]	7.7969(6)	16.0332(12)	5.4767(5)	6.4061(3)	14.580(2)
b [Å]	12.0686(7)	6.8721(4)	24.405(2)	10.2430(6)	13.1345(19)
c [Å]	10.9819(6)	10.7030(7)	7.9829(8)	16.3818(8)	5.7684(6)
α [°]	90	90	90	90	90
β [°]	103.056(6)	105.264(7)	97.370(9)	90	90.465(13)
γ [°]	90	90	90	90	90
Z	4	2	4	4	4
V [Å^3]	1006.66(11)	1137.67(14)	1058.17(17)	1074.94(10)	1104.6(2)
D_{calc} [g cm^{-3}]	1.499	1.653	1.621	1.706	1.760
μ [mm^{-1}]	0.132	0.589	0.153	0.169	0.392
total reflns	2667	4654	2743	1902	2923
unique reflns	2291	2783	2373	1740	2092
Observed reflns	1548	2153	1171	1585	933
R_1 [$I > 2\sigma(I)$]	0.0566	0.0688	0.0741	0.0332	0.0651
wR_2 [all]	0.1789	0.2299	0.2283	0.0892	0.2132
GOF	1.075	1.586	1.162	1.057	0.845
Diffractometer	Xcalibur Gemini Eos CCD	SMART APEX CCD	SMART APEX CCD	SMART APEX CCD	Xcalibur Gemini Eos CCD

Table 3.6. Crystallographic data for compounds **5, 7, 10, 11** and **12**

Compound	**5**	**7**	**10**	**11**	**12**
CCDC	949065	949066	949067	949069	949068
Formula	$C_{11}H_7F_3N_6$	$C_{13}H_8F_3N_9$	$C_{13}H_8F_3N_9$	$C_{13}H_8F_3N_9$	$C_{13}H_8F_3N_9$
M_w	280.23	347.28	347.28	347.28	347.28
Crystal system	monoclinic	orthorhombic	triclinic	monoclinic	monoclinic
Space group	$P2_1/n$	$Pca2_1$	$P\bar{1}$	$P2_1/c$	$C2/c$
T [K]	273	298	293	293	298
a [Å]	7.445(2)	17.315(4)	8.5034(13)	13.2240(8)	18.596(5)
b [Å]	15.889(5)	8.8212(18)	10.042(2)	10.7927(7)	10.898(3)
c [Å]	10.638(3)	19.147(4)	10.289(2)	20.8619(10)	28.644(8)
α [°]	90	90	61.31(2)	90	90
β [°]	109.220(5)	90	84.601(15)	93.504(5)	90.480(4)
γ [°]	90	90	72.454(16)	90	90
Z	4	8	2	8	16
V [Å^3]	1188.3(6)	2924.5 (11)	733.5(3)	2971.9(3)	5805 (3)
D_{calc} [g cm^{-3}]	1.566	1.577	1.572	1.552	1.589
μ [mm^{-1}]	0.136	0.133	0.132	0.131	0.134
total reflns	2282	5972	3951	4261	5746
unique reflns	2270	5940	3281	4251	5726
Observed reflns	1622	3795	2253	2874	4204
R_1 [$I > 2\sigma(I)$]	0.0404	0.0904	0.0657	0.0571	0.0650
wR_2 [all]	0.1073	0.2563	0.2196	0.2066	0.2175
GOF	1.011	1.021	1.315	0.814	1.063
Diffractometer	SMART APEX CCD	SMART APEX CCD	Xcalibur Gemini Eos CCD	Xcalibur Gemini Eos CCD	SMART APEX CCD

3.4. Energetic Properties

We have demonstrated the synthesis of trifluoromethyl substituted aryl triazoles (**2a**–**2m**), –CF_3 and –NO_2/–azido substituted *N*-aryl triazole derivatives (**3a**–**3m**, **16** and **19**), nitrogen-rich –CF_3 substituted *N*-aryl-poly-1,2,3-triazoles and tetrazoles (**5**–**13** and **15**). The physical properties of these synthesized compounds are summarized in Table 3.7. The molecules bearing the –CF_3 group showed negative HOFs owing to the presence of the F atoms. Importantly, the introduction of the azole backbone increases the energy of the molecules leading to an enhanced HOF.[4] Thus, the –CF_3 and polyazole-containing compounds showed positive HOFs. Due to the absence of an additional triazole ring, the enthalpies of compounds **5** and **6** are lower than for compounds **7**–**13**. The HOFs of the –CF_3 and three triazole bearing compounds **7**–**13** were 370–400 kJ mol^{-1}. The high nitrogen content of the substituted triazoles allows enhancement of the heat of formation of the molecules from negative to positive. The calculated densities of the synthesized compounds (**2a**–**2m**, **3a**–**3m**, **5**–**13**, and **15**) lie in the range between 1.53 to 1.71 g cm^{-3} (Table 3.7). Generally, the introduction of –NO_2 groups enhances the density of the compounds;[4,5] for instance, the density of **3a** (1.69 g cm^{-3}) is higher than for **2a** (1.59 g cm^{-3}). An identical trend in the variation of density is observed for **3b**, **3b'**, **3i**, **3c**, and **3e** over **2b**, **2i**, **2c** and **2e**, respectively. However, the position of –NO_2 and –CF_3 groups on the molecule did not lead to significant changes in the density (**3a** and **3b**, **3b'** and **3i**). Gratifyingly, the nitro and nitrogen rich heterocycles **16** and **19** had densities of 1.72 and 1.80 g cm^{-3}, respectively. The velocity of detonation (*vD*) and detonation pressure (*P*) are dependent on density rather than HOF.[3] Although compounds **3c** and **16** possess lower HOFs than **3b**, **3b'** and **3i**, however, the former molecules show better detonation performance due to better densities. The physical properties in Table 3.7 revealed that **19** (*vD* = 7673 m s^{-1}, *P* = 24.95 GPa) exhibited comparable detonation performance to TNT (*vD* = 6881 m s^{-1}, *P* = 19.50 GPa) and the previously reported –CF_3 derivatives.[1,2a]

The thermal stabilities of the –CF_3 substituted aryl triazole derivatives are determined by DSC-TGA measurements. The DSC-TGA plots for **3a** and **13** are depicted in Figure 3.2. The compounds **2a**–**2m**, **3a**–**3m**, **5**, **7**, **10**, **15**, and **16** exhibit an endothermic effect due to the lack of high nitrogen content. In contrast, the triazole/azido-bearing compounds **6**, **11**–**13** and **19** reflect an exothermic effect. The synthesized triazole derivatives decompose between 195–308 ^{o}C. Interestingly, **2f** and **3b'** showed good thermal stabilities (Td > 300 ^{o}C). Owing to a

large variation of the melting point (mp < 101 °C) and decomposition temperature (Td > 195 °C), the molecules **2b**, **2c**, **2f**, **2h**, **3a**, **3b'**, **3c** and **3i** might be useful as melt-cast explosives.

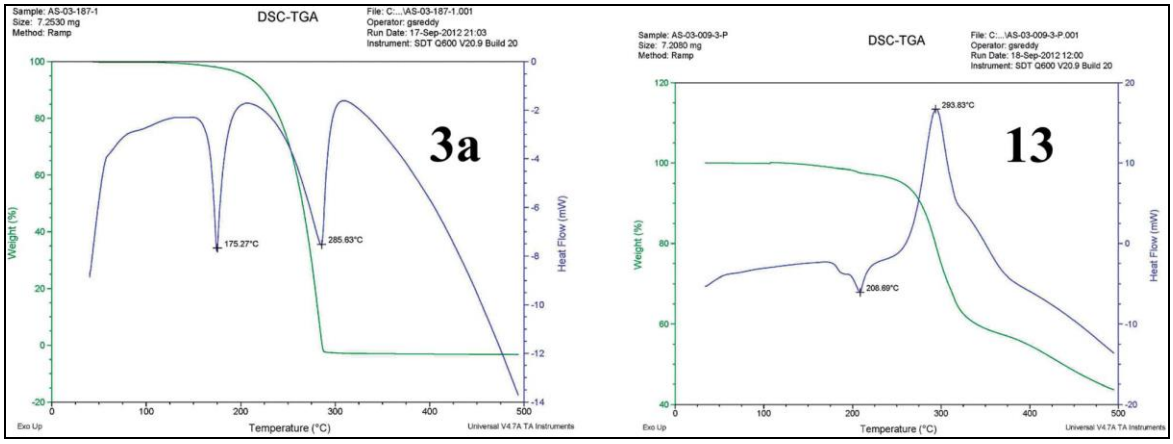

Figure 3.2. DSC-TGA plots for **3a** and **13**.

Table 3.7. Energetic properties of the triazole derivatives

Comp.	ρ[a] [g cm^{-3}]	vD[b] [m s^{-1}]	P[c] [GPa]	T_m[d] [°C]	T_d[e] [°C]	HOF[f] [kJ mol^{-1}]
2a	1.59	5249 (6332)	11.28 (17.27)	125	199	–278.52
2b	1.60	5278 (6358)	11.44 (17.33)	69	200	–276.37
2c	1.66	5459 (6177)	12.55 (17.21)	91	212	–475.85
2f	1.70	6276 (6866)	16.82 (20.61)	81	301	–271.74
2g	1.54	5185 (6210)	10.78 (16.82)	122	254	–124.64
2h	1.53 (1.49)	5039 (6347)	10.12 (16.86)	92	228	–302.71
2i[f]	1.59	5301 (6370)	11.53 (17.43)	–	–	–253.71
2j	1.69	6229 (6822)	16.49 (20.38)	109	228	–285.97
2k	1.65	5458 (6170)	12.48 (17.22)	142	195	–467.63
3a	1.69 (1.62)	6252 (6844)	16.67 (20.51)	101	237	–266.52
3b	1.67	6141 (6755)	15.99 (19.94)	129	213	–297.78
3b'	1.70	6279 (6866)	16.82 (20.61)	73	308	–271.74
3c	1.71 (1.71)	6348 (6693)	17.30 (19.71)	101	238	–470.67
3g[f]	1.65	6146 (6724)	15.86 (19.56)	–	–	–113.00
3h	1.64	5935 (6790)	14.71 (19.76)	122	233	–308.25
3i	1.69	6223 (6822)	16.49 (20.38)	87	252	–285.97

5	1.59 (1.56)	5636 (6725)	13.02 (18.60)	141	263	45.23
6	1.58	5644 (6720)	13.02 (18.46)	133	297	67.05
7	1.54 (1.57)	5741 (6798)	13.23 (18.26)	150	253	372.01
8	1.57	5852 (6915)	13.91 (18.96)	109	280	400.14
9	1.57	5824 (6898)	13.80 (18.87)	109	280	380.56
10	1.55 (1.57)	5761 (6830)	13.41 (18.53)	175	286	373.53
11	1.56 (1.55)	5809 (6870)	13.64 (18.75)	118	282	384.36
12	1.54 (1.58)	5751 (6808)	13.30 (18.31)	206	278	384.49
13	1.57	5843 (6910)	13.88 (18.93)	208	294	394.95
15	1.68	6552 (7262)	18.22 (22.01)	161	261	100.40
16	1.72	6341 (6865)	17.36 (20.56)	166	254	–466.32
19	1.80	7279 (7673)	23.47 (24.95)	122	213	–71.11
TNT[5a]	1.65	6881	19.50	–	300	–67.0
RDX[5g]	1.82	8748	34.90	–	230	92.6

[a] Calculated density; the experimental crystal density is shown in parentheses. [b] Velocity of detonation calculated with Kamlet–Jacobs equations; the *vD* is calculated with Explo5 *version* 6.02 is shown in parenthesis.[25] [c] Detonation pressure calculated with Kamlet–Jacobs equations; the detonation pressure is calculated with Explo5 *version* 6.02 is shown in parenthesis.[25] [d] Melting point. [e] Decomposition temperature under nitrogen gas (10 ^{o}C min^{-1}). [f] Heat of formation.[14] [g] Compounds are liquid.

3.5. Potential Energy Diagrams

General electrostatic potential energy information for this Chapter is same as mentioned in Page No 47, Chapter 2.

In compounds **2a**–**2k**, a small electropositive region is located in the vicinity of the benzene and triazole rings because of its strong electron withdrawing nature of –CF_3 group. Similarly, in nitro-rich compounds **3a**–**3i**, a large electropositive potential generated over the benzene and triazole rings due to the high electron withdrawing nature of –CF_3 and –NO_2 groups. In nitro-rich derivatives **5**–**16,** the charge density is mostly located on the nitrogen atom of the triazole rings because of its strong electronegativity of nitrogens. Finally, in compound **19**, charge densities were found more positive on the benzene and 1,2,4-triazole ring due to the high electron withdrawing nature of –CF_3, –NO_2 and –N_3 groups. This is cleary shown in potential energy diagrams (Figure 3.3).

Negative potential ---------- Neutral potential ---------- Positive potential

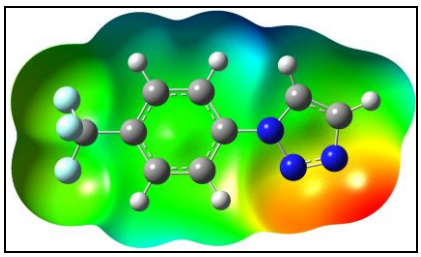

2a

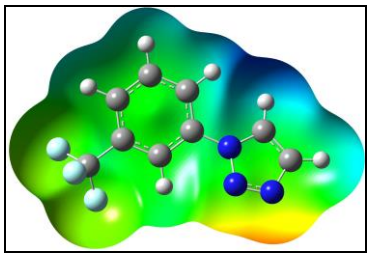

2b

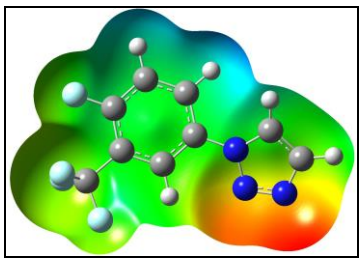

2c

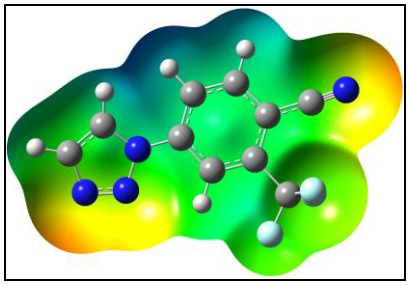

2g

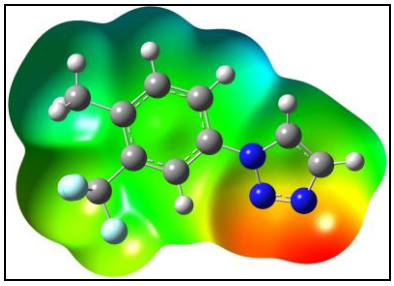

2h

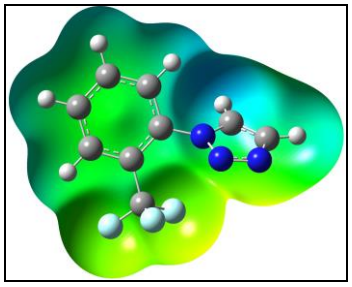

2i

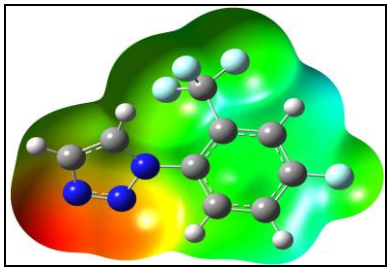

2k

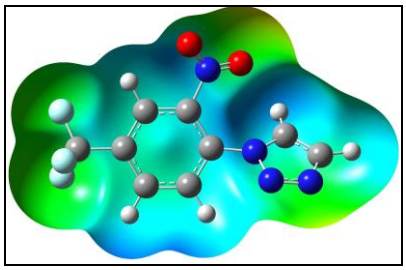

3a

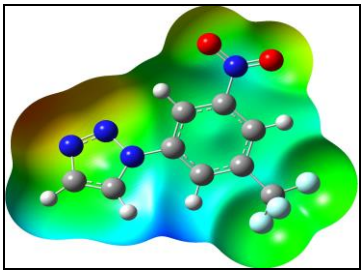

3b

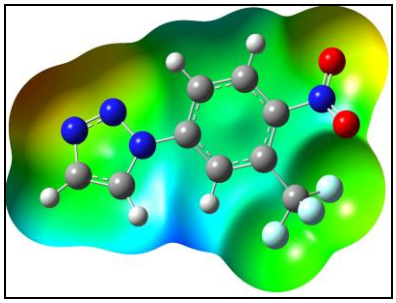

3b'

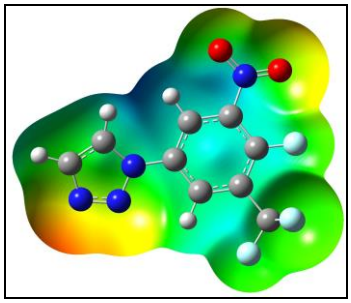

3c

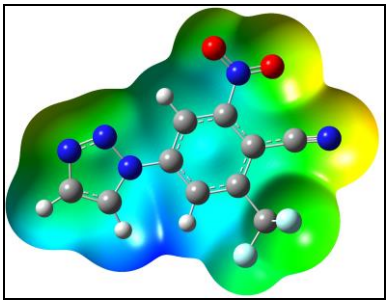

3g

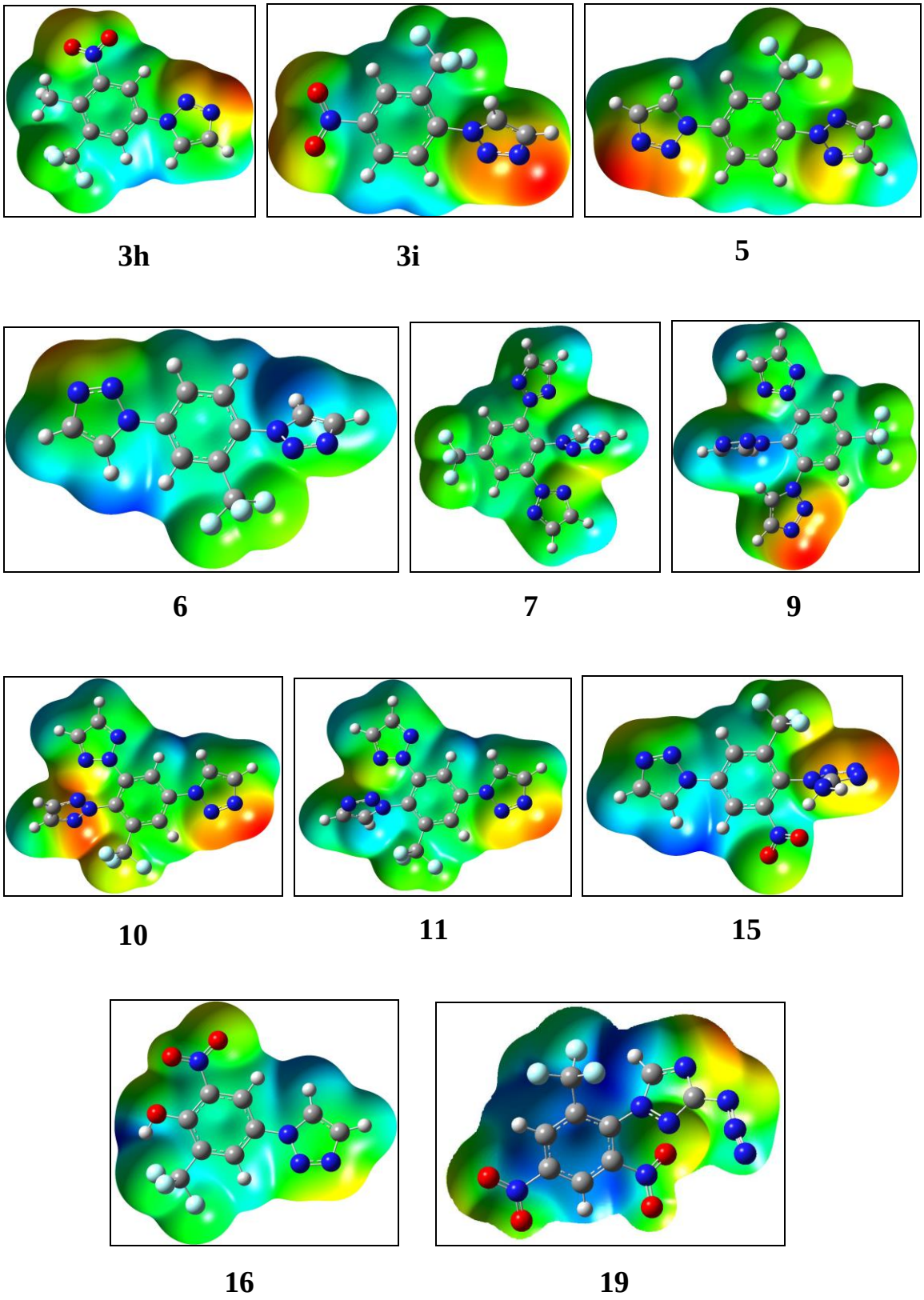

Figure 3.3. Optimized structures and electrostatic potential surfaces of compounds **2a**–**2c**, **2g**–**2i**, **2k**, **3a**–**3c**, **3g**–**3i**, and **5**–**19** (B3PW91/6-31G (d,p), 0.001 electron/bohr^3 isosurface. The red and blue regions of the ruler (from left to right) indicate regions of more negative (electron-rich) and positive (electron deficient) charges, respectively. Gray = carbon; white = hydrogen; blue = nitrogen; red = oxygen.

3.6. Conclusion

In summary, a wide array of $–CF_3$ and $–NO_2$ substituted *N*-arylpoly-1,2,3-triazoles and tetrazole compounds are efficiently synthesized. The Cu-catalyzed coupling of $–CF_3$, $–NO_2$ and halo substituted aryl triazole with 1H-1,2,3-triazole and amino-tetrazole delivered *N*-aryl-polytriazole derivatives. The molecules are characterized by analytical and spectroscopic methods. Structures of most of the newly synthesized molecules are determined by X-ray diffraction analysis. Most of the *N*-arylpoly-1,2,3-triazoles decomposes at 195–308 ^oC; these molecules are therefore considered thermally stable materials. Some of the compounds exhibit good density and acceptable detonation performance. The newly synthesized poly-1,2,3-triazole derivatives showed positive HOFs of 45–400 kJ mol^{-1}. Fabrications of novel $–CF_3$ or $–SF_5$ groups-containing pyridyl–triazole molecules are currently pursued.

3.7. Future Work

The present work successfully demonstrates the synthesis of trifluromethyl-substituted *N*-aryl-poly-1,2,3-triazole derivatives from readily accessible CF_3-substituted aryl azides and commercially available alkynes via click reaction, followed by a nitration sequence. The synthesized $–CF_3$ and $–NO_2$ substituted *N*-aryl-poly-1,2,3-triazoles and tetrazole derivatives exhibit positive heats of formation, high thermal stability and good density. However, most of molecules showed moderate detonation performances (*vD* & *P*). As nitro groups into a molecular backbone enhances the oxygen balance, and detonation performance,[5] we thus envisaged introducing NF_2, OCF_3 & SF_5 moieties along with the nitro group in the aryl-traizole skeleton to enhance the density and detonation performance of the material. Accordingly various new molecular entities **20–30** are designed (Scheme 3.4).

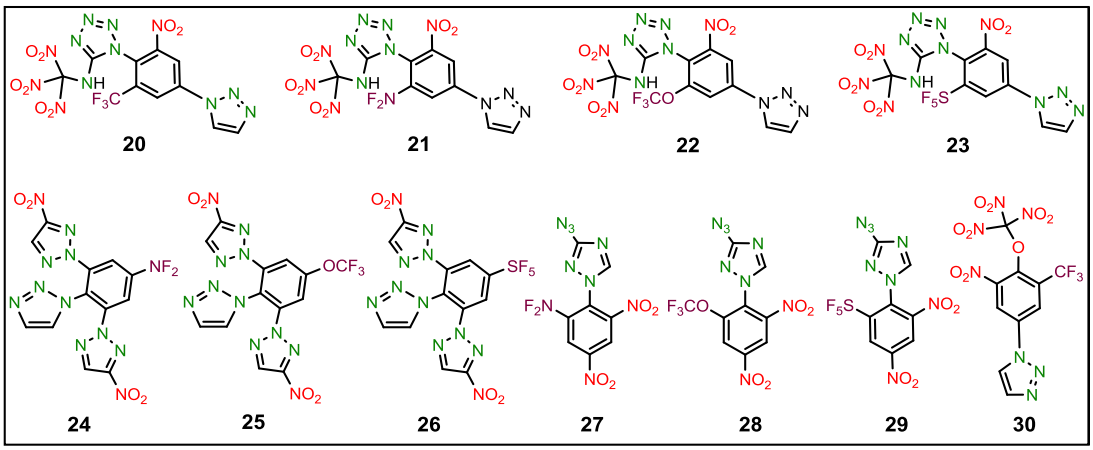

Scheme 3.4. Synthesis of OCF_3/NF_2/SF_5/trinitromethyl-substituted aminoaryl-triazole and tetrazole derivatives (**20-30)**

3.8. Experimental

3.8.1. General Experimental Information for this Chapter is same as mentioned in Page No 51-52, Chapter 2.

3.8.2. Caution!

Working with fluorinated azides should always be done carefully. Organic azides, particularly those of low molecular weight, or with high nitro and nitrogen content, are potentially-explosive substances that can and will decompose with the slightest input of energy from external sources (heat, light, pressure). Additionally, small molecules containing azido functionality tend to decompose violently which may result injury if proper safety precautions are not utilized. Furthermore, extra caution must be taken when azido compounds reacted with acids. Acids will protonate the azide ion and form the highly-toxic hydrogen azide (toxicity similar to that of hydrogen cyanide). Any experiments in which azides are to be heated in the presence of copper should involve the use of blast shield. Owing to the presence of high nitrogen content and strong oxidizers, the CF_3 and NO_2 containing triazole and tetrazole derivatives are considered to be dangerous, when heated at high temperature. All the fluorinated compounds are prepared in milligram quantity. We did not face any problem while handling these materials. The use of proper protective measurements (safety shields, safety glasses, face shields, ear plugs, body armor, leather gloves and earthen equipment) is therefore recommended at all times. Ignoring safety precautions can lead to serious injury.

3.8.3. X-ray crystallography

X-ray reflections for compounds **2m**, **3a**, **3c**, **5**, **7** and **12** were collected on a Bruker SMART APEX CCD diffractometer that was equipped with a graphite monochromator and Mo Kα fine-focus sealed tube (λ = 0.71073 Å). Data integration was done by using SAINT.[19] The Intensities of the absorption were corrected by using SADABS.[20] Structure solution and refinement were carried out by using Bruker SHELX-TL.[21] X-ray reflections for compounds **2h**, **3l**, **10** and **11** were collected on an Oxford Xcalibur Gemini Eos CCD diffractometer by using Mo-Kα radiation. Data reduction was performed using CrysAlisPro (*version* 1.171.33.55). The OLEX2-1.0[22] and SHELX-TL 97 programme were used to solve and refine the data. All non-hydrogen atoms were refined anisotropically, and C−H hydrogen atoms were placed at fixed positions.

CCDC-949060 (**2h**), CCDC-949061 (**2m**), CCDC-949062 (**3a**), CCDC-949063 (**3c**), CCDC-949064 (**3l**), CCDC-949065 (**5**), CCDC-949066 (**7**), CCDC-949067 (**10**), CCDC-949069 (**11**), CCDC-949068 (**12**) contains the supplementary crystallographic data for this paper. These data can be obtained free of charge from The Cambridge Crystallographic Data Centre via www.ccdc.cam.ac.uk/data_request/cif.

3.8.4. Theoretical study

All the calculations were performed using the Gaussian 03 program suite.[16] The geometric optimization of the structures and frequency analyses were carried out using the B3PW91 functional with 6-31G (d,p) basis set. The zero point energies (ZPEs) and the corresponding thermal corrections (HT) to the enthalpy at 298.15 K were obtained from frequency calculations and were subsequently added to the electronic energies. All of the optimized structures were characterized to be true local energy minima on the potential energy scale. The method of isodesmic reactions has been employed to calculate HOF from total energies obtained from DFT calculations. Crystal packing density was predicted by the molecular packing calculations using CVFF force field in the polymorph module of Material Studio Suite. The empirical Kamlet–Jacobs[17] equations were employed to estimate the values of detonation velocity (*vD*) and detonation pressure (*P*) [eqn (3)].

$$D = 1.01(NM^{0.5}Q^{0.5})^{0.5}(1 + 1.30\rho_o) \text{ and } P = 1.55\rho_o{}^2NM^{0.5}Q^{0.5} \quad (3)$$

where in the above equations, *vD* is the detonation velocity (m s^{-1}), *P* is detonation pressure (GPa), *N* is moles of gaseous detonation products per gram of explosives, *M* is the average molecular weight of gaseous products, *Q* is the chemical energy of detonation (cal g^{-1}) defined as the difference in the HOFs between products and reactants, and ρ is the density of explosive (g cm^{-3}).

3.8.5. Isodesmic reactions for the titled compounds:

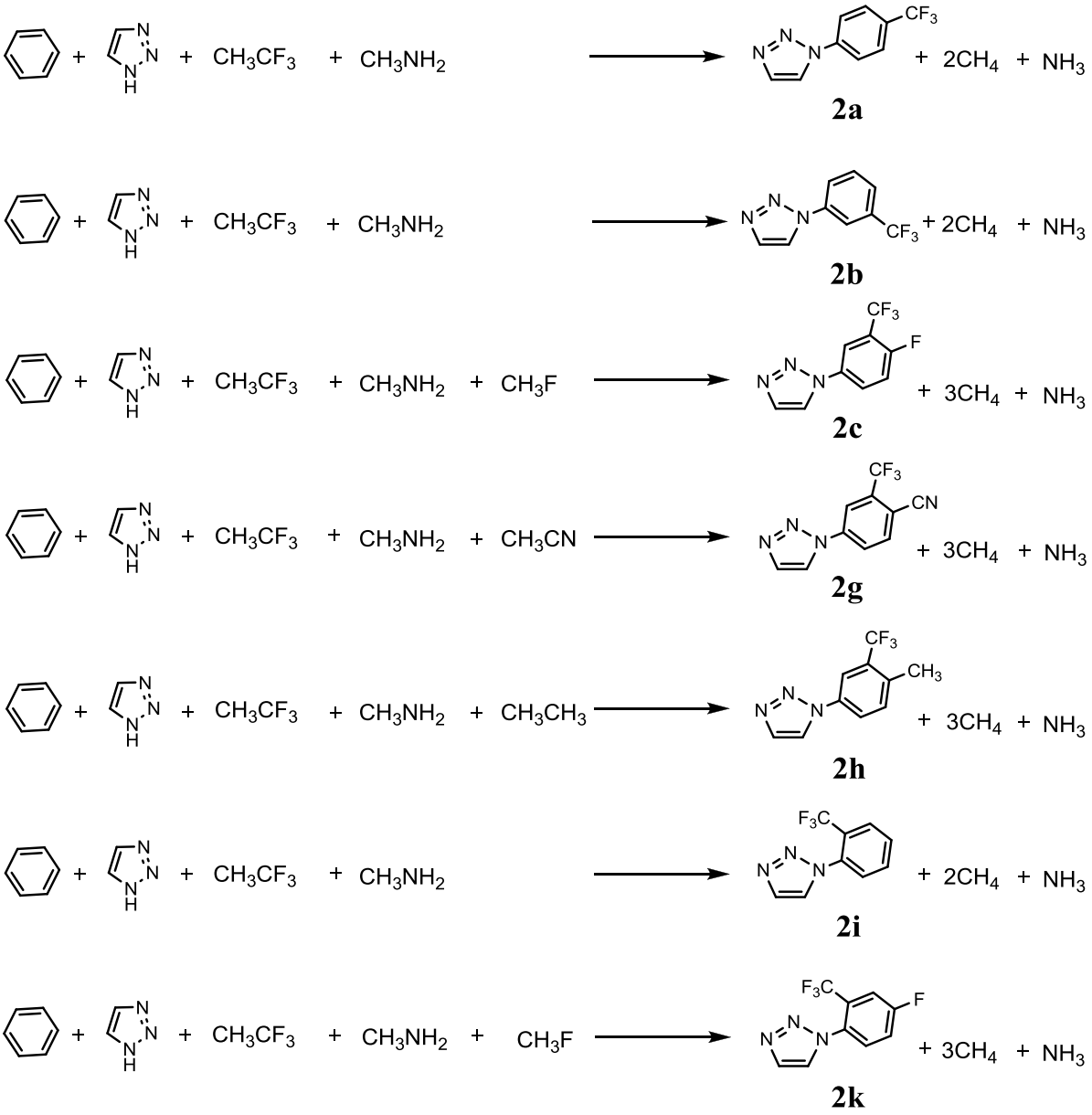

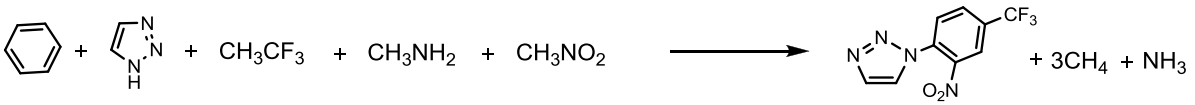

3a

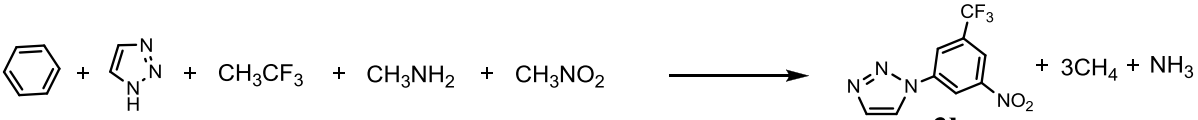

3b

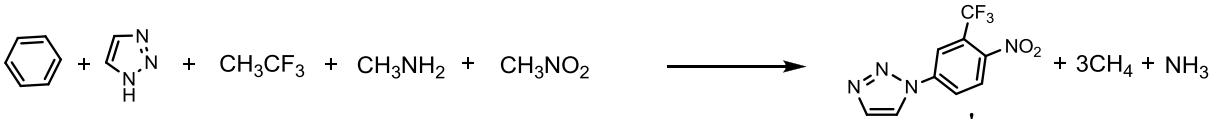

3b'

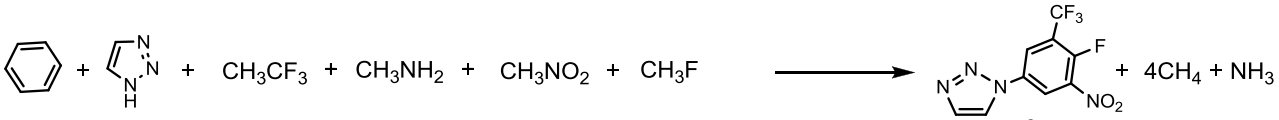

3c

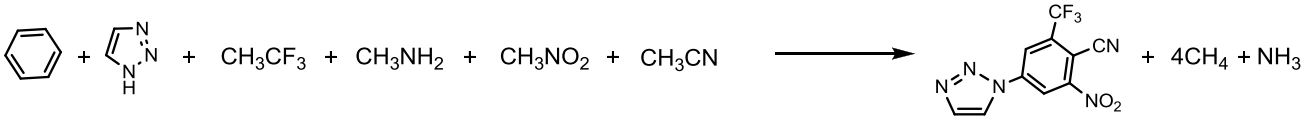

3g

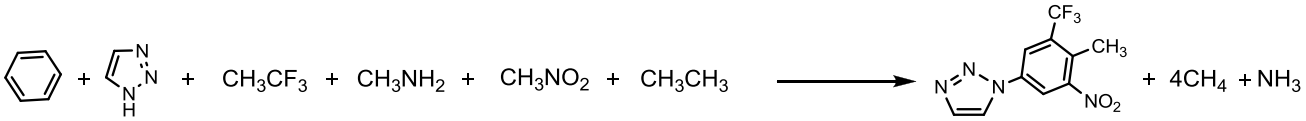

3h

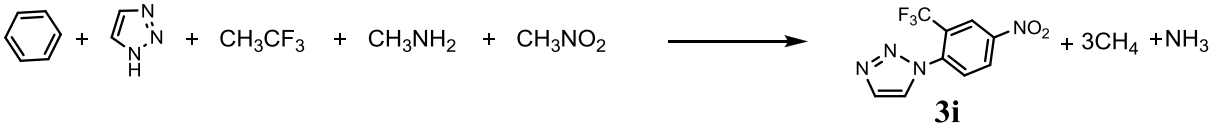

3i

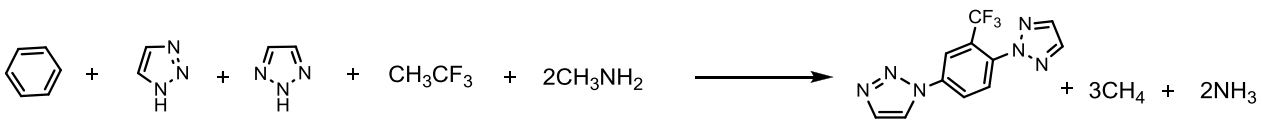

5

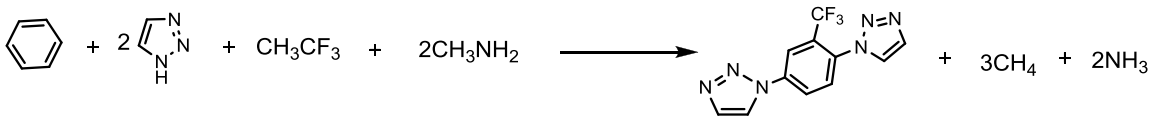

6

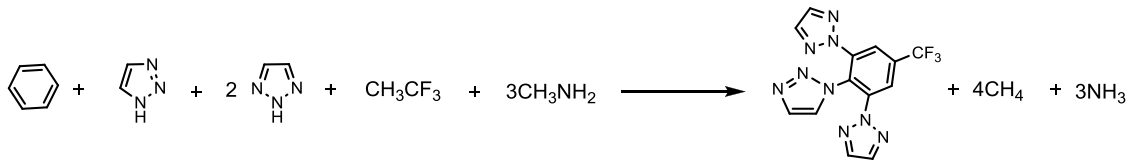

7

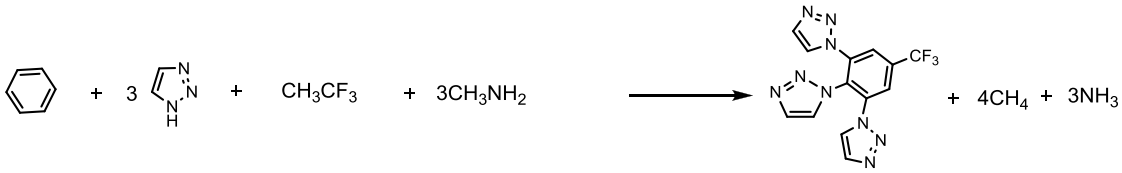

8

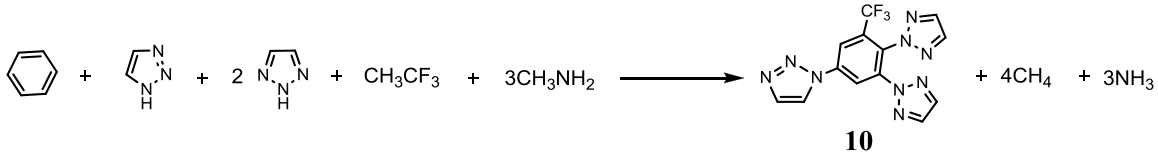

10

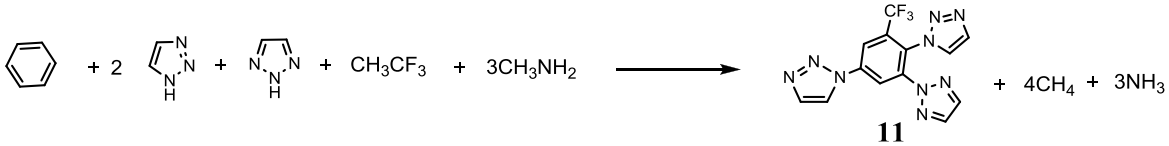

11

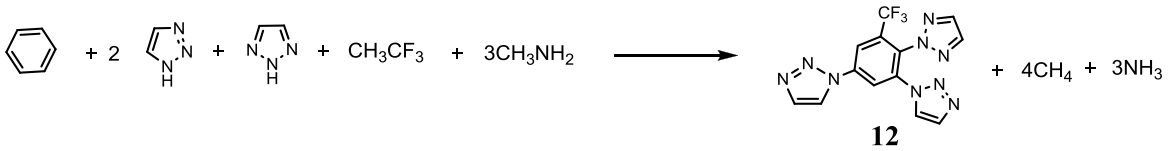

12

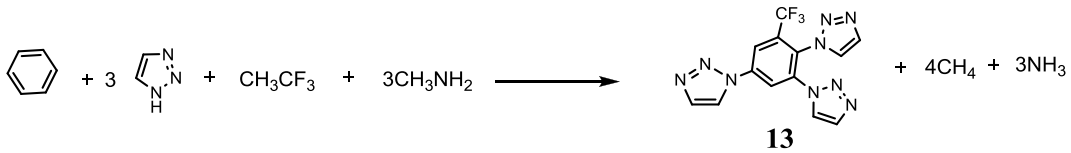

13

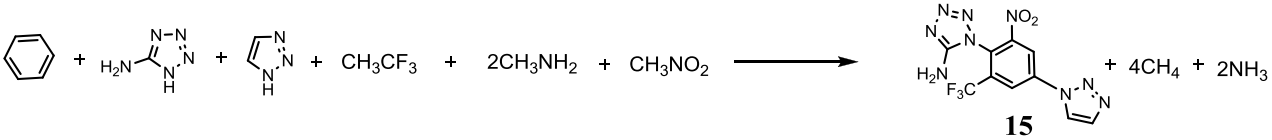

15

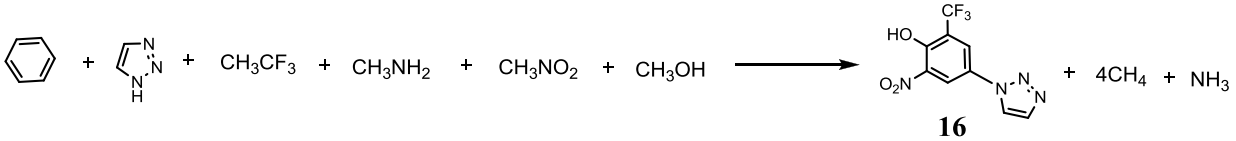

16

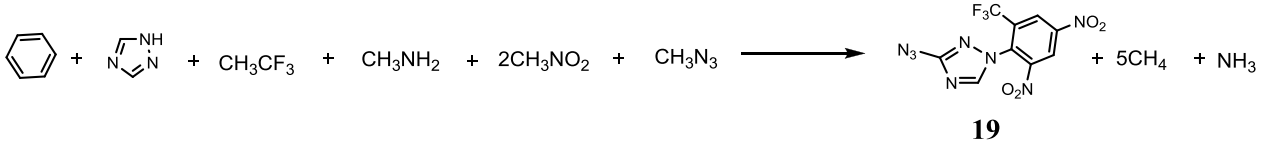

19

3.8.6. Materials

Unless otherwise noted, all the reagents and intermediates were obtained commercially and used without purification. Solvents were distilled prior to use. All the substrates 4-(trifluoromethyl)aniline, 3-trifluoromethyl)aniline, 2-(trifluoromethyl)aniline, 4-nitro-2-(trifluoromethyl)aniline, 4-nitro-3-(trifluoromethyl)aniline, 4-fluoro-2-(trifluoromethyl)aniline, 4-fluoro-3-(trifluoromethyl)aniline, 4-bromo-3-(trifluoromethyl)aniline, 4-chloro-2-(trifluoromethyl)aniline**,** 4-chloro-3-(trifluoromethyl)aniline**,** 4-methyl-3-(trifluoromethyl) aniline**,** 2,6-dichloro-4-(trifluoromethyl)aniline**,** 4-amino-2-(trifluoromethyl)benzonitrile**,** 1H-1,2,3-triazole**,** 2-chloro-1,5-dinitro-3-(trifluoromethyl)benzene, 5-amino tetrazole**,** 3-amino 1,2,4-triazole, trimethylsilylacetylene, potassium carbonate, potassium acetate, sodium ascorbate, copper sulphate pentahydrate purchased from Sigma Aldrich Ltd, and used as received.

3.8.7. General procedure for the synthesis of azides (**GP-1**)**:** All azides were prepared following the reported procedures.[15] 4-(trifluoromethyl)azide (**1a**), 3-(trifluoromethyl)azide (**1b**), 4-fluoro-3-(trifluoromethyl)azide (**1c**), 4-chloro-3-(trifluoromethyl)azide (**1d**)**,** 4-bromo-3-(trifluoromethyl)azide (**1e**), 4-nitro-3-(trifluoromethyl)azide (**1f**), 4-azido-2-(trifluoromethyl)benzonitrile (**1g**)**,** 4-methyl-3-(trifluoromethyl)azide (**1h**)**,** 2-(trifluoromethyl) azide (**1i**), 4-nitro-2-(trifluoromethyl)azide (**1j**), 4-fluoro-2-(trifluoromethyl)azide (**1k**)**,** 4-chloro-2-(trifluoromethyl)azide (**1l**), and 2,6-dichloro-4-(trifluoromethyl)azide (**1m**) were prepared through the diazotization of their corresponding anilines with $NaNO_2$ and HCl at room temperature. Physical characterization data of these compounds are exactly matching with the reported values.[15]

3.8.8. General cycloaddition procedure (GP-2):

A mixture of azide (1.0 equiv), trimethylsilyl acetylene (1.5 equiv), potassium carbonate (1.2 equiv), $CuSO_4$ (0.2 equiv), and sodium ascorbate (0.4 equiv) were taken in methanol: water (1:1) in a 20 mL vial. The vial was sealed with screw cap and the resulting mixture was stirred rapidly at room temperature for 24 h. Upon completion of the reaction, aqueous ammonium hydroxide (5%) was added to the reaction mixture. The organic layer was separated; the aqueous layer was extracted with EtOAc (3 × 10 mL). The combined extracts were washed with water (2 × 10 mL), brine (5.0 mL) and dried over Na_2SO_4. Solvent was filtered and evaporated under the reduced pressure. The crude residue was purified using column chromatography on silica gel.

3.8.9. General procedure for the synthesis of compounds 3a–3m (GP-3):

A mixture of 98% sulphuric acid and 95% nitric acid was added to **2** at 0 °C and the reaction was performed under the respective conditions shown in the Table 2. Upon completion, the reaction mixture was cooled by the addition of ice and neutralized with saturated aqueous solution of $NaHCO_3$. The organic layer was separated and the aqueous layer was extracted with the minimum amount of EtOAc (3 × 20 mL). The combined extracts were washed with water (2 × 20 mL) and brine (25 mL) and dried over Na_2SO_4. The Solvent was filtered off and evaporated under vacuum. The crude residue was purified by column chromatography on silica gel to afford the desired nitration products in overall good yields.

3.8.10. General procedure for the synthesis of compounds 5-15 (GP-4):

A mixture of CuI (0.2 equiv), Cs_2CO_3 (2 equiv), 1H-1,2,3-triazole (1.5 equiv), and aryl/nitro-aryl triazole were taken in DMF (2.0 mL for 1 mmol of aryl-triazole) in a 10 mL vial under an argon atmosphere. The vial was sealed with screw cap and the resulting mixture was stirred at the respective temperature shown in Table 3 & 4 for 24 h. Upon completion of the reaction, the mixture was diluted with EtOAc (30 mL for 1.0 mmol), filtered through a pad of Celite and the solution was extracted with water (10 mL) for removal DMF. The organic layer was separated and the aqueous layer was extracted with EtOAc (3 × 10 mL). The combined extracts were washed with water (2 × 10 mL) and brine (5.0 mL) and dried over Na_2SO_4. Solvent was filtered and evaporated under the reduced pressure. The crude residue was purified by column chromatography on silica gel.

3.9. Spectral and Analytical Data of the Compounds:

1-(4-(Trifluoromethyl)phenyl)-1H-1,2,3-triazole (2a):[23]

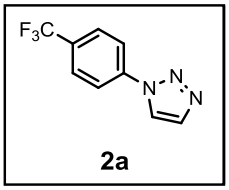

2a

Following the general procedure (GP-2); a mixture of 4-(trifluoromethyl)azide (**1a**; 2.0 g, 10.6 mmol), trimethylsilylacetylene (1.57 g, 16.0 mmol), K_2CO_3 (1.77 g, 12.8 mmol), sodium ascorbate (0.84 g, 4.27 mmol) and $CuSO_4$ (0.53 g, 2.13 mmol) in methanol : water (20 mL, 1:1) was stirred at room temperature for 24 h. Upon usual work-up, the crude mixture was purified by silica gel column chromatography eluting with hexane: ethyl acetate (2:1) to afford **2a** (1.79 g) in 79% yield as brown solid.

^{1}H NMR (400 MHz, $CDCl_3$): δ 8.11 (s, 1H), 7.90 (d, J = 8.4 Hz, 2H), 7.86 (s, 1H), 7.77 (d, J = 8.4 Hz, 2H); ^{13}C NMR (101 MHz, $CDCl_3$): δ 139.4, 134.9, 130.7 (q, J = 34.3 Hz), 127.1 (q, J = 2.0 Hz), 123.5 (q, J = 273 Hz), 121.8, 120.5; ^{19}F NMR (470 MHz, $CDCl_3$): δ −62.67.

1-(3-(Trifluoromethyl)phenyl)-1H-1,2,3-triazole (2b):[24]

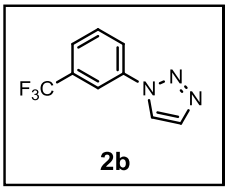

2b

Following the general procedure (GP-2); a mixture of 3-(trifluoromethyl)azide (**1b**; 5.0 g, 26.7 mmol), trimethylsilylacetylene (3.93 g, 40.0 mmol), K_2CO_3 (4.43 g, 32.0 mmol), sodium ascorbate (2.11 g, 10.6 mmol) and $CuSO_4$ (1.33 g, 5.34 mmol) in methanol : water (53 mL, 1:1) was stirred at room temperature for 24 h. Upon usual work-up, the crude mixture was purified by silica gel column chromatography eluting with hexane: ethyl acetate (2:1) to afford **2b** (3.10 g) in 55% yield as brown solid.

^{1}H NMR (400 MHz, $CDCl_3$): δ 8.10 (s, 1H), 8.04 (s, 1H), 7.99 (bd, J = 7.6 Hz, 1H), 7.91 (s, 1H), 7.76–7.66 (m, 2H); ^{13}C NMR (101 MHz, $CDCl_3$): δ 137.4, 132.3 (q, J = 33.3 Hz), 130.6, 125.3 (q, J = 3.0 Hz), 123.6, 123.3 (q, J = 274 Hz), 117.5 (q, J = 3.0 Hz); ^{19}F NMR (470 MHz, $CDCl_3$): δ −62.87.

1-(4-Fluoro-3-(trifluoromethyl)phenyl)-1H-1,2,3-triazole (2c):

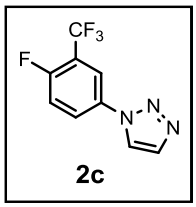

2c

Following the general procedure (GP-2); a mixture of 4-fluoro-3-(trifluoromethyl)azide (**1c**; 4.0 g, 19.5 mmol), trimethylsilylacetylene (2.87 g, 29.2 mmol), K_2CO_3 (3.23 g, 23.4 mmol), sodium ascorbate (1.54 g, 7.80 mmol) and $CuSO_4$ (0.97 g, 3.90 mmol) in methanol : water (40 mL, 1:1) was stirred at room temperature for 24 h. Upon usual work-up, the crude mixture was purified by silica gel column chromatography eluting with hexane: ethyl acetate (2:1) to afford **2c (**2.53 g) in 66% yield as brown solid.

2.53 g, 66% yield, brown solid, m.p. 91 °C; DTA = 212 °C; R_f = 0.70 (*n*-hexane/EtOAc, 2:1); ^{1}H NMR (400 MHz, $CDCl_3$): δ 8.09 (s, 1H), 8.04–7.98 (m, 1H), 7.98–7.92 (m, 1H), 7.85 (s, 1H), 7.38 (t, J = 8.8 Hz, 1H); ^{13}C NMR (101 MHz, $CDCl_3$): δ 159.2 (d, J = 260 Hz), 135.0, 133.2, 126.0 (d, J = 8.1 Hz), 122.2, 121.7 (q, J = 274 Hz), 119.9 (q, J = 35.3 Hz), 119.76 (q, J = 4.0 Hz), 119.74 (q, J = 32.3 Hz); ^{19}F NMR (376 MHz, $CDCl_3$): δ −61.77 (d, J = 15 Hz), −113.51 (m); IR (KBr): ν_{max} = 3084, 1631, 1340, 1236, 1043, 997, 839, 788, 680, 540 cm^{-1}; MS (EI): *m/z* (%): 232 (100) $[M+1]^+$; Elemental analysis calcd (%) for $C_9H_5F_4N_3$: C 46.76, H 2.18, N 18.18; found: C 46.58, H 2.25, N 18.26.

1-(4-Chloro-3-(trifluoromethyl)phenyl)-1H-1,2,3-triazole (2d):[23]

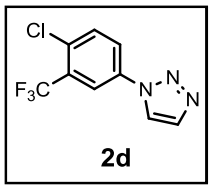

Following the general procedure (GP-2); a mixture of 4-chloro-3-(trifluoromethyl)azide (**1d**; 10.0 g, 45.1 mmol), trimethylsilylacetylene (4.67 g, 67.7 mmol), K_2CO_3 (7.48 g, 54.1 mmol), sodium ascorbate (3.57 g, 18.0 mmol) and $CuSO_4$ (2.25 g, 9.02 mmol) in methanol : water (90 mL, 1:1) was refluxed at 100 °C for 24 h. Upon usual work-up, the crude mixture was purified by silica gel column chromatography eluting with hexane: ethyl acetate (4:1) to afford **2d (**2.14 g) in 43% yield as brown solid.

^{1}H NMR (400 MHz, $CDCl_3$): δ 8.12 (bs, 2H), 7.93 (d, J = 8.0 Hz, 2H), 7.70 (d, J = 8.0 Hz, 1H); ^{13}C NMR (101 MHz, $CDCl_3$): δ 135.6, 133.1, 132.4 (q, J = 2.0 Hz), 130.6, 130.0 (q, J = 32.3 Hz), 125.4 (q, J = 2.02 Hz), 124.5, 122.1 (q, J = 275 Hz), 119.7 (q, J = 5.1 Hz); ^{19}F NMR (470 MHz, $CDCl_3$): δ −63.08.

1-(4-Bromo-3-(trifluoromethyl)phenyl)-1H-1,2,3-triazole (2e):

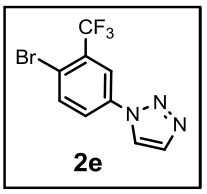

Following the general procedure (GP-2); a mixture of 4-bromo-3-(trifluoromethyl)azide (**1e**; 0.98 g, 3.70 mmol), trimethylsilylacetylene (0.54 g, 5.56 mmol), K_2CO_3 (0.61 g, 4.45 mmol), sodium ascorbate (0.29 g, 1.48 mmol) and $CuSO_4$ (0.18 g, 0.74 mmol) in methanol : water (8.0 mL, 1:1) was stirred at room temperature for 24 h. Upon usual work-up, the crude mixture was purified by silica gel column chromatography eluting with hexane: ethyl acetate (1:1) to afford **2e** (0.96 g) in 89% yield as brown solid.

0.96 g, 89% yield, brown solid, m.p. 83 °C; DTA = 220 °C; R_f = 0.61 (*n*-hexane/EtOAc, 1:1); ^{1}H NMR (400 MHz, $CDCl_3$): δ 8.10 (bs, 1H), 8.08 (bd, J = 1.6 Hz, 1H), 7.89–7.85 (m, 2H), 7.81 (dd, J = 2.4, 8.8 Hz, 1H); ^{13}C NMR (101 MHz, $CDCl_3$): δ 136.5, 136.1, 135.1, 131.8 (q, J = 32 Hz), 124.4, 122.2 (q, J = 275 Hz), 121.7, 119.8 (q, J = 6.1 Hz); ^{19}F NMR (376 MHz, $CDCl_3$): δ −63.10; IR (KBr): ν_{max} = 3123, 1500, 1334, 1259, 1141, 1030, 995, 777, 661 cm^{-1}; MS (EI): *m/z* (%): 293 (8) [M^++2], 292 (92) [M^++1], 291 (57) [M^+], 290 (100) [M^+−1], 275 (31); Elemental analysis calcd (%) for $C_9H_5BrF_3N_3$: C 37.01, H 1.73, N 14.39; found: C 37.12, H 1.86, N 14.25.

1-(4-Nitro-3-(trifluoromethyl)phenyl)-1H-1,2,3-triazole (2f):

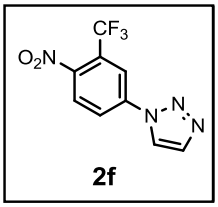

2f

Following the general procedure (GP-2); a mixture of 4-nitro-3-(trifluoromethyl)azide (**1f**; 4.57 g, 19.6 mmol), trimethylsilylacetylene (2.90 g, 29.4 mmol), K_2CO_3 (3.26 g, 23.5 mmol), sodium ascorbate (1.55 g, 7.84 mmol) and $CuSO_4$ (0.98 g, 3.92 mmol) in *t*-BuOH : water (40 mL, 1:1) was refluxed at 90 °C for 48 h. Upon usual work-up, the crude mixture was purified by silica gel column chromatography eluting with hexane: ethyl acetate (1:1) to afford **2f (**1.21 g) in 24% yield as yellow solid.

1.21 g, 24% yield, yellow solid, m.p. 81 °C; DTA = 301 °C; R_f = 0.69 (*n*-hexane/EtOAc, 1:1); ^{1}H NMR (400 MHz, $CDCl_3$): δ 8.31 (bs, 1H), 8.23 (s, 1H), 8.19 (dd, J = 1.6, 8.8 Hz, 1H), 8.14 (d, J = 8.8 Hz, 1H), 7.94 (s, 1H); ^{13}C NMR (101 MHz, $CDCl_3$): δ 146.9, 139.6, 135.5, 127.4, 126.0 (q, J = 35.3 Hz), 123.8, 121.9, 121.3 (q, J = 275 Hz), 119.6 (q, J = 5.0 Hz); ^{19}F NMR (376 MHz, $CDCl_3$): δ −60.18; IR (KBr): ν_{max} = 3142, 1543, 1358, 1182, 1145, 1032, 895, 846, 777 cm^{-1}; MS (EI): *m/z* (%): 259 (100) $[M+1]^+$, 241 (5), 225 (3), 117 (2), 95 (4); Elemental analysis calcd (%) for $C_9H_5F_3N_4O_2$: C 41.87, H 1.95, N 21.70; found: C 41.68, H 1.87, N 21.54.

4-(1H-1,2,3-Triazol-1-yl)-2-(trifluoromethyl)benzonitrile (2g):

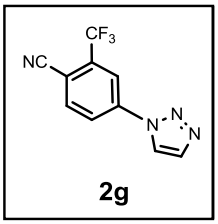

2g

Following the general procedure (GP-2); a mixture of 4-azido-2-(trifluoromethyl)benzonitrile (**1g**; 4.5 g, 21.2 mmol), trimethylsilylacetyl ene (3.12 g, 31.8 mmol), K_2CO_3 (3.51 g, 25.4 mmol), sodium ascorbate (1.68 g, 8.48 mmol) and $CuSO_4$ (1.05 g, 4.24 mmol) in methanol : water (42 mL, 1:1) was stirred at room temperature for 24 h. Upon usual work-up, the crude mixture was purified by silica gel column chromatography eluting with hexane: ethyl acetate (1:1) to afford **2g** (2.67 g) in 52% yield as yellow solid.

2.67 g, 52% yield, yellow solid, m.p. 122 °C; DTA = 254 °C; R_f = 0.70 (*n*-hexane/EtOAc, 1:1); ^{1}H NMR (400 MHz, $CDCl_3$): δ 8.29 (d, J = 1.6 Hz, 1H), 8.25 (s, 1H), 8.16 (dd, J = 2.0, 8.4 Hz, 1H), 8.05 (d, J = 8.4 Hz, 1H), 7.92 (s, 1H); ^{13}C NMR (101 MHz, $CDCl_3$): δ 139.8, 136.6, 135.5, 134.9 (q, J = 33.3 Hz), 123.1, 121.9, 121.6 (q, J = 278 Hz), 118.4 (q, J = 5.1 Hz), 114.5, 109.6; ^{19}F NMR (376 MHz, $CDCl_3$): δ −62.24; IR (KBr): ν_{max} = 3128, 2233, 1616, 1512, 1435, 1336, 1184, 1037, 850, 788, 677, 555 cm^{-1}; MS (EI): *m/z* (%): 240 (83) $[M+1]^+$, 237 (29), 147 (100); Elemental analysis calcd (%) for $C_{10}H_5F_3N_4$: C 50.43, H 2.12, N 23.52; found: C 50.31, H 2.18, N 23.43.

1-(4-Methyl-3-(trifluoromethyl)phenyl)-1H-1,2,3-triazole (2h):

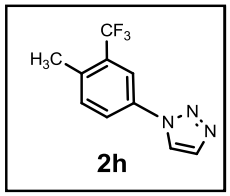

2h

Following the general procedure (GP-2); a mixture of 4-methyl-3-(trifluoromethyl)azide (**1h**; 3.1 g, 15.4 mmol), trimethylsilylacetylene (2.26 g, 23.1 mmol), K_2CO_3 (2.55 g, 18.4 mmol), sodium ascorbate (1.31 g, 6.16 mmol) and $CuSO_4$ (0.76 g, 3.08 mmol) in methanol : water (30 mL, 1:1) was stirred at room temperature for 24 h. Upon usual work-up, the crude mixture was purified by silica gel column chromatography eluting with hexane: ethyl acetate (2:1) to afford **2h** (1.84 g) in 53% yield as brown solid.

1.84 g, 53% yield, brown solid, m.p. 92 °C; DTA = 228 °C; R_f = 0.64 (*n*-hexane/EtOAc, 2:1); ^{1}H NMR (400 MHz, $CDCl_3$): δ 8.05 (s, 1H), 7.98 (s, 1H), 7.87 (s, 1H), 7.81 (dd, J = 2.0, 8.4 Hz, 1H), 7.46 (d, J = 8.4 Hz, 1H), 2.54 (s, 3H); ^{13}C NMR (101 MHz, $CDCl_3$): δ 137.5, 134.9, 133.4, 130.3 (q, J = 32.3 Hz), 125.0, 123.7 (q, J = 274.7 Hz), 123.5, 121.9, 118.2 (q, J = 6.1 Hz), 19.0; ^{19}F NMR (376 MHz, $CDCl_3$): δ −62.19; IR (KBr): ν_{max} = 3130, 1518, 1429, 1334, 1313, 1172, 1045, 837, 794, 677, 536 cm^{-1}; MS (EI): *m/z* (%): 228 (100) $[M+1]^+$, 161 (8), 147 (7), 109 (5), 91 (5), 65 (10); Elemental analysis calcd (%) for $C_{10}H_8F_3N_3$: C 52.87, H 3.55, N 18.50; found: C 52.71, H 3.63, N 18.39.

1-(2-(Trifluoromethyl)phenyl)-1H-1,2,3-triazole (2i):

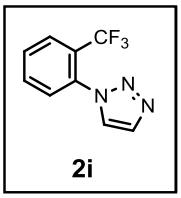

2i

Following the general procedure (GP-2); a mixture of 2-(trifluoromethyl)azide (**1i**; 0.50 g, 2.67 mmol), trimethylsilylacetylene (0.39 g, 4.01 mmol), KOAc (0.31 g, 3.20 mmol), sodium ascorbate (0.21 g, 1.06 mmol) and $CuSO_4$ (0.13 g, 0.53 mmol) in *t*-BuOH : water (6.0 mL, 1:1) was refluxed at 90 °C for 48 h. Upon usual work-up, the crude mixture was purified by silica gel column chromatography eluting with hexane: ethyl acetate (2:1) to afford **2i** (0.36 g) in 31% yield as brown liquid.

0.36 g, 31% yield, browm liquid, R_f = 0.59 (*n*-hexane/EtOAc, 2:1); ^{1}H NMR (400 MHz, $CDCl_3$): δ 7.91–7.86 (m, 3H), 7.80–7.68 (m, 2H), 7.58 (d, J = 7.6 Hz, 1H); ^{13}C NMR (101 MHz, $CDCl_3$): δ 134.9, 133.7, 133.1, 130.4, 129.1, 127.3 (q, J = 5.1 Hz), 126.2 (q, J = 32.3 Hz), 126.3, 122.6 (q, J = 275 Hz); ^{19}F NMR (470 MHz, $CDCl_3$): δ −64.18; IR (neat): ν_{max} = 3124, 1618, 1525, 1450, 1415, 1236, 1032, 856, 596 cm^{-1}; MS (EI): *m/z* (%): 214 (100) $[M+1]^+$, 201 (3), 174 (2), 156 (2); Elemental analysis calcd (%) for $C_9H_6F_3N_3$: C 50.71, H 2.84, N 19.71; found: C 50.61, H 2.79, N 19.58.

1-(4-Nitro-2-(trifluoromethyl)phenyl)-1H-1,2,3-triazole (2j):

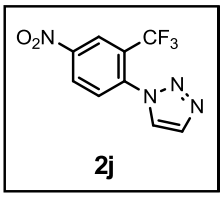

2j

Following the general procedure (GP-2); a mixture of 4-nitro-2-(trifluoromethyl)azide (**1j**; 2.0 g, 8.61 mmol), trimethylsilylacetylene (1.26 g, 12.9 mmol), KOAc (1.01 g, 10.3 mmol), sodium ascorbate (0.68 g, 3.44 mmol) and $CuSO_4$ (0.43 g, 1.72 mmol) in *t*-BuOH : water (18 mL, 1:1) was refluxed at 70 °C for 24 h. Upon usual work-up, the crude mixture was purified by silica gel column chromatography eluting with hexane: ethyl acetate (1:1) to afford **2j** (0.28 g) in 21% yield as brown solid.

0.28 g, 21% yield, brown solid, m.p.109 °C; DTA = 228 °C; R_f = 0.69 (*n*-hexane/EtOAc, 1:1); ^{1}H NMR (400 MHz, $CDCl_3$): δ 8.76 (bd, J = 2.0 Hz, 1H), 8.62 (dd, J = 2.0, 8.4 Hz, 1H), 7.98 (s, 1H), 7.92 (s, 1H), 7.88 (d, J = 8.8 Hz, 1H); ^{13}C NMR (101 MHz, $CDCl_3$): δ 148.1, 139.6, 134.4, 130.5, 128.0, 127.1 (q, J = 33.3 Hz), 126.1 (q, J = 2.0 Hz), 123.2 (q, J = 5.5 Hz), 121.4 (q, J = 275 Hz); ^{19}F NMR (376 MHz, $CDCl_3$): δ –59.44; IR (KBr): ν_{max} = 3138, 2924, 1626, 1539, 1352, 1236, 1053, 914, 794 cm^{-1}; MS (EI): *m/z* (%): 259 (100) $[M+1]^+$, 241 (21), 233 (13), 217 (18), 203 (4); Elemental analysis calcd (%) for $C_9H_5F_3N_4O_2$: C 41.87, H 1.95, N, 21.70; found: C 41.65, H 1.91, N 21.56.

1-(4-Fluoro-2-(trifluoromethyl)phenyl)-1H-1,2,3-triazole (2k):

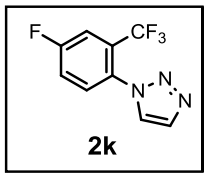

2k

Following the general procedure (GP-2); a mixture of 4-fluoro-2-(trifluoromethyl)azide (**1k**; 4.0 g, 19.5 mmol), trimethylsilylacetylene (2.87 g, 29.2 mmol), K_2CO_3 (3.23 g, 23.4 mmol), sodium ascorbate (1.54 g, 7.80 mmol) and $CuSO_4$ (0.97 g, 3.90 mmol) in methanol : water (40 mL, 1:1) was stirred at room temperature for 24 h. Upon usual work-up, the crude mixture was purified by silica gel column chromatography eluting with hexane: ethyl acetate (2:1) to afford **2k** (0.91 g) in 27% yield as brown solid.

0.91 g, 27% yield, brown solid, m.p. 142 °C; DTA = 195 °C; R_f = 0.67 (*n*-hexane/EtOAc, 2:1); ^{1}H NMR (400 MHz, $CDCl_3$): δ 7.82 (s, 1H), 7.74–7.73 (m, 1H), 7.48–7.45 (m, 2H), 7.38–7.34 (m, 1H); ^{13}C NMR (101 MHz, $CDCl_3$): δ 162.5 (d, J = 255 Hz), 134.8, 133.6, 131.4 (d, J = 9.09 Hz), 130.8, 128.2 (dq, J = 8.08, 33.3 Hz), 126.6, 126.0 (d, J = 9.1 Hz), 122.3, 121.7 (q, J = 276 Hz), 120.0 (q, J = 20.2 Hz), 118.5 (d, J = 23.2 Hz), 114.9 (qq, J = 5.1, 27.2 Hz); ^{19}F NMR (376 MHz, $CDCl_3$): δ –59.89, –106.89 (m); IR (KBr): ν_{max} = 3130, 1620, 1429, 1315, 1292, 1174, 1053, 904, 837, 787 cm^{-1}; MS (EI): *m/z* (%): 232 (100)

[*M*+1]$^+$, 214 (18), 200 (8); Elemental analysis calcd (%) for $C_9H_5F_4N_3$: C 46.76, H 2.18, N 18.18; found: C 46.65, H, 2.09, N 18.25.

1-(4-chloro-2-(trifluoromethyl)phenyl)-1H-1,2,3-triazole (2l):

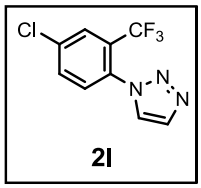

Following the general procedure (GP-2); a mixture of 4-chloro-2-(trifluoromethyl)azide (**1l**; 10.0 g, 45.1 mmol), trimethylsilylacetylene (4.67 g, 67.7 mmol), K_2CO_3 (7.48 g, 54.1 mmol), sodium ascorbate (3.57 g, 18.05 mmol) and $CuSO_4$ (2.25 g, 9.02 mmol) in methanol : water (90 mL, 1:1) was refluxed at 80 °C for 24 h. Upon usual work-up, the crude mixture was purified by silica gel column chromatography eluting with hexane: ethyl acetate (4:1) to afford **2l** (1.25 g) in 22% yield as dark brown liquid.

1.25 g, 22% yield, brown liquid, R_f = 0.54 (*n*-hexane/EtOAc, 4:1); ^{1}H NMR (400 MHz, $CDCl_3$): δ 7.88–7.87 (m, 3H), 7.73 (d, *J* = 8.4, 1H), 7.53 (d, *J* = 8.8, 1H); ^{13}C NMR (127 MHz, $CDCl_3$): δ 136.6, 133.1, 133.0 (q, *J* = 34.3), 130.3, 127.5 (q, *J* = 2.5 Hz), 124.4, 122.1 (q, *J* = 277 Hz), 121.7 (q, *J* = 277 Hz), 119.6 (q, *J* = 5.1); ^{19}F NMR (470 MHz, $CDCl_3$): δ –59.64; IR (KBr): ν_{max} = 3354, 1589, 1475, 1412, 889, 821, 719, 638, 561 cm^{-1}; MS (EI): *m/z* (%): 247 (100) [M^+]; elemental analysis calcd (%) for $C_9H_5ClF_3N_3$: C 43.66, H 2.04, N 16.97; found: C 43.52, H 2.12, N 16.85.

1-(2,6-Dichloro-4-(trifluoromethyl)phenyl)-1H-1,2,3-triazole (2m):

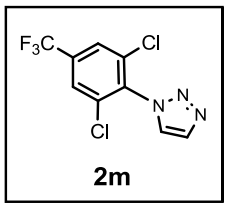

Following the general procedure (GP-2); reaction of 2,6-dichloro-4-(trifluoromethyl)azide (**1m**; 5.0 g, 19.5 mmol), trimethylsilylacetylene (2.02 g, 29.2 mmol), K_2CO_3 (3.23 g, 23.4 mmol), sodium ascorbate (1.54 g, 7.81 mmol) and $CuSO_4$ (0.97 g, 3.90 mmol) in methanol : water (40 mL, 1:1) was stirred at room temperature for 24 h. Upon usual work-up, the crude mixture was purified by silica gel column chromatography eluting with hexane: ethyl acetate (4:1) to afford **2m (**1.54 g) in 28% yield as brown solid.

1.54 g, 28% yield, brown solid, m.p. 162 °C; DTA = 206 °C; R_f = 0.59 (*n*-hexane/EtOAc, 4:1); ^{1}H NMR (400 MHz, $CDCl_3$): δ 7.92 (s, 1H), 7.81 (s, 1H), 7.78 (s, 2H); ^{13}C NMR (101 MHz, $CDCl_3$): δ 136.2, 134.9, 134.1 (q, *J* = 35.3 Hz), 133.9, 126.0 (q, *J* = 4.0 Hz), 125.7, 121.9 (q, *J* = 275 Hz); ^{19}F NMR (470 MHz, $CDCl_3$): δ –63.28; IR (KBr): ν_{max} = 3061, 1570, 1516, 1398, 1302, 1186, 1024, 883, 806, 709, 532 cm^{-1}; MS (EI): *m/z* (%): 283 (100) [*M*+2]$^+$, 255 (6), 249 (8), 221 (5); Elemental analysis calcd (%) for $C_9H_4Cl_2F_3N_3$: C 38.33, H 1.43, N 14.90; found: C 38.45, H 1.52, N 14.71.

1-(2-Nitro-4-(trifluoromethyl)phenyl)-1H-1,2,3-triazole (3a):

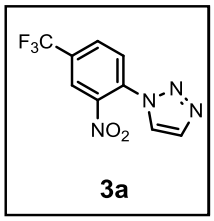

3a

Following the general procedure (GP-3); a mixture of 98% sulphuric acid (15 mL) and 95% nitric acid (10 mL) was added to 1-(4-(trifluoromethyl)phenyl)-1H-1,2,3-triazole (**2a**; 0.80 g, 3.75 mmol) at 0 °C. The resulting mixture was refluxed at 90 °C for 24 h. Upon usual work-up, the crude mixture was purified by silica gel column chromatography eluting with hexane: ethyl acetate (2:1) to afford **3a (**0.58 g) in 60% yield as yellow solid.

0.58 g, 60% yield, yellow solid, m.p. 101 °C; DTA = 237 °C; R_f = 0.57 (*n*-hexane/EtOAc, 2:1); ^{1}H NMR (400 MHz, $CDCl_3$): δ 8.32 (bd, J = 1.6 Hz, 1H), 8.07 (dd, J = 1.6, 8.4 Hz, 1H), 7.96 (bd, J = 0.8 Hz, 1H), 7.88 (bd, J = 1.2 Hz, 1H), 7.83 (d, J = 8.4 Hz, 1H); ^{13}C NMR (101 MHz, $CDCl_3$): δ 144.2, 134.6, 132.8 (q, J = 35.3 Hz), 132.6, 130.7 (q, J = 3.0 Hz), 128.5, 125.2, 122.2 (q, J = 275 Hz), 123.0 (q, J = 3.0 Hz); ^{19}F NMR (470 MHz, $CDCl_3$): δ –63.00; IR (KBr): ν_{max} = 3140, 1510, 1265, 1055, 1026, 914, 850, 792 cm^{-1}; MS (EI): *m/z* (%): 259 (100) $[M+1]^+$, 241 (21), 233 (11), 217 (16), 203 (3); Elemental analysis calcd (%) for $C_9H_5F_3N_4O_2$: C 41.87, H 1.95, N 21.70; found: C 41.96, H 1.91, N 21.82.

1-(3-Nitro-5-(trifluoromethyl)phenyl)-1H-1,2,3-triazole (3b) and 1-(4-Nitro-3-(trifluoromethyl)phenyl)-1H-1,2,3-triazole (3b'):

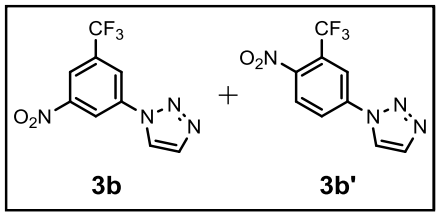

3b **3b'**

Following the general procedure (GP-3); a mixture of 98% sulphuric acid (15 mL) and 95% nitric acid (10 mL) was added to 1-(3-(trifluoromethyl)phenyl)-1H-1,2,3-triazole (**2b**; 2.0 g, 3.75 mmol) at 0 °C. The resulting mixture was refluxed at 80 °C for 12 h. Upon usual work-up, the crude mixture was purified by silica gel column chromatography eluting with hexane: ethyl acetate (2:1) to afford **3b** (0.46 g) in 19% yield and **3b'** (1.01 g) in 42% yield as yellow solids.

For **3b**: 0.46 g, 19% yield, yellow solid, m.p. 129 °C; DTA = 213 °C; R_f = 0.62 (*n*-hexane/EtOAc, 2:1); ^{1}H NMR (400 MHz, $CDCl_3$): δ 8.84 (s, 1H), 8.58 (s, 1H), 8.50 (s, 1H), 8.20 (bd, J = 1.2 Hz, 1H), 7.98 (bd, J = 1.2 Hz, 1H); ^{13}C NMR (101 MHz, $CDCl_3$): δ 149.2, 138.4, 135.5, 134.1 (q, J = 34.3 Hz), 122.2 (q, J = 275 Hz), 122.7 (q, J = 2.0 Hz), 121.9, 120.1 (q, J = 2.0 Hz), 118.1; ^{19}F NMR (470 MHz, $CDCl_3$): δ –63.00; IR (KBr): ν_{max} = 3105, 1601, 1433, 1240, 1045, 997, 862, 783, 692 cm^{-1}; MS (EI): *m/z* (%): 259 (100) $[M+1]^+$, 220

(5), 119 (3), 106 (46), 97 (14), 74 (8); Elemental analysis calcd (%) for $C_9H_5F_3N_4O_2$: C 41.87, H 1.95, N 21.70; found: C 41.72, H 2.05, N 21.85.

For **3b':** 1.01 g, 42% yield, yellow solid, m.p. 73 °C; DTA = 308 °C; R_f = 0.61 (*n*-hexane/EtOAc, 1:1); ^{1}H NMR (400 MHz, $CDCl_3$): δ 9.15 (bd, J = 0.8 Hz, 1H), 8.53 (s, 1H), 8.52 (bd, J = 2 Hz, 1H), 8.41 (d, J = 6.8 Hz, 1H), 8.07 (bd, J = 0.8 Hz, 1H); ^{13}C NMR (127 MHz, $CDCl_3$): δ 146.5, 139.8, 135.6, 128.3, 125.2, 124.6, 123.8 (q, J = 34.3 Hz), 122.0 (q, J = 277 Hz), 119.6 (q, J = 5.1 Hz); ^{19}F NMR (470 MHz, $CDCl_3$): δ –59.07; IR (KBr): ν_{max} = 3130, 1548, 1433, 1240, 1045, 997, 862, 783, 746, 692 cm^{-1}; MS (EI): *m/z* (%): 259 (100) $[M+1]^+$, 241 (3); Elemental analysis calcd (%) for $C_9H_5F_3N_4O_2$: C 41.87, H 1.95, N 21.70. found: C 41.73, H 1.91, N 21.82.

1-(4-Fluoro-3-nitro-5-(trifluoromethyl)phenyl)-1H-1,2,3-triazole (3c):

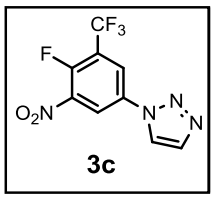

3c

Following the general procedure (GP-3); a mixture of 98% sulphuric acid (15 mL) and 95% nitric acid (10 mL) was added to 1-(4-fluoro-3-(trifluoromethyl)phenyl)-1H-1,2,3-triazole (**2c**; 1.0 g, 4.32 mmol) at 0 °C. The resulting mixture was refluxed at 95 °C for 12 h. Upon usual work-up, the crude mixture was purified by silica gel column chromatography eluting with hexane: ethyl acetate (2:1) to afford **3c** (0.52 g) in 44% yield as brown solid.

0.52 g, 44% yield, brown solid, m.p.101 °C; DTA = 238 °C; R_f = 0.72 (*n*-hexane/EtOAc, 2:1); ^{1}H NMR (400 MHz, $CDCl_3$): δ 8.67 (dd, J = 2.8, 6.0 Hz, 1H), 8.43 (dd, J = 2.8, 4.8 Hz, 1H), 8.19 (bd, J = 0.8 Hz, 1H), 7.94 (bd, J = 0.8 Hz, 1H); ^{13}C NMR (101 MHz, $CDCl_3$): δ 152.4 (d, J = 279 Hz), 138.7 (d, J = 8.1 Hz), 135.7, 132.9, 124.1, 123.2 (dd, J = 13.1, 35.3 Hz), 121.9, 121.0, 120.8 (q, J = 277 Hz); ^{19}F NMR (470 MHz, $CDCl_3$): δ –61.48 (d, J = 18.8 Hz), –119.1 (m); IR (KBr): ν_{max} = 1616, 1508, 1344, 1010, 895, 787, 682, 454 cm^{-1}; MS (EI): *m/z* (%): 277 (100) $[M+1]^+$, 261 (11), 247 (47), 219 (34), 202 (3), 89 (3); Elemental analysis calcd (%) for $C_9H_4F_4N_4O_2$: C 39.14, H 1.46, N 20.29; found: C 39.25, H 1.41, N 20.15.

1-(4-Chloro-3-nitro-5-(trifluoromethyl)phenyl)-1H-1,2,3-triazole (3d):

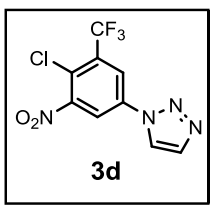

3d

Following the general procedure (GP-3); a mixture of 98% sulphuric acid (15 mL) and 95% nitric acid (10 mL) was added to 1-(4-chloro-3-(trifluoromethyl)phenyl)-1H-1,2,3-triazole (**2d**; 1.45 g, 5.85 mmol) at 0 °C. The resulting mixture was refluxed at 70 °C for 12 h. Upon usual

work-up, the crude mixture was purified by silica gel column chromatography eluting with hexane: ethyl acetate (2:1) to afford **3d** (0.51 g) in 30% yield as colorless solid.

0.51 g, 30% yield, colorless solid, m.p. 116 °C; DTA = 250 °C; R_f = 0.51 (*n*-hexane/EtOAc, 2:1); ^{1}H NMR (400 MHz, $CDCl_3$): δ 8.41 (bd, J = 2.4 Hz, 1H), 8.40 (bd, J = 2.4 Hz, 1H), 8.18 (bs, 1H), 7.94 (bs, 1H); ^{13}C NMR (101 MHz, $CDCl_3$): δ 150.8, 135.7, 132.8 (q, J = 32.3 Hz), 125.0, 121.8 (q, J = 6.1 Hz), 121.7, 121.3 (q, J = 276 Hz), 119.3, 118.1; ^{19}F NMR (376 MHz, $CDCl_3$): δ –62.70; IR (KBr): ν_{max} = 2924, 1554, 1493, 1361, 1232, 1194, 1047, 906, 815, 756, 690, 549 cm^{-1}; MS (EI) *m/z* (%) 293 (5) [M^++2], 292 (42) [M^++1], 291 (26) [M^+], 290 (100) [M^+–1], 275 (13); Elemental analysis calcd (%) for $C_9H_4ClF_3N_4O_2$: C 36.94, H 1.38, N 19.15; found: C 36.85, H 1.31, N 19.26.

1-(4-Bromo-3-nitro-5-(trifluoromethyl)phenyl)-1H-1,2,3-triazole (3e):

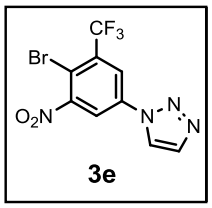

3e

Following the general procedure (GP-3); a mixture of 98% sulphuric acid (15 mL) and 95% nitric acid (10 mL) was added to 1-(4-bromo-3-(trifluoromethyl)phenyl)-1H-1,2,3-triazole (**2e**; 0.80 g, 2.73 mmol) at 0 °C. The resulting mixture was refluxed at 80 °C for 6 h. Upon usual work-up, the crude mixture was purified by silica gel column chromatography eluting with hexane: ethyl acetate (2:1) to afford **3e** (0.31 g) in 38% yield as pale yellow solid.

0.31 g, 38% yield, pale yellow solid, m.p.167 °C; DTA = 245 °C; R_f = 0.51 (*n*-hexane/EtOAc, 1:1); ^{1}H NMR (400 MHz, [D_6]DMSO): δ 9.07 (bd, J = 1.2 Hz, 1H), 8.93 (bd, J = 2.0 Hz, 1H), 8.58 (bd, J = 2.0 Hz, 1H), 8.04 (bd, J = 1.2 Hz, 1H); ^{13}C NMR (101 MHz, [D_6]DMSO): δ 153.5, 137.1, 135.6, 132.4 (q, J = 33.3 Hz), 124.5, 122.3 (q, J = 273 Hz), 122.2 (q, J = 5.1 Hz), 119.8, 110.6; ^{19}F NMR (470 MHz, [D_6]DMSO): δ –61.42; IR (KBr): ν_{max} = 3142, 1539, 1479, 1342, 1296, 1240, 1049, 1005, 912, 783, 696, 474 cm^{-1}; MS (EI): *m/z* (%): 340 (16) [M^++2], 339 (84) [M^++1], 338 (53) [M^+], 337 (100) [M^+–1], 335 (3), 309 (3); Elemental analysis calcd (%) for $C_9H_4BrF_3N_4O_2$: C 32.07, H 1.20, N 16.62; found: C 32.12, H 1.28, N 16.75.

2-Nitro-4-(1H-1,2,3-triazol-1-yl)-6-(trifluoromethyl)benzonitrile (3g):

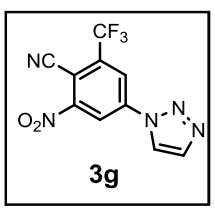

3g

Following the general procedure (GP-3); a mixture of 98% sulphuric acid (15 mL) and 95% nitric acid (10 mL) was added to 4-(1H-1,2,3-triazol-1-yl)-2-(trifluoromethyl)benzonitrile (**2g**; 0.30 g, 1.25 mmol) at 0 °C. The resulting mixture was refluxed at 60 °C for 6 h. Upon usual work-up, the

crude mixture was purified by silica gel column chromatography eluting with hexane: ethyl acetate (1:1) to afford **3g** (0.08 g) in 23% yield as dark brown oil.

0.08 g, 23% yield, dark brown oil, R_f = 0.72 (*n*-hexane/EtOAc, 1:1); ^{1}H NMR (400 MHz, [D$_6$]DMSO): δ 8.62 (s, 2H), 7.94 (s, 1H), 7.62–7.54 (m, 1H); ^{13}C NMR (101 MHz, [D$_6$]DMSO): δ 162.8, 159.2, 138.3, 132.5 (q, J = 2.0 Hz), 131.9 (d, J = 10 Hz), 129.7, 129.2 (d, J = 12 Hz), 127.5, 124.1, 121.2 (q, J = 277 Hz), 119.4 (q, J = 34.3 Hz); ^{19}F NMR (376 MHz, [D$_6$]DMSO): δ –56.73; IR (KBr): ν_{max} = 3128, 2233, 1616, 1512, 1435, 1315, 1182, 1037, 852, 790 cm^{-1}; MS (EI): *m/z* (%): 285 (53) [*M*+2]$^+$, 284 (100) [*M*+1]$^+$, 147 (5); Elemental analysis calcd (%) for $C_{10}H_4F_3N_5O_2$: C 42.42, H 1.42, N 24.73; found: C 42.51, H 1.38, N 24.65.

1-(4-Methyl-3-nitro-5-(trifluoromethyl) phenyl)-1H-1,2,3-triazole (3h):

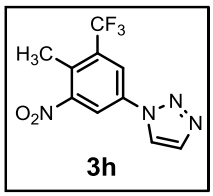

3h

Following the general procedure (GP-3); a mixture of 98% sulphuric acid (15 mL) and 95% nitric acid (10 mL) was added to 1-(4-methyl-3-(trifluoromethyl)phenyl)-1H-1,2,3-triazole (**2h**; 1.15 g, 5.06 mmol) at 0 °C. The resulting mixture was stirred at room temperature for 12 h. Upon usual work-up, the crude mixture was purified by silica gel column chromatography eluting with hexane: ethyl acetate (4:1) to afford **3h** (1.26 g) in 92% yield as pale yellow solid.

1.26 g, 92% yield, pale yellow solid, m.p. 122 °C; DTA = 233 °C; R_f = 0.61 (*n*-hexane/EtOAc, 4:1); ^{1}H NMR (400 MHz, $CDCl_3$): δ 8.36 (d, J = 8.0 Hz, 2H), 8.19 (s, 1H), 7.91 (s, 1H), 2.62 (s, 3H); ^{13}C NMR (101 MHz, $CDCl_3$): δ 152.5, 135.3, 133.3 (q, J = 32.3 Hz), 131.4, 122.6 (q, J = 278 Hz), 121.7, 121.2 (q, J = 6.1 Hz), 118.6, 14.7; ^{19}F NMR (376 MHz, $CDCl_3$): δ –61.12; IR (KBr): ν_{max} = 3034, 1545, 1504, 1334, 1286, 1170, 1051, 900, 790, 679 cm^{-1}; MS (EI): *m/z* (%): 273 (100) [*M*+1]$^+$; Elemental analysis calcd (%) for $C_{10}H_7F_3N_4O_2$: C 44.13, H 2.59, N 20.58; found: C 44.26, H 2.51, N 20.45.

1-(4-Nitro-2-(trifluoromethyl)phenyl)-1H-1,2,3-triazole (3i):

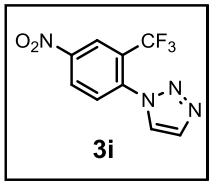

3i

Following the general procedure (GP-3); a mixture of 98% sulphuric acid (15 mL) and 95% nitric acid (10 mL) was added to 1-(2-(trifluoromethyl)phenyl)-1H-1,2,3-triazole (**2i**; 0.25 g, 1.17 mmol) at 0 °C. The resulting mixture was refluxed at 70 °C for 12 h. Upon usual work-up, the crude mixture was purified by silica gel column chromatography eluting with hexane: ethyl acetate (2:1) to afford **3i** (0.11 g) in 37% yield as pale brown solid.

0.11 g, 37% yield, pale brown solid, m.p. 84 °C; DTA = 252 °C; R_f = 0.69 (*n*-hexane/EtOAc, 1:1); ^{1}H NMR (400 MHz, $CDCl_3$): δ 8.76 (bd, J = 2.0 Hz, 1H), 8.62 (dd, J = 2.0, 8.4 Hz, 1H), 7.98 (s, 1H), 7.92 (s, 1H), 7.88 (d, J = 8.8 Hz, 1H); ^{13}C NMR (101 MHz, $CDCl_3$): δ 148.1, 139.6, 134.4, 130.5, 128.0, 127.1 (q, J = 33.3 Hz), 126.1 (q, J = 2.0 Hz), 123.2 (q, J = 5.5 Hz), 121.4 (q, J = 275 Hz); ^{19}F NMR (376 MHz, $CDCl_3$): δ –59.44; IR (KBr): ν_{max} = 3138, 1510, 1435, 1055, 914, 887, 790, 669 cm^{-1}; MS (EI): *m/z* (%): 257 (100) [M^+–1]; Elemental analysis calcd (%) for $C_9H_5F_3N_4O_2$: C 41.87, H 1.95, N, 21.70; found: C 41.68, H 1.88, N 21.86.

1-(4-Chloro-5-nitro-2-(trifluoromethyl)phenyl)-1H-1,2,3-triazole (3l):

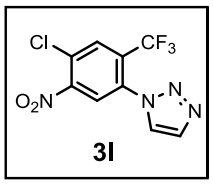

3l

Following the general procedure (GP-3); a mixture of 98% sulphuric acid (15 mL) and 95% nitric acid (10 mL) was added to 1-(4-chloro-2-(trifluoromethyl)phenyl)-1H-1,2,3-triazole (**2l**; 0.70 g, 2.82 mmol) at 0 °C. The resulting mixture was refluxed at 70 °C for 12 h. Upon usual work-up, the crude mixture was purified by silica gel column chromatography eluting with hexane: ethyl acetate (2:1) to afford **3l** (0.22 g) in 27% yield as colorless solid.

0.22 g, 27% yield, colorless solid, m.p. 138 °C; DTA = 274 °C; R_f = 0.65 (*n*-hexane/EtOAc, 2:1); ^{1}H NMR (400 MHz, $CDCl_3$): δ 8.14 (s, 1H), 8.10 (s, 1H), 7.95 (s, 1H), 7.90 (s, 1H); ^{13}C NMR (101 MHz, $CDCl_3$): δ 149.7, 134.4, 134.2, 131.4 (q, J = 5.1 Hz), 129.9 (q, J = 31.3 Hz), 129.5, 126.2, 126.1, 120.9 (q, J = 276 Hz); ^{19}F NMR (376 MHz, $CDCl_3$): δ –59.8; IR (KBr): ν_{max} = 3113, 2962, 1552, 1356, 1261, 1008, 898, 804, 706, 569 cm^{-1}; MS (EI): *m/z* (%): 293 (8) [M^++2], 292 (42) [M^++1], 291 (26) [M^+], 290 (100) [M^+–1], 275 (13); Elemental analysis calcd (%) for $C_9H_4ClF_3N_4O_2$: C 36.94, H 1.38, N 19.15; found: C 37.11, H 1.45, N, 19.06.

1-(2,6-Dichloro-3-nitro-4-(trifluoromethyl)phenyl)-1H-1,2,3-triazole (3m):

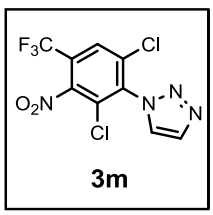

3m

Following the general procedure (GP-3); a mixture of 98% sulphuric acid (15 mL) and 95% nitric acid (10 mL) was added to 1-(2,6-dichloro-4-(trifluoromethyl)phenyl)-1H-1,2,3-triazole (**2m**; 0.10 g, 0.35 mmol) at 0 °C. The resulting mixture was refluxed at 110 °C for 48 h. Upon usual work-up, the crude mixture was purified by silica gel column chromatography eluting with hexane: ethyl acetate (2:1) to afford **3m** (0.04 g) in 32% yield as light brown solid.

0.04 g, 32% yield, light brown solid, m.p. 170 °C; DTA = 234 °C; R_f = 0.55 (*n*-hexane/EtOAc, 2:1); ^{1}H NMR (400 MHz, $CDCl_3$): δ 8.00 (s, 1H), 7.97 (s, 1H), 7.85 (s, 1H);

^{13}C NMR (127 MHz, $CDCl_3$): δ 145.8, 137.7, 136.5, 134.4, 128.3, 127.5 (q, J = 3.0 Hz), 126.0 (q, J = 35.6 Hz), 125.5, 120.3 (q, J = 278 Hz); ^{19}F NMR (470 MHz, $CDCl_3$): δ –61.06; IR (KBr): ν_{max} = 1552, 1363, 1290, 1155, 1006, 893, 792 cm^{-1}; MS (EI): *m/z* (%): 328 (37) [M^+], 327 (100) [M^+–1]; Elemental analysis calcd (%) for $C_9H_3Cl_2F_3N_4O_2$: C 33.05, H 0.92, N 17.13; found: C 33.12, H 0.96, N 17.25.

1-(triazol-1-yl)-4-(triazol-2-yl)-3-trifluoromethylbenzene (5) and 1,4-Bis(triazol-2-yl)-2-trifluoromethylbenzene (6):

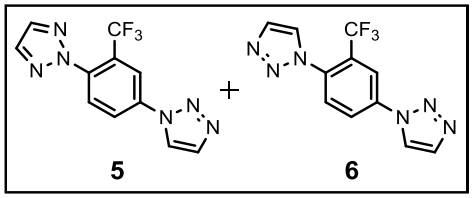

A mixture of 1-(4-bromo-3-(trifluoromethyl)phenyl)-1H-1,2,3-triazole (**2e**; 50 mg, 0.17 mmol), 1H-1,2,3-triazole (19 mg, 0.26 mmol), Cs_2CO_3 (111 mg, 0.34 mmol), CuI (6.0 mg, 0.03 mmol) in DMF (2.0 mL) was refluxed at 120 °C for 48 h. Upon usual work-up, the crude mixture was purified by silica gel column chromatography eluting with hexane: ethyl acetate (2:1) to afford **5** (13 mg) in 29% yield and **6** (24 mg) in 51% yield as colorless solids.

For **5**: 0.013 g, 29% yield, colorless solid, m.p. 141 °C; DTA = 263 °C; R_f = 0.69 (*n*-hexane/EtOAc, 2:1); ^{1}H NMR (400 MHz, $CDCl_3$): δ 8.28 (bd, J = 2.4 Hz, 1H), 8.17–8.15 (m, 1H), 8.13 (bd, J = 2.4 Hz, 1H), 7.96–7.91 (m, 4H); ^{13}C NMR (101 MHz, $CDCl_3$): δ 137.7, 137.1, 136.6, 135.2, 129.4, 126.9 (q, J = 34.3 Hz), 124.0, 122.0 (q, J = 275 Hz), 121.7, 119.6 (q, J = 5.1 Hz); ^{19}F NMR (470 MHz, $CDCl_3$): δ –59.72; IR (KBr): ν_{max} = 3070, 1533, 1408, 1305, 1049, 947, 833, 599 cm^{-1}; MS (EI): *m/z* (%): 281 (100) [M+1]$^+$, 249 (3); Elemental analysis calcd (%) for $C_{11}H_7F_3N_6$: C 47.15, H 2.52, N 29.99; found: C 47.26, H 2.56, N 29.92.

For **6**: 0.024 g, 51% yield, m.p. 133 °C; DTA = 297 °C (exothermic); R_f = 0.68 (*n*-hexane/EtOAc, 1:1); ^{1}H NMR (400 MHz, $CDCl_3$): δ 8.33 (bd, J = 2.4 Hz, 1H), 8.21 (bd, J = 1.2 Hz, 1H), 8.18 (dd, J = 2.4, 8.4 Hz, 1H), 7.93 (s, 2H), 7.89 (bd, J = 1.2 Hz, 1H); 7.77 (d, J = 8.4 Hz, 1H); ^{13}C NMR (101 MHz, $CDCl_3$): δ 138.1, 135.4, 134.5, 134.0, 130.9, 127.9 (q, J = 33.3 Hz), 126.3, 124.2, 121.9 (q, J = 276 Hz), 121.8, 119.2 (q, J = 5.1 Hz); ^{19}F NMR (470 MHz, $CDCl_3$): δ –59.55; IR (KBr): ν_{max} = 2852, 1523, 1338, 1290, 1143, 1033, 900, 790 cm^{-1}; MS (EI): *m/z* (%): 281 (100) [M+1]$^+$, 275 (5), 253 (5), 243 (3), 225 (3); Elemental analysis calcd (%) for $C_{11}H_7F_3N_6$: C 47.15, H 2.52, N 29.99; found: C 47.25, H 2.41, N 29.85.

1,3-Bis(triazol-2-yl)-2-(triazol-1-yl)-5-trifluoromethylbenzene (7):

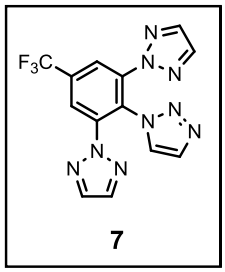

7

A mixture of 1-(2,6-dichloro-4-(trifluoromethyl)phenyl)-1H-1,2,3-triazole (**2m**; 0.72 g, 2.54 mmol), 1H-1,2,3-triazole (0.84 g, 12.2 mmol), Cs_2CO_3 (4.97 g, 15.2 mmol), CuI (0.29 g, 1.52 mmol) in DMF (10 mL) was refluxed at 90 °C for 12 h. Upon usual work-up, the crude mixture was purified by silica gel column chromatography eluting with hexane: ethyl acetate (2:1) to afford **7** (0.18 g) in 24% yield and **8** + **9** (0.38 g) in 43% yield (1:2 by NMR) as brown solids.

For **7**: 0.18 g, 24% yield, brown solid, m.p. 150 °C; 253 °C; R_f = 0.64 (*n*-hexane/EtOAc, 2:1); ^{1}H NMR (400 MHz, $CDCl_3$): δ 8.38 (s, 2H), 7.77 (s, 2H), 7.72 (bs, 4H); ^{13}C NMR (101 MHz, $CDCl_3$): δ 138.6, 136.9, 136.1, 133.4 (q, J = 34.3 Hz), 128.5, 124.9 (q, J = 4.0 Hz), 122.4 (q, J = 275 Hz), 121.6 (q, J = 3.0 Hz); ^{19}F NMR (376 MHz, $CDCl_3$): δ –63.18; IR (KBr): ν_{max} = 3067, 1601, 1529, 1408, 1302, 1182, 1143, 960, 825, 785, 549 cm^{-1}; MS (EI): *m/z* (%): 348 (100) [M+1]$^+$, 200 (13); Elemental analysis calcd (%) for $C_{13}H_8F_3N_9$: C 44.96, H 2.32, N 36.30; found: C 44.85, H 2.41, N 36.18.

1,2,3-Tris(triazol-1-yl)-5-trifluoromethylbenzene (8) and 1,2-Bis(triazol-1-yl)-3-(triazol-2-yl)-5-trifluoromethylbenzene (9):

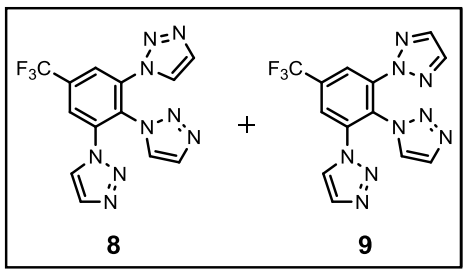

8 **9**

(For **8** (minor) + **9** (major)): 0.38g, 43% yield, brown solid, m.p. 109 °C; DTA = 280 °C (exothermic); R_f = 0.64 (*n*- hexane/EtOAc, 2:1); ^{1}H NMR (400 MHz, $CDCl_3$): δ 8.34 (s, 2H, major), 7.78 (s, 2H, major), 7.71 (bs, 4H, major), 8.51 (s, 1H, minor), 8.22 (s, 1H, minor), 7.83 (s, 1H, minor), 7.71 (bs, 3H, minor), 7.64 (s, 1H, minor), 7.26 (s, 1H, minor); ^{13}C NMR (101 MHz, $CDCl_3$): δ 138.5, 138.3, 137.2, 137.1, 136.9, 136.7, 134.2, 133.9, 133.8 (q, J = 34.3 Hz), 133.2, 128.6, 125.0 (q, J = 275 Hz), 124.7, 122.7 (q, J = 4.0 Hz), 122.2 (q, J = 4.0 Hz), 122.0 (q, J = 3.0 Hz), 120.9; ^{19}F NMR (376 MHz, $CDCl_3$): δ –63.21 (major), –63.16 (minor); IR (KBr): ν_{max} = 3067, 1601, 1529, 1408, 1302, 1182, 1143, 960, 825, 785, 549 cm^{-1}; MS (EI) *m/z* (%) 348 [M+1]$^+$, 200 (11); Elemental analysis calcd (%) for $C_{13}H_8F_3N_9$: C 44.96, H 2.32, N 36.30; found: C 45.06, H 2.28, N 36.43.

1,2-Bis(triazol-2-yl)-4-(triazol-1-yl)-6-trifluoromethylbenzene (**10**) and **1,4-Bis(triazol-1-yl)-2-(triazol-2-yl)-6-trifluoromethylbenzene** (**11**) and **1-(triazol-2-yl)-2,4-bis(triazol-1-yl)-6-trifluoromethylbenzene** (**12**) and **1,2,4-Tris(triazol-1-yl)-6-trifluoromethylbenzene (13):**

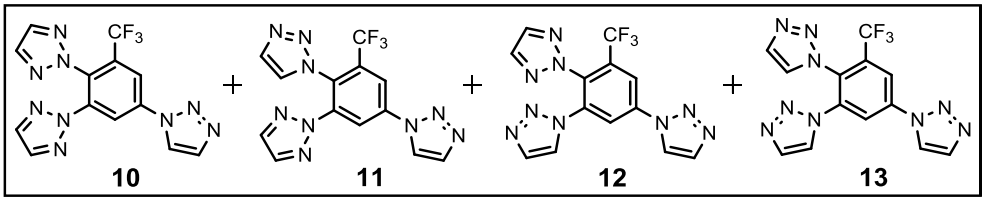

A mixture of 1-(4-bromo-3-nitro-5-(trifluoromethyl)phenyl)-1H-1,2,3-triazole (**3e**; 250 mg, 0.74 mmol), 1H-1,2,3-triazole (16 mg, 2.22 mmol), Cs_2CO_3 (98 mg 2.96 mmol), CuI (6.0 mg, 0.29 mmol) in DMF (6.0 mL) was refluxed at 120 °C for 48 h. Upon usual work-up, the crude mixture was purified by silica gel column chromatography eluting with hexane: ethyl acetate (3:1) to afford **10** (21 mg) in 8% yield**, 11** (52 mg) in 20% yield, **12** (92 mg) in 36% yield and **13** (74 mg) in 29% yield as pale yellow solids.

For **10**: 0.021 g, 8% yield, pale yellow solid, m.p. 175 °C; DTA = 286 °C; R_f = 0.60 (hexane/EtOAc, 3:1); ^{1}H NMR (400 MHz, $CDCl_3$): δ 9.00 (bd, J = 2.0 Hz, 1H), 8.64 (db, J = 2.4 Hz, 1H), 7.93 (bs, 2H), 7.84 (bs, 2H), 7.68 (bs, 2H); ^{13}C NMR (101 MHz, $CDCl_3$): δ 140.7, 139.2, 137.4, 136.8, 136.1, 131.1 (q, J = 32.3 Hz), 128.7, 121.8 (q, J = 276 Hz), 117.7, 116.3 (q, J = 5.1 Hz); ^{19}F NMR (376 MHz, $CDCl_3$): δ –60.42; IR (KBr): ν_{max} = 1624, 1521, 1439, 1284, 1097, 949, 825, 704, 590 cm^{-1}; MS (EI): *m/z* (%): 346 (100) [M^+–1], 328 (10); Elemental analysis calcd (%) for $C_{13}H_8F_3N_9$: C 44.96, H 2.32, N 36.30; found: C 44.85, H 2.28, N 36.21.

For **11**: 0.052 g, 20% yield, pale yellow solid, m.p. 118 °C; DTA = 282 °C (exothermic); R_f = 0.64 (*n*-hexane/EtOAc, 2:1); ^{1}H NMR (400 MHz, $CDCl_3$): δ 8.99 (bd, J = 2.0 Hz, 1H), 8.67 (bd, J = 2.0 Hz, 1H), 7.95 (bs, 2H), 7.88 (s, 1H), 7.83 (bs, 1H), 7.68 (bs, 2H); ^{13}C NMR (101 MHz, $CDCl_3$): δ 141.0, 139.2, 137.5, 137.0, 136.6, 133.3, 130.9 (q, J = 32.3 Hz), 128.4, 125.8, 121.7 (q, J = 276 Hz), 118.1, 116.3 (q, J = 5.1 Hz); ^{19}F NMR (376 MHz, $CDCl_3$): δ –59.80; IR (KBr): ν_{max} = 2924, 1521, 1406, 1138, 1028, 951, 831, 694, 515 cm^{-1}; MS (EI): *m/z* (%): 346 (100) [M^+–1], 332 (8), 315 (8), 300 (10), 291 (10), 260 (6), 233 (6); Elemental analysis calcd (%) for $C_{13}H_8F_3N_9$: C 44.96, H 2.32, N 36.30; found: C 45.08, H 2.38, N 36.43.

For **12**: 0.092 mg, 36% yield, pale yellow solid, m.p. 207 °C; DTA = 278 °C (exothermic); R_f = 0.66 (*n*-hexane/EtOAc, 2:1); ^{1}H NMR (400 MHz, $CDCl_3$): δ 8.71 (bd, *J* = 2.0 Hz, 1H), 8.41 (bd, *J* = 2.0 Hz, 1H), 8.26 (s, 1H), 7.99 (s, 1H), 7.87 (bs, 2H), 7.70 (bs, 2H); ^{13}C NMR (101 MHz, $CDCl_3$): δ 139.4, 138.3, 137.1, 136.3, 131.9 (q, *J* = 33.3), 129.6, 122.0, 121.6 (q, *J* = 278), 118.7, 117.8 (q, *J* = 3.0); ^{19}F NMR (376 MHz, $CDCl_3$): δ –60.45; IR (KBr): ν_{max} = 3067, 1601, 1529, 1408, 1302, 1182, 1143, 960, 825, 785, 549 cm^{-1}; MS (EI): *m/z* (%): 346 (100) [M^+–1], 328 (10); Elemental analysis calcd (%) for $C_{13}H_8F_3N_9$: C 44.96, H 2.32, N 36.30, found: C 44.91, H 2.36, N 36.43.

For **13**: 0.074 g, 29% yield, m.p. 208 °C; DTA = 294 °C (exothermic); R_f = 0.71 (*n*-hexane/EtOAc, 2:1); ^{1}H NMR (400 MHz, $CDCl_3$) δ 8.70 (s, 1H), 8.42 (s, 1H), 8.29 (s, 1H), 7.96 (s, 1H), 7.90 (s, 1H), 7.84 (s, 1H), 7.68 (bs, 2H); ^{13}C NMR (101 MHz, $CDCl_3$) δ 139.3, 138.6, 137.3, 137.0, 135.5, 133.5, 131.5 (q, *J* = 32.3 Hz), 128.4, 124.0, 122.0, 121.5 (q, *J* = 276 Hz), 119.2, 117.7 (q, *J* = 5.1 Hz); ^{19}F NMR (376 MHz, $CDCl_3$): δ –59.82; IR (KBr): ν_{max} = 3067, 1601, 1529, 1408, 1302, 1182, 1143, 960, 825, 785, 549 cm^{-1}; MS (EI): *m/z* (%): 346 (100) [M^+–1], 332 (8), 315 (8), 300 (10), 291 (10), 260 (6), 233 (6); Elemental analysis calcd (%) for $C_{13}H_8F_3N_9$: C 44.96, H 2.32, N 36.30; found: C 44.85, H 2.38, N 36.21.

1-(2-Nitro-4-(1H-1,2,3-triazol-1-yl)-6-(trifluoromethyl)phenyl)-1H-tetrazol-5-amine(15):

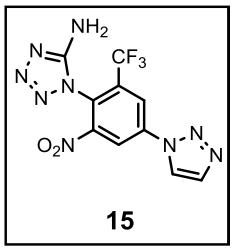

15

Following the general procedure (GP-4); a mixture of 1-(4-chloro-3-nitro-5-(trifluoromethyl)phenyl)-1H-1,2,3-triazole (**3d**; 0.20 g, 0.68 mmol), 5-amino-1H-1,2,3,4-tetrazole (0.09 g 1.02 mmol), Cs_2CO_3 (0.44 g 1.36 mmol), CuI (0.02 g, 0.13 mmol) in DMF (2.0 mL) was refluxed at 120 °C for 48 h. Upon usual work-up, the crude mixture was purified by silica gel column chromatography eluting with hexane: ethyl acetate (2:1) to afford **15** (0.03 g) in 23% yield as pale yellow solid.

0.03 g, 23% yield, pale yellow solid, m.p. 161 °C; DTA = 261 °C; R_f = 0.65 (*n*-hexane/EtOAc, 2:1); ^{1}H NMR (400 MHz, $CDCl_3$): δ 8.68 (bd, *J* = 2.4 Hz, 1H), 8.28 (bd, *J* = 2.4 Hz, 1H), 8.02 (s, 1H), 7.90 (s, 1H), 6.89 (bs, 2H); ^{13}C NMR (101 MHz, $CDCl_3$): δ 142.0, 135.0, 133.0, 129.5, 127.0 (q, *J* = 5.1 Hz), 125.4, 123.0 (q, *J* = 274 Hz), 122.1, 121.7, 118.5 (q, *J* = 31.3 Hz); ^{19}F NMR (376 MHz, $CDCl_3$): δ –63.5; IR (KBr): ν_{max} = 3375, 1539, 1267, 1124, 1084, 914, 775, 684 cm^{-1}; MS (EI): *m/z* (%): 342 (100) [M+1]$^+$, 65 (3); Elemental

analysis calcd (%) for $C_{10}H_6F_3N_9O_2$: C 35.20, H 1.77, N 36.95; found: C 35.11, H 1.86, N 37.05.

Synthesis of 2-Nitro-4-(1H-1,2,3-triazol-1-yl)-6-(trifluoromethyl)phenol (16):

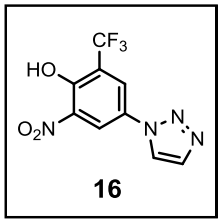

16

A mixture of 1-(4-fluoro-3-nitro-5-(trifluoromethyl)phenyl)-1H-1,2,3-triazole (**3c**; 0.10 g, 0.36 mmol), KOH (0.06 g, 1.08 mmol), H_2O_2 (0.03 g, 0.72 mmol) in THF–H_2O (4.0 mL, 1:1) was stirred at 100 °C for 48 h. Upon completion, the reaction mixture was extracted with EtOAc (3 × 10 mL). The combined extracts were washed with water (2 × 10 mL) and brine (5.0 mL) and dried over Na_2SO_4. The solvent was filtered and evaporated under the reduced pressure. The crude residue was purified by silica gel column chromatography eluting with hexane: ethyl acetate (1:1) to afford **16** (0.06 g) in 60% yield as yellow color solid.

0.06 g, 60% yield, yellow solid, m.p. 166 °C; DTA = 229 °C; R_f = 0.57 (*n*-hexane/EtOAc, 1:1); ^{1}H NMR (400 MHz, $CDCl_3$): δ 11.3 (s, 1H), 8.71 (d, J = 2.8 Hz, 1H), 8.41 (d, J = 2.4 Hz, 1H), 8.08 (s, 1H), 7.93 (s, 1H); ^{13}C NMR (101 MHz, $CDCl_3$): δ 152.9, 137.5, 135.3, 128.8, 127.4 (q, J = 4.04 Hz), 123.0 (q, J = 34.3 Hz), 121.5 (q, J = 275 Hz), 121.7, 120.1; ^{19}F NMR (470 MHz, $CDCl_3$): δ –63.13; IR (KBr): ν_{max} = 3117, 2926, 1641, 1554, 1444, 1336, 1240, 1087, 787, 690 cm^{-1}; MS (EI): *m/z* (%): 275 (100) $[M+1]^+$; Elemental analysis calcd (%) for $C_9H_5F_3N_4O_3$: C 39.43, H 1.84, N 20.44; found: C 39.26, H 1.76, N 20.32.

Synthesis of 3-azido-1-(2,4-dinitro-6-(trifluoromethyl)phenyl)-1H-1,2,4-triazole (19):

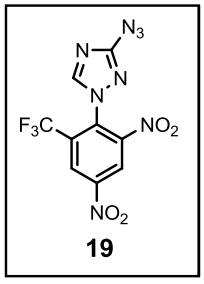

19

To a solution of 3-azido-1,2,4-triazole (**18**, 0.155 g, 1.4 mmol) in dry THF (5.0 mL) was added sodium hydride (60%, 0.05 g, 2.0 mmol) under an argon atmosphere at 0 ^{o}C. The resulting mixture was stirred for 30 min followed by the addition of 2-chloro-1,5-dinitro-3-(trifluoromethyl)benzene (**17**; 0.27 g, 1.0 mmol). The vial was sealed with screw cap and the resulting mixture was stirred rapidly at room temperature for 6 h. Upon completion, the reaction mixture was diluted with CH_2Cl_2 (30 mL) and filtered through a small pad of Celite. The filtrate was evaporated under the reduced pressure and the crude residue was purified by silica gel column chromatography eluting with hexane: ethyl acetate (4:1) to afford **19** (238 mg) in 69% yield as yellow color solid.

0.238 g, 69% yield, yellow solid, m.p. 122 °C; DTA = 213 °C (exothermic); R_f = 0.60 (*n*-hexane/EtOAc, 4:1); ^{1}H NMR (400 MHz, $CDCl_3$): δ 9.06 (s, 1H), 8.97 (s, 1H), 8.28 (s, 1H);

^{13}C NMR (127 MHz, $CDCl_3$): δ 161.5, 148.1, 148.0, 147.0, 132.9, 131.4 (q, J = 34.3 Hz), 125.9 (q, J = 5.0 Hz), 124.1, 120.7 (q, J = 279 Hz); ^{19}F NMR (470 MHz, $CDCl_3$): δ –58.90; IR (KBr): ν_{max} = 3106, 2926, 2854, 2153, 1736, 1627, 1550, 1463, 1353, 1293, 1156, 980 cm^{-1}; MS (EI): *m/z* (%): 344 (100) $[M+1]^+$, 345 (39) $[M^+]$, 195 (13); Elemental analysis calcd (%) for $C_9H_3F_3N_8O_4$: C 31.41, H 0.88, N 32.56; found: C 31.56, H 0.92, N 32.45.

3.10. References

1. S. Garg and J. M. Shreeve, *J. Mater. Chem.*, 2011, **21**, 4787–4797.

2. (a) C. Ye, G. L. Gard, R. W. Winter, R. G. Syvret, B. Twamley and J. M. Shreeve, *Org. Lett*., 2007, **9**, 3841–3844; (b) Y. Huang, G. L. Gard and J. M. Shreeve, *Tetrahedron*, 2010, **51**, 6551–6954; (c) S. Garg and J. M. Shreeve, *J. Fluorine Chem*., 2011, **132**, 241–243.

3. (a) H. Gao and J. M. Shreeve, *Chem. Rev*., 2011, **111**, 7377–7436; (b) R. P. Singh, R. D. Verma, D. T. Meshri andJ. M. Shreeve, *Angew. Chem., Int. Ed*., 2006, **45**, 3584–3601.

4. (a) V. Thottempudi, F. Forohor, D. A. Parrish and J. M. Shreeve, *Angew. Chem., Int. Ed*., 2012, **51**, 9881–9885; (b) Z. Zeng, Y. Guo, B. Twameley and J. M. Shreeve, *Chem. Commun*., 2009, 6014–6016; (c) T. M. Klapotke and C. M. Sabate, *Chem. Mater*., 2008, **20**, 3629–3637; (d) D. Srinivas, V. D. Ghule, S. P. Tewari and K. Muralidharan, *Chem.–Eur. J*., 2012, **18**, 15031–15037; (e) D. Srinivas, V. D. Ghule, S. P. Tewari, K. Muralidharan and H. D. B. Jenkins, *Chem. –Asian J*., 2013, **8**, 1023–1028; (f) N. Kommu, V. D. Ghule, A. S. Kumar and A. K. Sahoo, *Chem. –Asian J*., 2014, **9**, 166–178.

5. (a) Q. Zhang, J. Zhang, D. A. Parrish and J. M. Shreeve, *Chem.–Eur. J*., 2013, **19**, 11000–11006; (b) J. Kohler, R. Meyer and A. Homburg, *Explosives*, Wiley-VCH, Weinheim, 6th edn, 2007; (c) T. L. Davis, *The Chemistry of Powder and Explosives*, Angriff Press, Los Angeles, 1943; (d) J. P. Agrawal, *Propellants Explos. Pyrotech*., Wiley-VCH, Weinheim, 2010; (e) Y. Zhang, D. A. Parrish and J. M. Shreeve, *J. Mater. Chem. A*, 2013, **1**, 585–593; (f) M. Gobel and T. M. Klapotke, *Adv. Funct. Mater*., 2009, **19**, 347–365; (g) J. Zhang and J. M. Shreeve, *J. Am. Chem. Soc*. **2014**, *136*, 4437–4445.

6. (a) W. W. Wilson, A. Vij, V. Vij, E. Bernhardt and K. O. Christe, *Chem.–Eur. J*., 2003, **9**, 2840–2844; (b) M. E. Sitzmann, R. Gilardi, R. J. Butcher, W. M. Koppes, A. G. Stern, J. S. Thrasher, N. J. Trivedi and Z. Y. Yang, *Inorg. Chem*., 2000, **39**, 843–850.

7. (a) R. P. Singh and J. M. Shreeve, *J. Fluorine Chem*., 2012, **133**, 20–26; (b) G. S. Lal and K. E. Minnich, *US. Pat*., 6479645, 2002.

8. (a) Y. Suzuki, T. Hagiwara, I. Kawamura, N. Okamura, T. Kitazume, M. Kakimoto, Y. Imai, Y. Ouchi, H. Takezoe and A. Fukuda, *Liq. Cryst*., 2006, **33**, 1344–1349; (b) J. A. Smith, Jr, R. A. Distasio, N. A. Hannah, R. W. Winter, T. J. R. Weakley, G. L. Gard and S. B. Rananavare, *J. Phys. Chem. B*, 2004, **108**, 19940–19948; (c) P. Kirsch, M. Bremer, A. Taugerbeck and T. Wallmichrath, *Angew. Chem*., 2001, **113**, 1528; (d) P. Kirsch, M. Bremer, A. Taugerbeck and T. Wallmichrath, *Angew. Chem., Int. Ed*., 2001, **40**, 1480–1484.

9. (a) W. Li, G. Chen, S. Zhang, H. Wang and D. Yan, *J. Polym. Sci., Part A: Polym. Chem*., 2007, **45**, 3550–3561; (b) R. Winter, P. G. Nixon, R. J. Terjeson, J. Mohtasham, N. R. Holcomb, D. W. Grainger, D. Graham, D. G. Castner and G. L. Gard, *J. Fluorine Chem*., 2002, **115**, 107–204; (c) J. C. Hansen and P. M. Savu, *US. Pat*., 5286352, 1994. 10. (a) J. A. Schlueter, U. Geiser, H. H. Wang, M. E. Kelly, J. D. Dudek, J. M. Williams, D. Naumann and T. Roy, *Mol. Cryst. Liq. Cryst. Sci. Technol., Sect. A*, 1996, **284**, 195; (b) T. L. Clair, A. K. Clair and J. S. Thrasher, *US. Pat*., 5220070, 1993; c) H. G. Adolph, N. J. Trivedi, *US. Pat., 6,325,876,B1*, **2001**.

11. (a) A. S. Kumar, V. D. Ghule, S. Subrahmanyam and A. K. Sahoo, *Chem.–Eur. J*., 2013, **19**, 509–518; (b) V. R. Kamalraj, S. Senthil and P. Kannan, *J. Mol. Struct*., 2008, **892**, 210–215.

12. The cleavage of triazoles is responsible for the poor yield.

13. (a) V. D. Ghule, D. Srinivas and K. Muralidharan, *Asian J. Org. Chem*., 2013, **2**, 662–668; (b) J. Akhavan, *The Chemistry of Explosives*, RSC, Cambridge, 2nd edn, 2004; (c) T. M. Klapotke, C. Petermayer, D. G. Piercey and J. Stierstorfer, *J. Am. Chem. Soc*., 2012, **134**, 20827–20836; (d) A. A. Dippold and T. M. Klapotke, *J. Am. Chem. Soc*., 2013, **135**, 9931–9938; (e) Y. C. Li, C. Qi, S. H. Li, H. J. Zhang, C. H. Sun, Y. Z. Yu and S. Ping Pang, *J. Am. Chem. Soc*., 2010, **132**, 12172–12173; (f) A. A. Dippold, D. Izsak and T. M. Klapotke, *Chem.–Eur. J*., 2013, **19**, 12042–12051.

14. Heat of formation calculated in gaseous state (Gaussian 03) with isodesmic approach.

15. V. R. Kamalraj, S. Senthil and P. Kannan, *J. Mol. Struct*., 2008, **892**, 210–215.

16. M. J. Frisch, G. W. Trucks, H. B. Schlegel, G. E. Scuseria, M. A. Robb, J. R. Cheeseman, J. A. Montgomery, Jr, T. Vreven, K. N. Kudin, J. C. Burant, J. M. Millam, S. S. Iyengar, J. Tomasi, V. Barone, B. Mennucci, M. Cossi, G. Scalmani, N. Rega, G. A. Petersson, H. Nakatsuji, M. Ha da, M. Ehara, K. Toyota, R. Fukuda, J. Hasegawa, M. Ishida, T. Nakajima, Y. Honda, O. Kitao, H. Nakai M. Klene, X. Li, J. E. Knox, H. P. Hratchian, J. B. Cross, V. Bakken, C. Adamo, J. Jaramillo, R. Gomperts, R. E. Stratmann, O. Yazyev, A. J. Austin, R. Cammi, C. Pomelli, J. W. Ochterski, P. Y. Ayala, K. Morokuma, G. A. Voth, P. Salvador, J.

J. Dannenberg, V. G. Zakrzewski, S. Dapprich, A. D. Daniels, M. C. Strain, O. Farkas, D. K. Malick, A. D. Rabuck, K. Raghavachari, J. B. Foresman, J. V. Ortiz, Q. Cui, A. G. Baboul, S. Clifford, J. Cioslowski, B. B. Stefanov, G. Liu, A. Liashenko, P. Piskorz, I. Komaromi, R. L. Martin, D. J. Fox, T. Keith, M. A. Al-Laham, C. Y. Peng, A. Nanayakkara, M. Challacombe, P. M. W. Gill, B. Johnson, W. Chen, M. W. Wong, C. Gonzalez and J. A. Pople, Gaussian 03, Revision A.1, Gaussian, Inc., Pittsburgh, PA, 2003.

17. (a) M. J. Kamlet and S. J. Jacobs, *J. Chem. Phys*., 1968, **48**, 23–35; (b) M. J. Kamlet and J. E. J. Ablard, *J. Chem. Phys*., 1968, **48**, 36.

18. (a) M. W. J. Chase, NIST–JANAF Themochemical Tables, 4th Ed., *J. Phys. Chem. Ref. Data, Monograph* 1998, **9**, 1–1951; (b) J. D. Cox, D. D. Wagman and V. A. Medvedev, *CODATA Key Values for Thermodynamics*, Hemisphere Publishing Corp., New York, 1984, 1; (c) J. G. Aston, C. W. Siller and G. H. Messerly, *J. Am. Chem. Soc*., 1937, **59**, 1743–1817; (d) Y. K. Knobel, E. A. Miroshnichenko and Y. A. Lebedev, *Bull. Acad. Sci. USSR, Div. Chem. Sci*., 1971, 425-428; (e) E. Wu and A. S. Rodgers**,** *J. Phys. Chem***.,** 1974, **78**, 2315–2317; (f) X. An, M. Mansson, *J. Chem. Thermodyn***.,** 1983, **15**, 287–293; (g) P.Jimenez, M. V. Roux and C. Turrion, *J. Chem. Thermodyn.,* 1989, **21**, 759–764; (h) A. A. Balepin, V. P. Lebedev, E. A. Miroshnichenko, G. I. Koldobskii, V. A. Ostovskii, B. P. Larionov, B. V. Gidaspov and Yu. A. Lebedev, *Svoistva Veshchestv Str. Mol*., 1977, 93–98; (i) Values calculated using G3 calculations; (j) M. V. Roux, M. Temprado, J. S. Chickos and Y. Nagano, *J. Phys. Chem. Ref. Data*, 2008, **37**, 1855–1996.

19. *SAINT-Plus*, *version 6.45*, Bruker AXS Inc., Madison, WI, 2003.

20. G. M. Sheldrick, *SADABS*, Program for Empirical Absorption Correction of Area Detector Data, University of Gottingen, Germany, 1997.

21. (a) *SMART* (*version 5.625*), *SHELX-TL* (*version 6.12*), Bruker AXS Inc., Madison, WI, 2000; (b) G. M. Sheldrick, *SHELXL-97*, University of Gottingen, Germmany, 1997.

22. O. V. Dolomanov, A. J. Blake, N. R. Champness and M. Schroder, *J. Appl. Cryst*., 2003, **36**, 1283–1284.

23. S. A. Sandoz, *U. S. Patent* 4,499,280, 1983.

24. (a) Y. Jiang, C. Kuang and Q. Yang, *Tetrahedron* 2011, **67**, 289–292; (b) F. Reisser, *U.S. Patent* 4,499,280, 1985.

25. EXPLO5 *version* 6.02, M. Suceska, **2014**.

3.11. Spectra

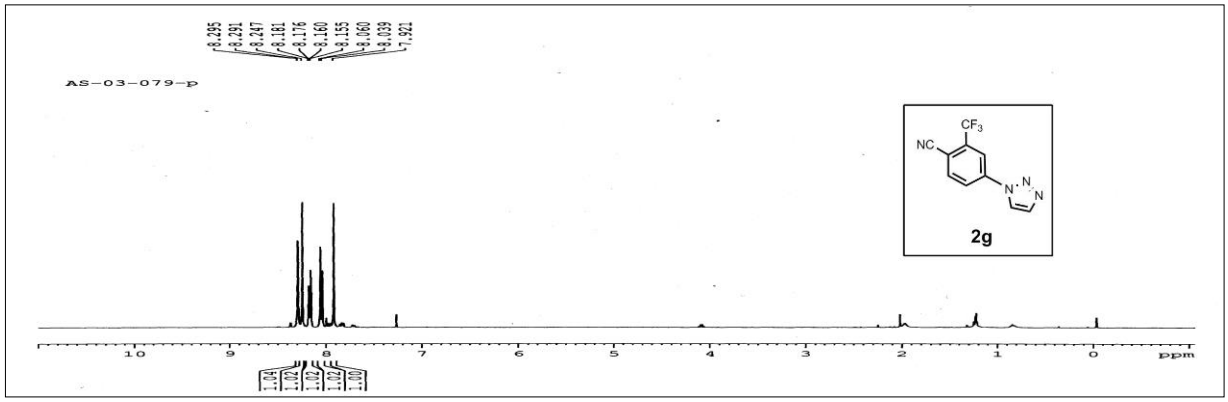
AS-03-079-p
2g
ppm

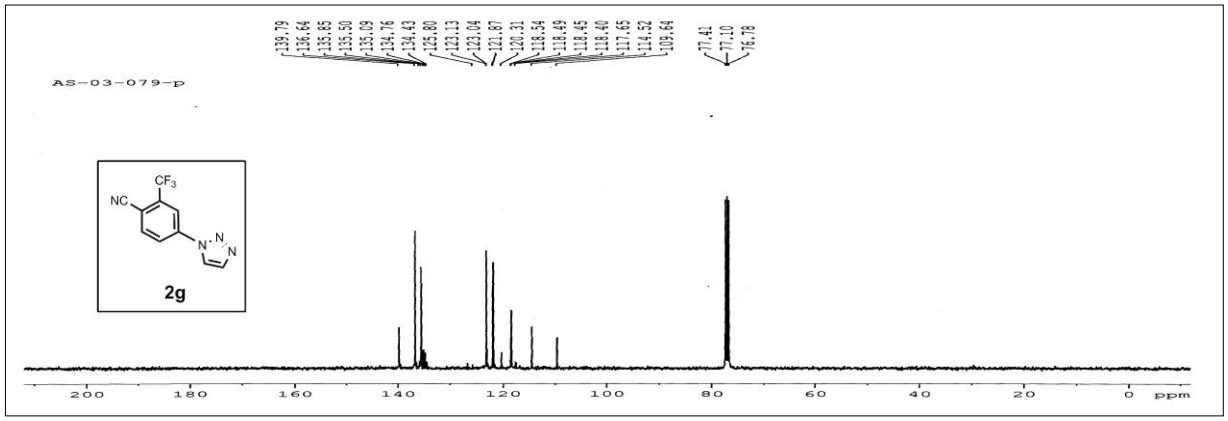
AS-03-079-p
2g
ppm

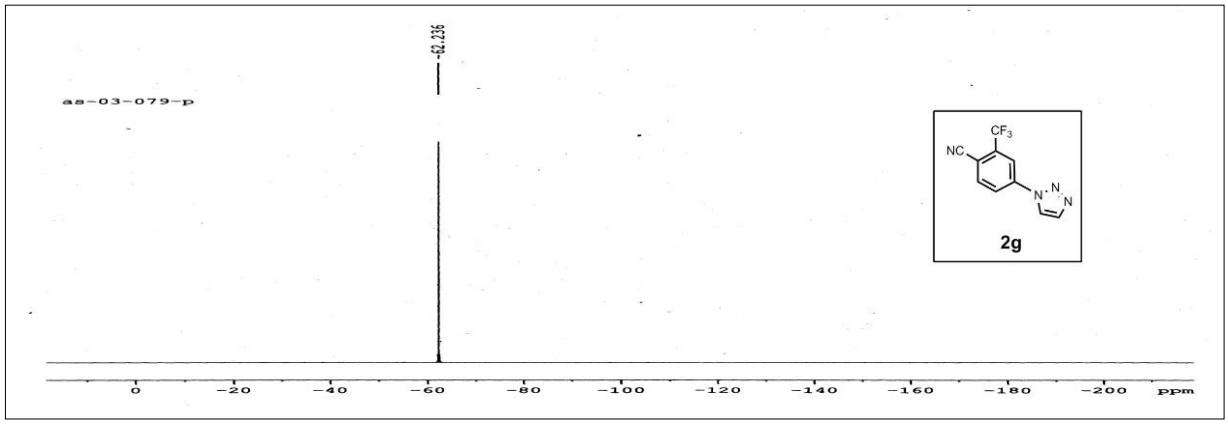
as-03-079-p
-62.236
2g
ppm

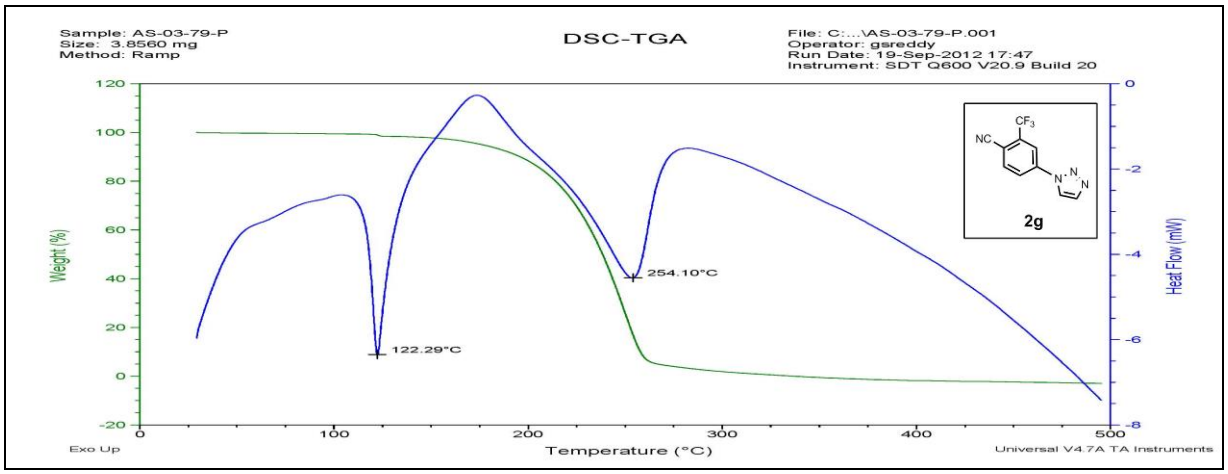
Sample: AS-03-79-P
Size: 3.8560 mg
Method: Ramp
DSC-TGA
File: C:...\AS-03-79-P.001
Operator: gsreddy
Run Date: 19-Sep-2012 17:47
Instrument: SDT Q600 V20.9 Build 20
2g
122.29°C
254.10°C
Weight (%)
Heat Flow (mW)
Temperature (°C)
Exo Up
Universal V4.7A TA Instruments

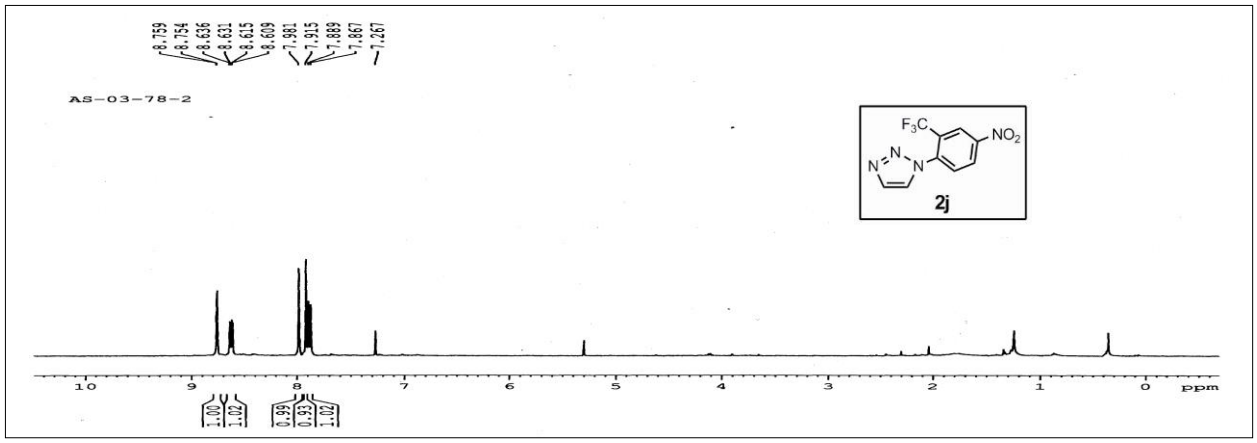
AS-03-78-2
8.159
8.154
8.636
8.631
8.615
8.609
7.981
7.915
7.889
7.867
7.267
1.00
1.02
0.99
0.93
1.02
2j
ppm

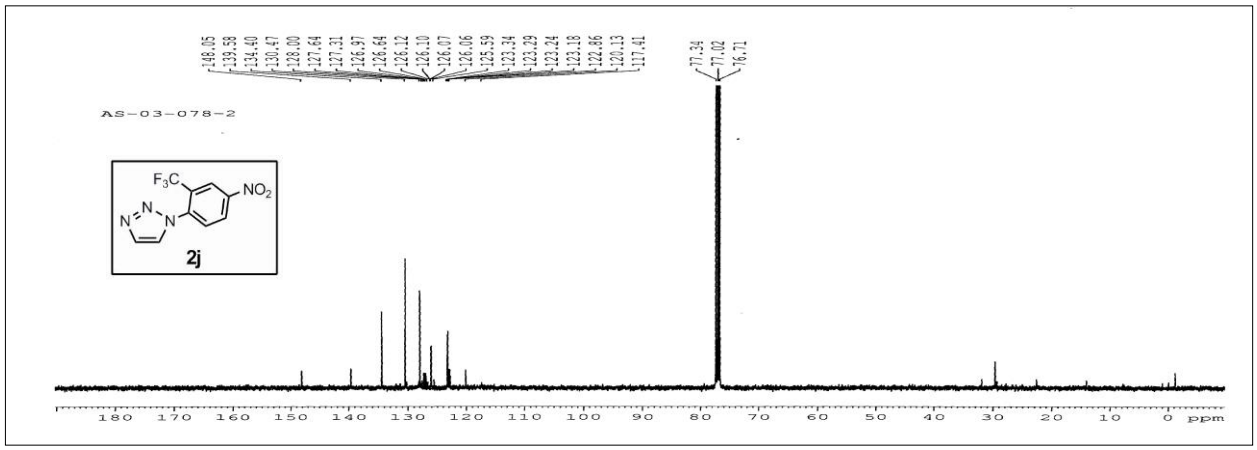
AS-03-078-2
148.05
139.58
134.40
130.47
128.00
127.64
127.31
126.97
126.64
126.12
126.10
126.07
126.06
125.59
123.34
123.29
123.24
123.18
122.86
120.13
117.41
77.34
77.02
76.71
2j
ppm

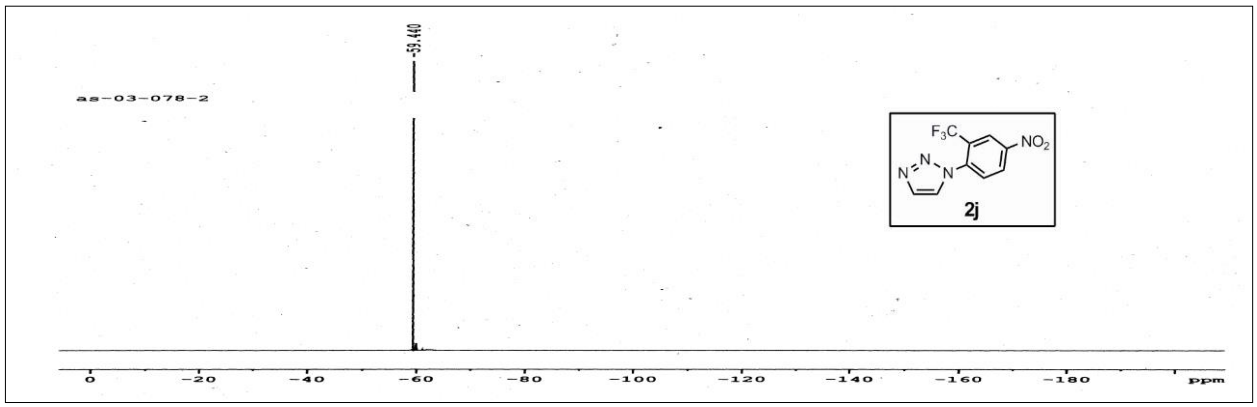
as-03-078-2
-59.440
2j
ppm

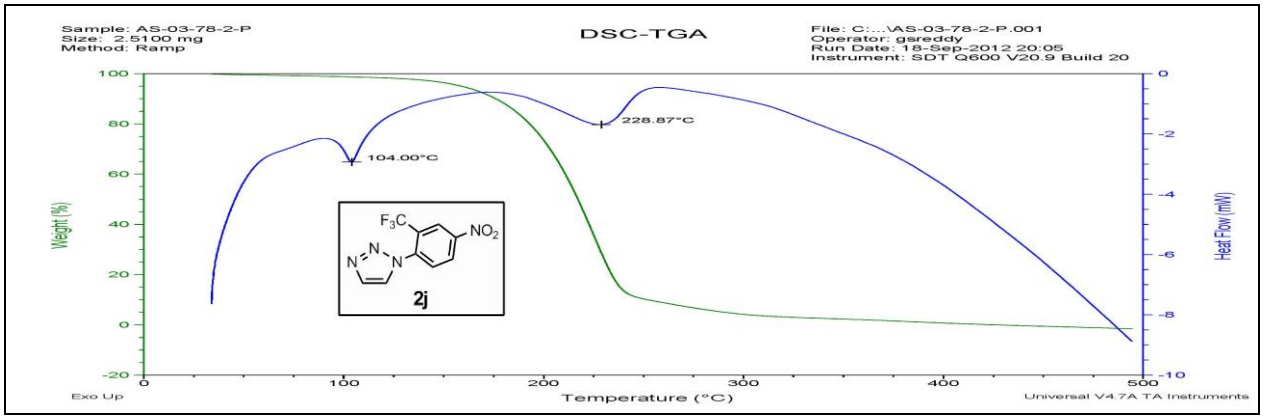
Sample: AS-03-78-2-P
Size: 2.5100 mg
Method: Ramp
DSC-TGA
File: C:...\AS-03-78-2-P.001
Operator: gsreddy
Run Date: 18-Sep-2012 20:05
Instrument: SDT Q600 V20.9 Build 20
104.00°C
228.87°C
2j
Weight (%)
Heat Flow (mW)
Temperature (°C)
Exo Up
Universal V4.7A TA Instruments

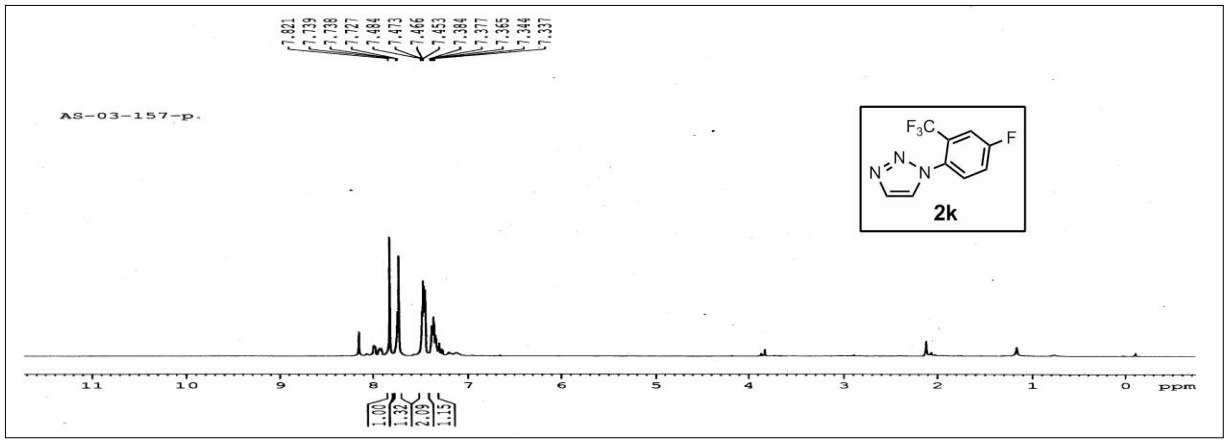
AS-03-157-p.
2k
ppm

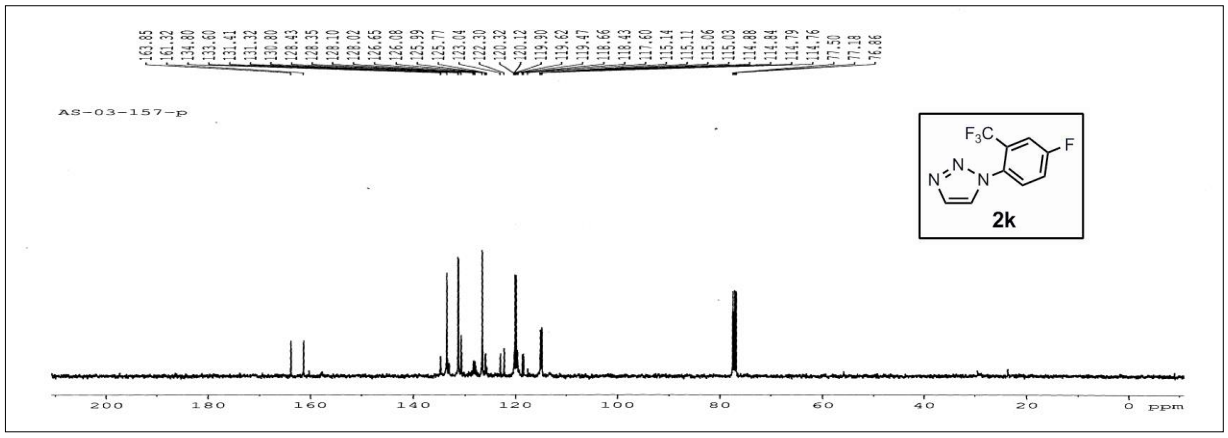
AS-03-157-p
2k
ppm

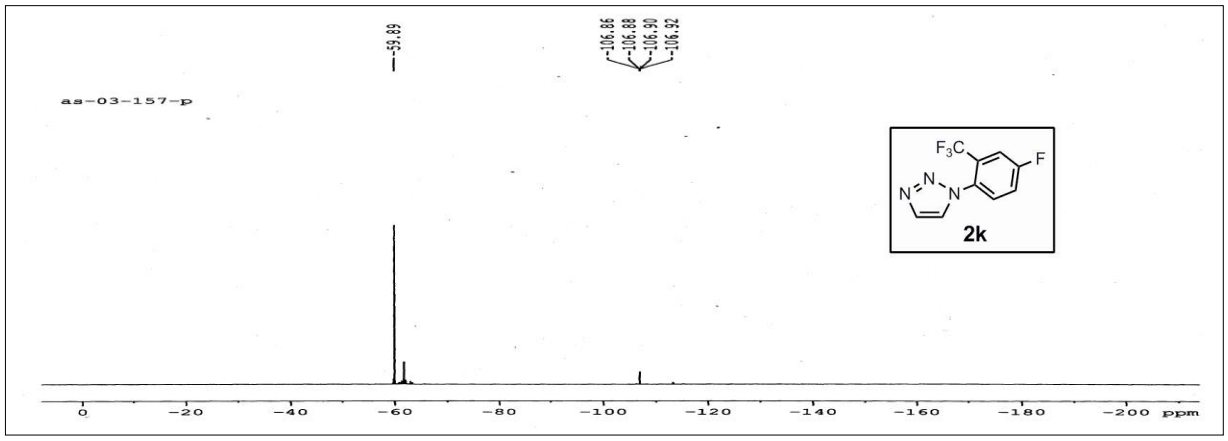
as-03-157-p
2k
ppm

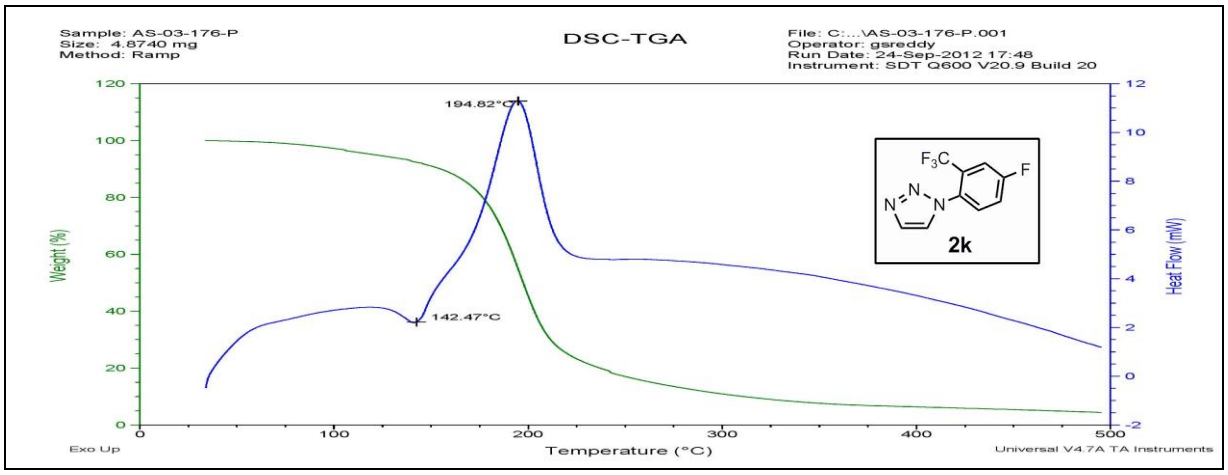
Sample: AS-03-176-P
Size: 4.8740 mg
Method: Ramp
DSC-TGA
File: C:...\AS-03-176-P.001
Operator: gsreddy
Run Date: 24-Sep-2012 17:48
Instrument: SDT Q600 V20.9 Build 20
194.82°C
142.47°C
2k
Weight (%)
Heat Flow (mW)
Temperature (°C)
Exo Up
Universal V4.7A TA Instruments

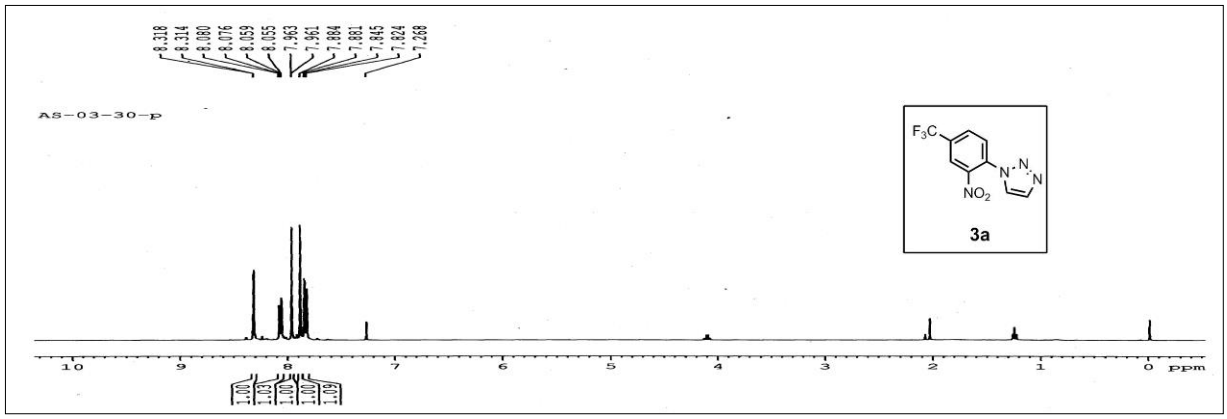
AS-03-30-P
8.318
8.314
8.080
8.076
8.059
8.055
7.963
7.961
7.884
7.881
7.845
7.824
7.268
1.00
1.03
1.00
1.00
1.09
10
9
8
7
6
5
4
3
2
1
0
ppm
F3C
NO2
N
N
N
3a

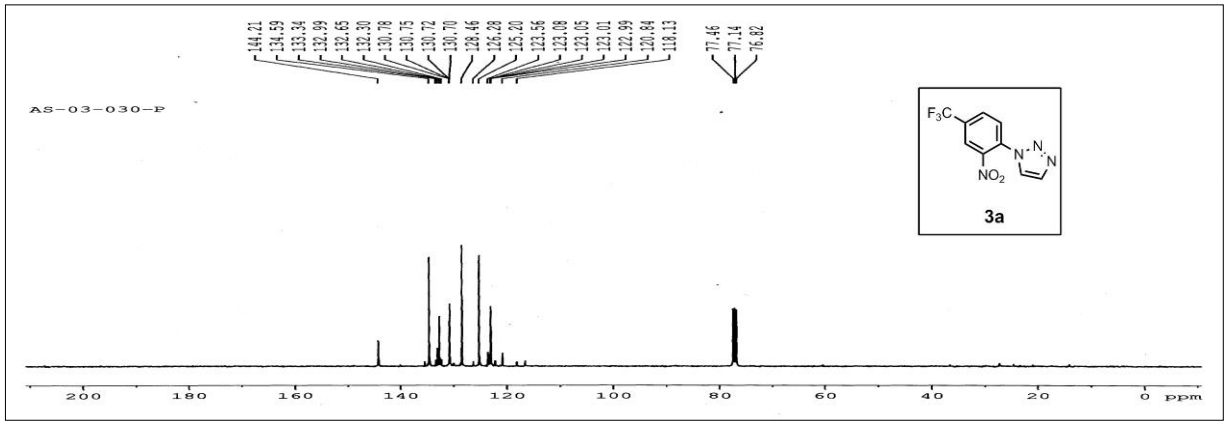
AS-03-030-P
144.21
134.59
133.34
132.99
132.65
132.30
130.78
130.75
130.72
130.70
128.46
126.28
125.20
123.56
123.08
123.05
123.01
122.99
120.84
118.13
77.46
77.14
76.82
200
180
160
140
120
100
80
60
40
20
0
ppm
F3C
NO2
N
N
N
3a

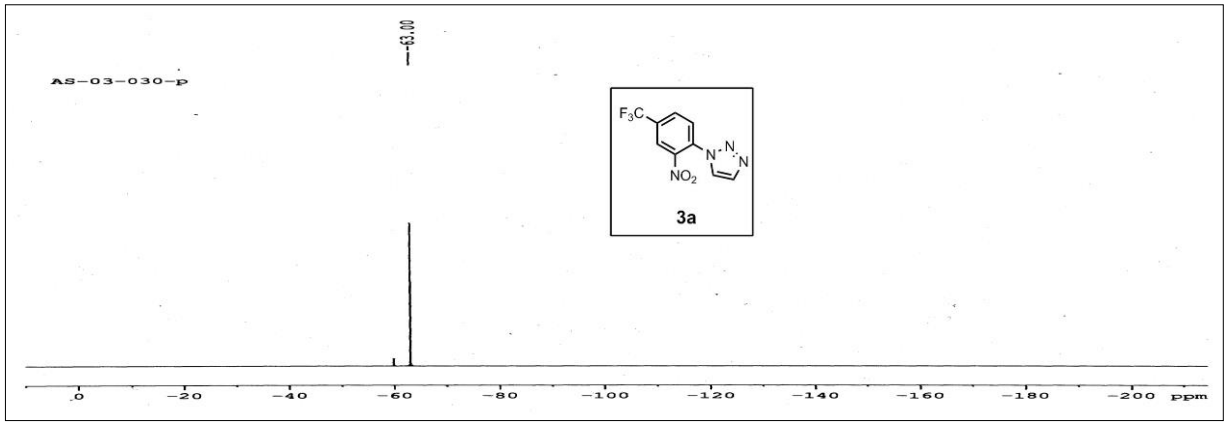
AS-03-030-P
-63.00
0
-20
-40
-60
-80
-100
-120
-140
-160
-180
-200
ppm
F3C
NO2
N
N
N
3a

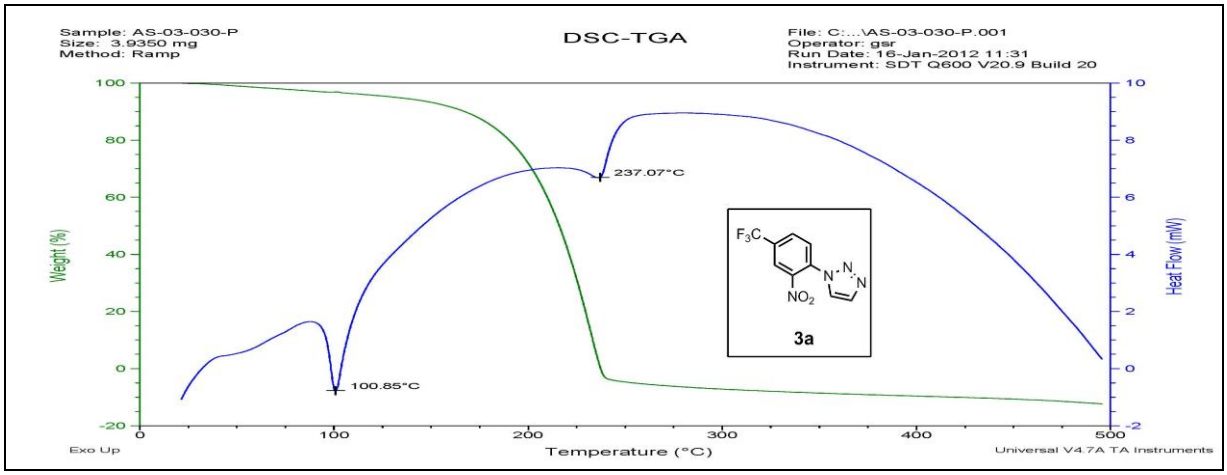
Sample: AS-03-030-P
Size: 3.9350 mg
Method: Ramp
DSC-TGA
File: C:...\AS-03-030-P.001
Operator: gsr
Run Date: 16-Jan-2012 11:31
Instrument: SDT Q600 V20.9 Build 20
Weight (%)
Heat Flow (mW)
237.07°C
100.85°C
Exo Up
Temperature (°C)
Universal V4.7A TA Instruments
F3C
NO2
N
N
N
3a

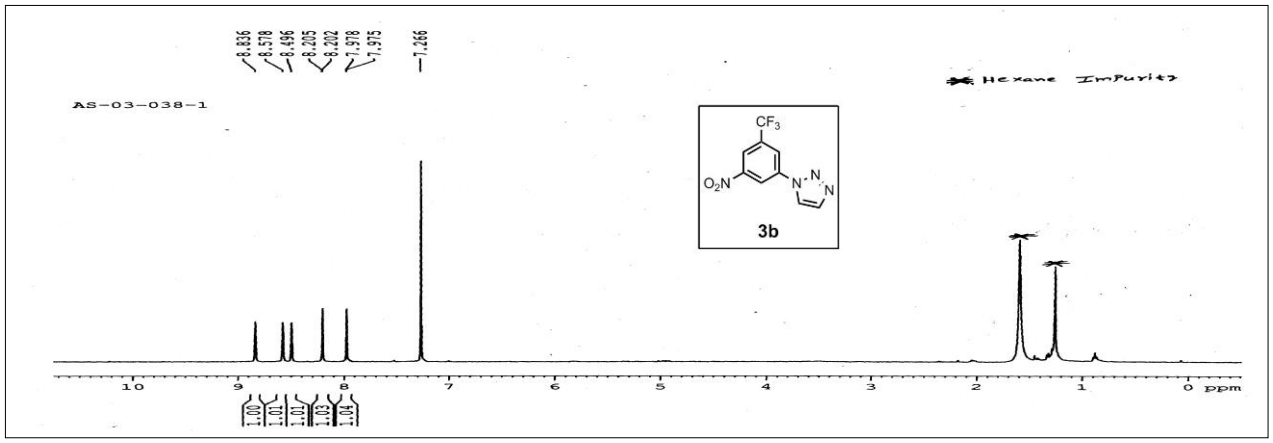
8.836
8.578
8.496
8.205
8.202
7.978
7.975
7.266
Hexane Impurity
AS-03-038-1
CF3
O2N
N
N
N
3b
1.00
1.01
1.01
1.03
1.04
10
9
8
7
6
5
4
3
2
1
0 ppm

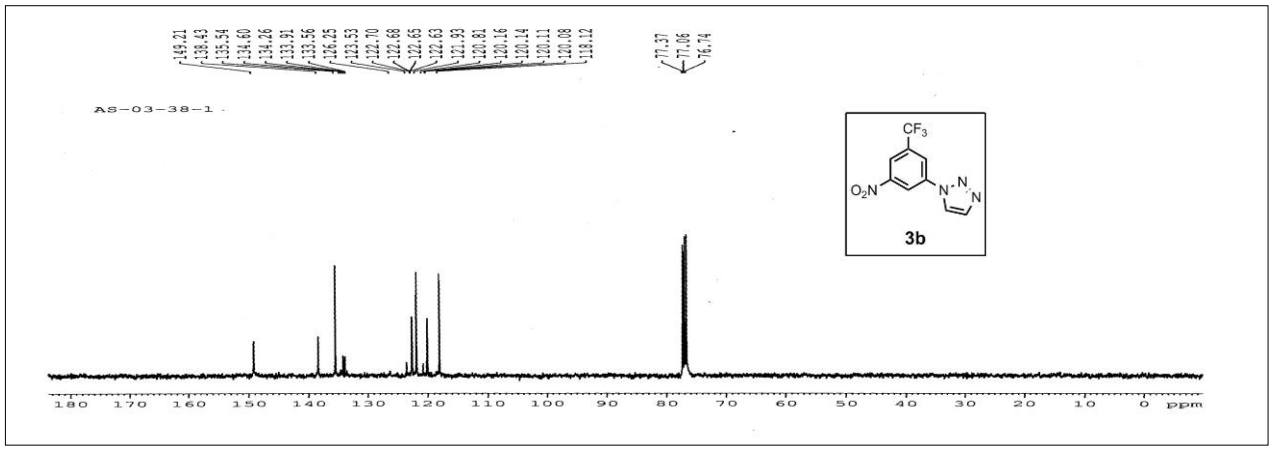
149.21
138.43
135.54
134.60
134.26
133.91
133.56
126.25
123.53
122.70
122.68
122.65
122.63
121.93
120.81
120.16
120.14
120.11
120.08
119.12
77.37
77.06
76.74
AS-03-38-1
CF3
O2N
N
N
N
3b
180 170 160 150 140 130 120 110 100 90 80 70 60 50 40 30 20 10 0 ppm

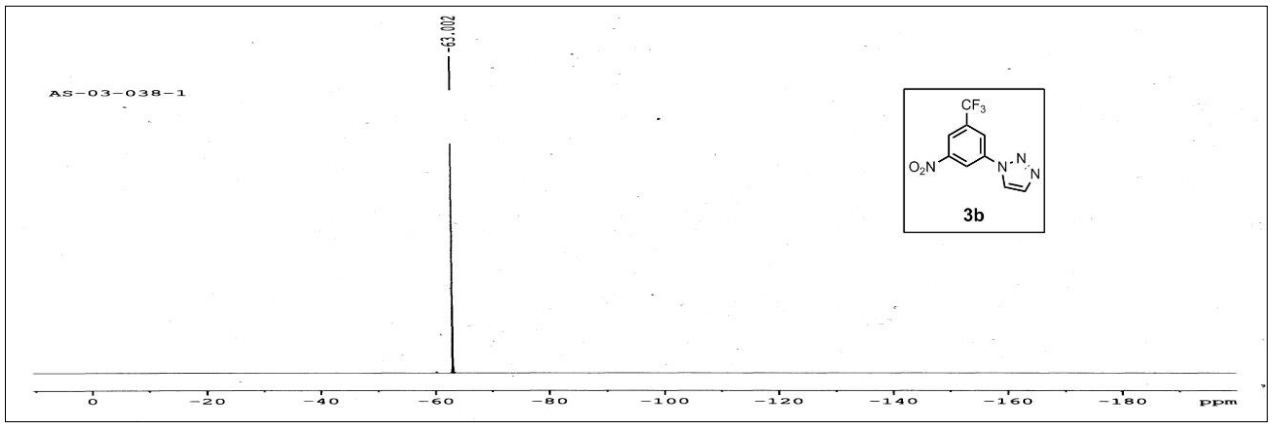
-63.002
AS-03-038-1
CF3
O2N
N
N
N
3b
0 −20 −40 −60 −80 −100 −120 −140 −160 −180 ppm

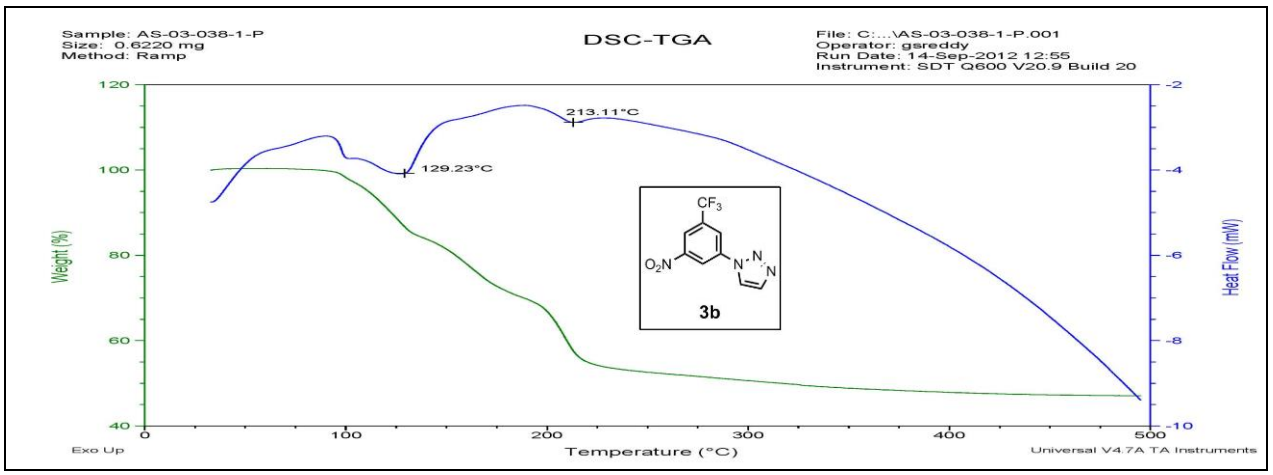
Sample: AS-03-038-1-P
Size: 0.6220 mg
Method: Ramp
DSC-TGA
File: C:...\AS-03-038-1-P.001
Operator: gsreddy
Run Date: 14-Sep-2012 12:55
Instrument: SDT Q600 V20.9 Build 20
213.11°C
129.23°C
CF3
O2N
N
N
N
3b
Weight (%)
Heat Flow (mW)
Exo Up
Temperature (°C)
Universal V4.7A TA Instruments

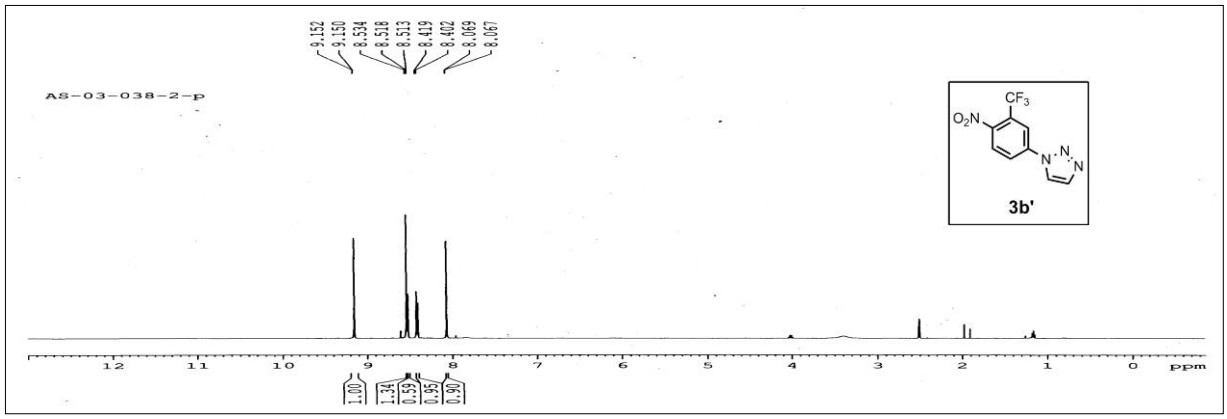
AS-03-038-2-p
9.152
9.150
8.534
8.518
8.513
8.419
8.402
8.069
8.067
1.00
1.34
0.59
0.95
0.90
CF3
O2N
3b'
ppm

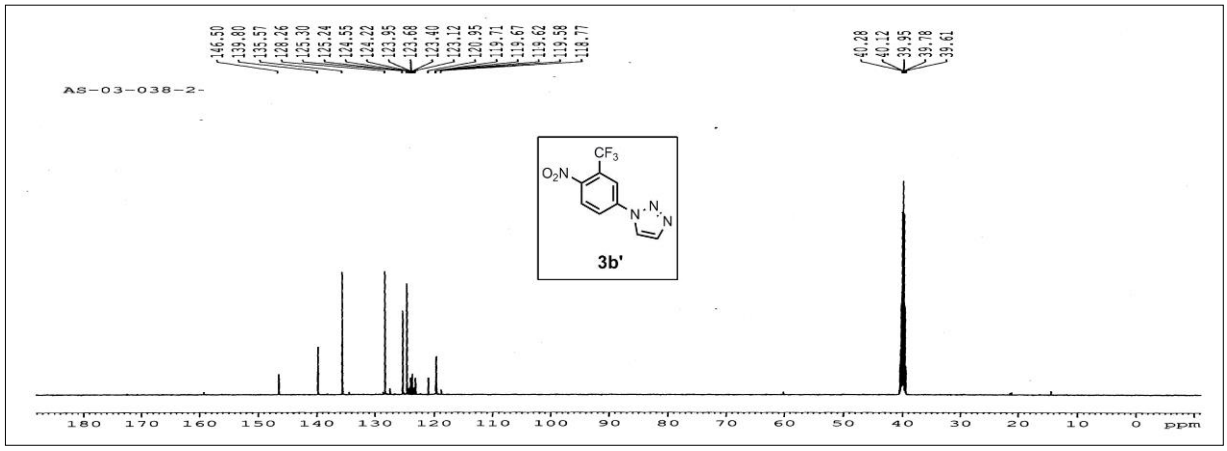
AS-03-038-2-
146.50
139.80
135.57
128.26
125.30
125.24
124.55
124.22
123.95
123.68
123.40
123.12
120.95
119.71
119.67
119.62
119.58
118.77
60.28
40.12
39.95
39.78
39.61
CF3
O2N
3b'
ppm

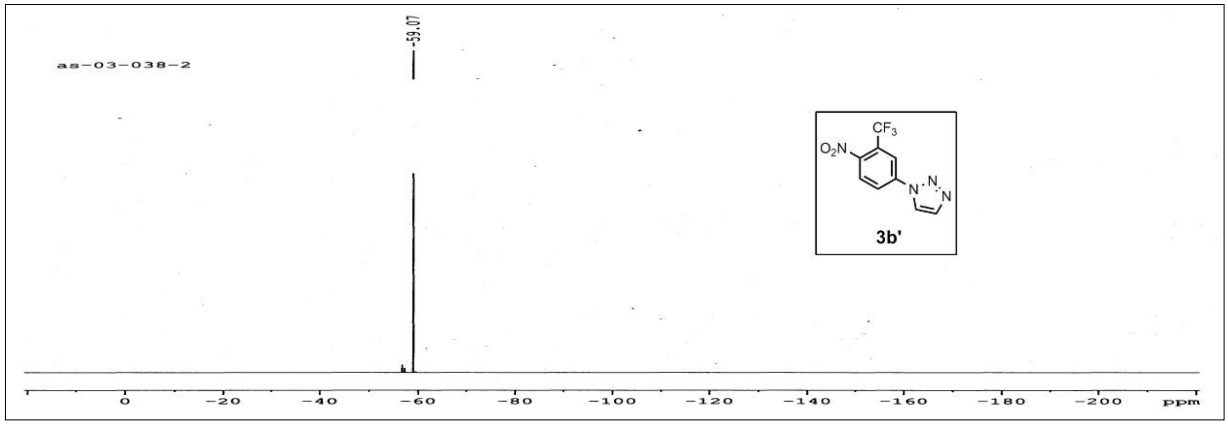
as-03-038-2
-59.07
CF3
O2N
3b'
ppm

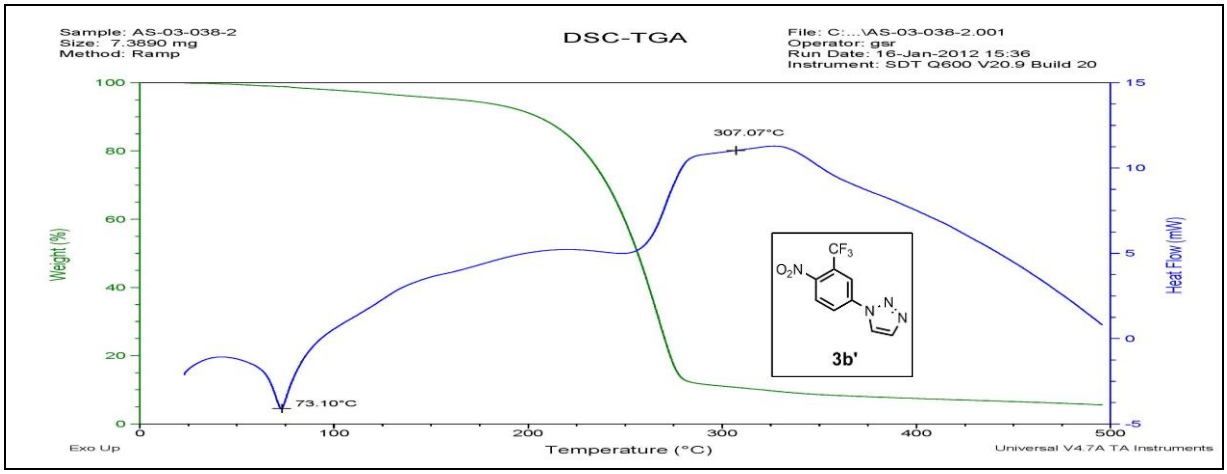
Sample: AS-03-038-2
Size: 7.3890 mg
Method: Ramp
DSC-TGA
File: C:...\AS-03-038-2.001
Operator: gsr
Run Date: 16-Jan-2012 15:36
Instrument: SDT Q600 V20.9 Build 20
307.07°C
73.10°C
Weight (%)
Heat Flow (mW)
Temperature (°C)
Exo Up
Universal V4.7A TA Instruments
CF3
O2N
3b'

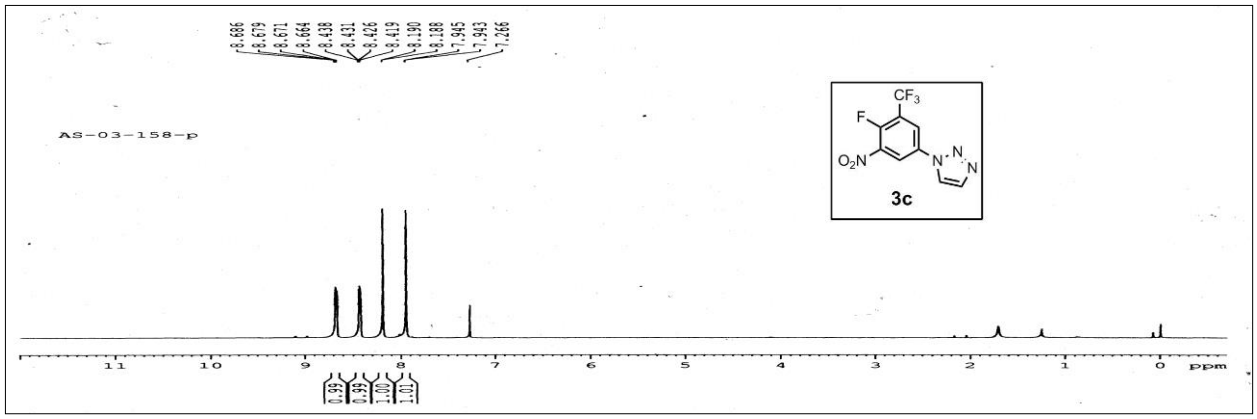
AS-03-158-p
8.666
8.679
8.671
8.664
8.438
8.431
8.426
8.419
8.190
8.188
7.945
7.943
7.266
CF3
F
O2N
N
N
N
3c
11
10
9
8
7
6
5
4
3
2
1
0
ppm
0.99
0.99
1.00
1.01

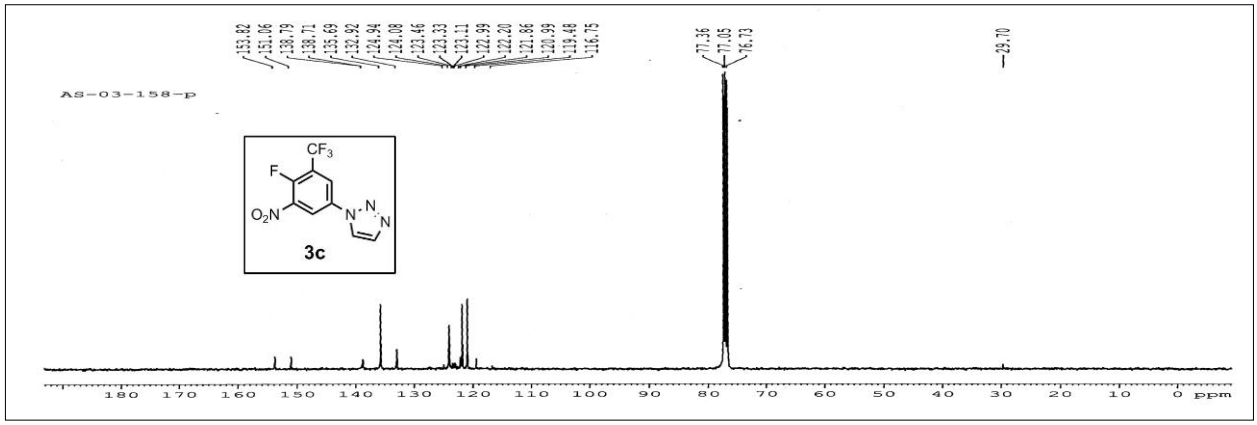
AS-03-158-p
153.82
151.06
138.79
138.71
135.69
132.92
124.94
124.08
123.46
123.33
123.11
122.99
122.20
121.86
120.99
119.48
116.75
77.36
77.05
76.73
29.70
CF3
F
O2N
N
N
N
3c
180
170
160
150
140
130
120
110
100
90
80
70
60
50
40
30
20
10
0
ppm

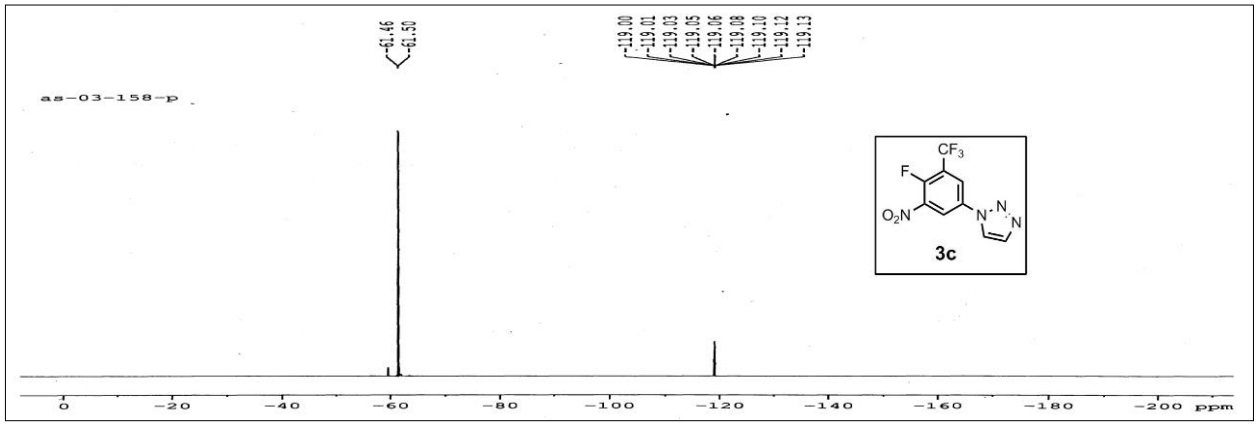
as-03-158-p
-61.46
-61.50
-119.00
-119.01
-119.03
-119.05
-119.06
-119.08
-119.10
-119.12
-119.13
CF3
F
O2N
N
N
N
3c
0
-20
-40
-60
-80
-100
-120
-140
-160
-180
-200
ppm

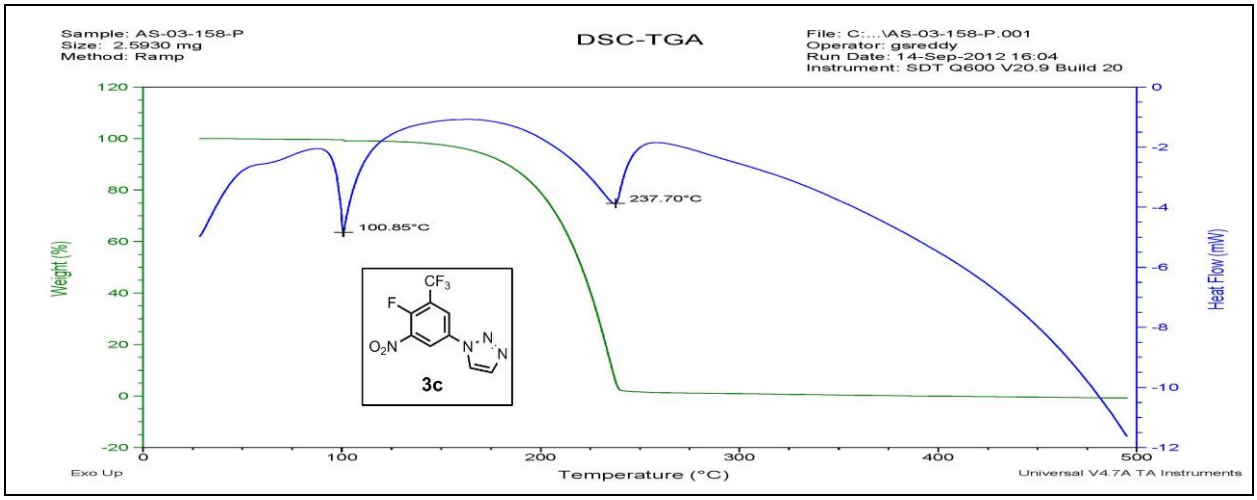
Sample: AS-03-158-P
Size: 2.5930 mg
Method: Ramp
DSC-TGA
File: C:...\AS-03-158-P.001
Operator: gsreddy
Run Date: 14-Sep-2012 16:04
Instrument: SDT Q600 V20.9 Build 20
100.85°C
237.70°C
CF3
F
O2N
N
N
N
3c
Weight (%)
Heat Flow (mW)
Exo Up
Temperature (°C)
Universal V4.7A TA Instruments

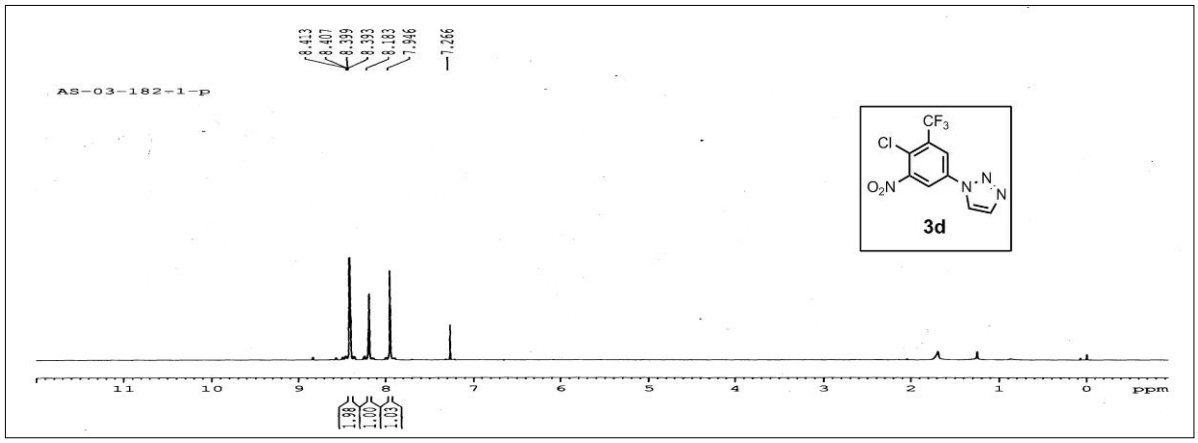
8.413
8.407
8.399
8.393
8.183
7.946
7.266
AS-03-182-1-p
CF3
Cl
O2N
N
N
N
3d
11
10
9
8
7
6
5
4
3
2
1
0
ppm
1.98
1.00
1.00
1.03

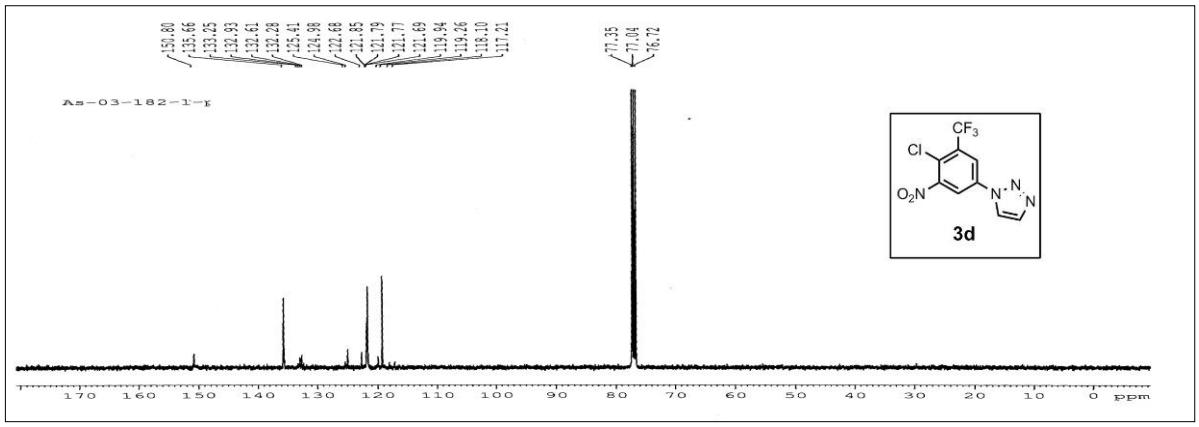
150.80
135.66
133.25
132.93
132.61
132.28
125.41
124.98
122.68
121.85
121.79
121.77
121.69
119.94
119.26
118.10
117.21
77.35
77.04
76.72
As-03-182-1-p
CF3
Cl
O2N
N
N
N
3d
170
160
150
140
130
120
110
100
90
80
70
60
50
40
30
20
10
0
ppm

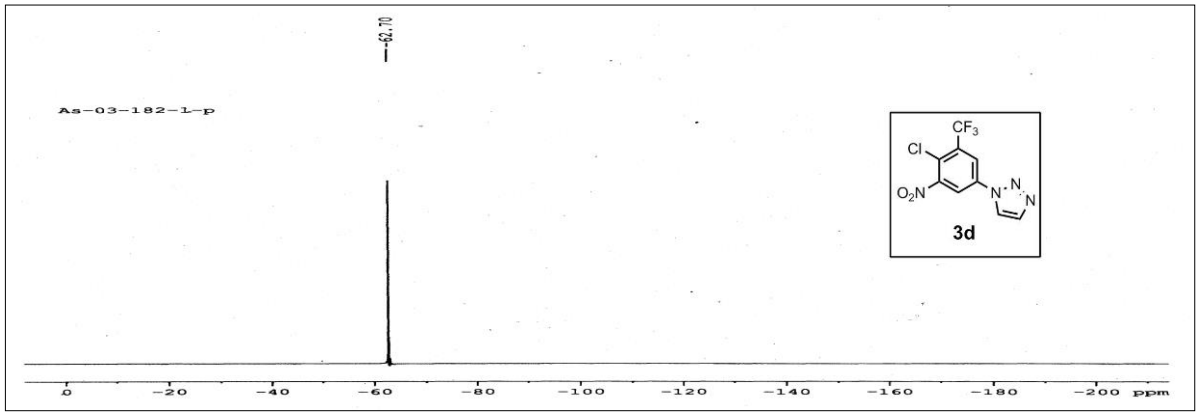
-62.10
As-03-182-1-p
CF3
Cl
O2N
N
N
N
3d
0
-20
-40
-60
-80
-100
-120
-140
-160
-180
-200
ppm

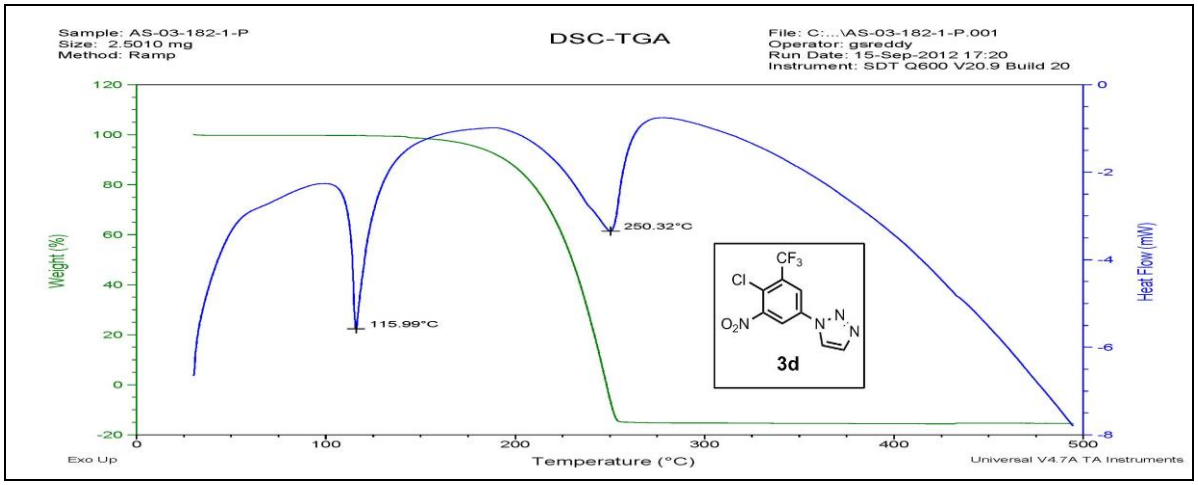
Sample: AS-03-182-1-P
Size: 2.5010 mg
Method: Ramp
DSC-TGA
File: C:...\AS-03-182-1-P.001
Operator: gsreddy
Run Date: 15-Sep-2012 17:20
Instrument: SDT Q600 V20.9 Build 20
Weight (%)
Heat Flow (mW)
115.99°C
250.32°C
CF3
Cl
O2N
N
N
N
3d
Exo Up
Temperature (°C)
Universal V4.7A TA Instruments

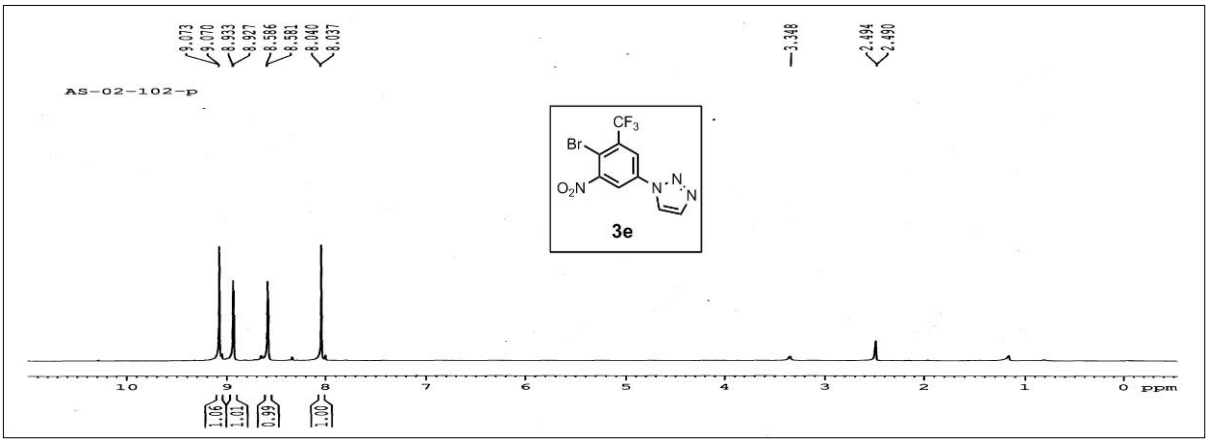
AS-02-102-p
9.073
9.070
8.933
8.927
8.586
8.581
8.040
8.037
3.348
2.494
2.490
3e
ppm

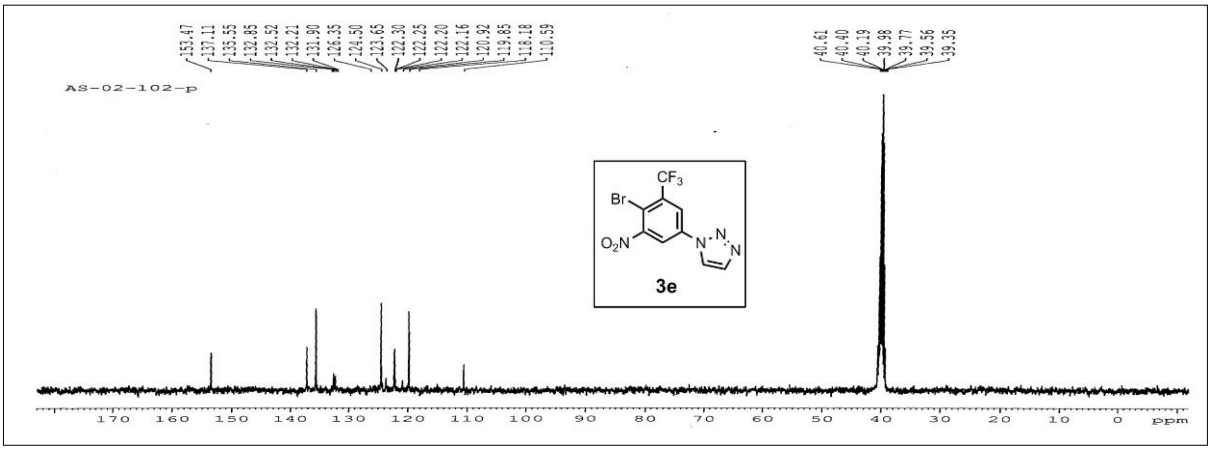
AS-02-102-p
153.47
137.11
135.55
132.85
132.52
132.21
131.90
126.35
124.50
123.63
122.30
122.25
122.20
122.16
120.92
119.85
118.18
110.59
40.61
40.40
40.19
39.98
39.77
39.56
39.35
3e
ppm

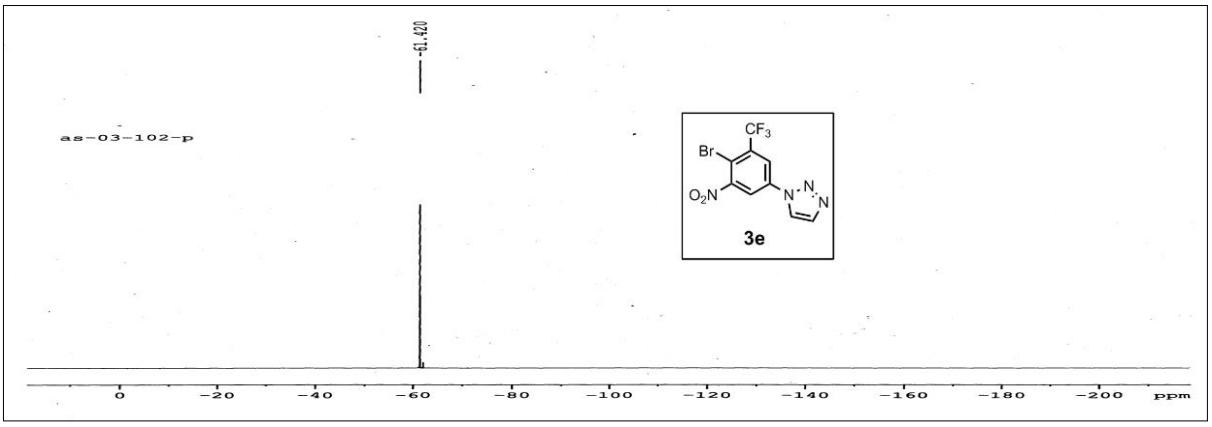
as-03-102-p
-61.420
3e
ppm

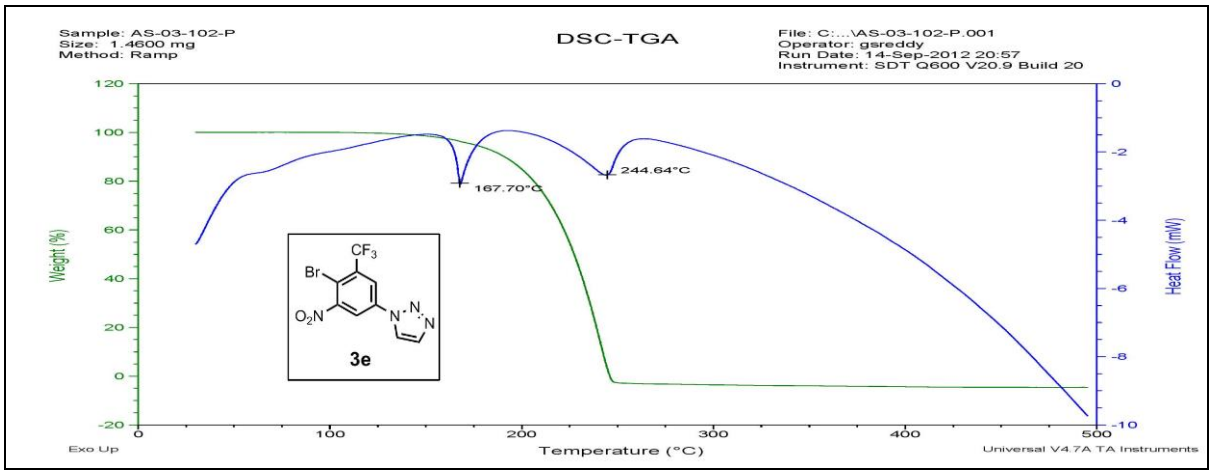
Sample: AS-03-102-P
Size: 1.4600 mg
Method: Ramp
DSC-TGA
File: C:...\AS-03-102-P.001
Operator: gsreddy
Run Date: 14-Sep-2012 20:57
Instrument: SDT Q600 V20.9 Build 20
167.70°C
244.64°C
3e
Weight (%)
Heat Flow (mW)
Temperature (°C)
Exo Up
Universal V4.7A TA Instruments

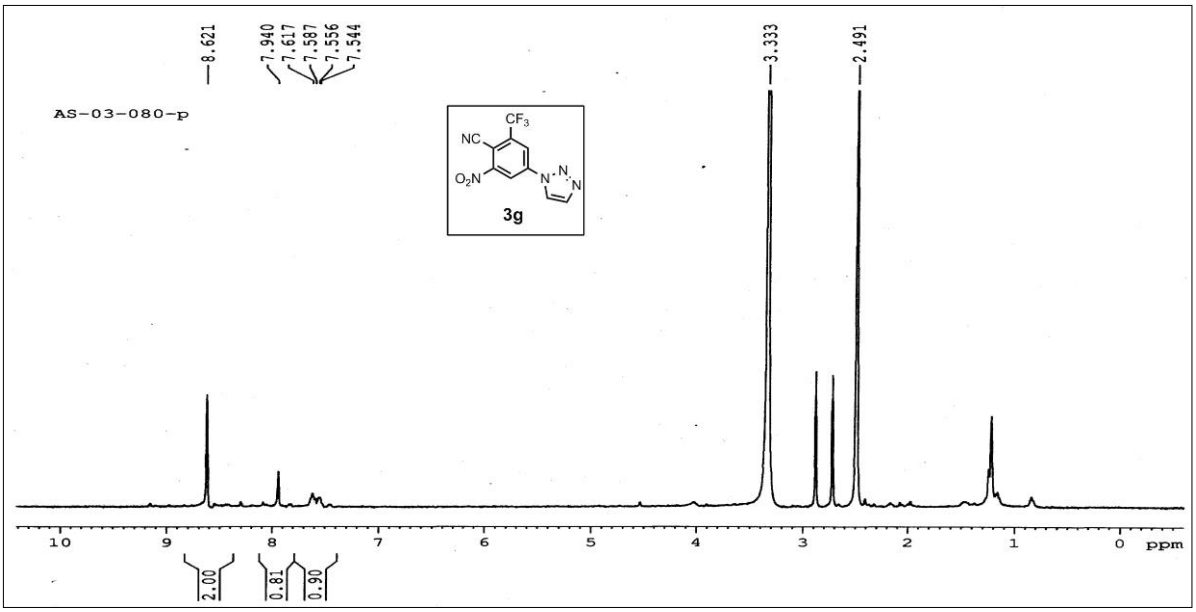
AS-03-080-p
8.621
7.940
7.617
7.587
7.556
7.544
3.333
2.491
3g
2.00
0.81
0.90
ppm

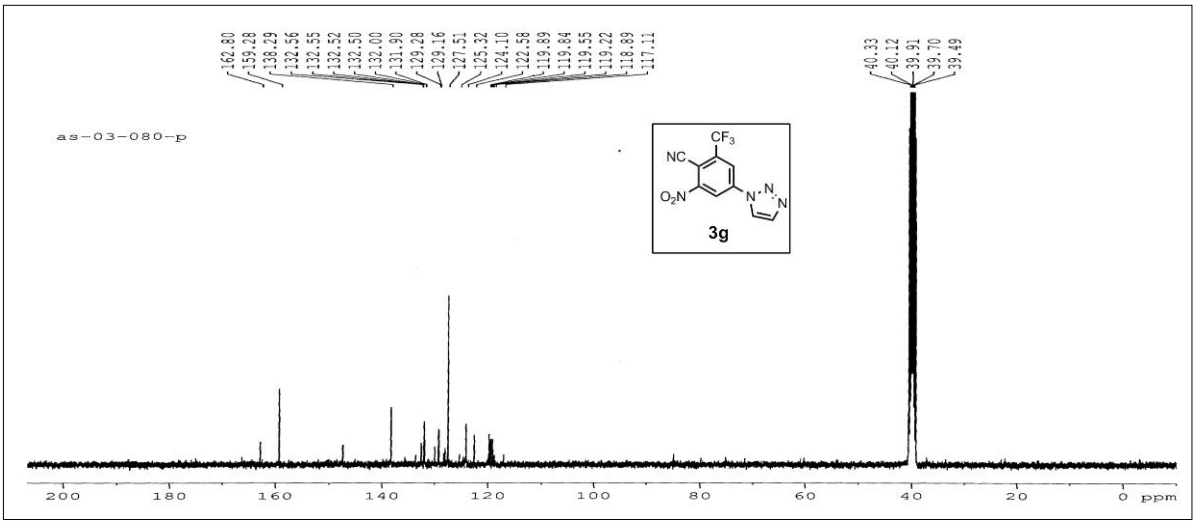
as-03-080-p
162.80
159.28
138.29
132.56
132.55
132.52
132.50
132.00
131.90
129.28
129.16
127.51
125.32
124.10
122.58
119.89
119.84
119.55
119.22
118.89
117.11
40.33
40.12
39.91
39.70
39.49
3g
ppm

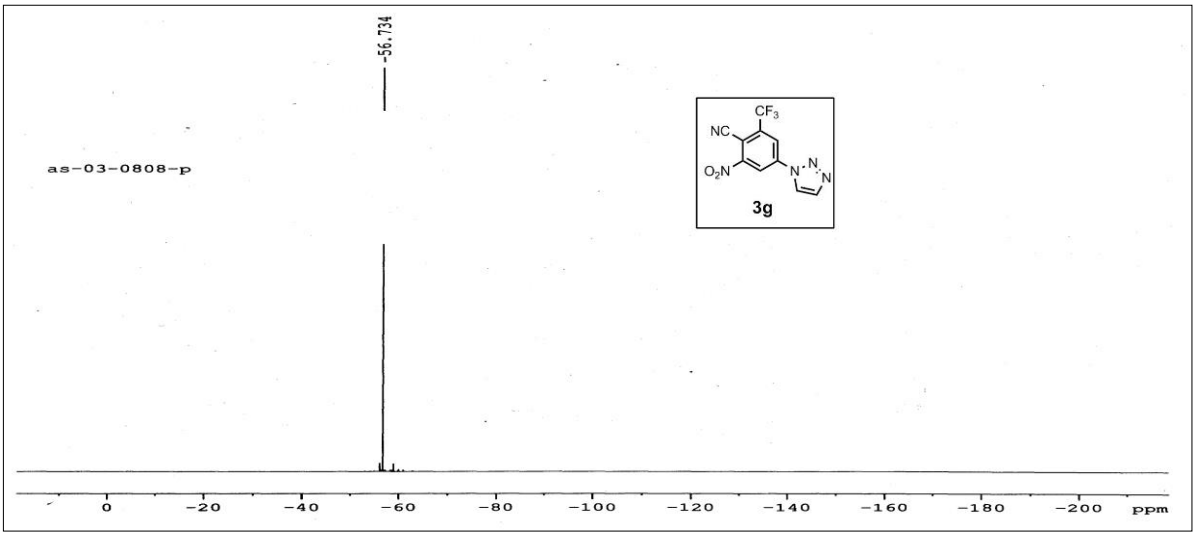
as-03-0808-p
-56.734
3g
ppm

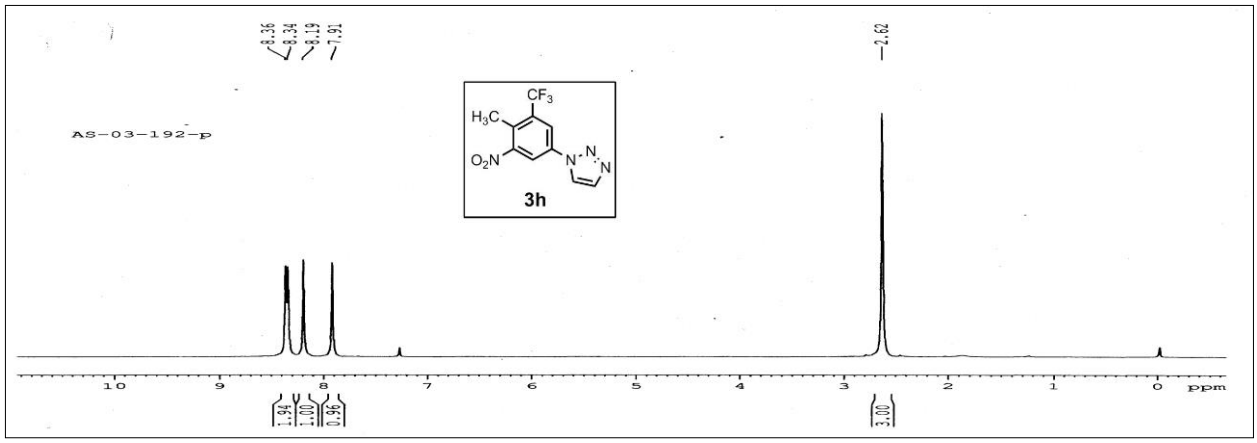
AS-03-192-p
8.36
8.34
8.19
7.91
2.62
1.94
2.00
0.96
3.00
ppm
3h

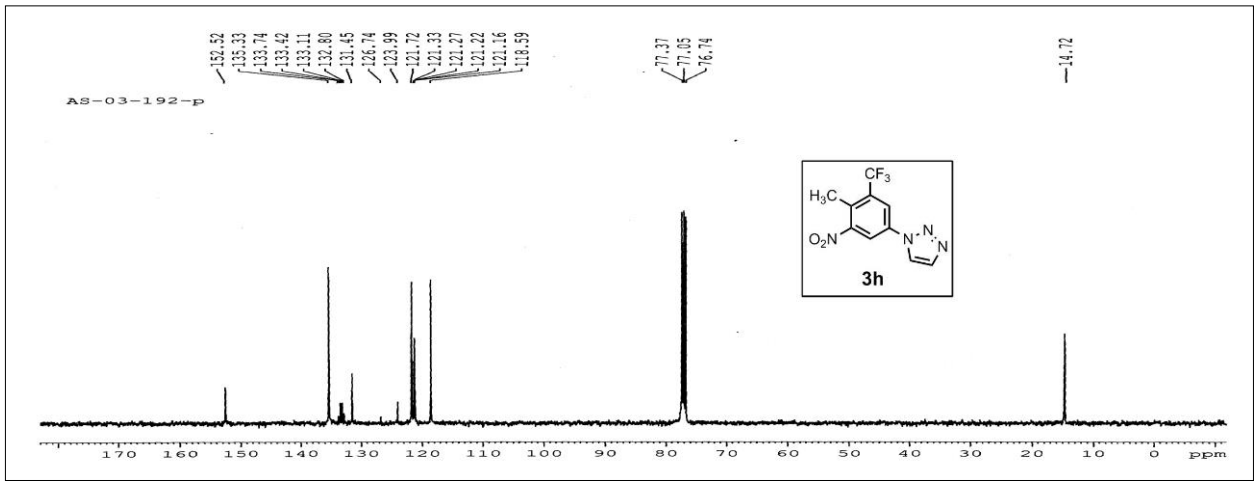
AS-03-192-p
152.52
135.33
133.74
133.42
133.11
132.80
131.45
126.74
123.99
121.72
121.33
121.27
121.22
121.16
118.59
77.37
77.05
76.74
14.72
ppm
3h

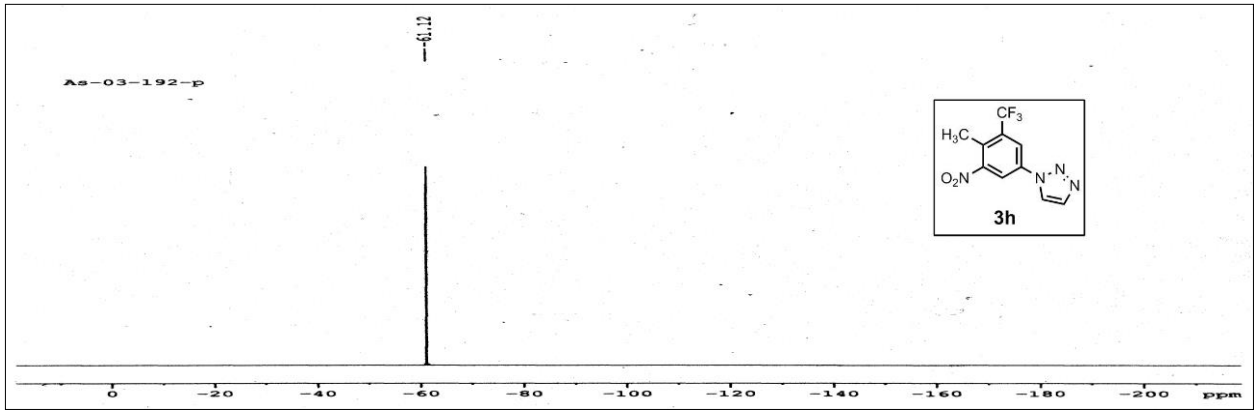
As-03-192-p
61.12
ppm
3h

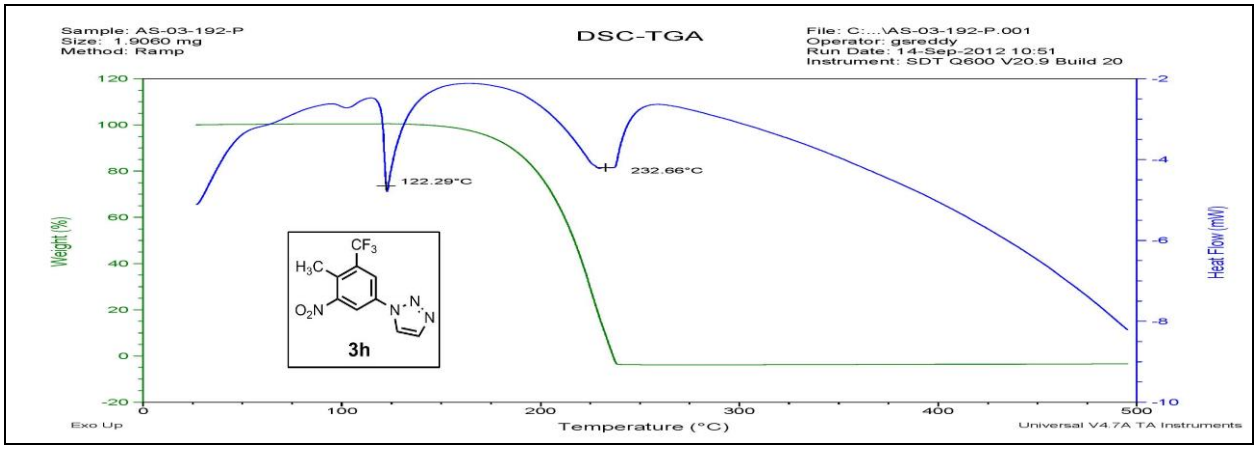
Sample: AS-03-192-P
Size: 1.9060 mg
Method: Ramp
DSC-TGA
File: C:...\AS-03-192-P.001
Operator: gsreddy
Run Date: 14-Sep-2012 10:51
Instrument: SDT Q600 V20.9 Build 20
122.29°C
232.66°C
Weight (%)
Heat Flow (mW)
Temperature (°C)
Exo Up
Universal V4.7A TA Instruments
3h

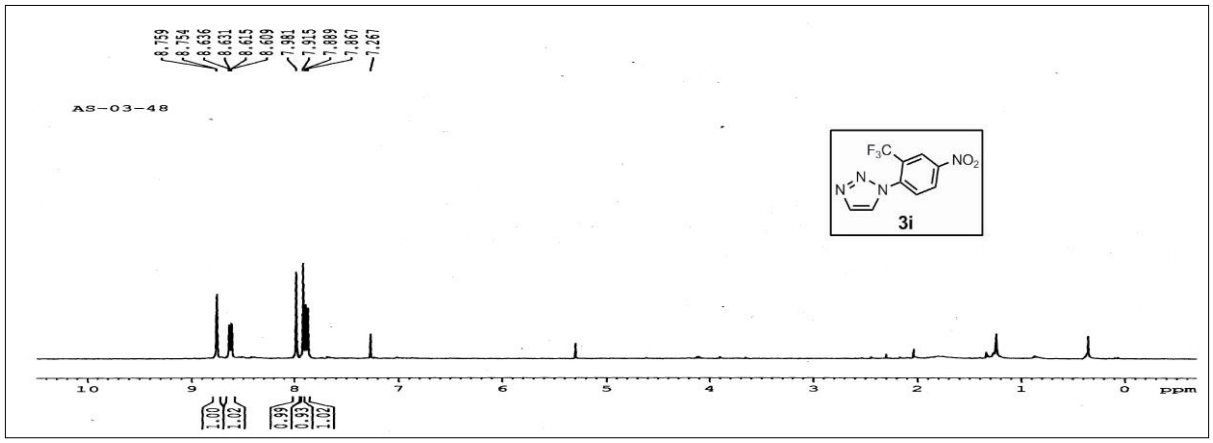
8.759
8.754
8.636
8.631
8.615
8.609
7.981
7.915
7.889
7.867
7.267
AS-03-48
3i
ppm

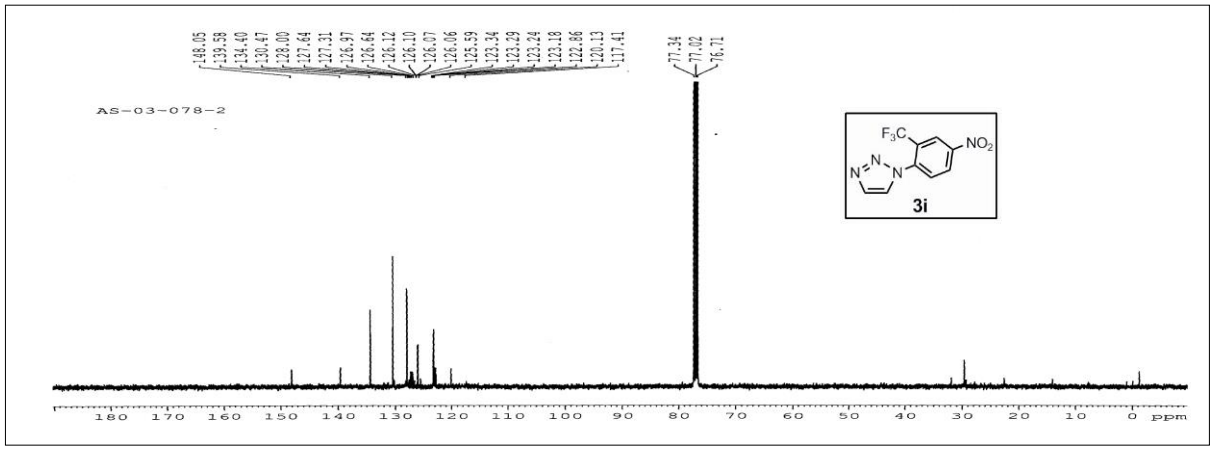
148.05
139.58
134.40
130.47
128.00
127.64
127.31
126.97
126.64
126.12
126.10
126.07
126.06
125.59
123.34
123.29
123.24
123.18
122.86
120.13
117.41
77.34
77.02
76.71
AS-03-078-2
3i
ppm

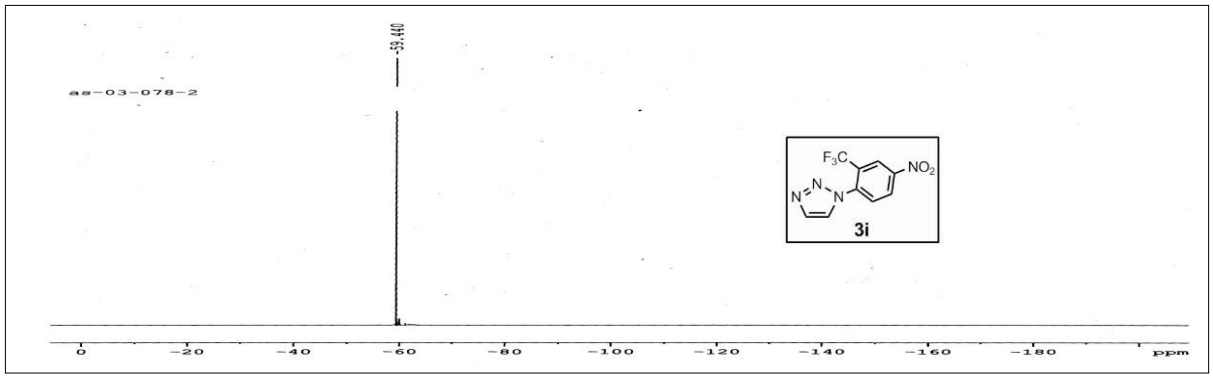
59.440
as-03-078-2
3i
ppm

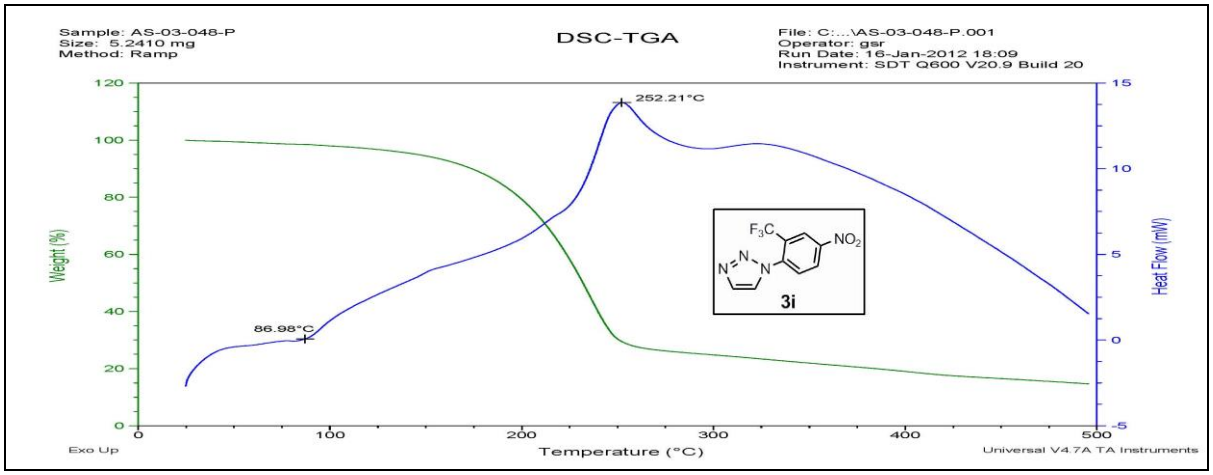
Sample: AS-03-048-P
Size: 5.2410 mg
Method: Ramp
DSC-TGA
File: C:...\AS-03-048-P.001
Operator: gsr
Run Date: 16-Jan-2012 18:09
Instrument: SDT Q600 V20.9 Build 20
252.21°C
86.98°C
3i
Weight (%)
Heat Flow (mW)
Exo Up
Temperature (°C)
Universal V4.7A TA Instruments

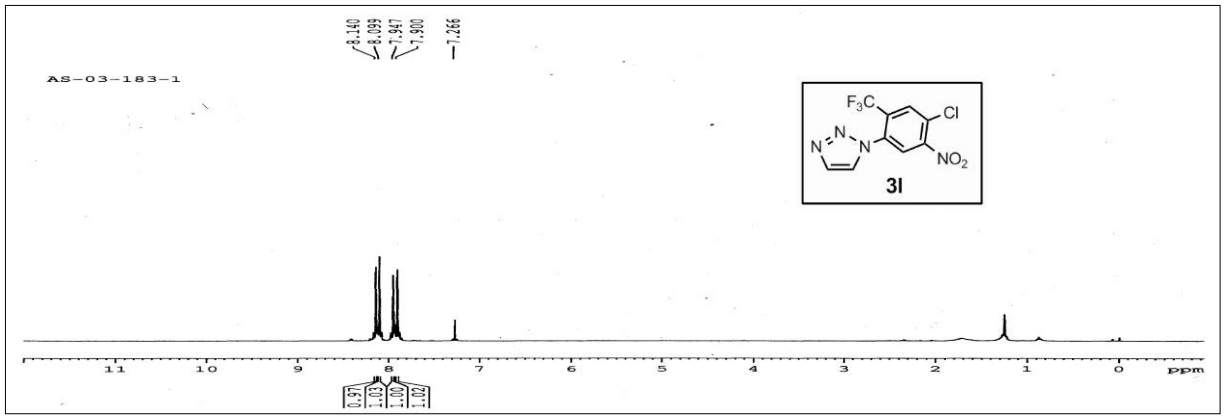
8.140
8.099
7.947
7.900
7.266
AS-03-183-1
3I
ppm

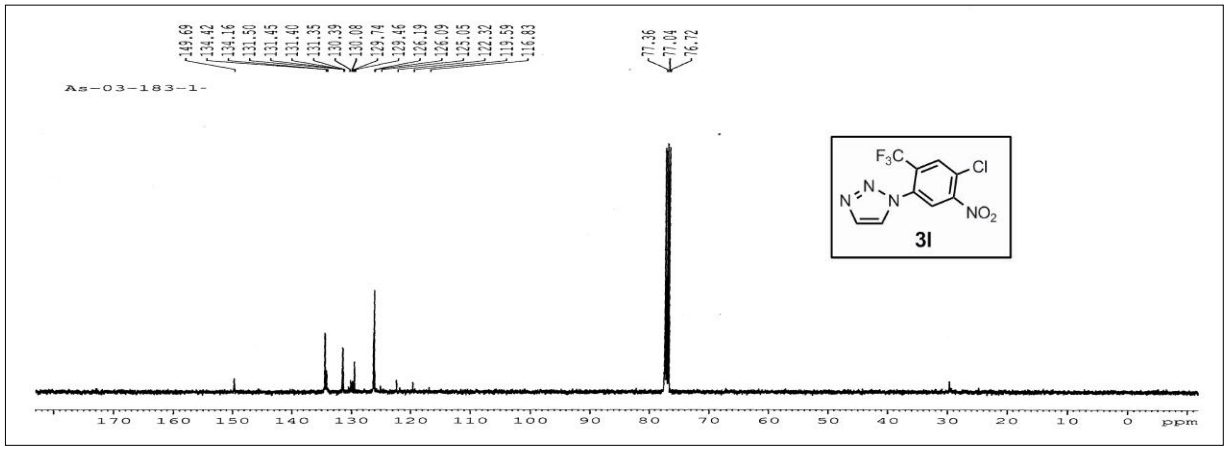
145.69
134.42
134.16
131.50
131.45
131.40
131.35
130.39
130.08
129.74
129.46
126.19
126.09
125.05
122.32
119.59
116.83
77.36
77.04
76.72
As-03-183-1-
3I
ppm

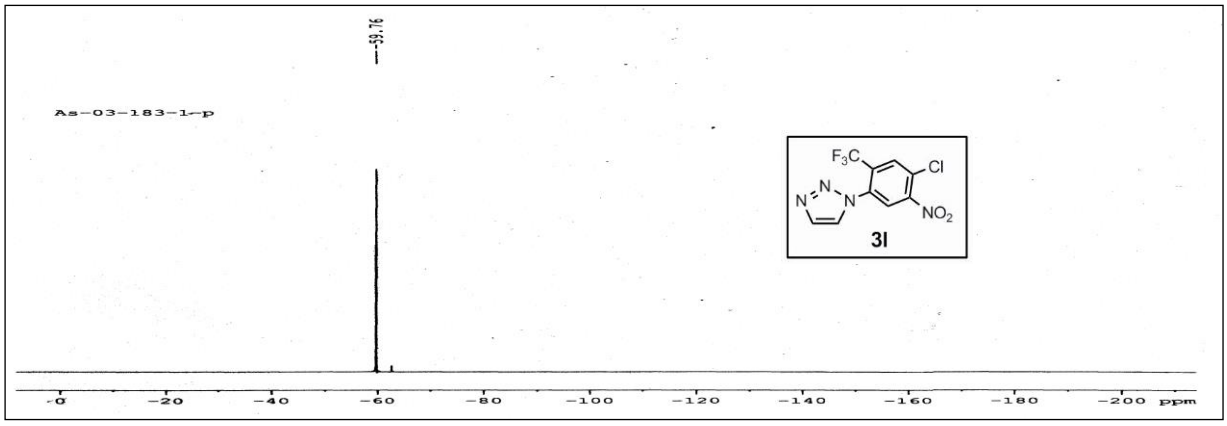
-59.76
As-03-183-1-p
3I
ppm

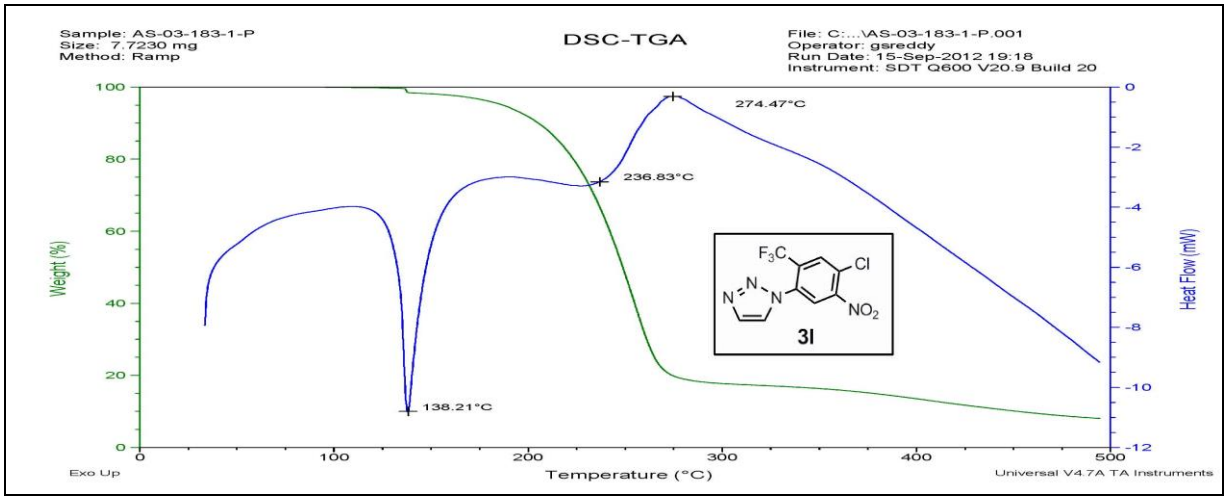
Sample: AS-03-183-1-P
Size: 7.7230 mg
Method: Ramp
DSC-TGA
File: C:...\AS-03-183-1-P.001
Operator: gsreddy
Run Date: 15-Sep-2012 19:18
Instrument: SDT Q600 V20.9 Build 20
274.47°C
236.83°C
138.21°C
3I
Weight (%)
Heat Flow (mW)
Exo Up
Temperature (°C)
Universal V4.7A TA Instruments

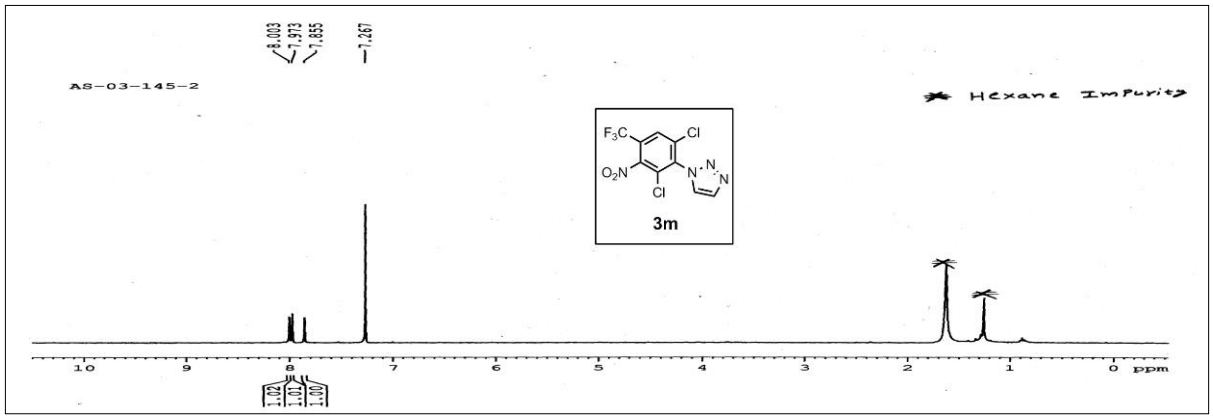
8.003
7.973
7.855
7.267
AS-03-145-2
Hexane Impurity
3m
1.02
1.01
1.00
ppm

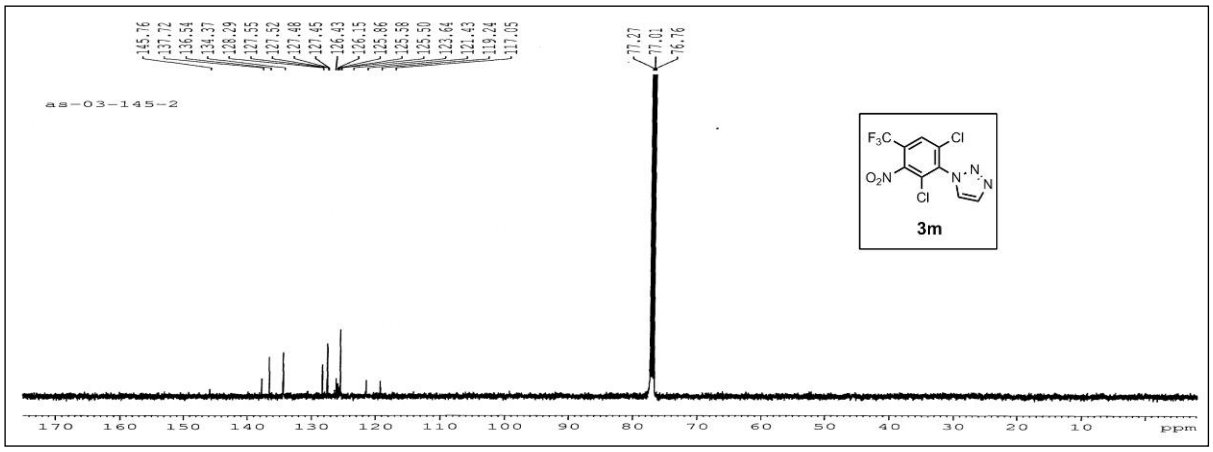
145.76
137.72
136.54
134.37
128.29
127.55
127.52
127.48
127.45
126.43
126.15
125.86
125.58
125.50
123.64
121.43
119.24
117.05
77.27
77.01
76.76
as-03-145-2
3m
ppm

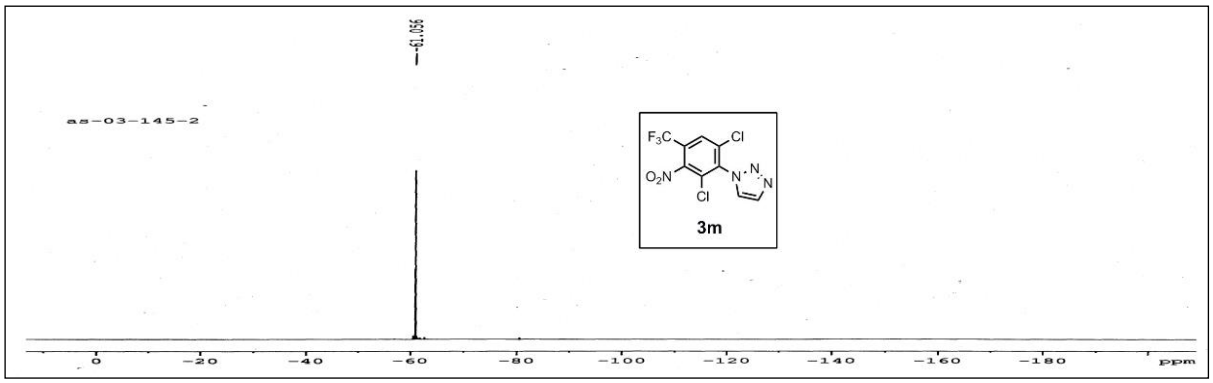
-61.056
as-03-145-2
3m
ppm

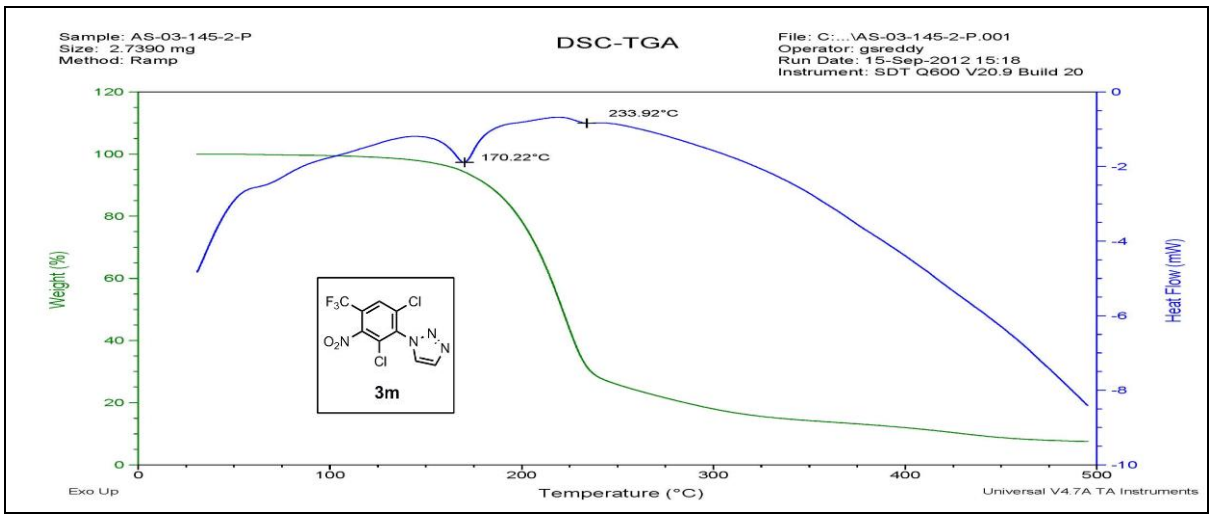
Sample: AS-03-145-2-P
Size: 2.7390 mg
Method: Ramp
DSC-TGA
File: C:...\AS-03-145-2-P.001
Operator: gsreddy
Run Date: 15-Sep-2012 15:18
Instrument: SDT Q600 V20.9 Build 20
233.92°C
170.22°C
3m
Weight (%)
Heat Flow (mW)
Exo Up
Temperature (°C)
Universal V4.7A TA Instruments

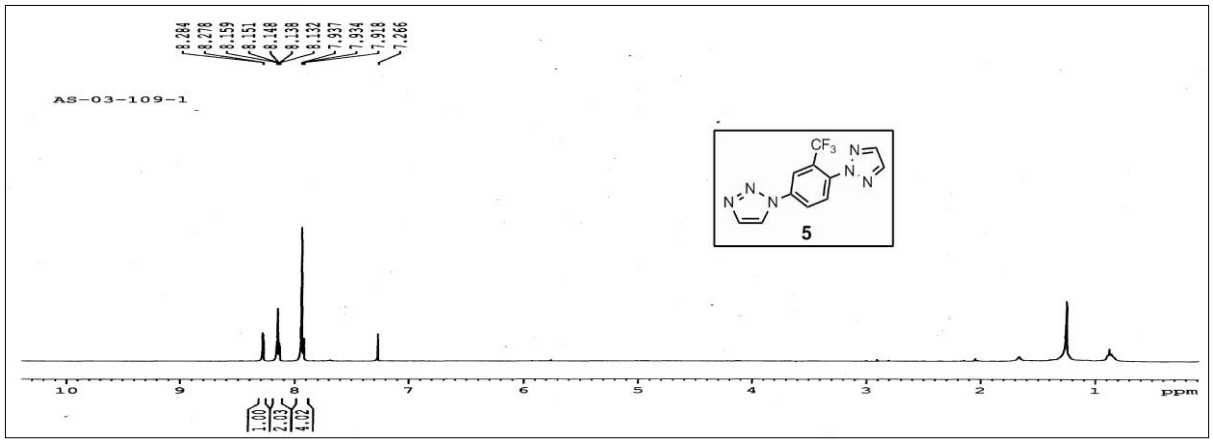
AS-03-109-1
8.284
8.278
8.159
8.151
8.148
8.138
8.132
7.937
7.934
7.918
7.266
1.00
2.03
4.02
CF3
5
ppm

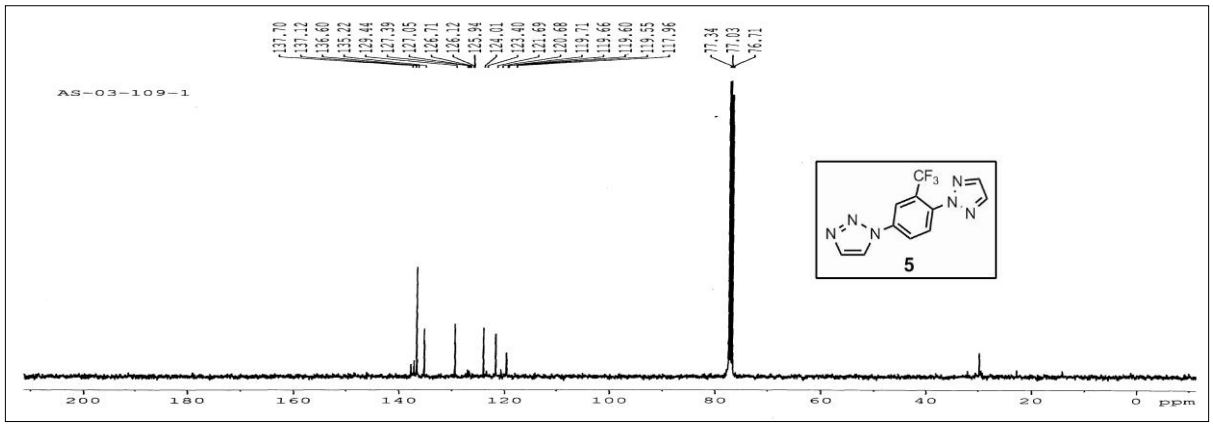
AS-03-109-1
137.70
137.12
136.60
135.22
129.44
127.39
127.05
126.71
126.12
125.94
124.01
123.40
121.69
120.68
119.71
119.66
119.60
119.55
117.96
77.34
77.03
76.71
CF3
5
ppm

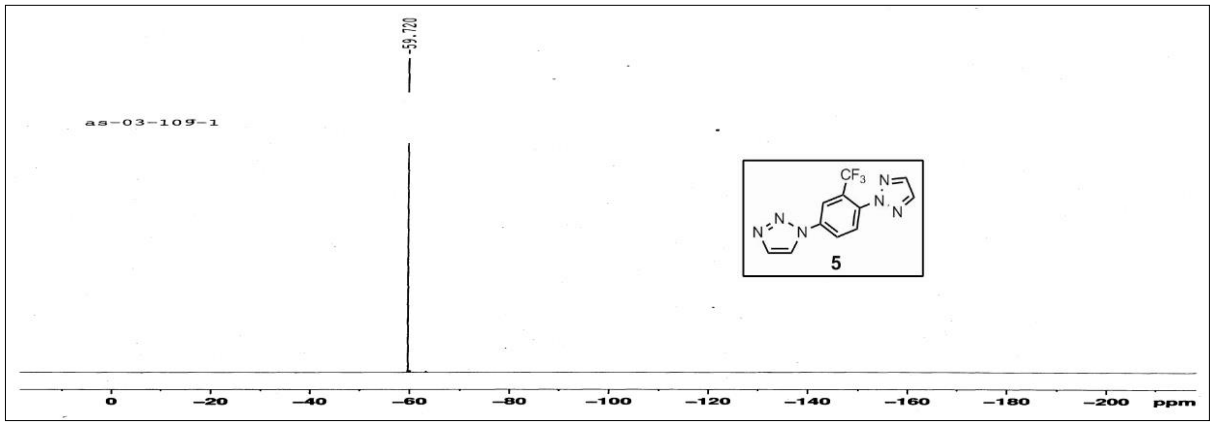
as-03-109-1
-59.720
CF3
5
ppm

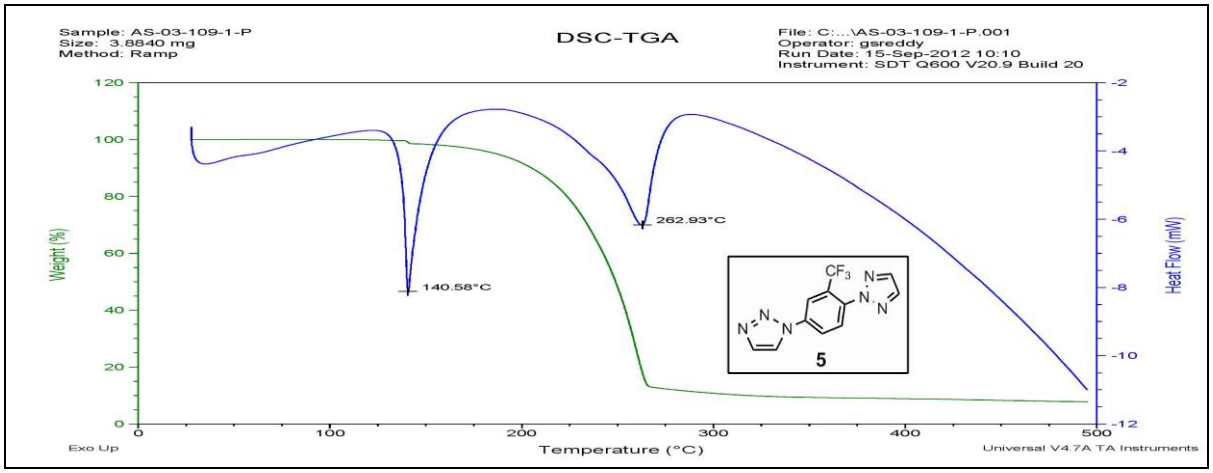
Sample: AS-03-109-1-P
Size: 3.8840 mg
Method: Ramp
DSC-TGA
File: C:...\AS-03-109-1-P.001
Operator: gsreddy
Run Date: 15-Sep-2012 10:10
Instrument: SDT Q600 V20.9 Build 20
140.58°C
262.93°C
CF3
5
Weight (%)
Heat Flow (mW)
Temperature (°C)
Exo Up
Universal V4.7A TA Instruments

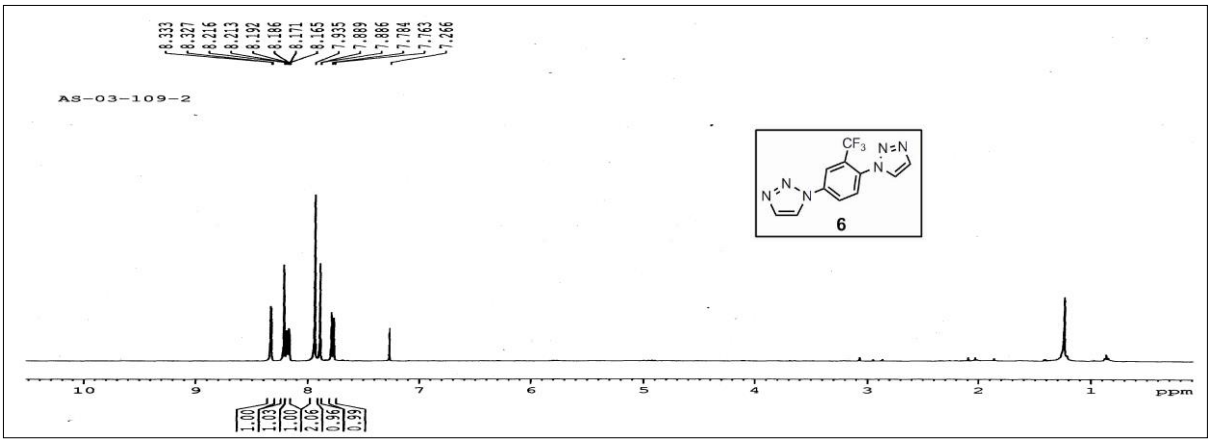
AS-03-109-2
8.333
8.327
8.215
8.213
8.192
8.186
8.171
8.165
7.935
7.889
7.886
7.784
7.763
7.266
1.00
1.03
1.00
2.06
0.96
0.99
10
9
8
7
6
5
4
3
2
1
ppm
CF3
N=N
6

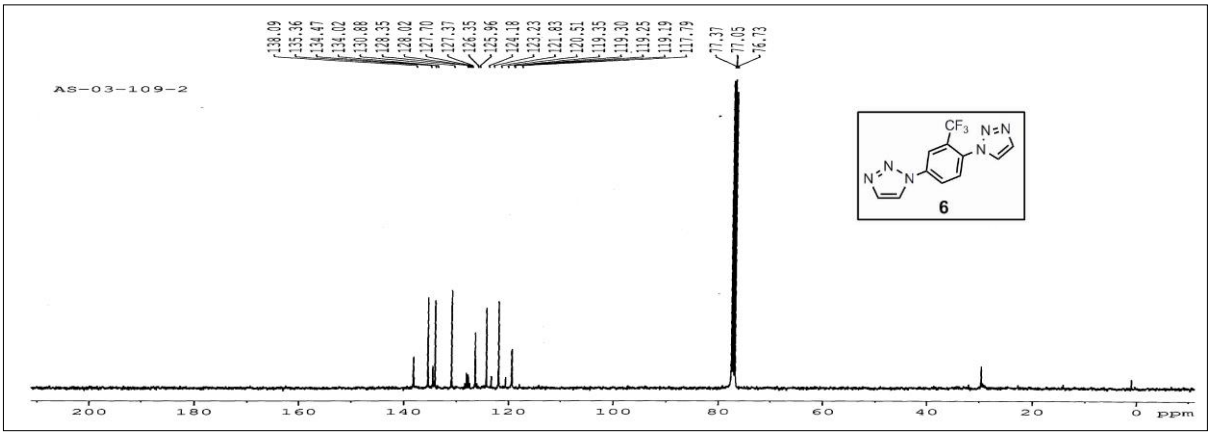
AS-03-109-2
138.09
135.36
134.47
134.02
130.88
128.35
128.02
127.70
127.37
126.35
125.96
124.18
123.23
121.83
120.51
119.35
119.30
119.25
119.19
117.79
77.37
77.05
76.73
200
180
160
140
120
100
80
60
40
20
0
ppm
CF3
N=N
6

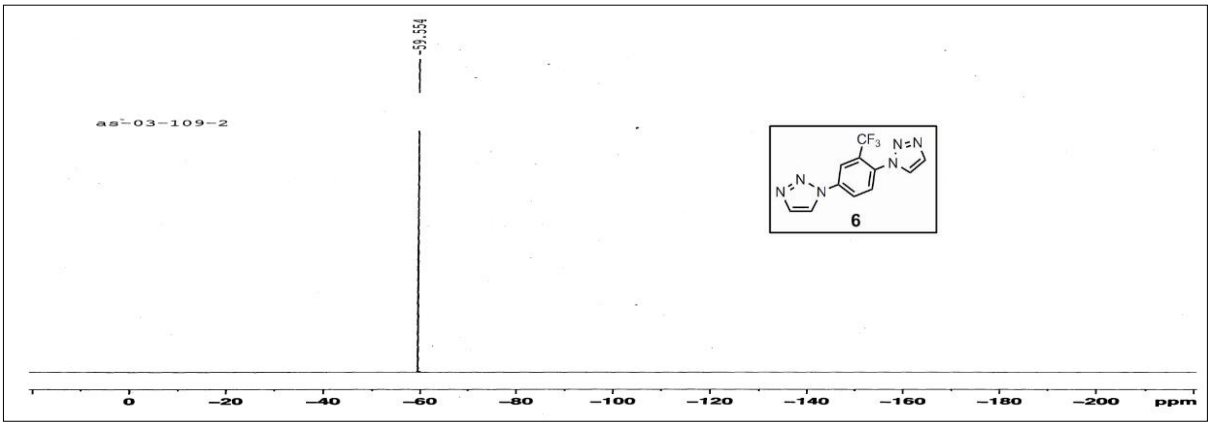
as-03-109-2
-59.554
0
-20
-40
-60
-80
-100
-120
-140
-160
-180
-200
ppm
CF3
N=N
6

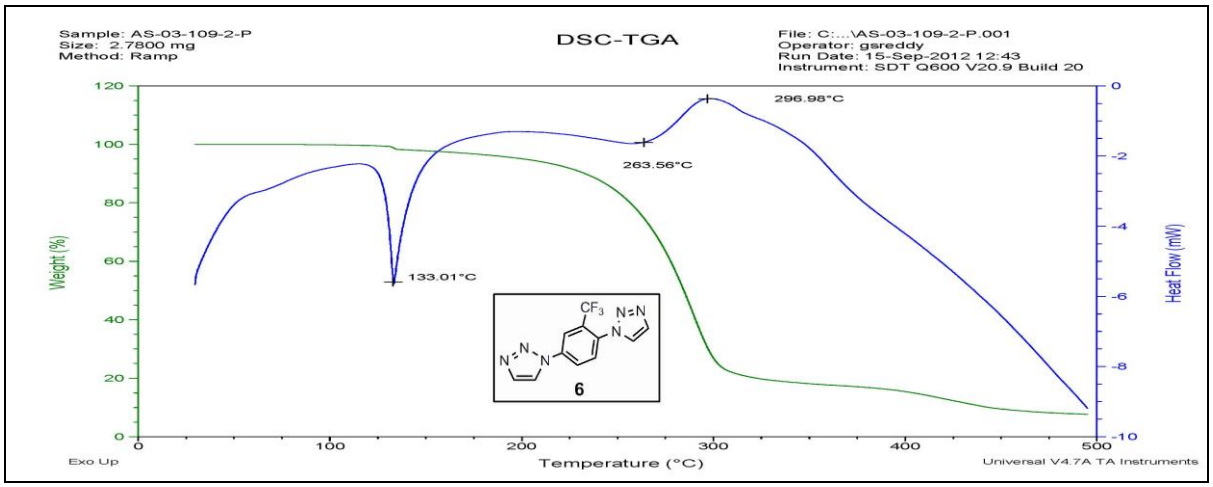
Sample: AS-03-109-2-P
Size: 2.7800 mg
Method: Ramp
DSC-TGA
File: C:...\AS-03-109-2-P.001
Operator: gsreddy
Run Date: 15-Sep-2012 12:43
Instrument: SDT Q600 V20.9 Build 20
296.98°C
263.56°C
133.01°C
Weight (%)
Heat Flow (mW)
Temperature (°C)
Exo Up
Universal V4.7A TA Instruments
CF3
N=N
6

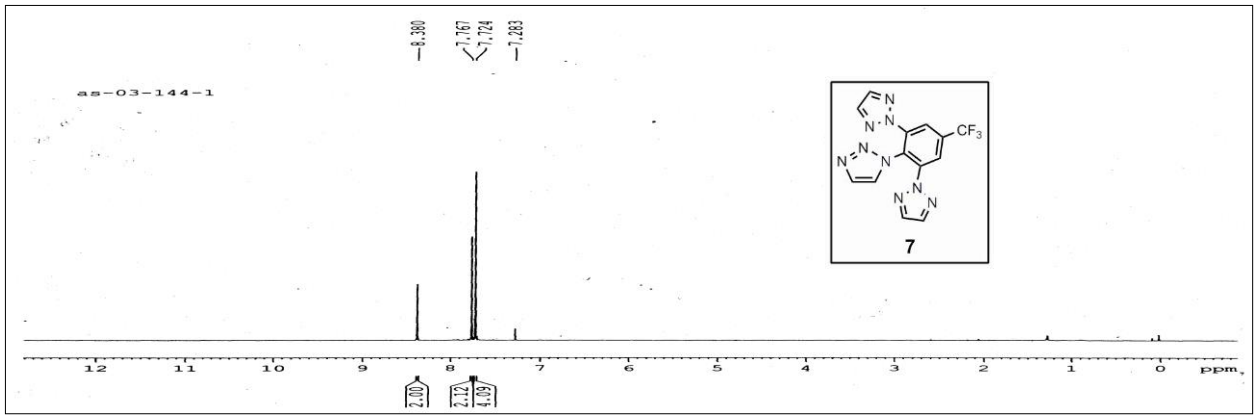
as-03-144-1
8.380
7.767
7.724
7.283
2.00
2.12
4.09
7
ppm

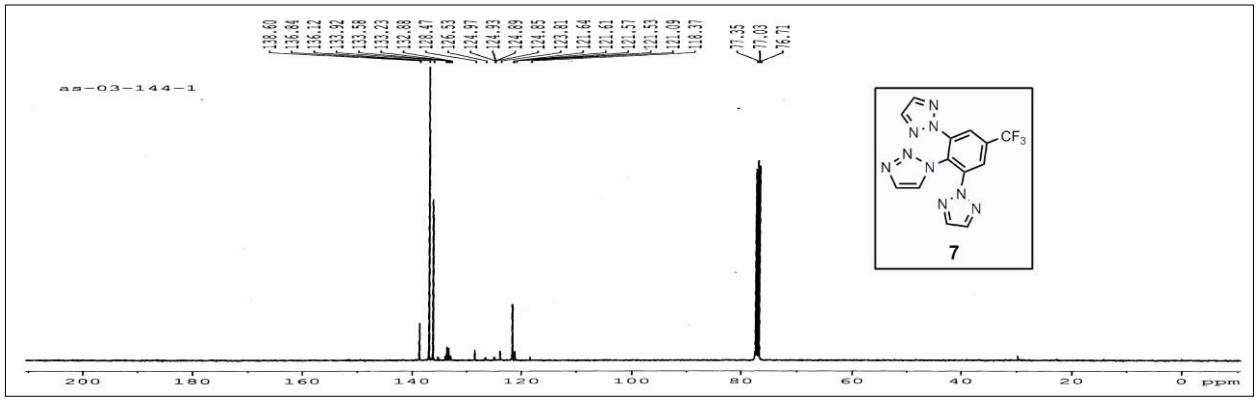
as-03-144-1
138.60
136.84
136.12
133.92
133.58
133.23
132.88
128.47
126.53
124.97
124.93
124.89
124.65
123.81
121.64
121.61
121.57
121.53
121.09
118.37
77.35
77.03
76.71
7
ppm

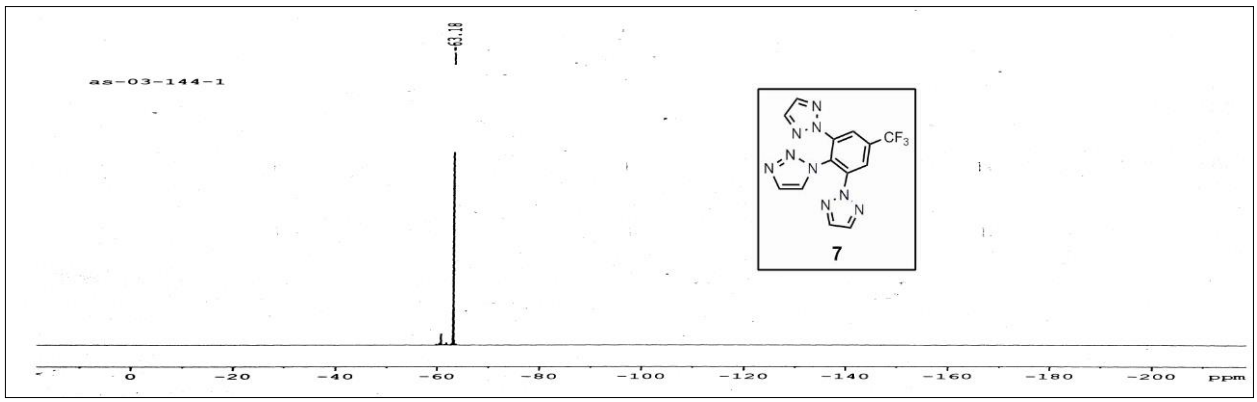
as-03-144-1
-63.18
7
ppm

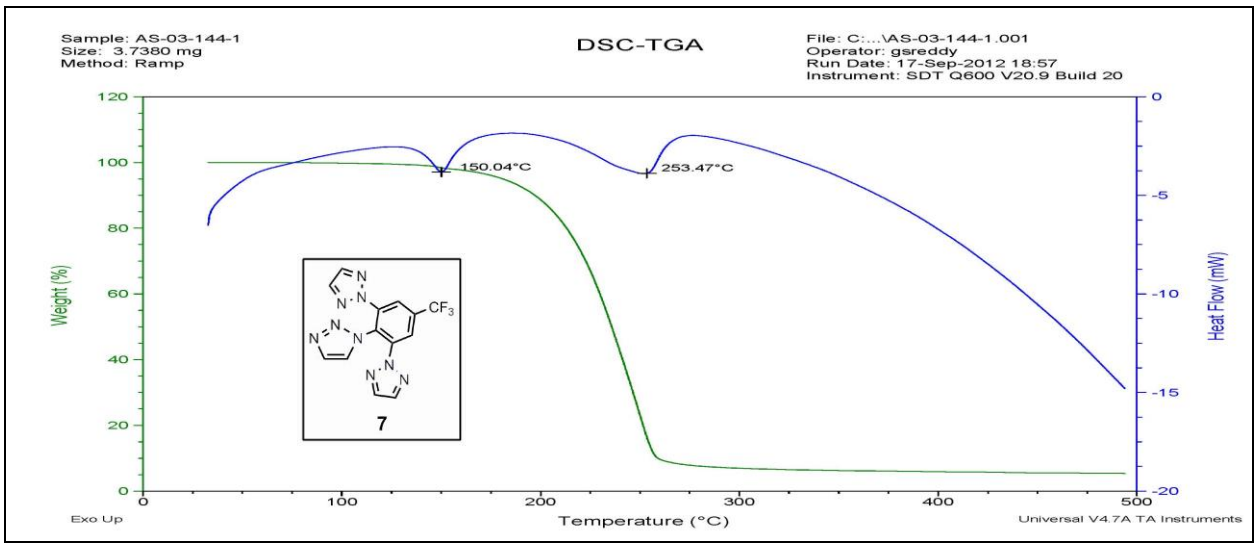
Sample: AS-03-144-1
Size: 3.7380 mg
Method: Ramp
DSC-TGA
File: C:...\AS-03-144-1.001
Operator: gsreddy
Run Date: 17-Sep-2012 18:57
Instrument: SDT Q600 V20.9 Build 20
150.04°C
253.47°C
Weight (%)
Heat Flow (mW)
Exo Up
Temperature (°C)
Universal V4.7A TA Instruments
7

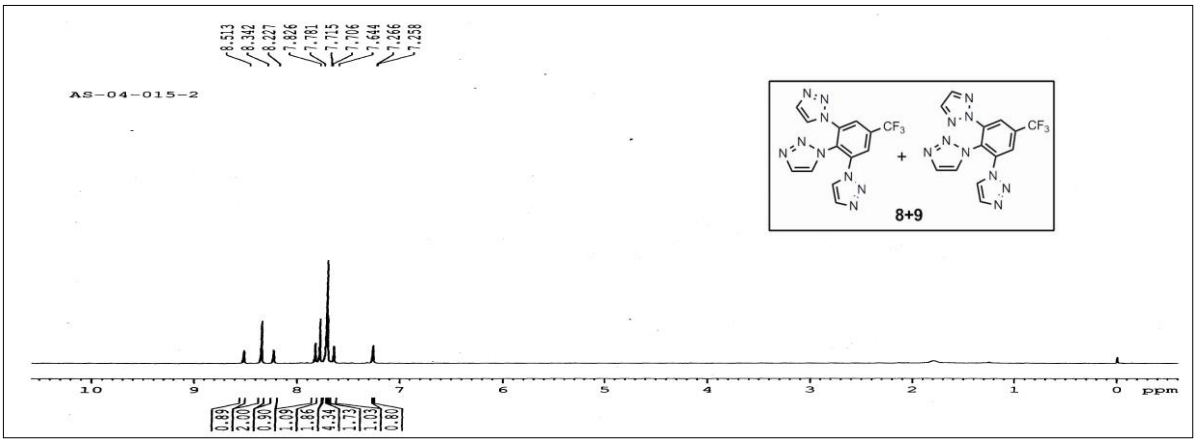
AS-04-015-2
8+9
ppm

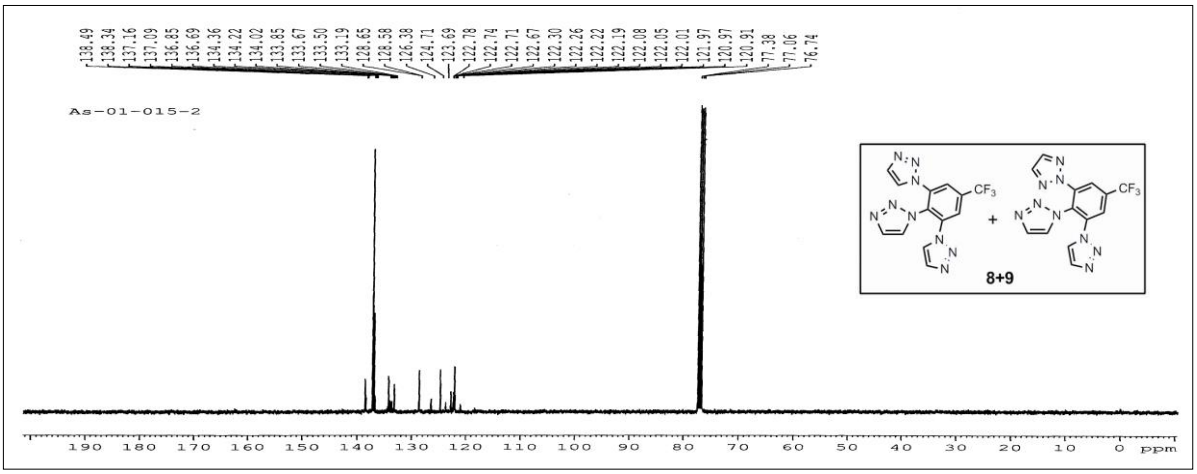
As-01-015-2
8+9
ppm

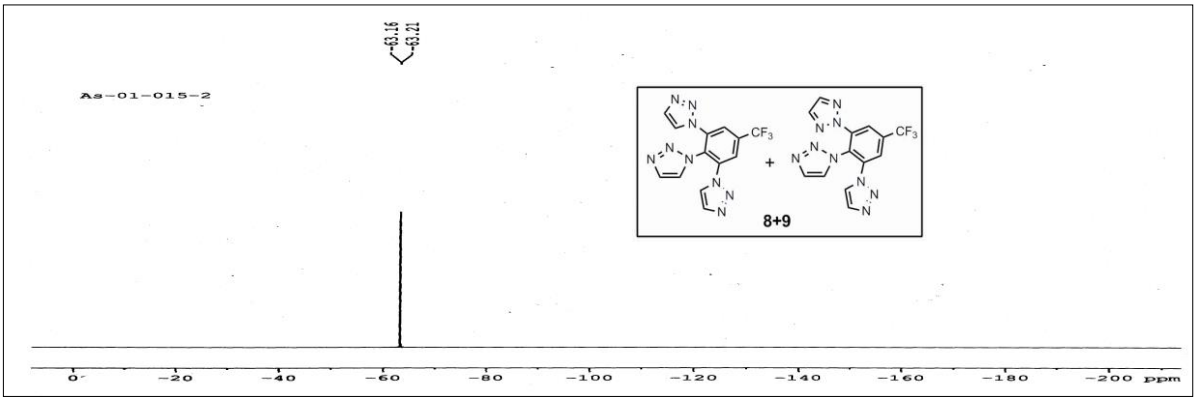
As-01-015-2
8+9
ppm

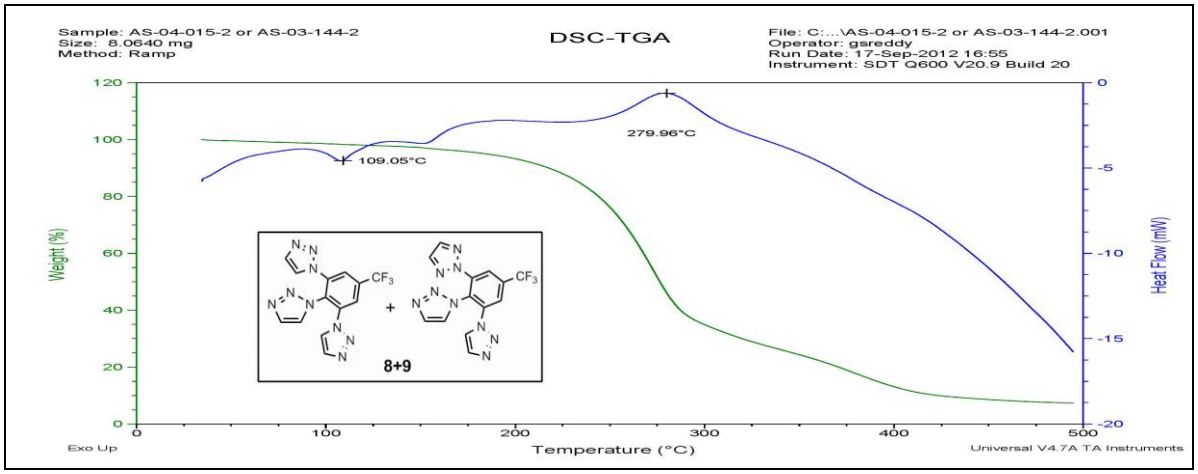
Sample: AS-04-015-2 or AS-03-144-2
Size: 8.0640 mg
Method: Ramp
DSC-TGA
File: C:...\AS-04-015-2 or AS-03-144-2.001
Operator: gsreddy
Run Date: 17-Sep-2012 16:55
Instrument: SDT Q600 V20.9 Build 20
109.05°C
279.96°C
8+9
Weight (%)
Heat Flow (mW)
Temperature (°C)
Exo Up
Universal V4.7A TA Instruments

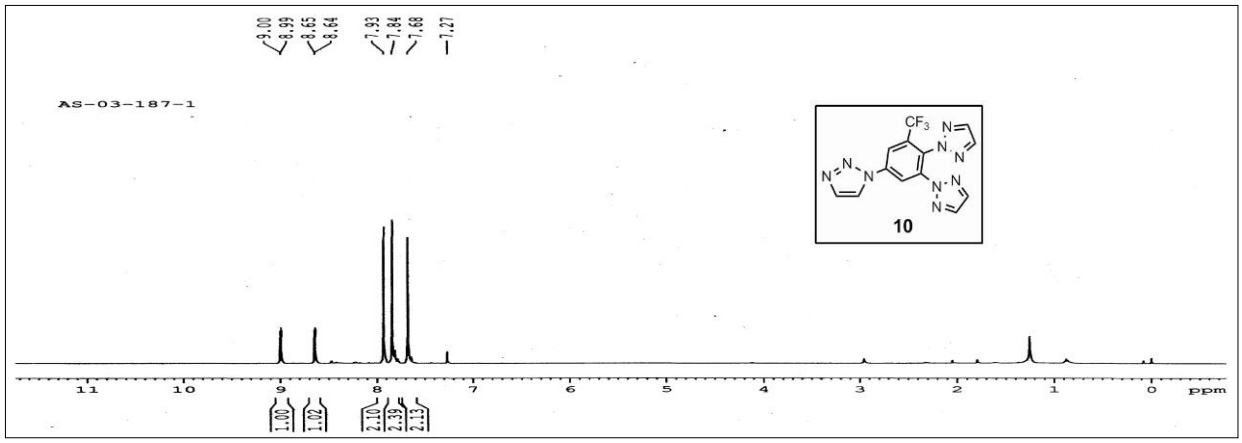
AS-03-187-1
9.00
8.99
8.65
8.64
7.93
7.84
7.68
7.27
1.00
1.02
2.10
2.39
2.13
ppm
10

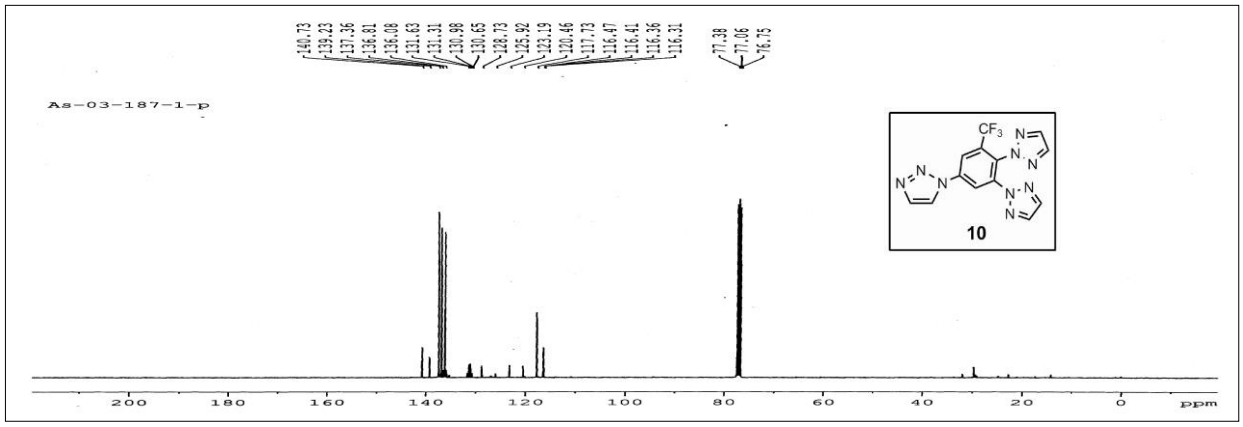
As-03-187-1-p
140.73
139.23
137.36
136.81
136.08
131.63
131.31
130.98
130.65
128.73
125.92
123.19
120.46
117.73
116.47
116.41
116.36
116.31
77.38
77.06
76.75
ppm
10

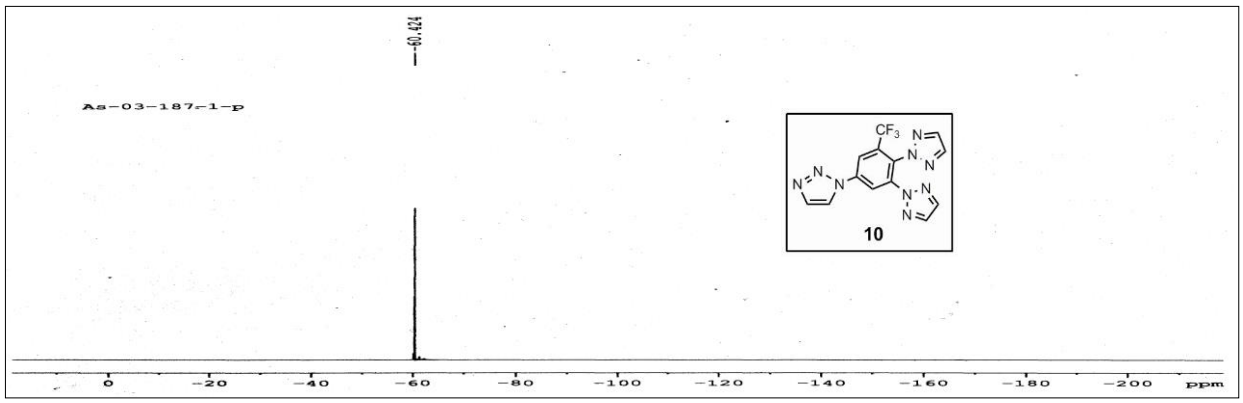
As-03-187-1-p
-60.424
ppm
10

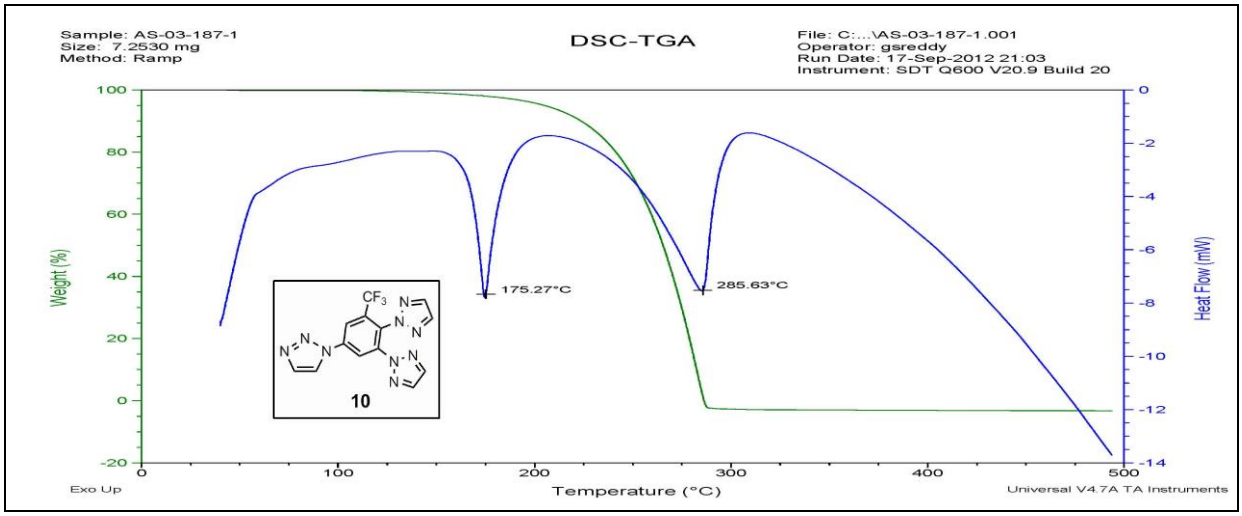
Sample: AS-03-187-1
Size: 7.2530 mg
Method: Ramp
DSC-TGA
File: C:...\AS-03-187-1.001
Operator: gsreddy
Run Date: 17-Sep-2012 21:03
Instrument: SDT Q600 V20.9 Build 20
Weight (%)
Heat Flow (mW)
175.27°C
285.63°C
10
Exo Up
Temperature (°C)
Universal V4.7A TA Instruments

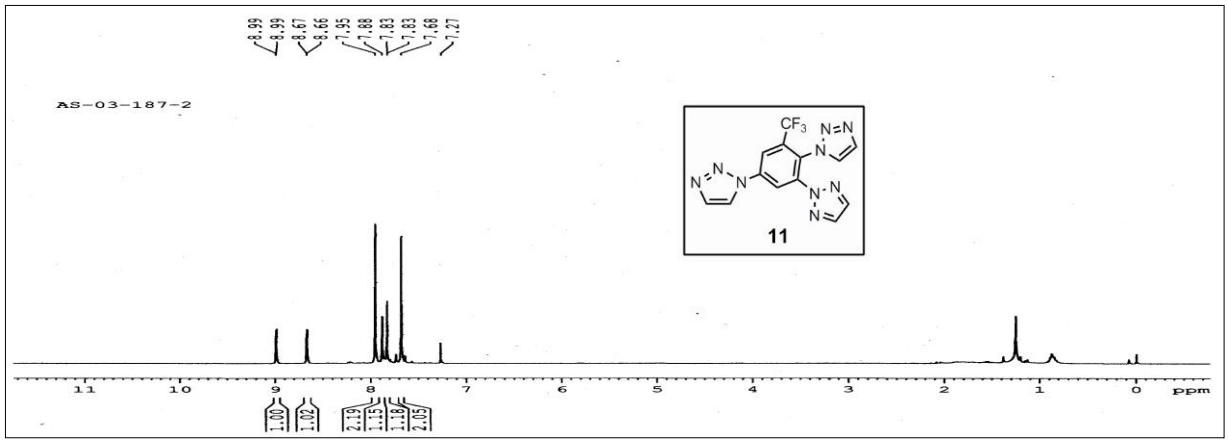
AS-03-187-2
11
ppm

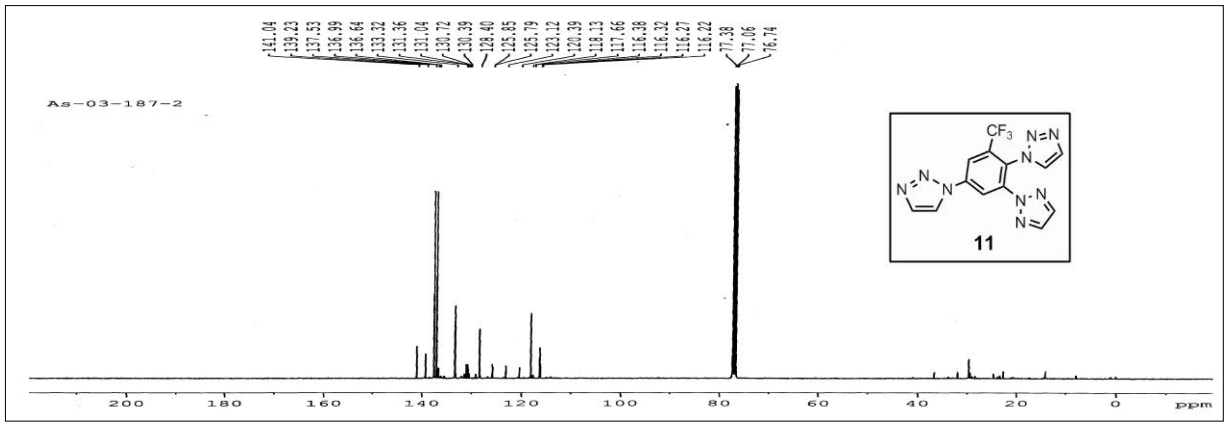
As-03-187-2
11
ppm

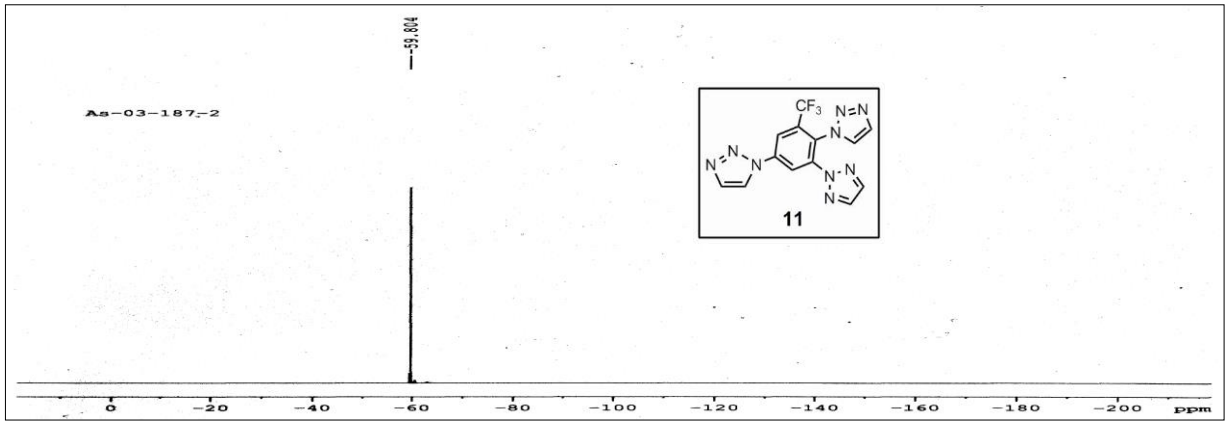
As-03-187-2
11
ppm

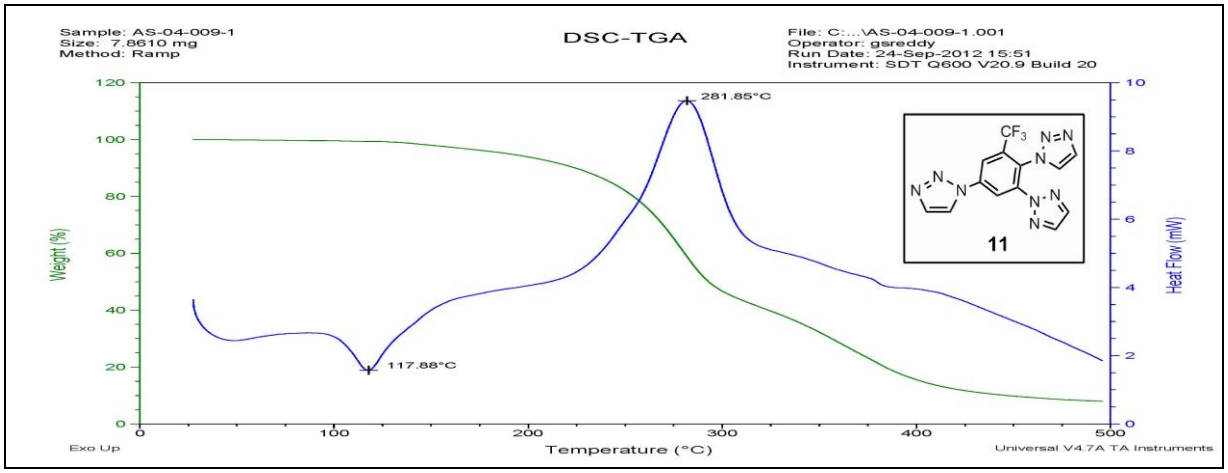
Sample: AS-04-009-1
Size: 7.8610 mg
Method: Ramp
DSC-TGA
File: C:...\AS-04-009-1.001
Operator: gsreddy
Run Date: 24-Sep-2012 15:51
Instrument: SDT Q600 V20.9 Build 20
281.85°C
117.88°C
11
Weight (%)
Heat Flow (mW)
Exo Up
Temperature (°C)
Universal V4.7A TA Instruments

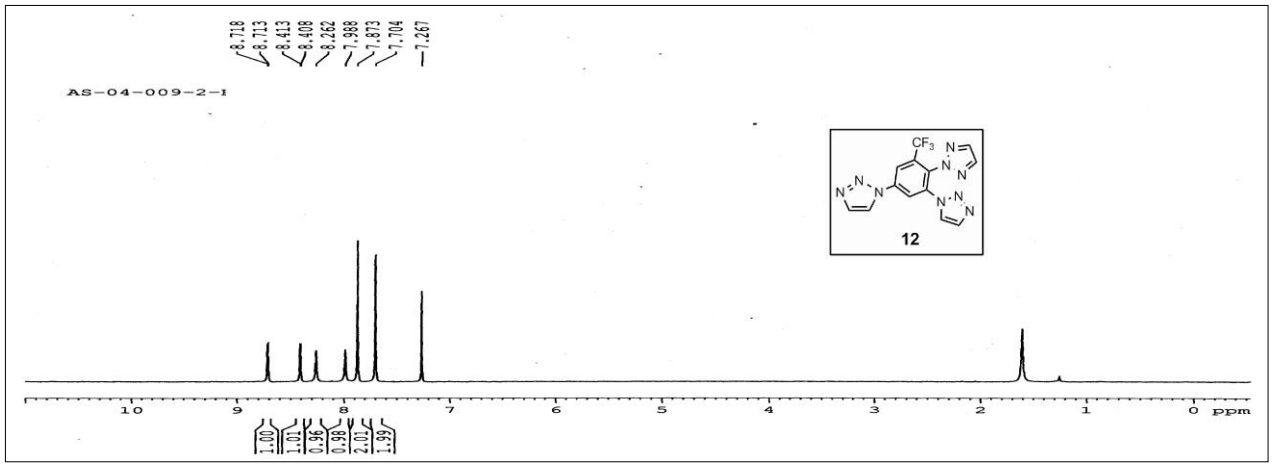
8.718
8.713
8.413
8.408
8.262
7.988
7.873
7.704
7.267
AS-04-009-2-I
CF3
12
1.00
1.01
0.96
0.98
2.01
1.39
ppm

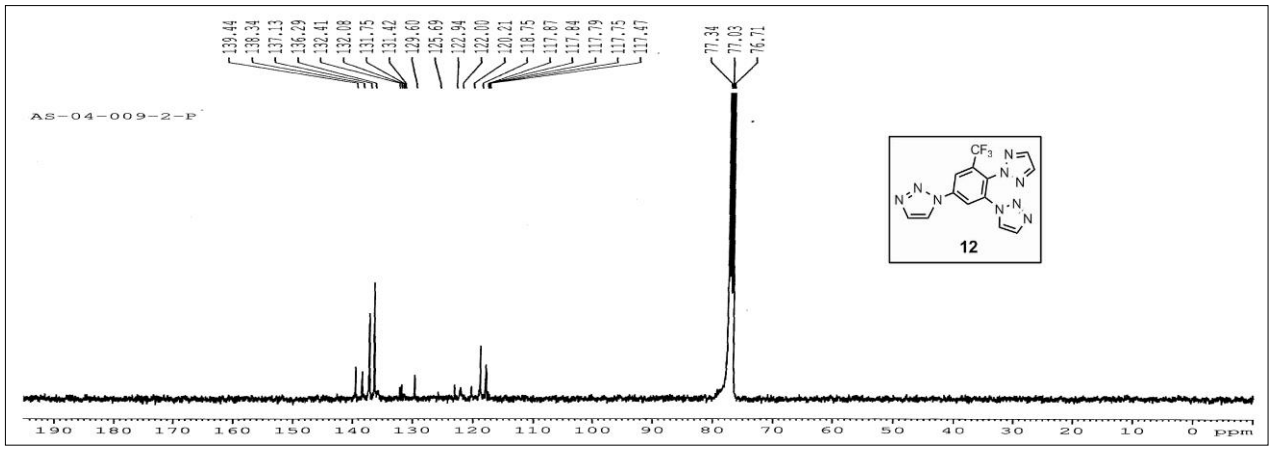
139.44
138.34
137.13
136.29
132.41
132.08
131.75
131.42
129.60
125.69
122.94
122.00
120.21
118.75
117.87
117.84
117.79
117.75
117.47
77.34
77.03
76.71
AS-04-009-2-P
CF3
12
ppm

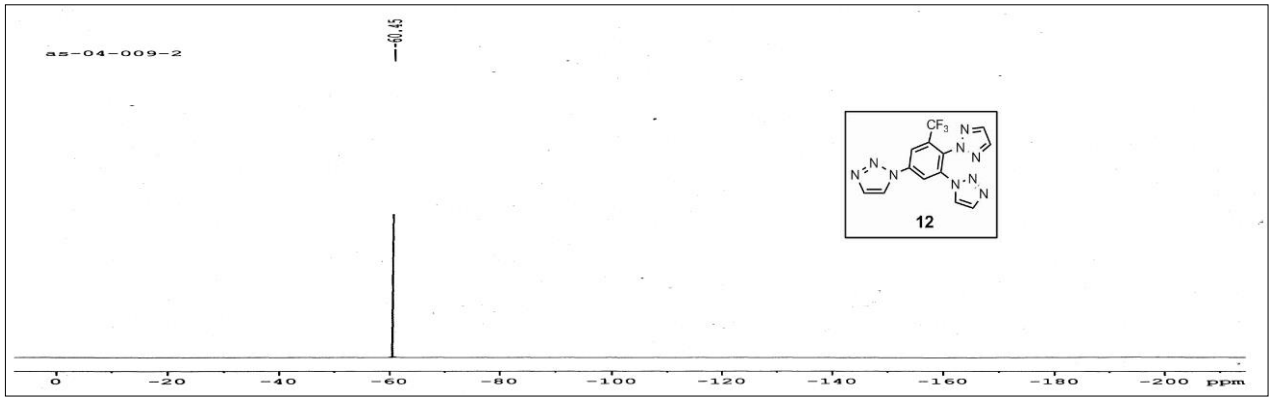
as-04-009-2
-60.45
CF3
12
ppm

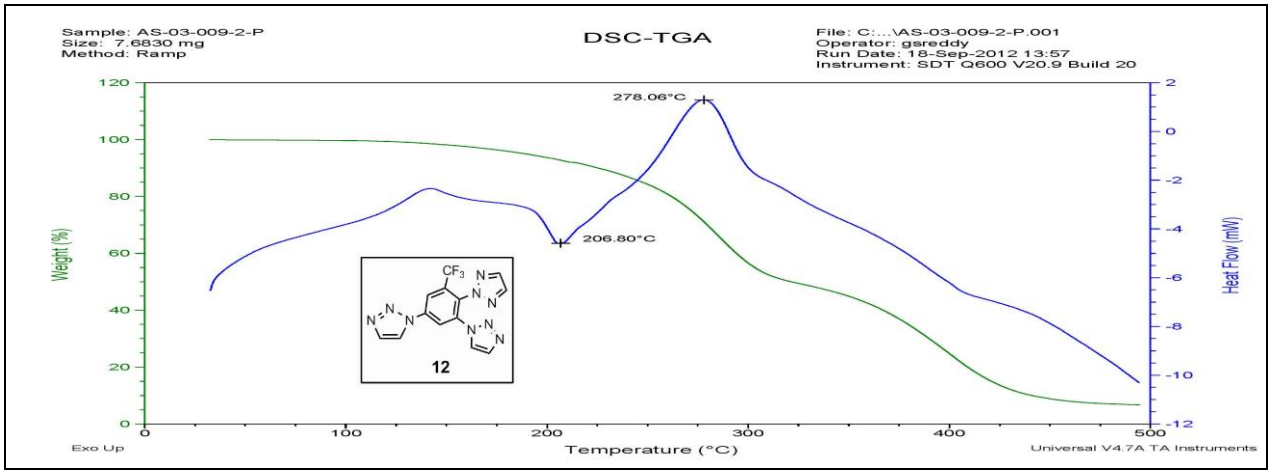
Sample: AS-03-009-2-P
Size: 7.6830 mg
Method: Ramp
DSC-TGA
File: C:...\AS-03-009-2-P.001
Operator: gsreddy
Run Date: 18-Sep-2012 13:57
Instrument: SDT Q600 V20.9 Build 20
278.06°C
206.80°C
CF3
12
Weight (%)
Heat Flow (mW)
Exo Up
Temperature (°C)
Universal V4.7A TA Instruments

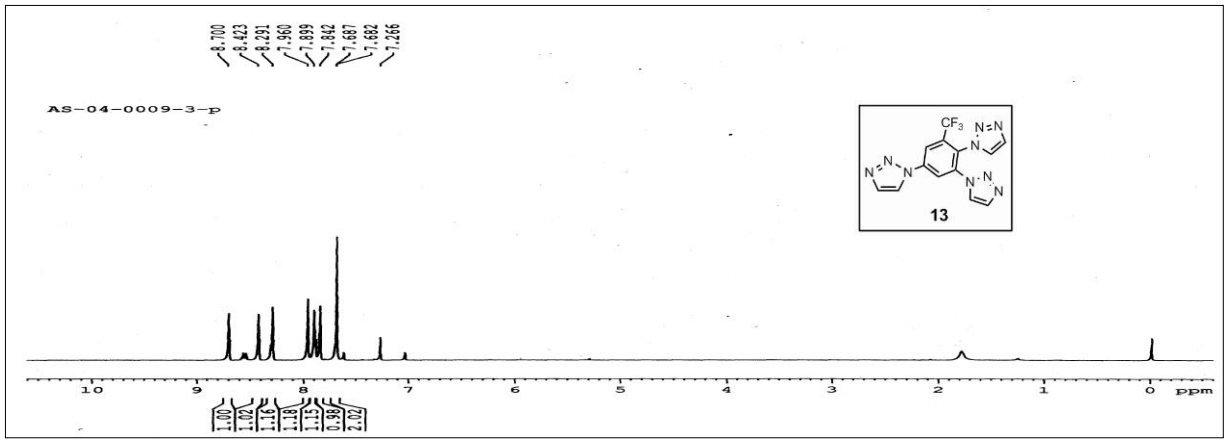
AS-04-0009-3-p
8.700
8.423
8.231
7.860
7.859
7.842
7.687
7.682
7.266
1.00
1.02
1.14
1.18
1.15
0.98
2.02
13
ppm

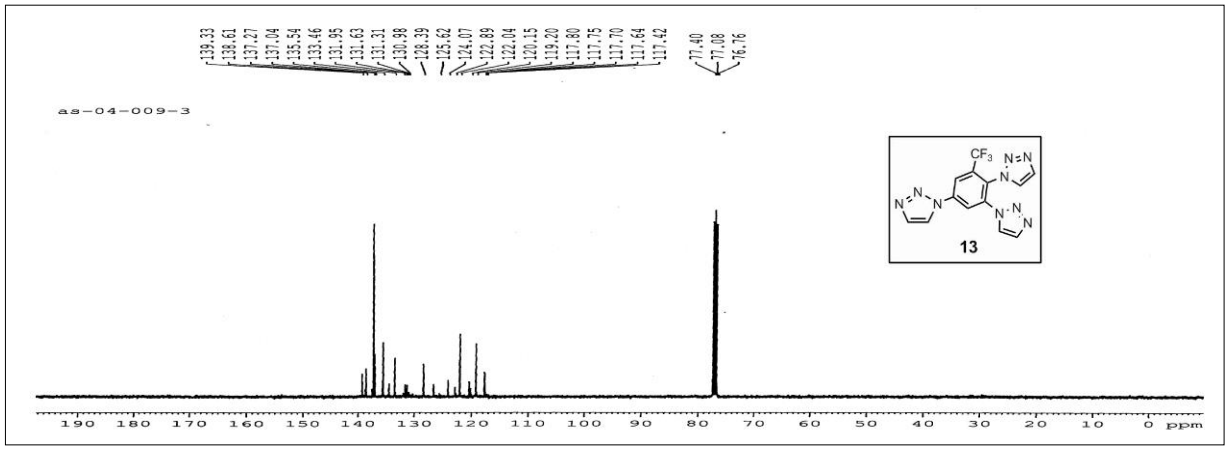
as-04-009-3
139.33
138.61
137.27
137.04
135.54
133.46
131.95
131.63
131.31
130.98
126.39
125.62
124.07
122.89
122.04
120.15
119.20
117.80
117.75
117.70
117.64
117.42
77.40
77.08
76.76
13
ppm

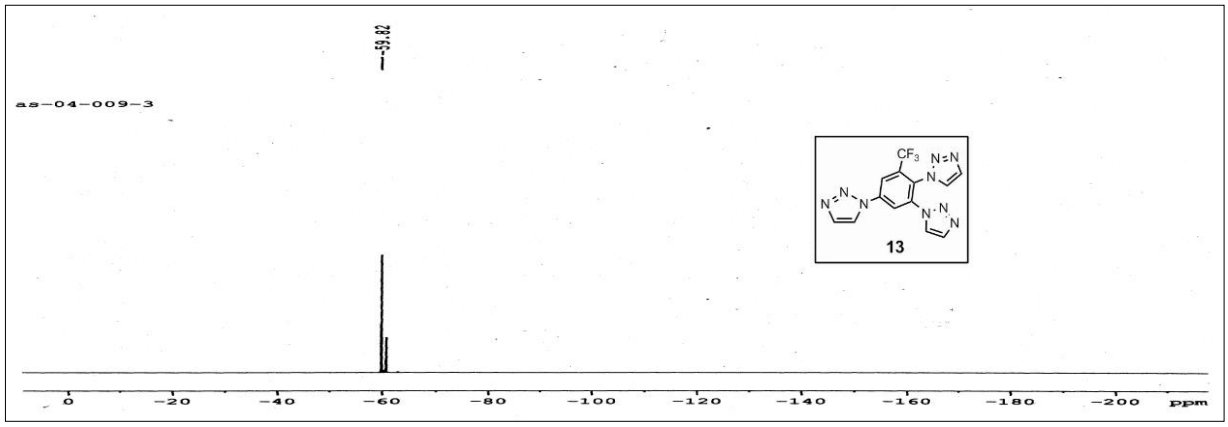
as-04-009-3
-59.82
13
ppm

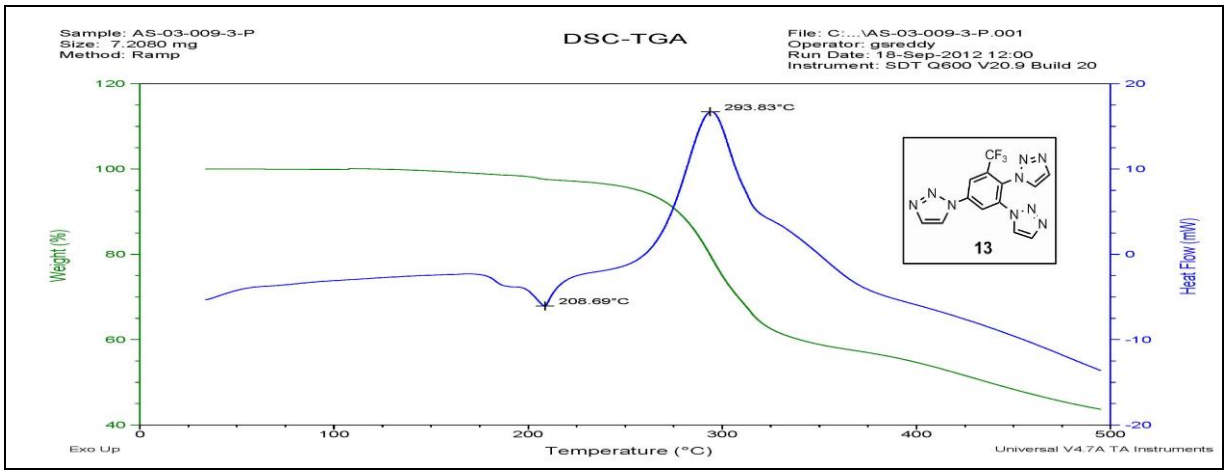
Sample: AS-03-009-3-P
Size: 7.2080 mg
Method: Ramp
DSC-TGA
File: C:...\AS-03-009-3-P.001
Operator: gsreddy
Run Date: 18-Sep-2012 12:00
Instrument: SDT Q600 V20.9 Build 20
293.83°C
208.69°C
13
Weight (%)
Heat Flow (mW)
Temperature (°C)
Exo Up
Universal V4.7A TA Instruments

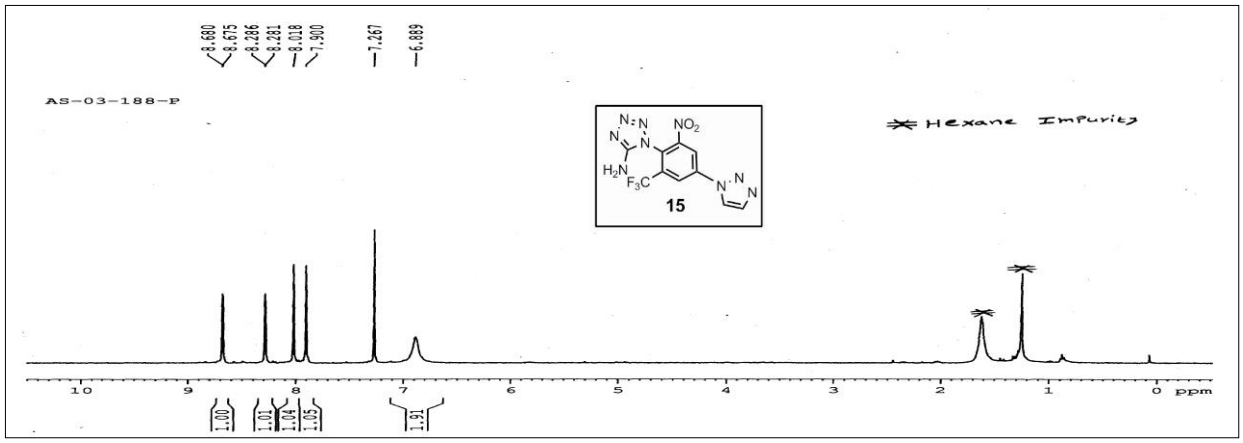
8.680
8.675
8.286
8.281
8.018
7.900
7.267
6.889
AS-03-188-P
Hexane Impurity
15
1.00
1.01
1.04
1.05
1.91
ppm

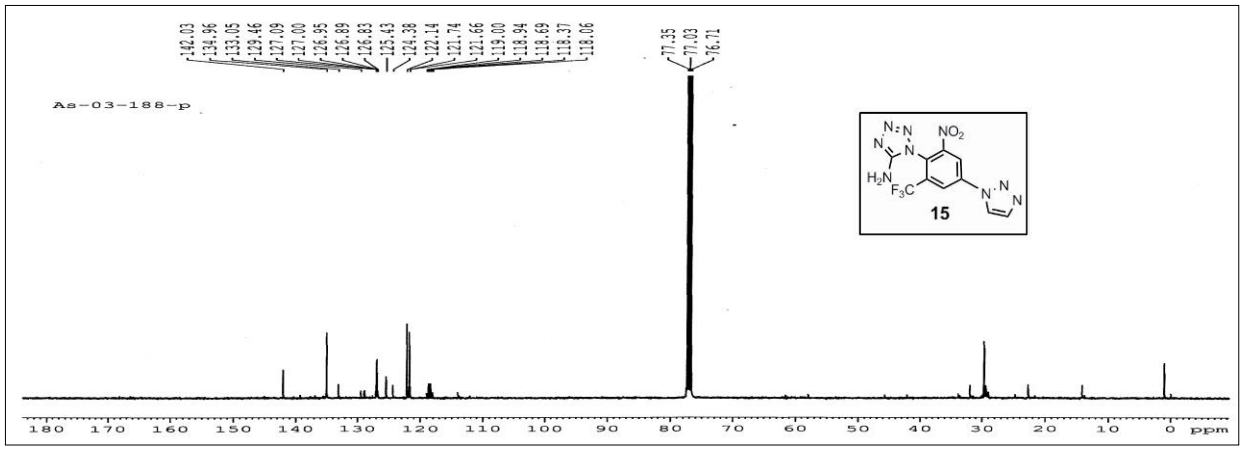
142.03
134.96
133.05
129.46
127.09
127.00
126.95
126.89
126.83
125.43
124.38
122.14
121.74
121.66
119.00
118.94
118.69
118.37
118.06
77.35
77.03
76.71
As-03-188-p
15
ppm

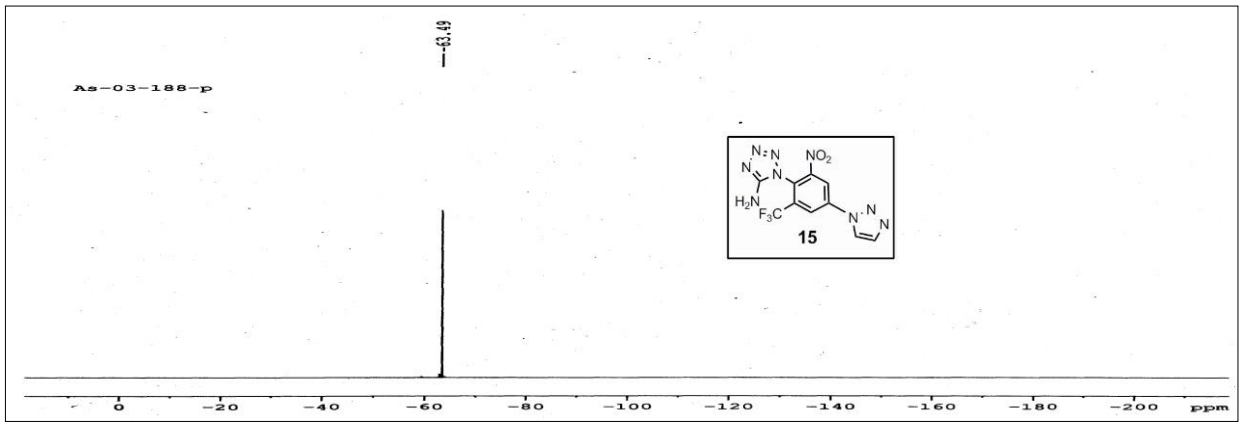
-63.49
As-03-188-p
15
ppm

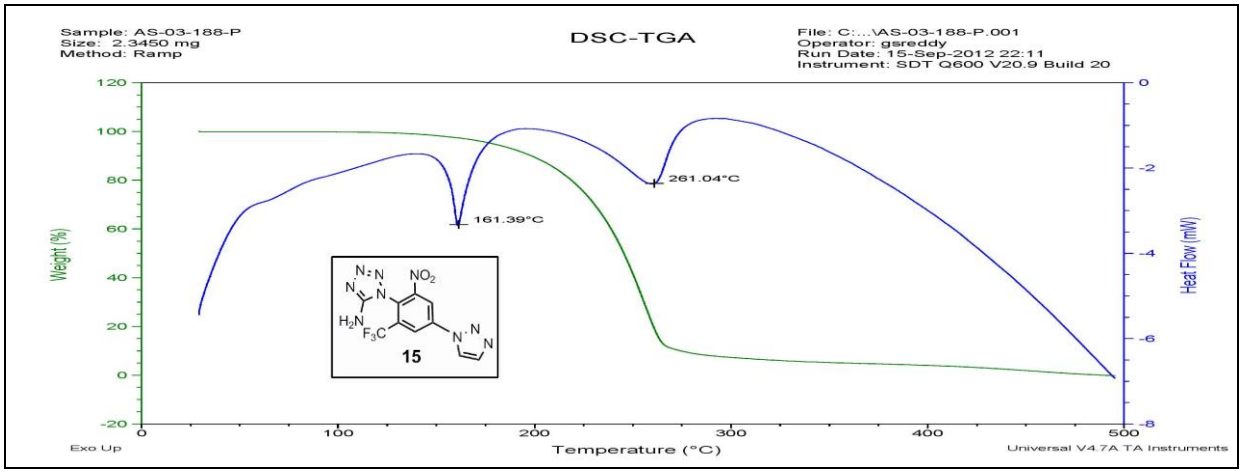
Sample: AS-03-188-P
Size: 2.3450 mg
Method: Ramp
DSC-TGA
File: C:...\AS-03-188-P.001
Operator: gsreddy
Run Date: 15-Sep-2012 22:11
Instrument: SDT Q600 V20.9 Build 20
161.39°C
261.04°C
15
Weight (%)
Heat Flow (mW)
Exo Up
Temperature (°C)
Universal V4.7A TA Instruments

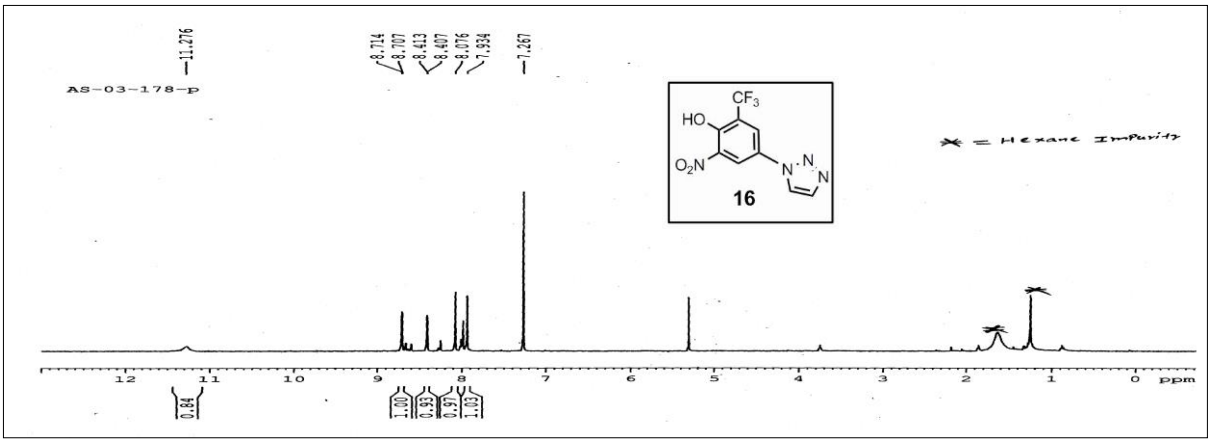
AS-03-178-P
11.276
8.714
8.707
8.413
8.407
8.076
7.934
7.267
CF3
HO
O2N
16
* = Hexane Impurity
ppm

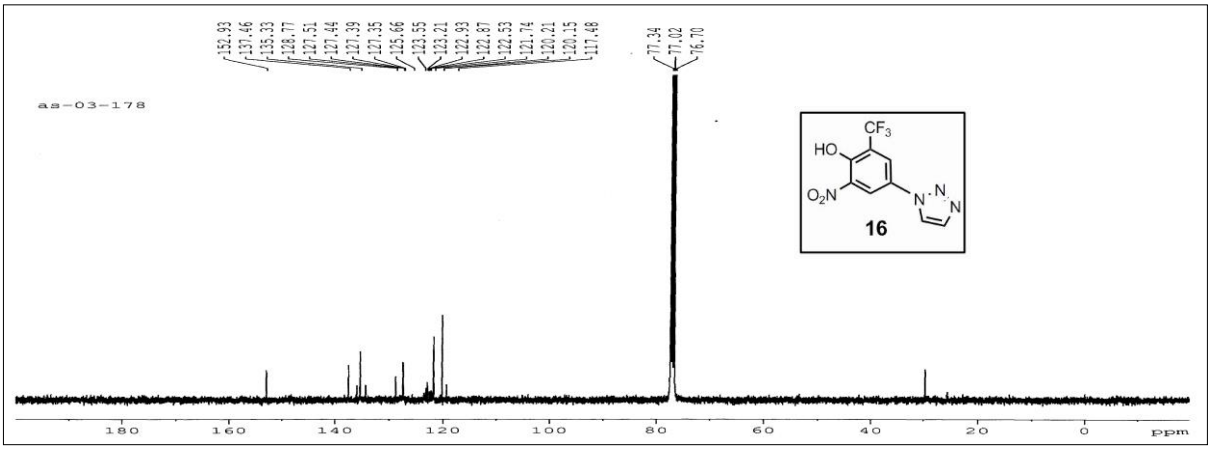
as-03-178
152.93
137.46
135.33
128.77
127.51
127.44
127.39
127.35
125.66
123.55
123.21
122.93
122.87
122.53
121.74
120.21
120.15
117.48
77.34
77.02
76.70
CF3
HO
O2N
16
ppm

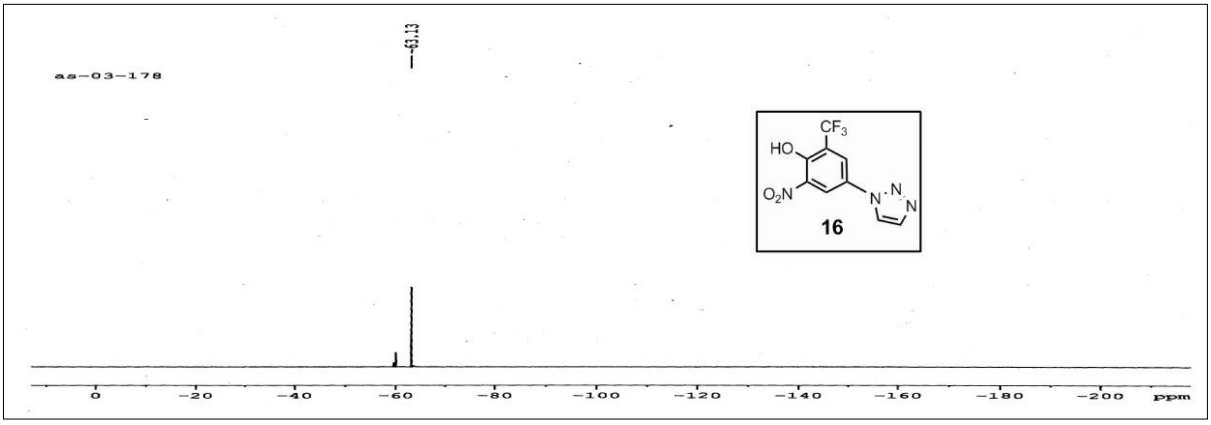
as-03-178
-63.13
CF3
HO
O2N
16
ppm

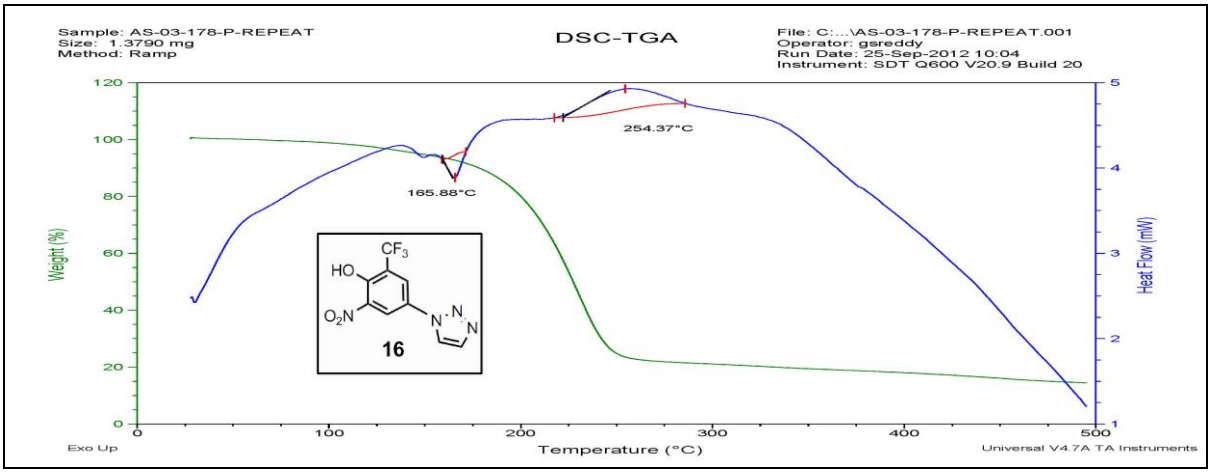
Sample: AS-03-178-P-REPEAT
Size: 1.3790 mg
Method: Ramp
DSC-TGA
File: C:...\AS-03-178-P-REPEAT.001
Operator: gsreddy
Run Date: 25-Sep-2012 10:04
Instrument: SDT Q600 V20.9 Build 20
254.37°C
165.88°C
CF3
HO
O2N
16
Weight (%)
Heat Flow (mW)
Exo Up
Temperature (°C)
Universal V4.7A TA Instruments

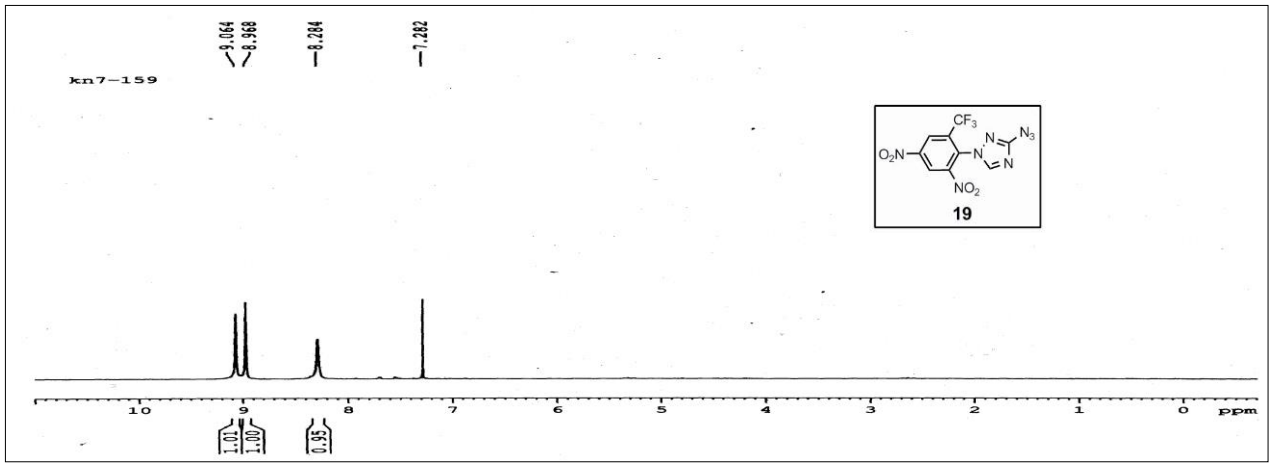
kn7-159
9.064
8.968
8.284
7.282
1.02
1.00
0.95
ppm
19

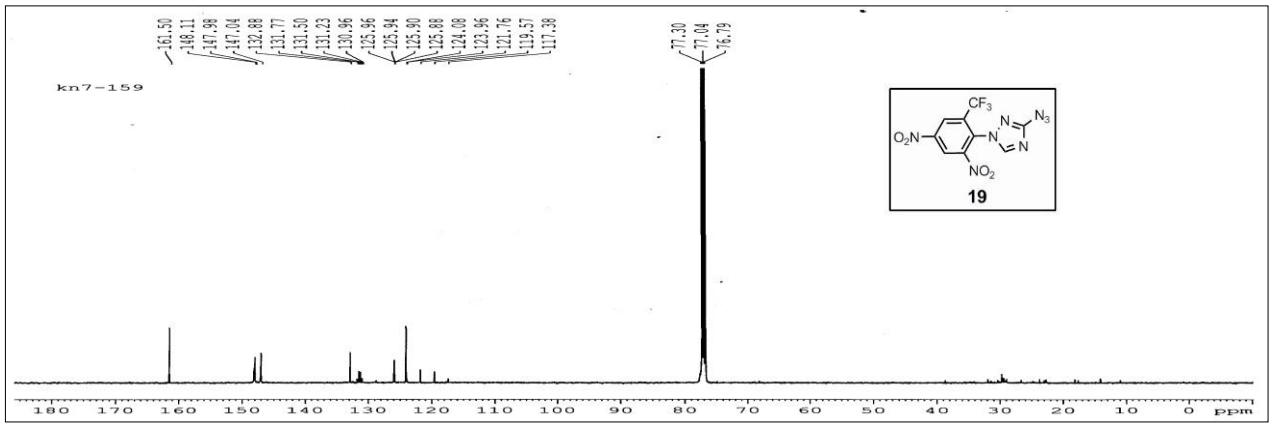
kn7-159
161.50
148.11
147.98
147.04
132.88
131.77
131.50
131.23
130.96
125.96
125.94
125.90
125.88
124.08
123.96
121.76
119.57
117.38
77.30
77.04
76.79
ppm
19

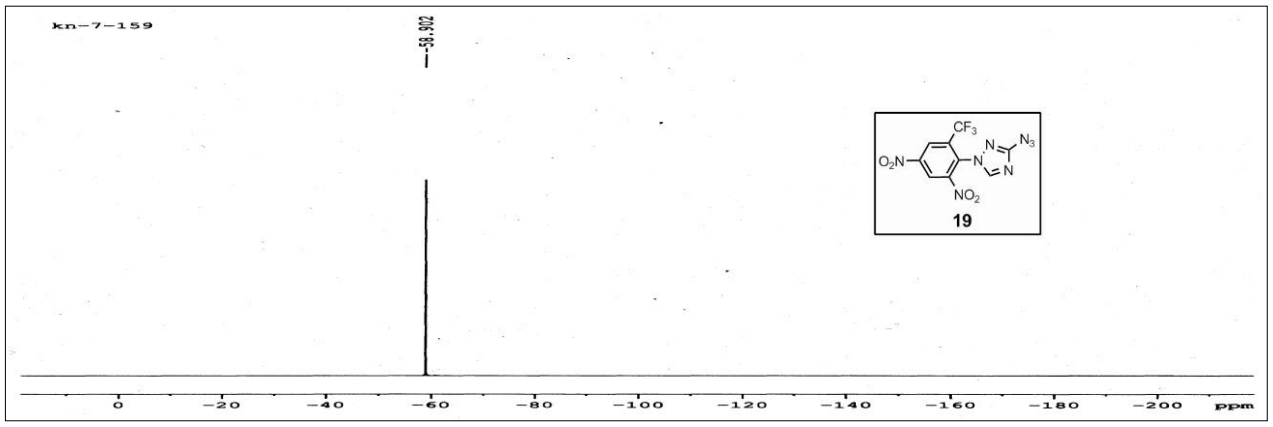
kn-7-159
-58.902
ppm
19

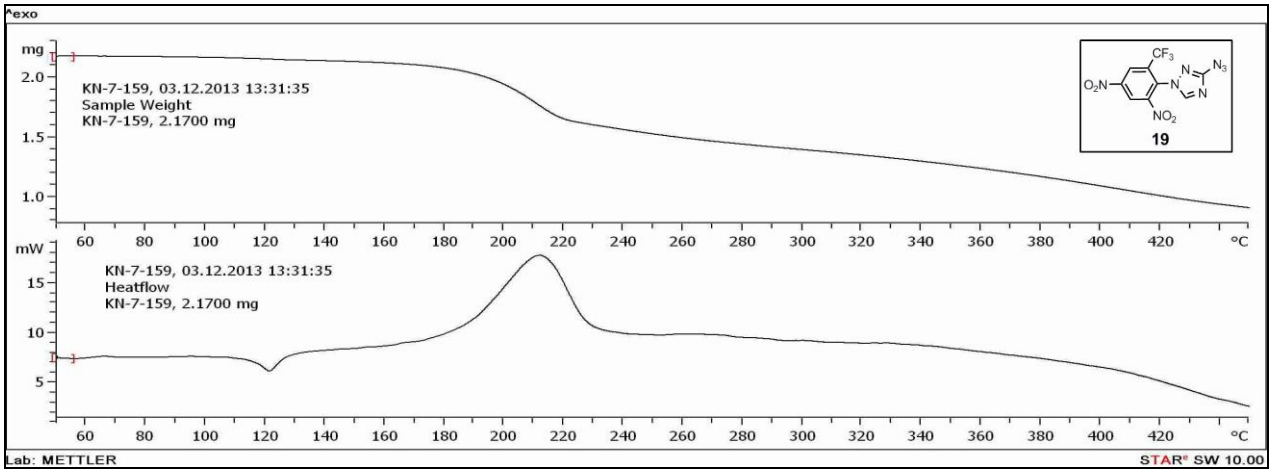
exo
mg
KN-7-159, 03.12.2013 13:31:35
Sample Weight
KN-7-159, 2.1700 mg
mW
KN-7-159, 03.12.2013 13:31:35
Heatflow
KN-7-159, 2.1700 mg
°C
Lab: METTLER
STAR° SW 10.00
19

Chapter 4

Synthesis and Energetic Studies of Nitrogen-Rich *N*-HeteroAryl-Azole Derivatives

Abstract

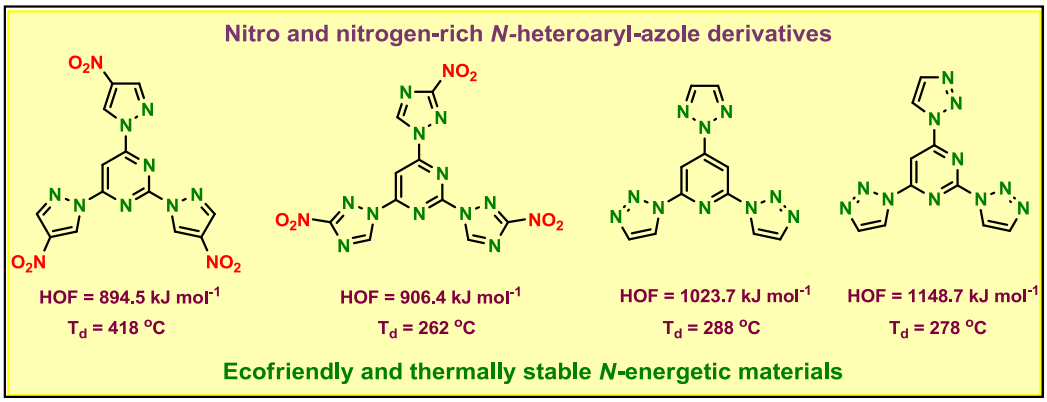

Various nitrogen-rich *N*-heteroaryl-pyrazole and triazole based energetic materials are synthesized and characterized. X-ray diffraction analysis studies establish the solid state structures of few representative molecules. Thermal properties are determined by DSC-TGA data. The synthesized nitrogen-rich pyridyl-/pyrimidyl-tethered-pyrazole and triazole derivatives exhibit excellent thermal stability, high positive heat of formation, good density and moderate detonation performance.

Reference:

A. Sudheer Kumar, Nagarjuna Kommu and Akhila K. Sahoo*

(*Manuscript under preparation***)**

4.1. Introduction

Nitrogen-rich energetic materials are enormously used in space, civil, and military applications.[1] The N–N and C–N bonds in the energetic materials specifically contributes to the positive heats of formation of the molecule. The common oxygen-rich energetic materials in fact produce large amounts of toxic CO and CO_2 gases decomposition product. On the other hand, nitrogen rich energetic materials release non-toxic molecular nitrogen (N_2) during decomposition. Consequently, the *N*-rich materials possess greater advantage.[2] Moreover, less number of hydrogen and carbon atoms in the molecular skeleton contributes to better oxygen balance than the respective carbocyclic analogues. This conceptual understanding has in fact been reflected in the development of novel propellants that would produce low/high flame temperature and less solid exhaust products.[3] The presence of nitrogen atoms in the energetic polynitrogen pyridines/pyrimidines contribute to the high energy-content of the molecule (pyrimidine = 196 kJ mol^{-1} and pyridine = 140 kJ mol^{-1} compare to the benzene = 82.9 kJ mol^{-1}) and in-sensitivity to impact, shock and friction.[4] Thus, polynitrogen containing pyridine/pyrimidine based energetic materials have consistently been used in propellant applications such as: rocket fuel, gun powder and gas generators and so on.[5] Furthermore, the pyridine and pyrimidine bearing energetic compounds showed high thermal and chemical stability.[6] Interestingly, incorporation of pyrazole and triazole skeletons on the six membered pyridine/pyrimidine heterocycles would further enhance positive heat of formation of the molecule.[7] Therefore, design and development of nitrogen-rich *N*-heteroaryl azole derivatives with positive heat of formation, high performance with good thermal stability is challenging and always attracts considerable attention.

4.1.1. Background of pirydyl-/pyrimidyl-tethered azoles for energetic material applications

The coburn group reported the synthesis of heat resistant high explosive 2,6-bis(picrylamino)-3,5-dinitropyridine (**4**) involving aromatic nucleophilic ipso substitution of 2,6-diamino-pyridine (**1**) with picryl chloride (**2**) followed by the electrophilic nitration sequence (Scheme 4.1).[10c] The density and detonation properties of compound **4** (ρ = 1.75 g cm^{-3}, *vD* = 7450 m s^{-1}) is comparable to TNT. Interestingly, PYX (**4**) showed excellent thermal stability (T_d = 460 ^{o}C) than TATB (T_d = 360 ^{o}C). However, it is more sensitive to impact (Is = 63 cm).

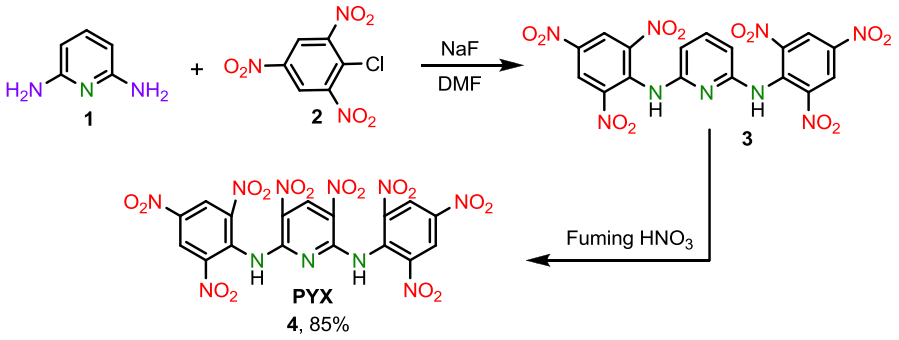

Scheme 4.1. Synthesis of 2,6-bis(picrylamino)-3,5-dinitropyridine (PYX)

In 1988, Licht and Ritter reported the synthesis of 2,4,6-trinitropyridine-1-oxide (**6**, TNPyOx) and 2,4,6-trinitropyridine (**7**, TNPy) with density 1.86 and 1.77 g cm^{-3}, respectively (Scheme 4.2).[8e] The acid mediated cyclization of potassium 2,2-dinitroethanol (**5**) led to **6**. De-oxygenation of **6** with $NaNO_2$ in dilute H_2SO_4 yielded TNPy (**7**) in 46% yield. Chlorination and azidation sequence of 2,6-dinitro moieties in TNPyOx (**6**) with PCl_3 and NaN_3 produced 2,6-diazido-derivative **8**. The detonation properties and heat of formation of compound **6** (*vD* = 8471 m s^{-1}, *P* = 32.2 GPa, HOF = 110.7 kJ mol^{-1}) is comparable to TNT.

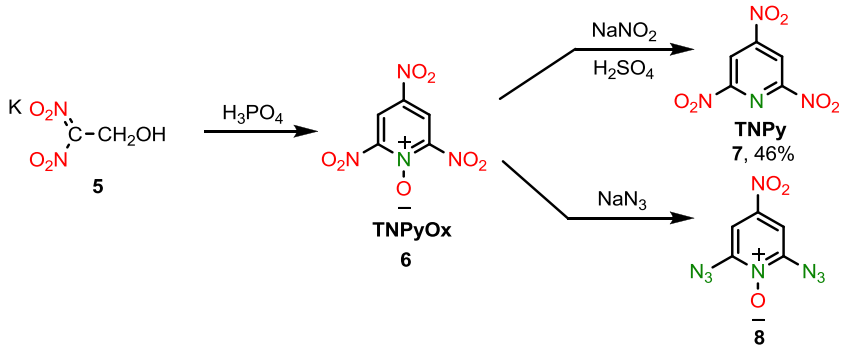

Scheme 4.2. Synthesis of TNPyOx (**6**) and TNPy (**7**)

Wilson and co-workers demonstrated synthesis of tetrazolo [1,5-*f*]furazano[4,5-*b*]pyridine-1-oxide (**11**) from 3-nitro-2,6-dichloropyridine (**9**) replacing chloro-group with the azide moiety followed by cyclization (Scheme 4.3).[9c] The reaction of **9** with NaN_3 in CH_3CN readily constructed tetrazole fused compound **10**. Next, refluxing **10** in benzene finally led to **11**. Compound **11** showed density (ρ = 1.72 g cm^{-3}) and velocity of detonation (*vD* = 7525 m s^{-1}) with poor thermal stability (T_d = 135 °C) and extremely sensitive towards friction and impact (Is = 8 cm).

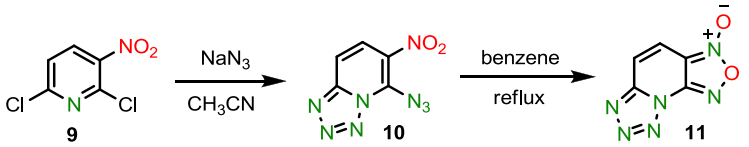

Scheme 4.3. Synthesis of tetrazolo [1,5-*f*]furazano[4,5-*b*]pyridine-1-oxide

The Nissan group reported the synthesis of 2,6-diamino-3,5-dinitropyridine (**13;** ANPy) through direct nitration of 2,6-diaminopyridine (**12**). Oxidation of **13** with peroxyacetic acid yielded ANPyO **14** (ρ = 1.80 g cm^{-3}, *vD* = 7840 m s^{-1}, *P* = 27.50 GPa). C-Amination of ANPyO (**14**) with hydroxylamine hydrochloride provided **15** (ρ = 1.88 g cm^{-3}, *vD* = 8010 m s^{-1}, *P* = 29.1 GPa), an impact insensitive explosive of high thermal stability. Disappointingly, compounds **14** (–132.2 kJ mol^{-1}) and **15** (–70.7 kJ mol^{-1}) showed negative heat of formation (Scheme 4.4).[10d]

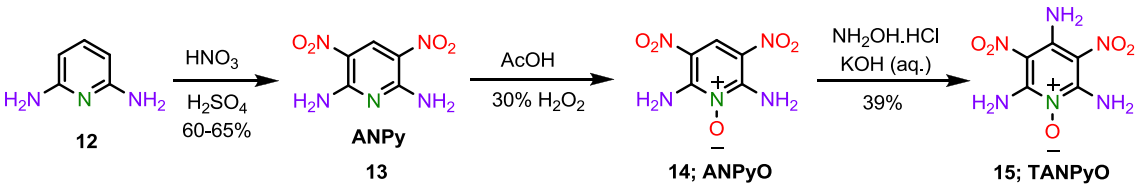

Scheme 4.4. Synthesis of 2,4,6-triamino-3,5-dinitropyridine-1-oxide (TANPyO)

In 1996, Cornago group described the synthesis of pentapyrazolylpyridines (pz5py), pentadimethylpyrazolylpyridines (dmpz5py) and tetrapyrazolyldimethylpyrazolylpyridines (pz4dmpzpy) (pz = pyrazol-l-yl, dmpz = 3,5-dimethylpyrazol-l-yl) via base assisted nucleophilic replacement of fluoro group in the pentafluoro pyridine **16** with the corresponding pyrazoles (Scheme 4.5).[14a] The structures of **18a** & **18b** are established through X-ray crystallographic analysis. The nitrogen-rich compounds showed high positive heat of formation (**18a**; 1961.04 kJ mol^{-1} and **18b**; 1654.7 kJ mol^{-1}) with poor density (**18a**; ρ = 1.41 g cm^{-3}; **18b**; ρ = 1.19 g cm^{-3}).

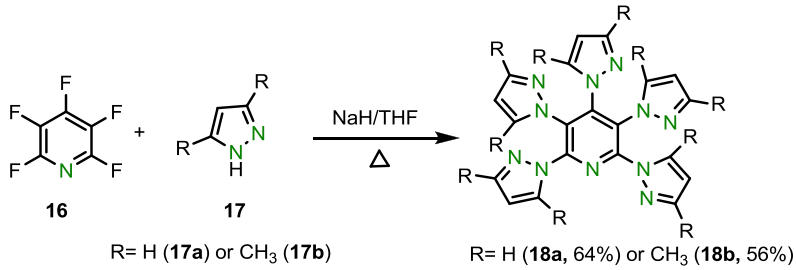

Scheme 4.5. Synthesis of Polypyrazolylpyridines

Synthesis of thermally stable tetranitrodipyridotetraazapentalene (**24**) from readily available 3,4-diaminopyridine (**19**) was demonstrated by Trudell and co-workers (Scheme 4.6).[14c] At first, diazotization of **19** in the presence of mixture of $NaNO_2$ and CH_3COOH produced triazole derivative **20.** Next, the Na_2CO_3 mediated *N*-arylation of **20** with 2-chloro-3-nitropyridine (**21**) in DMSO at 80 °C afforded 1-(3-nitro-2-pyridyl)-1,2,3-triazolo[4,5-*c*]pyridine (**22**) in 51% yield. Reductive cyclization of compound **22** with triethyl phosphate

in toluene at reflux furnished dipyridotetraazapentalene (**23**) in 74% yield. Finally, nitration of **23** with HNO_3/H_2SO_4 mixture at 80 °C afforded **24** in 58% yield. The aza-tacot derivative **24** exhibits excellent thermal stability and decomposed without explosion at 340–342 °C. In addition, this compound was found to be insensitive to impact in a hammer test. Based on calculated values, the aza-tacot derivative **24** displayed high density and good detonation properties (ρ = 1.88 g cm^{-3}, *vD* = 8011 m s^{-1}, *P* = 29.2 GPa).

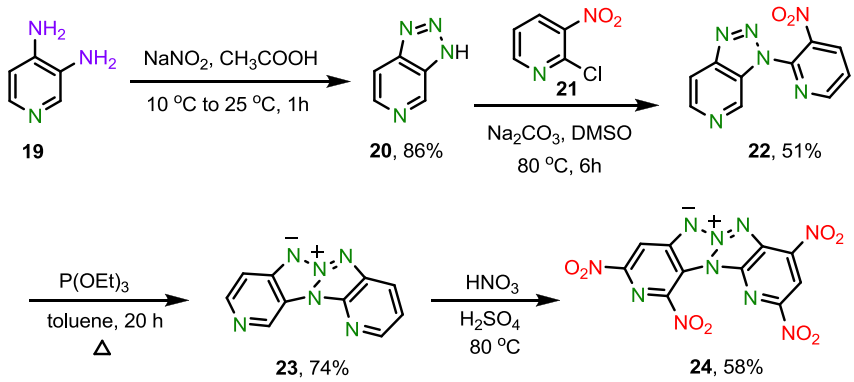

Scheme 4.6. Synthesis of tetranitrodipyridotetraazapentalene (aza-tacot)

Shreeve group synthesized a series of polyazidopyrimidine compounds **25**–**28**; the azidomethyl group contributes decreasing melting point of the compound (Scheme 4.7)[6b]. These polyazidopyrimidine compounds **25**–**28** exhibited high positive HOF (1087–1870 kJ mol^{-1}). However, these compounds are highly sensitive to impact and less-stable (T_d = 130–195 °C). The presence of three or four azido groups on the pyrimidine ring makes this synthetic method cumbersome. Interestingly, these molecular entities are useful for the fabrication of carbon nanotubes.

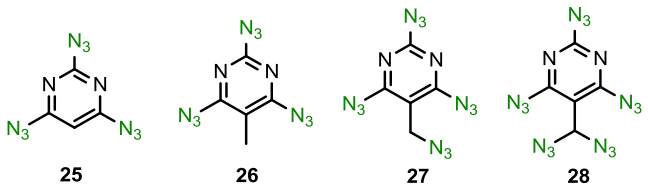

Scheme 4.7. Synthesis of polyazidopyrimidines: high energy compounds

Chapyshev group successfully constructed 2,6-diazido-3,5-dicyanopyridine (**29**), 2,4,6-triazido-3,5-dicyanopyridine (**30**), and 2,3,4,5-tetraazido-6-cyanopyridine (**31**) (Scheme 4.8).[10a] The replacement of azide-moiety in **31** with -CN fragment strongly reduces explosive risk of these compounds while retaining the energetic properties of the molecules. Dissapointongly, the synthesized compounds possesses poor thermal stabilty (T_d = < 200 °C)

with high positive heats of formation (HOF = 1047–1578 kJ mol^{-1}). The sensitivity (impact and friction) of the azide-bearing compounds substantially increases with the increase of azido groups in the pyridine ring.

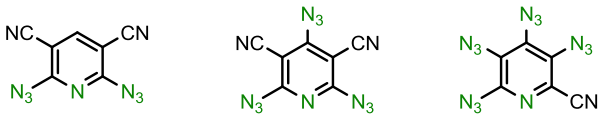

Scheme 4.8. Synthesis of cyano-substituted di-, tri-, and tetra-azidopyridines

The explosive PADP (**32**) is readily synthesized from 3,5-dinitro-2,6-bis- (hydrazino)pyridine and picryl chloride followed by the oxidation of the resulting compound with nitric acid. PADP (**32)** exhibited high thermal stability. Whereas compound 2,4,6-tris(picrylamino)-3,5-dinitropyridine (**33**) showed low thermal stability than PADP (Scheme 4.9).[10b]

Chemists at Los Alamos National Laboratory synthesized picrylamino-substituted pyrimidine **34** as thermally stable explosives. The pyrimidine-based explosive was synthesized involving aromatic nucleophilic substitution of 2,4,6-triaminopyrimidine with picryl fluoride followed by nitration sequence.

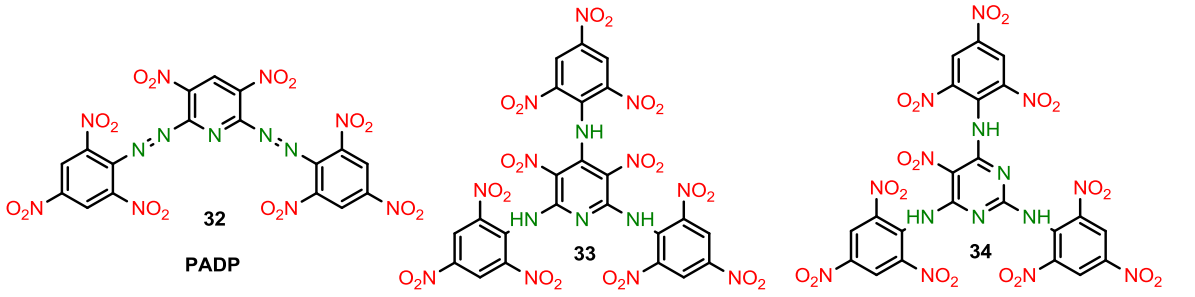

Scheme 4.9. Synthesis of picrylaminosubstituted pyridines/pyrimidines

4.1.2. Motivation and Design Plan

The common high-performance energetic materials release toxic gases during the decomposition of the compound, causing harmful effects to both humans and the environment. The synthesis of *N*-rich energetic materials could solve this problem as these molecules produce N_2 gas during decomposition. Thus, development of novel stable and insensitive *N*-rich molecules for energetic material applications is always desirable.

We thus envisaged to design and synthesis of nitrogen-rich pyridyl-/pyrimidyl-tethered-poly-pyrazole and triazole compounds as eco-friendly energetic materials. These molecules can readily be constructed through the substituion of the halo-moiety in pyridines/pyrimidines

with 3-nitro-1,2,4-triazole, 4-nitro-1H-pyrazole and 1,2,3-triazole. Alternatively, synthesis of pyrimidyl-tethered-1,2,3-triazoles can be realized through Cu-catalyzed [3+2]-cycloaddition between the corresponding azides and terminal-alkynes as shown in Scheme 4.10.

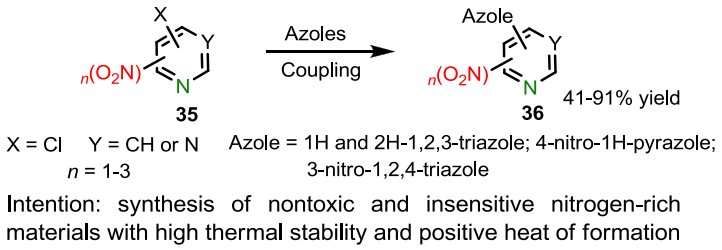

Scheme 4.10. Strategy for the nitrogen-rich *N*-hetero-aryl-azole derivatives

4.2. Results and Discussion

The development of thermally stable *N*-rich small-molecules with positive HOFs is highly desirable; thus, considerable attention has been paid to the synthesis of nitrogen-rich energetic molecules from readily available precursors by using cost-effective and efficient synthetic transformations.[10-14]

The coupling between electron rich heterocylces (pyrazole/triazole) and electron deficient nitro-group-bearing halopyridines can readily be performed.[5] With these facts in mind, the coupling between nitro substituted heteroaryl chlorides **37** and **38** in the presence of NaH in THF was conducted at room temperature for 6 h (Table 4.1). Accordingly, the reaction of **38** with 2,6-dichloro-3-nitropyridine (**37a**) gave the desired nitrogen-rich coupled product **39a** in 68% yield (Table 4.1, entry 1). Surprisingly, the NO_2 group in 2,6-dichloro-4-nitropyridine (**37b**) is easily replaced by **38** leaving the chloro group unaffected, producing a mixture of regioisomeres **39b** & **39b'** in overall good yield (entry 2).

Table 4.1. Coupling of 1H-1,2,3-triazole with nitro-substituted halopyridines.[a]

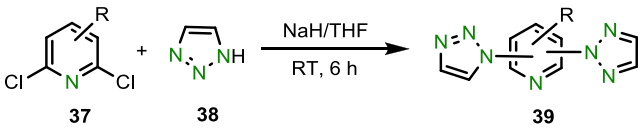

Entry	1	R	39a-39b[b]	
1	**37a**	3-NO_2	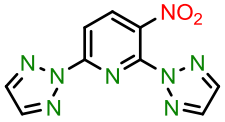 **39a** (68%)	–
2	**37b**	4-NO_2	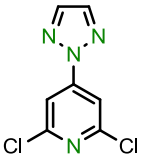 **39b** (17%)	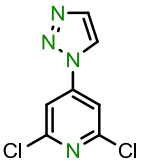 **39b' (78%)**

[a]All reactions were carried out using 1.0 equiv of nitro substituted dichloro pyridine, 4.0 equiv of 1H-1,2,3-triazole, 6.0 equiv of base (sodium hydride) in THF (5.0 mL for 1 mmol) at room temperature for 6 h; [b]Yield of the isolated product.

Next, the reaction of compound **39b** with 1H-1,2,3-triazole (**38**) under Cu-catalysts in the presence of Cs_2CO_3 in DMF at 80 ^oC (Scheme 4.11) provided **40** (63%); both chloro (–Cl) groups in **39b** are replaced. The reaction at room temperature led to poor consumption of **39b**. Disappointingly, introduction of more triazole skeletons by replacing –Cl groups on compound **39b'**[14b] were unsuccessful under the identical conditions.

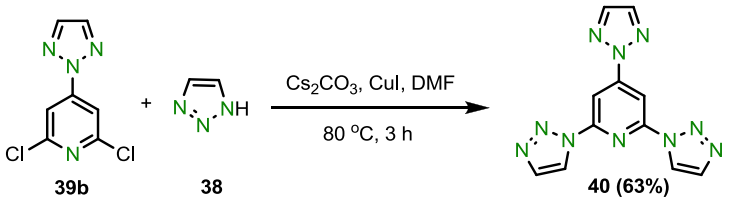

Scheme 4.11. Cu-catalyzed *N*-arylation of compound **39b** with 1H-1,2,3-triazole.

The synthesized pyridyl-tethered-1,2,3-triazoles **39a** & **40** showed positive HOFs (736–1023.7 kJ mol^{-1}). Thus, incorporation of more triazole rings in the molecular framework will significantly increase the HOF.[15] Thus, synthesis of nitrogen rich 2,4,6-polytriazolyl-pyridine is realized through the Cu-catalyzed coupling of trichloropyridine (**41**) with **38** in the presence of Cs_2CO_3 in DMF. Disappointingly, a regioisomeric mixture of **42** & **43+44** are obtained and purified by column chromatography (Table 4.2, entry 1).

Table 4.2. Coupling of trichloropyridine (**41**) with 1H-1,2,3-triazole.[a]

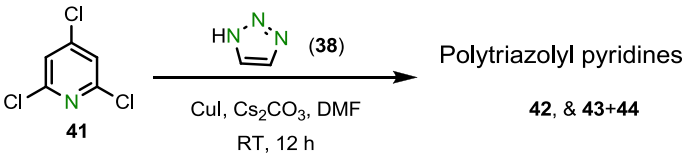

Entry	Comp.	Pyridyl-tethered poly 1,2,3-triazole derivatives[b]	
1	**41**	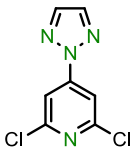 **42** (19%)	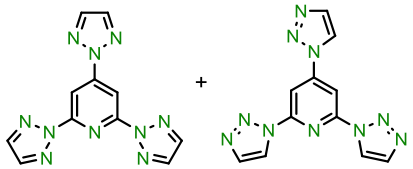 **43+44** (53%)

[a]The reaction was carried out using 1.0 equiv of 2,4,6-trichloropyridine, 6.0 equiv of 1H-1,2,3-triazole, 8.0 equiv of base (sodium hydride) in THF (5.0 mL for 1 mmol) at room temperature for 12 h; [b]Yield of the isolated product.

To accomplish the synthesis of penta(triazol-l-yl)pyridine (HOF: 1749.6 kJ mol^{-1}), the base assisted reaction between triazole and pentachloropyridine in 5:1 molar ratio was conducted. Surprisingly, formation of mixture of products comprising of mono-, bis-, and tris-triazolyl substituted pyridines **46**–**51** was noticed. These products were purified by silica gel column chromatography in overall 82% yield (Table 4.3, entry 1). Attempts to introduce five triazole skeletons on **45** were turned futile. X-ray diffraction analysis confirmed the structures of compounds **46**, **48,**[14b] **49,** & **50** as depicted in Figure 4.1.

Table 4.3. *N*-Arylation of pentachloropyridine (**45**) with 1H-1,2,3-triazole.[a]

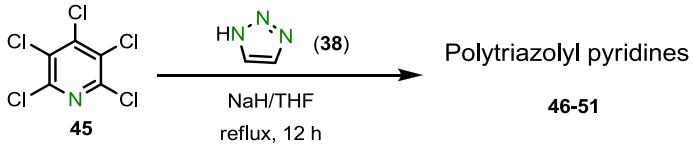

Entry	**45**	Pyridyl-tethered-1,2,3-triazole derivatives.[b]					
1	**45**	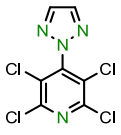 **46** (21%)	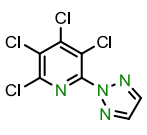 **47** (4%)	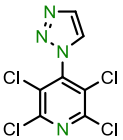 **48** (7%)	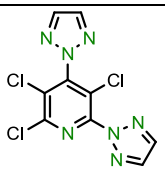 **49** (9%)	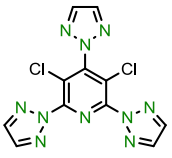 **50** (17%)	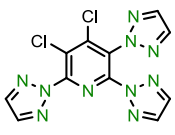 **51** (24%)

[a]The reaction was carried out using 1.0 equiv of pentachloro pyridine, 5.0 equiv of 1H-1,2,3-triazole, 7.0 equiv of base (sodium hydride) in a THF (5 mL for 1 mmol) at 65 ^{o}C for 12 h; [b]Yield of the isolated product.

Heat of formation (HOF) is a valuable factor that determines the nature and efficiency of high energy materials.[15] In general, pyrimidine (196 kJ mol^{-1}) contributes more energy than pyridine (140 kJ mol^{-1}) and benzene (82.9 kJ mol^{-1}).[15] We thus envisaged in the introduction of many *N*-bearing-moieties on pyrimidine moiety. Gratifyingly, triazidopyrimidine (**52**) was prepared from commercially available trichloropyrimidine through the nucleophilic displacement with NaN_3 in quantitative yield.[18a]

Next, the Cu-catalyzed [3+2]-cycloaddition of 2,4,6-triazidopyrimidine (**52**)[18] with trimethylsilylacetylene (**53**) was performed. We failed to obtaine tris-triazolyl pyrimidine derivative, when the reaction between **52** and **53** was carried out under Cu-catalysis in the presence of K_2CO_3 in MeOH/H_2O, rather compund **54** was isolated in 54% yield with the nucleophilic displacement of methoxy group on azido-moiety (Table 4.4, entry 1). While the identical reaction between **52** and **53** in *t*-BuOH/H_2O at room temperature delivered the corresponding pyrimidyl-tethered-tris-triazolyl product **55** in 72% yield (Table 4.4, entry 2).

Table 4.4. [3+2] cycloaddition between triazidopyrimidine and TMS-acetylene.[a]

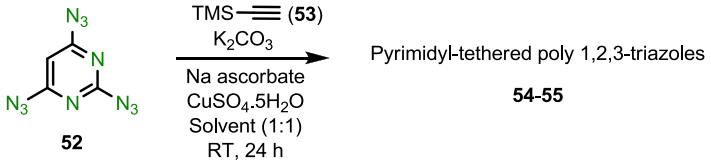

Entry	Solvent (1:1)	Pyrimidyl-tethered-1,2,3-triazoles[b]
1	MeOH/H_2O	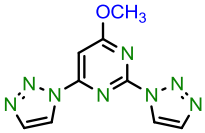 **54** (49%)
2	tBuOH/H_2O	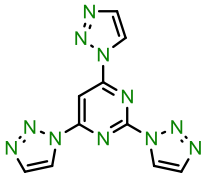 **55** (72%)

[a]All reactions were carried out with azide (1.0 equiv), TMS-acetylene (4.5 equiv), base (potassium carbonate 3.6 equiv), sodium ascorbate (1.2 equiv), and $CuSO_4 \cdot 5H_2O$ (0.6 equiv) in a mixture of MeOH or tBuOH/water (1:1, 1 mL for 1 mmol) at room temperature for 24 h. [b]Yield of the isolated product.

Until now, we have successfully introduced various nitrogen-bearing molecular entities on pyridyl-/pyrimidyl skeletons via coupling and click reactions. On the basis of theoretical

calculations, the nitrogen-rich pyridyl-/pyrimidyl-tethered 1,2,3-triazole derivatives shown in Table 4.1–4.4 and Scheme 4.11 displayed high positive HOF (635.9–1148.7 kJ mol^{-1}) and moderate detonation performance (5849–7205 m s^{-1}). As the presence of nitro groups on the molecular entity enhances the detonation performance of a molecule,[6] we next turned our attention to explore the coupling reactions between nitropyrazole skeleton and nitro-substituted heteroaryl halides. Accordingly, the base-promoted nucleophilic displacement of commercially available 4-nitro-1H-pyrazole (**57**) to nitro-rich halopyridine/pyrimidine (**56**) was investigated (Table 4.5).

Table 4.5. Coupling reactions of 4-nitro-1H-pyrazole (**57**) with various activated heteroaryl chlorides.[a]

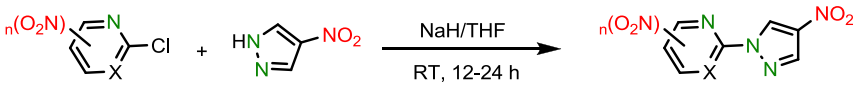

56 X = CH or N **57** **58a-d** *n* = 1-3

Entry	**56**	**58**	Yield [%][b]
1	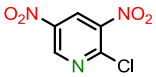 **56a**	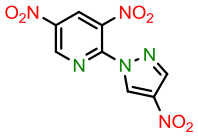 **58a**	65
2	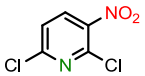 **56b**	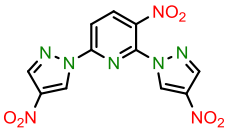 **58b**	62
3	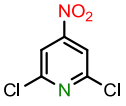 **56c**	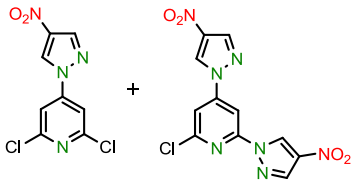 **58c+58c'**	54+17
4	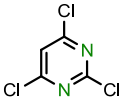 **56d**	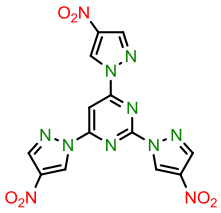 **58d**	82[d]

[a]Reaction conditions: heteroaryl chloride (**56**, 1.0 equiv), 4-nitro-1H-pyrazole (**57**, 4.0 equiv), and NaH (6.0 equiv) in THF (5.0 mL per 1.0 mmol) at RT for 12–24 h; [b]Yield of the isolated product; [c]**57** (2.0 equiv) and NaH (4.0 equiv) were used; [d]**57** (6.0 equiv) and NaH (8.0 equiv) were used.

Gratifyingly, coupling of 2-chloro-3,5-dinitropyridine (**56a**) with **57** was successfully conducted, when the reaction carried out with NaH in THF at room temperature to afford the desired trinitro-containing product **58a** in 65% yield (Table 4.5, entry 1). The NaH-assisted reaction of **57** with 2,6-dichloro-3-nitropyridine (**56b**) gave the desired nitro-rich coupled product **58b** in 62% yield (Table 4.5, entry 2). Surprisingly, compound **57** replaced the NO_2 group of 2,6-dichloro-4-nitropyridine (**56c**) leaving the chloro group unaffected to provide the regioisomers **58c** & **58c'** (Table 4.5, entry 3). Pleasingly, compound **58d (**82%) was synthesized from **57** and **56d**, when the reaction conducted in the presence of NaH in THF (Table 4.5, entry 4). The X-ray diffraction analysis confirmed the structure of compounds **58a**, **58b** and **58c** (Figure 4.1).

Next, we intend to prepare 1,2,4-triazole-containing molecules with high positive HOFs and improved thermal stabilities. Computational calculations studies reveals that 3-nitro-1,2,4-triazole (**60**) possesses HOF 181 kJ mol^{-1},[15b] whilst 4-nitro-1H-pyrazole (**57**) provided a HOF of 159 kJ mol^{-1}.[15c] Based on this information, incorporation of **60** onto the pyridyl/pyrimidyl-tethered halides through a base-promoted nucleophilic substitution reaction is envisioned (Table 4.6).

The NaH-assisted reaction of **60** with 2-chloro-3,5-dinitropyridine (**59a**) and 2,6-dichloro-3-nitropyridine (**59b**) in THF at room temperature gave the desired nitro-rich coupled products **61a** & **61b** and yields are depicted in Table 4.6. Surprisingly, skeleton **60** is inserted on 2,6-dichloro-4-nitropyridine (**59c**) through the replacement of NO_2 group leaving the chloro group untouched; compound **61c** was exclusively obtained in 67% yield at room temperature (Table 4.6, entry 3). Finally, the reaction of compound **59d** with an excess amount of **60** delivered polynitrogen-containing 1,2,4-triazole **61d** in 91% yield (Table 4.6, entry 4). These results revealed that 3-nitro-1,2,4-triazole (**60**) is a strong nucleophile and readily introduced on the heteroaryl motifs through the replacement of halo group. These newly synthesized heteroaryl-1,2,4-triazole derivatives (**61a-d**) showed HOFs within the range 368.7–906.4 kJ mol^{-1}. The structure of compound **61b** was elucidated by single-crystal X-ray-analysis (Figure 4.1).

Table 4.6. Coupling reactions of 3-nitro-1,2,4-triazole (**60**) with various heteroaryl chlorides.[a]

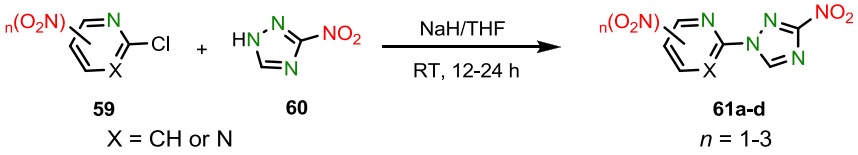

59 X = CH or N **60** **61a-d** *n* = 1-3

Entry	59	61	Yield [%][b]
1	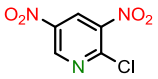 **59a**	 **61a**	74[χ]
2	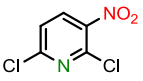 **59b**	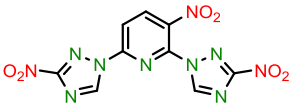 **61b**	86
3	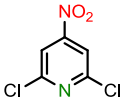 **59c**	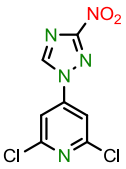 **61c**	67
4	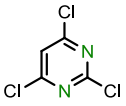 **59d**	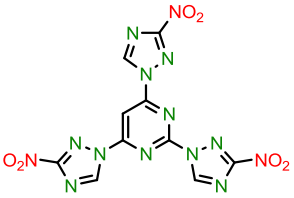 **61d**	91[d]

[a]Reaction conditions: heteroaryl chloride (**59**, 1.0 equiv), 3-nitro-1,2,4-triazole (**60**, 4.0 equiv), and NaH (6.0 equiv) in THF (5.0 mL per 1.0 mmol) at RT for 12–24 h; [b]Yield of the isolated product; [c]**60** (2.0 equiv) and NaH (4.0 equiv) were used; [d]**60** (6.0 equiv) and NaH (8.0 equiv) were used.

4.3. X-ray crystallography

The complete configurational assignment of the compounds **46**, **48, 49, 50, 58a, 58b, 58c** and **61b** were performed via single X-ray crystallographic analysis (Figure 4.1). Crystals are grown with the slow evaporation of a methanol and ethyl acetate solution of the compound at room temperature and atmospheric pressure.

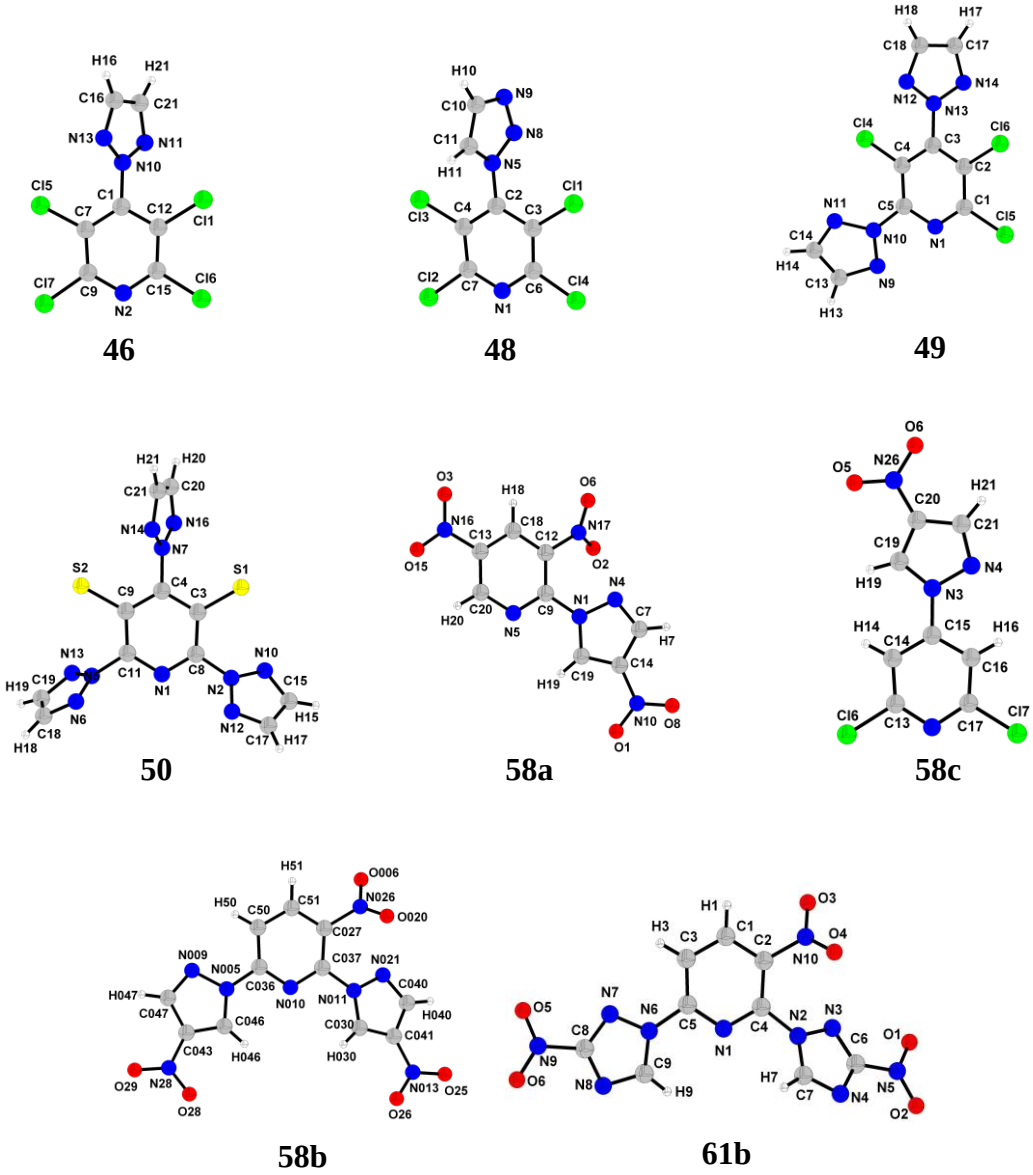

Figure 4.1. Molecular structures of compounds **46**, **48**, **49**, **50**, **58a**, **58b**, **58c** and **61b**; thermal ellipsoids are set at 50% probability.

Single-crystal X-ray analysis of **49, 50** and **58c** revealed triclinic ($P\bar{1}$) space group with cell volumes of 1232.5 (6), 703.25 (18) and 1020.2 (15) $Å^3$, respectively. Similarly, compounds **46, 48, 58b** and **61b** crystallized in monoclinic ($P2_1/c$) space group with cell volumes of 2233.9 (4), 1050.2 (3), 2219.16 (11) and 1354.7 (7) $Å^3$ whereas **58a** crystallized in the orthorhombic (*Pbca*) space group with cell volumes of 2219.16 (11) $Å^3$, respectively. The crystallographic data for all the compounds were detailed in Table 4.7 and Table 4.8.

Table 4.7. Crystallographic data for **46**, **48**, **49**, and **50**.

Compound	**46**	**48**	**49**	**50**
Formula	$C_7H_2Cl_4N_4$	$C_7H_2Cl_4N_4$	$C_7H_2Cl_4N_4$	$C_{11}H_6Cl_2N_{10}$
M_w	283.93	283.93	316.54	349.13
Crystal system	monoclinic	monoclinic	triclinic	triclinic
Space group	$P2_1/n$	$P2_1/c$	$P\bar{1}$	$P\bar{1}$
T [K]	293 K	293 K	273 K	273 K
a [Å]	11.9007 (12)	12.9718 (18)	5.6364 (15)	8.8357(13)
b [Å]	14.8924 (12)	7.5582 (14)	14.059 (4)	9.1432(14)
c [Å]	12.7282 (13)	10.7134 (14)	15.884 (4)	9.6553(14)
α [°]	90	90	88.034 (4)	84.394(2)
β [°]	97.987(10)	91.156 (16)	84.809 (4)	72.845(2)
γ [°]	90	90	74.549 (4)	70.657(2)
Z	8	4	4	2
V [$Å^3$]	2233.9 (4)	1050.2 (3)	1232.5 (6)	703.25 (18)
D_{calc} [g cm^{-3}]	1.688	1.796	1.706	1.649
μ [mm^{-1}]	1.029	1.094	0.739	0.478
total reflns	6020	2772	4799	2708
Unique reflns	4884	1950	4734	2684
Observed reflns	1540	1541	4218	2434
$R_1[I > 2\sigma(I)]$	0.0611	0.0746	0.0445	0.0387
wR_2 [all]	0.1296	0.2539	0.1304	0.1019
GOF	0.848	1.051	1.056	1.040
Diffractometer	X-calibur Gemini Eos CCD	X-calibur Gemini Eos CCD	SHELXL-97	SHELXL-97

Table 4.8. Crystallographic data for **58a**, **58b**, **58c** and **61b**.

Compound	**58a**	**58b**	**58c**	**61b**
Formula	$C_8H_4N_6O_6$	$C_{11}H_6N_8O_6$	$C_8H_4Cl_2N_4O_2$	$C_9H_4N_{10}O_6$
M_w	280.17	346.24	259.05	348.22
Crystal system	orthorhombic	monoclinic	triclinic	monoclinic
Space group	*Pbca*	$P2_1/c$	$P\bar{1}$	$P2_1/c$
T [K]	293 K	293 K	273 K	273 K
a [Å]	10.2457(3)	18.869(2)	9.534(8)	14.128(4)
b [Å]	21.0883(8)	19.0706(18)	10.062(8)	7.493(2)
c [Å]	90	7.7756(8)	10.657(9)	12.986(4)
α [°]	90	90	89.971(13)	90
β [°]	90	95.923(10)	86.262(13)	99.779(4)
γ [°]	90	90	89.768(13)	90
Z	8	8	4	4
V [Å^3]	2219.16 (11)	2783.1 (5)	1020.2 (15)	1354.7 (7)
D_{calc} [g cm^{-3}]	1.677	1.653	1.687	1.707
μ [mm^{-1}]	1.292	0.139	0.625	0.147
total reflns	2175	5687	4052	2687
Unique reflns	1879	5674	3939	2670
Observed reflns	1681	2397	2528	2316
$R_1[I > 2\sigma(I)]$	0.0473	0.0811	0.0601	0.0446
wR_2 [all]	0.1386	0.2601	0.1068	0.1423
GOF	1.068	1.022	0.993	0.802
Diffractometer	X-calibur Gemini Eos CCD	X-calibur Gemini Eos CCD	SHELXL-97	SHELXL-97

4.4. Energetic Properties

Energetic properties of nitrogen-rich poly-pyrazole and triazolyl-pyridines-/pyrimidines (**39a**, **40**, **43+44**, **54**, **55**, **58a, 58b, 58d, 61a, 61b** and **61d**) are illustrated in Table 4.9. Indispensable parameters such as: heat of formation (HOF), density, detonation velocity (*vD*) and detonation pressure (*P*) determine the nature and efficiency of the energetic materials. The density of the synthesized compounds were determined using Material Studio Suite programme, showing in the range of 1.48 to 1.74 g cm^{-3}. Among them, some of the compounds **58a, 58d, 61a, 61b** and **61d**, dispaly a higher density than TNT (1.65 g cm^{-3}). The variation of density for **39a** (1.58 g cm^{-3}) and **58a** (1.74 g cm^{-3}) suggests the effect of nitro group for the enhancement of density.

Oxygen balance (OB) is a significant index of energetic materials, as it indicates the deficiency or excess of oxygen in a compound required to convert all carbon into carbon dioxide and all hydrogen into water. Nitrogen-rich pyridyl-/pyrimidyl tethered 1,2,3-triazoles exhibit negative oxygen balance ranging from –117.8 to –148.5%, while nitro-rich pyrazoles and 1,2,4-triazoles possess good OB ranging from –54.0 to –91.0%; the introduction of nitro ($–NO_2$) groups effect this outcome.

As shown in Table 4.9, heats of formation of nitrogen-rich poly-1,2,3-triazolyl-pyridines-/pyrimidines are in the range of 635.9 to 1148.7 kJ mol^{-1}, whereas the heats of formation of nitro-rich poly-pyrazole/1,2,4-triazolyl-pyridine/pyrimidine compounds fall between 317.1 to 906.4 kJ mol^{-1}. Intrestingly, compound **55** exhibits high positive heats of formation (1148.7 kJ mol^{-1}) due to the high nitogen content. Next, the detonation pressures (*P*), and velocities (*vD*), were calculated by using EXPLO5 *version* 6.02. All nitro-rich pyridyl-/pyrimidyl-tethered poly-pyrazole/1,2,4-triazole derivatives show good detonation pressures (20.2–26.1 GPa) and detonation velocities (7305–8019 m s^{-1}), more than to trinitrotoluene (TNT, *P* = 19.50 GPa, *vD* = 6881 m s^{-1}). The oxygen and nitrogen rich compounds **58a, 58d, 61a, 61b** and **61d** holds high positive heats of formation as well as good detonation performances (**58a**, *vD* = 7787 m s^{-1}; **58d**, *vD* = 7465 m s^{-1}; **61a**, *vD* = 8019 m s^{-1}; **61b**, *vD* = 7685 m s^{-1}; **61d**, *vD* = 7781 m s^{-1}) more than triaminotrinitro benzene (TATB, *vD* = 7350 m s^{-1}).

Table 4.9. Energetic properties of *N*-heteroaryl-azole derivatives

Comp.	OB[a] [%]	ρ[b] [g cm^{-3}]	vD[c] [m s^{-1}]	P[d] [GPa]	T_m[e] [°C]	T_d[f] [°C]	HOF[g] [kJ mol^{-1}]
39a	-117.8	1.58	6221(7100)	15.79(17.02)	187	293	736.9
40	-148.5	1.49	5459(6892)	11.67(14.72)	–	288	1023.8
43	-148.5	1.46	5372(6861)	11.17(14.57)	266	284	1016.0
44	-148.5	1.48	5468(6902)	11.64(14.76)	266	284	1051.3
54	-137.7	1.48	5582(6858)	12.20(14.70)	249	276	635.9
55	-133.8	1.52	5849(7228)	13.60(16.74)	–	278	1148.7
58a	-68.5	1.74 (1.68)	7381(7787)	23.66(24.67)	117	324	317.1
58b	-87.8	1.66 (1.65)	6819(7305)	19.57(20.23)	228	379	510.6
58d	-91.0	1.70	6959(7465)	20.69(21.73)	315	418	894.5
61a	-54.0	1.74	7609(8019)	25.08(26.12)	148	310	368.7
61b	-64.3	1.70	7279(7685)	22.64(23.71)	220	392	606.3
61d	-61.5	1.73	7376(7781)	23.52(24.61)	–	262	906.4
TNT[11b]	-74.0	1.65	6881	19.50	80	300	-67.0
TATB[9]	-55.7	1.94	7350	30.01	350	360	137.9
RDX[11c]	-21.6	1.82	8748	34.90	–	230	92.6

[a] Oxygen balance. [b] Calculated density; the experimental crystal density is shown in the parenthesis. [c] Velocity of detonation calculated with Kamlet–Jacobs equations; the *vD* is calculated with Explo5 *version* 6.02 and shown in the parenthesis. [d] Detonation pressure calculated with Kamlet–Jacobs equations; the *P* is calculated with Explo5 *version* 6.02 and shown in the parenthesis. [e] Melting point. [f] Decomposition temperature under nitrogen gas (10 °C min^{-1}). [g] Heat of formation.

Thermal stability of the compounds were determined by differential scanning calorimetry–thermogravimetric (DSC-TGA) measurments (Table 4.9). Melting point of all the nitrogen-rich pyrazole and triazole compounds ranges from 117 °C to 266 °C. The pyridyl-/pyrimidyl-tethered-pyrazoles and triazoles show relatively high decomposition temperatures (262–418 °C). The pyrimidyl-tethered 1,2,3-triazole compound **55** decompose without melting at high temperature (278 °C). Most of the compounds show good thermal stabilities; gratifyingly, compound **58d** exhibits decomposition temperature 418 °C, thermally more stable than TATB (360 °C). The DSC thermograms of **54** and **55** for similar heating rates (10 °C/min) are presented in Figure 4.2. Interestingly, the

compounds **54** and **55** showed strong exothermic effect due to the presence of 1H-1,2,3-triazole moiety and pyrimidine ring.

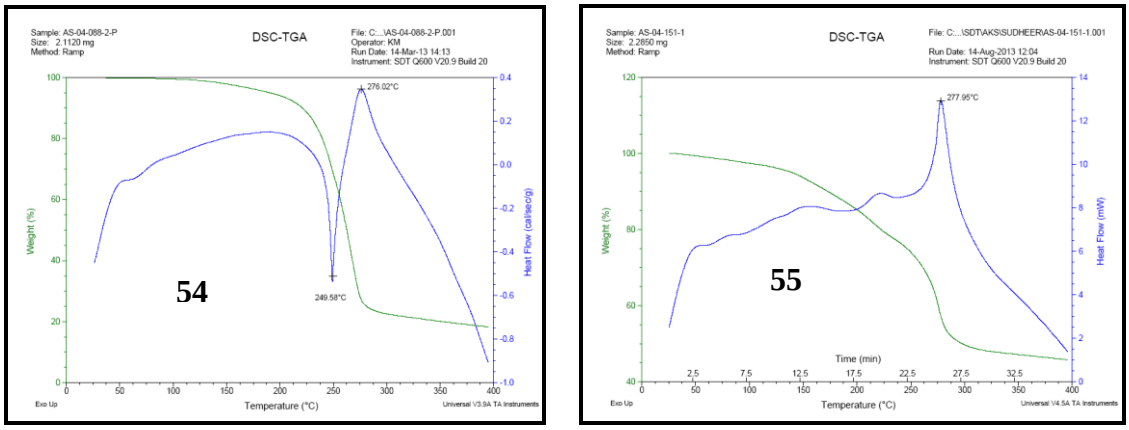

Figure 4.2. DSC thermograph for **54**, and **55** compounds

4.5. Potential Energy Diagrams

General electrostatic potential energy information is same as the information shown in Page No 47, Chapter 2.

A small electronegative region is located in the vicinity of the pyridine and triazole rings in the compounds **40** and **43** because of the strong electronegative nitrogen's. Whereas in pyrimidine derivatives **54** & **55**, more negative charge density is found on the triazole rings due to the strong electronegativity of pyrimidine ring. Likewise, large electropositive potential generated over the pyrazole and pyridine ring in the compounds **58a** & **58b** because of the strong electron withdrawing effect of the nitro ($-NO_2$) groups. This behavior is clearly shown in the potential energy diagrams (Figure 4.3).

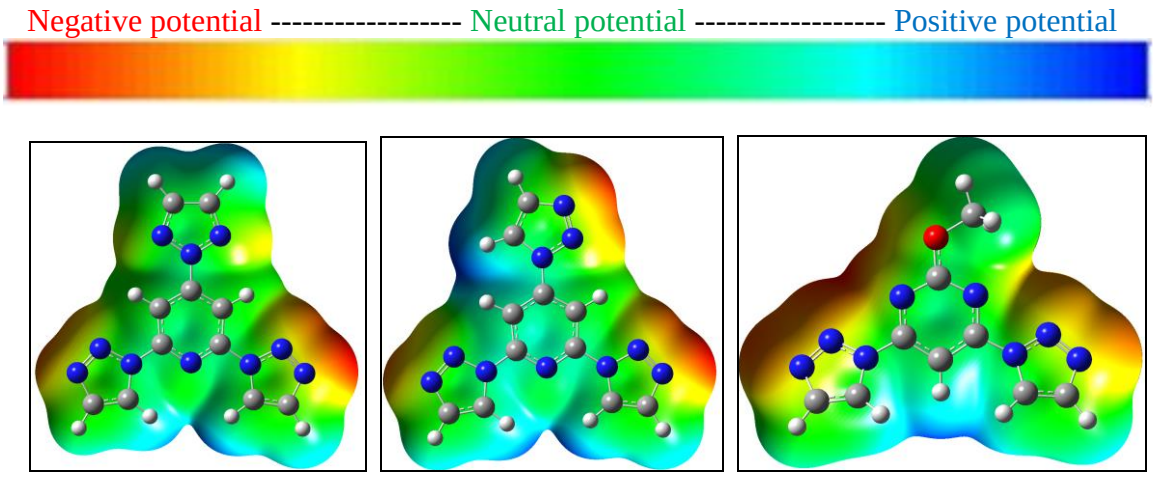

40 **43** **54**

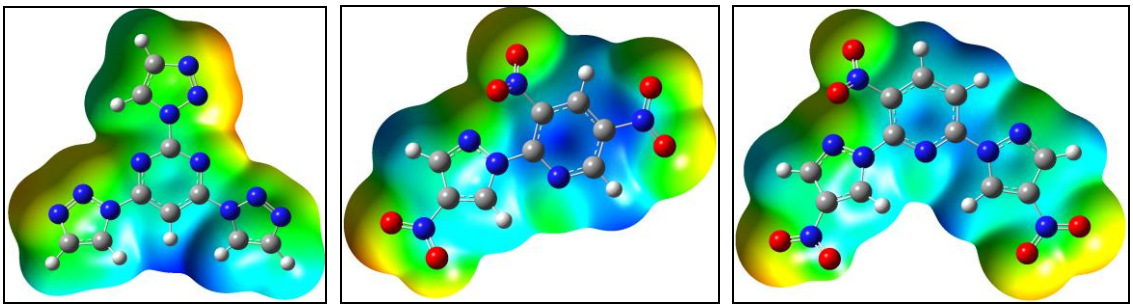

55 **58a** **58b**

Figure 4.3. Optimized structures and electrostatic potential surfaces of compounds **40**, **43**, **54**, **55, 58a** and **58b** (B3PW91/6-31G (d,p), 0.001 au electron/bohr^3 isosurface. The red and blue regions of the ruler (from left to right) indicate regions of more negative (electron-rich) and positive (electron deficient) charges, respectively. Gray = carbon; white = hydrogen; blue = nitrogen; red = oxygen.

4.6 Conclusion

In summary, a series of new nitrogen-rich pyridyl-/pyrimidyl-tethered-poly-pyrazole and triazole based energetic materials were successfully synthesized and characterized by analytical and spectroscopic methods. Furthermore, structures of some of the synthesized compounds were established by single-crystal X-ray diffraction. Most of the nitro-/nitrogen-rich pyrazole and triazole derivatives decomposed in the range 262–418 ^{o}C; consequently, these molecules are considered thermally stable energetic materials. Some of the synthesized nitro-rich pyrazole and triazole derivatives exhibit good density and detonation performance. Interestingly, compounds **58a** (ρ = 1.74 g cm^{-3}, *P* = 24.67 GPa, *vD* = 7787 m s^{-1}) and **61d** (ρ = 1.73 g cm^{-3}, *P* = 24.61 GPa, *vD* = 7781 m s^{-1}) showed high density and detonation properties than TNT (ρ = 1.65 g cm^{-3}, *P* = 19.50 GPa, *vD* = 6881 m s^{-1}) and TATB (*vD* = 7350 m s^{-1}). Gratifyingly, the tri-nitro group bearing compound **61a** possesses better density (1.74 g cm^{-3}), good detonation performance (*vD* = 8019 m s^{-1}), decompostion temperature (310 ^{o}C), and positive heat of formation (368.7 kJ mol^{-1}), an alternate thermally stable energetic material comparable to RDX. Our predicted results revealed that the synthesized compounds possess high positive HOFs due to the high nitrogen content; in particular, the pyrimidyl-tethered 1,2,3-triazole derivative **55** showed a *HOF of 1148.7 kJ mol^{-1}*. Owing to the high positive HOF, these compounds might be useful as environmentally friendly energetic materials.

4.7. Future Work

Heptazines play key role in the synthesis of high performance energetic materials. Heptazine is symmetrical heterocyclic azadienes, composed of three fused triazine rings. Owing to the high nitrogen content, fused triazine ring systems in symmetrical fashion, the heptazine skeleton possesses high positive heat of formation (ΔH^{o}_{f}) with enhanced density and detonation performance and high thermal stability. Thus, heptazine bearing molecular entities are extensively used in rocket fuel, gas generators, green explosives, rocket propellants and smoke-free pyrotechnic fuels. Therefore, we are interested in the design and synthesis of wide variety of heptazine-bearing molecular entities for energetic applications; some of the representative structures are shown in Scheme 4.12.

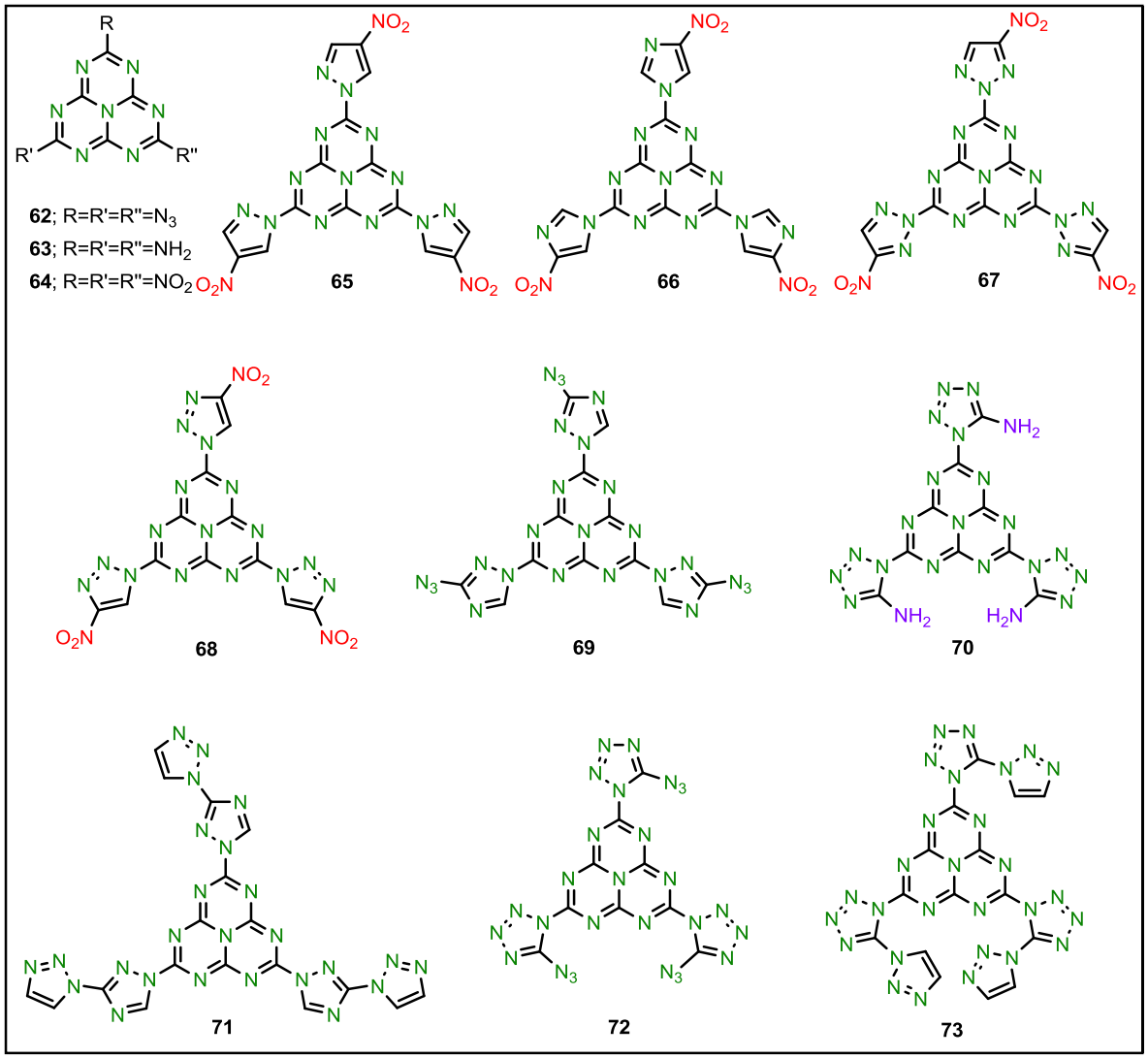

Scheme 4.12. Nitrogen-rich heptazine derivatives **62-73**

4.8. Experimental

4.8.1. General Experimental Information is shown in Page No 51-52, Chapter 2.

4.8.2. *Safety precautions!* Most of the high nitrogen content poly-pyrazole and triazole derivatives described in this report are typical representatives of high-energy materials that can show unpredictable behaviour. Especially, tirazidopyrimidine must be handled with extreme care and with appropriate safety precautions. Although we have not encountered any difficulties during the preparation of these compounds, manipulations must be carried out by using appropriate standard safety precautions. Eye protection & leather gloves must be worn.

4.8.3. X-ray crystallography

X-ray reflections **49, 50, 58c** and **61b** was collected on a Bruker SMART APEX CCD diffractometer equipped with a graphite monochromator and Mo-Kα fine-focus sealed tube (λ = 0.71073 Å). Data integration was done using SAINT.[19] Intensities for absorption were corrected using SADABS.[20] Structure solution and refinement were carried out using Bruker SHELX-TL.[21] X-ray reflections for compounds **46, 48, 58a** and **58b** were collected on an Oxford Xcalibur Gemini Eos CCD diffractometer using Mo-Kα, radiation. Data reduction was performed using CrysAlisPro (version 1.171.33.55). The OLEX2-1.0[22] and SHELX-TL 97 programme were used to solve and refine the data. All non-hydrogen atoms were refined anisotropically, and C−H hydrogens were fixed.

4.8.4. Theoretical Study Information is shown in Page No 106, Chapter 3

4.8.5. Isodesmic Reactions:

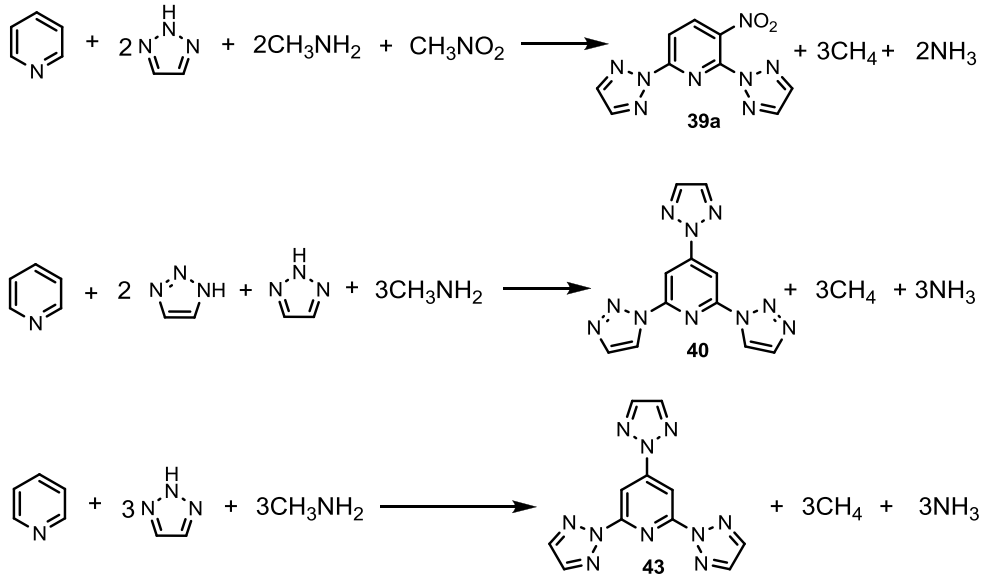

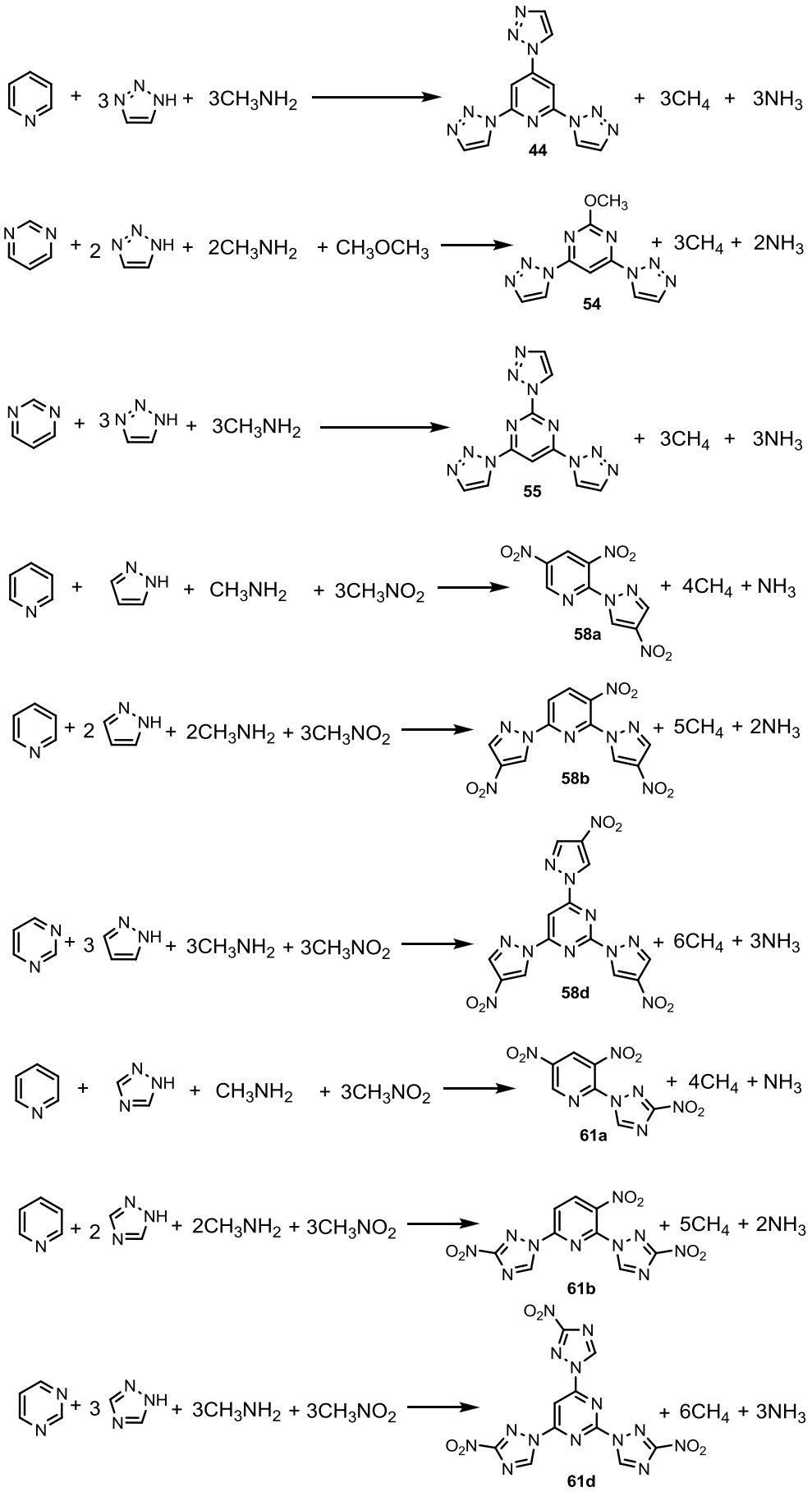
+ 3 + 3CH3NH2
+ 3CH4 + 3NH3
44
+ 2 + 2CH3NH2 + CH3OCH3
OCH3
+ 3CH4 + 2NH3
54
+ 3 + 3CH3NH2
+ 3CH4 + 3NH3
55
+ + CH3NH2 + 3CH3NO2
O2N
NO2
+ 4CH4 + NH3
58a
+ 2 + 2CH3NH2 + 3CH3NO2
+ 5CH4 + 2NH3
58b
+ 3 + 3CH3NH2 + 3CH3NO2
+ 6CH4 + 3NH3
58d
+ + CH3NH2 + 3CH3NO2
+ 4CH4 + NH3
61a
+ 2 + 2CH3NH2 + 3CH3NO2
+ 5CH4 + 2NH3
61b
+ 3 + 3CH3NH2 + 3CH3NO2
+ 6CH4 + 3NH3
61d

4.8.6. Materials: Unless otherwise noted, all the reagents and intermediates were obtained commercially and used without purification. Solvents were distilled. The substrates 2,6-dichloro-4-nitropyridine, 2,6-dichloro-3-nitropyridine, 2-chloro-3,5-dinitropyridine, 2,4,6-trichloropyridine, 2,4,6-trichloropyrimidine, pentachloropyridine, 3-nitro-1,2,4-triazole, 4-nitro-1H-pyrazole, 1H-1,2,3-triazole**,** trimethylsilylacetylene, potassium carbonate, sodium ascorbate, copper sulphate pentahydrate, copper iodide, cesium carbonate, sodium hydride were purchased from Sigma Aldrich Ltd, and used as received.

4.8.7. General procedure for the synthesis of compounds 39a, 39b-39b', 46-51, 58a-58d and 61a-61d (GP-1): A mixture of 1,2,3-triazole or 4-nitro-1H-pyrazole or 3-nitro-1,2,4-triazole (1.2 equiv) and NaH (60% oil dispersion) (2.0 equiv) was stirred in THF (5.0 mL for 1.0 mmol) in a 25 mL two-necked flask under an argon atmosphere at 0 ^{o}C for 30 min. The nitro-substituted halo pyridine (1.0 equiv) was then added and the mixture was stirred at RT for 6 h. Upon completion of the reaction, solvent was removed under the reduced pressure. The crude compound was dissolved in EtOAc. The organic layer was separated and the aqueous layer was extracted with EtOAc (3 times). The combined extracts were washed with water (twice) and brine and dried over Na_2SO_4. The solvent was filtered and evaporated under the reduced pressure. The crude residue was purified by column chromatography on silica gel.

4.8.8. General procedure for the synthesis of compounds 42 and 43+44 (GP-2): A mixture of CuI (0.2 equiv), Cs_2CO_3 (2.0 equiv), 1,2,3-triazole (1.4 equiv), and the heteroaryl halide (1.0 equiv) in DMF (2.0 mL per 1.0 mmol) was placed in a 10 mL vial under an argon atmosphere. The vial was sealed with a screw cap and the resulting mixture was stirred at the respective temperature (see Scheme 4.1 and Table 4.2). The reaction mixture was diluted with EtOAc (30 mL per 1.0 mmol) and filtered through a small plug of silica gel. The filtrate was washed with water (10 mL), the organic layer was separated, and the aqueous layer was extracted with EtOAc (3 ×10 mL). The combined organic extracts were washed with water (2 × 10 mL) and brine (5 mL) and dried over Na_2SO_4. The solvent was filtered and evaporated under reduced pressure. The crude residue was purified by silica gel column chromatography.

4.8.9. General procedure for the synthesis of azides (**GP-3**)**:** All azides were prepared following the reported procedures.[18] 2,4,6-triazidopyrimidine (**16**) was prepared from the corresponding bromides or chlorides by reacting with NaN_3 in DMSO at room temperature.

Physical characterization data of these compounds are exactly matching with the reported values.[18]

4.8.10. General cycloaddition procedure for the synthesis of compounds 54-55 (GP-4): A mixture of azide (1.0 equiv), trimethylsilylacetylene (9 equiv), potassium carbonate (7.2 equiv), sodium ascorbate (2.4 equiv) and $CuSO_4$ (1.2 equiv) were taken in MeOH/tBuOH: water (10 mL for 1 mmol, 1:1) in a 20 mL vial. The vial was sealed with a screw cap and the resulting mixture was stirred rapidly at room temperature for 24 h. Upon completion of the reaction, aqueous ammonium hydroxide (5%) was added to the reaction mixture. The organic layer was separated; the aqueous layer was extracted with ethyl acetate (3 times). The combined extracts were washed with water (2 times), brine and dried over Na_2SO_4. Solvent was filtered and evaporated under the reduced pressure. The crude residue was purified using silica gel column chromatography.

4.9. Spectral and Analytical Data of the Compounds:

3-Nitro-2,6-di(2H-1,2,3-triazol-2-yl)pyridine (**39a**)**:**

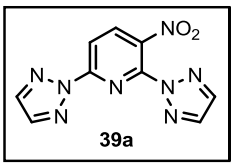

39a

Following the general procedure (**GP-1**); a mixture of 2,6-dichloro-3-nitropyridne (**37a**; 1.0 g, 5.18 mmol), 1H-1,2,3-triazole (1.43 g, 20.7 mmol), NaH (0.49 g, 20.7 mmol) in THF (10 mL) was stirred at room temperature for 6 h. Upon usual work-up, the crude mixture was purified by silica gel column chromatography eluting with hexane: ethyl acetate (2:1) to afford **39a** (0.91 g) in 68% yield as colorless solid.

m.p. 187 °C; DTA = 293 °C; R_f = 0.62 (*n*-hexane/EtOAc, 2:1); ^{1}H NMR (400 MHz, $CDCl_3$): δ = 8.43 (d, J = 8.8 Hz, 1H), 8.29 (d, J = 8.4 Hz, 1H), 8.01 (s, 2H), 7.98 (s, 2H); ^{13}C NMR (101 MHz, $CDCl_3$): δ = 150.1, 141.9, 138.5, 138.0, 137.7, 137.3; IR (KBr): ν_{max} = 3079, 1539, 1391, 1358, 1259, 1144, 1045, 936, 771, 645 cm^{-1}; MS (EI): *m/z* (%): 258 (100) $[M+1]^+$, 220 (23), 119 (23), 106 (57), 97 (30), 74 (28); Elemental analysis calcd (%) for $C_9H_6N_8O_2$: C 41.87, H 2.34, N 43.40; found: C 41.68, H 2.21, N 43.26.

2,6-Dichloro-4-(2H-1,2,3-triazol-2-yl)pyridine (**39b**) & **2,6-dichloro-4-(1H-1,2,3-triazol-1-yl)pyridine** (**39b'**)[14b]**:**

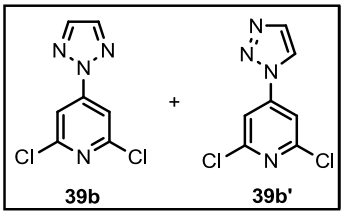

Following the general procedure (**GP-1**); a mixture of 2,6-dichloro-4-nitropyridne (**37b**; 2.0 g, 10.3 mmol), 1H-1,2,3-triazole (2.86 g, 41.4 mmol), NaH (0.99 g, 41.4 mmol) in THF (20 mL) was stirred at room temperature for 6 h. Upon usual work-up, the crude mixture was purified by silica gel column chromatography eluting with hexane: ethyl acetate (4:1) to afford **39b** (0.45 g) in 17% yield and **39b'**[14b] (2.04 g) in 78% yield as colorless solids.

For **39b**: m.p. 147 °C; DTA = 195 °C; R_f = 0.15 (*n*-hexane/EtOAc, 4:1); ^{1}H NMR (400 MHz, $CDCl_3$): δ = 7.96 (s, 3H), 7.90 (s, 3H); ^{13}C NMR (101 MHz, $CDCl_3$): δ = 151.7, 148.5, 137.8, 112.0; IR (KBr): ν_{max} = 3095, 1566, 1445, 1385, 1144, 930, 788, 656 cm^{-1}; MS (EI): *m/z* (%): 258 (100) $[M+1]^+$, 241 (46), 233 (38), 217 (41), 203 (30); Elemental analysis calcd (%) for $C_9H_6N_8O_2$: C 41.87, H 2.34, N 43.40; found: C 41.76, H 2.31, N 43.31.

For **39b'**:[14b] m.p. 94 °C; DTA = 246 °C; R_f = 0.69 (*n*-hexane/EtOAc, 4:1); ^{1}H NMR (400 MHz, $CDCl_3$): δ = 8.14 (s, 1H), 7.92 (s, 2H), 7.77 (s, 3H); ^{13}C NMR (101 MHz, $CDCl_3$): δ = 152.2, 146.1, 135.4, 121.7, 113.1; IR (KBr): ν_{max} = 3117, 1582, 1561, 1456, 1369, 1254, 1051, 859, 826, 777 cm^{-1}; MS (EI): *m/z* (%): 258 (100) $[M+1]^+$, 220 (32), 106 (46), 97 (38), 74 (35); Elemental analysis calcd (%) for $C_9H_6N_8O_2$: C 41.87, H 2.34, N 43.40; found: C 41.68, H 2.31, N 43.51.

2,6-Dichloro-4-(2H-1,2,3-triazol-2-yl)pyridine (**40**)**:**

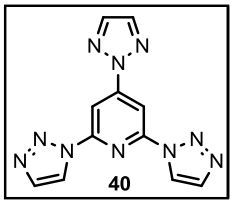

Following the general procedure (**GP-2**); a mixture of 2,6-dichloro-4-(2H-1,2,3-triazol-2-yl)pyridine (**39b**; 0.64 g, 3.31 mmol), 1H-1,2,3-triazole (**38**, 1.09 g 15.9 mmol), Cs_2CO_3 (6.48 g 19.8 mmol), CuI (0.37 g, 1.98 mmol) in DMF (20 mL) was heated at 80 ^{o}C for 3 h. Upon usual work-up, the crude mixture was purified by silica gel column chromatography eluting with hexane: ethyl acetate (1:1) to afford **40** (0.593 g) in 63% yield as colorless solid.

m.p. Not melting; DTA = 288 °C; R_f = 0.62 (*n*-hexane/EtOAc, 1:1); ^{1}H NMR (400 MHz, $CDCl_3$): δ = 9.33 (s, 2H), 8.60 (s, 2H), 8.42 (s, 2H), 8.12 (s, 2H); ^{13}C NMR (101 MHz, $CDCl_3$): δ = 150.0, 149.3, 139.7, 135.3, 123.6, 101.5; IR (KBr): ν_{max} = 3122, 1615, 1478, 1451, 1391, 1325, 1259, 1199, 996, 963, 870, 793 cm^{-1}; MS (EI): *m/z* (%): 280 (100) $[M+1]^+$,

274 (5), 249 (3), 222 (3); Elemental analysis calcd (%) for $C_9H_6N_8O_2$: C 47.14, H 2.88, N 49.98; found: C 47.21, H 2.81, N 49.85.

2,6-Dichloro-4-(2H-1,2,3-triazol-2-yl)pyridine (**42**), **2,4,6-tri(2H-1,2,3-triazol-2-yl)pyridine** (**43**) and **2,4,6-tri(1H-1,2,3-triazol-1-yl)pyridine** (**44**)**:**

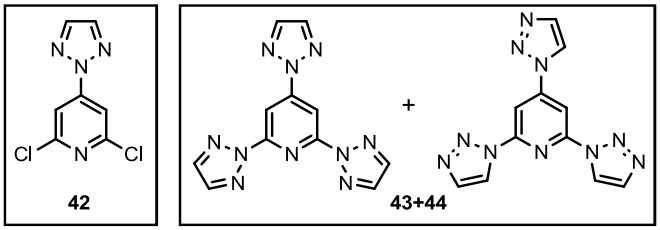

Following the general procedure (**GP-2**); a mixture of 2,4,6-trichloropyridine (**41**; 0.15 g, 0.82 mmol), 1H-1,2,3-triazole (**38**, 0.36 g 5.26 mmol), Cs_2CO_3 (2.14 g 6.57 mmol), CuI (0.12 g, 0.65 mmol) in DMF (5 mL) was stirred at room temperature for 12 h. Upon usual work-up, the crude mixture was purified by silica gel column chromatography eluting with hexane: ethyl acetate (1:1) to afford **42** (0.03 g) in 19% yield and **43**+**44** (0.83 g) in 53% yield as colorless solids.

For **42**: m.p. 147 °C; R_f = 0.15 (*n*-hexane/EtOAc, 4:1); ^{1}H NMR (400 MHz, $CDCl_3$): δ = 7.99 (s, 2H), 7.92 (s, 2H); ^{13}C NMR (101 MHz, $CDCl_3$): δ = 151.8, 148.5, 137.8, 112.1; IR (KBr): ν_{max} = 1561, 1419, 1232, 1161, 991, 827, 778, 712, 646 cm^{-1}; MS (EI): *m/z* (%): 215 (30) [M^+–1], 214 (100) [M^+], 127 (19), 122 (5), 95 (70); Elemental analysis calcd (%) for $C_9H_6N_8O_2$: C 39.10, H 1.87, N 26.05; found: C 39.16, H 1.83, N 26.12.

For **43+44**: m.p. 266 °C; DTA = 284 °C; R_f = 0.65 (*n*-hexane/EtOAc, 1:1); ^{1}H NMR (400 MHz, $CDCl_3$): δ = 8.87 (d, J = 1.6 Hz, 1H), 8.72 (s, 1H), 8.63 (s, 1H), 8.01 (m, 3H), 7.97 (m, 9H), 7.89 (s, 1H); ^{13}C NMR (101 MHz, $CDCl_3$): δ = 152.0, 151.6, 151.3, 149.8, 149.4, 149.2, 137.9, 137.7, 137.4, 112.7, 112.3, 101.9, 101.7; IR (KBr): ν_{max} = 3161, 2964, 2854, 1605, 1578, 1446, 1271, 1106, 1013, 810 cm^{-1}; MS (EI): *m/z* (%): 282 (13) [M^+], 281 (100) [M^+–1]; Elemental analysis calcd (%) for $C_9H_6N_8O_2$: C 47.14, H 2.88, N 49.98; found: C 47.23, H 2.82, N 49.85.

2,3,5,6-Tetrachloro-4-(2H-1,2,3-triazol-2-yl)pyridine (**46**) and **3,4,5-trichloro-2,6-di(2H-1,2,3-triazol-2-yl)pyridine** (**47**) and **3,4,5-trichloro-2,6-di(1H-1,2,3-triazol-1-yl)pyridine** (**48**)[14b] and **3,4,5-trichloro-2-(1H-1,2,3-triazol-1-yl)-6-(2H-1,2,3-triazol-2-yl)pyridine** (**49**) and **3,5-dichloro-2,4,6-tri(2H-1,2,3-triazol-2-yl)pyridine** (**50**) and **3-chloro-2,4,5,6-tetra(2H-1,2,3-triazol-2-yl)pyridine** (**51**):

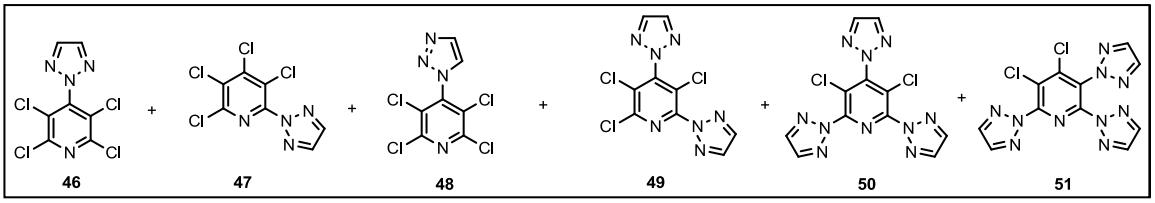

Following the general procedure (**GP-1**); a mixture of pentachloropyridine (**45**; 4.0 g, 15.9 mmol), 1H-1,2,3-triazole (**38**, 5.49 g, 79.5 mmol), NaH (1.91 g, 79.5 mmol) in THF (40 mL) was refluxed at 65 ^{o}C for 12 h. Upon usual work-up, the crude mixture was purified by silica gel column chromatography eluting with hexane: ethyl acetate (2:1) to afford **46** (0.91 g) in 21% yield and **47** (0.26 g) in 4% yield and **48** (0.40 g) in 7% yield and **49** (0.59 g) in 9% yield and **50** (0.96 g) in 17% yield and **51** (1.37 g) in 24% yield as colorless solids.

For **46**: m.p. 87 °C; R_f = 0.54 (*n*-hexane/EtOAc, 9:1); ^{1}H NMR (400 MHz, $CDCl_3$): 7.97 (br s, 2H); ^{13}C NMR (101 MHz, $CDCl_3$): δ = 147.2, 145.9, 136.9, 129.4; IR (KBr): ν_{max} = 2926, 1534, 1402, 1216, 1150 cm^{-1}; MS (EI): *m/z* (%): 286 (16) [M^++2], 285 (66) [M^++1], 284 (42) [M^+], 283 (100) [M^+–1], 255 (8), 249 (8), 221 (3); Elemental analysis calcd (%) for $C_7H_2Cl_4N_4$: C 29.61, H 0.71, N 19.73; found: C 29.56, H 0.76, N 19.65.

For **47**: m.p. 139 °C; R_f = 0.43 (*n*-hexane/EtOAc, 9:1); ^{1}H NMR (400 MHz, $CDCl_3$): δ = 8.04 (br s, 1H), 7.99 (s, 1H); ^{13}C NMR (101 MHz, $CDCl_3$): δ = 147.4, 139.3, 137.1 (d, *J* = 36 Hz, 1C); IR (KBr): ν_{max} = 2920, 1457, 1397, 1331, 1084, 942, 832, 794 cm^{-1}; MS (EI): *m/z* (%): 286 (15) [M^++2], 285 (65) [M^++1], 284 (40) [M^+], 283 (100) [M^+–1], 255 (8), 249 (8), 221 (3); Elemental analysis calcd (%) for $C_9H_4Cl_3N_7$: C 29.61, H 0.71, N 19.73; found: C 29.76, H 0.68, N 19.78.

For **48**: [14b] m.p. 170 °C; R_f = 0.48 (*n*-hexane/EtOAc, 6:1); ^{1}H NMR (400 MHz, $CDCl_3$): δ = 7.93 (d, *J* = 0.8 Hz, 1H), 7.89 (d, *J* = 1.2 Hz, 1H); ^{13}C NMR (101 MHz, $CDCl_3$): δ = 147.3, 143.3, 134.2, 128.7, 125.2; IR (KBr): ν_{max} = 2926, 1534, 1331, 1216, 1041, 723 cm^{-1}; MS (EI): *m/z* (%): 297 (16), 284 (21) [M^+], 283 (100) [M^+–1], 268 (18), 253 (10); Elemental analysis calcd (%) for $C_9H_4Cl_3N_7$: C 29.61, H 0.71, N 19.73; found: C 29.71, H 0.78, N 19.71.

For **49**: m.p. 143 °C; R_f = 0.45 (*n*-hexane/EtOAc, 3:1); ^{1}H NMR (400 MHz, $CDCl_3$): δ = 8.26 (d, *J* = 1.2 Hz, 1H), 8.01 (br s, 4H), 7.86 (d, *J* = 1.2 Hz, 1H); ^{13}C NMR (101 MHz, $CDCl_3$): δ = 147.5, 147.4, 143.9, 137.2, 133.7, 131.2, 124.7, 124.5; IR (KBr): ν_{max} = 3117, 1550, 1430, 1331, 1216, 958, 794, 652 cm^{-1}; MS (EI): *m/z* (%): 318 (32) [M^+], 317 (100) [M^+–1], 227

(8); Elemental analysis calcd (%) for $C_9H_4Cl_3N_7$: C 29.61, H 0.71, N 19.73; found: C 29.71, H 0.78, N 19.71.

For **50**: m.p. 101 °C; R_f = 0.55 (*n*-hexane/EtOAc, 2:1); ^{1}H NMR (400 MHz, $CDCl_3$): δ = 8.06 (s, 1H), 7.98 (br s, 3H), 7.76 (s, 2H); ^{13}C NMR (101 MHz, $CDCl_3$): δ = 148.6, 145.3, 137.3, 137.2, 131.0, 125.9; IR (KBr): ν_{max} = 3123, 1556, 1440, 1396, 1248, 1139, 843, 640 cm^{-1}; MS (EI): *m/z* (%): 351 (22), 349 (24) [M^+–1], 129 (7), 111 (20), 97 (100), 79 (13), 65 (19); Elemental analysis calcd (%) for $C_{11}H_6Cl_2N_{10}$: C 37.84, H 1.73, N 40.12; found: C 37.76, H 1.79, N 40.21.

For **51**: m.p. 189 °C; R_f = 0.50 (*n*-hexane/EtOAc, 1:1); ^{1}H NMR (400 MHz, $CDCl_3$): δ = 8.31 (s, 1H), 8.05 (br s, 2H), 7.99 (br s, 2H), 7.86 (s, 1H); ^{13}C NMR (101 MHz, $CDCl_3$): δ = 148.8, 145.6, 143.7, 137.3 (d, *J* = 20 Hz, 1C), 133.7, 126.4, 126.0, 124.9; IR (KBr): ν_{max} = 3117, 1566, 1440, 1402, 1160, 1002, 952, 837, 634 cm^{-1}; MS (EI): *m/z* (%): 351 (31), 349 (69) [M^+–1], 279 (6), 173 (12), 129 (24), 119 (16), 111 (100), 97 (37), 79 (41), 65 (20); Elemental analysis calcd (%) for $C_9H_5F_3N_4O_2$: C 37.84, H 1.73, N 40.12; found: C 37.88, H 1.71, N 40.07.

2-Methoxy-4,6-di(1H-1,2,3-triazol-1-yl)pyrimidine (**54**):

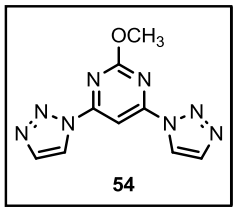

54

Following the general procedure (**GP-4**); a mixture of 2,4,6-triazidopyrimidine (**52**; 1.10 g, 5.41 mmol), trimethylsilylacetylene (**53**, 4.78 g, 48.7 mmol), potassium carbonate (5.38 g, 38.9 mmol), sodium ascorbate (2.57 g, 12.9), copper sulfate (1.62, 6.49) in MeOH:H_2O (100 mL) was stirred at room temperature for 12 h. Upon usual work-up, the crude mixture was purified by silica gel column chromatography eluting with hexane: ethyl acetate (1:1) to afford **54** (0.43 g) in 49% yield as yellow semi solid.

m.p. 249 °C; DTA = 276 °C (exothermic); R_f = 0.79 (*n*-hexane/EtOAc, 1:1); ^{1}H NMR (400 MHz, D_6[DMSO]): δ = 8.72 (s, 1H), 7.95 (s, 1H), 7.44 (s, 2H), 6.75 (s, 1H), 3.85 (s, 3H); ^{13}C NMR (101 MHz, D_6[DMSO]): δ = 167.6, 165.8, 155.4, 134.5, 122.6, 86.1; IR (KBr): ν_{max} = 3216, 1615, 1566, 1456, 1352, 1215, 1067, 996, 777 cm^{-1}; MS (EI): *m/z* (%): 246 (16) [M^+], 245 (100) [M^+–1], 209 (8); Elemental analysis calcd (%) for $C_9H_8N_8O$: C 44.26, H 3.30, N 45.88; found: C 44.32, H 3.26, N 45.71.

2,4,6-Tri(1H-1,2,3-triazol-1-yl)pyrimidine (**55**):

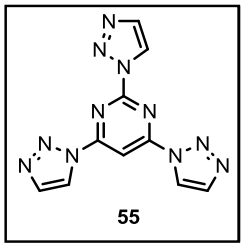

Following the general procedure (**GP-4**); a mixture of 2,4,6-triazidopyrimidine (**52**; 0.30 g, 1.47 mmol), trimethylsilylacetylene (**53,** 1.30 g, 13.29 mmol), potassium carbonate (1.50 g, 10.6 mmol), sodium ascorbate (0.70 g, 3.54), copper sulfate (0.44 g, 1.77) in *t*-BuOH:H_2O (20 mL) was stirred at room temperature for 12 h. Upon usual work-up, the crude mixture was purified by silica gel column chromatography eluting with hexane: ethyl acetate (4:1) to afford **55** (0.31 g) in 72% yield and as yellow solid.

m.p. Not melting; DTA = 278 °C (exothermic); R_f = 0.69 (*n*-hexane/EtOAc, 4:1); ^{1}H NMR (400 MHz, D6[DMSO]): δ = 9.04 (d, *J* = 6.8 Hz, 1H), 9.01 (d, *J* = 8.8 Hz, 1H), 8.04 (s, 2H), 7.97 (s, 2H), 7.13 (d, *J* = 3.6 Hz, 1H); ^{13}C NMR (101 MHz, D6[DMSO]): δ = 167.3, 154.8, 154.4, 134.9, 134.3, 124.6, 123.3, 90.9; IR (KBr): ν_{max} = 3194, 2953, 1660, 1556, 1463, 1375, 1249, 1046, 838 cm^{-1}; MS (EI): *m/z* (%): 282 (100) [M^+–1], 279 (16), 256 (11) 111 (29), 79 (34); Elemental analysis calcd (%) for $C_9H_8N_8O$: C 42.71, H 2.51, N 54.78; found: C 42.61, H 2.56, N 54.65.

3,5-Dinitro-2-(4-nitro-1H-pyrazol-1-yl)pyridine (**58a**)**:**

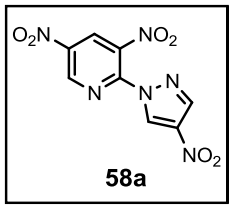

Following the general procedure (**GP-1**); a mixture of 2-chloro-3,5-dinitropyridne (**56a**; 1.0 g, 4.91 mmol), 4-nitro-1H-pyrazole (**57**, 0.72 g, 6.38 mmol), NaH (0.15 g, 6.38 mmol) in THF (20 mL) was stirred at room temperature for 6 h. Upon usual work-up, the crude mixture was purified by silica gel column chromatography eluting with hexane: ethyl acetate (4:1) to afford **58a** (0.90 g) in 65% yield as yellow solid.

m.p. 117 °C; DTA = 324 °C; R_f = 0.69 (*n*-hexane/EtOAc, 4:1); ^{1}H NMR (400 MHz, $CDCl_3$): δ = 9.50 (s, 1H), 9.21 (s, 1H), 8.93 (s, 1H), 8.30 (s, 1H); ^{13}C NMR (101 MHz, $CDCl_3$): δ = 146.1, 143.6, 142.6, 139.3, 138.6, 137.6, 130.3, 128.8; IR (KBr): ν_{max} = 3155, 3068, 1555, 1435, 1084, 1002, 919, 821, 749, 585 cm^{-1}; MS (EI): *m/z* (%):282 (18) [M^+–1], 280 (100) [M+1]$^+$, 249 (3); Elemental analysis calcd (%) for $C_9H_6N_8O_2$: C 34.30, H 1.44, N 30.00; found: C 34.26, H 1.38, N 30.12.

3-Nitro-2,6-bis(4-nitro-1H-pyrazol-1-yl)pyridine (**58b**)**:**

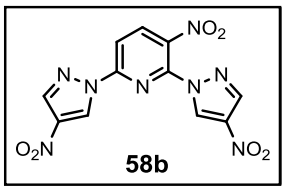

58b

Following the general procedure (**GP-1**); a mixture of 2,6-dichloro-3-nitropyridne (**56b**; 1.0 g, 5.18 mmol), 4-nitro-1H-pyrazole (**57**, 2.34 g, 20.7 mmol), NaH (0.49 g, 20.7 mmol) in THF (20 mL) was stirred at room temperature for 6 h. Upon usual work-up, the crude mixture was purified by silica gel column chromatography eluting with hexane: ethyl acetate (3:1) to afford **58b** (1.12 g) in 62% yield as yellow solid.

m.p. 228 °C; DTA = 379 °C (exothermic); R_f = 0.69 (*n*-hexane/EtOAc, 3:1); ^{1}H NMR (400 MHz, $CDCl_3$): δ = 10.3 (s, 1H), 10.2 (s, 1H), 8.76 (d, *J* = 8.8 Hz, 1H), 8.68 (s, 1H), 8.63 (s, 1H), 8.15 (d, *J* = 8.4 Hz, 1H); ^{13}C NMR (101 MHz, $CDCl_3$): δ = 149.2, 139.8, 139.7, 139.5, 139.2, 138.5, 138.1, 137.3, 131.3, 129.9, 113.6; IR (KBr): ν_{max} = 3128, 1593, 1489, 1407, 1319, 1188, 1002, 941, 865, 821, 749 cm^{-1}; MS (EI): *m/z* (%): 411 (7), 391 (3), 349 (3) [M^+–2], 348 (21) [M^+–1], 347 (100) [M^+–1]; Elemental analysis calcd (%) for $C_9H_6N_8O_2$: C 38.16, H 1.75, N 32.37; found: C 38.26, H 1.68, N 32.15.

2,6-Dichloro-4-(4-nitro-1H-pyrazol-1-yl)pyridine (**58c**) and **2-chloro-4,6-bis(4-nitro-1H-pyrazol-1-yl)pyridine** (**58c'**)**:**

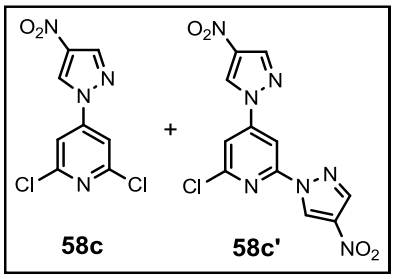

58c **58c'**

Following the general procedure (**GP-1**); a mixture of 2,6-dichloro-4-nitropyridne (**56c**; 1.0 g, 5.18 mmol), 4-nitro-1H-pyrazole (**57**, 2.34 g, 20.72 mmol), NaH (0.49 g, 20.72 mmol) in THF (20 mL) was stirred at room temperature for 6 h. Upon usual work-up, the crude mixture was purified by silica gel column chromatography eluting with hexane: ethyl acetate (4:1) to afford **58c** (0.75 g) in 54% yield and **58c'** (0.31 g) in 17% yield as colorless solids.

For **58c**: m.p. 160 °C; R_f = 0.15 (*n*-hexane/EtOAc, 4:1); ^{1}H NMR (400 MHz, $CDCl_3$): δ = 8.79 (s, 1H), 8.32 (s, 3H), 7.71 (s, 2H); ^{13}C NMR (101 MHz, $CDCl_3$): δ = 152.4, 148.0, 138.6, 138.2, 126.3, 112.4; IR (KBr): ν_{max} = 3139, 1539, 1418, 1325, 1166, 1111, 886, 821, 749 cm^{-1}; MS (EI): *m/z* (%): 259 (48) [M^+–2], 258 (15) [M^+–1], 257 (100) [M^++2]; Elemental analysis calcd (%) for $C_9H_6N_8O_2$: C 37.09, H 1.56, N 21.63; found: C 37.18, H 1.51, N 21.56.

For 58c': m.p. 198 °C; R_f = 0.69 (*n*-hexane/EtOAc, 1:1); ^{1}H NMR (400 MHz, $CDCl_3$): δ = 10.0 (s, 1H), 9.37 (s, 1H), 8.65 (d, *J* = 8.4 Hz, 2H), 8.39 (s, 1H), 8.23 (s, 1H); ^{13}C NMR (101

MHz, $CDCl_3$): δ = 151.1, 150.7, 149.5, 138.9, 138.8, 138.4, 137.8, 130.5, 128.0, 113.2, 101.9; IR (KBr): ν_{max} = 3139, 1604, 1544, 1402, 1319, 1040, 958, 821, 749 cm^{-1}; MS (EI): *m/z* (%): 337 (41) [M^+–2], 336 (28) [M^+–1], 335 (100) [M^++2]; Elemental analysis calcd (%) for $C_9H_6N_8O_2$: C 39.36, H 1.80, N 29.21; found: C 39.48, H 1.70, N 29.36.

2,4,6-Tris(4-nitro-1H-pyrazol-1-yl)pyrimidine (**58d**)**:**

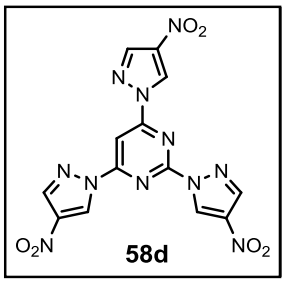

58d

Following the general procedure (**GP-1**); a mixture of 2,4,6-trichlropyrimidine (**56d**; 0.50 g, 2.72 mmol), 4-nitro-1H-pyrazole (**57**, 1.84 g, 16.3 mmol), NaH (0.39 g, 16.3 mmol) in THF (20 mL) was stirred at room temperature for 12 h. Upon usual work-up, the crude mixture was purified by silica gel column chromatography eluting with hexane: ethyl acetate (2:1) to afford **58d** (0.93 g) in 82% yield as colorless solid.

m.p. 315 °C; DTA = 418 °C (exothermic); R_f = 0.59 (*n*-hexane/EtOAc, 2:1); ^{1}H NMR (400 MHz, D6[DMSO]): δ = 10.2 (s, 1H), 9.75 (s, 2H), 8.72 (s, 2H), 8.56 (s, 1H), 8.06 (s, 1H); ^{13}C NMR (101 MHz, D6[DMSO]): δ = 159.9, 154.5, 140.1, 139.4, 138.8, 138.5, 131.7, 129.3, 96.2; IR (KBr): ν_{max} = 3139, 1599, 1550, 1396, 1314, 1182, 1002, 952, 821, 755 cm^{-1}; MS (EI): *m/z* (%): 412 (16) [M+1]$^+$, 414 (100) [M^+–1], 415 (29), 436 (8); Elemental analysis calcd (%) for $C_9H_6N_8O_2$: C 37.78, H 1.71, N 37.28; found: C 37.85, H 1.78, N 37.15.

3,5-Dinitro-2-(3-nitro-1H-1,2,4-triazol-1-yl)pyridine (**61a**)**:**

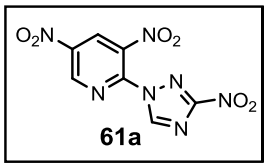

61a

Following the general procedure (**GP-1**); a mixture of 2-chloro-3,5-dinitropyridne (**59a**; 0.50 g, 2.45 mmol), 3-nitro-1,2,4-triazole (**60**, 0.36 g, 3.19 mmol), NaH (0.07 g, 3.19 mmol) in THF (20 mL) was stirred at room temperature for 12 h. Upon usual work-up, the crude mixture was purified by silica gel column chromatography eluting with hexane: ethyl acetate (4:1) to afford **61a** (0.51 g) in 74% yield as brown solid.

m.p. 148 °C; DTA = 310 °C (exothermic); R_f = 0.62 (*n*-hexane/EtOAc, 4:1); ^{1}H NMR (400 MHz, D6[DMSO]): δ = 9.82 (s, 1H), 9.70 (d, J = 2.0 Hz, 1H), 9.57 (d, J = 2.0 Hz, 1H); ^{13}C NMR (101 MHz, D6[DMSO]): δ = 163.5, 148.4, 147.6, 144.8, 141.3, 137.8, 132.3; IR (KBr): ν_{max} = 3090, 1610, 1555, 1467, 1418, 1341, 1314, 1111, 985, 925, 881, 760 cm^{-1}; MS (EI): *m/z* (%): 237 (16), 256 (16), 282 (100) [M^+–1], 283 (24) [M^+–2]; Elemental analysis calcd (%) for $C_9H_6N_8O_2$: C 29.90, H 1.08, N 34.87; found: C 30.06, H 1.12, N 34.71.

3-Nitro-2,6-bis(3-nitro-1H-1,2,4-triazol-1-yl)pyridine (61b):

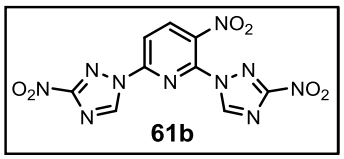

Following the general procedure (**GP-1**); a mixture of 2,6-dichloro-3-nitropyridne (**59b**; 0.50 g, 2.59 mmol), 3-nitro-1,2,4-triazole (**60**, 1.18 g, 10.3 mmol), NaH (0.24 g, 10.3 mmol) in THF (20 mL) was stirred at room temperature for 12 h. Upon usual work-up, the crude mixture was purified by silica gel column chromatography eluting with hexane: ethyl acetate (3:1) to afford **61b** (0.78 g) in 86% yield as yellow solid.

m.p. 220 °C; DTA = 392 °C (exothermic); R_f = 0.46 (*n*-hexane/EtOAc, 3:1); ^{1}H NMR (400 MHz, D6[DMSO]): δ = 10.1 (d, J = 1.6 Hz, 1H), 10.0 (d, J = 1.2 Hz, 1H), 9.02 (dd, J = 1.2, J = 8.8 Hz, 1H), 8.38 (dd, J = 1.2, 8.8 Hz, 1H); ^{13}C NMR (101 MHz, D6[DMSO]): δ = 163.7, 163.4, 148.4, 147.6, 147.0, 141.0, 137.9, 116.0; IR (KBr): ν_{max} = 2920, 1561, 1522, 1418, 1380, 1259, 1100, 804 cm^{-1}; MS (EI): *m/z* (%): 154 (16), 230 (11), 349 (100) [M^+–1], 350 (58) [M^+–2]; Elemental analysis calcd (%) for $C_9H_6N_8O_2$: C 31.05, H 1.16, N 40.23; found: C 31.16, H 1.26, N 40.07.

2,6-Dichloro-4-(3-nitro-1H-1,2,4-triazol-1-yl)pyridine (61c):

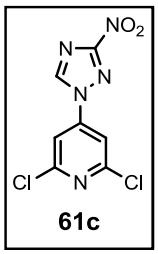

Following the general procedure (**GP-1**); a mixture of 2,6-dichloro-4-nitropyridne (**59c**; 0.30 g, 1.55 mmol), 3-nitro-1,2,4-triazole (**60**, 0.70 g, 6.21 mmol), NaH (0.14 g, 6.21 mmol) in THF (10 mL) was stirred at room temperature for 24 h. Upon usual work-up, the crude mixture was purified by silica gel column chromatography eluting with hexane: ethyl acetate (4:1) to afford **61c** (0.27 g) in 67% yield as yellow semi solid.

R_f = 0.15 (*n*-hexane/EtOAc, 4:1); ^{1}H NMR (400 MHz, $CDCl_3$): δ = 8.90 (s, 1H), 7.80 (s, 2H); ^{13}C NMR (101 MHz, $CDCl_3$): δ = 152.9, 145.1, 143.3, 143.2, 113.0; IR (KBr): ν_{max} = 3133, 1610, 1550, 1506, 1478, 1429, 1352, 1298, 1111, 985, 859 cm^{-1}; MS (EI): *m/z* (%): 105 (11), 156 (26), 260 (100) [M^+], 259 (63) [M^++1], 258 (26) [M^++2]; Elemental analysis calcd (%) for $C_9H_6N_8O_2$: C 32.33, H 1.16, N 26.93; found: C 32.41, H 1.21, N 26.82.

2,4,6-Tris(3-nitro-1H-1,2,4-triazol-1-yl)pyrimidine (61d):

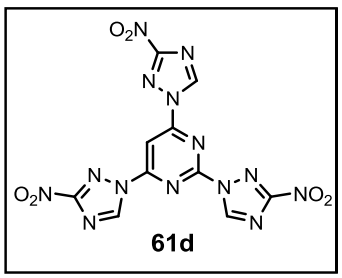

Following the general procedure (**GP-1**); a mixture of 2,4,6-trichlropyrimidine (**59d**; 0.50 g, 2.72 mmol), 3-nitro-1,2,4-triazole (**60**, 1.86 g, 16.3 mmol), NaH (0.39 g, 16.3 mmol) in THF (20 mL) was stirred at room temperature for 24 h. Upon usual work-up, the crude mixture was purified by silica gel

column chromatography eluting with hexane: ethyl acetate (1:1) to afford **61d** (1.03 g) in 91% yield as colorless solid.

m.p. 192 °C; DTA = 262 °C (exothermic); R_f = 0.72 (*n*-hexane/EtOAc, 1:1); ^{1}H NMR (400 MHz, D6[DMSO]): δ = 10.3 (s, 1H), 10.2 (s, 2H), 8.36 (s, 1H); ^{13}C NMR (101 MHz, D6[DMSO]): δ = 172.9, 164.4, 158.9, 153.5, 149.6, 148.2, 99.1; IR (KBr): ν_{max} = 3155, 1604, 1561, 1517, 1478, 1429, 1303, 1265, 1100, 980, 843, 799 cm^{-1}; MS (EI): *m/z* (%): 376 (5), 417 (100) [M^+–1], 416 (26) [M^+]; Elemental analysis calcd (%) for $C_9H_6N_8O_2$: C 28.26, H 0.97, N 47.11; found: C 28.72, H 1.06, N 47.21.

4.10. References

1) a) Q. Zhang, J. M. Shreeve, *Angew. Chem. Int. Ed.* **2013**, *52*, 2–5; b) J. P. Agrawal, R. D. Hodgson, *Organic Chemistry of Explosives*, Wiley–VCH, Weinheim, **2007**; c) J. Akhavan, *The Chemistry of Explosives*, 2nd ed., RSC, Cambridge, **2004**;

2) a) P. F. Pagoria, G. S. Lee, A. R. Mitchell, R. D. Schmidt, *Thermochimi. Acta.* **2002**, *384*, 187–204; b) M. B. Talawar, R. Sivabalan, M. Anniyappan, G. M. Gore, S. N. Asthana, B. R. Gandhe, *Combust. Explos. Shock Waves*, **2007**, *43*, 62–72.

3) C. K. L. Ma, R. A. Nissan, W. S. Wilson, *J. Org. Chem*. **1990**, *55*, 3755–3761.

4) S. V. Chapyshev, U. Bergstrdller, M. Regitz, *Chem. Heterocycl. Compd*., **1996**, *32*, 59–64.

5) a) J. M. Bakke, *Pure Appl. Chem*. **2003**, *75*, 1403–1415; b) N. Ishida, W. Ikemoto, M. Narumi, M. Murakami, *Org. Lett*. **2011**, *13*, 3008–3011.

6) a) G. H. Tao, B. Twamley, J. M. Shreeve, *J. Mater. Chem*. **2009**, *19*, 5850–5854; b) C. Ye, H. Gao, J. A. Boatz, G. W. Drake, B. Twamley, J. M. Shreeve, *Angew. Chem.* **2006**, *118*, 7420–7423; *Angew. Chem. Int. Ed.* **2006**, *45*, 7262–7265; c) A. Saikia, R. Sivabalan, G. Polke, G. M. Gore, A. Singh, A. S. Rao, A. K.Sikder, *J. Hazard. Mater*. **2009**, *170*, 306–313; d) O. Yu. Sapozhnikov, M. D. Dutov, M. A. Korolev, V. V. Kachala, V. I. Kadentsev, S. A. Shevelev, *Russ. Chem. Bull.* **2004**, *53*, 588–595.

7) a) D. Donati, S. Fusi, F. Ponticelli *J. Chem. Research (S)*, **1997**, 170–171. S. V. Chapyshev, *Chem. Heterocycl. Compd*., **2001**, *37*, 861–866; b) S. V. Chapyshev N. V. Chapysheva, *Chem. Heterocycl. Compd*. **1994**, *30*, 585–590.

8) a) R. P. Singh, J. M. Shreeve, *Chem. Eur. J*. **2011**, *17*, 11876 –11881; b) K. Karaghiosoff, T. M. Klapotke, P. Mayer, H. Piotrowski, K. Polborn,R. L. Willer, J. J. Weigand, *J. Org. Chem*. **2006**, *71*, 1295–1305; c) R. Damavarapu, *Propellants Explos. Pyrotech.* **2010**, *35*,

395–406; d) R. Damavarapu, C. R. Surapaneni, N. Gelber, R. G. Duddu, P. R.Dave, *U. S. Patent* 7304164, **2007**; e) H. H. Licht, H. Ritter, *Propell. Explos. Pyrotech.*, **1988**, *13*, 25.

9) a) P. Yin, J. Zhang, C. He, D. A. Parrish, J. M. Shreeve, *J. Mater. Chem. A*, **2014**, *2*, 3200–3208; b) C. He, J. Zhang, D. A. Parrish, J. M. Shreeve, *J. Mater. Chem. A*, **2013**, *1*, 2863–2868; c) C. K. L. Ma, R. A. Nissan, W. S. Wilson. *J. Org. Chem*. **1990**, *55*, 3761–3767.

10) a) Yu. M. Mikhailov, S. V. Chapyshev, V. V. Nedelko, *Russ. Chemical Bulletin*, **2009**, *58*, 2097–2102; b) S. V. Chapyshev, *Chem. Heterocycl. Compd*., **1993**, *29*, 1426–1427; c) M. D. Coburn, **1972**, *US Pat. 367806*; *Chem. Abstr*., **1972**, ***77***, 139812z; d) R. A. Nissan, W. S. Wilson, *Naval Air Warfare Centre*, **1995**, TR CA 3555-6001.

11) a) S. V. Chapyshev, *J. Fluorine Chem*. **2011**, *132*, 991–994; b) M. K. Elmkaddem, C. Fischmeister, C. M. Thomas, J. L. Renaud, *Chem. Commun*. **2010**, *46*, 925–927; (b) Q. Zhang, J. Zhang, D. A. Parrish and J. M. Shreeve, *Chem.–Eur. J*., 2013, **19**, 11000–11006; (c) J. Zhang and J. M. Shreeve, *J. Am. Chem. Soc*. **2014**, *136*, 4437–4445.

12) a) C. F. Foces, A. L. L. Saiz, R. M. Claramunt, N. Jagerovic, M. L. Jimeno, J. Elguero, *J. Chem. Soc. Perkin Trans.2* **1995**, 1359; b) C. F. Foces, A. L. L. Saiz, R. M. Claramunt, C. Escolhstico, R. M. Claramunt, *J. Phys. Org. Chem*. **1996**, *9*, 137.

13) a) A. J. Downard, G. E. Honey, P. J. Steel, *lnorg. Chem*. **1991**, *30*, 3733; (b) M. A. M. Garcfa, A. Gelling, D. R. Noble, K. G. Orrell, A. G. Osborne, V. Sik, *Polyhedron*, **1996**, *15*, 371.

14) a) P. Cornago, C. Escolistico, M. D. S. Maria, R. M. Ciaramunt, *Tetrahedron*, **1996**, *52*, 11075–11094; b) I. L. Knox, R. B. Rogers, US 4775762 A, **1988**; c) D. Balachari, M. L. Trudell, *Tetrahedron Lett*. **1997**, *38*, 8607–8610.

15) a) A. S. Kumar, V. D. Ghule, S. Subrahmanyam, A. K. Sahoo, *Chem. Eur. J*., **2013**, *19*, 509–518; b) N. Kommu, V. D. Ghule, A. S. Kumar, A. K. Sahoo, *Chem. Asian J*., **2014**, *9*, 166–178; c) A. S. Kumar, V. D. Ghule, N. Kommu, A. K. Sahoo, *J. Mater. Chem A*, **2014**, *2*, 7917-7926.

16) a) Y. Gao, C. Ye, B. Twamley, J. M. Shreeve, *Chem. Eur. J*. **2006**, *12*, 9010–9018; b) M. J. Crawford, K. Karaghlosoff, T. M. Klapotke, F. A. Martin, *Inorg. Chem*. **2009**, *48*, 1731–1743; c) M. V. Denffer, T. M. Klapotke, G. Kramer, G. Spiess, J. Welch, *Propellants. Explos. Pyrotech*. **2005**, *30*, 191–195; d) J. C. G. Ruiz, G. Holl, K. Karaghisoff, T. M. Klapotke, K. Lohnwitz, P. Mayer, H. Noth, K. Polborn, C. J. Rohbogner, M. Suter, J. J. Weigand, *Inorg. Chem*. **2005**, *44*, 4237–4253.

17) R. P. Singh, J. M. Shreeve, *Chem. Eur. J*. **2011**, *17*, 11876–11881; b) K. Karaghiosoff, T. M. Klapotke, P. Mayer, H. Piotrowski, K. Polborn, R. L. Willer, J. J. Weigand, *J. Org. Chem.*

2006, *71*, 1295–1305; c) R. Damavarapu, *Propellants Explos. Pyrotech*. **2010**, *35*, 395–406; d) R. Damavarapu, C. R. Surapaneni, N. Gelber, R. G. Duddu, P. R.Dave, *U. S. Patent* 7304164, **2007**.

18) a) S. Tadatake, N. Aiko, K. Yoshizo, N. Hiroyuki, B. Goetz, *Angew. Chem.Int. Ed*., **2003**, *42*, 5206–5209; b) Moulin, *Helvetica Chim. Acta*, **1952**, *35*, 167–175; c) V. R. Kamalraj, S. Senthil, P. Kannan, *J. Mol. Struct.* **2008**, *892*, 210–215.

19) *SAINT-Plus*, *version* 6.45, Bruker AXS Inc., Madison, **2003**.

20) G. M. Sheldrick, *SADABS*, Program for Empirical Absorption Correction of Area Detector Data, University of Gottingen, Gottingen, **1997**.

21) a) *SMART* (*version* 5.625), *SHELX-TL* (*version* 6.12), Bruker AXSInc., Madison, **2000**; b) G. M. Sheldrick, *SHELXS-97*, *SHELXL-97*, University of Gottingen, Gottingen, **1997**.

22) O. V. Dolomanov, A. J. Blake, N. R. Champness, M. Schroder, *J. Appl. Cryst*. **2003**, *36*, 1283–1284.

23) Gaussian 03, Revision A.1, M. J. Frisch, G. W. Trucks, H. B. Schlegel, G. E. Scuseria, M. A. Robb, J. R. Cheeseman, J. A. Montgomery, Jr., T. Vreven, K. N. Kudin, J. C. Burant, J. M. Millam, S. S. Iyengar, J. Tomasi, V. Barone, B. Mennucci, M. Cossi, G. Scalmani, N. Rega, G. A. Petersson, H. Nakatsuji, M. Hada, M. Ehara, K. Toyota, R. Fukuda, J. Hasegawa, M. Ishida, T. Nakajima, Y. Honda, O. Kitao, H. Nakai, M. Klene, X. Li, J. E. Knox, H. P. Hratchian, J. B. Cross, V. Bakken, C. Adamo, J. Jaramillo, R. Gomperts, R. E. Stratmann, O. Yazyev, A. J. Austin, R. Cammi, C. Pomelli, J. W. Ochterski, P. Y. Ayala, K. Morokuma, G. A. Voth, P. Salvador, J. J. Dannenberg, V. G. Zakrzewski, S. Dapprich, A. D. Daniels, M. C. Strain, O. Farkas, D. K. Malick, A. D. Rabuck, K. Raghavachari, J. B. Foresman, J. V. Ortiz, Q. Cui, A. G. Baboul, S. Clifford, J. Cioslowski, B. B. Stefanov, G. Liu, A. Liashenko, P. Piskorz, I. Komaromi, R. L. Martin, D. J. Fox, T. Keith, M. A. Al-Laham, C. Y. Peng, A. Nanayakkara, M. Challacombe, P. M. W. Gill, B. Johnson, W. Chen, M. W. Wong, C. Gonzalez, J. A. Pople, Gaussian, Inc., Pittsburgh, PA, **2003.**

24) EXPLO5 *version* 6.02, M. Suceska, **2014.**

4.11. Spectra

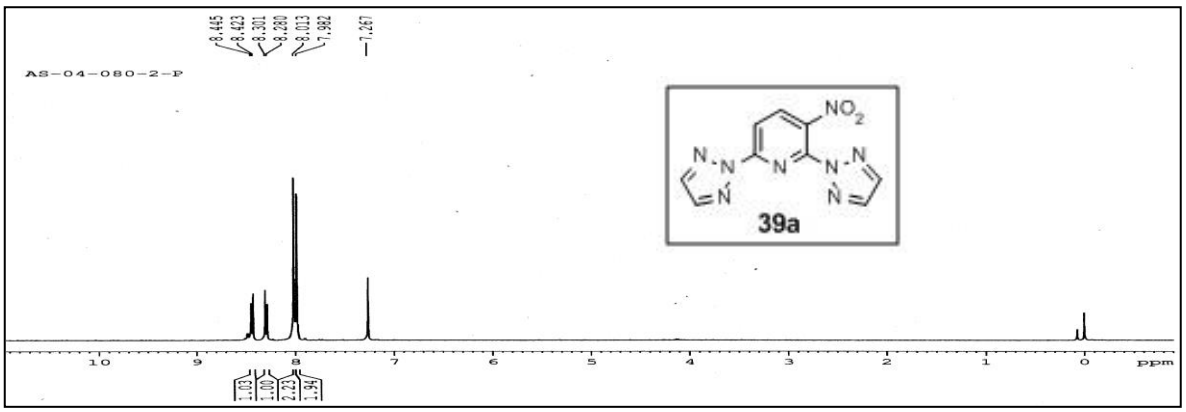
AS-04-080-2-P
8.445
8.423
8.301
8.280
8.013
7.982
7.267
39a
ppm

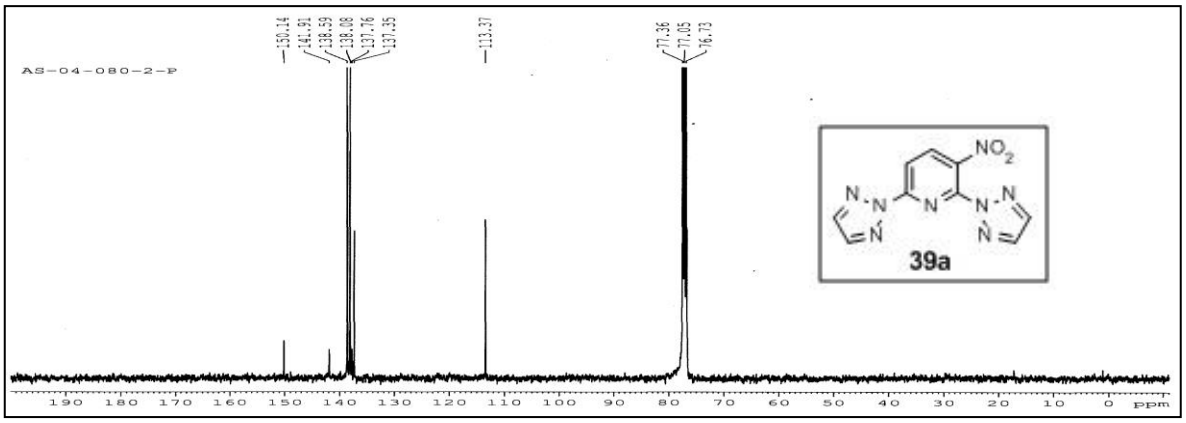
AS-04-080-2-P
150.14
141.91
138.59
138.08
137.76
137.35
113.37
77.36
77.05
76.73
39a
ppm

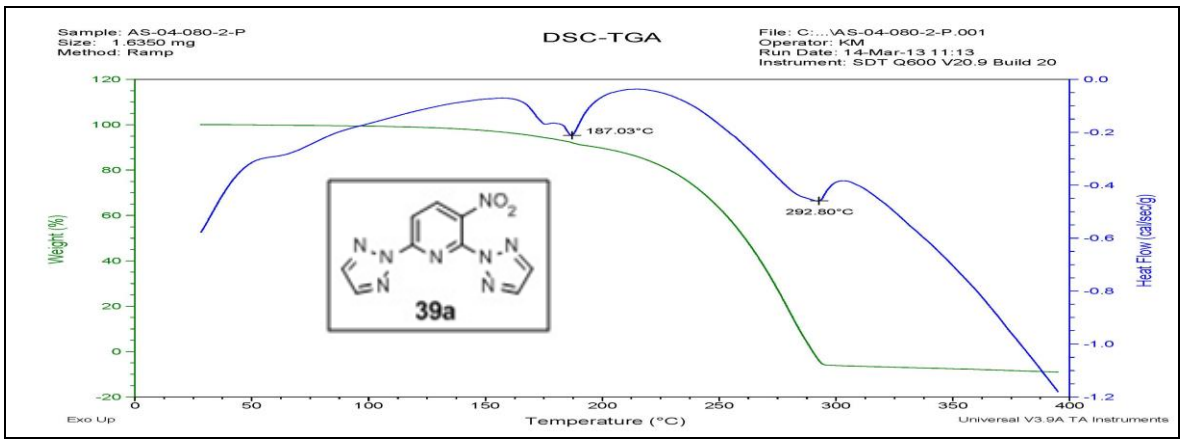
Sample: AS-04-080-2-P
Size: 1.6350 mg
Method: Ramp
DSC-TGA
File: C:...\AS-04-080-2-P.001
Operator: KM
Run Date: 14-Mar-13 11:13
Instrument: SDT Q600 V20.9 Build 20
187.03°C
292.80°C
39a
Weight (%)
Heat Flow (cal/sec/g)
Temperature (°C)
Exo Up
Universal V3.9A TA Instruments

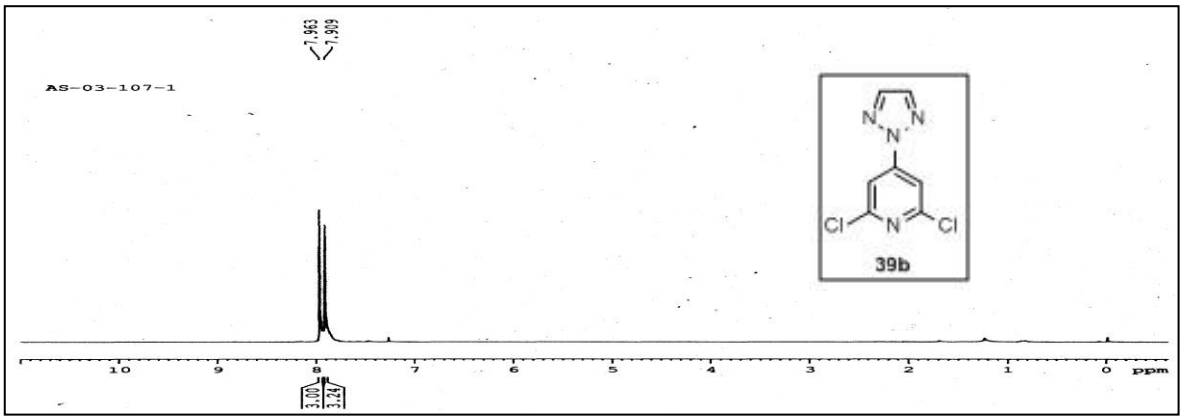
AS-03-107-1
7.963
7.909
39b
ppm

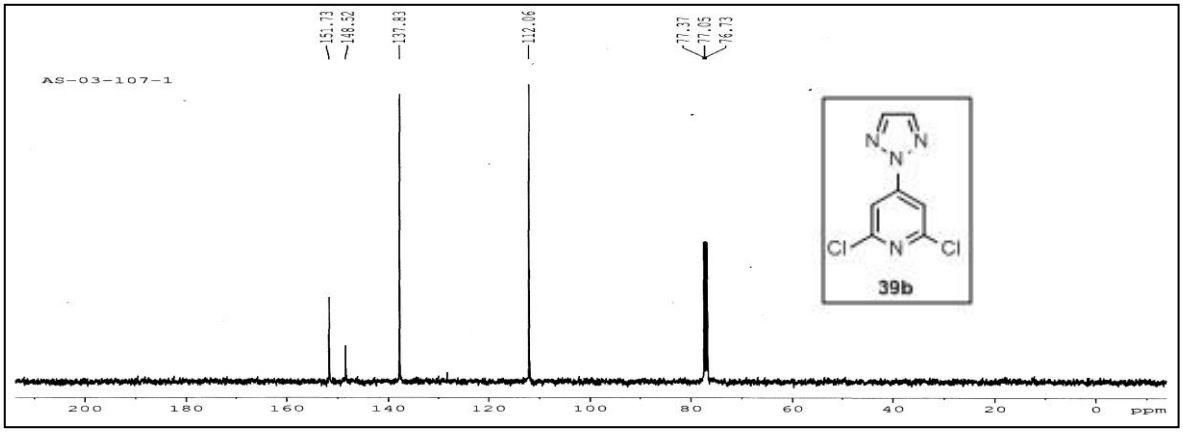
AS-03-107-1
151.73
148.52
137.83
112.06
77.37
77.05
76.73
39b
ppm

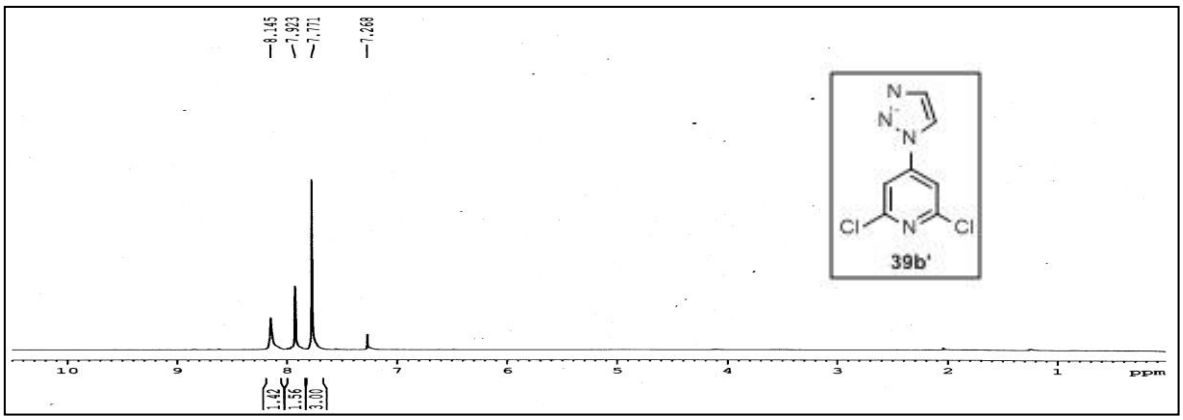
8.145
7.923
7.771
7.268
39b'
ppm

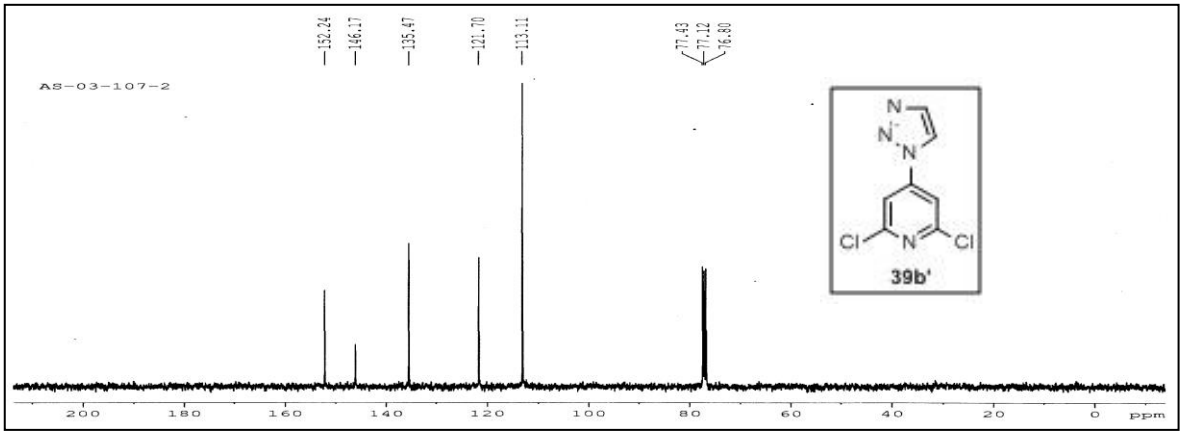
AS-03-107-2
152.24
146.17
135.47
121.70
113.11
77.43
77.12
76.80
39b'
ppm

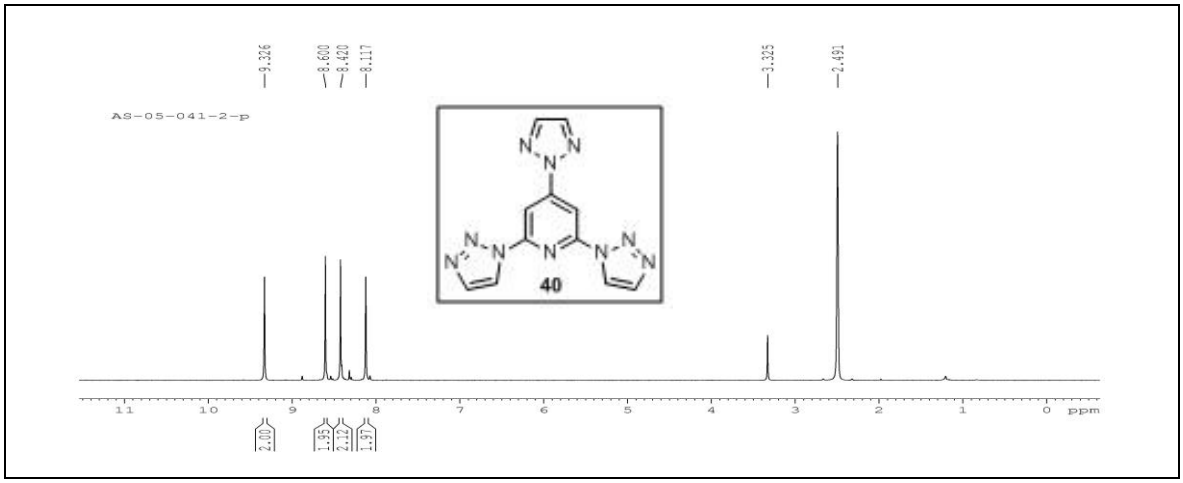
AS-05-041-2-p
9.326
8.600
8.420
8.117
3.325
2.491
40
ppm

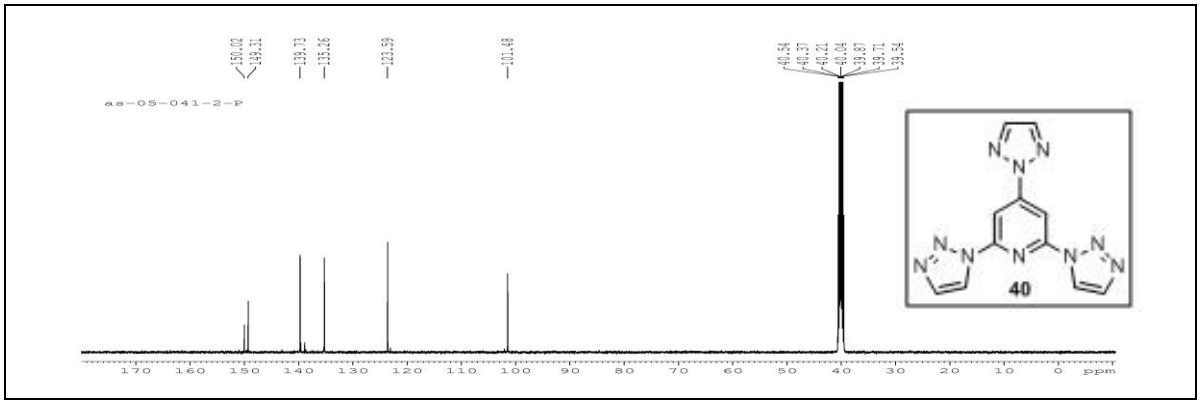
as-05-041-2-P
150.02
149.31
139.73
135.26
123.59
101.48
40.54
40.37
40.21
40.04
39.87
39.71
39.54
40
ppm

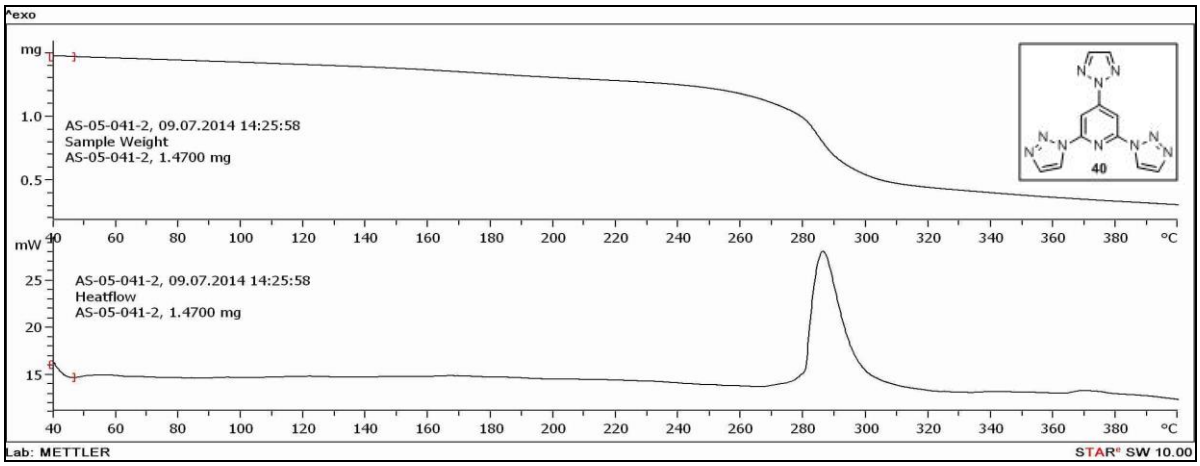
exo
mg
AS-05-041-2, 09.07.2014 14:25:58
Sample Weight
AS-05-041-2, 1.4700 mg
mW
AS-05-041-2, 09.07.2014 14:25:58
Heatflow
AS-05-041-2, 1.4700 mg
°C
Lab: METTLER
STARe SW 10.00
40

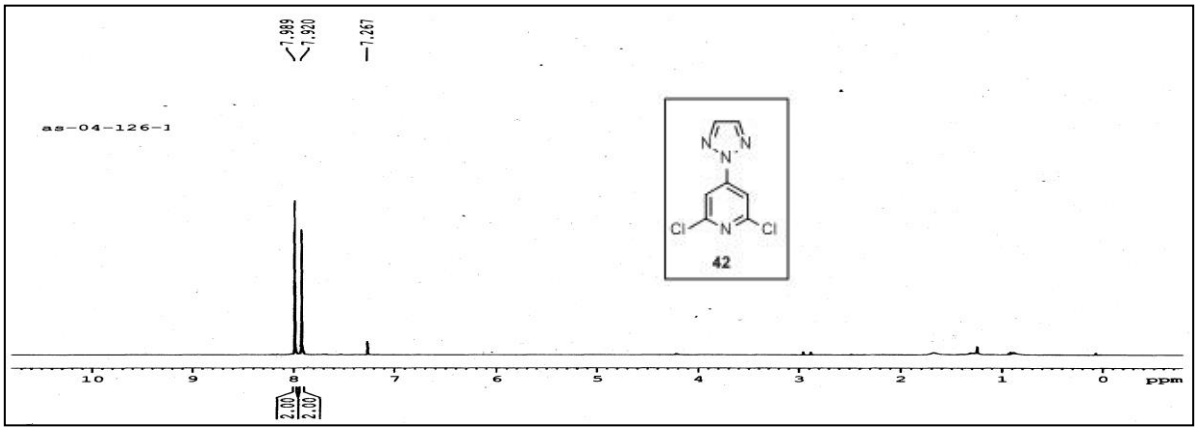
as-04-126-1
1.989
1.920
1.267
2.00
2.00
42
ppm

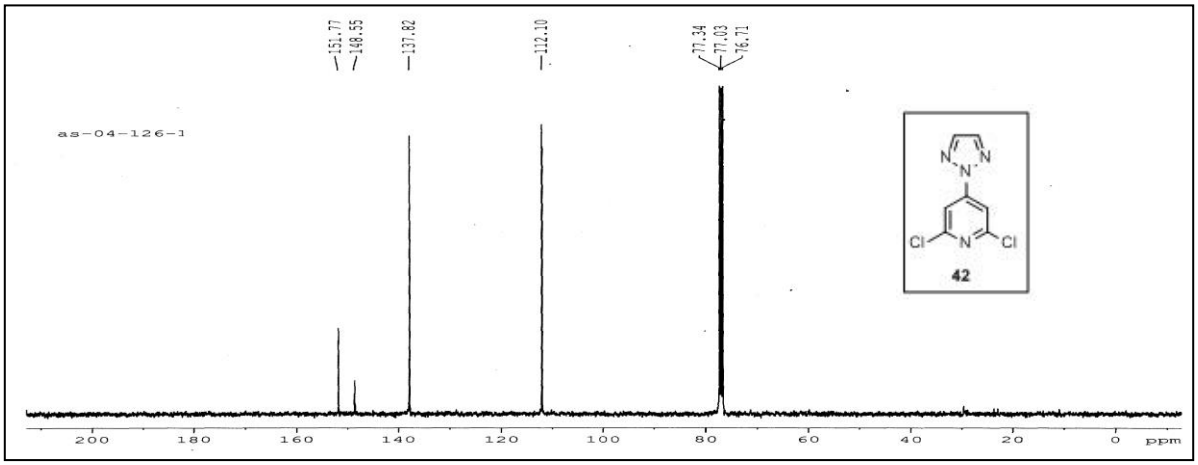
as-04-126-1
151.77
148.55
137.82
112.10
77.34
77.03
76.71
42
ppm

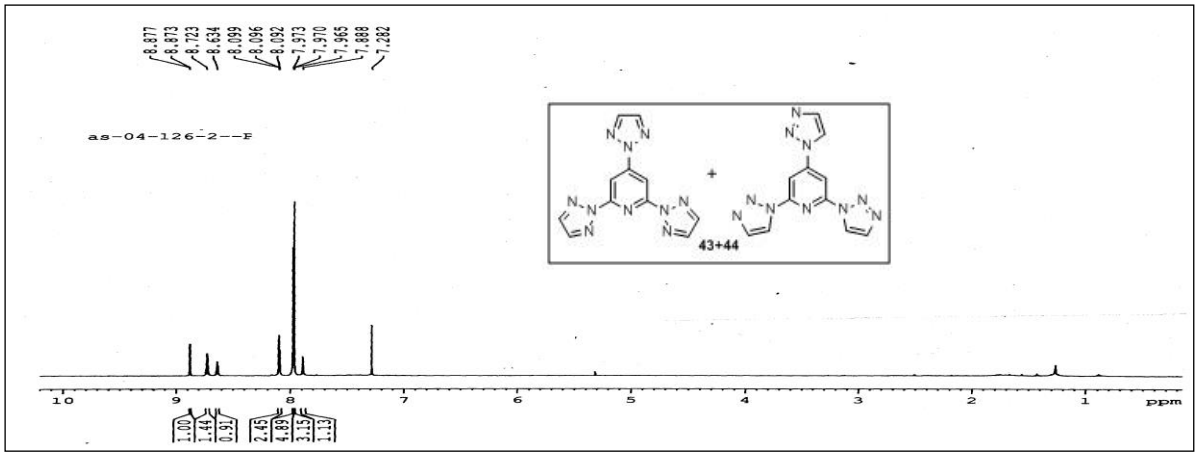
as-04-126-2--P
43+44
ppm

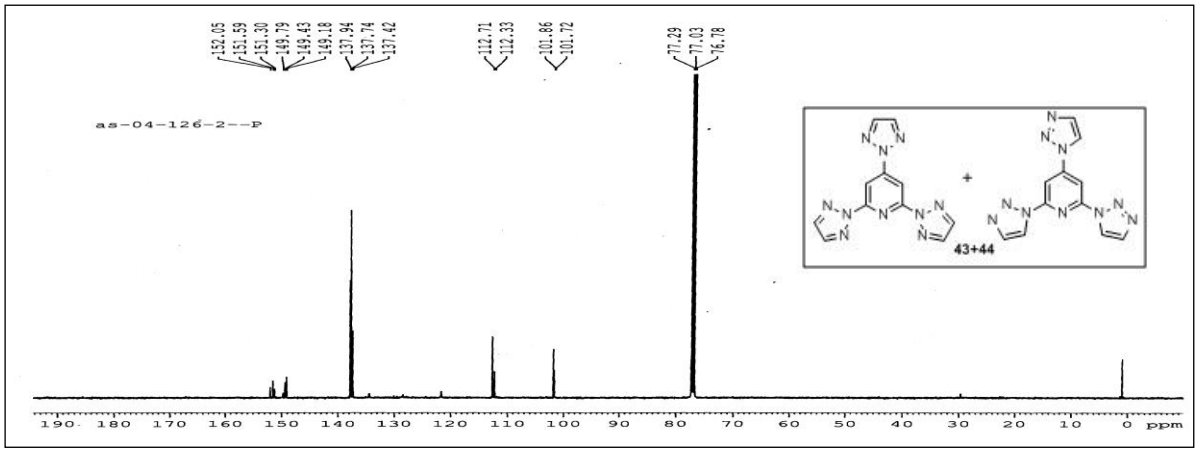
as-04-126-2--P
43+44
ppm

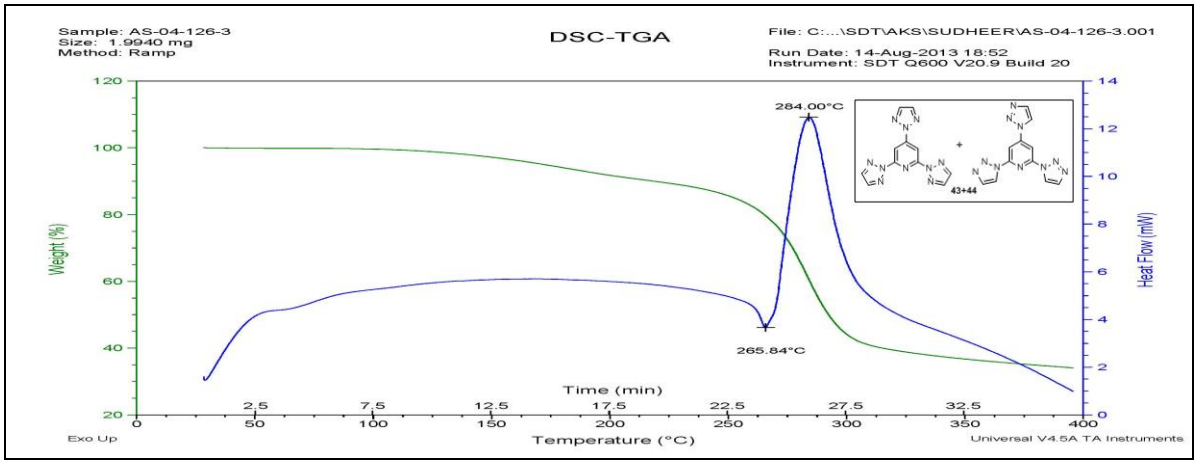
Sample: AS-04-126-3
Size: 1.9940 mg
Method: Ramp
DSC-TGA
File: C:...\SDT\AKS\SUDHEER\AS-04-126-3.001
Run Date: 14-Aug-2013 18:52
Instrument: SDT Q600 V20.9 Build 20
284.00°C
265.84°C
43+44
Weight (%)
Heat Flow (mW)
Time (min)
Temperature (°C)
Exo Up
Universal V4.5A TA Instruments

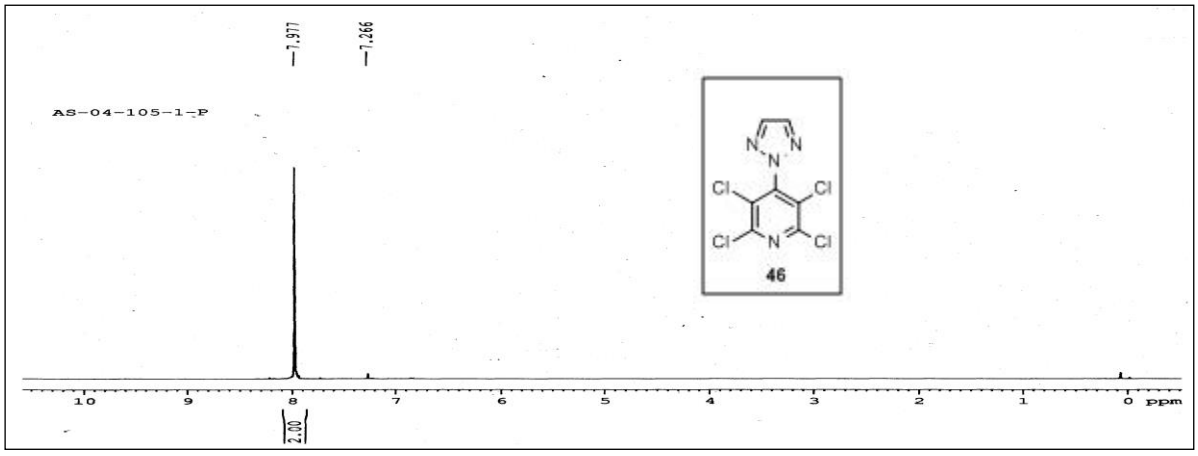
AS-04-105-1-P
46
ppm

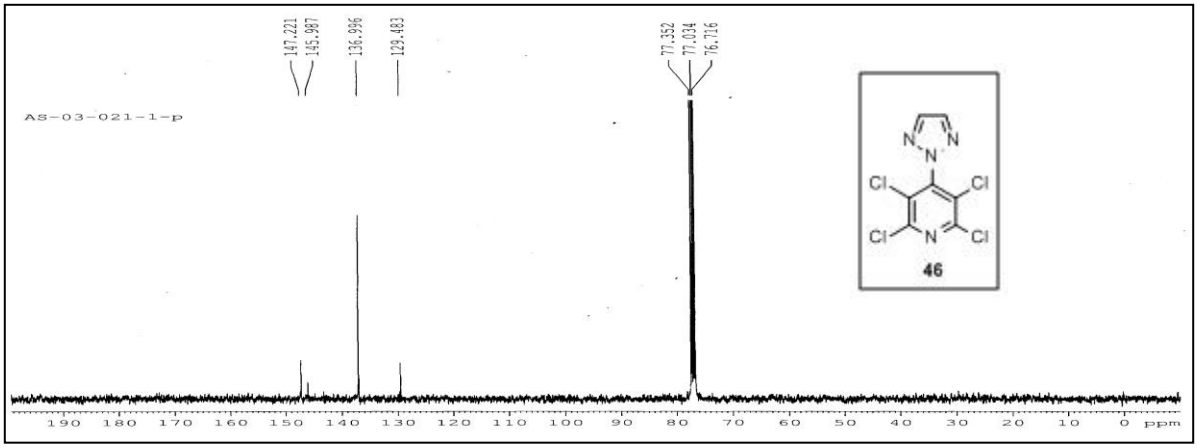
147.221
145.987
136.996
129.483
77.352
77.034
76.716
AS-03-021-1-p
46
190 180 170 160 150 140 130 120 110 100 90 80 70 60 50 40 30 20 10 0 ppm

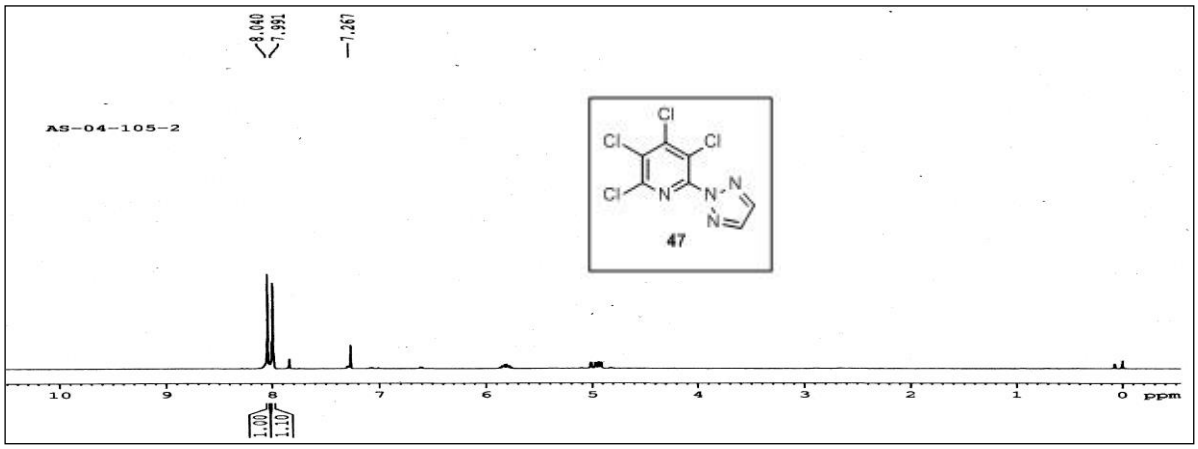
8.040
7.991
7.267
AS-04-105-2
47
10 9 8 7 6 5 4 3 2 1 0 ppm
1.00
1.10

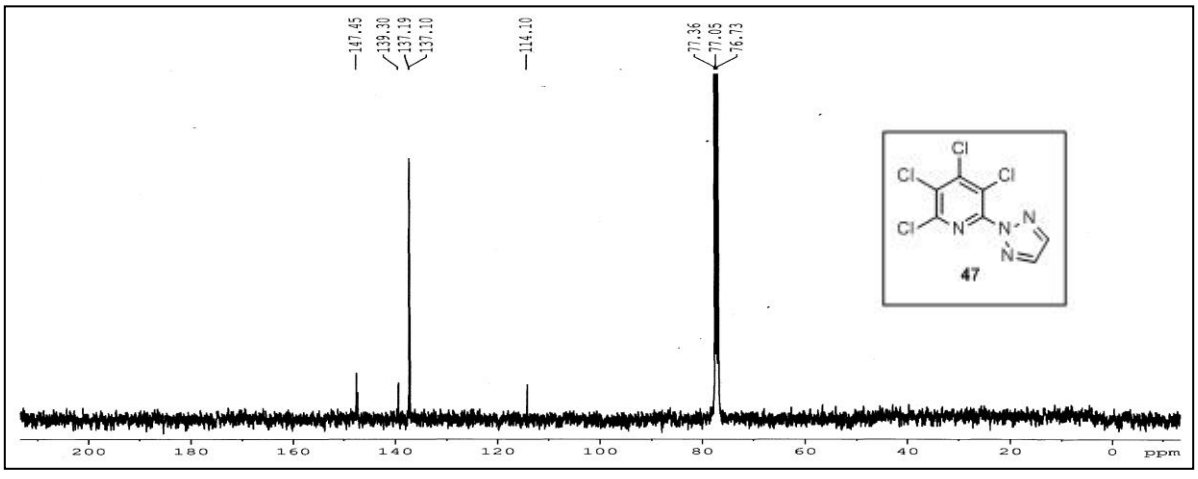
147.45
139.30
137.19
137.10
114.10
77.36
77.05
76.73
47
200 180 160 140 120 100 80 60 40 20 0 ppm

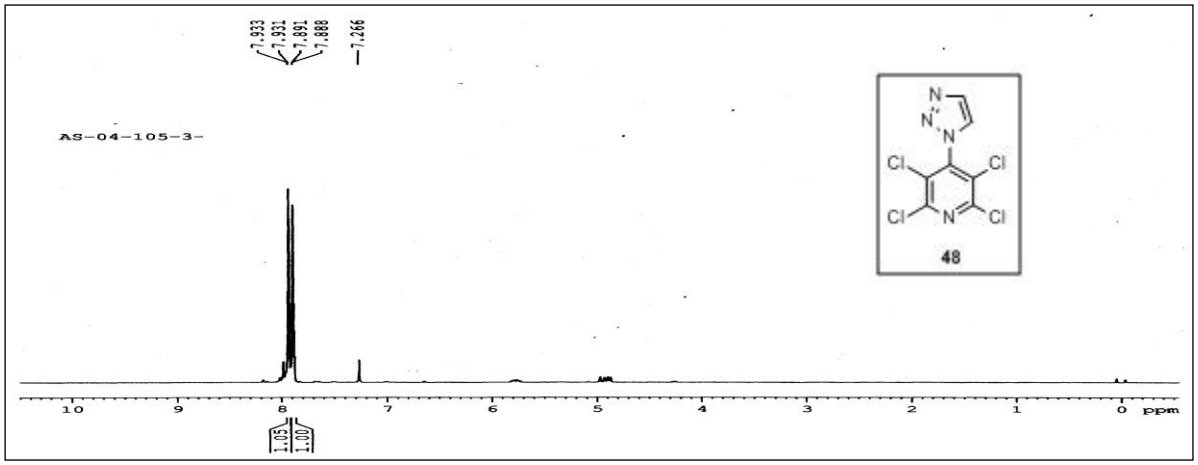
7.933
7.931
7.891
7.888
7.266
AS-04-105-3-
48
10 9 8 7 6 5 4 3 2 1 0 ppm
1.05
1.00

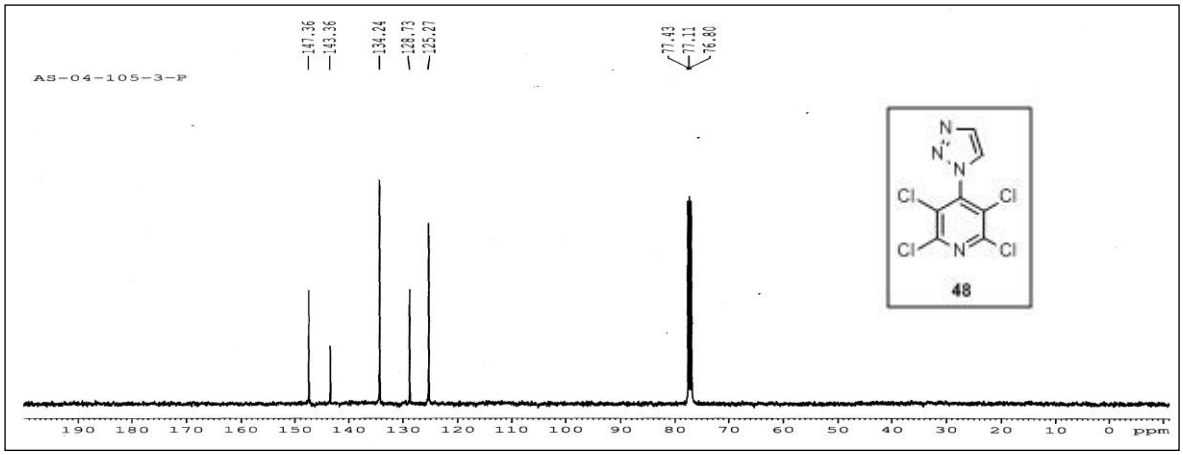
AS-04-105-3-P
147.36
143.36
134.24
128.73
125.27
77.43
77.11
76.80
48
ppm

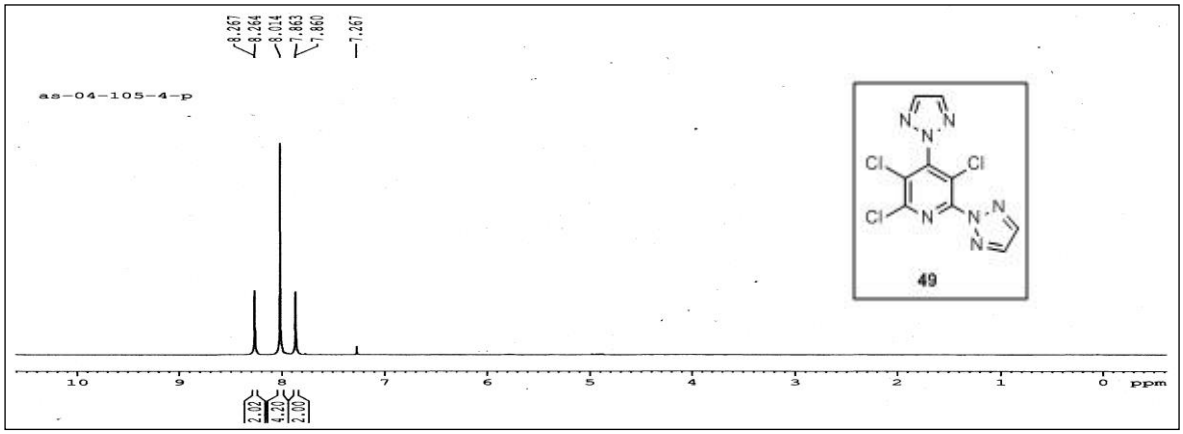
as-04-105-4-p
8.267
8.264
8.014
7.863
7.860
7.267
49
2.02
4.20
2.00
ppm

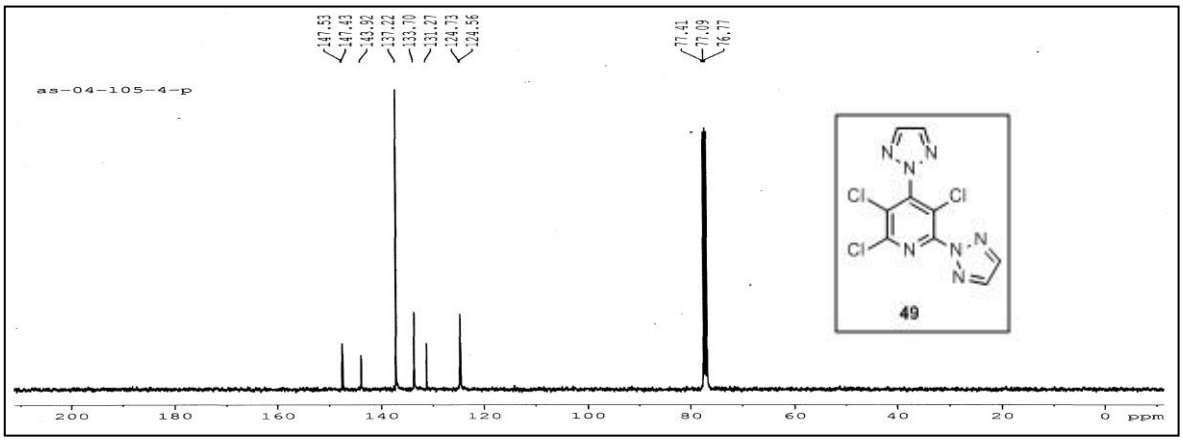
as-04-105-4-p
147.53
147.43
143.92
137.22
133.70
131.27
124.73
124.56
77.41
77.09
76.77
49
ppm

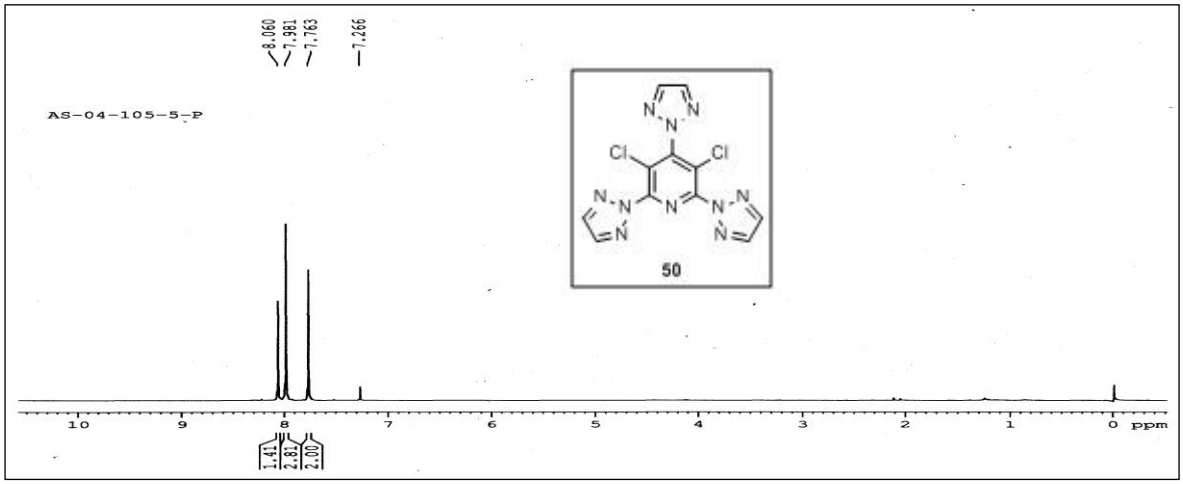
AS-04-105-5-P
8.060
7.981
7.763
7.266
50
1.41
2.82
2.00
ppm

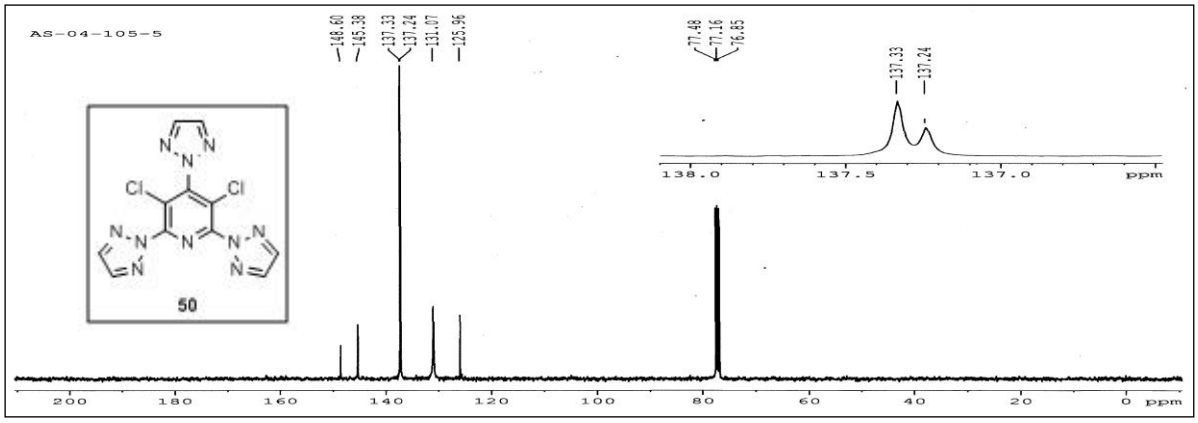
AS-04-105-5
148.60
145.38
137.33
137.24
131.07
125.96
77.48
77.16
76.85
131.33
131.24
138.0
137.5
137.0
ppm
Cl
Cl
50
200
180
160
140
120
100
80
60
40
20
0 ppm

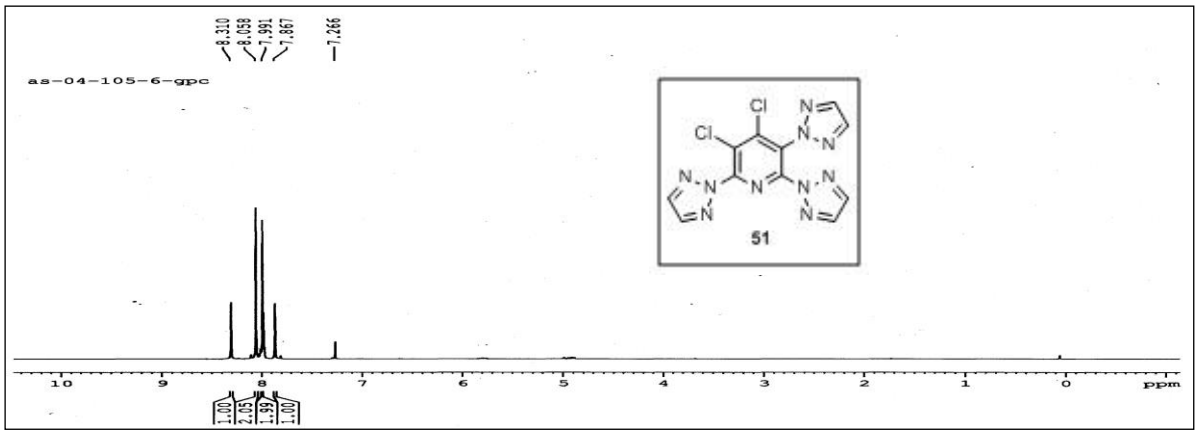
as-04-105-6-gpc
8.310
8.058
7.991
7.867
7.266
Cl
Cl
51
10
9
8
7
6
5
4
3
2
1
0
ppm
1.00
2.05
1.99
1.00

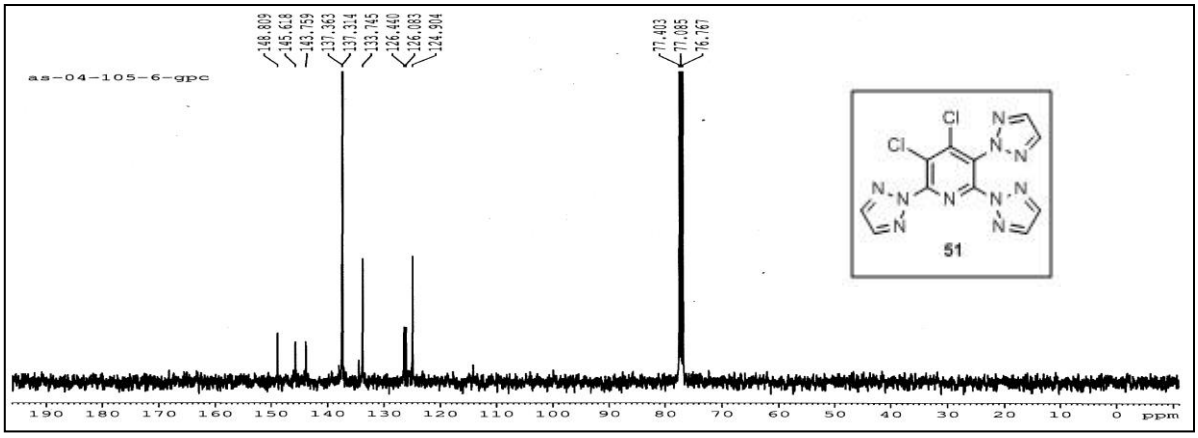
as-04-105-6-gpc
146.809
145.618
145.759
137.363
137.314
133.745
126.440
126.083
124.904
77.403
77.085
76.767
Cl
Cl
51
190
180
170
160
150
140
130
120
110
100
90
80
70
60
50
40
30
20
10
0
ppm

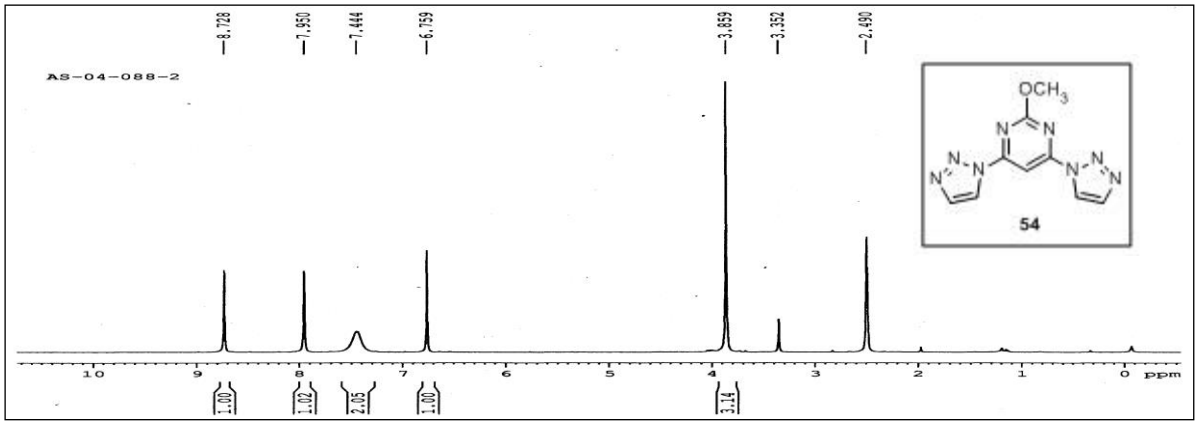
AS-04-088-2
8.728
7.950
7.444
6.759
3.659
3.352
2.490
OCH3
54
10
9
8
7
6
5
4
3
2
1
0
ppm
1.00
1.02
2.05
1.00
3.14

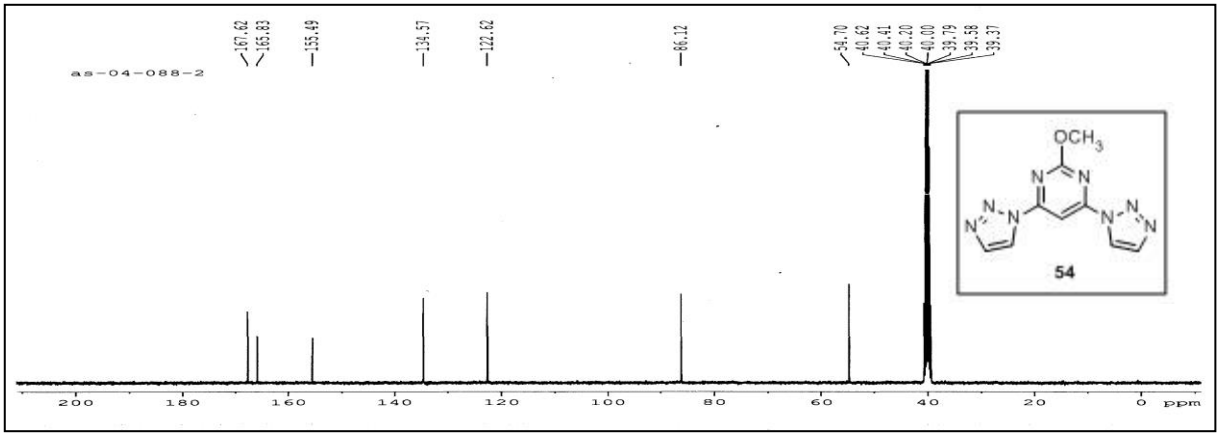
as-04-088-2
167.62
165.83
155.49
134.57
122.62
86.12
58.70
40.62
40.41
40.20
40.00
39.79
39.58
39.37
OCH3
54
200
180
160
140
120
100
80
60
40
20
0
ppm

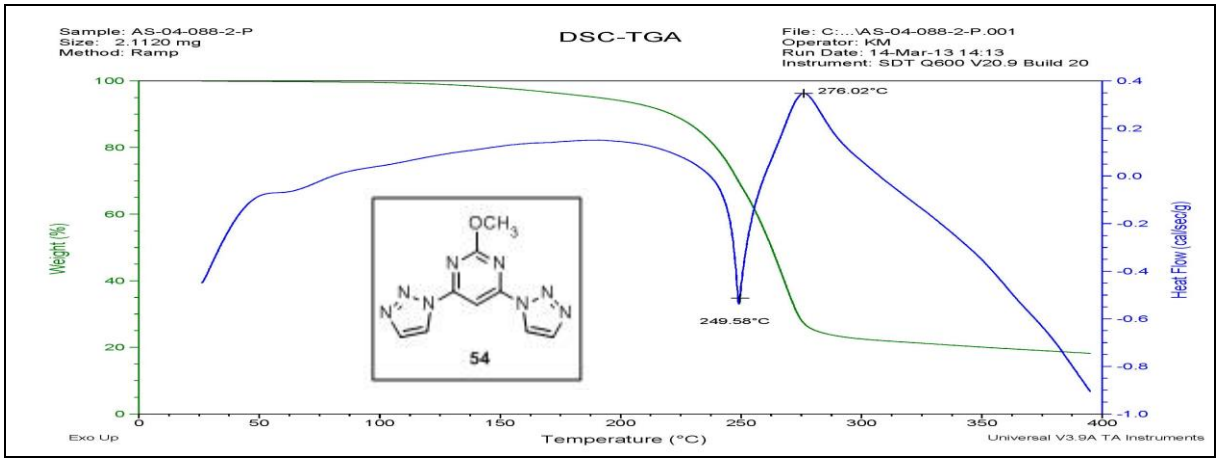
Sample: AS-04-088-2-P
Size: 2.1120 mg
Method: Ramp
DSC-TGA
File: C:...\AS-04-088-2-P.001
Operator: KM
Run Date: 14-Mar-13 14:13
Instrument: SDT Q600 V20.9 Build 20
276.02°C
249.58°C
OCH3
54
Weight (%)
Heat Flow (cal/sec/g)
Temperature (°C)
Exo Up
Universal V3.9A TA Instruments

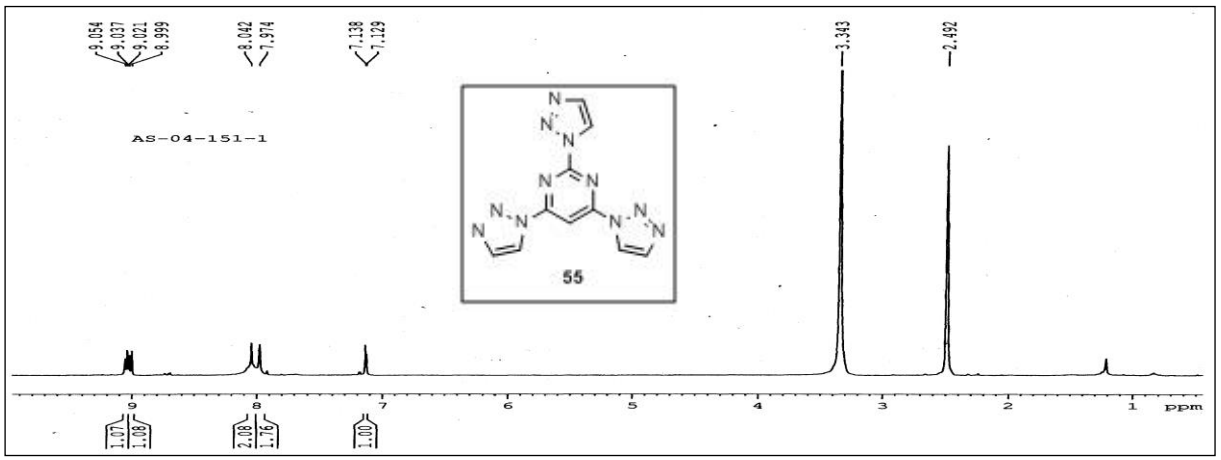
9.054
9.037
9.021
8.999
8.042
7.974
7.138
7.129
3.343
2.492
AS-04-151-1
55
1.07
1.08
2.08
1.76
1.00
ppm

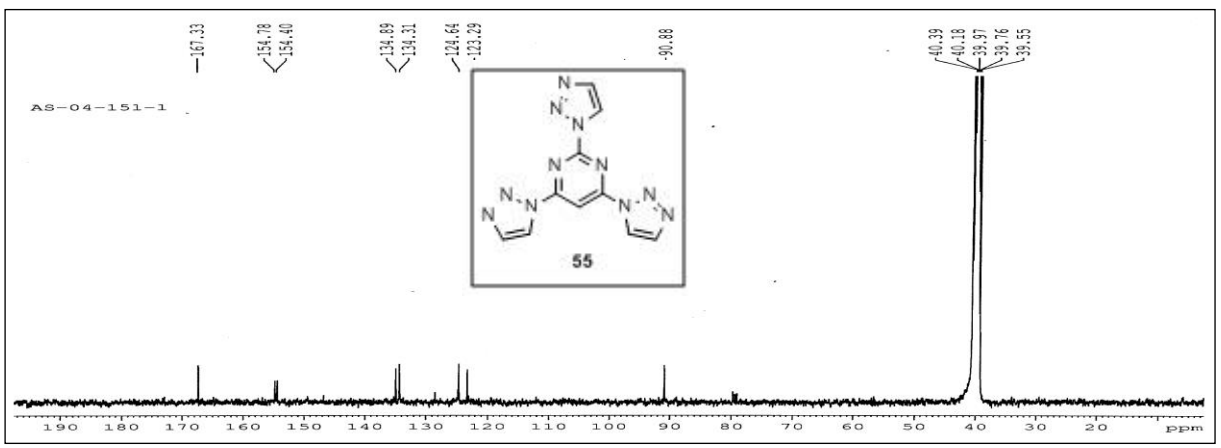
167.33
154.78
154.40
134.89
134.31
124.64
123.29
90.88
40.39
40.18
39.97
39.76
39.55
AS-04-151-1
55
ppm

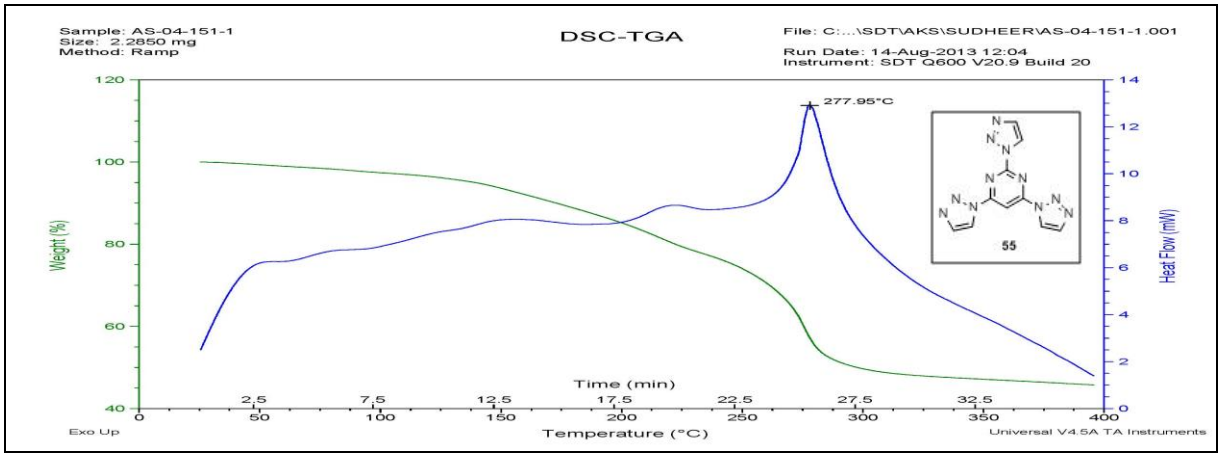
Sample: AS-04-151-1
Size: 2.2850 mg
Method: Ramp
DSC-TGA
File: C:...\SDT\AKS\SUDHEER\AS-04-151-1.001
Run Date: 14-Aug-2013 12:04
Instrument: SDT Q600 V20.9 Build 20
277.95°C
55
Weight (%)
Heat Flow (mW)
Time (min)
Temperature (°C)
Exo Up
Universal V4.5A TA Instruments

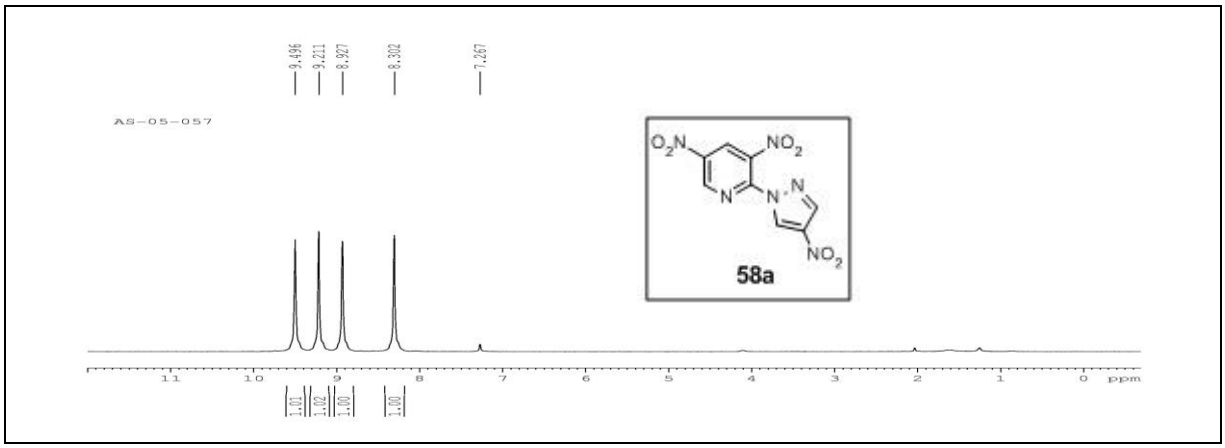
9.496
9.211
8.927
8.302
7.267
AS-05-057
58a
ppm

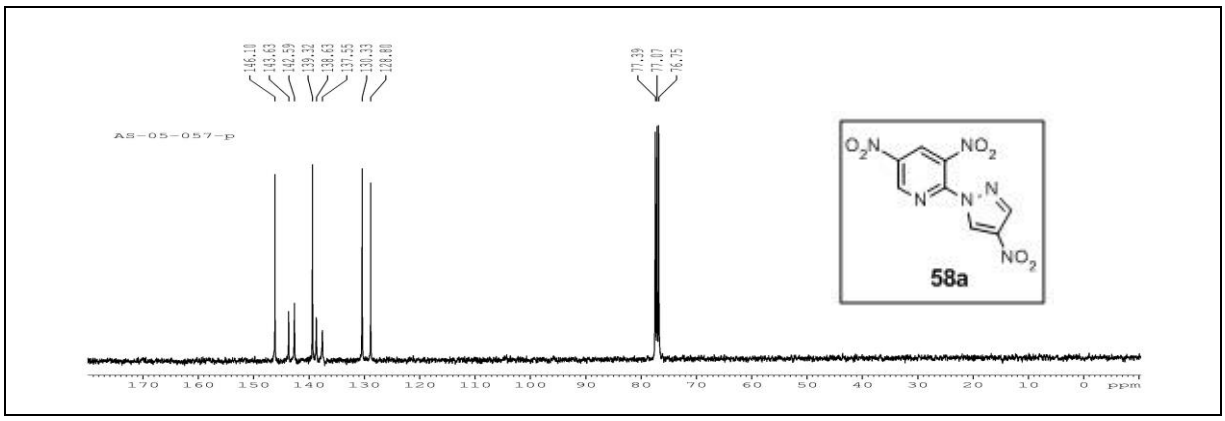
146.18
143.63
142.59
139.32
138.63
137.55
130.33
120.80
77.39
77.07
76.75
AS-05-057-p
58a
ppm

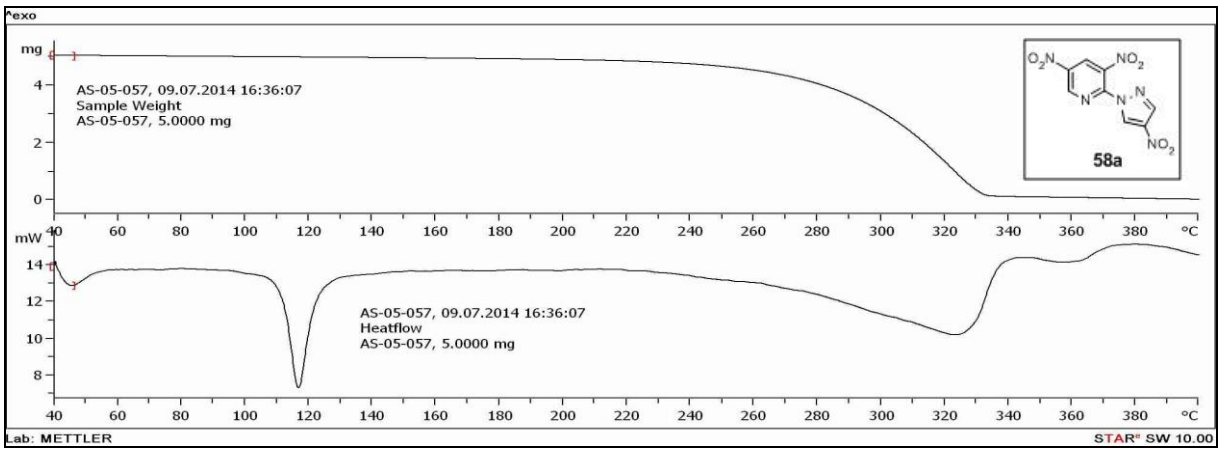
^exo
mg
AS-05-057, 09.07.2014 16:36:07
Sample Weight
AS-05-057, 5.0000 mg
58a
mW
AS-05-057, 09.07.2014 16:36:07
Heatflow
AS-05-057, 5.0000 mg
°C
Lab: METTLER
STAR° SW 10.00

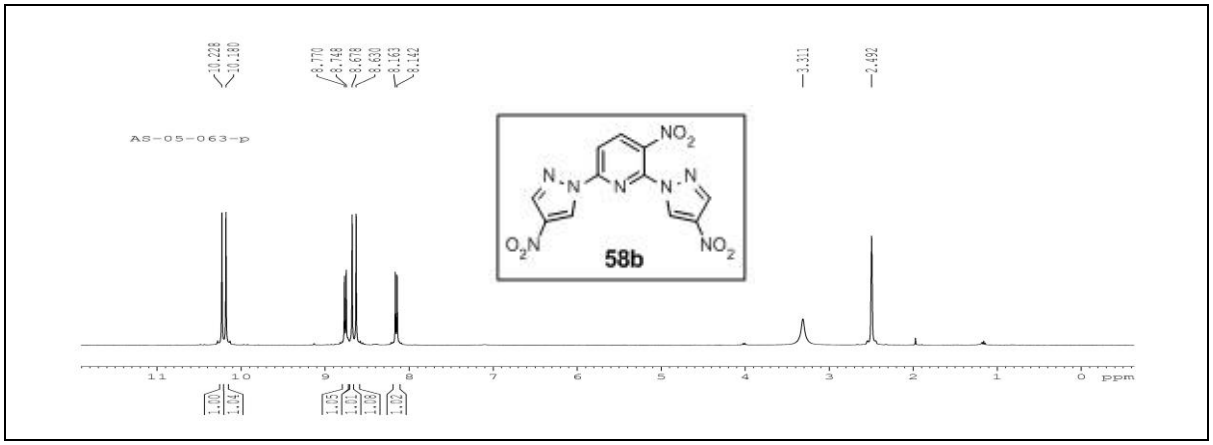
AS-05-063-p
58b

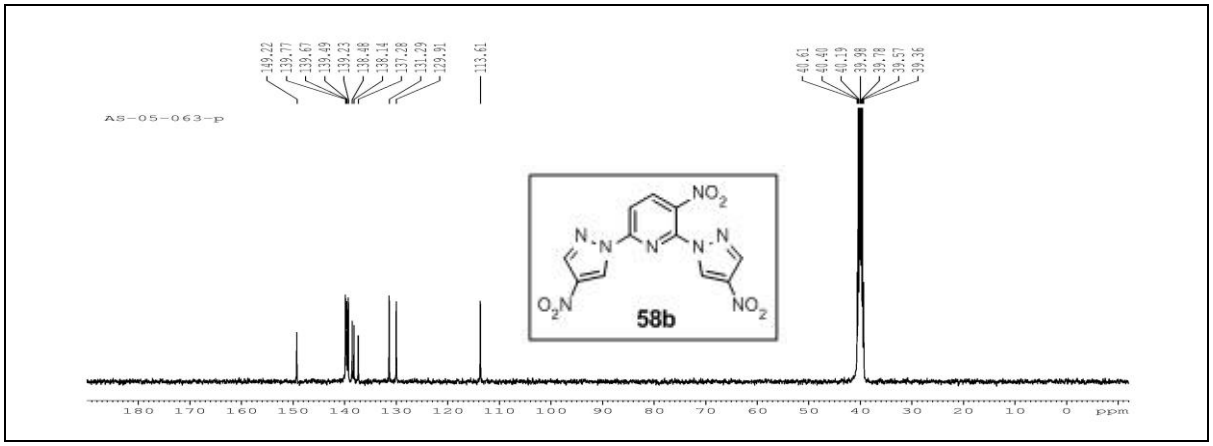
AS-05-063-p
58b

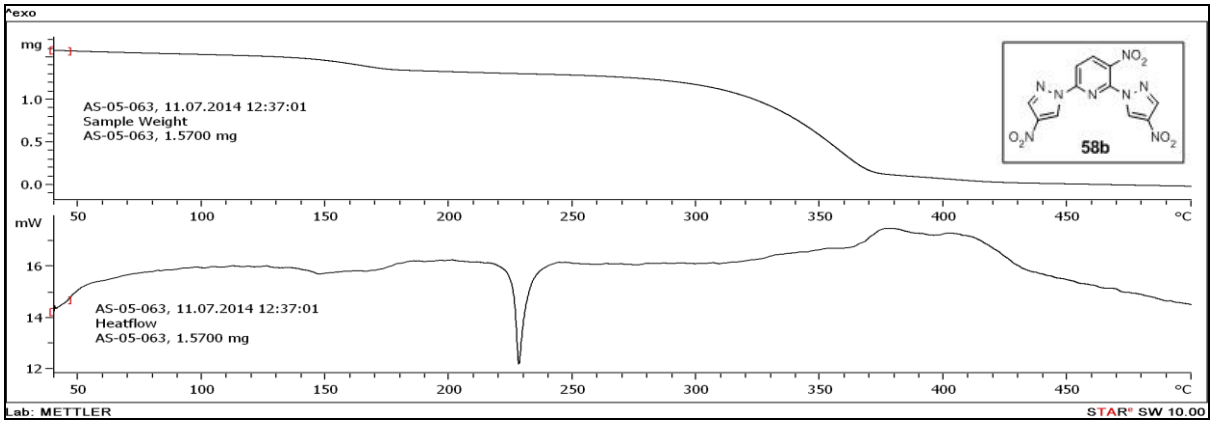
AS-05-063, 11.07.2014 12:37:01
Sample Weight
AS-05-063, 1.5700 mg
AS-05-063, 11.07.2014 12:37:01
Heatflow
AS-05-063, 1.5700 mg
58b
Lab: METTLER

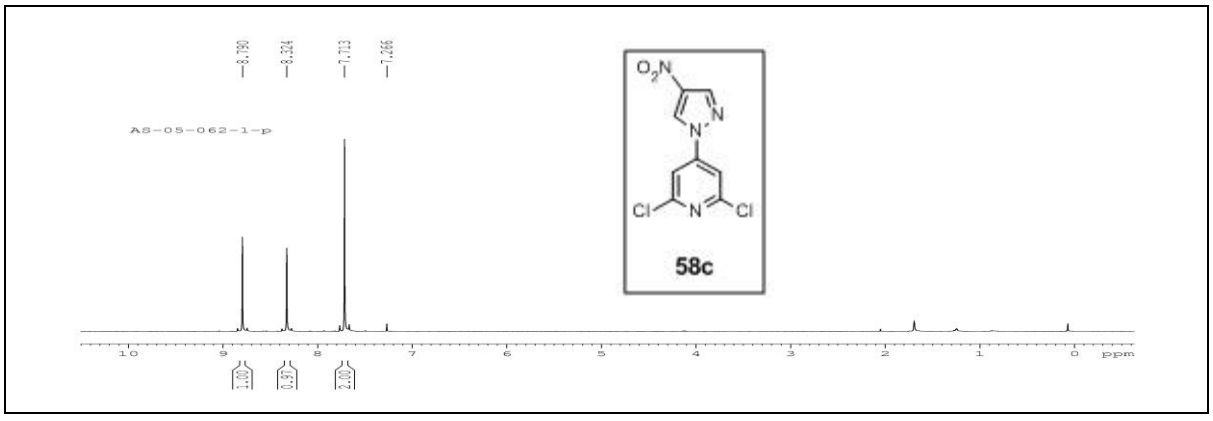
AS-05-062-1-p
58c

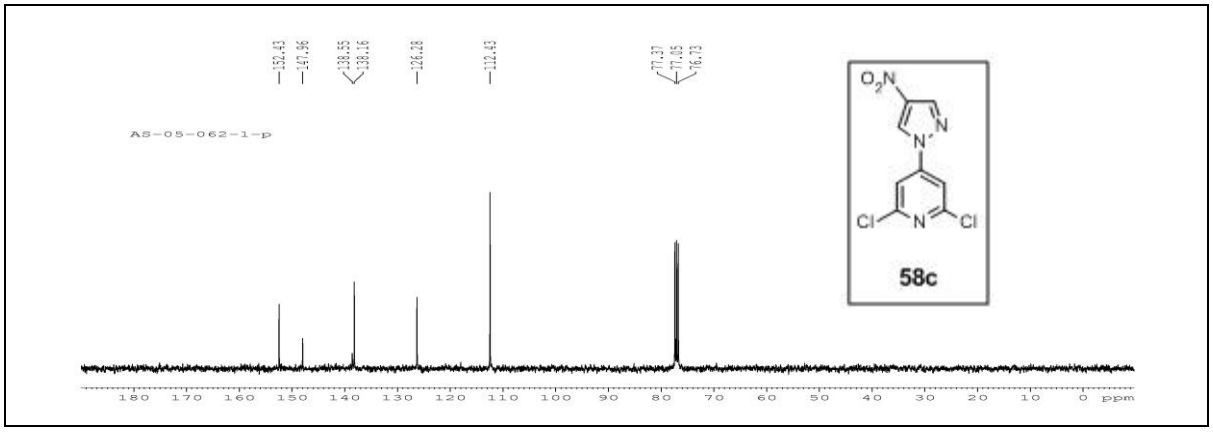
AS-05-062-1-p
58c

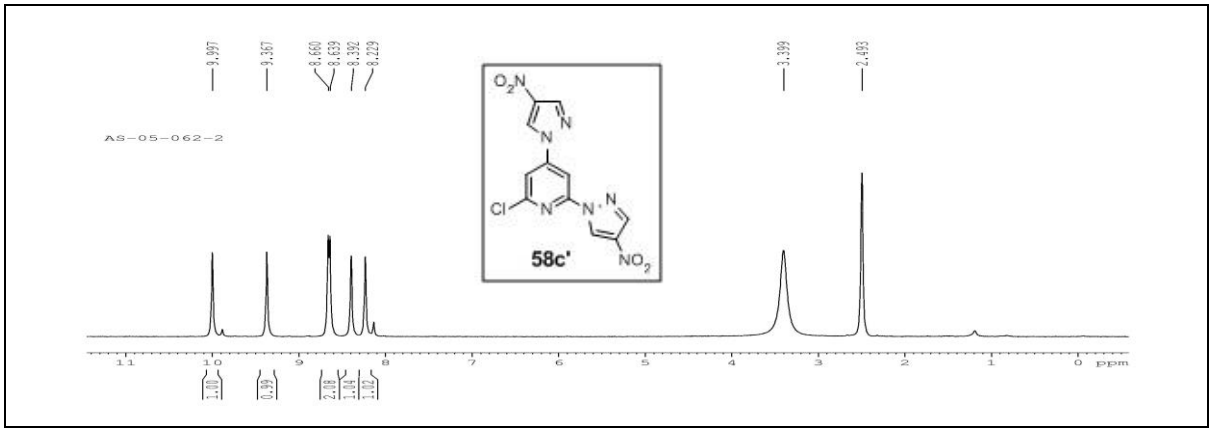
AS-05-062-2
58c'

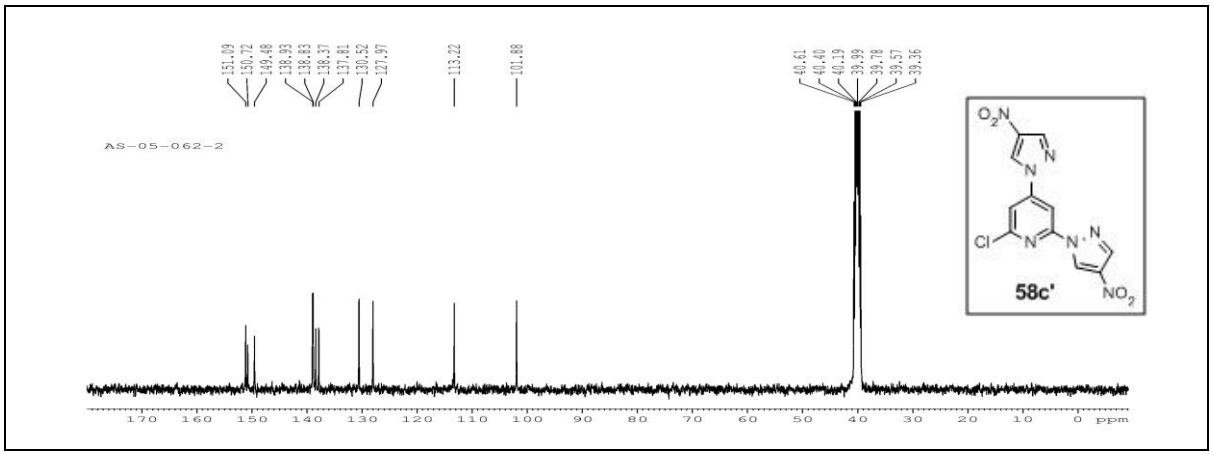
AS-05-062-2
58c'

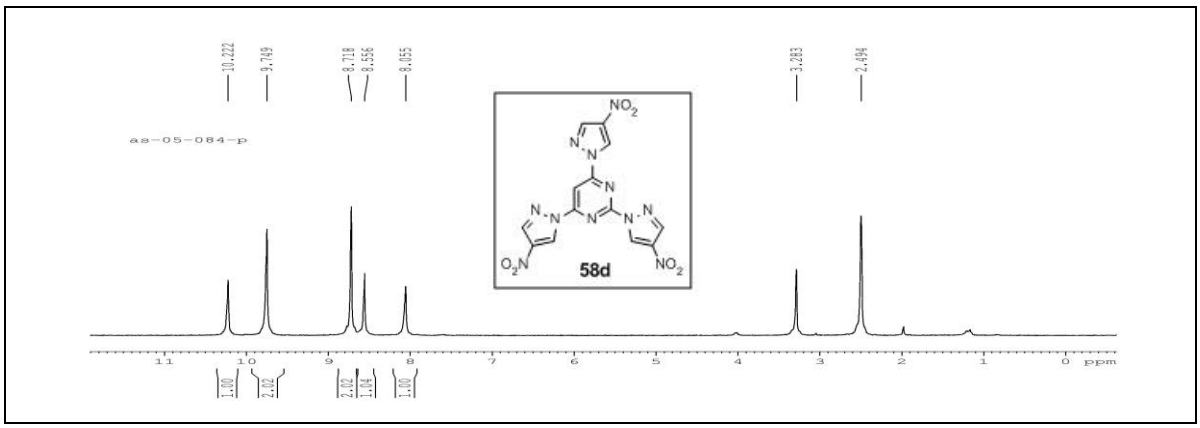
aa-05-084-p
58d

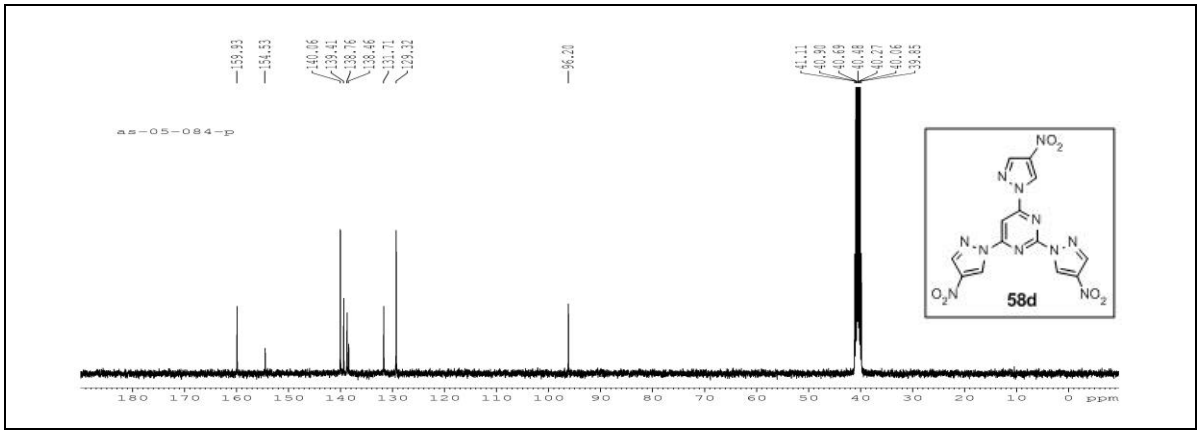
159.93
154.53
140.06
139.41
138.76
138.46
131.71
129.32
96.20
41.11
40.90
40.69
40.48
40.27
40.06
39.85
as-05-084-p
58d

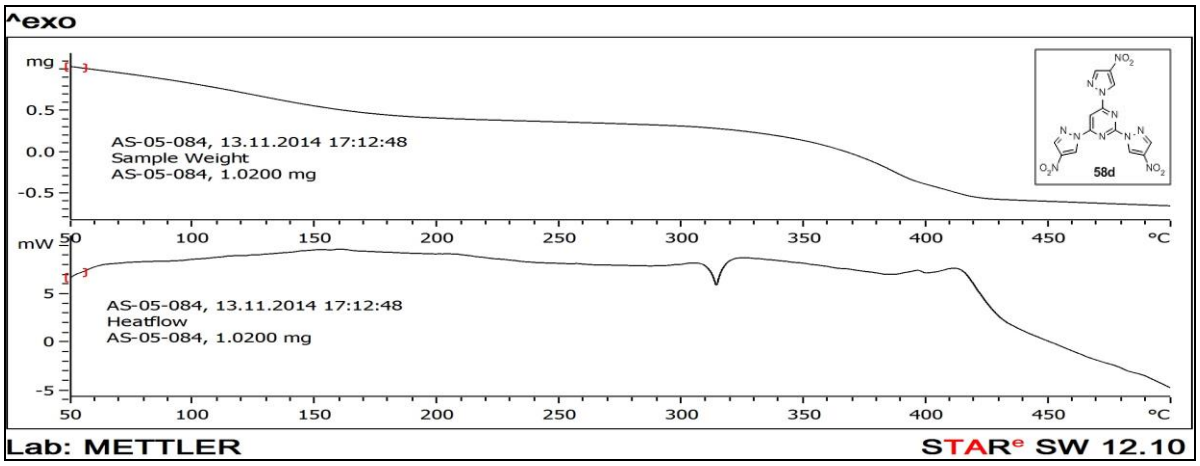
^exo
mg
AS-05-084, 13.11.2014 17:12:48
Sample Weight
AS-05-084, 1.0200 mg
mW
AS-05-084, 13.11.2014 17:12:48
Heatflow
AS-05-084, 1.0200 mg
°C
58d
Lab: METTLER
STARe SW 12.10

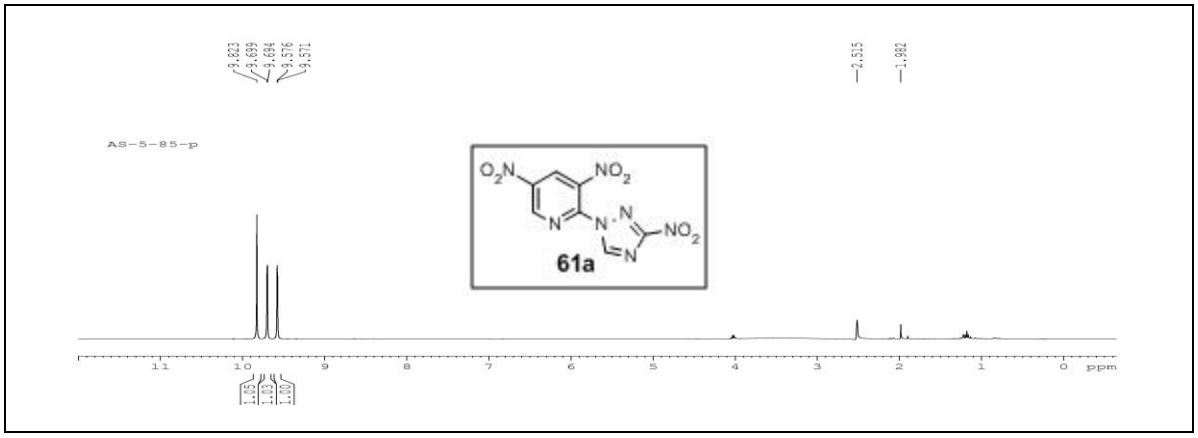
9.823
9.699
9.694
9.576
9.571
2.515
1.982
AS-5-85-p
61a
ppm

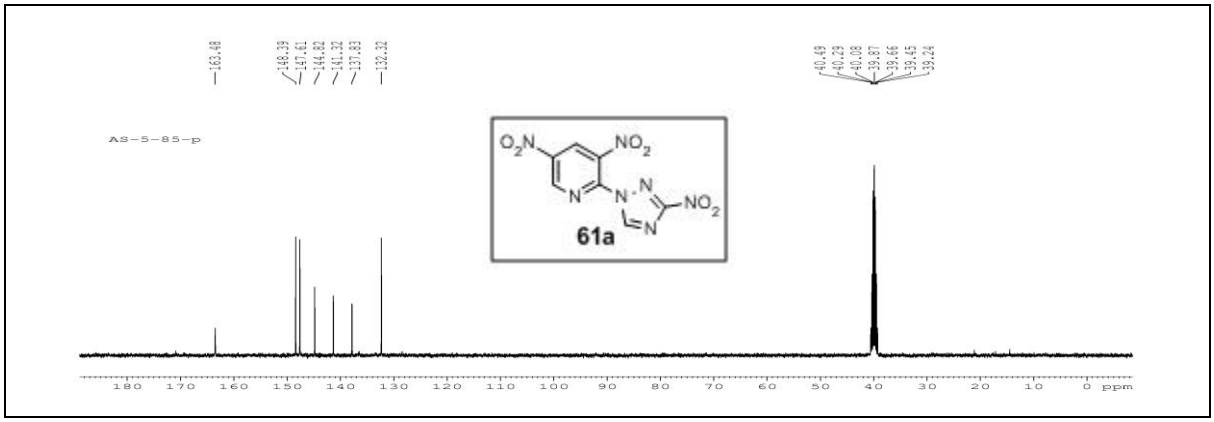
163.48
148.39
147.61
144.82
141.32
137.83
132.32
40.49
40.29
40.08
39.87
39.66
39.45
39.24
AS-5-85-p
61a
ppm

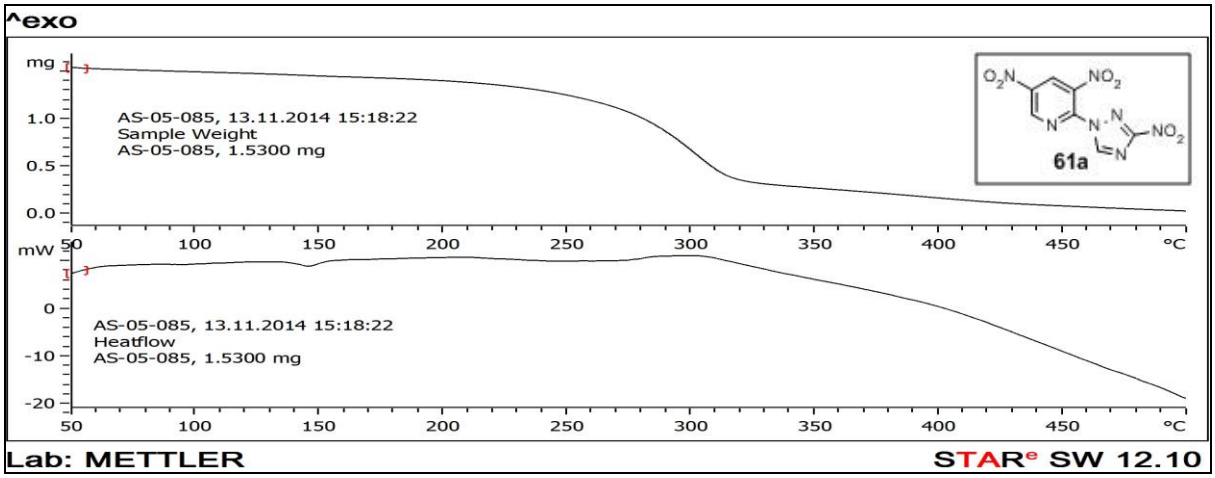
^exo
mg
AS-05-085, 13.11.2014 15:18:22
Sample Weight
AS-05-085, 1.5300 mg
61a
mW
AS-05-085, 13.11.2014 15:18:22
Heatflow
AS-05-085, 1.5300 mg
°C
Lab: METTLER
STARe SW 12.10

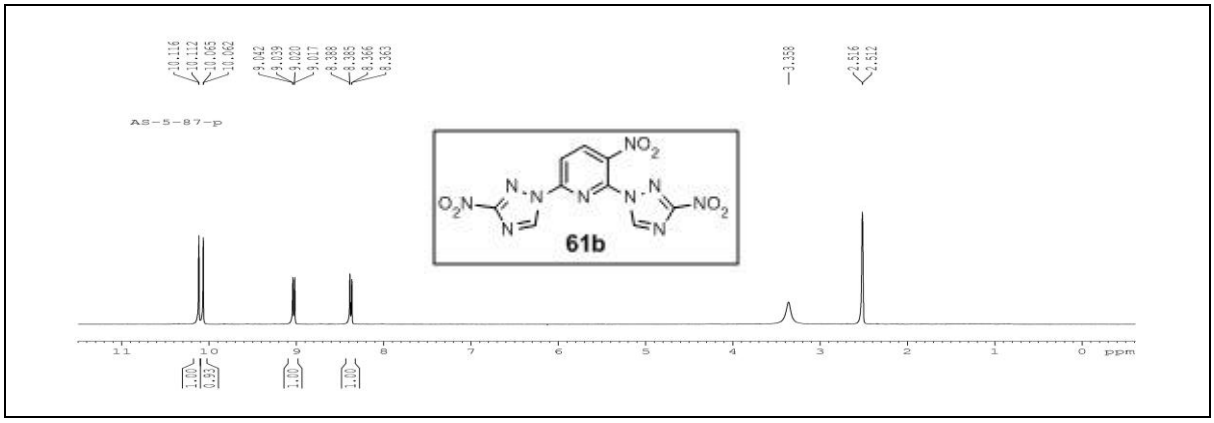
AS-5-87-p
61b
ppm

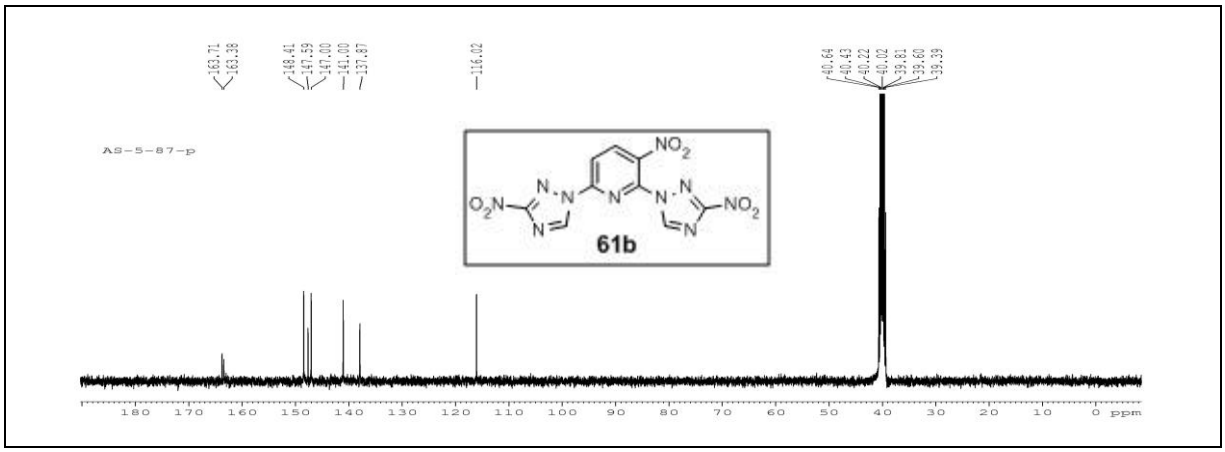
AS-5-87-p
61b
ppm

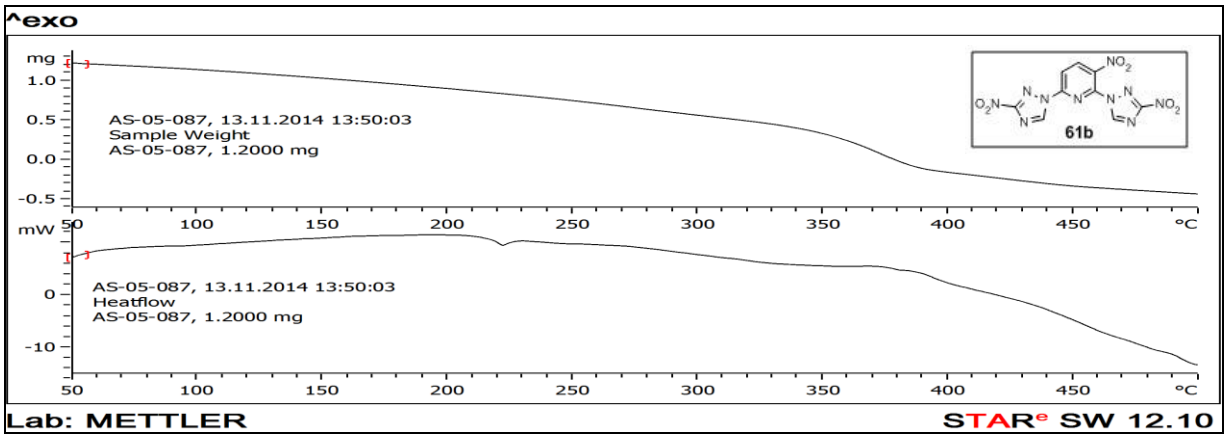
^exo
mg
AS-05-087, 13.11.2014 13:50:03
Sample Weight
AS-05-087, 1.2000 mg
61b
mW
AS-05-087, 13.11.2014 13:50:03
Heatflow
AS-05-087, 1.2000 mg
°C
Lab: METTLER
STARe SW 12.10

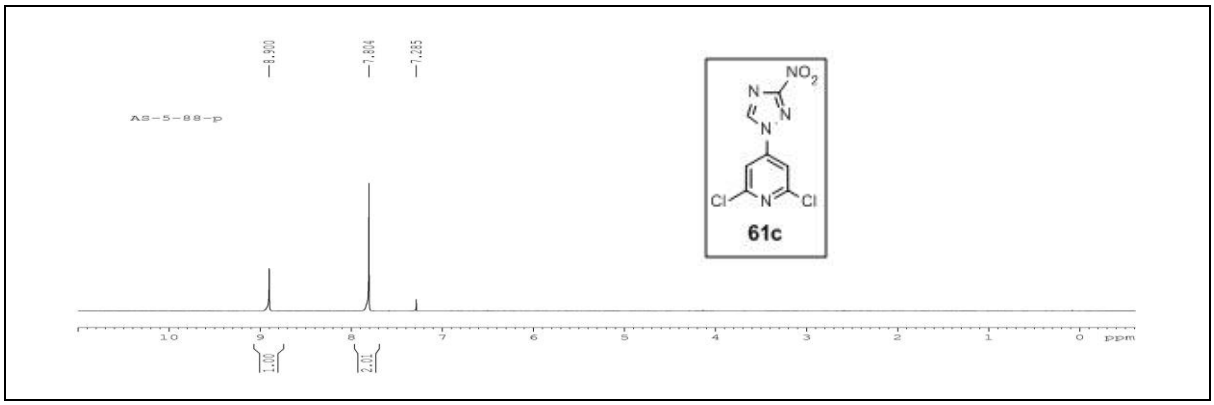
8.900
7.804
7.265
AS-5-88-p
61c
1.00
2.01
ppm

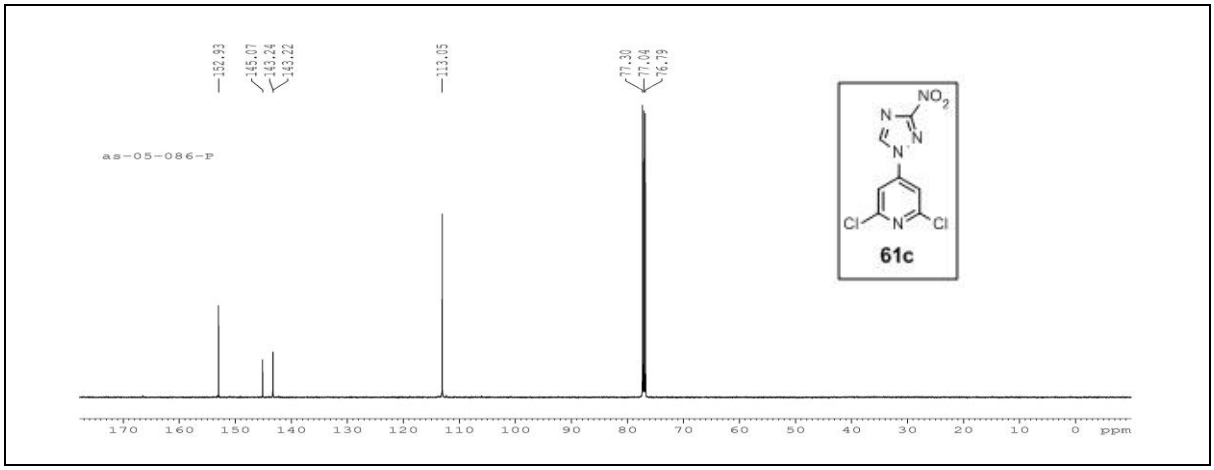
152.93
145.07
143.24
143.22
113.05
77.30
77.04
76.79
as-05-086-P
61c
ppm

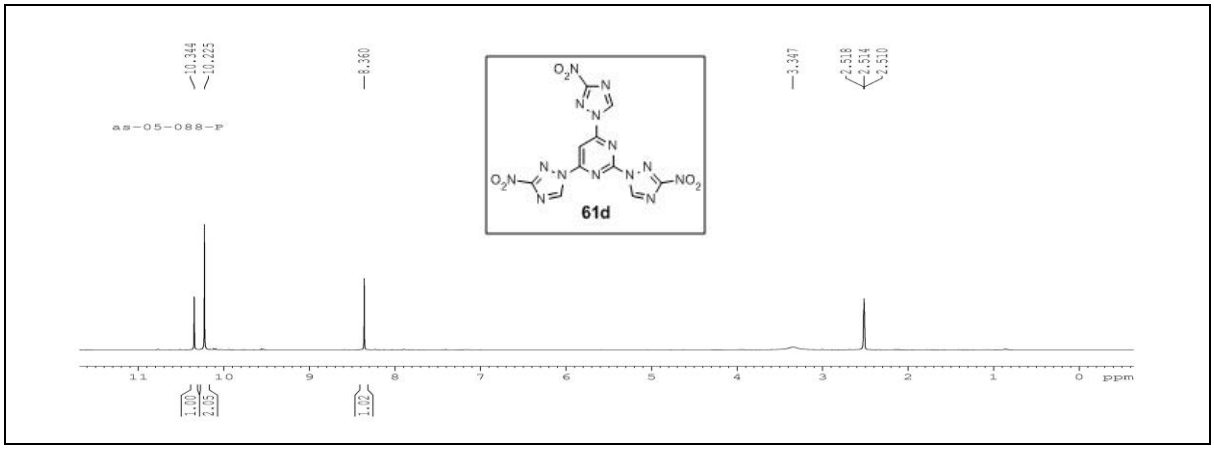
10.344
10.225
8.360
3.347
2.518
2.514
2.510
as-05-088-P
61d
1.00
2.05
1.02
ppm

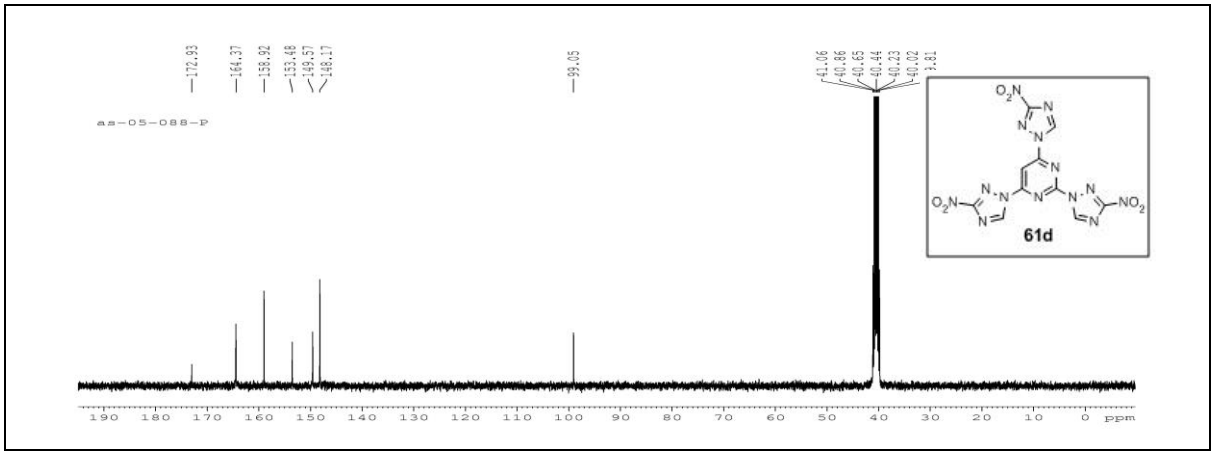
172.93
164.37
158.92
153.48
149.57
148.17
99.05
41.06
40.86
40.65
40.44
40.23
40.02
3.81
as-05-088-P
61d
ppm

List of Publications

1. Synthesis of Thermally Stable Energetic 1,2,3-Triazole Derivatives; A. Sudheer Kumar, Vikas D. Ghule, S. Subrahmanyam, Akhila K. Sahoo*, *Chem. Eur. J.* **2013**, *19*, 509-518.
2. Synthesis of Trifluromethyl-Substituted *N*-Aryl Poly-1,2,3-Triazole Derivatives; A. Sudheer Kumar, Vikas D. Ghule, Nagarjuna Kommu, Akhila K. Sahoo*, *J. Mater. Chem. A*, **2014**, *2*, 7917-7926.
3. Triazole Substituted Nitroarene Derivatives: Synthesis, Characterization, and Energetic Studies; Nagarjuna Kommu, Vikas D. Ghule, A. Sudheer Kumar, Akhila K. Sahoo*, *Chem. Asian J.* **2014**, *9*, 166-178.
4. Thermal Stability Study of Nitro-rich Triazole Derivatives using Temperature Dependent Time Resolved Pulsed Photoacoustic (PA) Technique; K. S. Rao, F. Yehya, A. K. Chaudhary*, A. Sudheer Kumar, Akhila K. Sahoo*, *J. Anal. . Appl. Pyrol.*, **2014**, *109*, 132-139.
5. Study of Acoustic Fingerprinting of Nitromethane and Some Triazole Derivatives Using UV266 nm Pulsed Photoacoustic (PA) Pyrolysis Technique; K. S. Rao, A. K. Chaudhary*, F. Yehya, A. Sudheer Kumar, *Spectrochim. Acta A*, **2015,** *147***,** 316-323.
6. Synthesis Characterization and Energetic Studies of Polynitro-Aryl-1,2,3-2*H*-Triazole Derivatives; Nagarjuna Kommu, A. Sudheer Kumar, J. Raveendra, Vikas D. Ghule, Akhila K. Sahoo* *"communicated"* (*Chem. Eur. J.*, **2015,** *DOI: 201502603*)
7. Synthesis and Energetic Studies of Nitrogen-Rich *N*-HeteroAryl-Azole Derivatives; A. Sudheer Kumar, Nagarjuna Kommu, Akhila K. Sahoo*, *"manuscript under preparation".*
8. Synthesis of Energetic Nitro-Substituted *N*-(Hetero)Aryl-Tetrazole Derivatives; Nagarjuna Kommu, A. Sudheer Kumar, M. Balaraju, Akhila K. Sahoo*, *"manuscript under preparation".*

Conference Attended

1. Synthesis of Trifluromethyl-Substituted *N*-Aryl Poly-1,2,3-Triazole Derivatives for Energetic Materials Applications"

   A. Sudheer Kumar, Nagarjuna Kommu, Vikas D. Ghule and Akhila K. Sahoo

   (i) *Oral and poster presentation* at "**18th International seminar on New Trends in Research of Energetic Materials (NTREM–2015)**" which was held on 15-April-2015 to 17-April-2015 in Institute of Energetic Materials, University of Pardubice, Pardubice, Czech Republic, European Union.

   (ii) *Oral presentation* at "**Chemfest-2015 (*In-house*)**" which was held on 20-Feb-2015 to 21-Feb-2015 in School of Chemistry, University of Hyderabad, Hyderabad, India.

   (iii) *Poster presentation* at "**9th International High Energy Materials Conference & Exhibit (HEMCE-2014)**" which was held on 13-Feb-2014 to 15-Feb-2014 in VSSC, Trivendrum, India.

   (iv) *Poster presentation* at "**Chemfest-2014 (*In-house*)**" which was held on 21-Feb-2014 to 22-Feb-2014 in School of Chemistry, University of Hyderabad, Hyderabad, India.

2. Synthesis of Thermally Stable Energetic 1,2,3-Triazole Derivatives

   A. Sudheer Kumar, Vikas D. Ghule, S. Subrahmanyam, and Akhila K. Sahoo

   (i) *Oral presentation* at "**8th International High Energy Materials Conference & Exhibit (HEMCE-2011)**" which was held on 10-Nov-2011 to 13-Nov-2011 in TBRL, Chandigarh, India.

3. *Participated* in "**7th International High Energy Materials Conference & Exhibit (HEMCE-2009)**" which was held on 08-Dec-2009 to 10-Dec-2009 in HEMRL, Pune, India.